GENETIC DETERMINANTS AND GENOTYPE-PHENOTYPE ASSOCIATIONS IN HYPERTROPHIC CARDIOMYOPATHY - CONTRIBUTION OF A HIGH-THROUGHPUT SEQUENCING APPROACH

LUÍS MIGUEL DA ROCHA LOPES

UNIVERSITY COLLEGE LONDON, UCL

DOCTOR OF PHILOSOPHY (PH.D.)

2015

DECLARATION

I, Luís Miguel da Rocha Lopes, confirm that the work presented in this thesis is my own. Where information has been derived from other sources, I confirm that this has been indicated in the thesis.

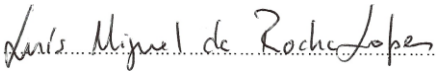

This thesis was evaluated using the online tool "Turnitin", accessed within UCL Moodle. The similarity index was 19%. According to the originality report, this percentage is due to already published work by the PhD candidate as the first author (**Appendix A**).

Some parts of the methodology used to obtain the data analysed in this work have been developed in collaboration with the following investigators, and this is indicated where appropriate throughout:

- Doctor Mike Hubank, Institute of Child Health, UCL: "Targeted gene enrichment and high-throughput sequencing of 41 cardiovascular genes" – "Library design and capture and sequencing protocol optimization" (Methods, Chapter 2); "Sequence data analysis of the non-coding regions" – "Expression study in patient samples vs controls" (Methods, Chapter 7);
- Doctor Vincent Plagnol, UCL Genetics Institute, UCL: "Sequence data analysis for targeted exonic regions" – "Bioinformatic analysis pipeline" (Methods, Chapter 3) and "Screening for copy number variation" – "Bioinformatic analysis for the detection of copy-number variation – ExomeDepth" (Methods, Chapter 6);
- Professor Mathias Gautel, King's College London: "Titin variants" – "Manual annotation and prediction of pathogenicity " (Methods, Chapter 3);
- Doctor Chiara Bachelli, GOSGene, Institute of Child Health, UCL: "Whole-exome sequencing and data analysis of sarcomere-negative families" (Methods, Chapter 8);
- Doctor Andrew Martin, Structural and Molecular Biology, UCL: "*In silico* analysis of *MYH7* missense variants – pathogenicity and phenotype prediction based in the structural impact of the mutation" –"Machine learning analysis to predict phenotype" (Methods, Chapter 9).

ACKNOWLEDGMENTS

I was supported by a grant from the Gulbenkian Doctoral Programme for Advanced Medical Education, sponsored by Fundação Calouste Gulbenkian, Ministério da Saúde and Fundação para a Ciência e Tecnologia, Portugal. I am deeply in depth to the Gulbenkian Foundation for this grant, which allowed me to enrol and conduct my research at University College London and for the initial 6 months of graduate courses, which influenced and inspired many ideas for the following 4 years. A special word of gratitude to Professors Leonor Parreira and João Ferreira, for their teaching, wise support and encouragement.

I am profoundly glad for the opportunity to thank my primary supervisor, Professor Perry Elliott. For his time, availability, encouragement, wisdom, patience and continued mentorship and example. Also for allowing me the ambition of participating in such a large and challenging project, which transformed this period of my life in a continuous learning experience. I also owe my supervisor a dept of gratitude for what was an intense period of clinical learning in the field of inherited heart disease.

I am also very grateful to my secondary supervisor, Professor William McKenna, for his encouragement, example, wisdom and intellectual contribution to my research and writing.

A special word of deep gratitude to Doctor Petros Syrris for his availability, teaching, friendship, support, wise advice and continuous encouragement along all this period.

I also thank all the collaborators of this project from outside the Institute of Cardiovascular Science, for their generous contribution and time and from whom I learned immensely in different areas of the Life Sciences. In particular, Doctor Vincent Plagnol, Doctor Mike Hubank, Doctor Andrew Martin and Professor Mathias Gautel.

I thank all my friends, fellows, graduate students, consultants, nurses and genetic counsellors at The Heart Hospital, for their help and companionship. Without the work of all present and past colleagues, my research project would not have been possible. I am also deeply grateful to all the patients and families who participated in this study and from whom I have learned so much.

I would like to dedicate this thesis to my parents, for their lifelong support and encouragement.

ABSTRACT

Background and Aims

The application of hypertrophic cardiomyopathy (HCM) genetics in clinical practice has been limited by an incomplete knowledge of the genetic background and a poor understanding of genotype-phenotype relationships. The aims of this study were to study genotype-phenotype relationships in HCM, expand the knowledge on the genetic architecture of the disease, explore genetic modifiers of the phenotype and develop a methodology for interpretation of variants detected by high-throughput sequencing platforms.

Methods

The study population consisted in consecutive and unrelated HCM patients. In order to analyze coding, intronic and regulatory regions of 41 cardiovascular genes, solution-based sequence capture was followed by massive parallel resequencing. Single-nucleotide variants, small insertion/deletions and copy number variants (CNVs) were called. For the analysis of variants in the coding region, rare, non-synonymous, loss-of-function and splice-site variants were defined as candidates. These variants were tested for associations with clinical phenotype and survival. For the analysis of non-coding variation, variants located in known transcription factor (TF) binding sites and 3'UTR miRNA targets were identified. The performance of an *insilico* pathogenicity prediction strategy incorporating structural features was explored for *MYH7* variants. Selected sarcomere-negative families were studied by whole-exome sequencing (WES).

Results

Eight-hundred-and-seventy-four patients (49.6±15.4 years, 67.8% males) were studied; likely disease-causing sarcomere protein (SP) gene variants were detected in 383 (43.8%). Patients with SP variants were characterized by younger age and higher prevalence of family history of HCM, family history of sudden cardiac death, asymmetric septal hypertrophy, higher maximal wall thickness (P-values<0.0005) and increased cardiovascular death (P-value=0.012). Similar associations were observed for individual SP genes. Patients with *ANK2* variants had greater maximum wall thickness (P-value=0.0005). Associations at a lower level of significance were demonstrated with variation in other non-SP genes. Four CNVs were detected in *MYBPC3*, *PDLIM3*, *TNNT2* and *LMNA*. Fourteen percent carried non-coding variants mapping to TF

binding sites. The pathogenicity prediction for *MYH7* missense variants had an accuracy of 0.93; the phenotype predictor had an accuracy of 0.79 and novel genotype-phenotype associations were suggested. Three families were studied using WES; in two of these families the main candidate variants were in *OBSCN* and *TTN*.

Conclusions

Patients with SP variants differed from those without with respect to age, family history, ventricular morphology and prognosis. Novel associations were demonstrated between individual sarcomeric genes and several phenotype traits and for the first time, associations between rare variants in non-SP genes and phenotype were described. CNVs and non-coding variation in SP genes can additionally contribute to the genetic architecture of HCM. Pathogenicity prediction incorporating structural features revealed additional genotype-phenotype associations. Whole-exome sequencing suggested new causal genes.

TABLE OF CONTENTS

LIST OF TABLES

LIST OF FIGURES

LIST OF ABBREVIATIONS

ABD: actin-binding domain
ABPRE: abnormal blood pressure response to exercise
aCGH: array comparative genomic hybridization
AF: atrial fibrillation
ALP: actinin-binding LIM protein
AMVL: anterior mitral valve leaflet
ANOVA: analysis of variance
ARVC: arrhythmogenic right ventricular cardiomyopathy
ASA: alcohol septal ablation
ASH: asymmetric septal hypertrophy
ATP: adenosine triphosphate
AUC: area under the curve
bp: base pairs
BP: blood pressure
BRC: Biomedical Research Centre
BWA: Burrows-Wheeler Alignment Tool
C/EBPß : CCAAT/enhancer binding protein beta
CARP: cardiac ankyrin repeat protein
CCDS: Consensus CDS database
ChIP-seq: chromatin immunoprecipitation - sequencing
CI: confidence interval
CMR:cardiovascular magnetic resonance
CNV: copy-number variant
CPEX: cardio-pulmonary exercise test
DCM: dilated cardiomyopathy
DHPLC: denaturating high pressure liquid chromatography
DNA: deoxyribonucleic acid
DS: direct sequencing
ECG: electrocardiography
EF: ejection fraction
ELC: essential light chain
ENCODE: Encyclopedia of DNA Elements
ESP: exome sequencing project
FFAs: free fatty acids
FH: family history
Fn: fibronectin
FS: fractional shortening;
GATK: Genome Analysis Toolkit
GEF: GTP-GDP exchange factor
GERP: genomic evolutionary rate profiling
GOSH: Great Ormond Street Hospital
GWAS: genome-wide association studies;
HCM: hypertrophic cardiomyopathy
HDAC2: histone deacetylase 2
HF: heart failure

HGMD: Human Gene Mutation Database
HTS: high-throughput sequencing
ICD: implantable cardioverter-defibrillator
ICH: Institute of Child Health
Ig: immunoglobulin
IGV: Integrative Genomics Viewer
Indel: insertion-deletion
IQR: interquartile range
LA: left atrium
LGE: late gadolinium enhancement
LMM: : myosin heavy chain's light meromyosin
LOF: loss-of-function
LV: left ventricle
LVEDV: left ventricular end-diastolic volume
LVEF: left ventricular ejection fraction
LVESV: left ventricular end-systolic volume
LVH: left-ventricular hypertrophy
LVNC: left ventricular non-compaction
LVOT: left ventricular outflow tract
LVOTO: left ventricular outflow tract obstruction
MAF: minor allele frequency
MAPK: mitogen-activated protein kinase
MLP: muscle LIM protein
MLVWT: maximal left ventricular wall thickness
MPLA: multiplex ligation-dependent probe amplification
Murf: Muscle specific Ring Finger
MyBPC: myosin bind protein C
NCBI: National Center for Biotechnology Information
ncSNV: non-coding single nucleotide variant
NFAT: nuclear factor of activated T-cells
NGS: next-generation sequencing
NHLBI: National Heart, Lung and Blood Institute
NIHR: National Institute for Health Research
NRSF : neuronrestrictive silencer factor
nsSNP: non-synonymous single nucleotide polymorphism
NSVT: non-sustained ventricular tachycardia
NYHA: New York Heart Association
OMIM: Online Mendelian Inheritance in Men
PDB: protein database
PKA: protein kinase A
PKC: protein kinase C
PICP: C-terminal propeptide of type I procollagen
QC: quality control
RAAS: renin-angiotensin-aldosterone system
RCM: restrictive cardiomyopathy
RFLP: restriction fragment length polymorphism
RHYME:Ranolazine for the Treatment of Chest Pain in HCM Patients
RLC: regulatory light chain
RNA: ribonucleic acid

ROC: receiver operating characteristics
RVH: right ventricular hypertrophy
SAAP:Single Amino Acid Polymorphism
SAAPbd:Single Amino Acid Polymorphism database
SAAPdap: Single Amino Acid Polymorphism data analysis pipeline
SAM: systolic anterior movement
SCD: sudden cardiac death
SERCA2: sarcoplasmic/endoplasmic reticulum calcium ATPase 2
SIFT: sorting intolerant from tolerant
SNP: single nucleotide polymorphism
SP: sarcomeric protein
SPB: systolic blood pressure
SRF: serum response factor
SSCP: single-strand conformation polymorphism
STAT3: signal transducer and activator of transcription 3
SV: systolic volume
TF: transcription factor
TFBS: transcription factor binding site
Tm: tropomyosin
TnC:troponin C
TnI:troponin I
TnT: troponin T
UCL: University College London
UTR: untranslated region
UPS: ubiquitine-proteosome system
VUS: variant of unkown significance
WES: whole-exome sequencing
WEKA: Waikato Environment for Knowledge Analysis
YY1: Yin Yang 1

SECTION I – INTRODUCTION

1. DEFINITION, PHENOTYPE AND EPIDEMIOLOGY OF HYPERTROPHIC CARDIOMYOPATHY

Cardiomyopathies (heart muscle diseases) are defined as myocardial disorders that are not solely explained by coronary artery disease or abnormal loading conditions [1]. They are classified according to ventricular function and morphology into four main subtypes: hypertrophic cardiomyopathy (HCM); dilated cardiomyopathy (DCM); restrictive cardiomyopathy (RCM) and arrhythmogenic (right) ventricular cardiomyopathy (ARVC). **Figure 1**. Diseases that do not fit into these categories are termed unclassified cardiomyopathies and include left ventricular (LV) noncompaction (LVNC) and Tako-Tsubo cardiomyopathy [1]. All cardiomyopathies can be caused by both genetic and non-genetic mechanisms [1].

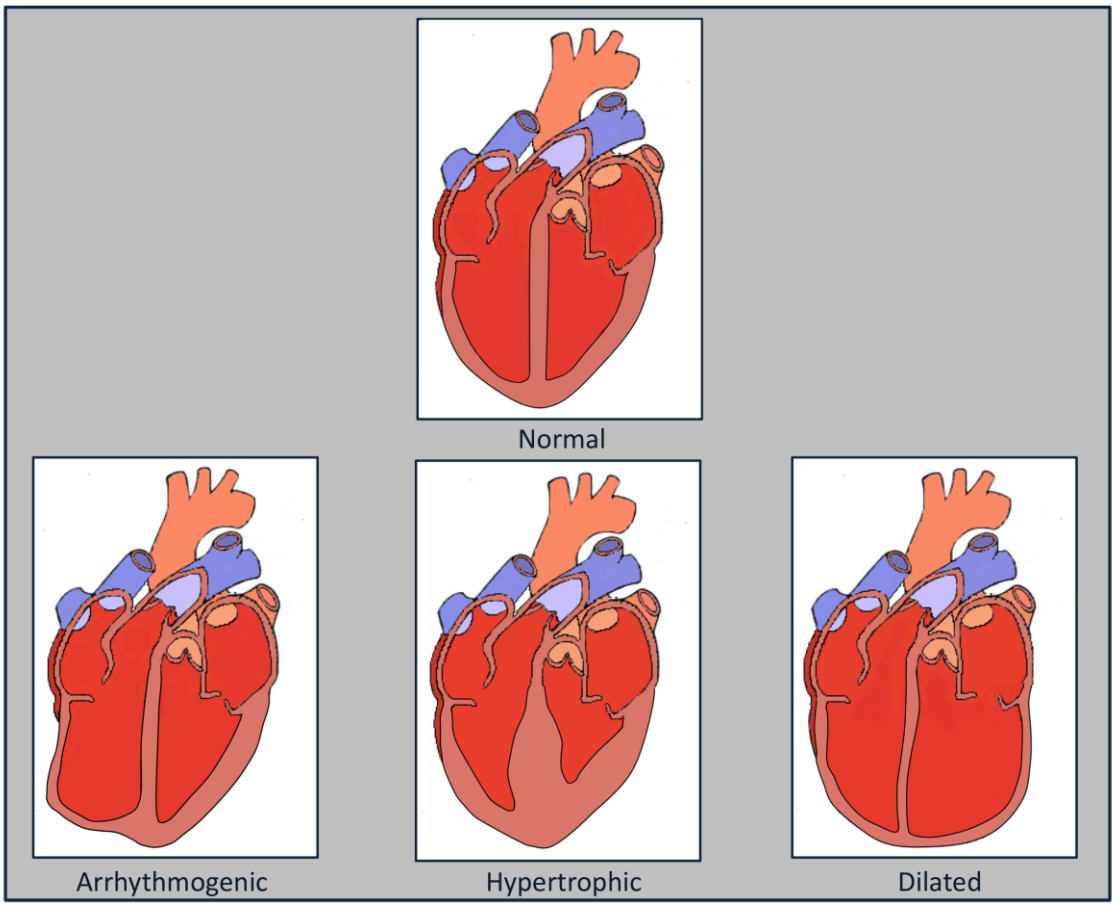

Figure 1. Schematic showing the different main cardiomyopathy phenotypes. Reproduced with permission from [2].

Hypertrophic cardiomyopathy (HCM) is defined as left ventricular hypertrophy in the absence of abnormal loading conditions, such as severe hypertension or valve disease, sufficient to provoke the observed phenotype. It occurs in approximately 1 in every 500 adults [3],[4],[5],[6],[7],[8].

The histopathology of HCM is characterized by cardiomyocyte hypertrophy and disarray, interstitial and replacement fibrosis and dysplastic arterioles [9].

Ventricular hypertrophy frequently develops during periods of rapid somatic growth, but can appear *de novo* at any time from infancy to old age. Presentation in infancy is associated with symptoms of heart failure and failure to thrive. In older children and adults the most common symptoms are dyspnoea, syncope and chest pain [3].

HCM is generally considered the commonest cause of sudden cardiac death (SCD) below 35 years of age, but SCD can happen at any age, with a peak incidence in adolescence and young adulthood, often in minimally symptomatic individuals [6],[7],[8]. The disease is associated with a lifelong risk of atrial fibrillation (AF) and stroke [3],[10],[11]. In the long-term, a significant proportion of patients (5-10%) develop progressive symptoms caused by gradual deterioration in left ventricular function [11]. This so-called “end-stage” is characterised by severe impairment of contractile performance and is associated with an annual mortality rate of 11% per year from sudden ventricular arrhythmia, stroke and severe heart failure (HF) [8, 12].

2. GENETIC BACKGROUND AND MECHANISMS OF DISEASE

In approximately half of adolescents and adults with the disease, HCM is inherited as an autosomal dominant trait, caused by mutations in cardiac sarcomere protein genes. This disease is characterized by a high locus and allelic diversity. More than 1000 mutations have been identified [13],[14],[15],[16],[17],[18], the majority of which (75% to 80%) involve cardiac myosin heavy chain (*MYH7*) and cardiac myosin binding protein C (*MYBPC3*). Mutations in cardiac troponin T (*TNNT2*), troponin I (*TNNI3*), alpha-tropomyosin (*TPM1*), myosin light chains (*MYL2*, *MYL3*) and cardiac actin (*ACTC1*), account for 15-20% of the identified sarcomere mutations. Mutations in other sarcomere or related genes, including alpha-myosin heavy chain (*MYH6*), titin (*TTN*), Z-disc protein genes like muscle LIM protein (*CSRP3*) or calcium-handling genes such as phospholamban (*PLN*), account for less than 1% of cases each. A further 5% of unexplained left ventricular hypertrophy (LVH) cases are caused by metabolic or storage disorders (for example, Anderson-Fabry disease, mitochondrial disorders, glycogen storage disorders), neuromuscular disorders, chromosome abnormalities and genetic syndromes such as cardio-facial-cutaneous disorders, including Noonan and LEOPARD syndrome. When all these disorders are excluded, approximately 30-40% of HCM remains unexplained [13], [14],[15],[16],[17],[18],[19, 20],[21, 22],[23].

2.1. NORMAL SARCOMERE STRUCTURE

Each cardiac myocyte is composed of a parallel arrangement of myofibrils that run longitudinally along the cell and are transversely sub-divided into contractile units called sarcomeres. [24]. The sarcomere is a highly specialized cytoskeletal structure, which constitutes the fundamental motor unit of the cardiomyocyte [25]. Each sarcomere is comprised of thin and thick myofilaments. The thick filament is composed of around 300 molecules of myosin, each made up of two protein units of beta- or alpha-myosin heavy chain and four myosin light chain molecules – two essential and two regulatory [25]. **Figure 2**. The thin filament is composed of repeating actin molecules, closely associated with the regulatory troponin complex (troponin T, troponin I and troponin C) which exerts its function in coordination with alpha-tropomyosin [26]. The protein cardiac myosin binding protein C also contributes to the regulation of actin-myosin interactions

The regular arrangement of the myofilaments delineates a number of discrete topographic zones in each sarcomere: the M-band in the middle of the sarcomere; the A-band which is made up of multiple and parallel thick filaments and includes a central region, the H-zone, devoid of cross-bridges and consisting only of myosin tails; the I-band in which there are only aligned thin filaments with no overlap with thick filaments; and finally, the Z-discs which constitute the lateral boundaries of the sarcomere [25]. **Figure 3**.

Myosin heavy chain is divided into three main domains: the globular head (the "motor domain"), which includes the adenosine triphosphate (ATP) and the actin binding sites; the neck, an alpha-helical domain where the light chains bind and which is further subdivided in a converter region and a lever arm involved in the amplification of mechanical energy required for the power-stroke of myosin along actin; and the tail or rod region, a helical coiled-coil protein that intertwines with the tail of another heavy chain molecule to form the thick filament [27]. There are two highly homologous isoforms of the myosin heavy chain, encoded sequentially by two genes located in tandem on chromosome 14: *MYH6* encodes alpha-myosin heavy chain and *MYH7* encodes beta-myosin heavy chain. *MYH7* is the dominantly expressed gene in the adult human ventricular cardiomyocytes (around 70-80% of beta-myosin heavy chain mRNA), while *MYH6* is expressed at higher levels in the developing heart, particularly in the atria [28],[27, 29].

Myosin light chains are part of the EF-hand family of calcium binding proteins. Their function is believed to be essentially mechanical, providing support to the heavy chain neck and possibly regulating the interaction of myosin head with actin and consequently the force and velocity of contraction. The essential light chain (ELC), encoded by *MYL3*, is located closer to the myosin head and the regulatory light chain (RLC), encoded by *MYL2,* binds to the neck closer to the rod domain [25].

Myosin-binding protein C (MyBPC) is made up of 11 domains (8 immunoglobulin-like and 3 fibronectin-like) numbered C0-C10; it also includes a proline/alanine-rich linker sequence between C0 and C1 and a regulatory motif between domains C1 and C2, that contains protein kinase A phosphorylation sites [27]. MyBPC interacts with the thick filament through 3 domains at its C terminus, which bind to both myosin and titin. The molecular stoichiometry is believed to be 2 - 4 MyBPC molecules per myosin. At the N-terminus, MyBPC may exert a regulatory role through its interaction with the myosin neck and actin [27].

The cardiac *thin filament* is composed by multiprotein complexes made of 7 actin monomers, 1 troponin complex - troponin I (TnI), troponin T (TnT) and troponin C (TnC) - and 1 alpha-tropomyosin (TM) coiled-coil dimer [26]. The overall structure of the troponins is similar, as they are composed by helical domains separated by linker sequences of varying lengths that confer a high degree of flexibility to the molecule [26]. *Alpha-tropomyosin* is an alpha-helical coiled coil dimer, which runs along the length of the actin filament and plays a key role in regulating contraction. *Alpha-cardiac muscle actin* is one of the isoforms of actin, a group of highly conserved proteins involved in cell motility. Globular actin (G-actin) polymerizes to form filament actin (F-actin), which is structurally organized as a two-stranded helix [30].

2.2. MECHANISM OF CONTRACTION – THE CROSS-BRIDGE CYCLE

The fundamental principle governing muscle contraction is that of the sliding filament theory, in which the sliding of actin past myosin generates muscle tension. The interaction between myosin and actin, in which the globular head of the myosin molecule bends towards and then binds to actin, contracts, releases actin, and then initiates a new cycle is known as myosin-actin cycling. The links between the myosin head and actin are called cross bridges; the contraction of the myosin S1 region is called the power stroke, which requires the hydrolysis of ATP to release energy.

Electrical activation of the heart and contraction are coupled through the intracellular movement of calcium. Depolarization of the cardiomyocyte cell membrane during the action potential activates the L-type voltage-dependent calcium channels in the T tubule; the influx of calcium into the cell then leads to the opening of ryanodine-receptor channels in the adjacent sarcoplasmic reticulum with a rapid increase in cytosolic calcium [31]. Calcium binds to TnC, inducing an allosteric conformational change in TnI and TnT that is transmitted to tropomyosin. This causes a transition from a "blocked" to a "closed" state, which then exposes the myosin binding sites of actin, which allows the cross-bridges to occur ("open" state) [26],[31]. The myosin heavy chain head, with ADP and inorganic phosphate bound to its nucleotide binding pocket, then interacts with the exposed actin binding sites. This is followed by the release of ADP and inorganic phosphate, which occurs concomitantly to the power stroke, resulting in force development via shortening of the sarcomere and the I-band and the approximation of the Z-discs. Following this, ATP binds to the nucleotide binding pocket of the myosin heavy

chain head, which detaches from actin. The myosin then hydrolyzes the ATP into ADP and inorganic phosphate once again [31], re-starting the cycle.

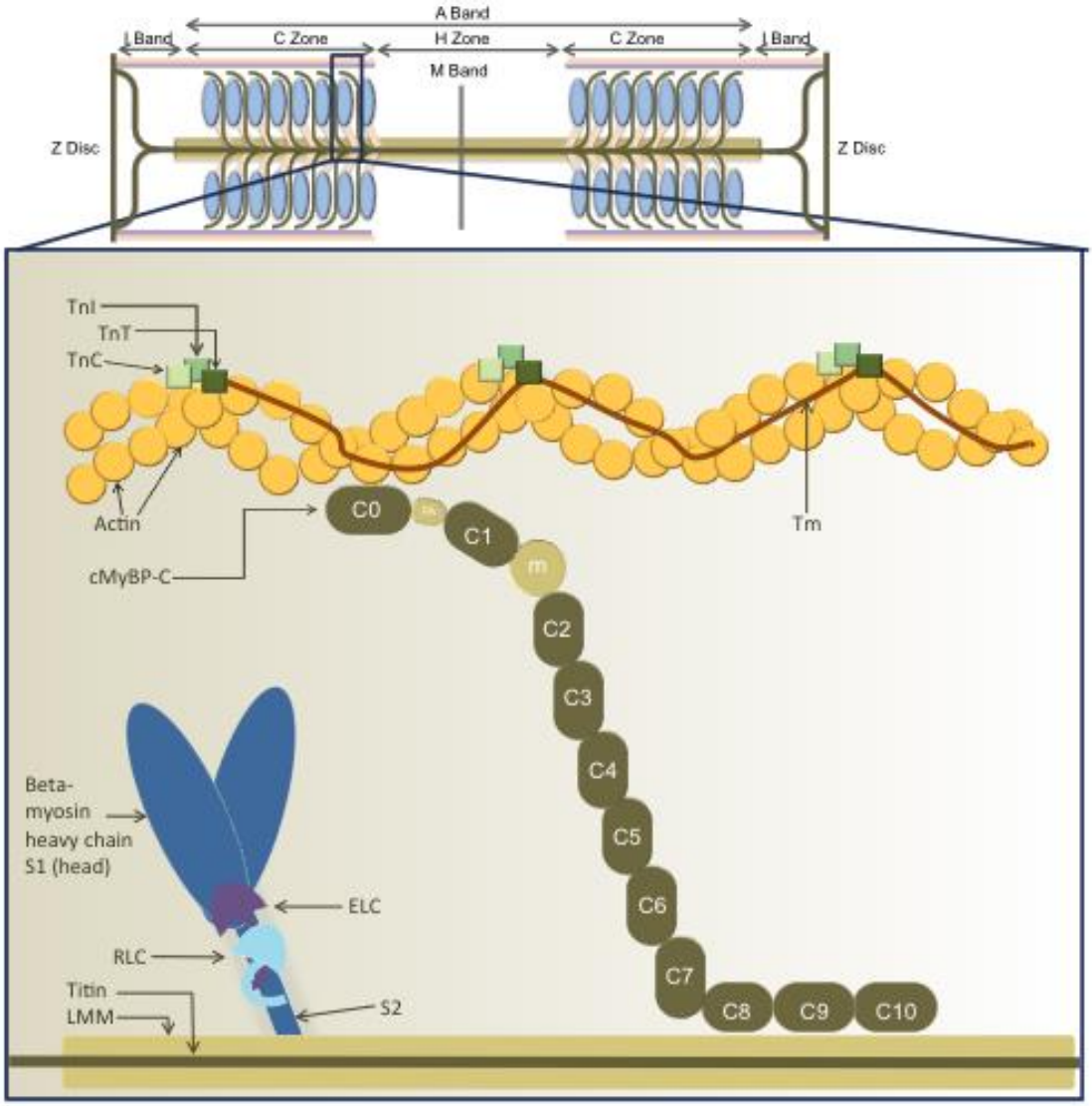

Figure 2. Schematic representation of the main eight sarcomere proteins and their interactions in the sarcomere. cMyBP-C: cardiac myosin binding protein C - domains are numbered C0 to C10, starting at the N terminus of cMyBP-C; m: regulatory motif between domains C1 and C2 that contains protein kinase A (PKA) phosphorylation sites; PA, a proline/alanine-rich linker sequence between C0 and C1; ELC: essential myosin light chain; LMM: myosin heavy chain's light meromyosin; RLC: regulatory myosin light chain; Tm: tropomyosin; TnC: troponin C; TnI: troponin I; TnT: troponin T. Reproduced with permission from [2].

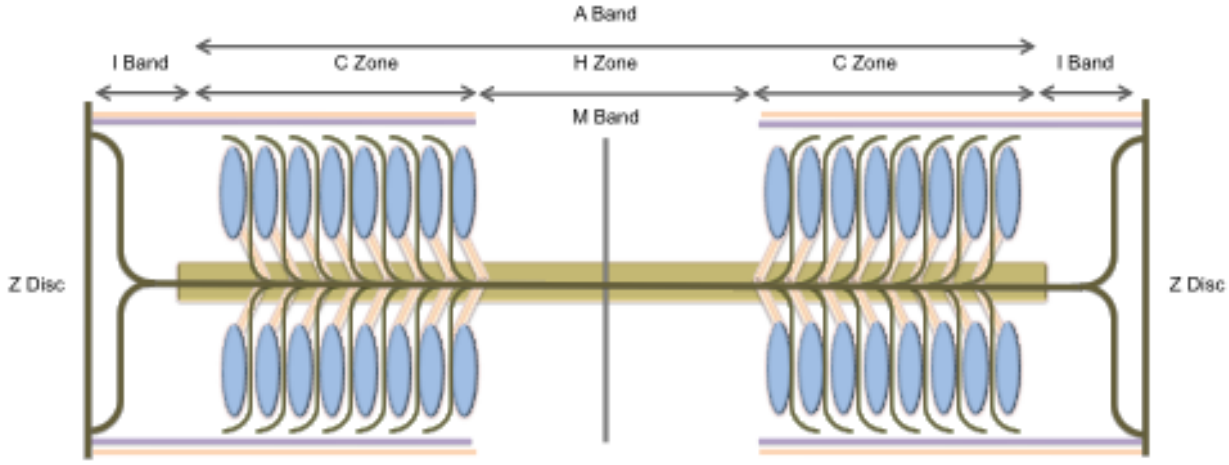

Figure 3. Schematic representation of the discrete topographic zones in each sarcomere. The M-band constitutes the middle of the sarcomere; the A-band is made up of multiple and parallel thick filaments and includes a central region, the H-zone, devoid of cross-bridges and consisting only of myosin tails; the I-band in which there are only aligned thin filaments, with no overlap with thick filaments; and finally, the Z-discs which constitute the lateral boundaries of the sarcomere. Reproduced with permission from [2].

2.3. CONTRACTILE PROTEIN GENE MUTATIONS

Mutations in proteins of the cardiac sarcomere comprise the main cause of hypertrophic cardiomyopathy (HCM). With the exception of the myosin light chains, genetic variation in all of these proteins can also cause dilated cardiomyopathy (DCM), although a larger percentage of cases remain genetically unsolved in DCM [32]. A proportion of restrictive cardiomyopathy (RCM) is also caused by mutations in sarcomere protein genes [33]. **Table 1** summarizes the sarcomeric and associated proteins, encoding genes, interactions, associated disease phenotypes and their respective prevalence.

Genetic mechanisms of disease

Two different basic pathogenic mechanisms are thought to account for disease associated with mutations in cardiac sarcomere proteins. Missense single nucleotide variants (a nucleotide change and hence codon change that results in an aminoacid being substituted by another aminoacid in the protein) predominantly lead to a *dominant negative effect* (described as a "poison peptide" mechanism) in which the mutated protein is not destroyed but rather

integrates into the sarcomere, leading to the disease phenotype. This is thought to be characteristic of *MYH7* variants [18]. Alternatively, nonsense single nucleotide variants or small frameshift insertion-deletions can introduce a premature stop codon and hence result in *haploinsufficiency*, due to nonsense mRNA mediated decay or proteolysis of a truncated (just partially translated) protein [34]. This mechanism is believed to be typical of the majority of *MYBPC3* disease-causing mutations [35].

Myosin heavy chain

The first cardiomyopathy-causing mutation was described in *MYH7* in 1990 in a large family with hypertrophic cardiomyopathy [13]. Since then more than 400 mutations have been reported in patients with HCM, DCM, RCM and LVNC, most of which affect residues in the head and neck regions of the molecule [27],[36]. The various effects of individual variants on fibre contractile velocity, force and calcium-sensitivity have been proposed as an explanation for the existence of dramatically different phenotypes arising from genetic variation in the same molecule [27],[36]. A paradigm has been proposed, whereby mutations that increase motor activity and power output lead to HCM, while those that diminish motor function and decrease power output lead to DCM[27],[36].

Myosin light chains

Mutations in both *MYL2* and *MYL3* were first associated with HCM in 1996 [16]. A small number of disease-causing mutations are located in two of the four EF-hand domains for *MYL3.* For *MYL2*, the reported variants are mostly located in two regions: a) an EF-hand domain that has the ability to bind calcium and magnesium or b) around the phosphorylated serine-15 residue. *In vitro* and *in vivo* functional studies predominantly show an increase in motor activity and power output and are consistent with the 'gain of function' hypothesis for HCM pathogenesis caused by mutations in these proteins [27]. There is no report associating *MYL2* or *MYL3* mutations with phenotypes other than HCM.

Cardiac myosin-binding protein C

Mutations in cardiac myosin-binding protein C were first associated with HCM in 1995 in two separate reports [37],[14]. Since then, more than 300 variants have been described in association with HCM and variation in this protein is reported as the most common cause of the disease in large cohorts of unrelated patients [38]. Most of the DNA variants result in potentially truncated proteins (nonsense or frameshift insertion-deletions) and are believed to

lead to haploinsufficiency [27]. Others (around 40%) are missense variants, of more unpredictable effect. Possible mechanisms of disease for missense mutations include protein misfolding–which can lead to a poison-peptide mechanism (dominant-negative effect)–or haploinsufficiency through activation of protein surveillance/degradation systems [27] that destroy the misfolded proteins.

Troponin-Tropomyosin complex and Actin

Alpha-tropomyosin (encoded by *TPM1*) and troponin T (encoded by *TNNT2*) were the first thin filament proteins to be linked to HCM [15]. This discovery was rapidly followed by reports of mutations in troponin I (encoded by *TNNI3*) in 1997 [17] and actin (*ACTC1*) in 1999 [39] and later troponin C (*TNNC1*) in 2008 [40]. Troponin T variation has been associated with HCM (around 50 mutations) and also with DCM and RCM phenotypes. Troponin I mutations have been linked to HCM, RCM and, more recently, to DCM. Around 40 mutations have been published to date. A homozygous troponin C variant was first described in a family with DCM [41] but suggested associations with HCM [40] are unproven. Genetic variation in both alpha-tropomyosin and actin is associated with HCM and DCM.

2.4. ROLE OF THE NON-CONTRACTILE SARCOMERE PROTEINS IN DISEASE

Mutations in the non-contractile elements of the sarcomere may also result in a cardiomyopathy phenotype. Some of the most important are as follows:

2.4.1. TITIN

Titin is a giant macromolecule that consists almost entirely of hundreds of immunoglobulin and fibronectin-like domains, which interact with sarcomeric proteins at the Z-disc, the myosin filament and the M-band, while other specific domains provide the elastic spring connection to myosin and actin filaments in the I-band [42], [43], [44, 45]. **Figures 3 and 4**. It spans an entire half-sarcomere, bound at the N-terminus to the Z-disc and at the C-terminus to myosin and myosin-binding protein C. Titin has a major role in determining the mechanical properties of the heart through its effects on passive tension during myocardial stretch and restoring forces during early ventricular filling and is an important biomechanical sensor and organisational element within the sarcomere [44].

The protein is encoded by the *TTN* gene on chromosome 2, which undergoes complex differential splicing, resulting in isoforms with variable elastic properties [46]. The two main isoform classes of the adult cardiac muscle are N2B and N2BA, which have different I-region lengths. N2BA contains an additional and unique N2A element and a larger spring-like PEVK (rich in proline, glutamic acid, valine, and lysine) element. Isoform switches, with increased expression of longer and more compliant isoforms (increasing the ratio N2BA:N2B), have been reported in heart failure associated with either reduced or preserved ejection fraction [46].

Titin stiffness can be regulated even faster by phosphorylation of the PEVK element by protein kinase C-alpha (activated by the alpha-1 adrenergic pathway), which results in increased passive tension or the N2B by protein kinases A (activated by the beta-adrenergic pathway) and G, which results in decreased passive tension [46].

Titin also has a serine/threonine kinase domain, in the transition of the M to the A-band [47]. Some of its targets include ubiquitin ligases that act on pathways relevant to cell survival and autophagy, such as Nbr, p62 or Murf.

Variation in *TTN* was linked to DCM for the first time in 2002 [48],[49]; ten years later truncating titin mutations were reported to be the most common genetic cause of dilated cardiomyopathy [50]. Although more debatable, there are also published reports of an association with HCM [51], RCM [52] and arrhythmogenic cardiomyopathy [53].

2.4.2. Z-DISC AND ASSOCIATED PROTEINS

The Z-disc corresponds to the lateral borders of the sarcomere. Besides its mechanical function, this structure is composed of proteins that have signaling functions related to the transcriptional regulation of muscle growth and mechano-transduction [24], [54]. Mutations in Z-disc associated proteins (**figure 4**) are predominantly associated with DCM rather than HCM:

- *Alpha-actinin* (encoded by *ACTN2*) is composed of four spectrin repeats at its centre as well as an actin-binding domain (ABD) at its N-terminus and two EF hands (calmodulin homology domains) at the C-terminus, which enable *α* actinin to cross-link actin filaments within the Z-disc [24]. **Figure 4**. It seems to serve an important role in actin localization and forms the principal cross-links at the Z-disc between actin filaments of

opposite polarity, originating from contiguous sarcomeres. Alpha-actinin mutations have been described in both HCM and DCM [55], [56].

- *Muscle LIM protein* (MLP, encoded by *CSRP3*) is a LIM-domain protein that interacts with *α* actinin, calcineurin, and telethonin. It is also localized in the nucleus and has been implicated in various pathways, including mechano-sensation and mechano-transduction, calcium metabolism, myofibrillogenesis and actin polymerization. Genetic variation is associated with HCM and DCM [56],[57].

- *Telethonin* (encoded by *TCAP*) binds the N-terminal domain of two adjacent titin molecules and is a substrate of titin kinase; it interacts with various proteins such as ankyrin repeat protein 2, T-tubular system components, and ion channels. It is also implicated in regulation of myocardial hypertrophy by interacting with calsarcin-1 (myozenin-2), and myostatin. Variation in this gene has been observed in HCM and DCM [58].

- *Calsarcin 1 or Myozenin 2* (encoded by *MYOZ2*) is involved in the transcriptional regulation of muscle growth. Variation in this gene has been proposed as a cause of HCM [59].

- *Four-and-a-half-LIM-domains-1* (encoded by the X-chromosome gene *FHL1*) localizes to the sarcomeric Z-disc/I-band area and the nucleus. This protein is important in sarcomerogenesis, structural maintenance of the sarcomere and transcriptional regulation. Both HCM and DCM phenotypes have been described, in isolation or in association with neuromuscular disease (e.g. Emery-Dreifuss muscular dystrophy) [60].

- *Cypher/ZASP or LIM domain binding protein 3* (encoded by *LDB3*) has an amino-terminal PDZ domain that interacts with alpha-actinin; it also interacts with protein kinase C at the C-terminal. Mutations in *LDB3* were reported in DCM and LVNC [61] and also HCM [62], although evidence for the latter is debated.

- *Actinin-Binding LIM Protein* (ALP) or PDZ/LIM domain protein 3, encoded by *PDLIM3*, belongs to the ALP family of proteins, characterized by an N- terminal PDZ domain and a C-terminal LIM domain. It has been proposed as a candidate gene for HCM, but no convincing evidence has been found as yet [63].

- *Desmin* (encoded by *DES*) is an intermediate filament, which connects to desmosomes and interacts with the Z-disc. Pathological variation in this gene leads to a number of phenotypes, including muscular disease, RCM with conduction abnormalities [64] and DCM [65]. An arrhythmogenic cardiomyopathy phenotype has also been described [66], [67].

- *Myopalladin* (*MYPN*) interacts with several proteins including α-actinin, titin, nebulette and cardiac ankyrin repeat protein (CARP). Variation in this gene has been described in association with DCM, HCM and RCM [68].

- *Nexilin* (*NEXN*), which contributes to maintain the integrity of the Z-discs against the tension generated within the sarcomere, interacts with actin and mutations have been associated with HCM [69] and DCM [70].

- *Ankyrin repeat domain 1* (*ANKRD1*)-encoded cardiac adriamycin responsive protein, or cardiac ankyrin repeat protein (CARP) is a protein localized in the I-band, that interacts with the N2A domain of titin and the N-terminal region of myopalladin. It can also be found in the nucleus, where it functions as a transcription co-factor in the embryonic and fetal heart; an increased expression was detected in advanced heart failure. Genetic variation has been associated with HCM [51] and DCM [71],[72].

2.4.3. M-BAND AND ASSOCIATED PROTEINS

The M-band is located in the centre of the A-band (**figure 3 and 4**) and is important in distributing tension along the sarcomere. The two main proteins of the M-band are myomesin and M-protein. Both myomesin and M-protein interact with other sarcomere proteins, such as titin and myosin and with M-band associated structural proteins, such as obscurin and regulatory proteins, for example Nrb1 or FHL1. A mutation in myomesin has been associated with the development of HCM [73].

Obscurin (encoded by *OBSCN*) is a giant muscle-specific protein that contains multiple structural motifs, including hundreds of immunoglobulin-like and fibronectin-like domains and a GTP-GDP exchange factor (GEF) domain that can interact with two serine/threonine protein

kinase domains. Alternative splicing of *OBSCN* results in different isoforms. Additionally, obscurin interacts at the M-band with ankyrin-1 (involved in sarcolemma-cytoskeleton interactions) and interacts with the sarcoplasmic reticulum [24],[74]. A single report suggested that an obscurin mutation could be a cause of HCM, but this remains to be confirmed [75].

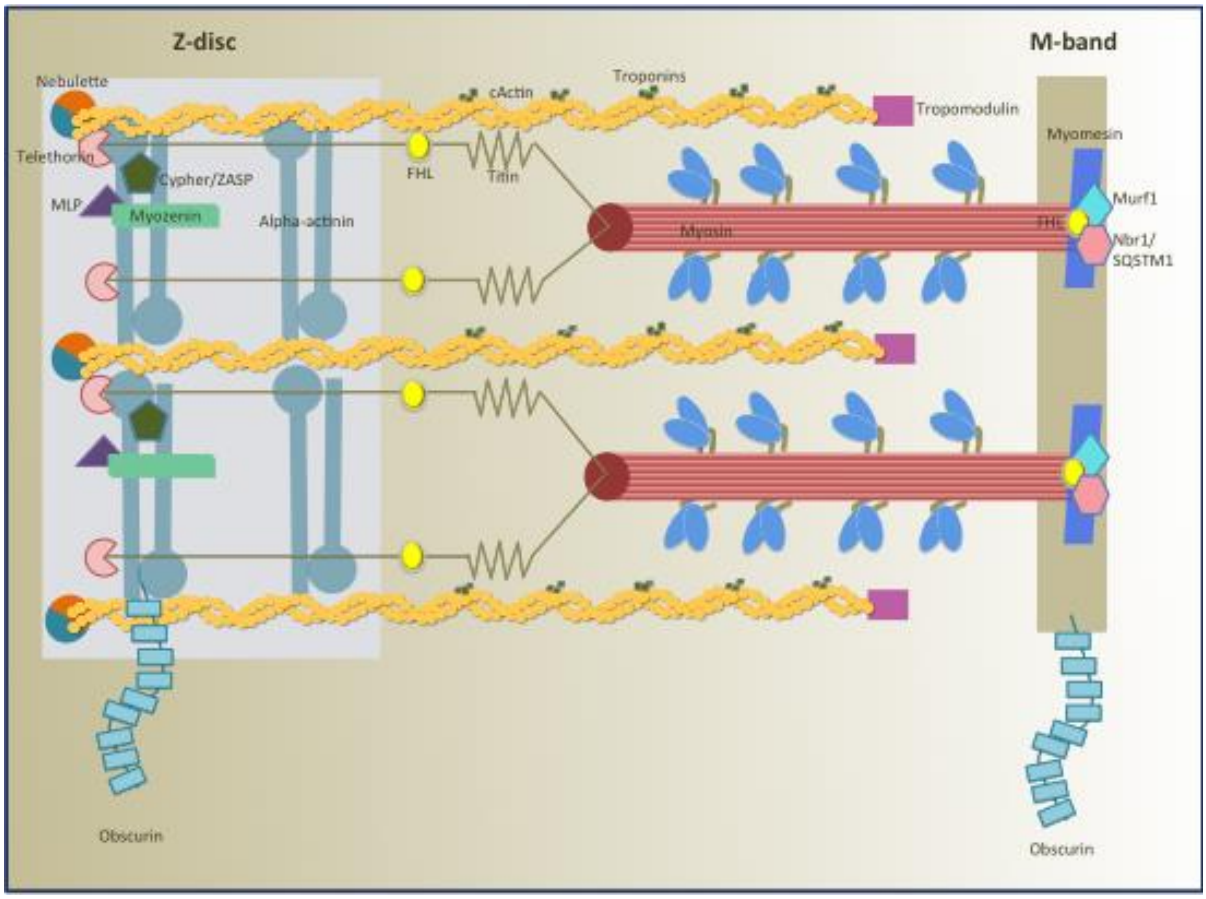

Figure 4. Schematic representation of the sarcomere, focusing on the Z-disc and the M-band proteins and its interactions. Reproduced with permission from [2].

Table 1. Summary of the sarcomeric and associated proteins, encoding genes, interactions, associated disease phenotypes and respective prevalence. For HCM: only percentages for the strongest established genes are shown. OMIM: Online Mendelian Inheritance in Men. DCM: dilated cardiomyopathy; HCM: hypertrophic cardiomyopathy; RCM: restrictive cardiomyopathy; LVNC: left ventricular non-compaction.X means that mutations in the gene have been associated with the phenotype.

Gene	OMIM	Protein	Interactions	DCM	HCM	RCM	LVNC
Sarcomere - contractile proteins							
MYH7	160760 192600	Myosin heavy chain, cardiac muscle beta isoform	myosin-binding protein C, myosin light chains, actin, titin, myomesin	X (4%)	X (20%)	X	X
MYH6	160710	Myosin heavy chain, cardiac muscle alpha isoform	myosin-binding protein C, myosin light chains, actin, titin	X (4%)	X		
MYL2	160781 608758	Myosin regulatory light chain 2, ventricular/cardiac muscle isoform	myosin heavy-chain		X (<1%)		
MYL3	160790 608751	Myosin light polypeptide 3	myosin-heavy chain		X (<1%)	X	
MYBPC3	600958	Myosin-binding protein C, cardiac-type	myosin-heavy chain, titin, actin	X (2%)	X (20%)		X
TNNT2	115195	Troponin T, cardiac muscle	troponin I, tropomyosin	X (3%)	X (2.5%)	X	X
TNNI3	191044	Troponin I, cardiac muscle	actin, troponin C, troponin T	X (<1%)	X (2.5%)	X	
TNNC1	191040	Troponin C, slow skeletal and cardiac muscles	troponin I	X (<1%)	X		
TPM1	115196 191010	Tropomyosin 1 alpha chain	troponin T, actin	X (<1%)	X (1%)		X
ACTC1	102540	Actin, alpha cardiac muscle 1	myosin heavy-chain, tropomyosin, troponin I, myosin-binding protein C, alpha-actinin 2	X (<1%)	X (<1%)	X	X
Sarcomeric cytoskeleton							
TTN	188840	Titin	multiple (see text)	X (25%)	X		

ACTN2	102573	Alpha-actinin-2	actin	X (1%)	x		
CSRP3	600824	Muscle LIM protein	α actinin, calcineurin, telethonin	X (<1%)	X		
TCAP	604488	Titin-cap or telethonin	myozenin-2, myostatin	X (1%)	X		
ILK	602366	Integrin-linked kinase	muscle LIM protein	X (<1%)			
MYOZ2	606602	Myozenin	telethonin		X		
FHl1	300163	Four-and-a-half-LIM-domains 1					
LDB3	605906	LIM domain binding protein 3/Cypher/ZASP	alpha-actinin, PKC	X (1%)	X		X
PDLIM3	605889	PDZ LIM domain protein 3		X (<1%)			
BAG3	603883	BCL2-associated athanogene 3		X			
DES	125660	Desmin		X (<1%)		X	
CRYAB	123590	Alpha B crystalin	desmin, vimentin, actin	X (< 1%)		X	
NEBL	605491	Nebullete	actin				
MYPN	608517	Myopalladin	α-actinin, titin, nebulette, cardiac ankyrin repeat protein	X (3-4%)			
NEXN	613121	Nexilin		X (<1%)	X		
ANKRD1	609599	Cardiac ankyrin repeat protein	myopalladin/titin	X (2%)	X		

2.5. DOWNSTREAM MECHANISMS OF DISEASE AND POSSIBLE DRUG TARGETS

It is striking that while the first sarcomeric protein gene mutations were reported over 20 years ago, the treatment of patients with cardiomyopathy is still largely palliative. Fortunately, greater understanding of the biological consequences of sarcomere mutations is leading to new ideas on the treatment of genetic heart muscle diseases. Downstream disease pathways and possible drug targets are illustrated in **figure 5**.

2.5.1. CROSS-BRIDGE KINETICS

Much research has focused on an exploration of the consequences of sarcomeric protein gene mutations on myofilament contraction, mostly using recombinant proteins or cellular/molecular studies from engineered animal models and less frequently, patient tissue

from myectomies or explanted hearts. Based on these findings, it has been hypothesized that small molecule inhibitors or activators of acto-myosin cross-bridge formation might be able to correct one of the fundamental pathophysiological mechanisms in cardiomyopathy [74] [76])[77], however acknowledging that other mechanisms may account for low force generation, including lower myofibril density and higher cardiomyocyte area, which are aspects of cardiomyocyte remodeling that vary between mutated genes [78].

2.5.2. CALCIUM SENSITIVITY AND CYCLING

Based on a hypothesis in which the differential effects of mutations on calcium homeostasis explain phenotypic variation [36],[27], manipulation of myofilament calcium sensitivity is being explored as a potential therapy. A recent paper, using a knock-in rodent model of a tropomyosin mutation, demonstrated that correction of increased calcium sensitivity, by co-expressing a pseudo-phosporylated troponin I, prevented the development of the phenotype, including a correction of diastolic dysfunction [79].

Deranged calcium cycling is a feature of heart failure of various aetiologies and is the consequence of changed expression or post-translational modifications of sarcoplasmic/endoplasmic reticulum calcium ATPase 2 (SERCA2) and the ryanodine receptor 2 (RYR2) [80]. Altered calcium cycling has been proposed as a fundamental aspect of HCM at the cellular level, possibly as a consequence of calcium being retained at the sarcomere [81, 82],[83]. Altered calcium cycling in HCM and other cardiomyopathies may also be explained by reduced uptake into the sarcoplasmic reticulum by the SERCA2 pump due to a cellular energetic defect [84]. The main clinical consequences of altered calcium dynamics are early and delayed after-depolarizations, arrhythmia and diastolic dysfunction [85], [86].

Animal models have shown that de-sensitization to calcium corrects the arrhythmogenic phenotype [86] and in a recent study using induced pluripotent stem cells as a model for HCM [87], pharmacological inhibition of calcium and sodium entry attenuated the arrhythmogenic cellular phenotype.

In two rodent models of HCM, an alpha- myosin heavy-chain missense mutant mouse and a transgenic mouse model expressing a cardiac troponin T mutation, inhibition of plasma sarcolemmal L-type calcium channel by diltiazem prevented fibrosis and improved LV diastolic function [81, 88]. Another recent paper focused on altered electro-mechanical coupling, using

cardiomyocytes from HCM patients undergoing myectomy. In a comparison with cardiomyocytes from non-hypertrophic non-failing tissue, the authors demonstrated that late sodium current inhibition with ranolazine improved a cellular phenotype provoked by increased calmodulin kinase II activity and increased phosphorylation of its targets, resulting in a reduction in early and delayed after-depolarisations [89]. A clinical trial of ranolazine in HCM is in progress (Ranolazine for the Treatment of Chest Pain in HCM Patients (RHYME); NCT01721967; clinicaltrials.gov).

2.5.3. SIGNALING PATHWAYS AND PROTEIN DEGRADATION PATHWAYS

Protein phosphatases and kinases

Many of the sarcomere, Z-disc and M-band proteins, as well as titin, are linked to cardiomyocyte survival/growth pathways, via nuclear factor of activated T-cells (NFAT) transcription factor, mitogen-activated protein kinases (MAPKs) and other protein kinases and transcription/co-transcription factors. This places the contractile and associated proteins as intermediaries between these downstream pathways and the mechanical processes of muscular tension, contractility and energy consumption [24],[74], [80]. These downstream pathways are also being considered in the search for new therapies. Possible targets include *protein kinases*, enzymes that catalyze the phosphorylation of various substrates (the most frequent post-translational modification of proteins) and that are key-mediators of cell activity via signal transduction pathways vital for metabolism, cell cycle, motility, survival/apoptosis and cell-cell communication [90]. *Protein phosphatases* have the opposite role; by dephosphorylating the same substrates as the kinases, they contribute to the regulation of the same pathways, as the activity of a signal transduction protein depends on the ratio between phosphorylated and dephosphorylated state [91].

Calcineurin, co-localized with MLP at the Z-disc, is a Ser/Thr phosphatase involved in the pathways leading to maladaptive remodeling/hypertrophy and heart failure. It acts through transcription factors such as NFAT, which also localizes at the Z-disc, but can translocate into the nucleus [74], [24]. Other Z-disc proteins described previously, such as MLP or FHL1, can also act in the nucleus as cofactors of transcription.

MAPKs, such as Erk2, are also localized at the Z-disc and interact with co-factors such as FHL1 [24]. They are involved in cardiomyocyte hypertrophy-promoting pathways.

Protein kinase C epsilon is a Ser/Thr kinase localized at the Z-disc; it can translocate into the nucleus, activating pathways leading to physiological hypertrophy [24].

Protein degradation and autophagy pathways

There is a growing interest in protein degradation pathways including the ubiquitine-proteosome system (UPS) and degradation by lysosomes via autophagy [92]. The ubiquitine-proteosome system has the task of flagging misfolded /truncated proteins, by adding poly-ubiquitin chains on them. Proteins become marked for degradation by the proteasome, an ATP consuming process. This system is also importantly involved in the control of cell growth/survival [74].

Calpain 1, a protease involved in cell-cycle regulation and apoptosis pathways, together with caspases, is also located at the Z-disc and M-band [74], [24].

Ubiquitinated proteins that are not disposed by the proteasome can form aggregates, that are then marked for autophagy by p62 (SQSTM1) and Nbr1, proteins present at the Z-disc and M-band. Autophagy can also dispose of entire damaged organelles [74].

Others, such as the TRIM ("tripartite motif") proteins, including Murf (Muscle specific Ring Finger proteins) 1 and 3 localize to the Z-disc and Murf 1 and 2 to the M-band. Murf1 ubiquitylates and degrades sarcomeric proteins such as myosin heavy chain or troponin I. Murf1 also inhibits the protein kinase C (PKC) dependent hypertrophy pathway and has been described as having a transcription repressor activity of c-jun in the heart. Finally, Murf2 can also have a developmental role in myofibrillogenesis [74],[24]. Mutations in Murf1 have been associated with HCM [93], but this was recently contested [94].

The presence of these proteins at the Z-disc and M-band, their ability to concomitantly interact with ubiquitin and autophagosome-associated proteins, together with the fact that they are targets for titin-kinase, strongly suggests a link between contractile function / mechano-sensing and the processes that regulate cell survival and growth; they can therefore eventually be involved in the pathogenesis of cardiomyopathy at the cellular level and therefore constitute ideal candidate targets for pharmacological intervention.

2.5.4. CARDIOMYOCYTE-FIBROBLAST CROSS-TALK: FIBROSIS

Interstitial fibrosis is one of the defining histological characteristics of cardiomyopathy [9] and

is thought to contribute to arrhythmia and LV diastolic and systolic dysfunction. In an animal (mouse) model of HCM, sarcomere protein gene mutations activated proliferative and pro-fibrotic signals in fibroblasts to produce pathologic remodelling; fibroblasts also demonstrated increased expression of TGF-beta and other pro-fibrotic proteins, like periostin [95]; administration of neutralizing antibodies or losartan attenuated fibroblast proliferation and fibrosis, and in the case of losartan, hypertrophy in mutation-positive pre-hypertrophic mice was prevented [95].

In human HCM, an increased level of C-terminal propeptide of type I procollagen (PICP), a biomarker of type I collagen biosynthesis, has been described in mutation carriers without left ventricular hypertrophy and in patients with overt HCM [96].

2.5.5. CARDIOMYOCYTE ENERGETICS

The myocardium depends on oxygen for high-energy phosphate production by oxidative phosphorylation. In the normal heart, adenosine triphosphate (ATP) is produced primarily by the metabolism of free fatty acids (FFAs) and carbohydrates, with FFAs accounting for approximately 70% of total ATP production. Importantly, FFAs are less efficient as a source of myocardial energy, as they require approximately 10% more oxygen than glucose in order to produce an equivalent amount of ATP [97]. Evidence from animal and human studies suggest that HCM (and perhaps other cardiomyopathies) is characterised by a reduction in the concentration of high-energy phosphates in the myocardium [98]. This might be partly explained by myocardial ischaemia caused by microvascular dysfunction, but may also be a direct consequence of sarcomere protein gene mutations on myocardial contractile efficiency [99]. A trial of perhexiline, that acts by inhibiting carnitine palmitoyl transferase (CPT-1/2), involved in mitochondrial uptake of long-chain fatty acids, versus placebo, showed an improvement of diastolic function and increased exercise capacity [100]. A number of other studies are evaluating the effect of drugs that stimulate glucose oxidation and reduce fatty acid oxidation and thereby improve myocardial efficiency and lower oxygen demand in patients with HCM and DCM.

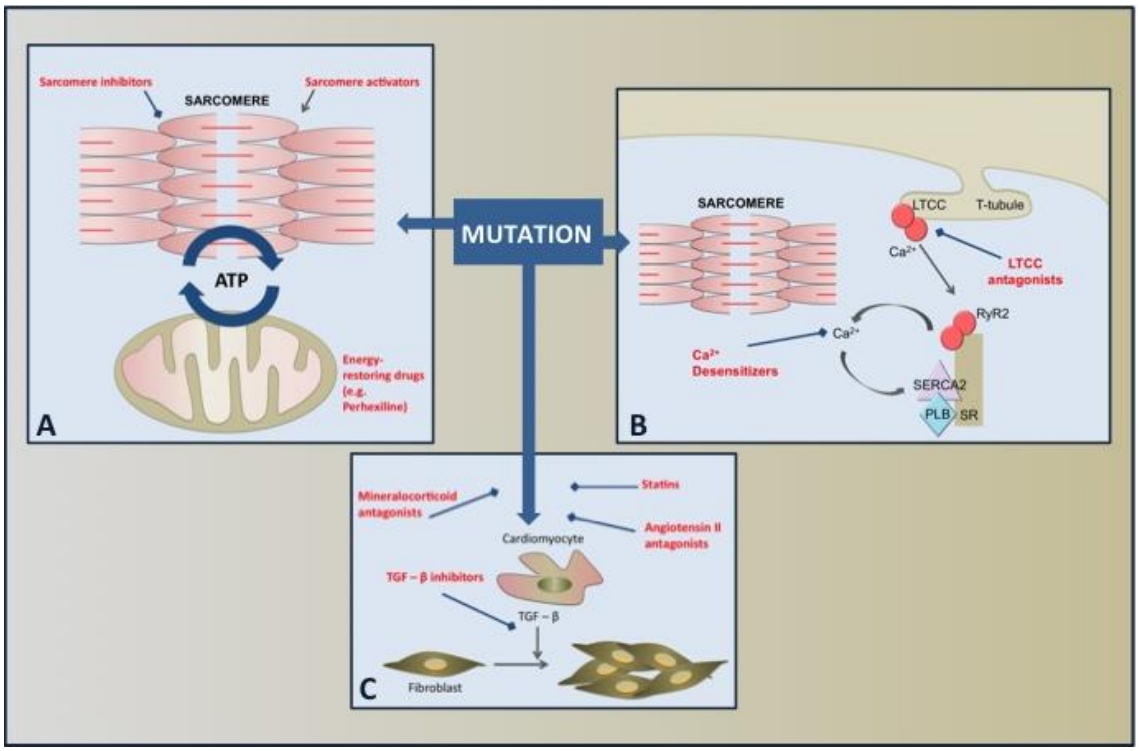

Figure 5. Mechanisms of disease in hypertrophic cardiomyopathy and possible drug targets. Reproduced with permission from [2].

3. COMPLEXITY AND CHALLENGES IN HYPERTROPHIC CARDIOMYOPATHY GENETICS

Mutations in the main sarcomeric proteins, that constitute the motor unit of the cardiomyocyte, are well established as causes of cardiomyopathy [18]. Animal models and functional studies have provided sound evidence of causality for some of the increasingly large number of variants associated with these diseases. However, there are still a considerable number of unsolved issues that merit research.

3.1. GENETIC TESTING STRATEGIES, HIGH-THROUGHPUT SEQUENCING AND INTERPRETATION OF RARE VARIATION

Most clinical guidelines [101, 102] recommend routine molecular genetic testing of HCM probands. Given the high level of biological discrimination afforded by genetic testing, the finding of an established disease-causing mutation adds weight to the diagnostic confirmation, and allows differentiation of geno- and phenocopies that could benefit from specific therapeutic strategies [103]. Genetic testing is also justified by the assumption that genotype information can be used to guide therapy and counselling strategies for families and to provide pre-symptomatic diagnosis of family members and thereby offer clinical surveillance, early medical intervention and reproductive advice [101],[102].

In clinical practice, the use of genetic testing has been limited by the cost and complexity of conventional sequencing technologies. The yield of genetic testing is also relatively limited, with the identification of a causal variant in less than 50% of the cardiomyopathy cases. The emergence of high-throughput sequencing (HTS) technologies has promised to tackle both limitations.

HTS or massively parallel sequencing is able to sequence substantially larger genomic regions at the same or lower cost compared to conventional Sanger (capillary) sequencing [104]. These also called next-generation sequencing (NGS) platforms allow the interrogation of many genes simultaneously – an improvement from the existing strategy of examining a fixed subset of genes (e.g. sarcomeric). This is relevant given the increasingly recognized overlap between the genetic background of different cardiomyopathy phenotypes and the locus heterogeneity that characterizes these diseases.

A pilot study exploring the use of targeted NGS in ten patients with cardiomyopathy (five HCM and five DCM patients) has demonstrated accuracy equivalent to conventional sequencing [105], with a sensitivity of 96%, which was comparable with other reports focussing on non-cardiac inherited diseases [106].

Limitations of HTS accuracy are mainly related to the sequencing of repetitive regions - which are prone to create false positives - and insertion-deletions, for which HTS can have limited sensitivity [107]. However HTS can have increased sensitivity compared with conventional screening strategies such as denaturating high pressure liquid chromatography (DHPLC), when variants are homozygous [108] or can be even superior to Sanger sequencing when variants occur in specific locations such as close to the end of analysed segments or untranslated regions [109].

As technological advances facilitate faster and more complete genetic testing, there arise new challenges regarding the interpretation of genetic variants. The establishment of pathogenicity of a new variant classically rests on the demonstration of co-segregation of the variant with disease in affected families. However, in most instances, families are too small to establish causality beyond reasonable doubt. High throughput sequencing technologies have amplified this problem through the sequencing of large panels of genes or even entire exomes - the coding part of the genome - and genomes, i.e. the entire DNA sequence [107]. These sequencing strategies generate large numbers of potentially pathogenic variants, only some of which are obviously related to the phenotype of patients undergoing testing [107]. *In silico* prediction tools are frequently used to determine pathogenicity of novel variants in this situation, but these are known to have poor accuracy and have not been developed or validated for specific diseases. [110].

Large-scale population studies, designed to explore the scope of genetic variation in humans, have recently been published, after the beginning of my research. The 1000 genomes project (http://www.1000genomes.org), published as a pilot report [111] and phase I data [112], studied the genomes of 1,092 non-phenotyped individuals from 14 populations, reporting that each individual carries approximately 250 to 300 loss-of-function variants in annotated genes and 50 to 100 variants previously implicated in inherited disorders. Another report on data generated by the 1000 genomes project confirmed that human genomes contain approximately 100 genuine loss-of-function variants, with around 20 genes being completely

inactivated [113]. Other projects aimed at building a database of variation from phenotyped disease populations and healthy controls were meanwhile launched. The NHLBI exome sequencing project completed the exome sequencing of 6503 individuals (data is publicly availble at http://evs.gs.washington.edu/EVS/) and a report based on part of these data showed similar findings to the ones from the 1000 genomes project [114]. A similar UK based project was launched in 2011, the UK10K project, that generated sequencing data for approximately 10000 individuals from the UK, including disease and control cohorts (www.uk10k.org).

Studies that described this previously unexplored and unexpected complexity in the inherited cardiac disease context have meanwhile been published. In a study [115] focussed on arrhythmogenic right ventricular cardiomyopathy (ARVC) associated genes, radical mutations were present in 0.5% of a control population versus 43% of ARVC cases, while 16% of controls carried missense mutations versus a similar 21% of ARVC cases. In another study, 33 missense variants previously associated with long-QT syndrome were identified in 1 of every 31 individuals in the population of the NHLBI Exome Sequencing Project [116].

3.2. GENOTYPE-PHENOTYPE ASSOCIATIONS

HCM is characterized by a highly heterogeneous phenotype, a highly variable intra and inter-familial expressivity and incomplete and age-dependent penetrance [117]. This genotype-phenotype plasticity is largely unexplained [118].

As stated in the previous section, patients are routinely offered genetic testing in order to provide them with information about the likely impact of disease on their lives and to facilitate lifestyle and medical interventions that improve prognosis [101]. However, for this strategy to succeed, there must be a predictable relation between specific genotypes and disease expression. One of the factors that still dramatically hampers the use of genetics in daily clinical decisions is the poor understanding of such genotype-phenotype relationships.

In clinical practice, the most robust associations between mutation and phenotypes are still relatively crude. This lack of knowledge is partly explained by the locus and allelic heterogeneity of all cardiomyopathies [32] and the small size of most reported patient cohorts.

In addition, novel variants with no established clinical phenotype information are increasingly common in the literature.

Following the identification of the first sarcomeric protein gene mutations, studies of large families explored the relationships between genetic variants and different sub-phenotypes. Specific associations were reported between individual mutations in ß-myosin heavy chain (*MYH7*) and troponin T (*TNNT2*) [119, 120, 121], [122, 123], [124] and prognosis and then some general correlations between particular genes and clinical phenotype were suggested. For example, a later onset and more benign prognosis for cardiac myosin binding protein C (*MYBPC3*) carriers [125], [126], [127], [128] and mild hypertrophy and higher risk of sudden cardiac death for *TNNT2* carriers [129],[130]. However, subsequent work [131],[132],[133] in large cohorts of mostly unrelated and consecutive probands [134, 135, 136] [137], [138], [139] yielded contradictory and inconsistent findings.

It has been hypothesized that the impressive genotype-phenotype plasticity and the challenge in finding reproducible genotype-phenotype associations could be explained by modifier genes, epigenetics, post-transcriptional and post-translational modifications and environmental effects [140, 141], [142]. Previous work looking for common variants/polymorphisms acting as modifiers has proven to be relatively unhelpful [143], [144], [145], [146]. A paper [147] explored the role of renin-angiotensin-aldosterone system (RAAS) in the phenotypic expression of HCM. The authors did not find major effects of genetic variation within the genes of the RAAS system on the phenotypic expression of HCM. Similar to that report, several studies have examined the role of common genetic variants on the expression of sarcomere mutations using GWAS or more commonly a candidate gene approach, but have failed to show any major effect on disease expression 41, 42 [143], [144], [145], [146] [147].

Given the substantial genetic overlap between different cardiomyopathies and knowledge from other genetic diseases, other authors have predicted the possible modifier effect of genes acting in common downstream pathways (e.g. other cardiomyopathy genes), but this has not been systematically explored before my studies [32], [142].

3.3. STRUCTURAL VARIATION

Copy-number variants (CNVs), usually defined as genomic deletions and duplications greater than 1 K base pairs, are an important cause of genetic variation in the general population [112, 148] and contribute to both simple Mendelian and complex genetic traits [149, 150]. Hypertrophic cardiomyopathy (HCM) is predominantly caused by missense mutations in cardiac sarcomeric protein genes [117]. Small insertion-deletions (denoted as indels, which are usually less than 10 base pairs) in sarcomeric protein genes are also relatively common [117], but the importance of major structural variation as a cause or modifier of the HCM phenotype is unknown.

This deficiency is important, as most diagnostic genetic laboratories have used Sanger sequencing strategies when screening patients with the disease and are, therefore, unable to detect this type of genetic variation. Even with the introduction of high-throughput sequencing, variant calling pipelines are usually directed for the detection of single nucleotide variants or small insertion-deletions.

Recently, bioinformatic algorithms have been developed to allow the detection of structural variation from high-throughput short-read sequencing data [151]-[152]. While several analytical approaches are available [152], read depth based strategies are most effective for targeted sequencing because they do not require the sequencing of the DNA region surrounding the CNV breakpoints.

3.4. NON-CODING VARIATION

Current genetic diagnostic strategies in hypertrophic cardiomyopathy and other Mendelian diseases are based on the screening of the exons and intron-exon flanking regions of the most commonly associated genes, looking for potentially pathogenic mutations. This approach is based upon the fact that the coding region, corresponding to 1% of the genome, is considered to harbour the pathogenic variation responsible for Mendelian disease. Nevertheless, recent estimates from the ENCODE (“Encyclopedia of DNA Elements”) project suggest that around 80% of the genome has a biochemically relevant role [153]. Importantly, it has already been

demonstrated that variation in the non-coding regions can be the cause in a proportion of other genetic diseases, such as nonsyndromic intellectual disability [154].

It seems very likely therefore that a proportion of cardiomyopathies may also result from regulatory gene mutations. Additionally, through a putative interference in epigenetic and other regulatory mechanisms, non-coding variation could potentially modify the phenotype when added to the effects of a "main" coding variant, and partially explain the extremely variable expressivity that has contributed to a poor understanding of genotype-phenotype relationships in HCM.

However, prediction of the functional consequence of non-coding variation is more difficult than that of coding variation, due to the unknown function of the great majority of the non-coding DNA. The recent efforts of the ENCODE project [153] allowed a significant amount of experimentally validated data to be generated and made available, including ChIP (chromatin immunoprecipitation) -sequencing [155],[156] data for TF binding sites, that helps predict the possible consequences of non-coding variants.

These challenges of interpretation are increased by the growing awareness that a large amount of variation is present in the general population. This was recently shown for coding variation [111],[113, 114], but also for non-coding variation, as reported in the publication of phase 1 results from the 1000 genomes project project [112]. According to these report, individuals carry between 18 and 69 rare variants in conserved TF binding motifs.

3.5. *IN SILICO* PREDICTION OF THE PATHOGENICITY OF A CODING VARIANT

The high genetic heterogeneity that characterizes HCM makes determination of the pathogenicity of individual genetic variants problematic [157]. These variants are often novel and missense variants with uncertain effects on gene function. The effects of a missense variant on molecular function, phenotype, and organism fitness can be extremely diverse [158]. The use of high-throughput sequencing approaches is likely to result in even greater complexity, by identifying multiple variants in individual patients. Given the almost impossible task of developing massively parallel functional studies to match massively parallel sequencing platforms, new interpretative tools are needed.

Among some of the tools that can be used to estimate the effect of a variant and prioritize further analysis are *in silico* prediction software. The best known are PolyPhen ("Polymorphism Phenotyping"), PolyPhen2 and SIFT ("Sorting Intolerant from Tolerant") [159],[160]. More recently, Condel ("Consensus Deleteriousness Score") [161] a tool developed by combining Polyphen and SIFT algorithms, was reported to achieve increased accuracy. These software packages can be used to predict the damaging effect of a missense variant based on features that include species conservation and the physicochemical difference between the aminoacids. Nevertheless, the accuracy is largely unknown, because they were not designed for clinical use or for specific diseases and have not been validated against thoroughly annotated locus-specific databases or phenotype datasets [110]. Moreover, they frequently give conflicting results that limit their clinical utility [162].

Another major drawback of existing prediction softwares is the fact that they make use of limited structural information. SAAPdb ("Single Amino Acid Polymorphism" database) and SAAPdap ("Single Amino Acid Polymorphism" data analysis pipeline), developed by Martin et al [163],[164],[165],[166] uses a combination of rule-based structural measures to assess whether a modification is likely to alter or destroy the function of the protein. This software has already been used to study structural differences between disease-causing mutations and neutral polymorphisms [163], to analyse mutations in glucose-6-phosphate dehydrogenase [167] and in tumour suppressor p53 [168].

In HCM, different functional consequences have been suggested to depend on the specific domain/region where the variant is localized [169]. Nevertheless, the hypothesis that the structural impact of a missense variant could influence phenotype and disease severity and outcome has never been tested before my work.

4. SYSTEMATIC REVIEW OF THE LITERATURE AND META-ANALYSIS OF GENOTYPE-PHENOTYPE ASSOCIATIONS

As part of the background preparation for my PhD thesis, I summarised and critically reviewed the current literature on genotype–phenotype associations in patients with HCM and performed a meta-analysis on selected clinical features.

4.1. METHODS

The methodology and presentation of the review is based on the recommendations of the PRISMA statement [170].

4.1.1. STUDY SELECTION AND ELECTRONIC SEARCH METHODS

I searched PubMed/Medline up to December 2012, for the terms “genotype” or “genetics” combined with either “phenotype”, “age”, “family history”, “histology”, “wall thickness”, “geometry”, “morphology”, “left ventricular function”, “heart failure”, “stroke”, “risk factor”, “sudden cardiac death”, “syncope”, “abnormal blood pressure response”, “implantable cardioverter-defibrillator”, “myectomy”, “alcohol septal ablation”, “death”, “prognosis” or “outcome”, each combined either with “hypertrophic cardiomyopathy” or “HCM”. Duplicates were eliminated. References from the retrieved original articles and reviews were searched for missing studies.

I selected observational English language human studies, with a cross-sectional or prospective design, that compared phenotypic features in patients with and without sarcomere mutations and between specific genes or individual mutations. The first selection was made by reading abstracts and the final selection by reading full articles.

In order to reduce ascertainment biases, the pooled analysis was confined to studies reporting on cohorts of unrelated and consecutive patients, where at least two sarcomere genes were sequenced. Some of these studies also included data on relatives; those data were excluded from the pooled analyses. Studies that compared specific individual mutations, data that

incorporated relatives and publications in which patients were selected on the basis of a certain phenotypic/clinical feature were excluded from the pooled analysis but were used to inform the narrative review.

4.1.2. STATISTICAL ANALYSIS

I extracted data on the following phenotypic features to a table: age; family history of HCM; histology; morphology and function evaluated by cardiac imaging (extent and pattern of hypertrophy, late gadolinium enhancement, atrial and ventricular dimensions and function, left ventricular outflow tract obstruction, mitral valve abnormalities); clinical risk factors for sudden cardiac death (maximum left ventricular wall thickness ≥ 30mm, abnormal exercise blood pressure response, non-sustained ventricular tachycardia, family history of sudden cardiac death, syncope); interventions, outcome and prognosis (all death, cardiovascular death, SCD, non-fatal heart failure, AF, non-fatal stroke, implantable cardioverter-defibrillator (ICD) implantation, myectomy and alcohol septal ablation).

A random effect meta-regression model [171] was used to combine the data and to obtain the pooled (overall) estimate for a set of clinical features that were most frequently reported in the final selected studies: age at presentation, gender, family history of HCM, family history of sudden cardiac death (SCD) and maximum left ventricular wall thickness (MLVWT). Other clinical parameters, including the majority of the risk factors for SCD, were inconsistently reported or not rigorously defined in the great majority of the selected studies.

The overall prevalence was the weighted average of the prevalence across different studies. The pooled estimate is the weighted average of study specific estimates, where weights were calculated using measures of precision (inverse of the variance). Intra- and inter-study variances were used in the calculation of precision. The intra-study variance was the variance of the prevalence/proportion/mean obtained for each study. The between study variance, a parameter of the random effects meta-regression model, was estimated using method of moments. The inter-study variance was used to adjust for the heterogeneity in prevalence/proportion/mean between studies. Heterogeneity between studies was further assessed using I^2 statistic, which represents the proportion of total variability in the prevalence/proportion data attributable to the heterogeneity between the studies. This statistical analysis was conducted in collaboration with Dr. Shafiqur Rahman, Institute of

Statistical Research and Training, University of Dhaka, Bangladesh.

4.2. RESULTS

The initial search resulted in a total of 242 studies after removing duplicates. Twenty-two additional studies were added after reviewing the references of the retrieved articles. Reviews (n=29) and editorials (n=6) were excluded from the systematic review and publications that did not fulfil the pre-specified inclusion criteria were excluded from the meta-analysis. In particular, 53 family based studies were judged to be unsuitable for pooled analyses (**table 2**) as they included small numbers of patients and were characterised by marked variability in the methods and scope of genetic testing, the extent of family screening and the definition of clinical penetrance. The selection and filtering process is summarised in **figure 6**.

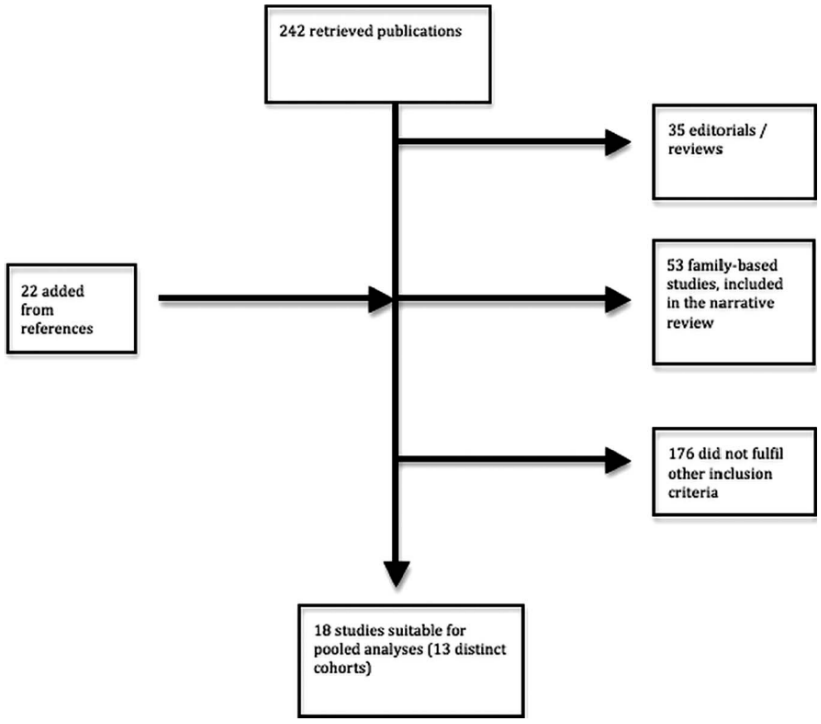

Figure 6. Flow chart of study selection process for the meta-analysis. Reproduced with permission from [172].

The 18 studies [23],[173],[174],[21, 175, 176, 177],[178],[179],[180],[181],[182],[22],[183, 184],[185],[186] selected for the pooled analyses (corresponding to 13 distinct cohorts and a

total of 2459 patients) are described in **table 3**. The pooled analysis for the percentage of individuals that are sarcomere mutation-positive (42.5%, 95% CI: 35.2%-46.7%) is shown in **figure 7**. Different publications were used in the analysis of individual clinical parameters, according to the completeness of the required data

Table 2. Family-centred studies reporting on penetrance, severity and prognosis. Reproduced with permission from [172]. SCD: sudden cardiac death (in some studies this includes aborted SCD); CS: cross-sectional; L: longitudinal; NR: not reported; * values calculated from the data provided on the publication; # deceased not tested.

Study	Number of families	Number of genotype-positive	Number of phenotype-positive	Penetrance	Follow-up (years)	Number of disease-related deaths	Number of SCD in the famlily	Mutations	Design
MYBPC3									
Niimura et al 1998 [125]	16	228	137	60%	-	36	34	12	CS
Charron et al 1998 [187]	2	33	23	69%	-	7	4	1 (SASint20 or IVS20-2A>G)	CS
Charron et al 1998 [126]	9	69	49*	71% (adults)	-	9	4	7	CS
Moolman et al 2000 [133]	1	27	10 (excluding deaths)	-	-	5	2	1	CS
Konno et al 2003 [188]	7	16	16	100% (above 50y)	-	NR	NR	1(R820G)	CS
Kubo 2005 [189]	15	39	30	77% (100% above 50y)	9.2±5.5	9	6 (CS assessment)	1(V592fs/8 or Ser593Profs*9)	L
Konno et al 2006 [190]	5	15	11	73% (90% above 30y)	-	NR	4	1 (IVS21+1G>A)	CS
Saltzman et al 2010 [191]	34	77	60*	78%	-	-	18	1 (R502W)	CS
Oliva-Sandoval et al 2010 [192]	18	65	40	61.5%	-	9	17 (+2 appropriate shocks)	1 (IVS23+1G>A)	CS
Choi et al 2010 [193]	1	7	6	86%	-	-	2	1 (L1238P)	CS
Hirota et al 2010 [194]	2	9	8	89%*	NR	0	0	1 (S297X)	CS
Page et al 2012 [138]	57	167	95	56.9% (34.5% relatives)	7.9±4.5	5	3	42	L
MYH7									
Watkins et al 1992 [121]	12	121	121	100%	-	47	24	7	CS
Epstein et al 1992 [119] + Fananapazir et al 1994 [120]	4	108	73	68%*	-	NR	13	4	CS
Anan et al 1994 [195]	6	75	75	100%	-	37	24	3	CS

Consevage et al 1994 [196]	1	4	4	-	-	NR	0	1(R719G)	CS
Marian et al 1994 [197]	2	10 #	21	86%	-	11	8	1 (G1208A)	CS
Marian et al 1995 [131]	3	23 #	33	-	-	14	10	2	CS
Posen et al 1995 [198]	2	42	-	60% for R403W 80% for R249Q (adults)	-	NR	0	2	CS
Ko et al 1996 [199]	1	NR	11	NR	-	5	3	1 (R453C)	CS
Tesson et al 1998 [195]	4	25	15	*	-	NR	4	4	CS
Charon et al 1998 [187]	5	35 (adults)	23 (adults)	66% (adults)	-	9	4	5	CS
Charron et al 1998 [126]	7	45 (adults)	32	71% (adults)	-	12	8	7	CS
Hwang et al 1998 [200]	1	5 #	13	100%	-	8	7	1 (G716R)	CS
Enjuto et al 2000 [201]	3	30	NR	NR	-	9	6	1 (R723G)	CS
Hvandrup et al 2001 [202]	1	5	5	100%	-	NR	3	1 (V606M)	CS
Huang et al 2001 [203]	1	1	1	-	-	NR	2	1 (R719G)	CS
Brito et al 2003 [204]	2	16	14	100% in one of the families and 50% in the other (adults)	11.2 in one family and 7.8 in the other	NR	2	1 (I263T)	L
Liu et al 2005 [205]	1	9	4	44%	-	NR	2	1 (A26V)	CS
Perrot et al 2005 [206]	5	17	11	65%*	-	NR	0	5	CS
Choi et al 2010 [193]	1	15	15	100%	-	NR	8	1 (G716R)	CS
TNNT2									
Watkins et al 1995 [123]	11	112	-	75% (above 16)	-	50	39	8	CS
Moolman et al 1997 [130]	2	22	17*	80% (above 16)	-	7	7	1(R92W)	CS
Nakajima-Taniguchi et al 1997 [207]	1	4	4 (excluding deaths)	NR	-	2	2	1 (A104V)	CS
Anan et al 1998 [208]	6	16 #	13	81%	-	2	2	1 (F110I)	CS
Varnava et al 1999 [209]	1	-	5	-	-	NR	4	1 (R94L)	CS
Torricelli et al 2003 [210]	5	10 #	-		-	NR	2	5	CS
Theopistou 2004 [211]	1	5 #	-	-	-	NR	5	1 (R278C)	CS
Gimeno et al 2009 [212]	4	16 #	24	-	-	11	7	3	CS

Pasquale et al 2011 [139]	20	92	-	91% (adults)	9.9±5.2	NR	6 (+1 appropriate shock)	12	L
TNNI3									
Kokado et al 2000 [132]	7	25	-	96% (above 20)	8.7±2.5		7	1 (K183 del)	L
Shimizu et al 2002 [213]	10	46	-	-	-	NR	4	1 (K183 del)	CS
Mogensen et al 2004 [137]	23	100	48	48%	-	12	6	13	CS
Doolan et al 2005 [214]	4	15	11	73% *	-	NR	4	4	CS
Choi et al 2010 [193]	1	12	12	100%	-	8	2	1 (R145G)	CS
MYL2									
Flavigny et al 1998 [215]	3	17 #	16 (excluding deaths)	-	-	NR	2	2	CS
Kabaeva et al 2002 [216]	2	8 #	7	-	-	NR	2	2	CS
MYL3									
Lee et al 2001 [217]	2	14	-	78% (adults)	-	NR	2	1 (A57G)	CS
Choi et al 2010 [193]	1	12	5	63% (adults)	-	2	1	1 (A57G)	CS
TPM1									
Yamauchi-Takihara et al 1996 [218]	3	-	8 (excluding deaths)	-	-	7	6	3	CS
Coviello et al 1997 [219]	3	-	21	-	-	2	2	1 (D175N)	CS
Karibe et al 2001 [220]	1	14 #	26	53%	-	13	11	1 (V95A)	CS
Jongbloed et al 2003 [221]	1	-	12	-	-	9	9	1 (E62Q)	CS
Makhoul et al 2011 [222]	1	4	4	100%	-		1 (+2 appropriate shocks)	1 (L185R)	CS

Table 3. Studies selected for pooled analyses. Frequency of mutations in each sarcomere gene and sequencing methodology for each study. Reproduced with permission from [172]. * indicates that only part of the gene was sequenced. SSCP: single-strand conformation polymorphism; DS: direct sequencing; RFLP: restriction fragment length polymorphism.

Cohort	**N patients**	**N genes**	**Sarcomeric positive (%)**	***MYBPC3* (%)**	***MYH7* (%)**	***TNNT2* (%)**	***TNNI3* (%)**	***MYL2* (%)**	***MYL3* (%)**	***ACTC1* (%)**	***TPM1* (%)**	**Sequencing methodology**
Richard et al 2003 [23]	197	9	63	26.4	25.4	4	4	2.5	0.5	0	0	SSCP+DS
Morner et al 2003 [173]	46	8	28	20	2.2 *	0	2.2	2.2	0	0	0	SSCP / DHPLC
Erdmann et al 2003 [174]	108	6	33.3	18.5	13 *	0.9	0.9	-	-	-	0.9	SSCP+DS or RFLP
Van Driest et al 2003-2005 [21, 175, 176, 177]	389	8	37.7	18.2	14.9	2.3	1.3	1.8	0	0.3	0.8	DHPLC+DS
Olivotto et al 2008 [178]	203	8	62	34	17	3.5	0.49	3.5		0.49	0.99	DHPLC+DS+RFLP
Garcia-Castro et al 2009 [179]	120	5	26.7	16	8	0.8	0				0.8	DS
Andersen et al 2009 [180]	90	11	36	10	10	2.2	2.2		1.1	1.1	1.1	SSCP+DS
Laredo et al 2006 + Rodriguez-Garcia et al 2010 [181],[182]	130	2	23	15	8	-	-	-	-	-	-	SSCP+DS+RFLP
Millat et al 2010 [22]	192	4	48	25	12	3.1	3.1	-	-	-	-	DHPLC+DS
Waldmuller et al 2011 [183]	236	2	41	24	17	-	-	-	-	-	-	DS
Brito et al 2012 [184]	77	5	53	35	11.7	6.5	2.6	0	-	-	-	DS
Gruner et al 2012 [185]	471	8	35	14.9	13.6	2.3	0.85	0.2	0.6	0.4	0.64	DS
Yobau Zou et al 2013 [186]	200	8	51	18	26	4	3.5	1	1.5	1.5	1.5	DS

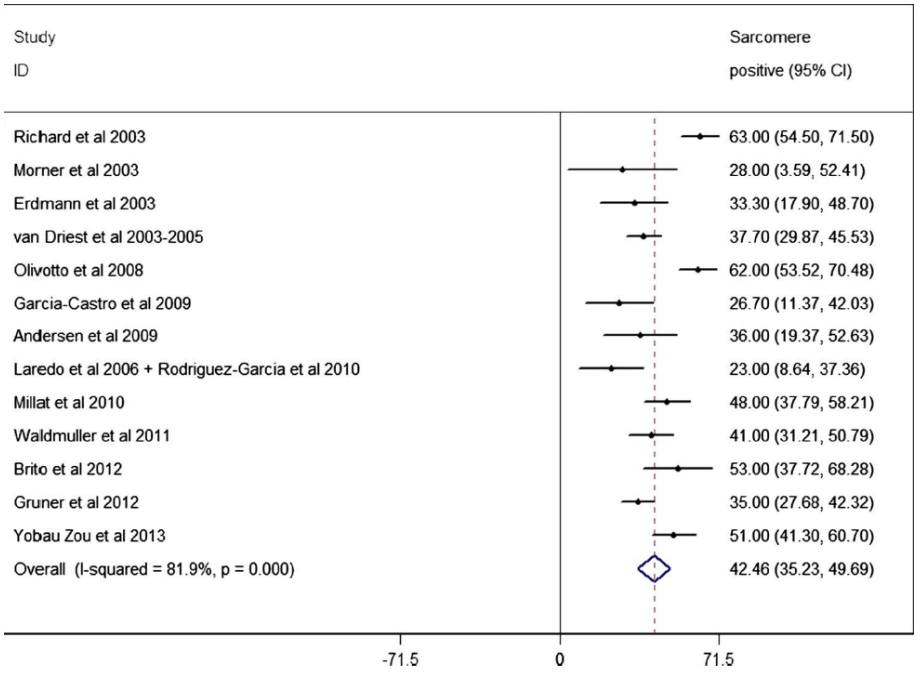

Figure 7. Pooled analysis for the proportion of individuals that are sarcomere gene mutation-positive. The overall proportion was 42.5% (95% CI 35.2% to 49.7%). The analysis shows significant heterogeneity. Reproduced with permission from [172].

4.2.1. DEMOGRAPHIC CHARACTERISTICS AND FAMILY HISTORY

Age

Younger age at presentation in carriers of sarcomere protein gene mutations is a common finding in many studies [185] [174],[21, 183, 184] and [186]. The presence of multiple sarcomere gene mutations (double or triple heterozygosity, compound heterozygosity or homozygosity) was associated with a younger age compared to a single mutation or to the absence of mutations in a single report [21]. In contrast, some other publications have reported a non-significant association between age and the presence of sarcomere mutations [178], [179], [182] and [22].

In the pooled analysis (**figure 8**), the presence of a sarcomere gene mutation was associated with a younger age at presentation. The age for sarcomere-positive individuals was 38.4 years (95% CI of 28.1-48.7). The age for sarcomere-negative individuals was 46.0 years (95% CI 35.6-56.4). The overall mean difference was statistically significant ($p < 0.0005$). There were no significant heterogeneity effects ($I^2 = 45.4\%$ with P-value=0.07) between studies.

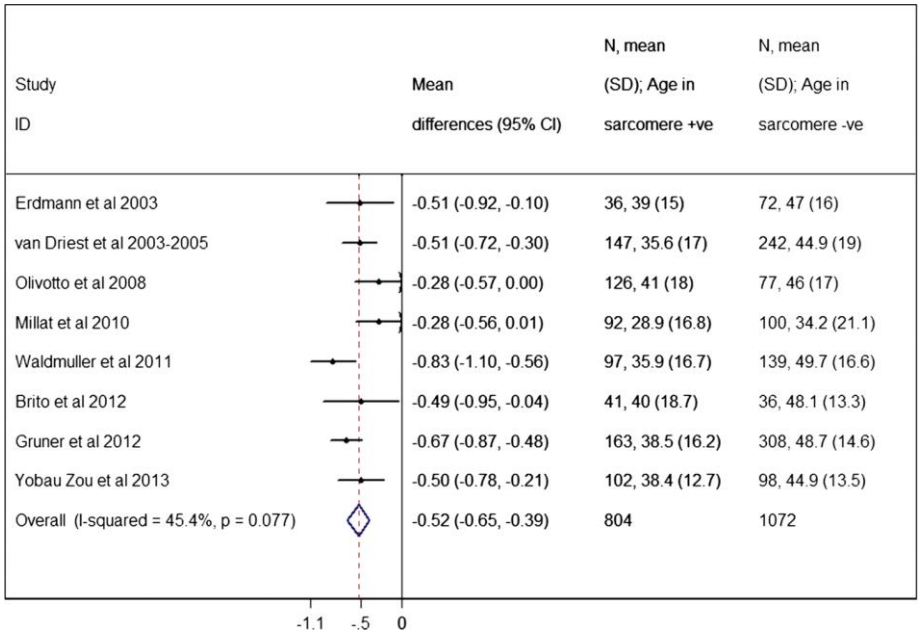

Figure 8. Forest plot from random effect meta-analysis showing that the presence of a sarcomere gene mutation was associated with a younger age at presentation. The age for sarcomere-positive individuals was 38.4 years (95% CI 28.1 to 48.7 years). The age for sarcomere-negative individuals was 46.0 years (95% CI 35.6 to 56.4 years) (P-value<0.0005). There were no significant heterogeneity effects (I^2 = 45.4% with P-value=0.07) between studies. Reproduced with permission from [172].

Some studies reported that patients with mutations in *MYH7* present earlier than *MYBPC3* mutation patients: [126], [22], [223], but others have failed to show such a difference [174], [183], [184] [176], [179], [182] or even describe a younger age at diagnosis for patients with truncating mutations in *MYBPC3* [174].

The pooled analysis (**figure 9**) showed no statistically significant difference in the age at presentation between the *MYBPC3* (37.6 years, 95% CI: 27.1- 48.2) and *MYH7* (35.3 years, 95% CI: 22.1 - 48.5) sub-cohorts, P-value=0.316.

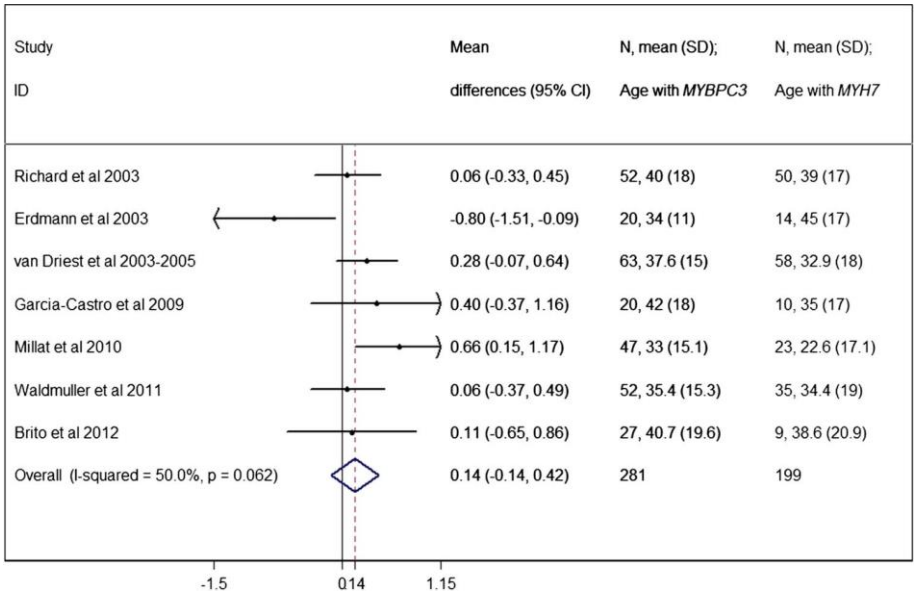

Figure 9. Forest plot from random effect meta-analysis showing no statistically significant difference regarding the age of presentation between *MYBPC3* (37.6 years, 95% CI 27.1 to 48.2 years) and *MYH7* (35.3 years, 95% CI 22.1 to 48.5 years) sub-cohorts, p = 0.316. There was no significant effect of heterogeneity between studies (I^2 = 50.0% with p = 0.062). Reproduced with permission from [172].

Three studies have compared age at presentation between patients harbouring *MYH7* mutations and patients without mutations in this gene. In one [177], patients with a *MYH7* mutation presented earlier than patients without a mutation (with or without mutations in other genes), but this was not replicated in two other studies [224],[181]. One study [9] reported a younger age at presentation in *TNNT2* patients than other patients with HCM. One further publication [225] reported that patients with mutations in *MYBPC3* were older at presentation than individuals harbouring mutations in *MYH7* or *TNNT2*.

Gender

A higher frequency of male patients is reported in the great majority of HCM cohorts. An association between the absence of a sarcomere mutation and an even higher proportion of males is reported in two studies [185] [182], but not in others [174], [21], [178], [179], [183].

The pooled analysis (**figure 10**) showed no statistically significant difference in the proportion of males in patients with sarcomere gene mutations compared with those without (57.5% vs 61.5% respectively, P-value=0.422).

There is no reported difference in the proportion of males between *MYH7* and *MYBPC3* mutation patients [126], [174], [176] [195], [179], [182],[223], except for a single study that reported a higher frequency of male patients with *MYBPC3* truncating mutations compared to *MYH7* [174]. There was no difference in the prevalence of males in two studies that compared *MYH7*-positive to *MYH7*-negative patients [177], [181].

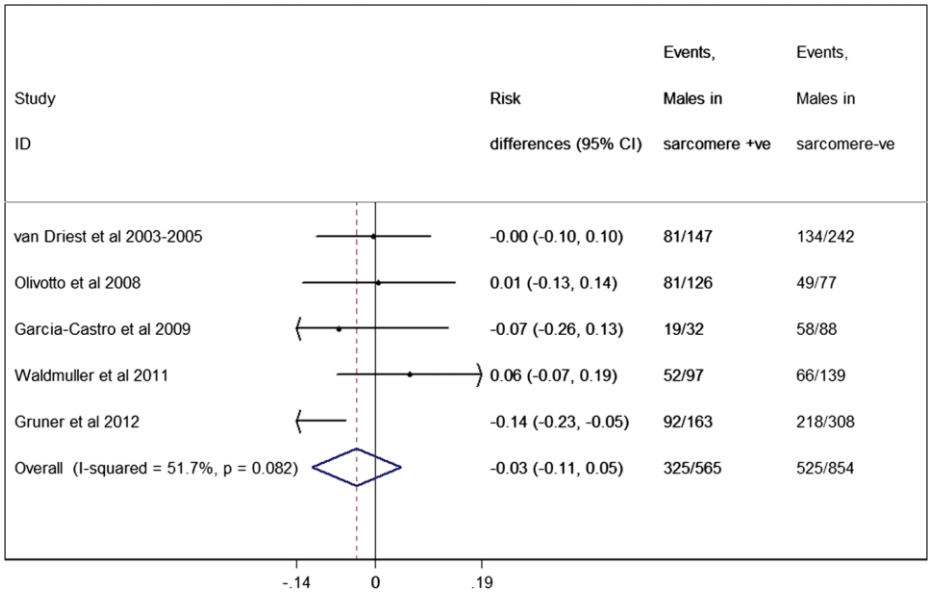

Figure 10. Forest plot from random effect meta-analysis showing the absence of a statistically significant difference between the proportion of males in sarcomere-positive (57.5%, 95% CI 53.4 to 61.6) compared with sarcomere-negative patients (61.5%, 95% CI 58.2 to 64.8, P-value=0.422). No significant heterogeneity effect was observed (I^2 = 51.7%, p = 0.082). Reproduced with permission from [172].

Family history

A family history of HCM has been associated with the presence of a sarcomere mutation [185], [174], [21], [183], [178], [226], [180]. The pooled analysis (**figure 11**) showed a significantly higher proportion of a family history of HCM within the mutation-positive subgroup (50.6%, 95% CI of 46.8%-54.4%) compared to mutation-negative individuals (23.1%, 95% CI of 20.6%-25.6%), P-value<0.0005. There were significant heterogeneity effects (I^2= 73.1%, P-value=0.001) between studies.

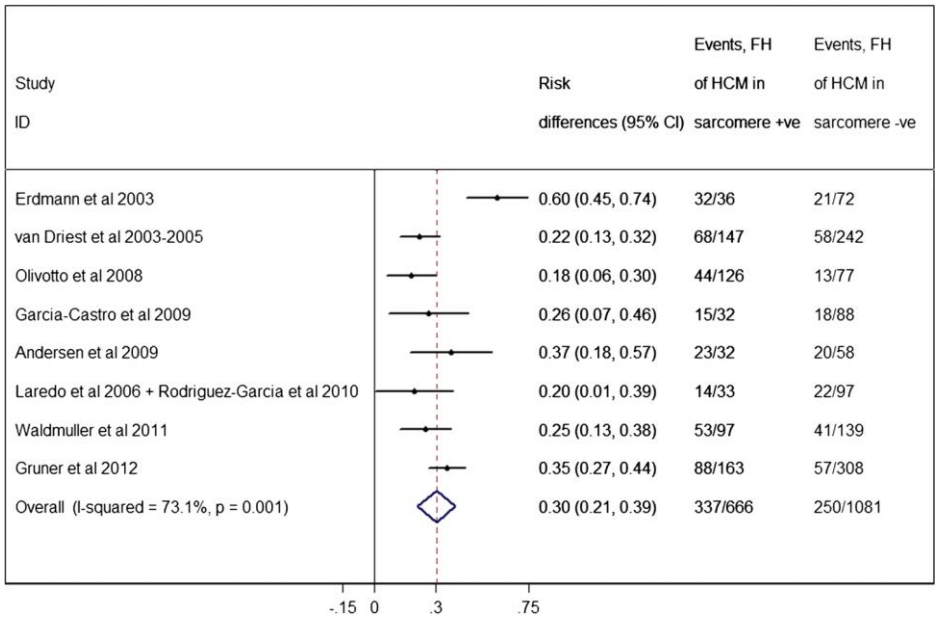

Figure 11. Forest plot from random effect meta-analysis showing a significantly higher proportion of a family history (FH) of hypertrophic cardiomyopathy (HCM) within the sarcomere-positive subgroup (50.6%, 95% CI 46.8% to 54.4%) compared to the sarcomere-negative individuals (23.1%, 95% CI 20.6% to 26.6%) (P-value<0.0005). There were significant heterogeneity effects (I^2=73.1%, P-value=0.001) between studies. Reproduced with permission from [172].

MYH7-positive patients are more likely to present with a family history of HCM, compared with patients without mutations in this gene [177],[181],[179]. The last study [179] compared against sarcomere-negative patients.

No study has reported a significant difference in the proportion of a positive family history in patients harbouring *MYBPC3* versus *MYH7* mutations [174], [176], [182], [183]. The pooled analysis is shown in **figure 12**.

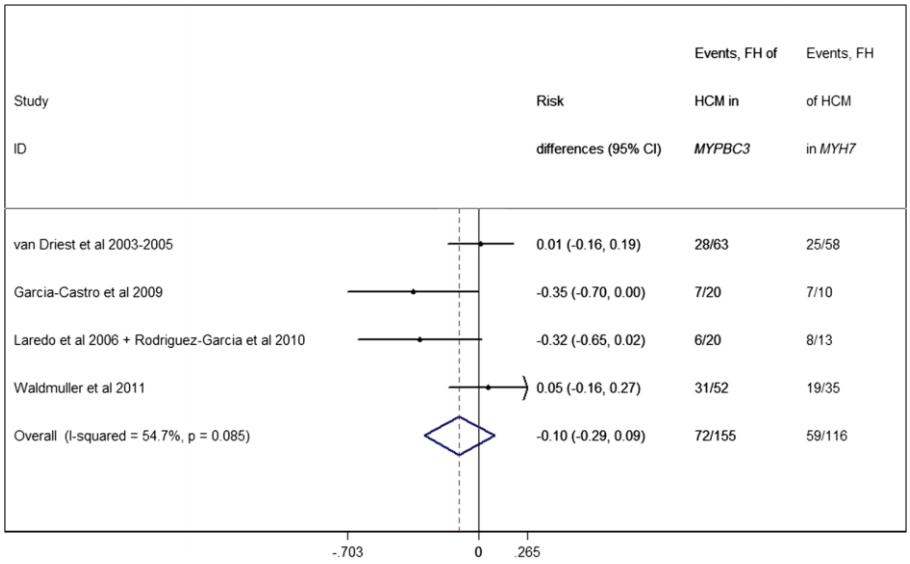

Figure 12. Forest plot from random effect meta-analysis showing no difference between the proportion of family history (FH) of hypertrophic cardiomyopathy (HCM) in patients with *MYPBC3* mutations (46.5%, 95% CI 38.6% to 54.3%), compared to the frequency of FH of HCM in patients with *MYH7* (50.9%, 95% CI 41.8% to 59.9%) (P-value=0.284). There were no significant heterogeneity effects between studies (I^2= 54.7%, P-value=0.085). Reproduced with permission from [172].

In one study, patients carrying mutations in the thin myofilament genes – troponin T (*TNNT2*), troponin I (*TNNI3*), actin (*ACTC1*) and alpha-tropomyosin (*TPM1*) - had a similar frequency of a family history of HCM compared to the rest of rest of the cohort [175].

Arterial hypertension

Four studies in three different cohorts reported on the prevalence of arterial hypertension in sarcomere-positive versus negative individuals [180],[181],[182],[185]. Only one of those studies found a significant association [185], reporting a higher prevalence amongst sarcomere-negative individuals. The pooled analysis showed an overall proportion of hypertensive patients amongst sarcomere-positive individuals of 22.8% (95% CI 17.3-28.2%), compared with a proportion of 41.7% amongst sarcomere-negative (95% CI 37.2, 46.2%, p = 0.004) (**figure 13**).

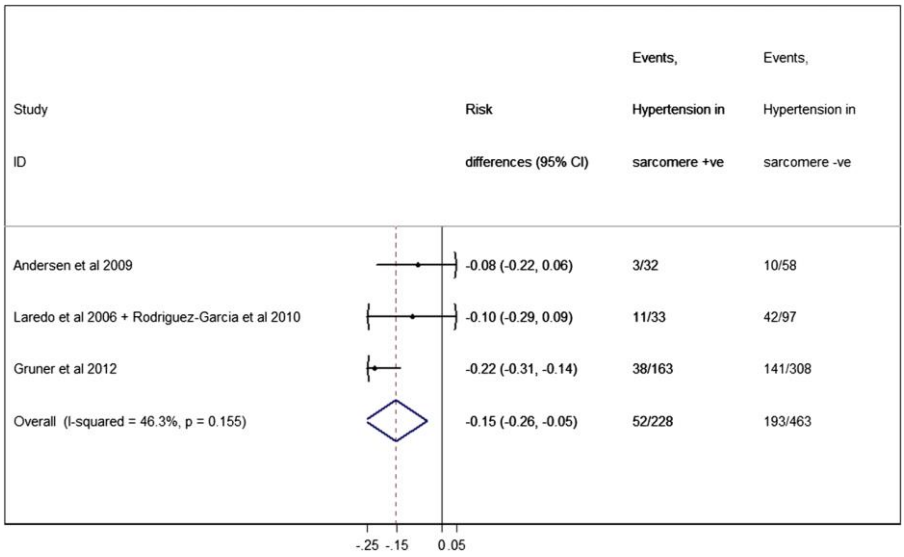

Figure 13. Forest plot from random effect meta-analysis showing that the proportion of patients with hypertension among sarcomere-positive individuals (22.8%, 95% CI 17.3% to 28.2%) is significantly less than the proportion among sarcomere-negative patients (41.7%, 95% CI 37.2% to 46.2%) (P-value=0.004). There were no significant heterogeneity effects (I^2=46.3%, P-value=0.155) between studies. Reproduced with permission from [172].

4.2.2. MORPHOLOGY AND FUNCTION

Maximum left ventricular wall thickness

The presence of any sarcomere gene mutation was associated with a greater maximum LV wall thickness (MLVWT) in several studies [185], [21], [184], [182]. Complex genotypes (multiple mutations in sarcomere genes) were associated with an even greater wall thickness compared to sarcomere negative patients in some but not all studies [21], [227], [186] [174], [178, 195], [179], [183].

The pooled analysis (**figure 14**) showed a greater MLVWT for patients carrying any sarcomere mutation (21.0 mm, 95% CI of 16.9-25.1 mm) compared to sarcomere-negative individuals (19.3 mm, 95% CI of 15.7-22.8 mm), P-value=0.03. The heterogeneity effects between studies were not significant (I^2=40.8%, P-value=0.133).

Differences in the prevalence of a maximum wall thickness ≥ 30 mm between sarcomere-positive and sarcomere-negative individuals were explored in two studies, that found no significant associations [21], [178].

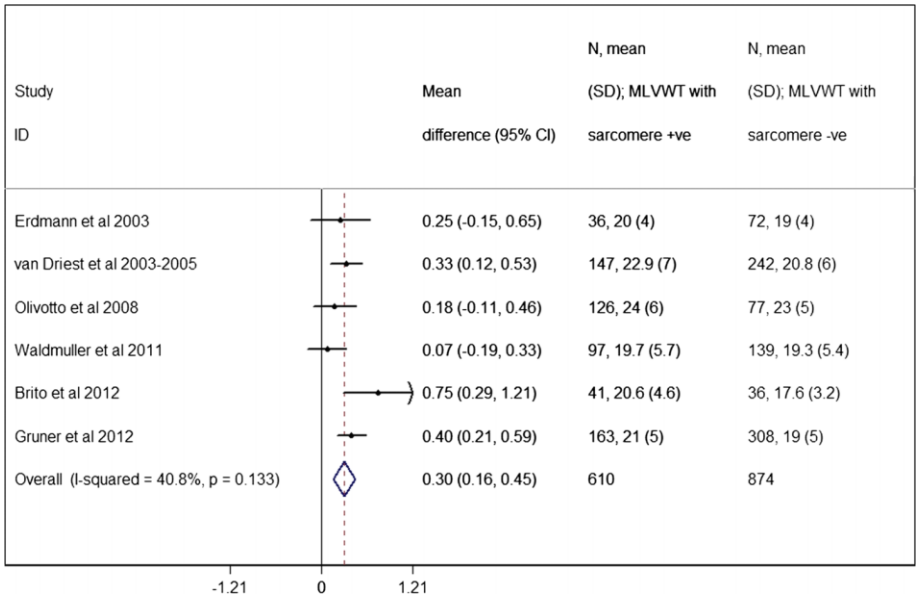

Figure 14. Forest plot from random effect meta-analysis showing a greater maximum left ventricular wall thickness (MLVWT) for patients carrying any sarcomere mutation (21.0 mm, 95% CI 16.9 to 25.1 mm) compared to sarcomere-negative individuals (19.3 mm, 95% CI 15.7 to 22.8 mm) (P-value=0.03). There were no significant heterogeneity effects (I^2=40.8% P-value=0.133). Reproduced with permission from [172].

Patients carrying mutations in *MYBPC3* seem to have a similar degree of hypertrophy when compared to *MYH7* patients [182], [184], [179], [176], [174], [126] with the exception of a single study [183], that described an increased average LV wall thickness for *MYBPC3* patients. The pooled analysis showed no difference in MLVWT between the *MYBPC3* and *MYH7* sub-cohorts, P-value=0.421 (**figure 15**).

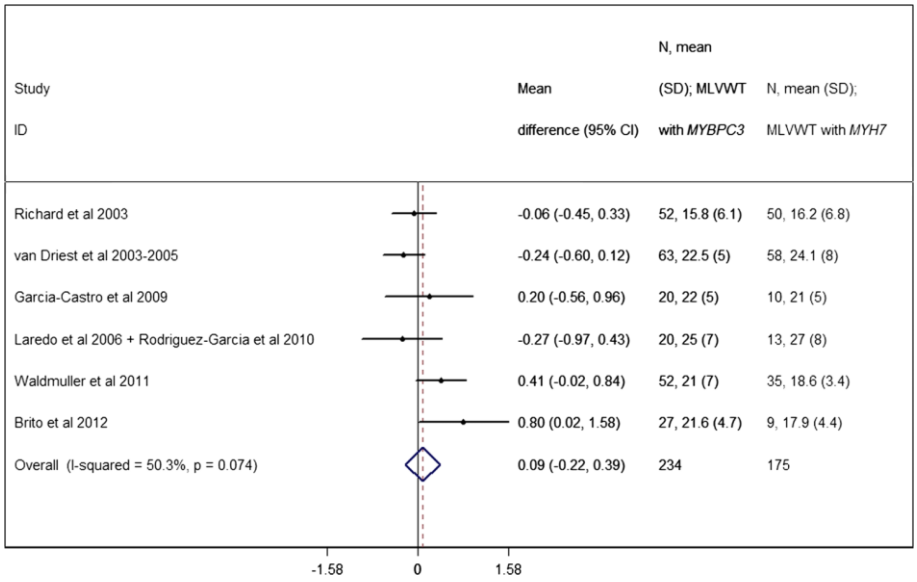

Figure 15. Forest plot from random effect meta-analysis showing no difference in maximum left ventricular wall thickness (MLVWT) between the *MYBPC3* (21.0 mm, 95% CI 17.1 to 24.8 mm) and *MYH7* (19.2 mm, 95% CI 15.6 to 22.9 mm) sub-cohorts (P-value=0.574). No significant effects of heterogeneity between the studies were observed (I^2=50.3%, P-value=0.074). Reproduced with permission from [172].

In a single study, there was no difference between the LV wall thickness of patients with thin filament mutations and the rest of the cohort [175].

In two studies that focus on the presence or absence of a *MYH7* mutation, a higher degree of hypertrophy in *MYH7* patients compared to the negative individuals is reported in one but not the other (40)[181]. Additionally, *MYH7*-head mutations were reported to be associated with increased wall thickness when compared to rod region mutations in another publication [223].

Ventricular morphology

Few studies have analysed the distribution of LV hypertrophy. Sarcomere protein mutations are reported to be much more frequent in patients with a reverse septal curvature phenotype compared with those with sigmoidal septum in two studies [228] [185], where this morphology was described as an independent predictor of genotype-status. Another publication [62] described an association between Z-disc mutations and sigmoidal septum. One study [224] did not find a significant difference in the prevalence of asymmetrical hypertrophy versus other sub-phenotypes in patients harbouring *MYH7* mutations.

Two studies have examined the genetic background of apical HCM. One [229] reported the absence of an association between genotype and apical HCM, with some of the mutations giving rise to different hypertrophy patterns within the same family. In the second study [230] there was a lower percentage of mutation-positive patients in apical HCM (13%) compared to non-apical HCM (40%).

LV dimensions and function

Most studies have not demonstrated an association between genotype and LV end-diastolic diameter, fractional shortening (FS) and ejection fraction [178], [185], [186]. One publication [224] reported a higher FS for *MYH7*-positive versus negative patients and another [181] reported an increased ejection fraction in patients harbouring *MYH7* mutations. In a single longitudinal study [178], patients with a sarcomere protein mutation were more likely to develop LV systolic or diastolic dysfunction during follow-up.

Microvascular function and myocardial fibrosis

One study [231] has reported reduced myocardial blood flow in patients carrying a sarcomeric mutation, compared with mutation-negative patients. Mutation-positive status was also associated with a higher prevalence of late gadolinium enhancement [231]. Another recent publication [96] described an increased level of C-terminal propeptide of type I procollagen, a biomarker of type I collagen biosynthesis, in *MYH7* carriers compared to *MYBPC3* carriers without hypertrophy; this association was not present in patients with LV hypertrophy.

Left ventricular outflow tract obstruction and mitral valve abnormalities

Most studies have shown no significant association between left ventricular outflow tract obstruction and genotype status [126], [173], [21], [175, 176, 177], [178], [179], [181], [182], [223], [184]. One study [185] reported an increased prevalence of left ventricular outflow tract obstruction in genotype-negative patients (48% vs 37%), but it was not an independent predictor of genotype-status.

The only study to report on the association between genetic background and mitral regurgitation found an increased prevalence of mitral regurgitation in *MYH7* patients compared to genotype-negative patients [183].

Histology

Very few studies have analysed the correlation between genotype and histologic findings. One study [9] described less fibrosis and more severe myocyte disarray in patients with *TNNT2* mutations; but no difference between genotype-positive and negative patients was found in a series of genotyped patients undergoing septal myectomy [195, 232]. In a study [219], reporting on a *TPM1* missense mutation, histopathological features were indistinguishable between the reported family and patients with mutations in other genes. Another report [233] described an association between the presence of a sarcomere mutation and the severity of cardiomyocyte hypertrophy, but not with other histologic features of HCM.

4.2.3. RISK FACTORS FOR SUDDEN CARDIAC DEATH

Syncope

Two studies described an association between the presence of *MYH7* mutations and an increased prevalence of syncope in comparison to carriers of *MYBPC3* mutations [225] or *MYH7*-negative patients [224].

Abnormal blood pressure response to exercise

Two studies report an association between genotype and an abnormal blood pressure response to exercise (ABPRE). In one [182], sarcomere-positive patients had a higher prevalence of ABPRE (32% in *MYBPC3* and 61% in *MYH7*) than sarcomere-negative patients (11%). In a second, [234] patients with the *TNNT2* R92W mutation had a lower exercise blood pressure response compared to patients with any mutation in *MYH7*.

Family history of SCD

Patients carrying sarcomere mutations have a higher proportion of family history of SCD in some cohorts [178], [22], [185], but not others [21], [179], [182], [184]. Pooled analysis (**figure 16**) showed a significant difference in the proportion of patients with a family history of SCD between sarcomere-positive (27.0%, 95% CI of 23.5%-30.3%) and sarcomere-negative individuals (14.9%, 95% CI of 12.6%-17.2%, P-value<0.0005). Heterogeneity effects between studies were not significant (P-value=0.650).

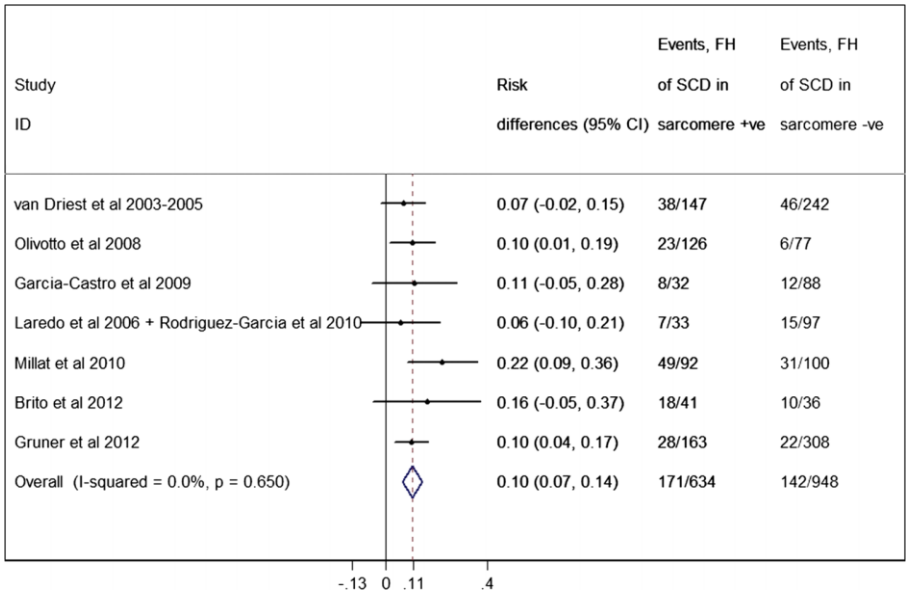

Figure 16. Forest plot from random effect meta-analysis showing a significant difference for the proportion of a family history (FH) of sudden cardiac death (SCD) between sarcomere-positive (27.0%, 95% CI 23.5% to 30.5%) and sarcomere-negative individuals (14.9%, 95% CI 12.6% to 17.2%) (P-value<0.0005). There were no significant heterogeneity effects (I^2=0%, P-value=0.650). Reproduced with permission from [172].

In studies comparing *MYBPC3* and *MYH7* mutations, only one described an increased frequency of a family history of SCD in *MYH7* patients [223]; this was not the case in others [176], [179], [182], [184]. The pooled analysis (**figure 17**) showed no difference between *MYH7* and *MYBPC3* sub-groups regarding family history of SCD (P-value=0.651).

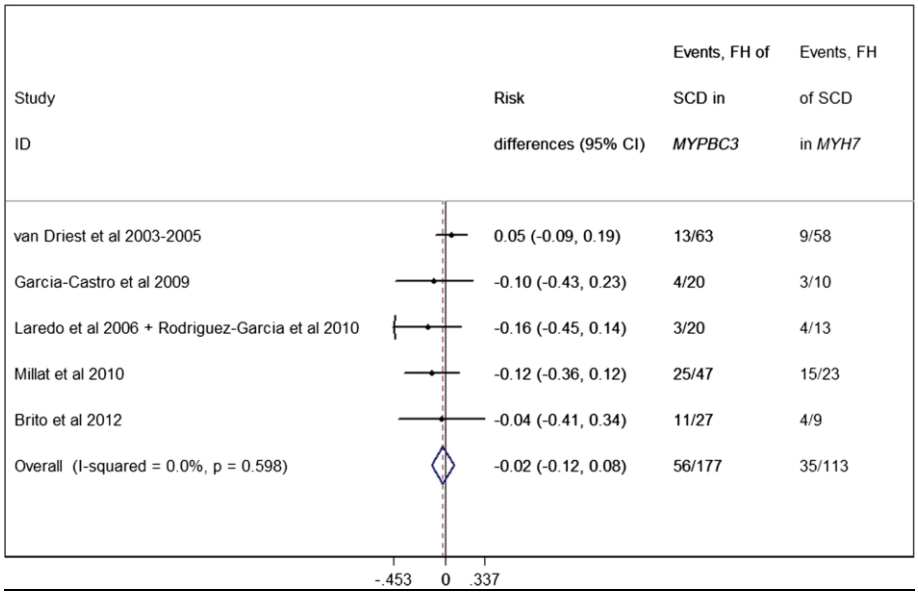

Figure 17. Forest plot from random effect meta-analysis showing that the proportion of a family history (FH) of sudden cardiac death (SCD) is not different between *MYBPC3* (31.6%, 95% CI 24.7% to 38.5%) and *MYH7* patients (31.0%, 95% CI 22.5% to 39.5%) (P-value=0.651). No significant heterogeneity effects were observed (I^2=0%, P-value=0.598). Reproduced with permission from [172].

Patients harbouring mutations in *MYH7* had an increased family history of SCD compared to *MYH7*-negative individuals in one publication [181], although the same association was not described in another [177].

4.2.4. INTERVENTIONS AND PROGNOSIS

Implantable cardioverter-defibrillator (ICD) implantation

Data on the frequency of ICD implantation in mutation carriers are contradictory, with some reporting an increased prevalence of implanted ICDs in sarcomere-positive patients compared to sarcomere-negative [21] and others no association with mutation status [178], [179],[184]. As studies reporting ICD implants are very heterogeneous with respect to design and data presentation, a pooled analysis was not possible.

In the majority of studies comparing *MYBPC3* and *MYH7* mutation carriers, there were no differences in the frequency of ICD implantations [176], [179], [183]. One study, [174] reported an increased frequency of ICD implantation in patients with *MYBPC3* truncating mutations and another [223] a higher number of ICD implantations in *MYH7* mutations. Finally,

a study [177] reported an increased implantation of ICDs in *MYH7*-positive patients compared to *MYH7*-negative individuals, which was not observed in another report [224].

Septal myectomy and alcohol septal ablation

A higher frequency of sarcomere mutations is reported in patients undergoing invasive septal reduction therapies alone in one study [183] and in another that combined treatment for left ventricular outflow tract obstruction with ICD implantation [174]. In contrast, three studies reported no relation between sarcomeric mutation status and septal reduction therapy [21], [178], [179].

Atrial fibrillation

The majority of studies have found no association between genetic background and the prevalence of atrial fibrillation –[184], [185], [179], [224]. In one [178], chronic atrial fibrillation was significantly more prevalent at baseline evaluation in genotype-positive patients.

Severity of disease, prognosis and outcome

The great majority of genotype-phenotype correlation studies reporting on outcome are family focussed, analyse fewer than 100 individuals and are cross-sectional in design (**table 2**). A pooled analysis of outcomes was not performed.

Four studies provided longitudinal follow-up data. One was confined to individuals with *MYBPC3* mutations [195] (57 families and 167 genotype-positive individuals) and one to families with *TNNT2* mutations [195] (20 families and 92 genotype-positive individuals). Another, reporting on unrelated probands, described a poorer prognosis in sarcomere mutation-positive patients, with an increased incidence of a combined endpoint of cardiovascular death, evolution to NYHA class III or IV heart failure and non-fatal stroke [178]; a fourth study [223] reported an increased incidence of SCD in *MYH7* probands compared to *MYBPC3* patients.

Some familial studies describe a particularly severe phenotype and poor prognosis in individuals with multiple mutations (homozygous or compound and double heterozygous) [235], [236], [237], [238], [239], [240], [241]. An increased burden of risk factors for SCD and

higher likelihood of an evolution to a dilated phenotype was also reported in a series of triple mutation carriers [242].

Clinical Penetrance

Penetrance is very variably reported in family studies. Some describe penetrance for the whole family, while others only for adults. Some examples of general associations between genotype and penetrance are reported for *MYBPC3* [195], [243] (late onset and higher rate of incomplete penetrance in females), *MYH7* [206], (age-dependent penetrance) and *TNNI3* (high rate of incomplete penetrance) [195]. One study [126] reported later penetrance in *MYBPC3* families compared to *MYH7* families, but another [133] described a higher than expected penetrance for a *MYBPC3* mutation that generated a cryptic donor splice site.

4.3. SUMMARY OF RESULTS

Given the genetic and clinical heterogeneity that characterise HCM, it is not surprising that very few genotype-phenotype relationships have been shown to be reproducible. As the great majority of mutations are private (unique to each family) [195], studies lack statistical power to demonstrate correlations between individual mutations and phenotype. The variable expression of the same or similar mutations with respect to age at presentation, severity of hypertrophy and prognosis is another important confounder [204],[195] [140].

As this systematic review shows, this genetic complexity has led to an exploration of genotype-phenotype effects based on the affected gene rather than individual mutations. The advantage of this approach is that it increases the sample size and power to detect associations, but as we show in this review, there are still substantial differences with respect to study design, case ascertainment and the depth of clinical phenotyping. In addition, the assignment of pathogenicity to genetic variants varies considerably and there is little consideration of other factors that might influence disease expression such as comorbidity and ethnic background.

In spite of these limitations, the meta-analysis of pooled data does show that a small number of clinical variables are consistently associated with genotype; specifically, age at presentation,

maximum left ventricular wall thickness, and family history of HCM or SCD. For each of these parameters, the pooled association is significant for the comparison between sarcomere mutation-positive and negative patients, but not when comparing the two most frequently affected genes, *MYBPC3* and *MYH7*. Patients carrying a sarcomere mutation seem to present earlier, have more severe hypertrophy, and have higher prevalence of a family history of the disease and SCD. Although data are limited, it does seem that patients with more than one sarcomere mutation also present earlier or with a more severe phenotype [21],[186, 227] and a higher likelihood of an evolution to a dilated phenotype [242], but this last observation requires further study.

The consistent differences observed between sarcomere-positive and sarcomere-negative patients suggest that, in spite of heterogeneity across different genes and mutations, sarcomeric protein disease might be characterised by a class-effect. The corollary would be that HCM not caused by sarcomeric protein mutations has different clinical characteristics, natural history and prognosis, reflecting the large number of potential genetic and non-genetic mimics of HCM. The pooled data showing an increased prevalence of hypertension in sarcomere-negative individuals provides some circumstantial evidence for this hypothesis.

The clinical value of the associations demonstrated in this meta-analysis is probably confined at present to the general counselling of families, and in particular relatives that are considering predictive genetic testing or parents seeking reproductive advice. Specific advice on therapeutic interventions requires more robust data than exist at present, particularly in relation to the natural history of individual mutations. This requires large-scale genotyping combined with new bioinformatic approaches that take into account the mutation type (e.g. missense versus truncating mutations) and the biological effect of the mutation on protein structure and function, including the functional domain [169]. The relatively high frequency of rare sarcomeric variation in general population databases [244],[245],[246],[247],[248] also makes attribution of causality extremely challenging. Finally, more sophisticated phenotyping tools that can detect early disease manifestations (intermediate phenotypes) are required to improve understanding of genotype-phenotype correlations.

5. AIMS

1- Improve understanding of genotype-phenotype relationships in patients with hypertrophic cardiomyopathy.
2- Identify novel genetic causes and modifiers of the disease phenotype, using a high-throughput sequencing approach.
3- Develop methodologies for the interpretation of variants called by high-throughput technologies.

6. HYPOTHESES

- Distinct individual rare candidate variants in sarcomere and associated genes are associated with specific sub-phenotypes
- Distinct sarcomeric genes are associated with specific sub-phenotypes;
- Non-sarcomeric genes associated with other cardiomyopathies or channelopathies act as modifiers of the phenotype;
- Copy-number variation explains some "genotype-negative" cases;
- Evaluation of the structural impact of missense variants improves the accuracy of *in silico* prediction of pathogenicity;
- Sarcomere gene expression can be modified by variation in the non-coding regulatory regions of the DNA.

SECTION II – METHODS

1. STUDY COHORT AND ETHICAL APPROVAL

The study cohort comprised unrelated and consecutively evaluated patients with HCM referred to an inherited cardiovascular disease unit at The Heart Hospital, University College London (UCL), London, U.K.

HCM was diagnosed in probands when the maximum left ventricular wall thickness (MLVWT) on two dimensional echocardiography measured 15 mm or more in at least one myocardial segment or when MLVWT exceeded two standard deviations corrected for age, size and gender in the absence of other diseases that could explain the hypertrophy. In individuals with unequivocal disease in a first degree relative, a diagnosis was made using extended familial criteria for HCM [249].

The project was approved by the UCL/UCLH Joint Research Ethics Committee (ethical approval is included in **Appendix B**). Before enrolment and venesection, all patients provided written informed consent (consent form is included in **Appendix B**) and received genetic counselling in accordance with international guidelines [101]. Blood samples were collected at routine clinic visits and DNA was isolated from peripheral blood lymphocytes, as published [250].

2. TARGETED GENE ENRICHMENT AND HIGH-THROUGHPUT SEQUENCING OF 41 CARDIOVASCULAR GENES

The library design, capture protocol and sequencing platform development and optimization were coordinated by Dr. Mike Hubank, UCL Genomics, UCL Institute of Child Health, in collaboration with Dr. Petros Syrris, UCL Institute of Cardiovascular Science. Dr. Syrris conducted all the protocolized laboratory work from DNA extraction to the preparation of plates for the sequencing platform (phases I and II) at Paul O'Gorman building laboratory, UCL and Dr. Hubank coordinated the sequencing platform tasks at Institute of Child Health. My role consisted in: a) confirming that each individual sample already longitudinally collected for sequencing was from a case that strictly complied with diagnostic criteria for hypertrophic cardiomyopathy (as described above); b) prospectively selecting new samples while checking for those criteria and organizing the consent, counselling and sample collection at the outpatient clinic; b) prospectively organizing the collection of new samples in the outpatient clinic for Sanger confirmation, whenever the patient carried a variant that had criteria for confirmation (as described below); c) consenting and participating in genetic counselling for all the prospectively collected samples. I did not directly participate in the protocolized laboratory activities, i.e. DNA extraction, plate construction and sequencing platform tasks, but the methodology is included here for completion.

The study was designed to screen 2.1Mb of genomic DNA sequence per patient, covering coding, intronic and selected regulatory regions of 20 genes known to be associated with HCM and dilated cardiomyopathy (DCM), 17 genes implicated in other inherited cardiomyopathies and arrhythmia syndromes, and a further 4 candidate genes (**Table 4**).

Table 4. Name of the targeted genes, Ensembl accession number, chromosomal position and size. (Ensembl: Feb 2009 (GRCh37/hg19). The total size of genomic sequence for 41 loci was approximately 3Mb, which was reduced to 2.1Mb of capture sequence following the exclusion of repetitive DNA regions in the custom RNA bait library design with eArray (Agilent). Reproduced with permission from [251].

Gene	Ensembl no	Location Chromosome: base range	Dimension (base-pairs)
MYBPC3	ENSG00000134571	chr11:47352958-47374253	21,295
MYH7	ENSG00000092054	chr14:23881948-23904870	22,922
TNNI3	ENSG00000129991	chr19:55663137-55669100	5,963
TNNT2	ENSG00000118194	chr1:201328143-201346805	18,662
TPM1	ENSG00000140416	chr15:63334838-63364111	29,273
MYL2	ENSG00000111245	chr12:111348626-111358404	9,778
MYL3	ENSG00000160808	chr3:46899357-46904973	5,616
ACTC	ENSG00000159251	chr15:35080297-35087927	7,630
TNNC1	ENSG00000114854	chr3:52485108-52488057	2,949
MYH6	ENSG00000197616	chr14:23851199-23877482	26,283
TTN	ENSG00000155657	chr2:179390720-179672150	281,430
PDLIM3	ENSG00000154553	chr4:186422852-186456712	33,860
CSRP3	ENSG00000129170	chr11:19203578-19223589	20,011
DES	ENSG00000175084	chr2:220283099-220291459	8,360
LMNA	ENSG00000160789	chr1:156084461-156109878	25,417
LDB3	ENSG00000122367	chr10:88428426-88495822	67,396
VCL	ENSG00000035403	chr10:75757872-75879912	122,040
TCAP	ENST00000309889	chr17:37821599-37822806	1,207
PLN	ENSG00000198523	chr6:118869442-118881586	12,144
RBM20	ENSG00000203867	chr10:112404155-112599227	195,072
JUP	ENSG00000173801	chr17:39910859-39942964	32,105
DSP	ENSG00000096696	chr6:7541870-7586946	45,076
PKP2	ENSG00000057294	chr12:32943682-33049780	106,098
DSG2	ENSG00000046604	chr18:29078027-29128813	50,786
DSC2	ENSG00000134755	chr18:28645944-28682388	36,444
RYR2	ENSG00000198626	chr1:237205702-237997288	791,586
TMEM43	ENST00000306077	chr3:14166440-14185180	18,740
TGF-beta3	ENST00000238682	chr14:76424442-76448092	23,650

KCNQ1	ENSG00000053918	chr11:2466221-2870339	404,118
KCNH2	ENSG00000055118	chr7:150642050-150675014	32,964
SCN5A	ENSG00000183873	chr3:38589554-38691164	101,610
KCNE1	ENSG00000180509	chr21:35818989-35828063	9,074
KCNE2	ENSG00000159197	chr21:35736323-35743440	7,117
ANK2	ENST00000394537	chr4:113970785-114304894	334,109
CASQ2	ENSG00000118729	chr1:116242628-116311426	68,798
CAV3	ENSG00000182533	chr3:8775496-8788450	12,954
KCNJ2	ENSG00000123700	chr17:68165676-68176181	10,505
PLEC1	ENSG00000178209	chr8:144989321-145025044	35,723
GJA1	ENST00000282561	chr6:121756745-121770872	14,127
PKP4	ENSG00000144283	chr2:159313476-159537938	224,462
PNN	ENSG00000100941	chr14:39644387-39652421	8,036
			3,285,390

2.1. PHASE I – LIBRARY DESIGN AND CAPTURE AND SEQUENCING PROTOCOL OPTIMIZATION

A web-based design tool, eArray (Agilent Technologies, Santa Clara, CA, USA) was employed to design an initial SureSelect (Agilent) capture library of oligonucleotides (RNA bait groups) based on the target gene sequences using the following parameters: library size 1x55K; length 120; tiling 1x.

Control samples from patients with HCM who were known to carry disease-causing sequence variants, previously detected with conventional Sanger sequencing, were used in pilot studies to validate the method (data not shown, as this was an integral part of another Ph.D. thesis supervised by Dr. Mike Hubank, UCL Genomics). The library was used to capture the target regions from 8 patients, which were then sequenced (single end) on an Illumina GAIIx platform with 35 base-pair (bp) read length. Single-end sequencing of control samples with known HCM-related variants identified regions of low coverage possibly associated with suboptimal sample processing steps or low capture efficiency. The pilot study was used to optimise the protocol and to redesign the capture library, introducing double density cover to regions of low coverage and increase cover at the 5' regulatory ends of genes. The following steps were adopted: single-end adapters were replaced with paired-end adapters; sequencing read length

was increased from 35 bp to 75 bp and the capture RNA bait library was redesigned with eArray to enrich regions with low coverage. The new design included an additional 965 RNA baits at 2x tiling for all <30 read depth regions, 2x tiling for 20 genes associated with HCM and DCM and redesigned sequence regions were extended 5-10Kb upstream of all genes. As a result 23,637 120 bp RNA baits were redesigned to target a total of 2.1Mb of genomic DNA.

In order to increase efficiency and reduce costs, we adopted a 75 bp paired-end multiplexed sequencing method which allowed us to pool 12 samples into a single lane of an Illumina GAIIX flow cell and thus, taking into account internal controls, sequence a total of 84 samples in a single instrument run. The multiplex sequencing protocol was also tested using control samples. In early sequencing test runs, a total of 21 samples from HCM patients were sequenced as part of developing and optimising the method (data not shown – Dr. Mike Hubank, UCL Genomics).

2.2. PHASE II – SEQUENCING OF THE STUDY COHORT

For phase two, sample preparation was carried out as recommended by Agilent and initially based on the SureSelect Target Enrichment for Illumina paired-end multiplexed sequencing method. Genomic DNA shearing (3µg) per patient was performed on a Covaris E220 instrument in 96-well plates. Fragmented DNA was end-repaired and "A" base addition was performed using the NEBNext DNA Sample Prep Master mix Set 1 (New England BioLabs). Ligation of indexing-specific paired-end adapters to DNA samples was performed using the Illumina Paired-End Genomic DNA Sample Prep Kit and the subsequent amplification of the adapter-ligated library was carried out with Herculase II Fusion DNA Polymerase (Agilent). Hybridization of amplified libraries to the SureSelect biotinylated RNA library (baits) was performed at 65ºC for 24 hours on a GeneAmp PCR System 9700 (AppliedBiosystems). Addition of index tags to the library preparation was achieved by PCR using the Illumina Multiplex Sample Preparation Oligonucleotide Kit and Herculase II Fusion DNA Polymerase (Agilent). Following the introduction of the SureSelectXT Target Enrichment protocol, all the above steps were performed with Agilent reagents as recommended by the manufacturer. Clean-up of DNA samples was performed according to the protocol using Agencourt AMPure XP beads and Dynal MyOne Streptavidin T1 magnetic beads (Invitrogen, hybridisation step). Quality of DNA samples throughout the protocol was assessed with Agilent 2100 Bioanalyzer DNA assays. All steps were performed manually using individual PCR tubes or 96-well plates

except the incubation of the hybrid-capture/bead solution (hybridisation step) on 96-well plates, which was carried out on the Bravo Automated Liquid Handling Platform (Agilent) using an Agilent instrument protocol with small modifications. Samples were subjected to standard Illumina protocols for cluster generation and sequencing. Paired-end multiplexed sequencing was performed on an Illumina GAIIX with twelve samples tagged with different index sequences (Illumina) combined in each lane.

From plate 4 (234th patient) onwards, successive updated versions of the Agilent sample preparation protocol were used according to the manufacturer's instructions. The latest version of SureSelect Target Enrichment for Illumina paired-end multiplexed sequencing protocol was v1.6 released in October 2013. (SureSelect^{XT} Target Enrichment for Illumina paired-end sequencing library. Illumina HiSeq and MiSeq multiplexed sequencing platforms. Protocol. Agilent. version 1.6; October 2013). The main scientific principles of the updated versions remained the same but they contained a number of improvements in sample preparation compared to the initial protocol. The main changes referred to smaller initial quantities of genomic DNA (200ng to 3µg), use of Agilent enzymes and reagents throughout the protocol, optimisations of hybridisation steps and replacement of in-solution PCR procedure with an on-bead PCR method. Introduction of additional SureSelect indexes allowed multiplexing of 16 samples in a single pool. The resulting index-tagged sample pools were sequenced on the Illumina HiSeq 2000 system, a more powerful sequencer compared to GAIIX, which can generate up to 200Gb of sequencing data per run. (HiSeq^{TM} 2000 sequencing system. Specification sheet: Illumina sequencing. Pub. No. 770-2009-036. 17 June 2010). Cluster generation on Illumina cBot was carried out according to the manufacturer's protocol. A total of 128 HCM samples (16 multiplexed samples x 8 lanes) were sequenced (100bp, paired end) per instrument run, using standard methods (Illumina).

2.3. SEQUENCING AND ANALYSIS OF UK10K CONTROL SAMPLES

The UK10K project was designed to study the scope of rare genetic variation in longitudinally followed-up U.K. general population cohorts (e.g. the Avon Longitudinal Study of Parents and Children - ALSPAC), cohorts of individuals with neurodevelopmental disorders and rare disease cohorts. Details regarding the selection of the study samples can be found at www.uk10k.org. None of the UK10K control samples was recruited on the basis of a cardiac phenotype.

Sequencing results for the first 223 patients were compared with a set of 1,287 UK controls with exome sequence data generated by the UK10K project. These samples are the subset of UK10K whole-exomes for which ethics enabled their use as control samples as of November 2012.

The sequencing protocol for the UK10K project is available through its website (www.uk10k.org).

3. SEQUENCE DATA ANALYSIS FOR TARGETED EXONIC REGIONS

The alignment and variant calling steps from the raw sequencing data, that generated initial datasets of variants, as well as the data extraction from UK10K and UCLexome and the related case-control analyses, were all developed and conducted by Dr. Vincent Plagnol, UCL Genetics Institute. The detailed methodology for Dr. Plagnol's bioinformatic work is included in this thesis for completion (chapters 3.1, 3.4, 3.5). My work consisted in all the downstream manual filtering, manual annotation, in silico prediction of pathogenicity and further analysis of each individual variant (part of chapter 3.1 and all chapter 3.2). At each time a new dataset of variants was generated through the bioinformatic pipeline, I checked the data for quality, discrepancies and errors, based in clinical judgment and results from the Sanger confirmation. I also confirmed the annotated frequency at available databases, i.e. 1000 genomes and exome sequencing server. My close interaction and continuous guiding of the bioinformatic work led to several improvements of the pipeline during the development of my thesis, leading to a higher accuracy of the generated data.

3.1. BIOINFORMATIC ANALYSIS PIPELINE

For the case samples, paired-end reads were aligned using the Novoalign software v2.7.19 on the human reference genome build hg19 using quality score calibration, soft clipping and Illumina adapter trimming.

On an initial stage (for the first 233 samples), following the exclusion of PCR duplicate reads (Picard MarkDuplicate tool), insertion-deletions (indels) and single-nucleotide polymorphisms (SNPs) were called using the software SAM ("Sequence Alignment/Map") tools (version 0.1.18) [252]. Variants were filtered on the basis of the SAMtools Phred scale quality score greater than 20.

At a later stage (for all samples), our calling strategy followed closely the Genome Analysis Toolkit (GATK) best practices as of January 2014 [253]. Following BAM file (defined as a binary version of a SAM file) compression using the GATK ReduceReads module [254], multi-sample calling was performed on all probands jointly with a set of 1,492 unrelated whole exomes ("UCL-exomes consortium") using the GATK Unified Genotyper [254]. After GATK variant recalibration (separately for SNPs and indels) calls were annotated using the ANNOVAR

software (with the Ensembl gene definitions) [255]. For all association tests, we filtered variants for the GATK recalibration PASS filter.

Candidate variants for further analysis were defined using frequency and predicted functional effect. For the functional filter, exonic non-synonymous, loss-of-function and splice-site variants were included.

Initially, we used the allele frequency estimates from the 1,000 genomes project database [111] and we used a 0.5% minor allele frequency cut off (based on the November 2010 and May 2011 releases).

All sequence data were later filtered using a minor allele frequency threshold of ≤ 0.2%, based on the National Heart, Lung and Blood Institute (NHLBI) exome variant server data (computed through the ANNOVAR annotations). To provide a more accurate estimate of variant frequency in controls that is not affected by potential differences in calling strategy in the NHLBI dataset, we randomly selected 25% of the 1,492 UCL-exomes samples as an "external control set" and removed variants that appeared more than twice in these 372 "external controls". These samples were only used to define a variant frequency and were not included in the subsequent case-control test to avoid a previously noted statistical issue, where variant frequency is defined in the same set that is used for case-control testing [256].

3.2. MANUAL ANNOTATION OF THE VARIANTS AND *IN SILICO* PREDICTION OF PATHOGENICITY

I identified all variants present in the dbSNP build 137 database [257], published in the literature and includd in general and locus-specific genetic databases using ClinVar (http://www.ncbi.nlm.nih.gov/clinvar/), Human Gene Mutation Database – trial version (http://www.hgmd.org) and Health in Code Inc. mutation database (access allowed for the purpose of this research, courtesy of Dr. Lorenzo Monserrat, https://mutaciones.healthincode.com). The latter is a curated and annotated database of inherited cardiovascular disease genes, built within a genetic testing laboratory and to be used as a tool for reporting, that includes a review of the available literature on most of the published mutations.

In silico prediction of pathogenicity for novel missense variants was performed using Polyphen2, SIFT and Condel [159],[160],[161]. A variant was predicted to be pathogenic if: a) classified as "damaging" by SIFT and simultaneously "possibly" or "probably damaging" by Polyphen2, or b) predicted to be damaging by Condel.

When a variant was not confirmed by Sanger sequencing or the quality of the call was in doubt, I used Integrative Genomics Viewer [258] (http://www.broadinstitute.org/igv/UserGuide) software to visualize the genomic region in detail (BAM files containing SNP and indels calls) to ascertain the veracity of the call.

I plotted all the rare variants (MAF ≤ 0.5%) encountered in the 8 main sarcomere genes (*MYBPC3*, *MYH7*, *TNNT2*, *TNNI3*, *MYL2*, *MYL3*, *ACTC1*, *TPM1*) in a 2D graphic representation for better visualization, using the Plot Protein software (https://sites.google.com/site/plotprotein/) [259].

3.3. TITIN VARIANTS - MANUAL ANNOTATION AND PREDICTION OF PATHOGENICITY

This part of the work was done in collaboration with Professor Mathias Gautel, King's College London, who helped to generate a list of prioritized variants based in in-house built tools, including homology modelling for some of titin domains and prediction of interference with ligand binding. Prof. Gautel also coordinated the case-control comparison of the frequency of titin variants to look for enrichment. My role consisted in: a) providing and organizing the initial lists of rare/candidate titin variants; b) manually annotating those lists as to an initial prediction of the probable impact of the variants, including in silico prediction of pathogenicity of the missense variants and flagging potentially truncating vs others; c) checking for the frequency of the variants in general population variation databases; d) exploring the distribution of the variants along titin; e) organizing the collection of samples that allowed the confirmation of prioritized titin variants with Sanger sequencing.

Due to the complexity of *TTN* structure and the number of encountered variants, the absence of adequate *in silico* pathogenicity prediction tools and the scarcity of pathogenicity annotation in the literature/ genetic databases, we opted for a strategy of prioritizing missense variants for further analysis, based on the physicochemical difference of the amino acid change, domain location, predicted structural effect and possible impact on interaction with titin ligands.

Titin variants that were predicted to cause degradation or a truncated form of the protein were also flagged. These included splice-site disrupting, frameshift insertion-deletions and stop-codon variants.

The MAF of each individual titin variant was also compared with the MAF of the same variant in the 1000 genomes database [111], to calculate an enrichment score, and thereby define a sub-population of enriched variants for further analysis.

3.4. ANALYSIS OF UK10K CONTROL SAMPLES AND CASE-CONTROL COMPARISON OF CANDIDATE NSSNPS

Work done in collaboration with Dr. Vincent Plagnol, UCL Genetics Institute, as described above.

For the UK10K samples, alignment was performed using Bowtie [260] and the calling algorithm merged the output of SAMtools (version 0.1.17) and GATK Unified Genotyper (version 1.3-21).

To limit the technical difficulties associated with comparing sets of variants in controls and cases generated using different protocols and analyzed in different laboratories, we restricted our comparison to non-synonymous single nucleotide polymorphisms (nsSNPs), hence excluding insertion-deletions (indels) and larger copy number variants. We retrieved the data from the UK10K project and annotated nsSNPs as candidates using the same protocol and thresholds that were applied to the set of HCM cases.

This analysis was restricted to the first 180 Caucasian HCM cases, which could be matched to the 1,287 UK10K control samples. All computations were performed using the statistical software 'R'. Frequencies of candidate nsSNPs were compared between cases and controls. We then used the case-control data to infer the proportion of HCM cases explained by rare nsSNPs variants in each gene. We used a profile likelihood approach to estimate this parameter of interest (**Appendix C** - additional statistical methods).

For genes showing a significant excess of rare nsSNPs, point estimates for the probability that a rare nsSNP is causal for HCM were estimated using the formula: (proportion of carriers of rare nsSNPs in cases - proportion of carriers of rare nsSNPs in controls)/ proportion of carriers of rare nsSNPs in cases (**Appendix C** - additional statistical methods).

3.5. CASE CONTROL COMPARISON OF CANDIDATE NSSNPS WITH UCL-EXOMES COHORT

Work done in collaboration with Dr. Vincent Plagnol, UCL Genetics Institute, as described above.

Using a similar statistical approach, we compared the frequency of rare variants in each of the 41 genes in the total HCM cohort of 874 individuals with the frequency of rare variants in each gene in the UCL-exomes cohort.

4. CLINICAL VALIDATION AND ASSESSMENT OF THE ACCURACY OF THE HIGH-THROUGHPUT SEQUENCING PLATFORM AND ANALYSIS PIPELINE

Work done in collaboration with Dr. Petros Syrris, who performed the laboratory work related to Sanger sequencing. My role consisted in: a) prospectively organizing the collection of new samples in the outpatient clinic for Sanger confirmation, whenever the patient carried a variant that had criteria for confirmation (as described below); b) consenting and participating in the genetic counselling for sample collection; c) analysing the results from the Sanger confirmation and comparing with the high-throughput sequencing data to assess accuracy. This process led to improvements of the pipeline during the development of my thesis, allowing a higher accuracy of the generated data.

Following improvement of coverage using the pilot control samples (Phase I as described above, chapter 2.1.), I designed a two-step continuous clinical validation of the HTS sequencing platform and analysis pipeline, mainly directed at the clinical exclusion/detection of false positives (specificity). However, in exons with a low mean coverage, Sanger sequencing was still performed because of the possibility of low sensitivity.

4.1. STEP 1 –SYSTEMATIC VALIDATION OF ACCURACY FOR PLATES 1-3 (FIRST 223 PATIENTS)

The following variants were submitted to conventional dideoxy sequencing using BigDye Terminator v3.1 sequencing chemistry (AppliedBiosystems) on a 3130xl capillary sequencer (AppliedBiosystems): all variants with a read depth below 15; potentially pathogenic variants in sarcomeric and associated genes as well as published and potentially disrupting ion-channel and ARVC-associated variants.

We also sequenced, using conventional dideoxy sequencing, those exons with an average read depth below 15: *MYBPC3* exons 5 and 13; *TNNI3* exon 1; *KCNH2* exons 1 and 13. All *MYH6* variants present in the first three plates were also confirmed using dideoxy sequencing, due to the high homology between *MYH7* and *MYH6* at DNA level, which could potentially generate false positive results. *TTN* variants judged to be relevant for further study (as described under chapter 3.3) were also confirmed by Sanger sequencing.

4.2. STEP 2 – APPLICATION - VALIDATION OF CLINICALLY ACTIONABLE VARIANTS (ALL PATIENTS)

We carried out confirmations by conventional dideoxy sequencing using BigDye Terminator v3.1 sequencing chemistry (AppliedBiosystems) on a 3130xl capillary sequencer (AppliedBiosystems) on the following: potentially pathogenic rare variants in sarcomeric and associated genes as well as published and potentially disrupting ion-channel and ARVC-associated variants. Accuracy was calculated according to conventional formulae.

5. PHENOTYPE DATA COLLECTION AND GENOTYPE-PHENOTYPE ANALYSIS

An observational, retrospective, longitudinal cohort study design was used. Initial evaluation and follow-up data were collected prospectively and registered in a relational database. All patients were evaluated every 6–12 months or earlier if there was a clinical event. Follow-up data was collected until the 31st September 2013.

The initial/baseline observation and physical examination of the patients, performance of the diagnostic tests and collection of the data into the database were prospectively conducted by various clinicians and researchers. I reviewed all the data, collected missing values, re-coded the variables as needed for the analyses, collected follow-up clinical, imaging and survival data, and collected and coded new parameters that were not present in the original database. I designed and performed all the statistical analyses.

5.1. DEMOGRAPHIC DATA AND SYMPTOMS

Dyspnoea was coded according to the New York Heart Association (NYHA) classification. Chest pain was classified as exertional, if precipitated by physical activity and relieved by rest, or atypical. Palpitations were coded as a binary variable. Unexplained syncope was defined as unexplained transient loss of consciousness at or prior to first evaluation, suggestive of arrhythmic origin.

Ethnicity was self-reported and was classified using a modified National Health Service ethnic categorization.

5.2. ELECTROCARDIOGRAPHY

All patients underwent 12 lead electrocardiography (ECG). Standard 12-lead ECG was performed in the supine position during quiet respiration. The following data was recorded and analysed for this work: heart rate, rhythm, QRS axis, PR interval and QRS duration.

5.3. CARDIO-PULMONARY EXERCISE TESTING

Patients were exercised on a treadmill using the Bruce or modified Bruce protocols or on an upright bicycle ergometer using an incremental ramp protocol. Simultaneous 12-lead electrocardiography was performed throughout. Blood pressure was measured by auscultation of the brachial artery during deflation of a mercury sphygmomanometer at rest, every minute during exercise and for the first 5 min of recovery. Simultaneous respiratory gas analysis was performed using previously published methods [261]. Recorded heart rate and systolic blood pressure at rest and peak exercise was used in this work, as well as the blood pressure response (difference between maximal and rest systolic blood pressure). An abnormal response is defined below.

5.4. AMBULATORY ECG MONITORING

Patients underwent two or three channel 24 to 48 h ambulatory electrocardiogram monitoring, while performing unrestricted daily activities. The presence or absence of non-sustained ventricular tachycardia (NSVT) episodes, defined below, was used in the analysis as a binary variable.

5.5. ECHOCARDIOGRAPHY

Two-dimensional and M-mode echocardiography were performed using standard methods for chamber quantification [262], [263]. All dimensions were analysed as continuous variables. The end-diastolic dimension of the left ventricle was re-coded as a binary variable for analysis (dilated versus non-dilated), using a cut-off of 55mm. Fractional shortening was also analysed as both a continuous and a binary variable; a FS ≤ 25% was used to define systolic left ventricular dysfunction.

End-diastolic LV wall thickness was recorded at mitral valve and papillary muscle level in the anterior and inferior septum and in the anterior, lateral, inferior and posterior LV wall using short-axis two-dimensional echo images. Wall thickness at the apex was measured in the two-chamber, four-chamber and short-axis apical views. The pattern of hypertrophy was classified as asymmetric septal, predominantly apical or concentric [262]. The definitions of the pattern

and severity of the left ventricular hypertrophy (LVH) were as previously published [6].

Left ventricular outflow tract velocities were measured using continuous wave Doppler, and LV outflow tract gradients were calculated using the modified Bernoulli equation. A maximal left ventricular outflow tract gradient (LVOT) ≥ 30 mmHg at rest was used to define obstructive HCM and allowed re-coding of this continuous parameter into a binary variable (obstructive versus non-obstructive). When the maximal LVOT was ≥ 50 mmHg, the phenotype was recoded as severely obstructive.

Quantification of diastolic function and valvular regurgitation followed established guidelines [264], [265]. The severity of diastolic dysfunction and mitral regurgitation were re-coded as binary variables, with a cut-off of ≥ moderate to define the sub-groups.

The presence of right ventricular hypertrophy was defined as a right ventricular free wall thickness ≥ 6mm measured at the parasternal or subcostal view [266].

5.6. Definition of the clinical risk factors for sudden cardiac death

Major risk factors for SCD [5, 139],[267],[261] were defined as: family history of sudden cardiac death at an age ≤ 40 years or SCD in a relative with confirmed HCM at any age; unexplained syncope (defined above); NSVT during ambulatory ECG monitoring, defined as 3 or more ventricular premature complexes at a rate of ≥ 120 bpm, lasting <30 s [268]; maximum left ventricular wall thickness ≥ 30 mm; an abnormal blood-pressure response during symptom limited upright exercise testing, defined as a failure of systolic blood pressure to rise by > 25 mm Hg from baseline values or a fall of > 10 mm Hg from the maximum blood pressure during upright exercise [269].

5.7. Cardiac magnetic resonance protocol

Approximately one-third of the cohort (N=271, 31%) was submitted to cardiac magnetic resonance imaging as part of the clinical assessment. Standard clinical scans (localizers, three long-axis views, black and white blood images, full LV short-axis stack) were performed using a 1.5-T magnet (Avanto, Siemens Medical Solutions, Erlangen, Germany). CMR short-axis

volumetric studies [270] were acquired from retrospectively-gated, breath-held, balanced, steady-state free-precession cines. LV volumes, ejection fraction (EF) and LV mass were determined according to standardized CMR methods [271] (papillary muscles were included in the LV mass). LV wall thickness was calculated for the septum and posterior wall on end-diastolic and end-systolic short-axis cine frames. End-systolic left atrial areas were measured by planimetry on 4-chamber view. AMVL length was measured using the method described in [272]. Presence of rest LV outflow tract obstruction and systolic anterior motion of the mitral valve leaflet were noted. Breath-held, delayed contrast enhancement images acquired through an inversion recovery sequence were obtained 7-15 min after injection of 0.1 mmol/kg gadolinium-DTPA.

5.8. STATISTICAL ANALYSIS

R (version 3.0.0) and IBM SPSS (version 22.0.0.0) were used for the analyses.

5.8.1. DESCRIPTIVE STATISTICS AND COMPARISON OF MEANS AND PROPORTIONS BETWEEN GROUPS

Clinical phenotype data are presented as frequency (and percentage) for non-continuous variables and mean +/- standard deviation or median and interquartile range (IQR) for continuous variables where appropriate. Normally distributed continuous variables were compared using unpaired two-tailed Student t test. Multiple groups were compared using analysis of variance (ANOVA). Categorical variables were compared using Chi-squared or Fisher exact tests. When appropriate, non-parametric tests were used.

Group comparisons were made for the prevalence and severity of each phenotypic trait (at baseline and final follow-up) and for survival (see below) in patients with versus without a candidate rare (MAF≤0.2%) variant in one or more of the eight most common sarcomeric protein (SP) genes (*MYH7, MYBPC3, TNNI3, TNNT2, MYL2, MYL3, ACTC1, TPM1*). We also compared the prevalence and severity of each phenotypic trait between patients carrying only one compared to more than one variant in SP genes. The same comparisons were made for the presence versus absence of rare variation in each SP-associated gene and non-SP gene.

All the above was done 1) for the whole cohort and 2) only within in the subgroup of sarcomere-positive individuals. This was based on the hypothesis that by selecting a more

homogeneous group in terms of biological cause, additional genotype-phenotype associations could be discovered, namely regarding possible modifier effects of non-SP genes.

Direct comparisons were also made between the four most frequent SP genes- *MYBPC3*, *MYH7*, *TNNT2* and *TNNI3* for each phenotypic trait. Additionally, I repeated all the above comparisons, only using the variants *in silico* predicted to be pathogenic, to test the relevance of such tools for genotype-phenotype association discovery, hypothesizing that such a filtering would generate a dataset of variants with an increased biological effect, that could reveal additional correlations, despite the slightly decreased statistical power (due to a lower number of variants).

For *TTN* variants, additional genotype-phenotype analysis were conducted using linear discriminant analysis and multivariate logistic regression (stepwise backward selection and an alpha-value of 0.05 for model retention).

5.8.2. MULTIPLE COMPARISON CORRECTION STRATEGY

For each clinical trait of interest we tested the effect of variants in several genes: 8 SP genes and 28 non-SP genes (excluding the 4 candidate genes *GJA1*, *PKP4*, *PNN* and *PLEC1* - and TTN). Therefore, a nominal P-value of 0.05 was not appropriate. In addition, the Bonferroni correction for the number of phenotypes multiplied by the number of genes is too stringent, because it tests the global null of no association between any pair of gene/trait. We therefore took an intermediate approach, correcting for each phenotype for the number of gene tests. For SP genes, we performed 9 tests (one per SP gene, plus an additional test for all SP mutations combined). Therefore, we used $P < 0.0056$, which is 0.05/9. For non-SP genes, we corrected for 28 tests, which translates into $P < 0.0018 = 0.05/28$. Data on associations that did not fulfil these thresholds but met a nominal P-value of < 0.05 are also presented in the results section.

5.8.3. LOGISTIC REGRESSION ANALYSIS AND CONSTRUCTION OF A MODEL AND SCORE TO PREDICT THE PRESENCE OF A SARCOMERE PROTEIN GENE MUTATION

The parameters that were found to be significantly associated with the presence of a candidate variant in any of the 8 main SP genes were used to build a model and a score for prediction of genotype status. Continuous variables were transformed in categorical binary

variables, by applying cut-off values based on receiver operating characteristic (ROC) curve analysis. Logistic regression used a stepwise backward selection and an alpha-value of 0.05 for model retention. The weights of each parameter in the final model / genotype prediction score were calculated by dividing each regression coefficient by the lowest regression coefficient and rounding to the nearest integer. Hosmer-Lemeshow goodness-of-fit statistic was used to evaluate model precision and the diagnostic accuracy was analysed by ROC curve analysis.

5.8.4. SURVIVAL ANALYSIS

Survival from cardiovascular death (combining sudden cardiac death, heart failure related death and stroke related death) and sudden cardiac death (SCD)/appropriate implantable cardioverter-defibrillator (ICD) shocks was modelled using Kaplan-Meier analysis and log-rank test, from the first clinical evaluation at The Heart Hospital and from birth. Definition of the endpoints and outcome was performed as previously published [6],[261]. Sudden cardiac death was defined as witnessed sudden cardiac death with or without documented ventricular fibrillation or death within 1 h of new symptoms; nocturnal deaths with no antecedent history of worsening symptoms were included in this category. Progressive heart failure was defined as death preceded by signs and/or symptoms of heart failure, including cardiogenic shock. Heart transplantation was defined as orthotopic heart transplantation performed for end-stage disease with systolic impairment and refractory congestive symptoms. Other cardiovascular death was defined as stroke, pulmonary or systemic embolism and myocardial infarction. Non-cardiovascular death was defined as death secondary to non-cardiovascular events and of unknown cause.

6. SCREENING FOR COPY NUMBER VARIATION

Work done in collaboration with Dr. Vincent Plagnol, UCL Genetics Institute, who developed the read-depth methodology for CNV calling that was here applied to the HCM samples and also analysed the aCGH data using R software (snapCGH). My work consisted in: a) visual analysis and filtering of the initial results from read-depth analysis; b) selection of the CNVs for confirmation with aCGH; c) contribution to the design of the CGH array; d) analysis of the aCGH validation results with Cytosure Software; e) search publicly available databases (e.g. dbVar) for the presence of the validates CNVs and f) clinical characterization of patients carrying CVNs.

Given the recent development of bioinformatic algorithms that allow the detection of structural variation from high-throughput short-read sequencing data [151]-[152] and considering my hypothesis that structural variation could explain at least part of the sarcomere-negative cases, we have screened the available HTS data with the aim of detecting CNVs in cardiac sarcomeric protein genes.

6.1. STUDY POPULATION

The population comprised the first 505 unrelated and consecutively evaluated patients of the studied cohort.

6.2. BIOINFORMATIC ANALYSIS FOR THE DETECTION OF COPY-NUMBER VARIATION – EXOMEDEPTH

Raw sequence reads in fastq format were aligned against the National Center for Biotechnology Information (NCBI) build 37 of the human reference genome using Novoalign (v2.08.03). We used a custom bed file summarizing the exons of the 41 targeted genes and the R package ExomeDepth v0.97 to count the reads overlapping each exon. ExomeDepth [273] uses a read depth approach, and compares the observed number of reads mapping to each exon with its expectation based on a comparison set (called the “aggregate reference set”) built based on other samples processed within the same experiment and designed to technically match the test sample as closely as possible. For each test sample, we used

ExomeDepth to build this aggregate reference set and called CNVs using the default ExomeDepth parameters.

I focused my analysis in 19 genes previously associated with cardiomyopathy – *MYBPC3, MYH7, TNNT2, TNNI3, MYL2, MYL3, TPM1, ACTC1, TNNC1, MYH6, LDB3, PDLIM3, CSRP3, DES, TCAP, VCL, PLN, LMNA, RBM20*.

For further confirmation, we prioritized CNVs found in these genes for which the statistical evidence was convincing (log likelihood ratio in favour of a CNV event, as determined by ExomeDepth, greater than 7).

6.3. ARRAY COMPARATIVE GENOMIC HYBRIDIZATION

An aCGH was designed to validate the ExomeDepth called CNVs and to verify that its algorithm identified all CNVs. This was done via the Agilent eArray server (https://earray.chem.agilent.com/earray/). This was designed to cover 2.1Mbp of sequence across the target genes, with 3 probes per exon.

To determine if the aCGH called any CNVs in the selected samples, results were first analysed using the Cytosure Interpret software (http://www.ogt.co.uk/products/246_cytosure_interpret_software).

Additionally, the Log_2 ratios were processed in R, using the package snapCGH [274], which uses a Hidden Markov Model based segmentation algorithm for the aCGH intensity data. An experiment without measurement or normalization errors run on a normal copy number variant null clone would yield a Log_2 aCGH probe intensity ratios of 0 because the test and reference sample would be equivalent. The Log_2 ratio of a heterozygous deletion is $Log_2(1/2)$ = -1 and a heterozygous gain is $Log_2(3/2)$= 0.58. To limit the background noise, we used the "minimum" snapCGH method which simply subtracts the background value from that of the foreground.

7. ANALYSIS OF THE NON-CODING REGIONS

The available non-coding sequence data from the targeted genes have been screened for putative functional variants, with the aim of testing the hypotheses that sarcomere gene expression could be changed by variation in the non-coding regulatory regions of the DNA and that this variation could be the direct cause of at least a proportion of the unexplained familial cases.

The bioinformatic steps of variant alignment and calling, that generated an initial raw list of non-coding variants, were done by Dr. Vincent Plagnol, UCL Genetics Institute. My work consisted in all the methodology developed and described in 7.2, including downstream filtering, manual annotation, in silico analysis of the non-coding variants and generation of a list of putative functional non-coding variants.

7.1. STUDY COHORT

This analysis was performed in the first 233 patients of the cohort.

7.2. ANALYSIS OF THE NON-CODING VARIANTS

The noncoding regions of the 8 sarcomere genes most commonly associated with HCM (*MYH7, MYBPC3, TNNT2, TNNI3, MYL2, MYL3, ACTC1, TPM1*) were analysed. Variants present in the dbSNP build 135 database [257] were identified.

I buildt the candidate regulatory variant dataset by mapping non-coding variants onto known transcription factor (TF) binding sites, identified by ChIP-seq as part of the ENCODE project [155],[156] using the UCSC genome browser (http:/genome.ucsc.edu/) [275]. RegulomeDB (http://regulome.stanford.edu/) was used to assess the level of evidence supporting those transcription factor binding sites, according to available datatypes [276]. Targetscan (http://www.targetscan.org/) [277] and miRTar (http://mirtar.mbc.nctu.edu.tw/human/) were utilized to identify predicted 3'UTR miRNA target regions. I assessed cardiomyocyte expression levels of potentially relevant transcription factors and miRNAs using BioGPS annotation portal

(http://biogps.org/#goto=welcome) [278],[279] and mimiRNA (http://mimirna.centenary.org.au/mep/formulaire.html) [280] respectively. Evolutionary conservation of the variant position at the DNA was analysed using genomic evolutionary rate profiling (GERP) conservation score [281].

Transcription factors previously experimentally proven to be involved in relevant pathways for cardiomyocyte hypertrophic signaling, were then identified through a literature search. I used a Pubmed search that combined the name of each transcription factor with either "heart", "cardiac", hypertrophy", "cardiomyocyte" or "cardiomyopathy".

7.3. EXPRESSION STUDY IN PATIENT SAMPLES VERSUS CONTROLS

The laboratory work for this chapter, consisting in RNA extraction from the selected samples, followed by array quantification, was done by Dr. Mike Hubank, UCL Genomics, Institute of Child Health, following the protocol described below. I identified the samples carrying potentially functional non-coding variants; data analysis for comparison with controls was done as part of my own work, in collaboration with Dr. Hubank.

Paraffin embedded cardiac tissue samples were available for two patients with potentially functional (Results Section, chapter 8) non-coding variants, that had undergone surgical septal myectomy for relief of left ventricular outflow tract obstruction. Local ethical approval had been obtained from University College London Hospitals/UCL joint ethical committee for collection of tissue samples.

Total RNA was prepared from 8 x 10 um sections from paraffin blocks using the ReliaPrep FFPE total RNA mini prep kit (Promega, cat Z1001). Following RNA quality check on an Agilent Bioanalyser, 50 ng was amplified and labelled using the SensationPlus FFPE amplification and labelling module (Affymetrix, 902042) before hybridising to Affymetrix HuGene 1.0 ST arrays.

Labelling and scanning was performed following standard Affymetrix protocols to generate .cel files. Data analysis was performed in Genespring 12. Briefly, cel file data from experimental material was combined with data from cel files from GEO submission GSE22253 (Gene expression and genotype in normal heart; samples GSM954999_VC_A1.cel-

GSM955004_VC_A6.cel; available at http://www.ncbi.nlm.nih.gov/geo/query/acc.cgi?acc=GSE22253) [282] and re-normalised using RMA to generate comparable expression profiles. Individual genes were then compared for normalised expression values against the control database samples.

8. WHOLE-EXOME SEQUENCING AND DATA ANALYSIS OF SARCOMERE-NEGATIVE FAMILIES

High-throuhgput capture platforms that allow the sequencing of the entire coding region of the genome (the "exome") have been applied both in the research and clinical contexts and advocated as a possible alternative to targeted gene sequencing for diagnostic purposes and/or novel causal gene discovery. We have applied a whole-exome sequencing strategy to three sarcomere-negative families with 2 or more relatives affected, to test the hypothesis that novel causal genes could be the genetic cause of the disease in HCM sarcomere-negative families. The preliminary results are presented as part of this thesis.

8.1. SAMPLES

Three families with at least two affected members without any candidate sarcomere candidate variants from the targeted HTS were selected for whole-exome sequencing.

8.2. GOSGENE APPLICATION AND COLLABORATION

The Centre for Translational Genomics-GOSgene initiative funded by the Great Ormond Street Hospital (GOSH) Biomedical Research Centre (BRC) of the National Institute for Health Research (NIHR) offers clinicians and PIs at the joint GOSH, ICH and UCL collaborators a comprehensive service to facilitate gene identification in uncharacterised genetic disorders. Due to the nature of this project, an application to GOSgene was submitted and approved by the GOSgene Access Committee in November 2012. The collaborative agreement was for GOSgene to perform exome next generation sequencing in 6 samples, two affected individuals from each of 3 families.

The steps described in 8.3 to 8.5, from sequencing to variant calling, that allowed a raw dataset of whole-exome variants to be generated, were conducted by GOS gene; the methodology, which followed established protocols, is briefly described below.

My work consisted in all the downstream filtering, prioritization, annotation and analysis of the detected variants, as well as the initial selection and clinical phenotyping of the enrolled families.

8.3. DNA QUANTIFICATION AND QUALITY

DNA from peripheral blood of the patients was received and the GOSgene team run quality controls (QCs) measurement required for next generation sequencing technologies. DNA concentration and purity was assessed by a Thermo Scientific NanoDrop™ 1000 spectrophotometer according to the manufacturer's protocol. DNA concentration from all individuals sequenced was also assessed by fluorometric assay using a Qubit® 2.0 Fluorometer (Life Technologies) following manufacturer's instructions. Exome sequencing was performed by Beckman Coulter Genomics (Danvers, MA, USA). As per Beckman Coulter Genomics' requirements, 3ug of DNA at 100ng/µl according to Qubit reading were prepared in 30µl of H2O. Only samples with an A_{260}/A_{280} ratio of 1.8-2.0 were sent. To assess DNA integrity, 1µl of diluted DNA (100ng/µl) was run on a 1% agarose gel with 1Kb ladder alongside.

8.4. EXOME CAPTURE AND SEQUENCING

Samples were processed using Agilent 51Mb SureSelect Target Enrichment, Human All Exon version 4 (Agilent Technologies). The SureSelect Human All Exon kit design covers 1.22% of human genomic regions corresponding to the NCBI Consensus CDS database (CCDS). Samples were processed according to the SureSelect target Enrichment System for Illumina Paired-End Sequencing Library Protocol and run on an Illumina HiSeq2000 sequencer, paired end 2x100bp read length with an aimed median coverage of 89x. Samples were multiplexed 4 per lane on the HiSeq2000 flowcell to aim for 89x coverage. FASTQ files generated from the sequencing run were shipped back from Beckman Coulter Genomics to UCL on an external hard drive.

8.5. EXOME ANALYSIS

The sequencing reads resulting from the HiSeq2000 were aligned by the GOSgene Bioinformatics team to the human reference genome (GRCh37 release, downloaded from the ENSEMBL database, corresponding to Hg19 NCBI built 37.1) with BWA (Burrows-Wheeler Alignment Tool) software [283]. The GATK tool suite was used to further process the alignments (base quality score recalibration, indels realignment, duplicate removal, using standard hard filtering parameters). Variant calling was also performed using GATK Unified

Genotyper multi-sample SNP caller [253]. A summary of the sequencing coverage produced by GATK DepthOfCoverage profiler is shown in Results, chapter 9.

8.6. FILTERING AND PRIORITIZATION OF VARIANTS

BAM files containing SNP and indels calls were visualised using the Integrative Genomics Viewer IGV (http://www.broadinstitute.org/igv/UserGuide).

SNPs and small insertions/deletions (indels) annotation and interpretation analysis were generated through the use of Ingenuity Variant Analysis™ software (www.ingenuity.com/variants) from Ingenuity Systems.

In summary, starting with 7259895 variants spanning 21421 genes, variants were kept with call quality at least 20.0 in cases or at least 20.0 in controls.

Initial downstream variants analysis included the assessment of the quality of the reads from the BAM files, existing structural variations in the chromosomal region, assessment of the novelty against internal GOSgene databases (for common currently not submitted variants), details of gene functions (review of databases and literature), affected domains and prediction of the biological impact (SIFT, Polyphen and Mutation Taster), amino acid conservation, expression pattern, existing animal models and any other relevant information (including phenotype indications via OMIM and HGMD).

Variants were then prioritised by predicted frequency starting from “novel” variants (i.e. not annotated in databases including dbSNP, NHLBI Exome Sequencing Project (ESP) and 1000genomes) and predicted effect (starting from essential splice site, stop gained, stop lost, frameshift indels and non-synonymous variants).

Parameters used in the Ingenuity Variant Analysis software for filtering of the variants, in order to generate an initial candidate dataset for each family, were:

- MAF ≤ 1% in the 1000 genomes database AND exome sequencing project
- absent from dbSNP
- absent from controls
- absent from in-house GOSgene database

- in common for the family members affected
- non-synonymous, splicing, frameshift
- localization in genes previously related to cardiomyopathy

I used the detailed script, as follows:

"Excluded those variants that are observed with an allele frequency greater than or equal to 1.0% of the genomes in the 1000 genomes project OR greater than or equal to 1.0% of the public Complete Genomics genomes OR greater than or equal to 1.0% of the NHLBI ESP exomes (All) OR present in dbSNP.

Kept those variants that are experimentally observed to be associated with a phenotype: Pathogenic, Possibly Pathogenic, Unknown Significance, Possibly Benign, Benign OR established gain of function in the literature OR gene fusions OR inferred activating mutations by Ingenuity OR predicted gain of function by BSIFT OR in a microRNA binding site OR Frameshift, in-frame indel, or stop codon change OR Missense OR disrupt splice site upto 10.0 bases into intron OR deleterious to a microRNA OR structural variant

Kept those variants which are associated with gain of function OR compound_heterozygous OR hemizygous OR heterozygous_alt OR homozygous OR heterozygous_amb OR heterozygous OR haploinsufficient AND occur in at least 2 of the case samples at the gene level in the Case samples AND not which are associated with gain of function OR compound_heterozygous OR hemizygous OR heterozygous_alt OR homozygous OR heterozygous_amb OR heterozygous OR haploinsufficient AND occur in at least 1 of the control samples at the variant level in the Control Samples

Kept those that are within 2 hops upstream and that are known or predicted to affect: cardiomyopathy, cardiomyocyte abnormalities, cardiomyocyte acidosis, cardiomyocyte activation (activation of cardiomyocytes), cardiomyocyte adhesion (adhesion of cardiomyocytes), cardiomyocyte aging, cardiomyocyte apoptosis, cardiomyocyte area, cardiomyocyte atrophy, cardiomyocyte autophagy, cardiomyocyte beat, cardiomyocyte beating, cardiomyocyte binucleation (binucleation of cardiomyocytes), cardiomyocyte chemoinvasion (chemotaxis of cardiomyocytes), cardiomyocyte cleavage, cardiomyocyte content, cardiomyocyte contractility, cardiomyocyte contraction (contraction of cardiomyocytes), cardiomyocyte coupling, cardiomyocyte cytokinesis, cardiomyocyte cytonecrosis, cardiomyocyte damage, cardiac abnormality, cardiac abnormality (organismal abnormalities of heart), cardiac activation, cardiac anterior wall hypertrophy, cardiac apoptosis, cardiac arrhythmia, cardiac arrhythmia of cardiac ventricle, cardiac arrhythmia of heart atrium, cardiac atrophy, cardiac beating, heart abnormality, heart abnormality (organismal abnormalities of heart), heart activation (activation of heart), heart apex hypertrophy, heart apoptosis, myocardial cells activation, myocardial cells adhesion,

myocardial cells binucleation, myocardial cells chemoinvasion, myocardial cells contraction, myocardial cells degeneration, myocardial cells desensitization, myocardial cells differentiation, myocardial cells division, myocardial cells dysfunction, myocardial cells function, myopathy, myopathy of heart, ZASP-related myofibrillar myopathy (myofibrilliar myopathy ZASP-related) or diseases consistent with these phenotypes"

All candidate genes in the obtained list were checked for cardiac expression using GeneCards (http://www.genecards.org) and BioGPS (www.biogps.org) [278].

Prioritised candidates variants were confirmed by PCR and Sanger sequencing using the methodology previously described in chapter 4.

9. *IN SILICO* ANALYSIS AND STRUCTURAL IMPACT PREDICTION OF MISSENSE VARIANTS IN *MYH7*

My work consisted in: a) manually curating a list of MYH7 variants detected in this cohort and extracted from the mentioned databases; b) assessing the degree of evidence for the pathogenicity of these variants and the frequency of the variants in general population databases; c) annotating the associated phenotypes; d) manually introducing each variant at the SAAPdap software and annotating the predicted impact in protein structure; e) manually analysing the relationship between the obtained impact and the phenotype. The results and data generated from the manual analysis inspired a machine-learning work developed by Dr. Andrew Martin, Structural and Molecular Biology, UCL. The methodology developed and applied by Dr. Martin is described below for completion and the results presented in the Results section. During the development of the machine learning work, I continuousy discussed the obtained results and data with Dr. Martin, which lead to several optimizations of the algorithm

9.1. DATASET OF *MYH7* VARIANTS

I built a dataset of beta-myosin heavy chain variants detected in this cohort of consecutively evaluated unrelated HCM patients (as described in previous chapters). To increase the number of variants analysed, I enriched this dataset with other established disease-causing or likely pathogenic variants in *MYH7*, for which limited phenotypic data was available from a genetic testing company database (Health in Code, Inc. - courtesy Dr. Lorenzo Monserrat) and from the Human Gene Mutation Database (free trial version, accessed Abril 2012). These additional variants were associated not only with HCM but also with dilated cardiomyopathy (DCM), left ventricular non-compaction (LVNC), various skeletal myopathies and congenital heart disease. All selected variants were rare as defined by a minor allele frequency (MAF) ≤ 0.5% in the Heart, Lung and Blood Institute (NHLBI) exome sequencing project database.

I analysed the distribution of the mutations throughout the different domains of the protein (P12883), based on the boundaries for the different domains and sub-domains available at UniProtKB/SwissProt (http://www.uniprot.org) and Pfam (http://pfam.xfam.org)

The expected number of mutations for each residue (Ea) was calculated based on Ea =Na x Mt/Nt, where: Ea is the expected number of mutations for amino acid a, Na is the total number of amino acids of type a in the protein, Mt is the total number of mutations observed and Nt is the total number of residues.

9.2. PREDICTION OF *IN SILICO* PATHOGENICITY

Prediction was performed using Polyphen2 [160], SIFT [159] and SAAP (single amino acid polymorphism) data analysis pipeline (SAAPdap) [166] (http://www.bioinf.org.uk/saap/dap/), which indicates whether a mutation is likely to have a detrimental effect on structure using cutoff values, and also provides continuous values for each of the analyses. SAAPdap-based evaluated features were: a) Interface: Residue is in an interface according to difference in solvent accessibility between complexed and un-complexed forms; b) Binding: Residue makes specific interactions with a different protein chain or ligand; c) SProtFT: Residue is annotated as functionally relevant by UniProtKB/SwissProt; d) Clash: Mutation introduces a steric clash with an existing residue; e) Void: Mutation introduces a destabilizing void in the protein core; f) CisPro: Mutation from cis-proline, introducing an unfavorable ω torsion angle; g) Glycine: Mutation from glycine, introducing unfavorable torsion angles; h) Proline: Mutation to proline, introducing unfavorable torsion angles; i) HBond: Mutation disrupts a hydrogen bond; j) CorePhilic: Introduction of a hydrophilic residue in the protein core; k) SurfacePhobic: Introduction of a hydrophobic residue on the protein surface; l) BuriedCharge: Mutation causes an unsatisfied charge in the protein core; m) SSGeom: Mutation disrupts a disulphide bond; n) Impact: Residue is significantly conserved.

9.3. MANUAL ANALYSIS OF ASSOCIATIONS BETWEEN STRUCTURAL CONSEQUENCES AND PHENOTYPE

I tested the association between each of three available phenotype parameters (maximum wall thickness (MLVWT), age at presentation and HCM versus other phenotypes) and: a) effect of each of the SAAPdap predicted structural features; b) effect of any of the predicted SAAPdap structural features versus absence of any structural effect; c) number of SAAPdap structural features affected; d) *in silico* prediction by SIFT, Polyphen2 or both; e) functional domain affected.

I also tested for associations between functional domain affected and: a) the presence of each of the predicted structural features; b) presence of any of the predicted structural features versus none; c) number of SAAPdap structural features affected.

All these associations were tested using Chi-square tests.

9.4. MACHINE LEARNING ANALYSIS TO PREDICT PATHOGENICITY AND PHENOTYPE

Initial pathogenicity prediction was performed using the SAAPpred (predictor), trained on HumVar, which is constituted by all human disease-causing mutations from UniProtKB, together with common human nsSNPs (MAF>1%) without annotated involvement in disease, which were treated as non-damaging [166]. SAAPpred makes use of the analyses from SAAPdap to make a prediction of pathogenicity; thus a mutation with no analyses individually expected to be damaging can still be predicted to be pathogenic as a result of the accumulation of a number of more subtle effects. Ten pre-built models were used and the performance results were averaged.

The same approach was used in phenotype prediction for separating mutations associated with HCM and DCM. As a starting point, any mutations associated with multiple phenotypes or causing phenotypes other than HCM or DCM (i.e. restrictive cardiomyopathy, left ventricular non-compaction, congenital heart disease, distal myopathies) were discarded. The major problem encountered was the unbalanced nature of the dataset; many more mutations existed for HCM than for DCM. Perl code was written to limit the size of each class by selecting examples at random. For example, if the class size was limited to 21, the complete DCM class was retained while 21 mutations were selected at random from the HCM class. This random selection process was repeated 10 times to provide a representative sample of the HCM class and the results were averaged. Because the available dataset was limited in size, it was desirable to use mapping to multiple structure. For that a Perl program was written to split the HCM and DCM unique mutations with available PDB (Protein Data Bank, http://www.rcsb.org/pdb/home/home.do) structures into 10 sets of approximately the same size. Each of these 10 sets in turn was chosen as a test set and enlarged with all the available PDB/chain structures. The remaining 9 sets were used for training by randomly drawing balanced datasets of different sizes from the mutations as mapped to protein chains. Results

were averaged across the 10 models built using all DCM and different subsets of HCM.

Mutations were represented by a total of 47 'features' from the structural analysis. Of these, 13 were found to be redundant (i.e. they had the same value for all examples in the dataset), thus reducing the number to 34 features. These data were then used to train Random Forest models in WEKA. Then, a simple cut-off for each of the 14 major features was used to suggest whether they were damaging using SAAPdap results. Chi-square tests were performed to investigate which features were most informative.

After determining the optimum number of features and trees, together with exploration of the most informative feature subsets, different numbers of models were also investigated (5, 10 and 20 models).

Addition of the 'clustering' feature (see Results Section, chapter 10.3) was also explored. To use this information in machine learning, the centroid of each cluster was calculated and the feature vector for each mutation was expanded by the addition of the distances from the C-alpha of the mutated residue to each of the three centroids.

SECTION III – RESULTS

1. STUDY COHORT CHARACTERIZATION

Eight-hundred-and-seventy-four unrelated and consecutive patients with HCM were studied. Mean follow-up time was 4.8±3.5 years. **Table 5** summarizes the demographic and clinical characteristics of the patients.

Table 5. Demographic and clinical characteristics of the study cohort. HCM: hypertrophic cardiomyopathy; SCD: sudden cardiac death; NYHA: New York Heart Association; ECG: electrocardiography; CPEX: cardiopulmonary exercise test; SBP: systolic blood pressure; LVH: left-ventricular hypertrophy; RVH: right ventricular hypertrophy; FS: fractional shortening; LVOT: left ventricular outflow tract; NSVT: non-sustained ventricular tachycardia.

	Frequency (percentage) or mean ± standard deviation (range) or median (IQR)
DEMOGRAPHICS	
Age at initial evaluation (years)	49.6±15.4 (6-87)
Male	590/874 (67.8%)
Ethnicity – Caucasian – Indian and other Asian – African/Caribbean – Chinese – Other	 622 (71.2%) 68 (7.8%) 39 (4.5%) 6 (0.7%) 20 (2.3%) 119 (13.6%)
PRESENTATION	
Family history of HCM	226/853 (26.5%)
Family history of SCD	182/872 (20.9%)
NYHA class III or IV	100/850 (11.8%)
Syncope	140/856 (16.4%)
Chest pain	205/854 (24.0%)
INITIAL ECG	
Atrial fibrillation	43/874 (4.9%)
PR interval (msec)	174.8±32.4 (108-320)

QRS duration (msec)	101.0±25.5 (64-238)
INITIAL CPEX	
SBP rest (mmHg)	128.8±21.0 (80-210)
SBP difference (mmHg)	48.5±24.2 (-5 - 150)
Abnormal systolic blood pressure response to exercise	92/662 (13.9%)
INITIAL ECHOCARDIOGRAPHY	
Maximal left ventricular wall thickness (mm)	18.5±4.4 (9-38)
Severe LVH (≥30mm)	17/601 (2.8%)
Right ventricular hypertrophy (>5mm)	184/864 (21.3%)
Asymmetric septal hypertrophy pattern	643/850 (75.6%)
Left atrial diameter (mm)	44.0±7.5 (18-90)
Left ventricular end-diastolic diameter (mm)	45.9±5.9 (29-65)
Left ventricular dilatation (> 55 mm)	38/851 (4.5%)
Left ventricular end-systolic diameter (mm)	28.5±5.6 (9-50)
Fractional shortening (%)	38.3±8.2 (16-70)
Systolic dysfunction (≤ 25% FS)	29/829 (3.5%)
E wave Deceleration time (ms)	221.0 (184-268)
Mitral regurgitation – moderate/severe	163/851 (19.2%)
Peak LVOT gradient (mmHg)	12.0 (4.0-60.0)
LVOT gradient > 30 mmHg	328/812 (40.4%)
NSVT – Holter	127/566 (22.4%)
FOLLOW-UP	
New-onset atrial fibrillation	216/874 (24.7%)
Implantable cardioverter-defibrillator	177/874 (20.3%)
Myectomy	130/874 (14.9%)
Alcohol septal ablation	46/874 (5.3%)

Myectomy and/or alcohol septal ablation and/or pacemaker implantation for LVOT gradient reduction	182/874 (20.8%)
Cardiovascular death	25/874 (2.9%)
Sudden cardiac death	16/874 (1.8%)

2. TARGETED GENE ENRICHMENT AND HIGH-THROUGHPUT SEQUENCING – COVERAGE AND READ DEPTH DATA

The mean value of the per-sample average read depth in the exonic target region across the samples was 472.27±127.68. Thirty-four samples had an average read depth lower than 40, with a minimum of 8. Combining all samples and taking the mean value across all samples, 93.5% of the target region was covered to a read depth of 15 or more.

2.1. ANALYSIS PER PLATE

Considering that there were differences in sequencing platform, multiplexing methodology and sample preparation between different plates, particularly from plate 4 onwards compared to the previous plates (see Methods Section, chapter 2), it is informative to analyse the average read depth per plate, which was: 73.39±108.0 for plate 1, 203.0±223.95 for plate 2, 351.86±222.17 for plate 3, 494.13±84.21 for plate 4, 480.02±112.64 for plate 5, 486.13±104.56 for plate 6, 495.34±80.09 for plate 7, 40.12±53.14 for plate 8, 500.30±67.50 for plate 9. **Figure 18, A-G**.

When analysing the percentage of acceptable coverage (>15x) per plate, I obtained an average of 89.79% in plate 1; 85.78% in plate 2; 87.55% in plate 3; 97.09% in plate 4; 97.90% in plate 5; 96.35% in plate 6; 97.05% in plate7; 88.39% in plate 8; 98.06% in plate 9.

The significantly lower average read depth for plate 8 was due to sub-optimal clustering, prior to the sequencing process. However, the coverage is similar to the first three plates, from which the calls were submitted to a process of systematic validation as described on the Methods Section, chapter 4; results are presented in the next chapter. From that validation process we concluded that even for low read depths the accuracy was acceptable. Therefore, even with lower read depth, the calls from plate 8 were considered of adequate quality and are under continuous clinical validation.

A

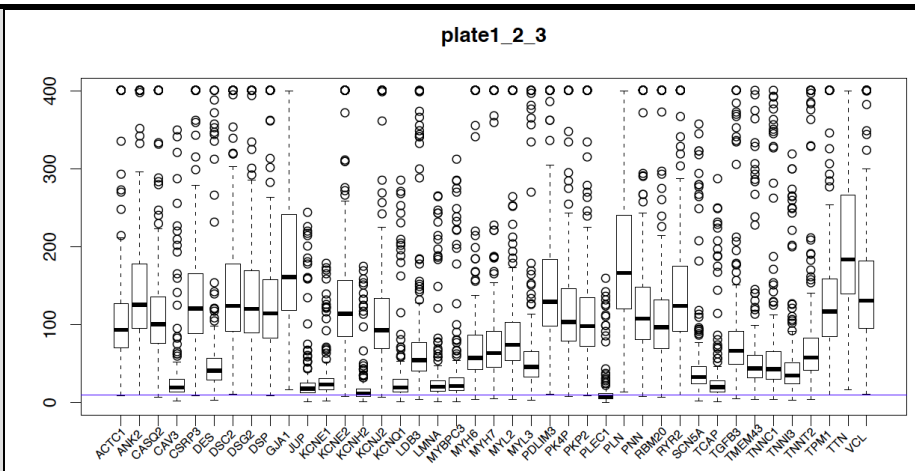
plate1_2_3
0
100
200
300
400
ACTC1 ANK2 CASQ2 CAV3 CSRP3 DES DSC2 DSG2 DSP GJA1 JUP KCNE1 KCNE2 KCNH2 KCNJ2 KCNQ1 LDB3 LMNA MYBPC3 MYH6 MYH7 MYL2 MYL3 PDLIM3 PKP4 PKP2 PLEC1 PLN PNN RBM20 RYR2 SCN5A TCAP TGFB3 TMEM43 TNNC1 TNNI3 TNNT2 TPM1 TTN VCL

B

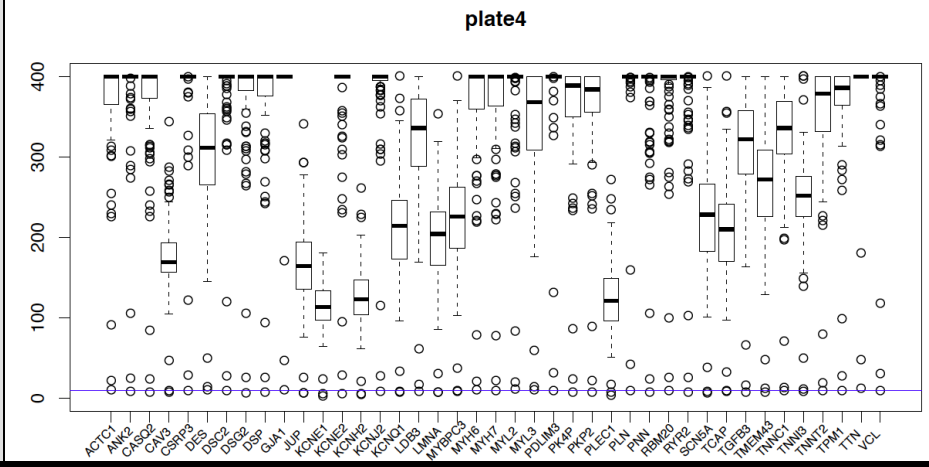
plate4
0
100
200
300
400
ACTC1 ANK2 CASQ2 CAV3 CSRP3 DES DSC2 DSG2 DSP GJA1 JUP KCNE1 KCNE2 KCNH2 KCNJ2 KCNQ1 LDB3 LMNA MYBPC3 MYH6 MYH7 MYL2 MYL3 PDLIM3 PKP4 PKP2 PLEC1 PLN PNN RBM20 RYR2 SCN5A TCAP TGFB3 TMEM43 TNNC1 TNNI3 TNNT2 TPM1 TTN VCL

C

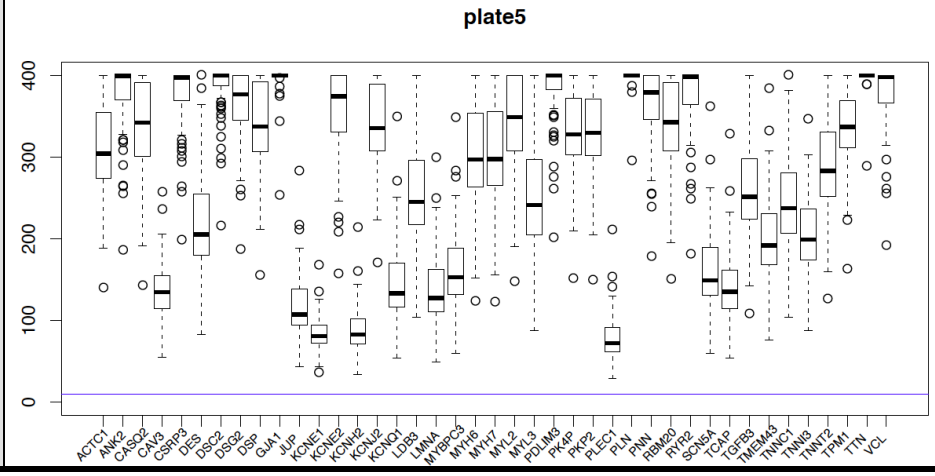
plate5
0
100
200
300
400
ACTC1 ANK2 CASQ2 CAV3 CSRP3 DES DSC2 DSG2 DSP GJA1 JUP KCNE1 KCNE2 KCNH2 KCNJ2 KCNQ1 LDB3 LMNA MYBPC3 MYH6 MYH7 MYL2 MYL3 PDLIM3 PKP4 PKP2 PLEC1 PLN PNN RBM20 RYR2 SCN5A TCAP TGFB3 TMEM43 TNNC1 TNNI3 TNNT2 TPM1 TTN VCL

D

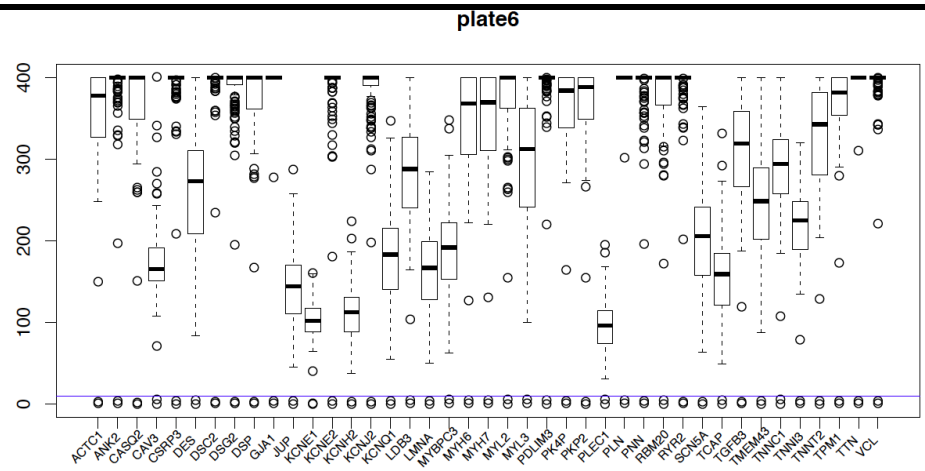
plate6
0
100
200
300
400
ACTC1 ANK2 CASQ2 CAV3 CSRP3 DES DSC2 DSG2 DSP GJA1 JUP KCNE1 KCNE2 KCNH2 KCNJ2 KCNQ1 LDB3 LMNA MYBPC3 MYH6 MYH7 MYL2 MYL3 PDLIM3 PKP4 PKP2 PLEC1 PLN PNN RBM20 RYR2 SCN5A TCAP TGFB3 TMEM43 TNNC1 TNNI3 TNNT2 TPM1 TTN VCL

E

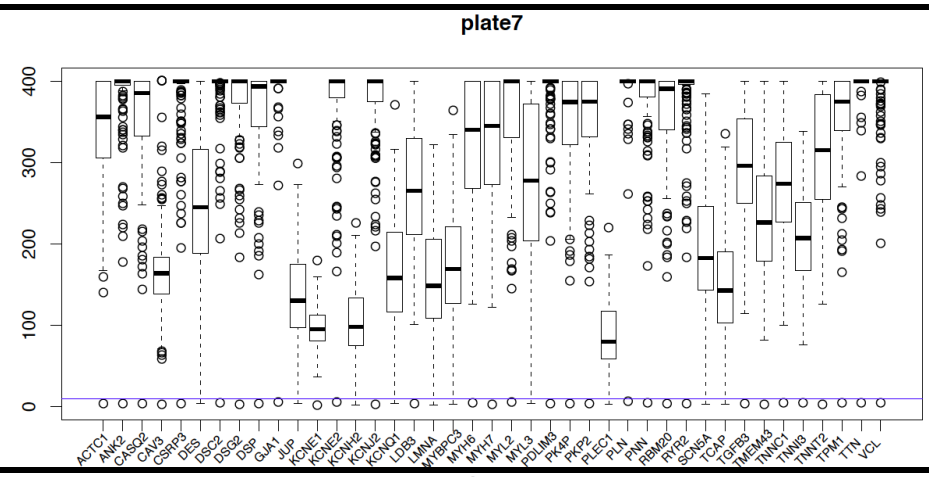
plate7
0
100
200
300
400
ACTC1 ANK2 CASQ2 CAV3 CSRP3 DES DSC2 DSG2 DSP GJA1 JUP KCNE1 KCNE2 KCNH2 KCNJ2 KCNQ1 LDB3 LMNA MYBPC3 MYH6 MYH7 MYL2 MYL3 PDLIM3 PKP4 PKP2 PLEC1 PLN PNN RBM20 RYR2 SCN5A TCAP TGFB3 TMEM43 TNNC1 TNNI3 TNNT2 TPM1 TTN VCL

F

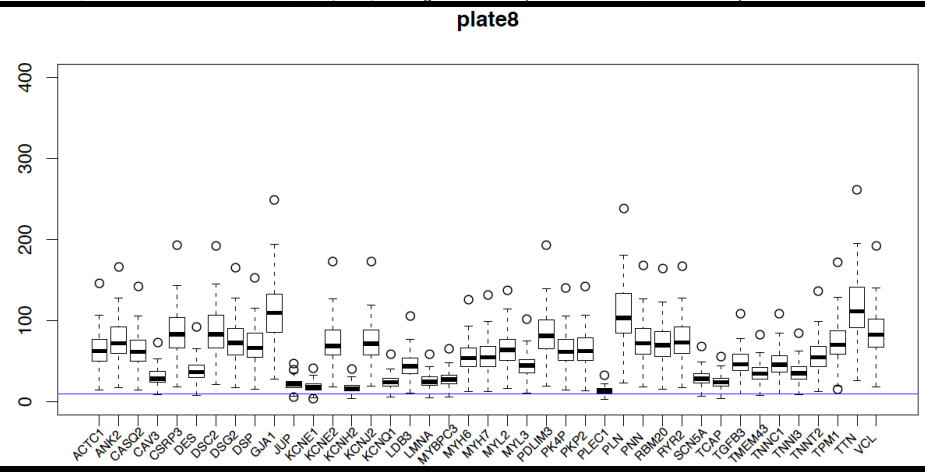
plate8
0
100
200
300
400
ACTC1 ANK2 CASQ2 CAV3 CSRP3 DES DSC2 DSG2 DSP GJA1 JUP KCNE1 KCNE2 KCNH2 KCNJ2 KCNQ1 LDB3 LMNA MYBPC3 MYH6 MYH7 MYL2 MYL3 PDLIM3 PKP4 PKP2 PLEC1 PLN PNN RBM20 RYR2 SCN5A TCAP TGFB3 TMEM43 TNNC1 TNNI3 TNNT2 TPM1 TTN VCL

G

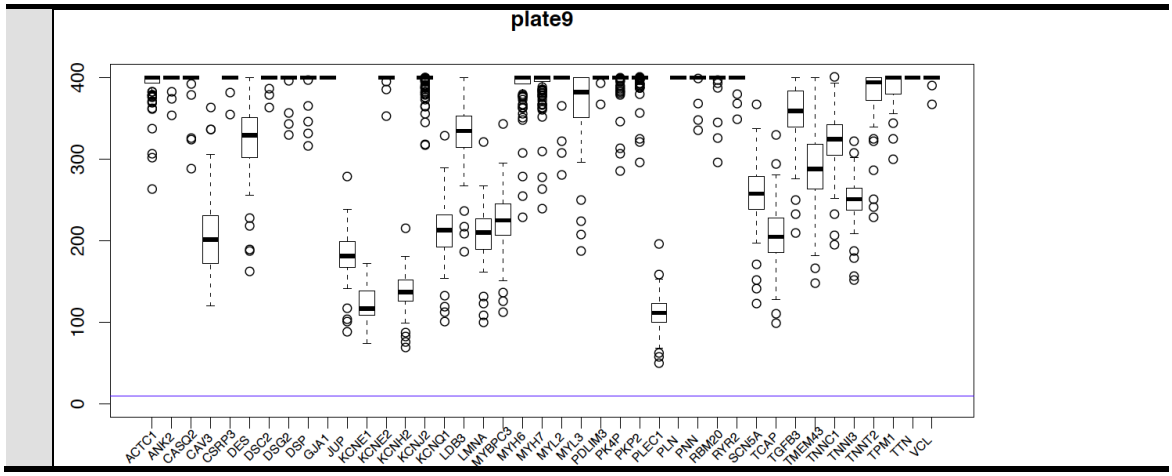

Figure 18. Box-and-whisker plots, representing the read-depths across the targeted genes, for A: plate 1-3, B: plate 4, C: plate 5, D: plate 6, E: plate 7, F: plate 8, G: plate 9. The horizontal line on each graph represents the read-depth=15 cut-off. Panel A is adapted with permission from [251].

2.2. ANALYSIS PER GENE

The read depth for each gene, across all plates/samples and subdivided in plates 1-3 and 4-9 - due to differences in the sequencing platform and multiplexing - is shown in **table 6**.

Table 6. Pooled analysis of read depth per gene, across all plates and subdivided in plates 1-3 and 4-9. Plate 8 was excluded from this analysis due to a significant lower average read depth caused by sub-optimal clustering prior to the sequencing process, as explained in the previous sub-chapter.

Gene	Read depth (mean±standard deviation) – total cohort	Read depth (mean±standard deviation) – plates 1-3	Read depth (mean±standard deviation) – plates 4-9 excluding 8
CASQ2	276.86±163.48	126.95±99.70	391.11±82.55
LMNA	116.34±86.23	32.50±46.02	173.85±56.23
TNNT2	234.43±153.91	81.56±85.81	341.91±84.69
RYR2	311.07±171.42	153.40±106.43	433.83±72.35
PKP4	268.08±150.95	131.27±93.27	374.64±70.35
TTN	376.94±178.59	218.07±116.64	505.87±60.86
DES	185.88±132.31	61.02±77.34	274.28±82.96

CAV3	117.82±86.32	33.68±52.06	174.66±55.85
TMEM43	170.76±117.21	61.48±67.04	249.40±72.92
SCN5A	142.33±102.01	48.86±60.92	209.05±67.06
MYL3	213.23±151.42	69.19±85.89	314.77±95.05
TNNC1	198.68±132.39	64.44±75.64	292.00±69.31
ANK2	313.00±170.80	157.36±105.40	435.29±71.96
PDLIM3	309.38±161.18	159.17±98.17	426.44±61.34
DSP	283.53±159.19	141.66±102.65	394.43±77.07
PLN	331.15±156.14	194.99±104.16	441.72±62.00
GJA1	350.13±171.19	196.60±121.24	471.72±63.13
KCNH2	75.90±57.41	19.28±29.25	114.22±37.88
PLEC	64.98±52.40	13.73±24.94	99.22±36.94
VCL	319.27±171.78	159.17±105.74	442.56±72.44
LDB3	201.48±131.64	75.29±75.99	292.39±74.02
RBM20	280.49±165.02	122.52±104.01	397.17±77.90
KCNQ1	121.80±92.20	32.27±47.45	183.22±60.97
CSRP3	320.32±179.02	149.94±110.10	448.48±78.68
MYBPC3	130.06±96.00	35.44±51.90	194.83±60.43
PKP2	264.55±150.21	122.76±90.03	372.11±67.03
MYL2	287.29±186.78	102.85±106.25	418.70±98.32
MYH7	250.14±163.68	90.86±98.35	364.02±87.74
PNN	300.39±171.86	135.88±98.53	423.83±78.38
MYH6	247.17±163.90	84.89±95.16	361.91±87.46
TGFB3	215.83±137.01	87.01±78.46	310.46±76.79
ACTC1	260.42±152.83	118.23±91.69	367.46±77.61
TPM1	274.76±149.64	141.47±100.48	378.85±70.43
TCAP	115.25±87.35	31.47±44.98	172.66±59.65
JUP	100.27±75.15	28.12±40.50	149.81±50.35
KCNJ2	286.38±168.03	118.36±88.90	408.33±77.16
DSC2	310.41±164.50	152.45±96.81	430.88±61.82
DSG2	297.71±162.81	147.85±99.22	414.17±70.51
TNNI3	153.16±101.62	49.77±54.90	225.15±53.44
KCNE2	317.72±191.15	144.69±118.00	448.93±104.02
KCNE1	73.01±46.85	30.25±29.03	104.31±28.37

3. CLINICAL VALIDATION AND ASSESSMENT OF THE ACCURACY OF THE HIGH-THROUGHPUT SEQUENCING PLATFORM AND ANALYSIS PIPELINE

3.1. STEP 1 – SYSTEMATIC VALIDATION OF ACCURACY FOR PLATES 1-3 (FIRST 223 PATIENTS)

We successfully validated by Sanger sequencing:

- all novel and/or potentially pathogenic variants in desmosomal or ion-channel disease genes;
- 48 out of 50 variants with a sufficient quality score but a read depth lower than 15; the two exceptions were one missense variant in *LDB3* and one frameshift deletion in *KCNH2*;
- all the *MYH6* and *MYH7* variants;
- 45 out of 46 *TTN* variants were confirmed (one insertion-deletion was wrongly annotated).

In total, 123 out of 126 variants were confirmed, including 16 insertions and deletions and 110 single base-pair substitutions. This indicated that the approach has a very low false positive rate even with a lower read depth.

Regarding the screening of exons with low average read depth (Methods Section, chapter 4), only one false negative was found, c.459delC, p.P153fsX5 in MYBPC3. This indicated that the sequencing protocol has a very low rate of false negatives, even for lower read depths.

3.2. STEP 2 – APPLICATION - VALIDATION OF CLINICALLY ACTIONABLE VARIANTS (ALL PATIENTS)

As part of the application phase, we obtained the results for 117 of the variants flagged for validation, counselling and clinical use, for which 85 were confirmed and 28 were already known from clinical Sanger sequencing conducted in other laboratories. This is equivalent to 113 true positives (positive predictive value of 96.58%); four variants (2 from the same patient) were not confirmed.

4. CODING SEQUENCE DATA ANALYSIS

Initial genotype calling generated 90551 exonic and splice-site calls distinct from the reference sequence, that corresponded to a total of 7261 distinct variants present in the 874 patients. After exclusion of synonymous substitutions, we found 37913 non-synonymous exonic and splice-site calls (4105 distinct variants).

After filtering for frequency (for a minor allele frequency (MAF) ≤ 0.5%), we selected 1555 distinct rare variants (2502 calls); when excluding titin, 826 distinct rare non-synonymous exonic or splice-site variants (1236 calls) were obtained as candidates for further analysis. The list of candidate variants is provided in **Appendix D**. In total, 830 patients (95.0%) carried at least one variant in the targeted genes, 701 patients (80.2%) when excluding TTN. Six-hundred-and-thirty-eight (73.1%) patients carried multiple variants, 392 when excluding TTN (44.8%).

4.1. SARCOMERE PROTEIN GENE VARIANTS

Using a cut-off MAF of 0.5%, 411 patients (47.03%) carried 272 rare distinct variants in one or one or more of the eight sarcomeric protein genes most commonly associated with HCM *(MYH7, MYBPC3, TNNT2, TNNI3, MYL2, MYL3, ACTC1* and *TPM1*) (**table 7**). One-hundred-and-forty-five (53.3%) of these variants were previously published [20],[23],[284],[285],[128],[173],[176],[286],[125],[287],[288],[289],[188],[123],[130],[218],[17],[16],[290],[291],[121],[292],[293],[294],[169],[174],[196],[224],[295],[250],[296],[297],[126],[298],[227],[181],[299],[178],[300],[212]. Forty-five (16.5%) were novel missense variants predicted *in silico* to be pathogenic and 43 (15.8%) were novel potential loss-of-function variants. As such, a majority (85.6%) of these variants are strong candidates for pathogenicity and were present in 394 patients (45% of the cohort).

At a cut-off for rarity of minor allele frequency (MAF) ≤ 0.2%, three-hundred-and-eighty-three patients (43.8%) had 265 distinct rare variants in the same eight main sarcomere protein genes. One-hundred-and-forty-two (53.5%) of these rare variants were previously published as

disease-causing mutations, 44 (16.6%) were novel missense variants predicted *in silico* to be pathogenic and 40 (15%) were novel potential loss-of-function variants.

Table 7. Prevalence of rare variants in the eight main sarcomere genes. The number and proportion of individuals for each individual gene excludes patients carrying more than one variant, who are grouped under "multiple". MAF: minor allele frequency.

Gene	Number of cases (MAF ≤ 0.2%)	Percentage of sarcomere-positive individuals (MAF ≤ 0.2%)	Number of cases (MAF ≤ 0.5%)	Percentage of sarcomere-positive individuals (MAF ≤ 0.5%)
ACTC1	3	0.8	3	0.73
MYBPC3	191	49.9	199	48.4
MYH7	99	25.9	104	25.3
MYL2	6	1.6	5	1.2
MYL3	4	1.0	5	1.2
TNNI3	15	3.9	15	3.7
TNNT2	20	5.2	20	4.9
TPM1	8	2.1	12	2.9
Multiple	37	9.7	48	11.7
Total	383	100	411	100

Thirty-four patients (3.9%) carried multiple candidate variants in these sarcomere protein genes, if considering a MAF cut-off of 0.2%. Forty-eight (5.5%) carried multiple candidate variants for a MAF cut-off of 0.5%. The distribution of sarcomere variants in patients with multiple variants considering a MAF ≤ 0.5% is shown in **Figure 19**. Thirty-two (66.7%) of the compound, double and triple heterozygotes carried a cardiac myosin binding protein C (*MYBPC3*) variant as one of the candidate sarcomere variants. Twelve patients were compound heterozygotes for *MYBPC3*, one patient was homozygous for a *MYBPC3* variant and seven patients were compound heterozygotes for *MYH7*.

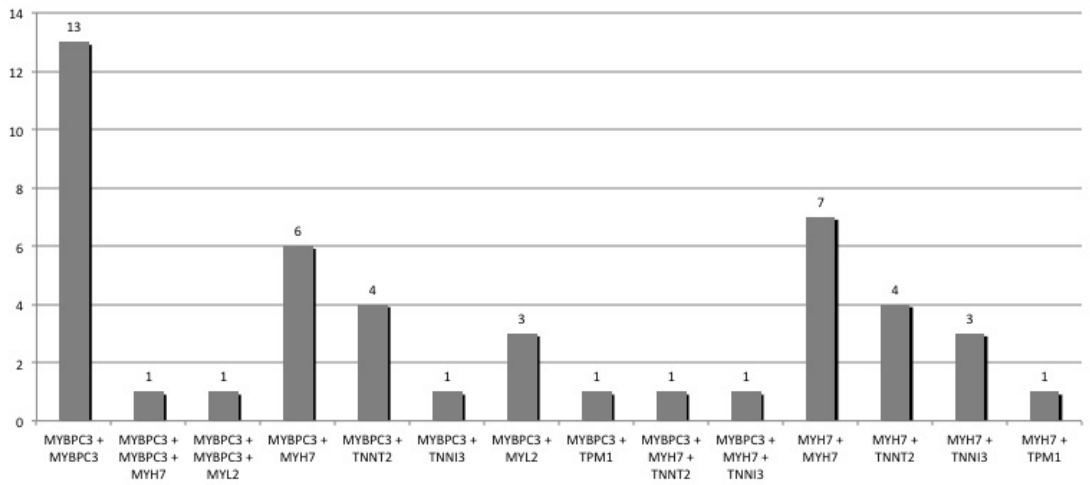

Figure 19. Number of patients with different combinations of multiple sarcomere variants (MAF≤0.5%). Adapted with permission from [251].

In order detect possible clustering of rare variation in certain domain/regions of the sarcomere proteins, I plotted the tabulated variants (≤0.5% MAF) in simple models (Plot Protein application; Methods Section, chapter 3), shown in **figure 20, panels A-G.**

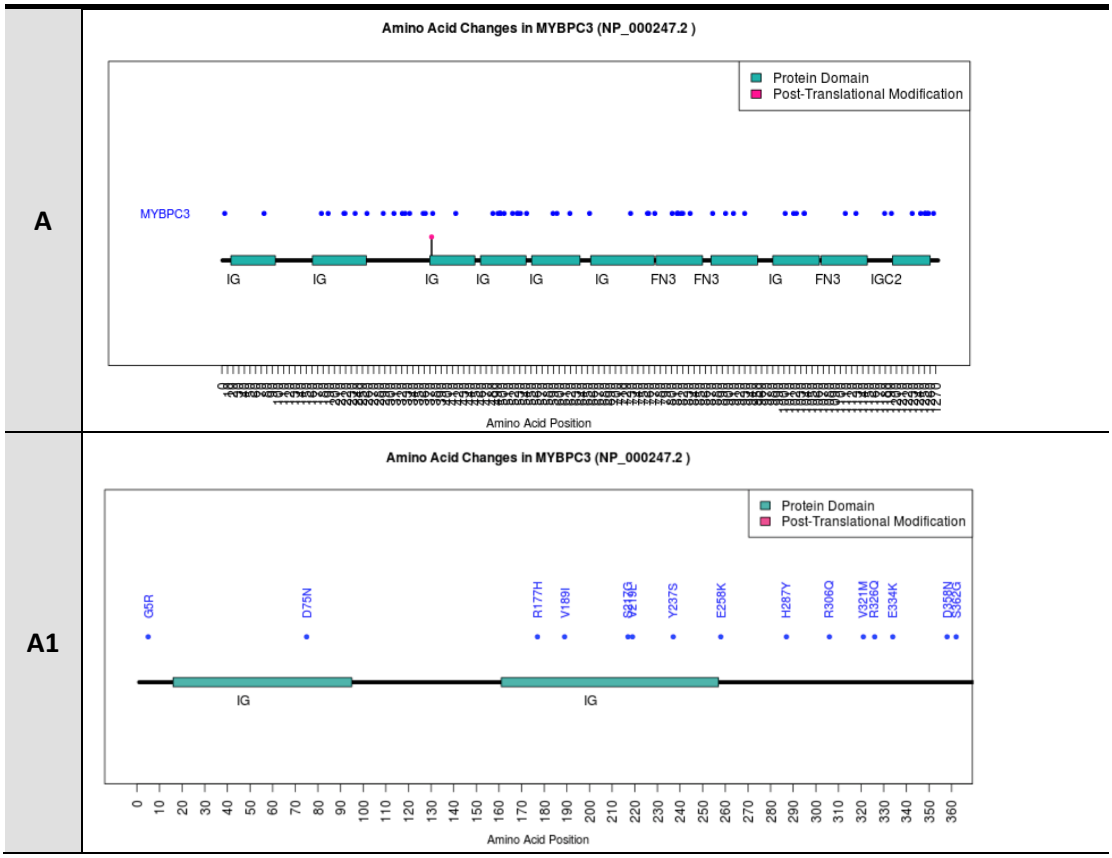

A2

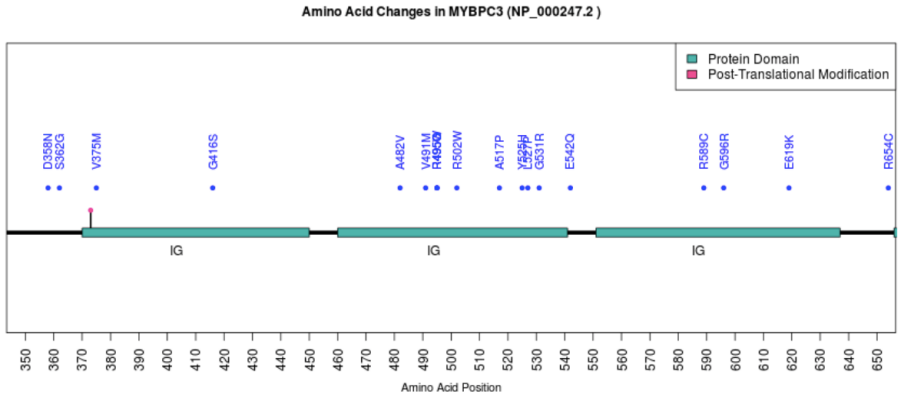
Amino Acid Changes in MYBPC3 (NP_000247.2)
Protein Domain
Post-Translational Modification
D358N
S362G
V375M
G416S
A482V
R502W
A517P
G531R
E542Q
R589C
G596R
E819K
R654C
IG
IG
IG
Amino Acid Position

A3

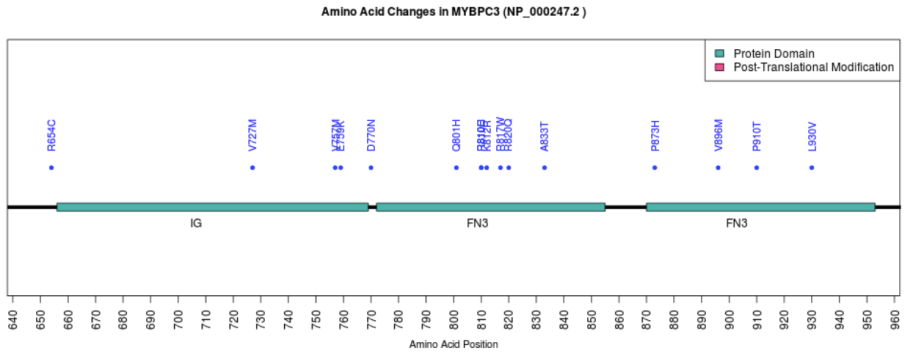
Amino Acid Changes in MYBPC3 (NP_000247.2)
Protein Domain
Post-Translational Modification
R654C
V727M
D770N
Q801H
A833T
P873H
V896M
P910T
L930V
IG
FN3
FN3
Amino Acid Position

A4

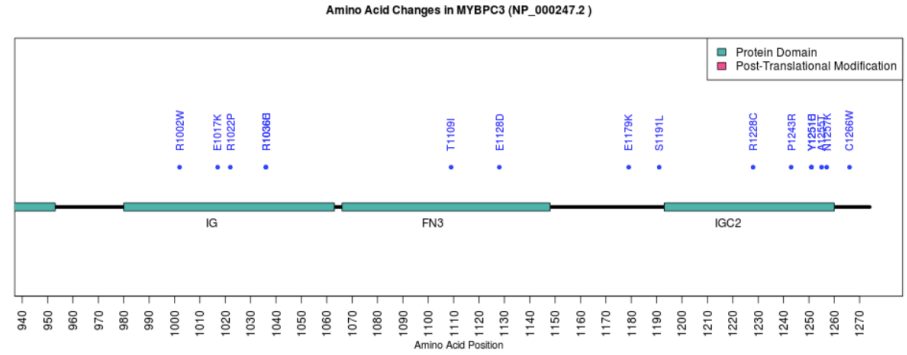
Amino Acid Changes in MYBPC3 (NP_000247.2)
Protein Domain
Post-Translational Modification
R1002W
E1017K
R1022P
T1109I
E1128D
E1179K
S1191L
R1226C
P1243R
C1266W
IG
FN3
IGC2
Amino Acid Position

B

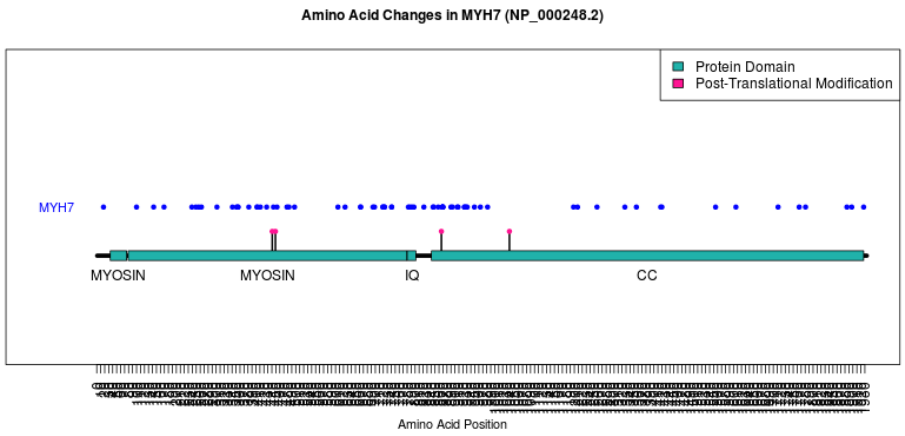
Amino Acid Changes in MYH7 (NP_000248.2)
Protein Domain
Post-Translational Modification
MYH7
MYOSIN
MYOSIN
IQ
CC
Amino Acid Position

B1

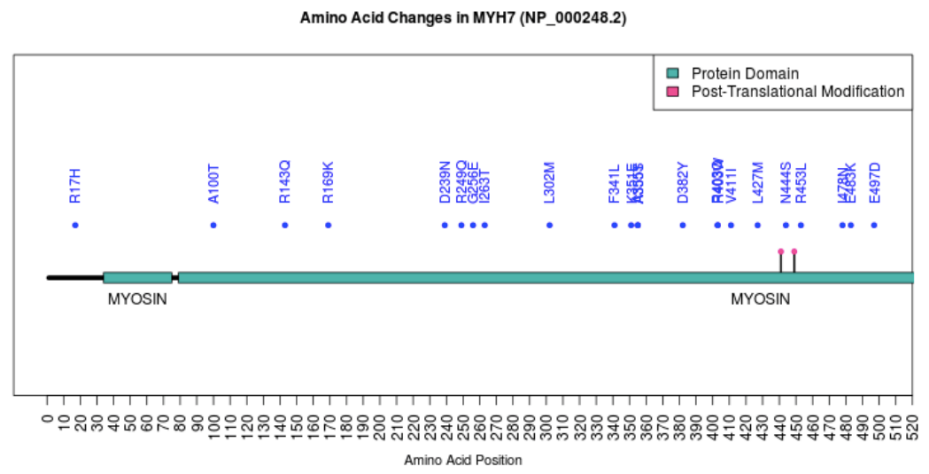
Amino Acid Changes in MYH7 (NP_000248.2)
Protein Domain
Post-Translational Modification
R17H
A100T
R143Q
R169K
D239N
L302M
F341L
D382Y
V411I
L427M
N444S
R453L
E497D
MYOSIN
MYOSIN
Amino Acid Position

B2

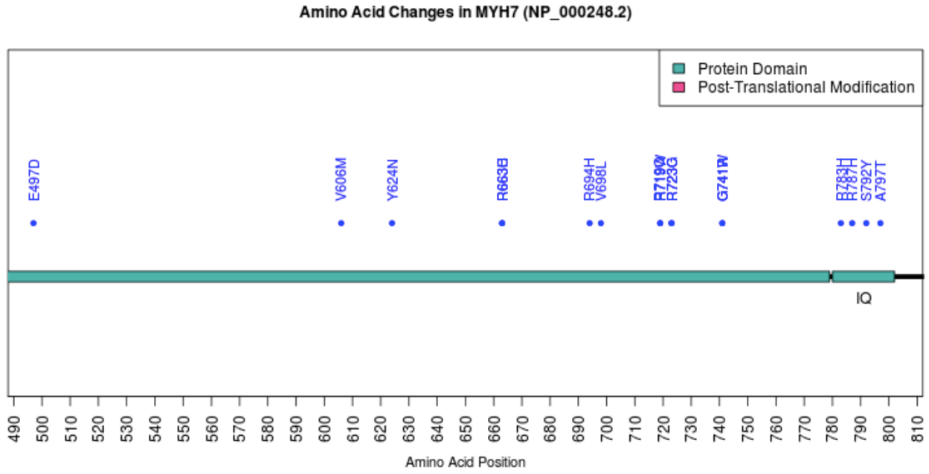
Amino Acid Changes in MYH7 (NP_000248.2)
Protein Domain
Post-Translational Modification
E497D
V606M
Y624N
R694H
V698L
S792Y
A797T
IQ
Amino Acid Position

B3

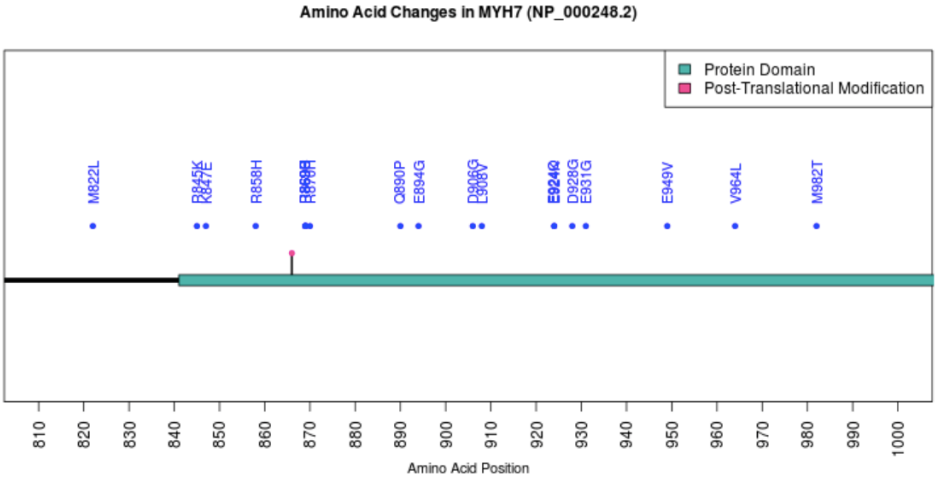
Amino Acid Changes in MYH7 (NP_000248.2)
Protein Domain
Post-Translational Modification
M822L
R858H
Q890P
E894G
D928G
E931G
E949V
V964L
M982T
Amino Acid Position

B4

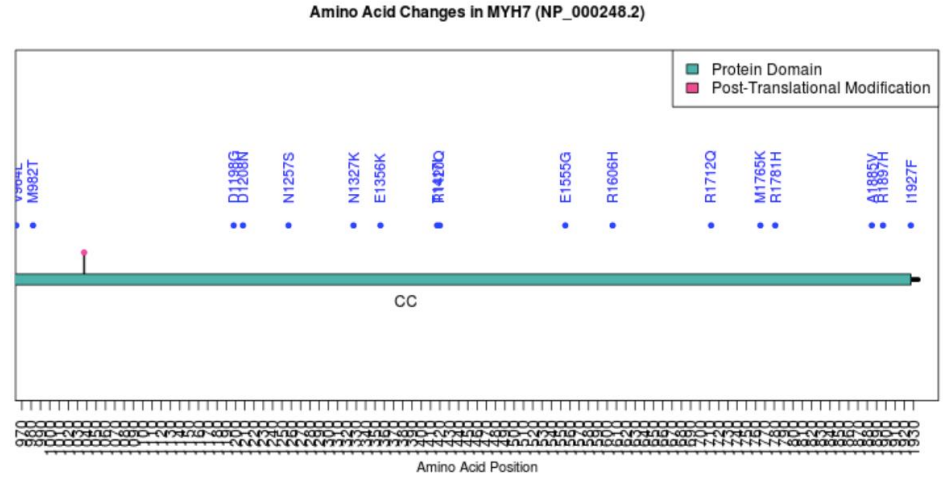
Amino Acid Changes in MYH7 (NP_000248.2)
Protein Domain
Post-Translational Modification
M982T
N1257S
N1327K
E1356K
E1555G
R1606H
R1712Q
M1765K
R1781H
I1927F
CC
Amino Acid Position

C

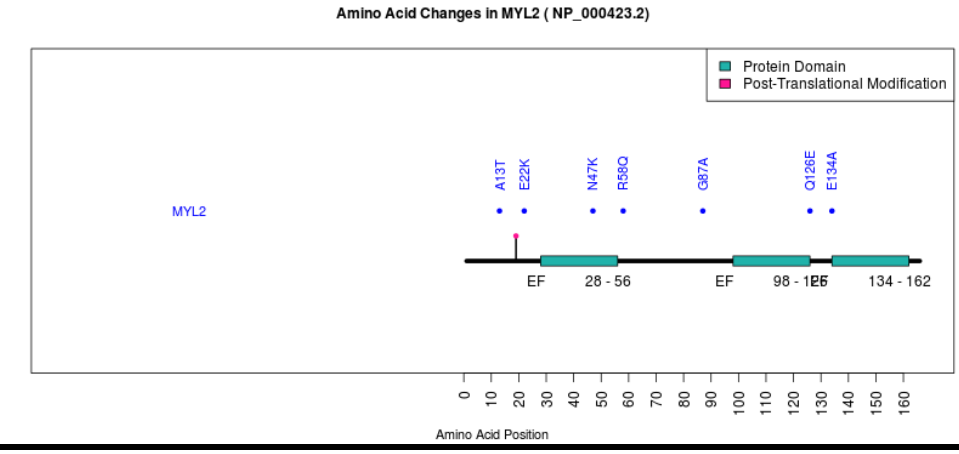
Amino Acid Changes in MYL2 (NP_000423.2)
Protein Domain
Post-Translational Modification
MYL2
A13T
E22K
N47K
R58Q
G87A
Q126E
E134A
EF
28 - 56
EF
134 - 162
Amino Acid Position

D

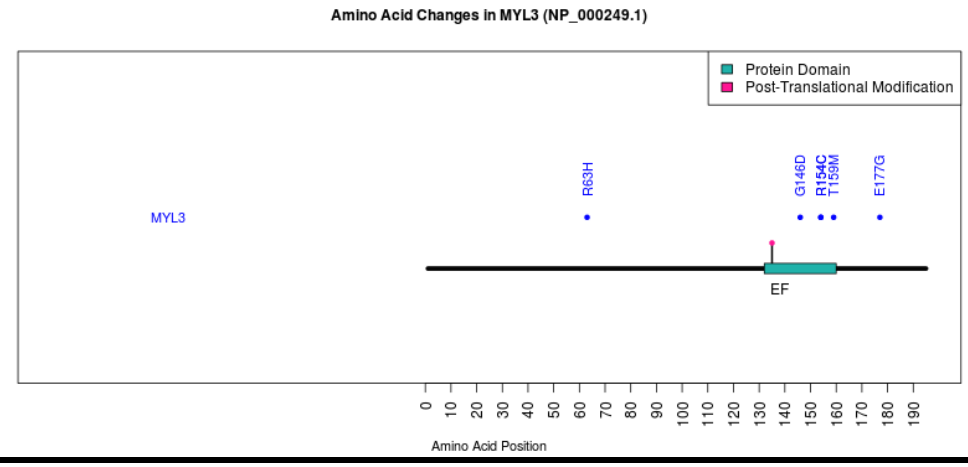
Amino Acid Changes in MYL3 (NP_000249.1)
Protein Domain
Post-Translational Modification
MYL3
R63H
G146D
R154C
T159M
E177G
EF
Amino Acid Position

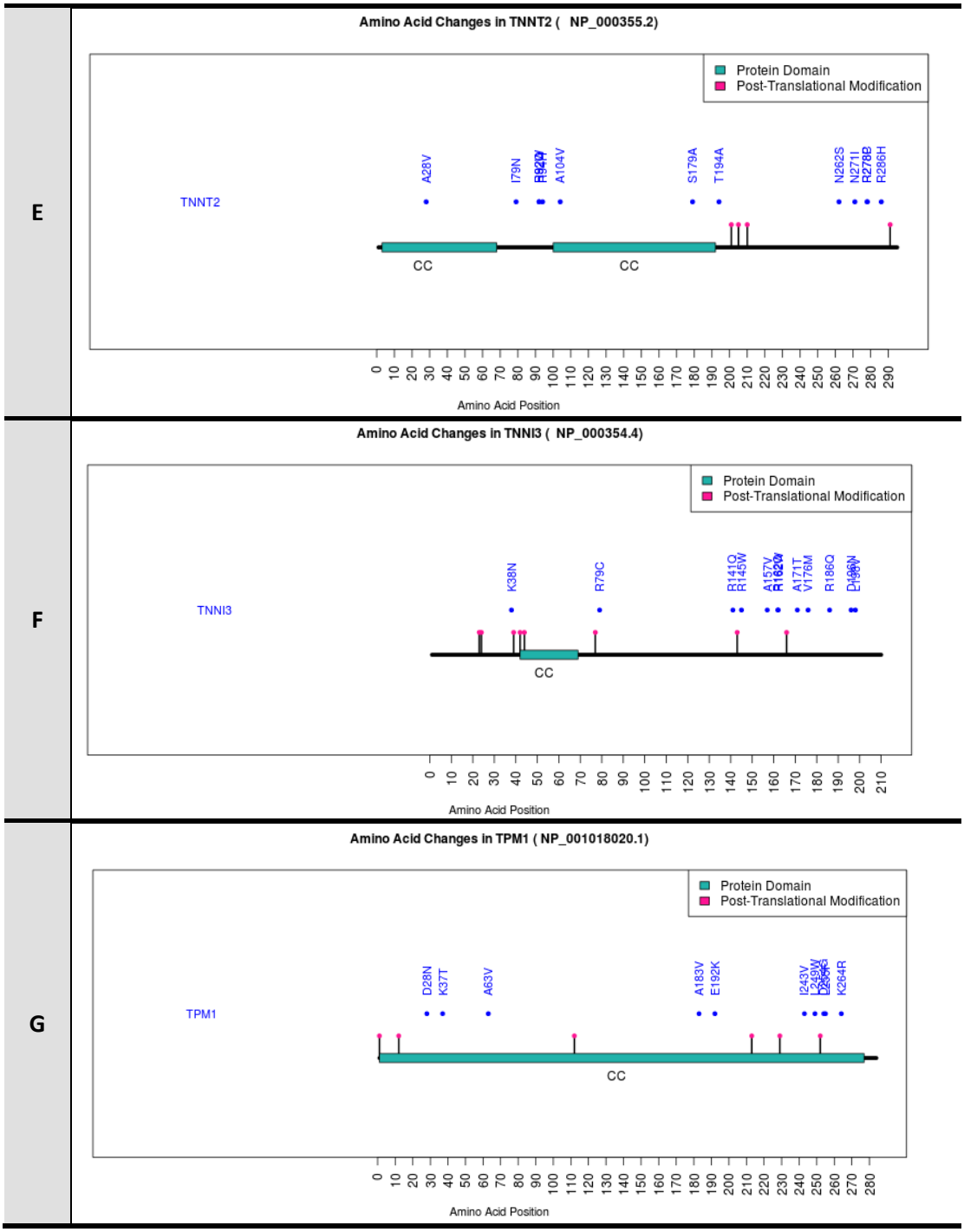

Figure 20. Illustrations of the distribution of mutations across the domains of seven of the eight main sarcomeric proteins. *ACTC1* is not represented due to the very low number of variants in that gene (three). For *MYBPC3* and *MYH7*, sub-panels are used in order to cover the entirety of the protein, given the high number of variants and the larger size of those two proteins. CC: coiled-coil; EF: EF-hand domain; IG: immunoglobulin domain; FN: fibronectin domain.

For *MYBPC3*, *MYH7*, *MYL2* and *MYL3* variants tended to be located in functionally annotated domains rather than inter-linker regions. In *MYH7* the great majority of variants reside in the myosin-head region and neck compared with the coiled-coil rod domain. For *TNNT2* and *TNNI3*, a clustering of variants was observed at the C-terminal region.

4.2. OTHER SARCOMERE AND ASSOCIATED GENES

Expanding the analysis to 19 sarcomeric and related / cytoskeletal genes previously associated with HCM or DCM – excluding the highly variable titin – resulted in the detection of 446 distinct rare variants in 549 patients (62.8%) at a 0.5% MAF cut-off. At a 0.2% MAF cut-off, 432 distinct variants were detected in 457 patients (52.3%). The number of variants found in each gene, as well as the predicted functional consequence, is summarised in **table 8**.

From the 446 variants, 163 (36.6%), present in 322 patients (36.9%), have been previously published as pathogenic mutations [297], [295], [296]. Ninety-eight (22.0%) were novel missense variants predicted *in silico* to be pathogenic and 57 (12.8%) were novel nonsense, frameshift insertion-deletions or splice-site variants predicted to cause loss-of-function (**table 8**). In total, a majority (71%) of these variants are strong candidates for pathogenicity and were present in 515 patients (58.9% of the cohort).

Fifty-nine rare (MAF≤0.5%) variants in *MYH6*, six previously published as disease-causing mutations [301], 5 predicted to cause loss-of-function and 26 predicted *insilico* to be pathogenic, were present in 85 patients (9.7%).

Table 8 Number of distinct rare variants in sarcomeric, Z-disc and calcium-handling genes (MAF cut-off 0.2%). Adapted with permission from [251].

Genes	Total number of distinct rare variants in each gene	Published	Novel	
			Misssense variants predicted *in silico* to be pathogenic	Nonsense, frameshift or splice- site variants predicted to cause loss-of-function
Sarcomere genes				
MYBPC3	126	64	14	32
MYH7	78	48	15	3
TNNI3	12	9	2	
TNNT2	20	13		4
MYL2	7	4	3	
MYL3	5		5	
ACTC1	3	1	1	
TPM1	13	3	4	1
Subtotal	**264**	**142**	**44**	**40**
Z disc/ sarcomere related, calcium handling				
MYH6	53	6	23	5
TNNC1	4		2	1
PLN	7		2	2
CSRP3	9	1	4	2
TCAP	7	1		
LDB3	13	5	2	1
VCL	20	3	4	1
PDLIM3	9		1	
DES	3		1	1
LMNA	9		1	1
RBM20	33	1	10	
Subtotal	**167**	**17**	**49**	**14**
TOTAL	**432**	**159**	**93**	**54**

Table 9 shows the distribution of patients according to the strength of the evidence supporting causality for the detected candidate variants.

Table 9. Level of evidence for the pathogenicity of the distinct variants ("others" – novel missense variants not predicted to be pathogenic *insilico*) . Adapted with permission from [251].

	N of patients (%)
Sarcomere genes (*MYH7, MYBPC3, TNNT2, TNNI3, MYL2, MYL3, ACTC1, TPM1*)	**411 (47.03%)**
Published mutation	291 (33.3%)
Loss of function / *insilico* predicted to be damaging	103 (54/49) (11.79%)
Others	17 (2.0%)
Other sarcomere and sarcomere-associated genes (titin excluded): *TNNC1, MYH6, VCL, CSRP3, DES, LDB3, LMNA, RBM20, TCAP, PLN, PDLIM3*	**138 (15.8%)**
Published mutation	31 (3.6%)
Loss of function/ *insilico* predicted to be damaging	90 (18/72) (10.3%)
Others	17 (1.9%)
Total	**549 (62.8%)**

4.3. First case – control analysis: comparison of nsSNPs between the first 223 HCM cases and UK10K controls

For the first 223 patients we combined non-synonymous single nucleotide polymorphims (nsSNPs) to test for an overall enrichment in HCM cases compared to the general population. For the control set and in a first phase, we used the UK10K exome sequence dataset (see Methods Section, chapter 3). To avoid technical artefacts associated with indel calling, and to properly match cases and controls, we restricted this analysis to nsSNPs and the first 180 HCM Caucasian HCM cases. Data for the 19 sarcomere and associated genes is summarised in **table 10** and for the eight sarcomere genes most commonly implicated in HCM in **figure 21**.

Four of the sarcomere genes (*MYH7, MYBPC3, TNNI3, TNNT2*) and also *PLN* showed an excess of rare nsSNP in cases compared to controls (two-tailed Fisher exact $P < 0.05$), which is consistent with the established causal role of rare nsSNPs in these genes. We used these case-control data to extrapolate the proportion of HCM cases in the general population explained by variants in each of these genes (see Methods Section, chapter 3 and **table 10**). Rare nsSNPs in *MYH7* explained the largest fraction, with between 9.6 and 20.7% of HCM cases (95% confidence interval (CI)). *MYBPC3* harbours a significant number of loss-of-function indels that are excluded in this first case-control analysis, therefore underestimating the contribution of *MYBPC3*.

Assuming that an excess of candidate variants in HCM cases reflects their disease-causing potential, these data can be used to estimate the probability that a candidate nsSNP found in a HCM case is disease causing (see Methods Section, chapter 3 and **table 10**). We found that these estimates are largely dependent of the genetic variability for each gene in the general population. As an example, nsSNPs in *MYH7* explain between 9.6 and 20.7% of HCM cases and a rare nsSNP in *MYH7* found in a HCM case is estimated to have 86% probability to be causal for HCM (**table 10**). Higher estimates are obtained for rare nsSNPs in the genes *TNNT2* and *TNNI3*, even though the contribution of these genes to HCM cases is lower. This is a consequence of the much lower presence of nsSNPs in these genes in the control population (0,3% and 0% respectively) compared to *MYH7* (2.5%) – **table 10**.

Table 10. Rare nsSNPs frequency comparison between my sequencing results and a set of 1,287 UK controls with exome sequence data generated by the UK10K project (www.uk10k.org) for 19 HCM/DCM associated genes. To avoid technical artefacts associated with indel calling, and to properly match cases and controls, we restricted this analysis to nsSNPs and the first 180 HCM UK Caucasian HCM cases. The columns show: the proportion of the 1,287 UK controls with exome sequence data generated by the UK10K project (www.uk10k.org) and 180 HCM cases that carry rare nsSNPs (rare defined by frequency less than 0.5% in the 1000 Genomes dataset), a Fisher exact test P-value to quantify the case-control difference, the 95% confidence interval for the estimated proportion of HCM cases explained by rare nsSNPs variants in each gene (Appendix C - additional statistical methods), and (in the rightmost column) the estimated probability that a rare nsSNP found in a HCM case in each gene is disease causing (Appendix C - additional statistical methods). nsSNP: nonsynonymous single nucleotide polymorphism; CI: confidence interval. Significant P-values in bold. Adapted with permission from [251].

Gene	Rare nsSNPs – Frequency in controls	Rare nsSNPs – Frequency in patients	P-value	95% CI for the proportion of cases explained	Probability that a nsSNP is causal
MYH7	0.025	0.172	**3.86E-13**	[0.0964-0.207]	0.856
TNNT2	0.003	0.044	**8.41E-05**	[0.0136-0.0708]	0.930
TNNI3	0.000	0.017	**0.002**	[0.00333-0.0415]	1.000
MYBPC3	0.045	0.106	**0.007**	[0.014-0.104]	0.570
PLN	0.001	0.022	**0.001**	[0.006-0.0498]	0.965
MYL2	0.007	0.022	0.065	[0-0.044]	NA
MYL3	0.004	0.011	0.208	[0-0.0301]	NA
ACTC1	0.001	0.006	0.230	[0-0.0167]	NA
TPM1	0.000	0.006	0.123	[0-0.0167]	NA
CSRP3	0.012	0.028	0.168	[0-0.0467]	NA
MYH6	0.053	0.056	0.608	[0-0.0501]	NA
DES	0.005	0.011	0.256	[0-0.0294]	NA
TNNC1	0.000	0.000	1.000	[0-0]	NA
LDB3	0.012	0.011	1.000	[0-0.0228]	NA
TCAP	0.004	0.000	1.000	[0-0]	NA
LMNA	0.005	0.000	1.000	[0-0]	NA
RBM20	0.061	0.056	0.871	[0-0.0361]	NA
PDLIM3	0.011	0.000	0.241	[0-0]	NA
VCL	0.038	0.028	0.677	[0-0.0244]	NA

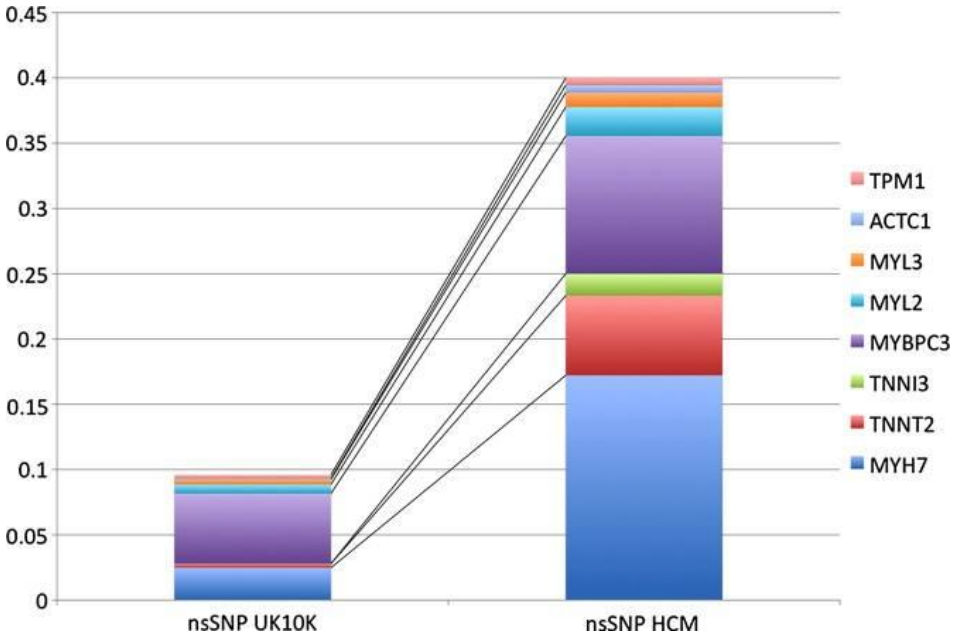

Figure 21 Rare nsSNPs frequency comparison between my sequencing results and a set of 1,287 UK controls with exome sequence data generated by the UK10K project (www.uk10k.org) for the 8 sarcomere genes most commonly associated with HCM. The frequency of *MYH7, MYBPC3, TNNT2* and *TNNI3* candidate nsSNPs is significantly higher in this cohort as also shown in table 10. nsSNP: nonsynonymous single nucleotide polymorphism. Reproduced with permission from [251].

4.4. SECOND CASE – CONTROL ANALYSIS: COMPARISON OF ALL TYPES OF VARIANTS BETWEEN ALL THE 874 HCM CASES AND UCL-EXOME CONTROLS

In a second phase, we compared the aggregated frequency of all types of rare variation in sarcomere and associated genes, between the total HCM cohort and the UCL-exome sequencing dataset. Because the sequencing methodology and also the variant calling and annotation pipeline are similar for the case and control population, the analysis was not restricted to nsSNPs.

The results were similar to the first case-control analysis and are summarized in **table 11** and **figure 22**. The same four sarcomere genes showed a significant difference between cases and controls, now with *MYBPC3* as the most significantly different, which is due to the inclusion of missense, splice-site and frameshift variants (and not only missense). In this second phase, *CSRP3* and *PLN* also showed a significantly higher prevalence of rare variants compared with controls.

Table 11. Case-control comparison for the frequency of very rare (MAF<0.2%) variants between the 874 cases and UCL-exome controls for sarcomere and associated genes, ordered by P-value. Significant P-values in bold. Adapted with permission from [251].

Gene	Ensembl ID	Frequency – cases	Frequency - controls	P-value
MYBPC3	ENSG00000134571	0,322	0,058	**4,23E-36**
MYH7	ENSG00000092054	0,148	0,030	**9,75E-19**
TNNT2	ENSG00000118194	0,038	0,005	**0,000000956**
TNNI3	ENSG00000129991	0,025	0,001	**0,00000409**
CSRP3	ENSG00000129170	0,016	0,005	**0,0151**
PLN	ENSG00000198523	0,007	0,001	**0,0377**
TPM1	ENSG00000140416	0,011	0,005	0,122
PDLIM3	ENSG00000154553	0,013	0,007	0,188
MYL2	ENSG00000111245	0,010	0,006	0,256
TNNC1	ENSG00000114854	0,005	0,002	0,26
MYL3	ENSG00000160808	0,007	0,004	0,299
MYH6	ENSG00000197616	0,075	0,068	0,329
ACTC1	ENSG00000159251	0,003	0,002	0,427
RBM20	ENSG00000203867	0,051	0,056	0,7
DES	ENSG00000175084	0,003	0,003	0,766
LMNA	ENSG00000160789	0,011	0,016	0,854
LDB3	ENSG00000122367	0,021	0,031	0,896
VCL	ENSG00000035403	0,030	0,040	0,909
TCAP	ENSG00000173991	0,012	0,021	0,939

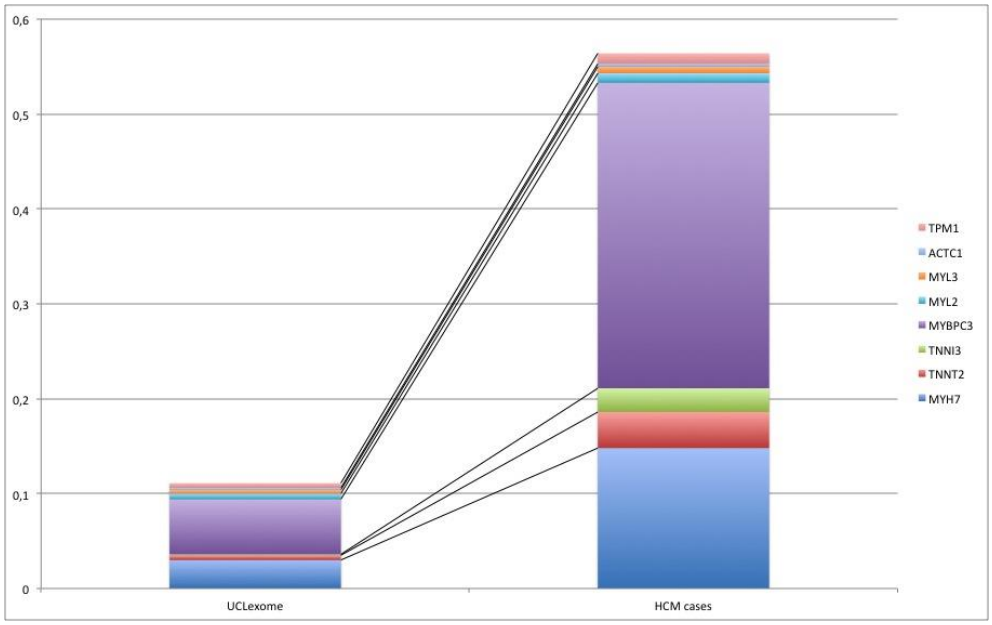

Figure 22. Rare variant (nsSNPs+LOFs+splice-site) frequency comparison between my sequencing results and the UCL-exome dataset as controls, for the eight sarcomere genes most commonly associated with HCM. The frequency of *MYH7, MYBPC3, TNNT2* and *TNNI3* candidate variants is significantly higher in this cohort, as also shown in table 11. Due to the inclusion of LOF and splice-site variants, the prevalence and statistical significance of *MYBPC3* variants increased compared to figure 21. Adapted with permission from [251].

4.5. RECURRENT VARIANTS IN HCM CASES

We also investigated whether nsSNP variants were found in multiple HCM cases, suggesting individual mutations as potentially common genetic causes of HCM.

For the first set of 223 patients, we found 3 rare nsSNPs for which the single SNP case-control P-value was less than 0.05 compared with the UK10K population, in *MYPC3*, *MYH7* and *TNNT2* (**table 12**). All were previously published as disease-causing mutations.

Table 12. Candidate variants present in the first 223 HCM cases for which the single nsSNP case-control P-value between HCM cases and UK10K controls was < 0.05. MAF: minor allele frequency. Adapted with permission from [251].

Gene	Amino acid change	N calls	Frequency in patients	UK10K MAF	P-value	Published as disease-causing
MYBPC3	NM_000256:c.G1484A:p.R495Q	3	0.008333333	0	0.001833766	Yes
TNNT2	NM_001001432:c.C296T:p.A104V	3	0.008333333	0	0.001833766	Yes
MYH7	NM_000257:c.G1988A:p.R663H	3	0.008333333	0	0.001833766	Yes

When analysing the whole cohort of 874 patients vs UCL-exome, four different individual variants showed a significant P-value for the difference between cases and controls, all in *MYBPC3* and all previously published. **Table 13**.

Table 13. Candidate variants present in 874 HCM cases for which the single case-control P-value between HCM cases and UCL-exome controls was < 0.05. MAF: minor allele frequency (results for MAF 0.2% are the same as for a cut-off of 0.5%). Adapted with permission from [251].

Gene	Amino acid change	N calls	MAF in patients	MAF in UCL-exome	P-value	Published as disease-causing
MYBPC3	NM_000256:c. C1504T:p.R502W	16	0.01038	0	1.8636 e-06	Yes
MYBPC3	NM_000256: c.1624+4A>T	15	0.01346	0.00132	0.000206	Yes
MYBPC3	NM_000256: c.G772A:p.E258K	9	0.00616	0	0.001613	Yes
MYBPC3	NM_000256: c.G655C:p.V219L	6	0.00442	0	0.009914	Yes

4.6. TITIN VARIANTS

Seven-hundred-and-twenty-nine rare (MAF <0.5%) titin variants were identified in 786 probands (89.9%). The distribution of rare *TTN* variants is shown in **figure 23**, illustrating a widespread distribution across the different regions.

One missense variant was previously described as pathogenic in HCM (R8500H) [51]. Twenty-seven variants (0.005% of the total number of *TTN* variants) were predicted to cause loss-of-function and were detected in 46 patients (5.3%): 6 were small frameshift insertions or deletions potentially leading to a truncated protein; 4 were nonsense variants that probably lead to the synthesis of a truncated protein and 17 more were splice-site variants predicted to cause exon skipping (list of titin variants provided in **Appendix E**).

Considering all *TTN* variants, four-hundred and twenty-eight patients (54% of the patients with *TTN* variants) carried a *TTN* rare variant in association with a variant in one of the eight main sarcomere protein genes. Three hundred and fifty eight patients (46%) had titin candidate variants in isolation or only in association with other sarcomere-related, desmosomal or ion channel disease associated gene variants.

From the 46 patients carrying potentially truncating variants**,** 20 patients (43%) carried the *TTN* variant together with a main causal sarcomere variant and 26 patients (57%) isolated or only associated with ion-channel/desmosome/sarcomere-associated genes.

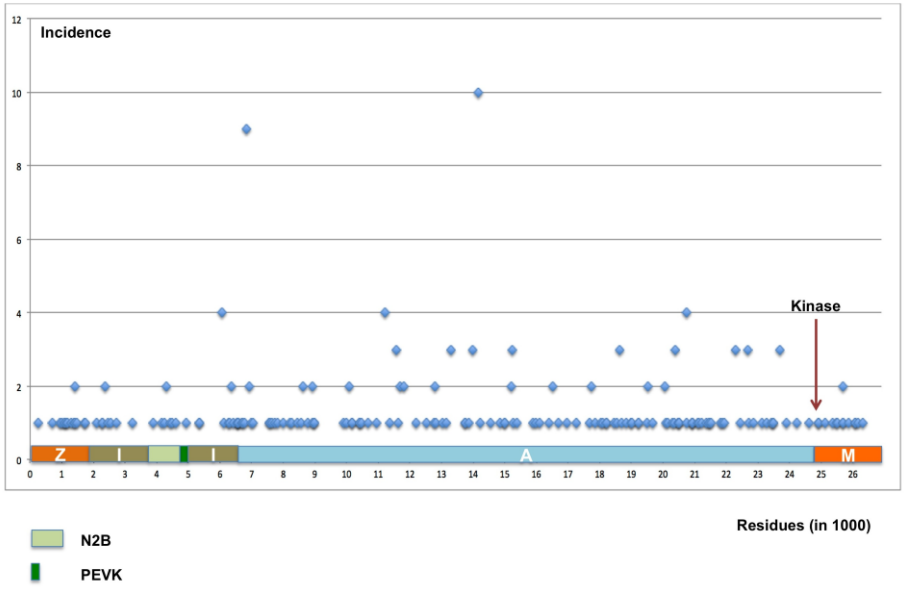

Figure 23. Distribution of titin rare variants along the multiple regions/domains of the protein. The N2B isoform is represented. Z: Z-disc region; I: I-band region; A: A-band region; M:M-band region.

Prioritization of TTN variants for further analysis

We prioritized 29 *TTN* variants, present in 29 patients, based on the physicochemical difference of the amino acid change, domain location, predicted structural effect and possible

impact on interaction with titin ligands. **Table 14**. This includes variants in A-band fibronectin (Fn3) and immunoglobulin (Ig) domains where homology modelling confidently suggests a disruptive effect on the protein fold due to the highly conserved position of the affected residues in the beta-barrel fold (e.g. L14984P in A72) or due to involvement of the highly conserved proline-rich first beta-strand of A-band Fn3 domains (e.g. P11209L in A34) but also such domains where frequent HCM-associated variants (occurrences of up to 9 in the cohort) are surface exposed or are unclassifiable due to weak existing homology models (e.g. S14161G in A63). One of these domains, A150, carries 2 missense mutations (I22692T and S22701F). In this same domain, clearly disrupting mutations have been identified in numerous families with the strictly skeletal muscle disease entity Human Myopathy with early Respiratory Failure (HMERF) [302, 303, 304].

Two variants were identified in the activation loop of the catalytic protein kinase domain of titin (P24914R and R24899H), suggesting that altered kinase activity might also contribute to the HCM phenotype (**figure 24**). Several clearly disruptive variants were identified in the Ig- and Fn3 domains immediately flanking the kinase-domain (e.g. a 4-residue insertion-deletion at 24709 in A170).

Table 14. Prioritized *TTN* variants and predicted effect.

Variant	Predicted effect
NM_003319:c.C41935T:p.P13979S	disruption of protein fold
NM_003319:c.G20528A:p.R6843H	surface exposed- ligand interaction
NM_003319:c.T68075C:p.I22692T	disruption of protein fold (A150 domain)
NM_003319:c.T44951C:p.L14984P	disruption of protein fold
NM_003319:c.C68102T:p.S22701F	disruption of protein fold (A150 domain)
NM_003319:c.C33626T:p.P11209L	highly conserved proline
NM_003319:c.G35080A:p.E11694K	surface exposed- ligand interaction
NM_003319:c.47401_47403del:p.15801_15801del	truncating
NM_003319:c.A3557T:p.D1186V	disruption of protein fold
NM_133378:c.G19937T:p.R6646I	disruption of protein fold
NM_003319:c.A64742G:p.N21581S	surface exposed- ligand interaction
NM_003319:c.C3910T:p.R1304C	surface exposed- ligand interaction
NM_003319:c.G74696A:p.R24899H	kinase domain
NM_133378:c.30508_30510del:p.10170_10170del	truncating
NM_003319:c.G77056C:p.A25686P	disruption of protein fold
NM_133379:c.C16321T:p.R5441X	truncating
NM_003319:c.G78524A:p.R26175Q	phosphorylation site
NM_003319:c.C26729G:p.T8910S	surface exposed- ligand interaction
NM_003319:c. c.C75076T:p.R25026W	kinase domain
NM_003319:c.C74741G:p.P24914R	kinase domain
NM_003319:c.16639_16644del:p.5547_5548del	truncating
NM_003319:c.T39904C:p.S13302P	disruption of protein fold
NM_003319:exon44:c.9977-4G>A	truncating
NM_003319:c.G23419C:p.A7807P	disruption of protein fold
NM_003319:c.G62231A:p.R20744Q	surface exposed- ligand interaction
NM_003319:c.74120_74121insAGCCTTCAG:p.K24707delinsKPSE	disrupting/flanking kinase domain
NM_003319:c.C26953T:p.R8985C	surface exposed- ligand interaction
NM_003319:c.A44954G:p.E14985G	surface exposed- ligand interaction
NM_003319:exon178:c.69998-3T>C	truncating

Some of the individual titin variants occur with a particularly high frequency in our cohort. We have therefore also looked for evidence of enrichment of those variants, as an indirect evidence of pathogenicity, comparing with the frequency of the same variants in the 1000 genomes population, to discard the possibility that the observed high prevalence in the HCM cohort could simply be due to high background variation in the general population. **Table 15**. Enriched variants were tested for genotype-phenotype correlations (chapter 5).

Table 15. Comparison between the frequency of individual *TTN* variants in this cohort and the 1000 genomes population, looking for enrichment. MAF: minor allele frequency. Variants with enrichment factor > 3 are represented.

Amino acid change	Frequency in 874 patients	per 1000	MAF in 1000 genomes	per 1000	Enrichment
S21937I	6	6.87	0.000459137	0.46	14.95
V20731M	5	5.72	0.000459137	0.46	12.46
P11209L	4	4.58	0.000459137	0.46	9.97
A23700G	4	4.58	0.000459137	0.46	9.97
A25686P	3	3.43	0.000459137	0.46	7.48
R6666C	9	10.30	0.00183655	1.84	5.61
S14161G	10	11.44	0.00229568	2.30	4.98
R8634H	4	4.58	0.000918274	0.92	4.98
R23683C	4	4.58	0.000918274	0.92	4.98
M10083V	2	2.29	0.000459137	0.46	4.98
R10163H	2	2.29	0.000459137	0.46	4.98
R19226C	2	2.29	0.000459137	0.46	4.98
G19307E	2	2.29	0.000459137	0.46	4.98
M26794T	2	2.29	0.000459137	0.46	4.98
R6843H	9	10.30	0.00229568	2.30	4.49
R23522H	3	3.43	0.000918274	0.92	3.74
R6707Q	5	5.72	0.00183655	1.84	3.12

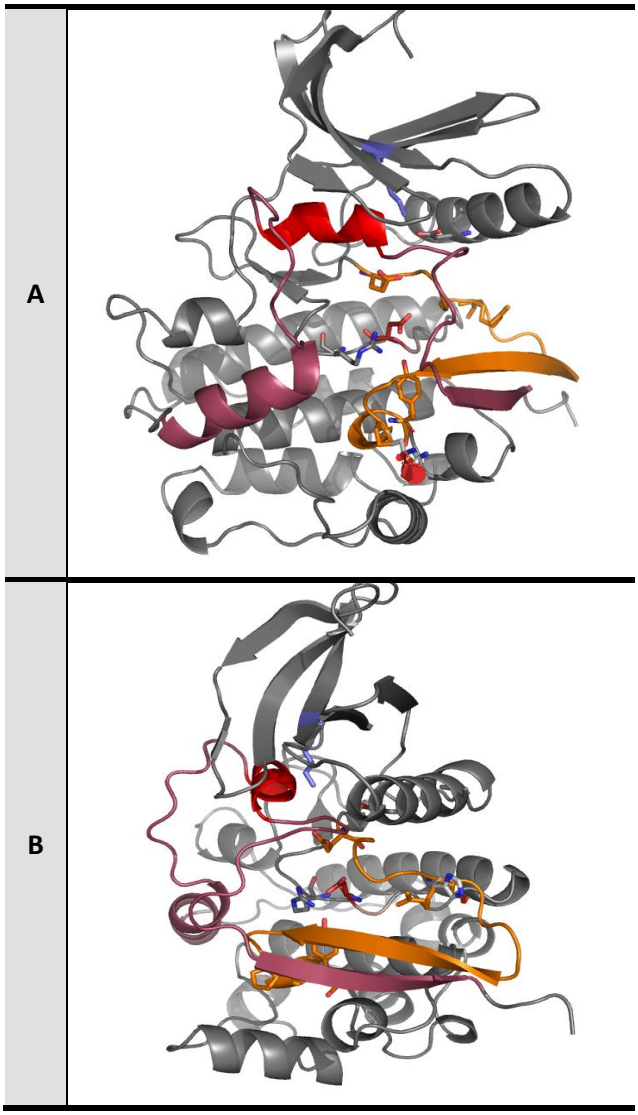

Figure 24. Structural modelling of the two *TTN* variants located in the activation loop of the kinase domain. A: P24914R: this variant is at the end of the activation loop segment and replaces a completely conserved proline with arginine (element-coded side chain; N= blue, C= white, O= red). The exchange is predicted to disrupt the turn at the position at the proline, and to result in a sterical clash; it is predicted to be disruptive (sterical clash shown as red volumes). Key residues in the active site are shown as stick models. Image generated using PDB entry 1TKI and PyMOL; B: R24899H: this variant is at the beginning of the activation loop segment and replaces a completely conserved arginine with histidine (element-coded side chain; N= blue, C= white, O= red). The exchanged residue is surface-exposed, and this variant is therefore structurally not disruptive; however, arginine 24899 is engaged in local salt bridges and hydrogen bonds, a minor destabilising local effect is possible. The loss of positive charge possibly affects the interaction with ligands like nbr1. Image generated using PDB entry 1TKI and PyMOL. (courtesy of Prof. Mathias Gautel, King's College London).

4.7. NON-SARCOMERE PROTEIN GENE VARIANTS

At a MAF cut-off of 0.5%, 132 rare ARVC associated variants were present in 193 patients (22.1%) and 210 ion-channel disease variants were found in 238 patients (27.2%). Thirty-seven (28.0%) of the ARVC associated and 46 (21.9%) of the ion-channel variants were previously published. A further 85 (24.9%) of these non-sarcomere variants were novel missense variants predicted *in silico* to be pathogenic and 24 (7%) were potential loss-of-function variants. In total, slightly over half of these non-sarcomere variants are predicted to have a biological effect. One-hundred-and-fifty-seven of the 371 patients (42.4%) carrying these non-sarcomere gene variants also carried variants in sarcomere or related genes.

At a MAF cut-off of 0.2%, one-hundred-and-fourteen distinct rare desmosomal protein gene variants were present in 122 (14.0%) patients and one-hundred-and-ninety-two rare ion-channel disease gene variants were present in 196 patients (22.4%). Twenty-nine (25.4%) of the desmosomal variants and 38 (19.8%) of the ion channel variants were previously published [305],[66],[306],[307],[308],[309],[310],[311],[312],[313],[314],[315],[316],[115],[317],[318]. A further 74 (24.2%) of these non-sarcomere variants were novel missense variants predicted *in silico* to be pathogenic and 20 (6.5%) were potential loss-of-function variants. In total, slightly over half these non-sarcomere variants are predicted to have a biological effect. One-hundred-and-twenty-two patients (43.0% of 284) with these non-sarcomere protein variants also carried a sarcomere protein variant.

Table 16 summarizes the number and type of variant in each non-sarcomere gene, while **table 17 and 18** illustrate the case-control comparison for the same genes, using the same methodology as for sarcomere genes. None of the non-sarcomere genes showed a statistically significant difference for the frequency of rare variation between cases and controls.

Table 16. Number of distinct rare variants in genes associated with arrhythmogenic cardiomyopathy and ion channel disease (MAF cut-off 0.2%). Adapted with permission from [251].

Genes	Total number of distinct rare variants in each gene	Published	Novel	
			Misssense variants predicted *in silico* to be pathogenic	Nonsense, frameshift or splice- site variants predicted to cause loss-of-function
Genes associated with arrhythmogenic cardiomyopathy				
DSC2	20	8	2	1
DSG2	20	10	4	1
PKP2	18	6	3	1
DSP	38	5	11	1
JUP	7		2	
TMEM43	6	2		
TGF-beta3	5	1		
Subtotal	**114**	**29**	**25**	**4**
Genes associated with ion-channel disease				
KCNQ1	15	5	1	1
KCNH2	15	2	4	
SCN5A	33	19	2	2
KCNE1	4	1		
KCNE2	6	4		1
KCNJ2	1			
ANK2	63	5	21	5
CASQ2	8		1	1
CAV3	2	1		
RYR2	45	1	20	6
Subtotal	**192**	**38**	**49**	**16**
TOTAL	**306**	**67**	**74**	**20**

Table 17. Rare nsSNPs frequency comparison between my sequencing results and a set of 1,287 UK controls with exome sequence data generated by the UK10K project (www.uk10k.org) for genes associated with arrhythmogenic right ventricular cardiomyopathy and ion channel disease. To avoid technical artefacts associated with indel calling, and to properly match cases and controls, we restricted this analysis to nsSNPs and the first 180 HCM UK Caucasian HCM cases. The columns show: the proportion of the 1,287 UK controls with exome sequence data generated by the UK10K project (www.uk10k.org) and 180 HCM cases that carry rare nsSNPs (rare defined by frequency less than 0.5% in the 1000 Genomes dataset) and a Fisher exact test P-value to quantify the case-control difference. nsSNP: nonsynonymous single nucleotide polymorphism; CI: confidence interval. Adapted with permission from [251].

Gene	Rare nsSNPs - Frequency in controls	Rare nsSNPs - Frequency in patients	P-value
DSP	0.040	0.061	0.240
ANK2	0.039	0.044	0.690
DSG2	0.040	0.044	0.842
KCNE1	0.004	0.006	0.544
KCNQ1	0.012	0.011	1.000
CAV3	0.001	0.000	1.000
TGFB3	0.002	0.000	1.000
KCNJ2	0.003	0.000	1.000
JUP	0.014	0.011	1.000
SCN5A	0.043	0.039	1.000
CASQ2	0.006	0.000	0.607
DSC2	0.034	0.028	0.828
TMEM43	0.013	0.006	0.716
KCNH2	0.014	0.006	0.500
KCNE2	0.019	0.000	0.064
PKP2	0.049	0.028	0.264
RYR2	0.068	0.028	0.037

Table 18. Case-control comparison for the frequency of rare (MAF<0.2%) variants between the 874 HCM cases vs UCL-exome samples as controls for ARVC associated and ion-channel genes, ordered by P-value (all non significant). Adapted with permission from [251].

Gene	Ensembl ID	Frequency cases	Frequency controls	P-value
TGFB3	ENSG00000119699	0,006	0,002	0,144
SCN5A	ENSG00000183873	0,054	0,043	0,168
ANK2	ENSG00000145362	0,090	0,082	0,318
KCNE2	ENSG00000159197	0,007	0,006	0,486
KCNQ1	ENSG00000053918	0,024	0,025	0,613
PKP2	ENSG00000057294	0,034	0,038	0,723
KCNH2	ENSG00000055118	0,034	0,040	0,737
KCNE1	ENSG00000180509	0,005	0,006	0,765
CASQ2	ENSG00000118729	0,009	0,012	0,784
CAV3	ENSG00000182533	0,004	0,005	0,795
TMEM43	ENSG00000170876	0,008	0,012	0,85
DSG2	ENSG00000046604	0,029	0,037	0,858
JUP	ENSG00000173801	0,011	0,016	0,86
DSC2	ENSG00000134755	0,036	0,050	0,929
RYR2	ENSG00000198626	0,059	0,077	0,94
KCNJ2	ENSG00000123700	0,001	0,006	0,988
DSP	ENSG00000096696	0,057	0,089	0,996

5. PHENOTYPE DATA AND GENOTYPE-PHENOTYPE ANALYSIS

Genotype-phenotype associations significant at a more stringent threshold (as defined in the Methods Section, chapter 5) are summarised in **table 19** and **figure 25.** Additional pairs of traits/genes with P-values < 0.05 are shown in **table 20** for sarcomere protein (SP) genes and **table 21** for non-SP genes.

5.1. EFFECT OF MUTATIONS IN SARCOMERE GENES

Patients with at least one variant in one of the eight main sarcomere genes were younger at diagnosis and had a higher frequency of a family history of HCM or sudden cardiac death compared to those without sarcomere variants. Patients with sarcomere protein mutations were more likely to have asymmetric septal hypertrophy than apical or concentric patterns and had greater maximum LV wall thickness. The prevalence of male sex was lower in sarcomere-positive individuals (62.4 vs 72.0%, P-value=0.00213). SP-positive individuals were also more likely to have an ICD implanted. Patients with sarcomere mutations had a lower resting systolic blood pressure (SBP) (123.1±19.2 vs 133.7±21.3mmHg, P-value=1.54×10^{-9}) and a lower systolic blood pressure response to exercise (44.1±21.5 vs 52.2±26.9 mmHg, P-value=7.61×10^{-5}).

Similar and additional associations were observed when individual SP genes were considered (**table 19 and 20**).

The proportion of cardiovascular deaths during follow-up was higher in patients with at least one variant in one of the eight main sarcomere genes. The same was true for sudden death/aborted sudden cardiac death (**figure 26**). For individual genes, a decreased survival in the presence of *MYBPC3* variants was detected, when analysing the SCD end-point modelled for time from birth, but not when modelled for time of follow-up from first evaluation. The presence of rare variation in *MYH7* was significantly associated with an increased incidence of cardiovascular death when modelled for time from birth. Carriers of a rare *TNNT2* variant had a worse prognosis due to an increased incidence of cardiovascular death during follow-up, either modelled for age or for follow-up time. Survival curves for significant associations with

individual sarcomere genes are shown in **Figure 27**.

5.2. PATIENTS WITH MULTIPLE SARCOMERE PROTEIN GENE VARIANTS

Patients that carried more than one sarcomere variant had an increased prevalence of syncope when compared to individuals with only one sarcomere variant (35.1% vs 16.6%; 13/37 vs 56/337, P-value= 0.012). Systolic blood pressure (BP) response to exercise was lower in individuals with multiple sarcomere variants compared to a single variant (36.5±21.9 vs 45.1±21.2 mmHg, P-value=0.012) and there was a higher proportion of patients with an an abnormal blood pressure response to exercise (10/29 vs 39/276; 34.5% vs 14.1%, P-value=0.010). Finally, there was a tendency towards an increased proportion of ICDs implanted at baseline and during follow-up, amongst multiple variant carriers (42.3%; 11/26) vs single variant carriers (22.9%; 58/253), P-value=0.053. No other phenotype traits were significantly different for multiple SP variant individuals. Survival differences between multiple and single variant carriers are described in the sub-chapter 5.4 below.

5.3. ASSOCIATIONS WITH RARE VARIANTS IN DESMOSOMAL AND ION CHANNEL GENES

Seventy-one patients carried rare *ANK2* variants (of these, 36 also carried sarcomere protein variants). At a significance threshold of $P < 0.0018$, there was a higher proportion of patients with a maximum left ventricular wall thickness ≥30 mm amongst carriers of an *ANK2* rare variant (**Table 19**).

Additional phenotype-genotype correlations for non-sarcomere protein genes were identified at a less stringent $P < 0.05$. These are listed in **Table 21**, and include an increased mean MLVWT in *ANK2* variant carriers.

5.4. COMPARISONS BETWEEN SARCOMERIC GENES

MYH7 patients were characterized by a lower fractional shortening (37.19±8.48%) compared with patients harbouring all types of *MYBPC3* variants (39.71±8.85%, P-value=0.016) and with

the patients carrying *MYBPC3* loss-of-function (LOF) variants (40.24±8.87%, P-value=0.010). The blood pressure response to exercise was lower in the presence of *MYH7* rare variation (36.08±19.80mmHg) compared with the effect of any *MYBPC3* (46.60±21.60mmHg,P-value<0.0005) or *MYBPC3* LOF variation (48.97±22.19mmHg, P-value=0.008). *MYH7* patients had a longer QRS duration (103.57±24.03 msecs) compared to patients carrying any *MYBPC3* variant (94.08±14.58 msecs, P-value=0.004) or LOF variants (94.49±14.57 msecs, P-value=0.008). Left atrial size was larger at last evaluation in *MYH7* patients compared to individuals carrying any type of *MYBPC3* rare variant (45.86±9.13 vs 43.43±7.06 mm, P-value=0.011) or *MYBPC3* LOF variants (43.44±7.30 mm, P-value=0.034).

There were no other significant differences in the evaluated clinical parameters between patients carrying mutations in different sarcomeric protein genes.

Survival was compared between carriers of *MYBPC3* variants, carriers of *MYH7* variants, carriers of variants in both genes (double heterozygotes) and individuals without candidate variants in any of those two genes. **Figure 28**. No difference was observed between *MYBPC3* and *MYH7*. However, carriers of variants in both genes had a significantly reduced survival compared to none or each of the genes, either for cardiovascular death or for SCD, if modelled for time from birth. When survival was modelled for follow-up time, survival analysis showed the same significant difference between carrying variants in both genes vs none, but only the comparison between double heterozygozity vs *MYBPC3* reached statistical significance.

5.5. GENOTYPE-PHENOTYPE ASSOCIATIONS FOR VARIANTS PREDICTED *IN SILICO* TO BE PATHOGENIC

When repeating all the above comparisons for the variants that were predicted *insilico* to be pathogenic, no additional genotype-phenotype associations were revealed.

5.6. COMPARISONS WITHIN SARCOMERE POSITIVE INDIVIDUALS ONLY

By repeating all the above comparisons only within the sub-cohort of individuals that carry rare variants in sarcomere protein genes, no additional genotype-phenotype associations were found.

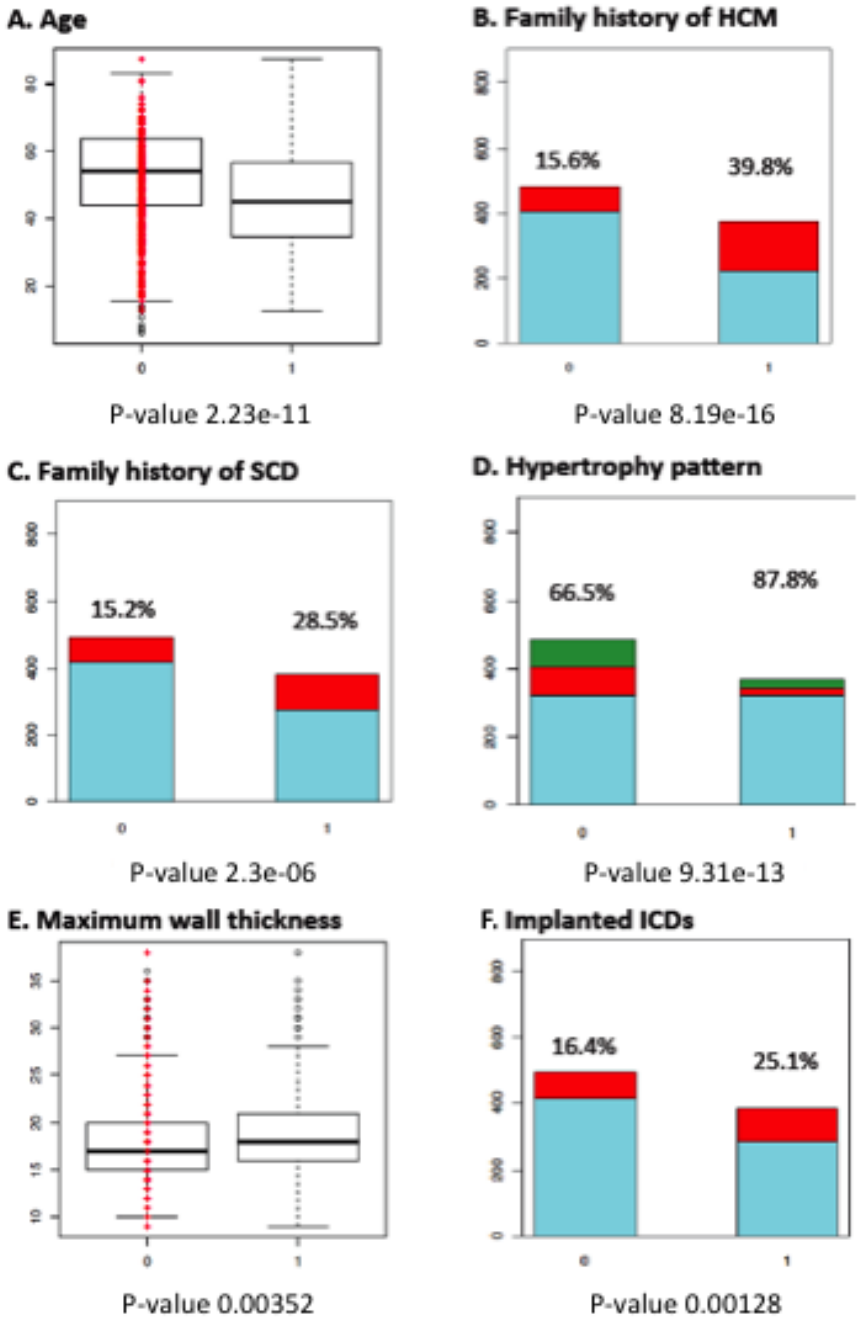

Figure 25. Comparison between sarcomere gene mutation-positive and negative patients. A. Age at initial evaluation (45.78±14.65 vs 53.05±14.94 years). B. Family history of HCM. C. Family history of SCD. D. Hypertrophy pattern. E. Maximum wall thickness (18.83±4.42 vs 18.12±4.08 mm). F. Implanted ICDs. Key: 0:sarcomere-negative; 1: sarcomere-positive. For B, C, F: red colour and percentages indicate the individuals with the trait within each genotype; for D light blue – asymmetric septal hypertrophy; red – apical hypertrophy; green – concentric hypertrophy.

Table 19. Genotype-phenotype associations for individual sarcomeric and related protein genes and non-sarcomere protein genes, meeting the predefined stringent statistical thresholds for multiple testing. P-values reflect the comparison for proportions or means, between the group of patients with versus the group of patients without a rare variant in a given gene (P-value thresholds of < 0.0056 for SP genes and < 0.0018 for non-SP genes). HCM: hypertrophic cardiomyopathy; SCD: sudden cardiac death; ASH: asymmetric septal hypertrophy; MLVWT: maximum left ventricular wall thickness; LV: left ventricle; LA: left atria; BP: blood pressure; LVOTO: left ventricular outflow tract obstruction.

Phenotype	Gene	Frequency or mean ± standard deviation Variant present	Frequency or mean ± standard deviation Variant absent	P-value
Age at initial evaluation (years)	*MYBPC3*	45.5±14.4	51.0±15.5	8.97×10^{-6}
	MYH7	43.9±15.4	50.5±15.2	1.91×10^{-5}
Family history of HCM	*MYBPC3*	40.4% (86/213)	21.9% (140/640)	2.7×10^{-7}
	MYH7	47.4% (54/114)	23.4% (173/740)	3.06×10^{-7}
Family history of SCD	*MYBPC3*	28.7% (62/216)	18.3% (120/656)	0.001
	MYH7	31.6% (37/117)	19.2% (145/775)	0.003
ASH pattern	*MYBPC3*	88.0% (184/209)	71.6% (459/641)	3.75×10^{-6}
	MYH7	89.2% (99/111)	73.6% (544/739)	0.001
MLVWT (mm)	*MYBPC3*	19.4±4.7	18.2±4.2	0.0005
MLVWT >30mm	*ANK2*	12.5% (6/48)	2% (11/553)	0.0005
LV end-diastolic diameter (mm)	*MYBPC3*	44.8±5.5	46.3±6.0	0.00089
LV end-systolic diameter (mm)	*MYBPC3*	27.4±6.0	28.8±5.4	0.005
LA diameter (mm)	*RBM20*	40.9±6.8	44.2±7.5	0.00239
Right ventricular hypertrophy	*TNNI3*	50% (10/20)	21.6% (174/806)	5.49×10^{-6}
BP response to exercise (mmHg)	MYH7	36.6±19.9	50.2±24.4	0.002
Abnormal BP response to exercise	*TNNT2*	40.9% (9/22)	13% (83/640)	3.0×10^{-4}
Myectomy and/or alcohol septal ablation and/or pacemaker	*MYBPC3* (splicing variants)	43.1% (22/51)	20.0% (160/799)	0.005

implantation for gradient reduction				
LVOTO (>30 mmHg)	*TNNI3*	10% (2/20)	41.2% (326/792)	5.49×10^{-6}

Table 20. Additional genotype-phenotype associations for individual sarcomere protein and related genes, with P-values <0.05, but not meeting the predefined threshold for significance, if correcting for multiple comparisons. P-values reflect the comparison for proportions or means, between patients with and without a rare variant in a given gene. HCM: hypertrophic cardiomyopathy; NYHA: New York Heart Association; LA: left atria; MLVWT: maximum left ventricular wall thickness; LV: left ventricular; ASH: asymmetric septal hypertrophy; LVOT: left ventricular outflow tract; LVOTO: left ventricular outflow tract obstruction; SCD: sudden cardiac death; BP: blood pressure.

Phenotype	Gene	Frequency or mean±standard deviation - Variant present	Frequency or mean±standard deviation – Variant absent	P-value
Age at initial evaluation (years)	*TNNT2*	43.5±14.7	49.8±15.4	0.031
	CSRP3	56.7±8.1	49.5±15.5	0.006
	VCL	43.2±17.6	49.8±15.3	0.0361
LV end-diastolic diameter (mm)	*RBM20*	43.6±5.2	46.1±6.0	0.00431
Fractional shortening (%)	*MYBPC3*	39.7±8.9	38.2±8.8	0.026
LV systolic dysfunction	*TNNI3*	15.8% (3/19)	3.2% (26/810)	0.020
ASH pattern	*MYH6*	81.2% (56/69)	75.2% (587/781)	0.025
Moderate-severe mitral regurgitation	*MYL2*	55.6% (5/9)	19.4% (158/814)	0.041
LVOT gradient (mmHg)	*TNNI3*	13.1±26.6	34.8±41.3	0.002
Family history of SCD	*TPM1*	62.5% (5/8)	20.5% (177/864)	0.012
Abnormal BP response to exercise	*MYH7*	22.5% (20/89)	12.6% (72/573)	0.020
Syncope	*MYH7*	22.8% (26/114)	15.4% (114/742)	0.045

Implanted cardioverter-defibrillator at baseline and during follow-up	*MYH7*	28.2% (33/117)	19.2% (145/756)	0.027

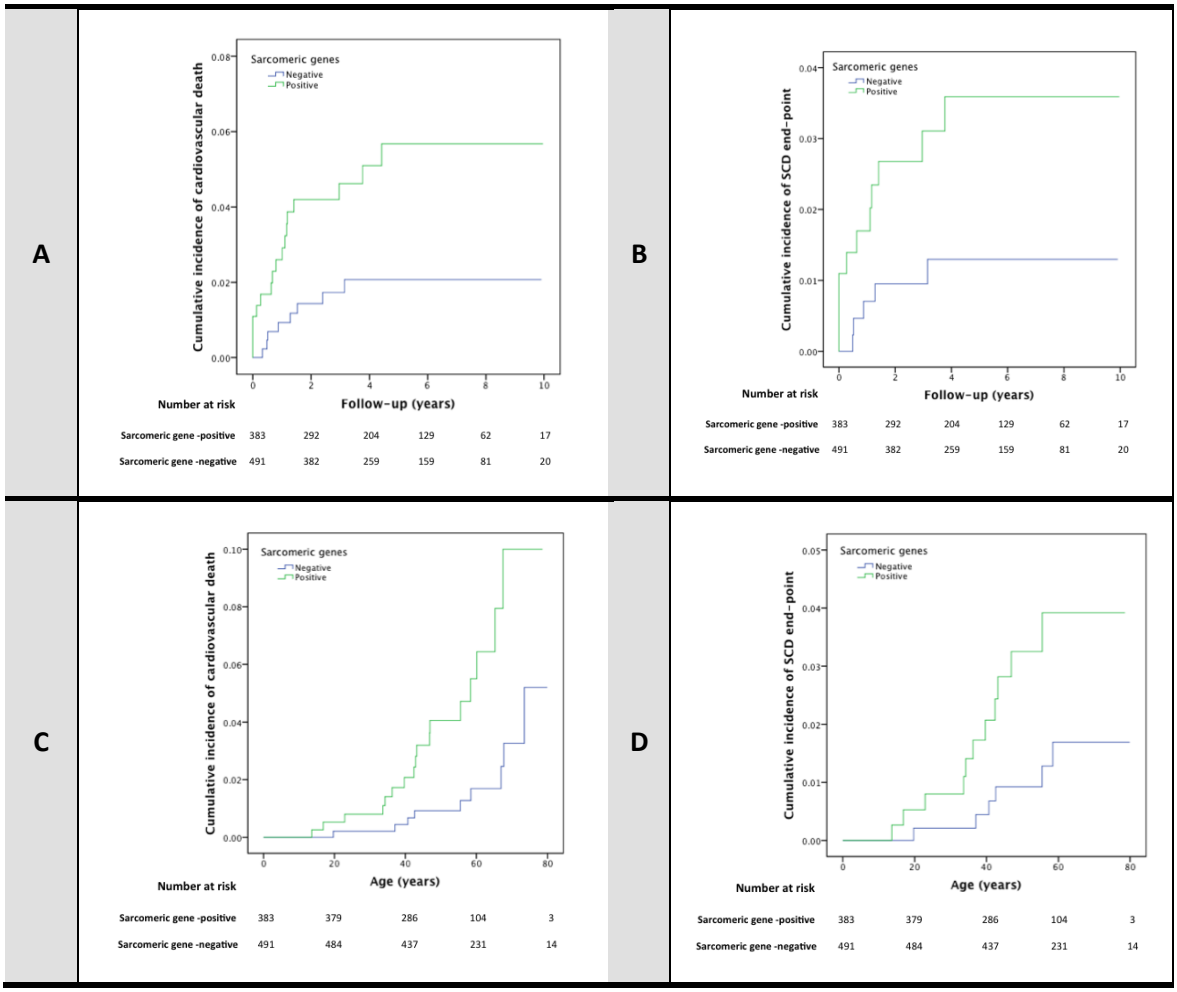

Figure 26. Kaplan-Meier cumulative incidence curves for cardiovascular death and SCD endpoint (see Methods Section), comparing sarcomere positive and sarcomere negative individuals. Modelled for follow-up from first evaluation (years): A: cardiovascular death, log-rank test P-value=0.012 (HR: 2.81; 95% CI:1.21-6.51); B: SCD/aborted SCD: log-rank test P-value=0.039 (HR: 2.89; 95% CI:1.01-8.33). Modelled for time from birth (years): C: cardiovascular death, log-rank test P-value=0.001 (HR: 3.99; 95% CI: 1.71-9.36); D: SCD/aborted SCD, log-rank test P-value=0.028 (HR: 3.44; 95% CI: 1.19-9.92). Y axis values indicate proportions.

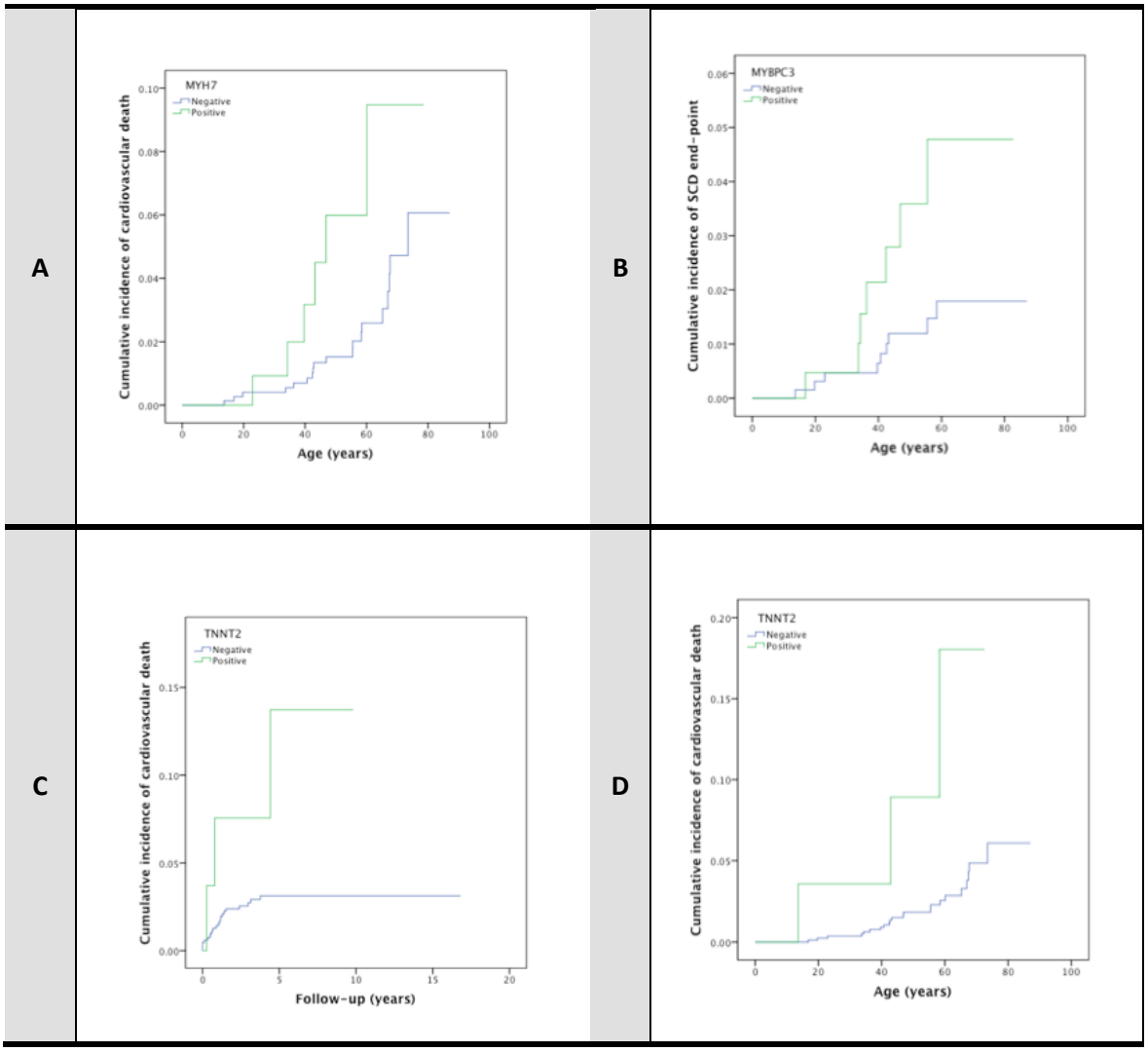

Figure 27. Kaplan-Meier cumulative incidence curves for cardiovascular death and SCD endpoint (see Methods Section), comparing individuals with versus without a candidate variant in individual sarcomeric genes. A: Cumulative incidence of cardiovascular death, modelled for time from birth (years), for *MYH7* positive vs negative patients, log-rank test P-value=0.022 (HR: 2.80; 95%CI:1.20-7.05). B: Cumulative incidence of SCD end-point, modelled for time from birth (years), for *MYBPC3* positive vs negative patients, log-rank test P-value=0.036 (HR: 2.77; 95%CI:1.03-7.45). C: Cumulative incidence of cardiovascular death, modelled for follow-up from first evaluation (years), for *TNNT2* positive vs negative patients, log-rank test P-value=0.016 (HR: 3.92; 95%CI:1.17-13.12). D: Cumulative incidence of cardiovascular death, modelled for time from birth (years), for *TNNT2* positive vs negative patients, log-rank test P-value=0.002 (HR: 5.46; 95%CI:1.62-18.39).

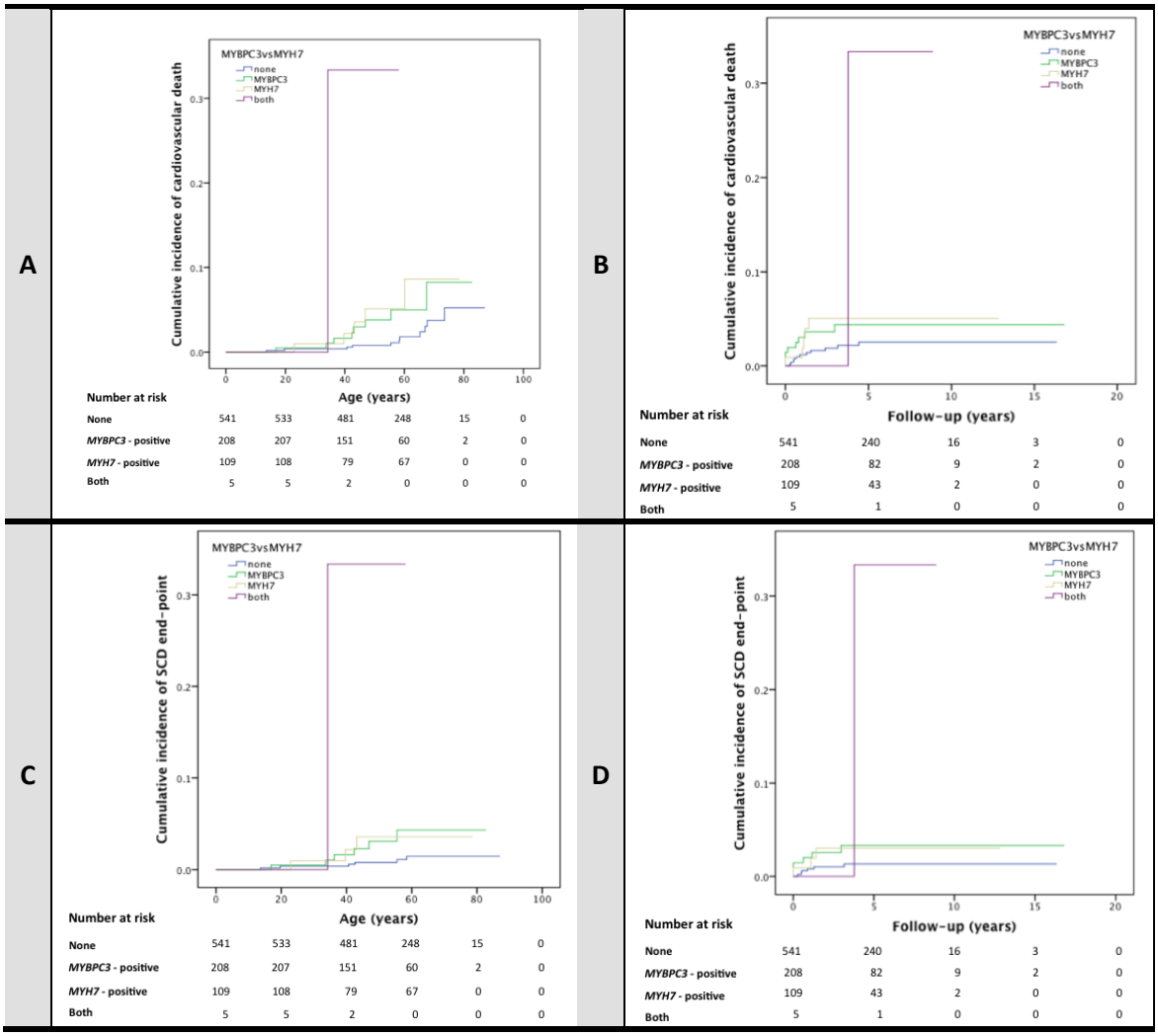

Figure 28. Kaplan-Meier cumulative incidence curves for cardiovascular death and SCD endpoint (see Methods Section), comparing carriers of rare variants in *MYH7*, *MYBPC3*, none or both genes. A: cardiovascular death, modelled for time from birth (years), log-rank test P-value=0.028 for none vs *MYBPC3*; P-value=0.018 for none vs *MYH7*; P-value<0.0005 for none vs both; P-value=0.693 (NS) for *MYH7* vs *MYBPC3*; P-value=0.009 for *MYBPC3* vs both; P-value=0.023 for *MYH7* vs both. B: cardiovascular death, modelled for follow-up from first evaluation, log-rank test P-value=0.139 (NS) for none vs *MYBPC3*; P-value=0.121 (NS) for none vs *MYH7*; P-value=0.007 for none vs both; P-value=0.815 (NS) for *MYH7* vs *MYBPC3*; P-value=0.101 (NS) for *MYBPC3* vs both; P-value=0.180 (NS) for *MYH7* vs both. C: SCD end-point, modelled for time from birth (years), log-rank test P-value=0.074 (NS) for none vs *MYBPC3*; P-value=0.188 (NS) for none vs *MYH7*; P-value<0.0005 for none vs both; P-value=0.917 (NS) for *MYH7* vs *MYBPC3*; P-value=0.045 for *MYBPC3* vs both; P-value=0.061 (NS) for *MYH7* vs both. D: SCD end-point, modelled for follow-up from first evaluation (years), log-rank test P-value=0.036 for none vs *MYBPC3*; P-value=0.095 (NS) for none vs *MYH7*; P-value<0.0005 for none vs both; P-value=0.983 (NS) for *MYH7* vs *MYBPC3*; P-value=0.005 for *MYBPC3* vs both; P-value=0.014 for *MYH7* vs both.

Table 21. Genotype-phenotype associations for non-sarcomeric protein genes not meeting the predefined statistical thresholds for multiple testing. P-values reflect the comparison for proportions or means, between the group of patients with versus the group of patients without a rare variant in a given gene. LA: left atria; LVOTO: left ventricular outflow tract obstruction; MLVWT: maximal left ventricular wall thickness; E/e´ratio: ratio between the maximal velocity of the E wave from the pulsed wave Doppler of the transmitral flow and the maximal velocity of the e' wave of tissue Doppler at the mitral annulus; NSVT: non-sustained ventricular tachycardia.

Phenotype	Gene	Frequency or mean±standard deviation - Variant present	Frequency or mean±standard deviation - Variant absent	P-value
LA diameter at the final follow-up (mm)	*SCN5A*	46.9±5.4	44.3±7.5	0.0418
LVOTO (>30 mmHg)	*SCN5A*	57.5% (23/40)	39.5% (305/772)	0.031
	Ion-channel	49.2% (89/181)	37.9% (239/631)	0.00595
MLVWT (mm)	*ANK2*	19.7±5.6	18.4±4.2	0.0152
E/e'	*CASQ2*	16.4±7.1	11.4±5.9	0.016
NSVT	*PLN*	100% (3/3)	22.1% (124/562)	0.011

5.7. LOGISTIC REGRESSION ANALYSIS AND CONSTRUCTION OF A MODEL AND SCORE TO PREDICT THE PRESENCE OF A SARCOMERE GENE MUTATION

Based on the previously described significant associations between phenotype traits and the presence of a rare variant in any of the 8 main SP genes, the variables selected to enter the model were: age at presentation, gender, family history of HCM, family history of SCD, left ventricular hypertrophy pattern (asymmetric septal hypertrophy vs others) and maximal left ventricular wall thickness (MLVWT).

Age was transformed into a categorical variable by using ROC curve analysis, which defined a cut-off of 50 years of age (AUC 0.643; sensitivity 60%; specificity 62%). MLVWT was also transformed into a categorical variable, with a cut-off of 17 mm defined by ROC curve analysis (AUC 0.556; sensitivity 60%, specificity 50%).

By multivariate logistic regression analysis, all the variables, with the exception of MLVWT, were still significantly associated with a SP-positive genotype and were retained in the model. **Table 22**.

Table 22. Multivariate logistic regression model for the presence of a rare variant in a SP gene. FH HCM: family history of hypertrophic cardiomyopathy; FH SCD: family history of sudden cardiac death; MLVWT: maximal left ventricular wall thickness; ASH: asymmetric septal hypertrophy; OR: odds ratio; CI: confidence interval.

					95% CI for OR	
		B	P-value	OR	Lower	Upper
Model 1	**Male**	-.442	0.007	.643	.467	.885
	FH HCM	.868	<0.0005	2.382	1.665	3.407
	FH SCD	.352	0.071	1.422	.970	2.087
	MLVWT≥17mm	.244	0.127	1.276	.933	1.747
	Age≥50	-.723	<0.0005	.485	.356	.661
	ASH	1.004	<0.0005	2.730	1.857	4.013
Model 2	**Male**	-.434	0.008	.648	.471	.891
	FH HCM	.852	<0.0005	2.343	1.640	3.348
	FH SCD	.342	0.079	1.408	.961	2.065
	Age≥50	-.739	<0.0005	.478	.351	.650
	ASH	1.046	<0.0005	2.846	1.944	4.167

As described in the methods, the weighted score for each variable was calculated from the regression coefficients and were as follows: male sex: -1; family history of HCM: 3; family history of SCD: 1; ASH: 3; age ≥ 50: -2.

Applying the score to the cohort, ROC curve analysis showed a reasonable AUC of 0.723 for the model, with a sensitivity of 77% and specificity of 55%, and a cut-off of 0.5 to predict a positive genotype. **Figure 29**.

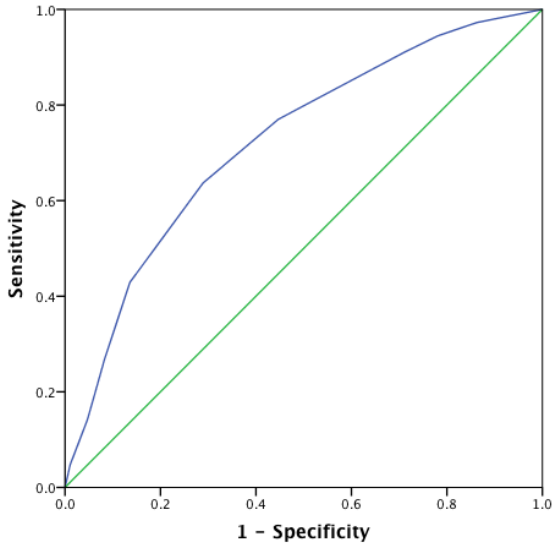

Figure 29. ROC curve analysis evaluating the diagnostic accuracy of the proposed model to predict the presence of a sarcomere variant.

5.8. TITIN GENOTYPE-PHENOTYPE ASSOCIATIONS

5.8.1. COMPARISON OF MEANS AND PROPORTIONS FOR THE DIFFERENT PHENOTYPIC TRAITS

Carriers of rare *TTN* variants were younger than patients without those variants : 49.37±15.27 vs 54.44±14.31, P-value=0.003 and had an increased incidence of ICD implantation during follow-up: 21.2% (162/763) vs 12.1% (12/99), P-value=0.033.

The presence of a potential loss-of-function (LOF) or splice-site variant in TTN was associated with poorer left ventricular systolic function (fractional shortening 35.3±7.0% vs 38.5±8.3%, P-value=0.012).

There was a higher prevalence of males among carriers of an enriched (as defined by an enrichment factor > 3, listed in chapter 4.6, table 15) variant (84.1% vs 66.5%, p = 0.003),

which were also characterized by a higher maximal LV wall thickness (19.4 ±4.7 vs 18.4±4.3 mm, p =0.023).

No other phenotype parameter was significantly different in the presence of a LOF, enriched or any *TTN* rare variant, either analysed for a cut-off of 0.5% or 0.2%.

5.8.2. DISCRIMINANT ANALYSIS AND LOGISTIC REGRESSION ANALYSIS

To reveal additional genotype-phenotype associations, a linear discriminant analysis and logistic regression was conducted to predict whether a patient was a carrier of a titin variant.

All TTN rare variants

No linear discriminant function was found as being able to significantly discriminate carriers vs non-carriers of a rare titin variant. Logistic regression analysis reproduced the previous findings regarding age and implantated ICDs.

TTN potentially truncating variants

A linear discriminant function significantly discriminated carriers of potentially truncating variants vs non-carriers (**Figure 30**).

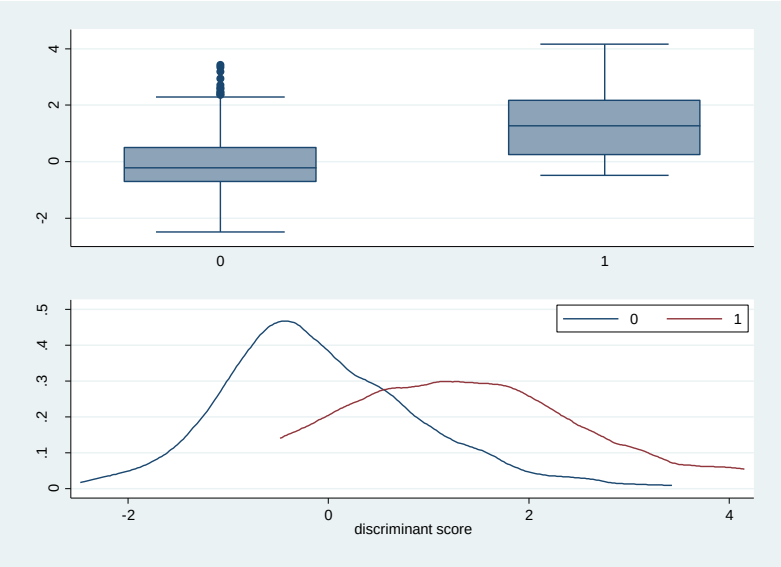

Figure 30. Discriminative ability of function 1 to distinguish between diagnostic groups. 0: non-carriers; 1:carriers of a *TTN* truncating variant.

The function was 70.4% sensitive and 78.6% specific at predicting carriage of a truncating variant.

Multivariate logistic regression analysis demonstrated that a lower fractional shortening (or ejection fraction), higher maximal left ventricular wall thickness and the presence of hypertrophy of the right ventricle were significant discriminators of carriers of a potentially truncating variant vs non-carriers (**Table 23**).

Table 23. Multivariate logistic regression analysis for the presence of a potentially truncating titin variant. CI: confidence interval.

	Coefficient	P-value	95% CI for coefficient
Ejection fraction	-0.0578368	0.005	-0.0981445-(-0.0175292)
Right ventricular hypertrophy	1.000587	0.016	0.1830905 - 1.818084
Maximal left ventricular wall thickness	0.146069	<0.0005	0.0640364 - 0.2281015

TTN enriched variants

A linear discriminant function significantly discriminated carriers of enriched variants vs non-carriers of enriched variants, as defined by an enrichment factor > 4 and listed in chapter 4.6, **table 15**.

The function was 70.0% sensitive and 77.5% specific at predicting the presence of an enriched variant.

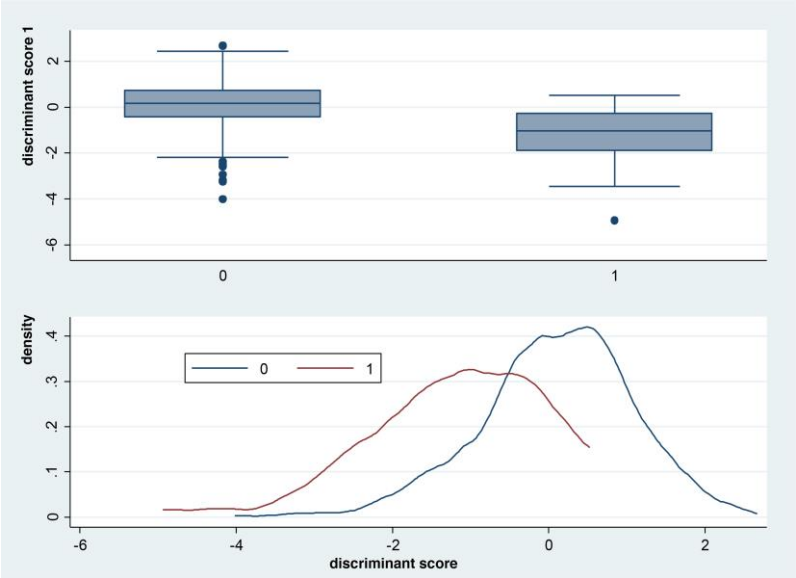

Figure 31. Discriminative ability of function 1 to distinguish between diagnostic groups. 0: non-carriers; 1:carriers of an enriched *TTN* variant.

Multivariate logistic regression analysis demonstrated that male sex, higher increase in left ventricular diastolic dimension between baseline and follow-up, larger left atrial diameter and higher maximal left ventricular wall thickness at last follow-up were significantly associated with carriers vs non-carriers of an enriched variant (**table 24**).

Table 24. Multivariate logistic regression analysis for the presence of an enriched titin variant. CI: confidence interval. LA: left atria. LVEDD: left ventricular end-diastolic dimension. MLVWT: maximal left ventricular wall thickness.

	Coefficient	P-value	95% CI for coefficient
Male	1.376369	0.008	0.3604189 -2.392319
LA diameter	0.0568337	0.010	0.0138598 - 0.0998077
Increase in LVEDD from baseline to follow-up	0.1043353	0.009	0.0266105 - 0.18206
MLVWT at last follow-up	0.0814253	0.033	0.0066106 - 0.1097004

6. CARDIAC MAGNETIC RESONANCE IMAGING PHENOTYPE DATA

As described in the methods, approximately one-third of the cohort - 271 patients (31%) - was submitted to cardiovascular magnetic resonance (CMR) to further characterize the phenotype. The main demographic and clinical characteristics are summarized in **table 25** and the main CMR parameters in **table 26**.

Table 25. Characterization of the subset of the total cohort studied with CMR (N=271). HCM: hypertrophic cardiomyopathy. SCD: sudden cardiac death. NYHA: New York Heart Association.

N=271	**Frequency (percentage) or mean ± standard deviation (range) or median (IQR)**
DEMOGRAPHICS	
Age at initial evaluation (years)	49.6±14.2 (13-81)
Male	185 (68.3%)
Ethnicity	
– Caucasian	170 (62.7%)
– Indian and other Asian	29 (10.7%)
– African/Caribbean	18 (6.6%)
– Chinese	0 (0.0%)
– Other	8 (3.0%)
	46 (17.0%)
PRESENTATION	
Family history of HCM	59 (21.8%)
Family history of SCD	47 (17.3%)
NYHA class III or IV	31 (11.4%)
Syncope	31 (11.4%)

Table 26. Cardiac magnetic resonance parameters. ASH: asymmetric septal hypertrophy; LVEDV: left ventricular end-diastolic volume; LVESV: left ventricular end-systolic volume; SV: systolic volume; LVEF: left ventricular ejection fraction; LA: left atrium; SAM: systolic anterior movement; LVOTO: left ventricular outflow tract obstruction.

CMR parameter	Mean±standard deviation or percentage
LVEDV (ml)	137.5±36.8
LVESV (ml)	35.7±21.2
Mass (g)	241.0±94.0
SV (ml)	100.0±26.5
LVEF (%)	75.2±9.2
MLVWT	19.9±5.2
LA area (cm2)	30.2±7.1
LVH pattern	
ASH	188 (69.4%)
Apical	33 (12.2%)
Concentric	44 (16.2%)
Mitral SAM	138 (49.9%)
LVOTO	105 (38.7%)
Late gadolinium enhancement	211 (77.9%)
Right ventricular hypertrophy	50 (18.5%)

Given the previously described genotype-phenotype findings and to optimize the statistical power with a reduced sample, we limited the analysis to a comparison between sarcomere negative and positive individuals, which is presented in **table 27**.

Table 27. Comparison between sarcomere gene mutation-positive and negative patients for the analysed CMR parameters. Significant or near-significant P-values are shown in bold. ASH: asymmetric septal hypertrophy; LVEDV: left ventricular end-diastolic volume; LVESV: left ventricular end-systolic volume; SV: systolic volume; LVEF: left ventricular ejection fraction; LA: left atrium; SAM: systolic anterior movement; LGE: late gadolinium enhancement; LVOTO: left ventricular outflow tract obstruction.

	Sarcomere-positive	**Sarcomere negative**	**P-value**
LVEDV	139.08±40.95	136.32±33.53	0.612
LVESV	39.23±26.43	33.17±15.95	**0.052**
SV	97.95±26.36	101.46±26.61	0.370
LVEF (%)	73.2±9.5	76.7±8.6	**0.009**
Mass (g)	218.0±83.6	257.8±97.9	**0.006**
MLVWT (mm)	20.8±6.0	19.4±4.6	**0.027**
LVH pattern - ASH	79.2% (84/106)	62.8% (103/164)	**0.006**
LA area	30.64±6.82	29.83±7.28	0.433
Presence of LGE	84.8% (89/105)	75.2% (121/161)	**0.066**
AMVL (mm) (N=31 vs N=36)	24.6±4.6	25.7±3.3	0.260

Sarcomere-positive patients had a higher maximal left ventricular wall thickness, lower ejection fraction, lower mass and a higher proportion of individuals with an asymmetric septal hypertrophy pattern. Late gadolinium enhancement tended to be more prevalent in sarcomere-positive individuals, without reaching statistical significance.

7. SCREENING OF COPY NUMBER VARIATION

At the selected confidence threshold level (see Methods Section, chapter 6), twelve CNVs in 12 patients (2.4% of the 505 patients screened for CVNs) were identified using ExomeDepth. Four of these CNVs in 4 patients (0.8%) were validated by array comparative genomic hybridization (aCGH): one large deletion in *MYBPC3* (involving 4 exons; **figure 32**), one large deletion in *PDLIM3* (involving the first 4 exons; **figure 33**), one duplication of the entire *TNNT2* gene (**figure 32**) and one large duplication in *LMNA* (involving 5 exons; **figure 33**).

Eight CNVs were not validated by the aCGH analysis, including three single exon duplications and one single exon deletion in *MYBPC3,* two two-exon deletions and one single exon duplication in *TNNI3* and one single exon duplication in *ACTC1*.

Figures 32 and 33 show the ExomeDepth generated graphs for each confirmed CNV (sarcomeric genes in **figure 32**, non-sarcomeric genes in **figure 33**) and the corresponding validation graphs generated from snapCGH. **Figures 34-41** show the non-validated CNVs.

Table 28 summarizes the clinical and genetic characteristics of the four patients with validated CNVs. Two did not harbour any rare variant in a potentially causal SP gene. The patient carrying the duplication of *TNNT2* is a carrier of a variant of unknown significance in the same gene. The analysis of the read count data at this variant shows that the rare variant occurs less frequently than the common allele, and therefore most likely occurs on the non-duplicated allele.

Table 28. Demographic, clinical and genetic characteristics of the patients harbouring CNVs. ASA: alcohol septal ablation; ASH: asymmetrical septal hypertrophy; del- deletion; dup – duplication; ICD: implantable cardioverter-defibrillator; MLVWT: maximal left ventricular wall thickness; NSVT: non-sustained ventricular tachycardia; SCD: sudden cardiac death; VUS: variant of unknown significance.

	Sex	**Age presentation (years)**	**NYHA III/IV**	**Family history of HCM**	**MLVWT (mm) and hypertrophy pattern**	**Risk factors for SCD**	**Events**	**Sarcomere variant**	**CNV**
H1	M	40	-	-	20 ASH	-	ASA	-	*MYBPC3 del*
H2	M	41	-	-	16 ASH	-	-	*TNNT2* N262S (VUS)	*TNNT2 dup*
H3	M	48	-	-	22 ASH	-	-	-	*PDLIM3 del*
H4	M	43	-	-	16 ASH	NSVT	ICD	*MYBPC3* R495G	*LMNA dup*

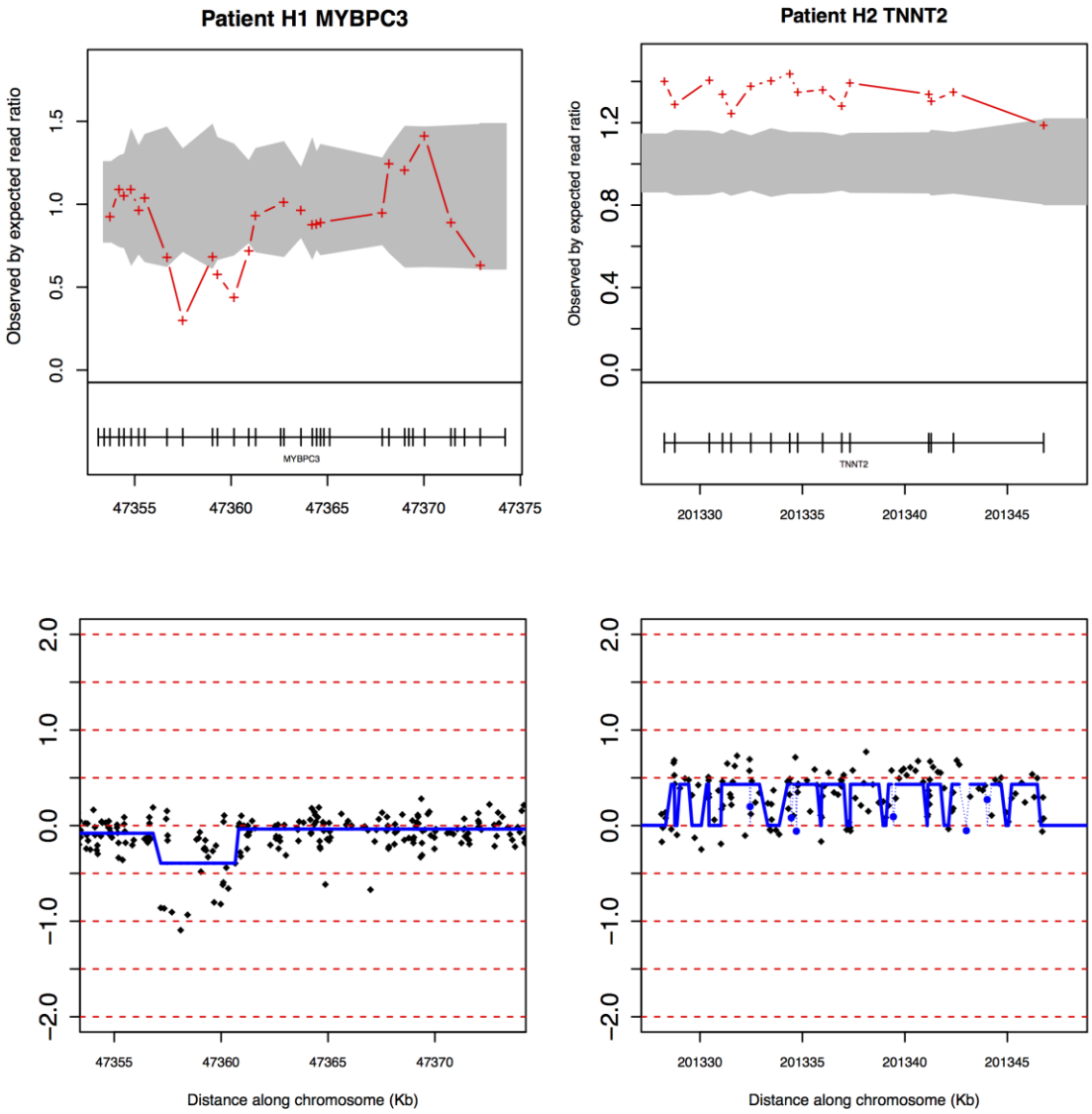

Figure 32. Large deletion in *MYBPC3* involving 4 exons (patient H1) and duplication of the entire *TNNT2* gene (patient H2). Upper figures generated through ExomeDepth analysis and lower figures generated through snapCGH.

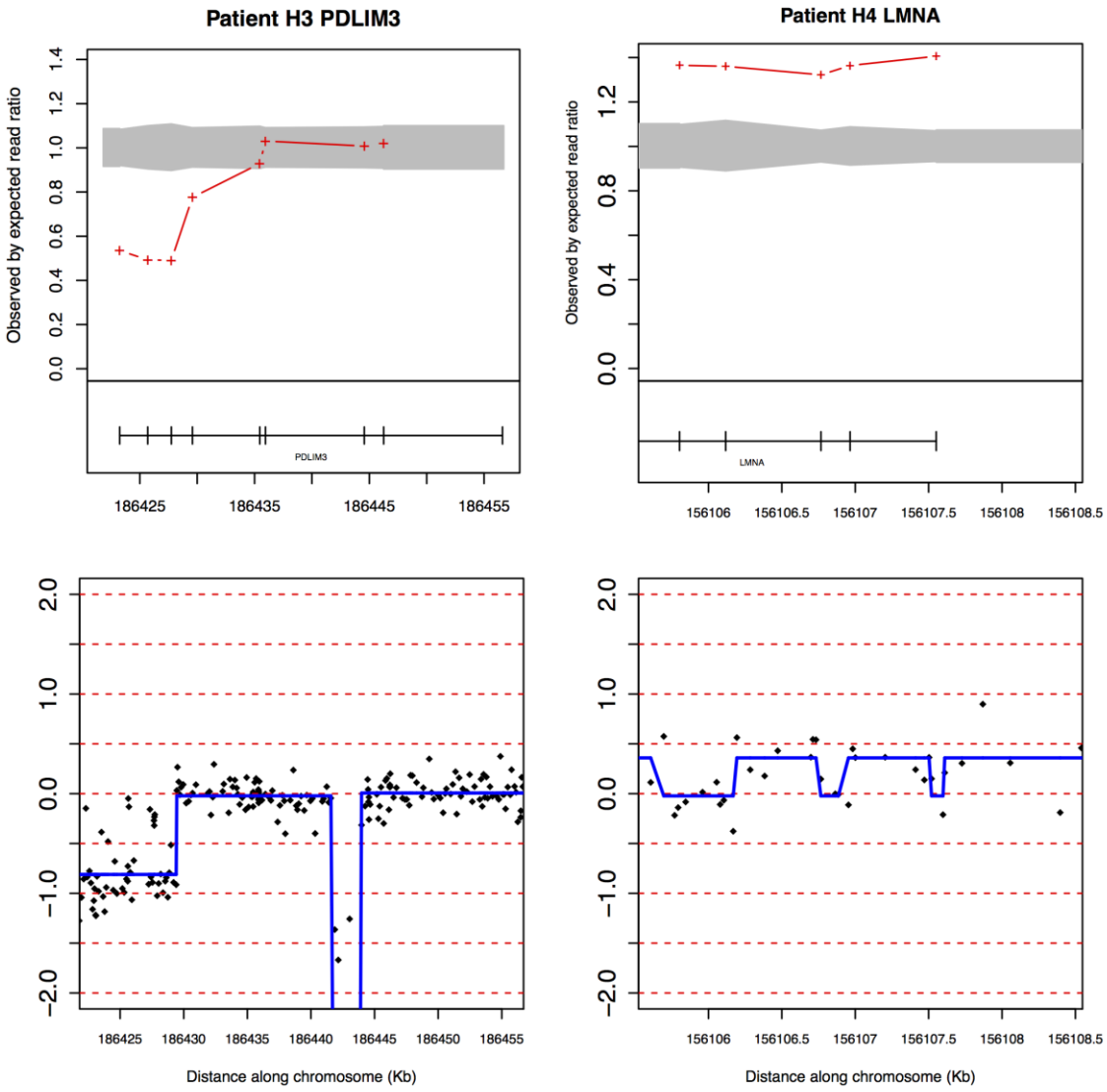

Figure 33. Large deletion of the first 4 exons of *PDLIM3* (patient H3) and large duplication in LMNA involving the last 5 exons (patient H4). Upper figures generated through ExomeDepth analysis and lower figures generated through snapCGH.

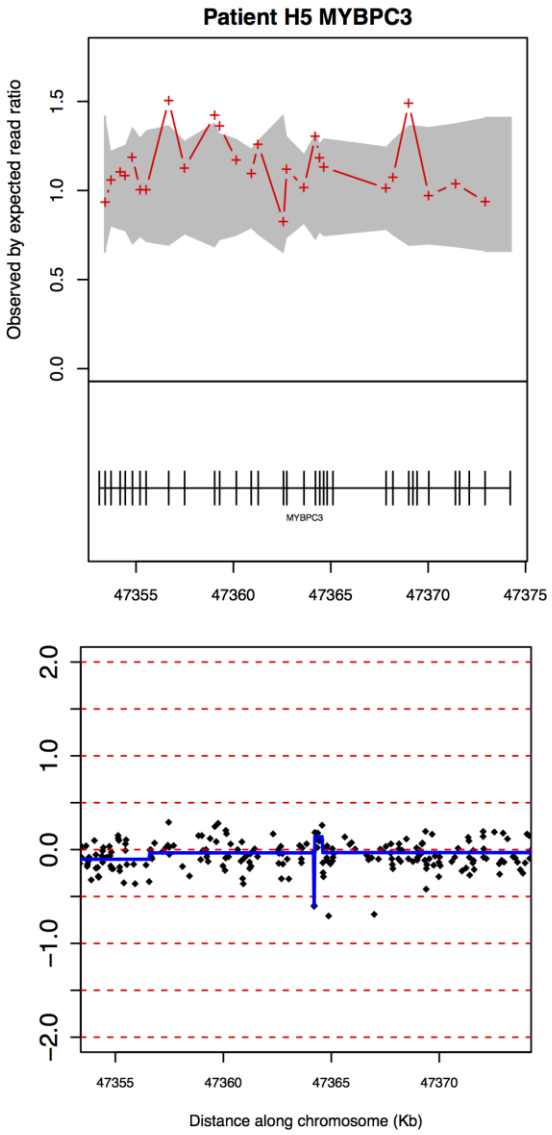

Figure 34. *MYBPC3* duplication of a single exon not confirmed by aCGH. Upper figure generated through ExomeDepth analysis and lower figure generated through snapCGH.

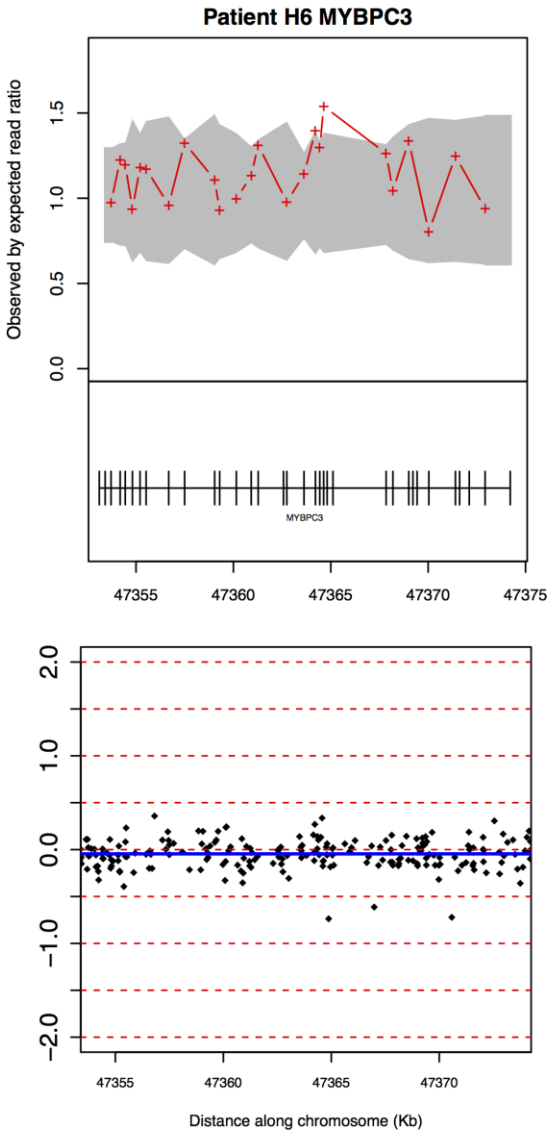

Figure 35. *MYBPC3* duplication of a single exon not confirmed by aCGH. Upper figure generated through ExomeDepth analysis and lower figure generated through snapCGH.

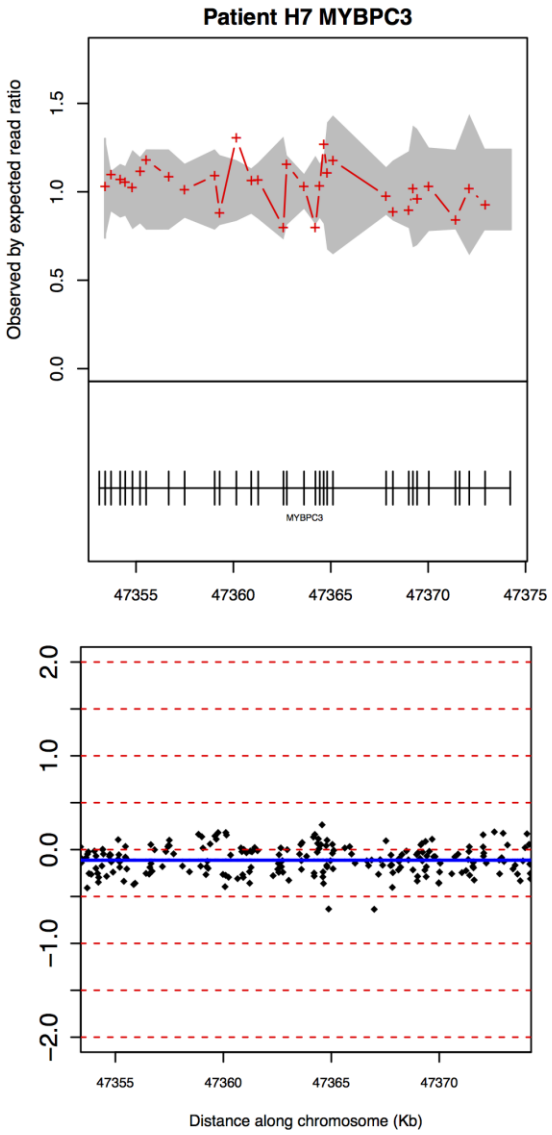

Figure 36. *MYBPC3* duplication of a single exon not confirmed by aCGH. Upper figure generated through ExomeDepth analysis and lower figure generated through snapCGH.

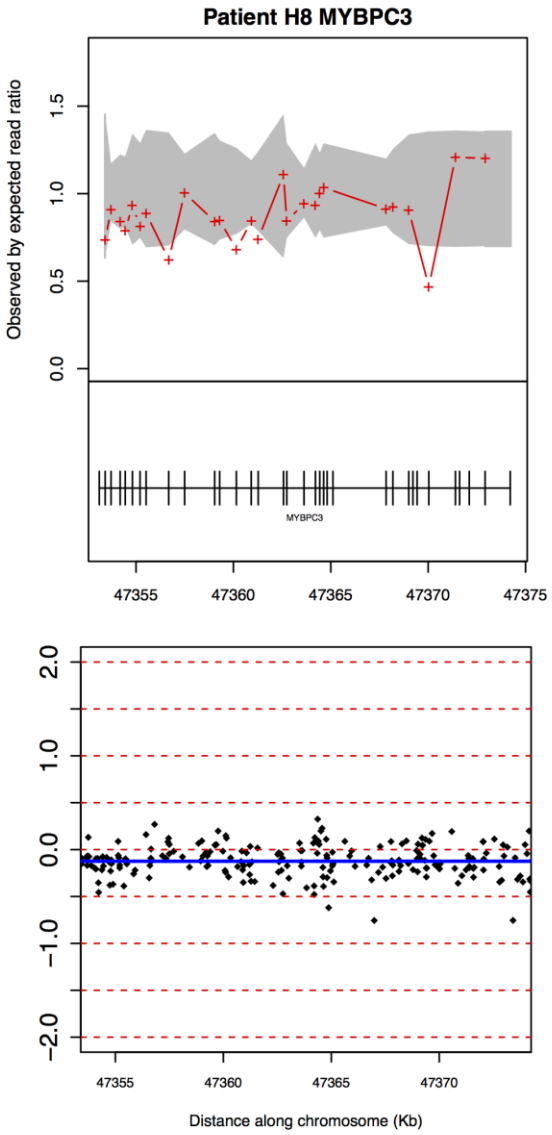

Figure 37. *MYBPC3* deletion of a single exon not confirmed by aCGH. Upper figure generated through ExomeDepth analysis and lower figure generated through snapCGH.

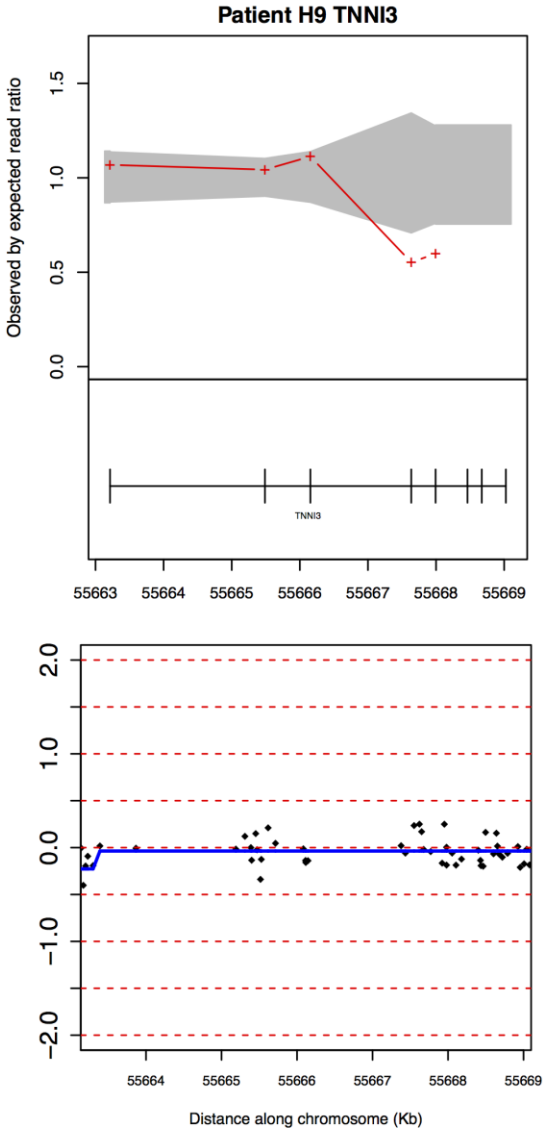

Figure 38. *TNNI3* deletion of two exons not confirmed by aCGH. Upper figure generated through ExomeDepth analysis and lower figure generated through snapCGH.

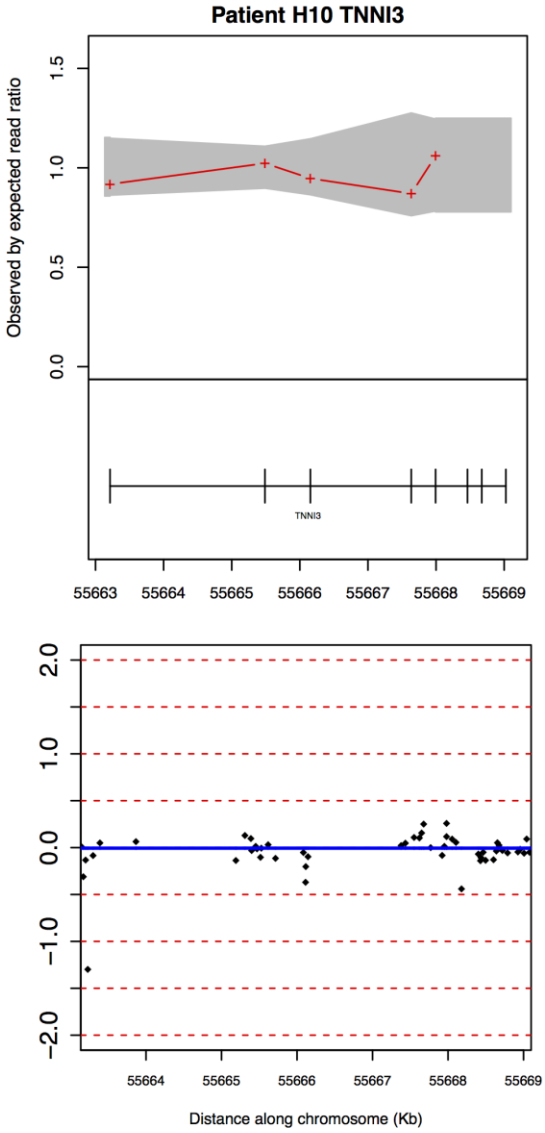

Figure 39. *TNNI3* deletion of two exons not confirmed by aCGH. Upper figure generated through ExomeDepth analysis and lower figure generated through snapCGH.

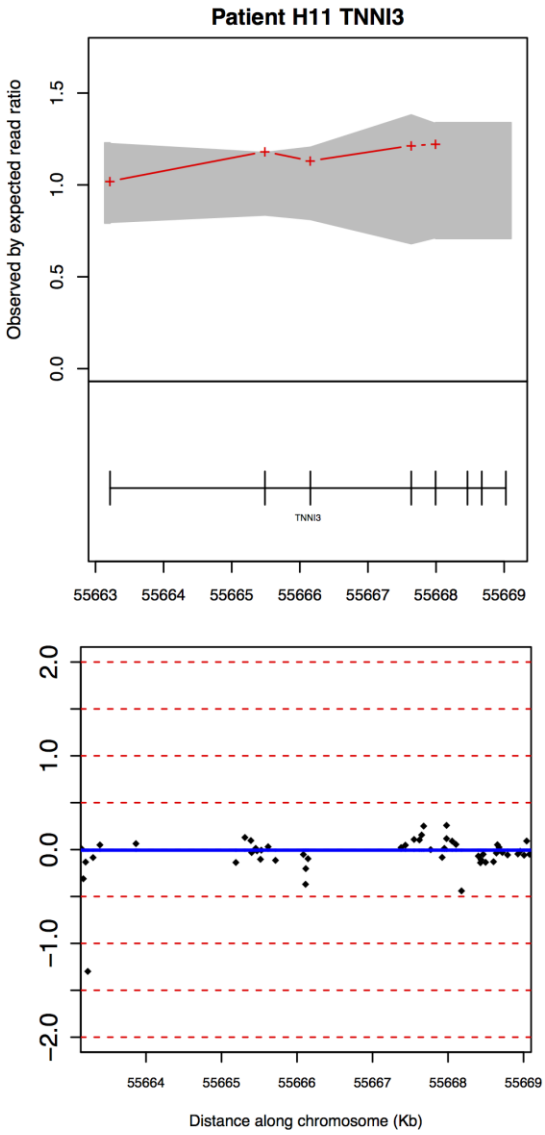

Figure 40. *TNNI3* duplication of one exon not confirmed by aCGH. Upper figure generated through ExomeDepth analysis and lower figure generated through snapCGH.

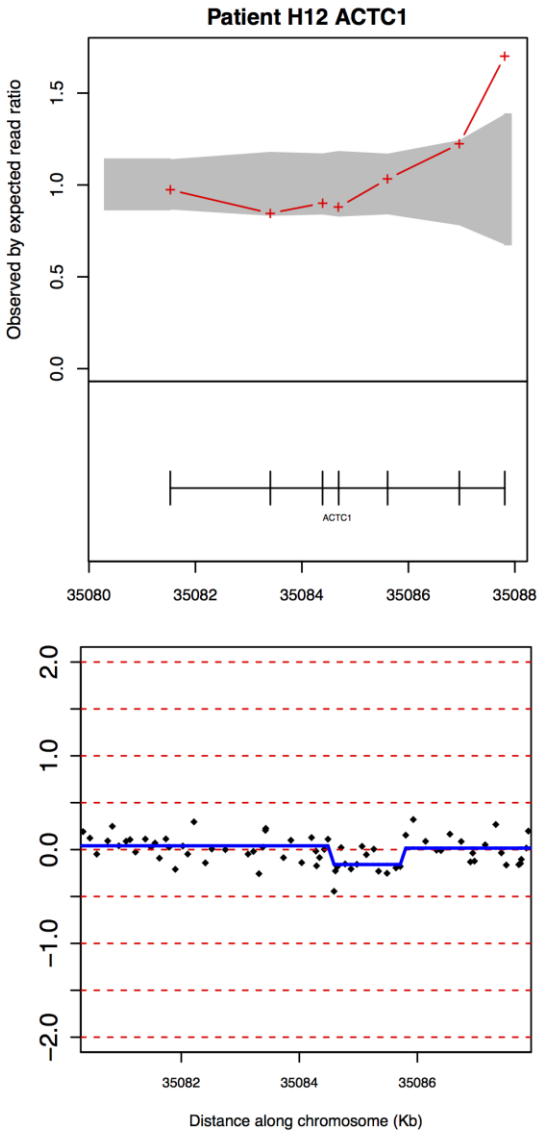

Figure 41. *ACTC1* duplication of one exon not confirmed by aCGH. Upper figure generated through ExomeDepth analysis and lower figure generated through snapCGH.

8. NON-CODING REGION ANALYSIS

A total of 1562 non-coding single nucleotide variant (ncSNV) calls were identified, distributed amongst the eight main sarcomere protein genes, in the first 233 patients of the study cohort.

8.1. VARIATION IN TRANSCRIPTION FACTOR BINDING SITES

Thirty-three distinct rare variants, present in 32 patients (14%), mapped to transcription factor (TF) binding sites localized in the 5' and 3' untranslated regions, upstream and downstream regions and introns. The majority of these patients (20, 63%) did not have any coding candidate variants in sarcomere genes. **Figure 42** illustrates the proportion of patients with coding and non-coding rare variants in sarcomeric genes.

Table 29 shows the ncSNVs found in TF binding sites, per gene. Twelve variants were present in *TPM1* (in 12 patients), six in *ACTC1* (in 6 patients), five in *TNNT2* (in 5 patients), three in *MYBPC3* (in 4 patients), three in *MYL3* (in 3 patients), two in *MYH7* (in 2 patients) and one in *TNNI3* and *MYL2* each. Three patients carried two different TF binding site variants each.

Two of the *TPM1* non-coding variants were present in both dbSNP135 and 1000 genomes project databases: rs146903018 (MAF of 0.1% in the 1000 genomes project and present in two of the patients) and rs188184852 (MAF of 0.2% in the 1000 genomes project and present in one of the patients). All the other non-coding variants were absent from those databases.

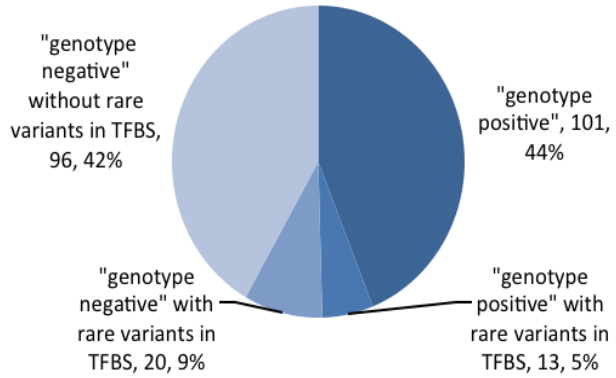

Figure 42. Proportion of patients with coding and non-coding variants in the eight main sarcomeric genes. TFBS: transcription factor binding sites.

Table 29. List of non-coding variants carried by HCM patients, that map onto transcription factors binding sites (TFBS). In bold, TFs described in the literature as part of cardiomyocyte survival/growth/hypertrophy pathways and conserved posititions as per GERP score. Ref: reference allele. Obs: observed allele. GERP: genomic evolutionary rate profiling. UTR5: 5' untranslated region. UTR3: 3' untranslated region. RegulomeDB score according to http://regulome.stanford.edu/.

Gene	Localization	Coding variants in sarcomere genes in the same patient	Frequency in 1000 genomes dataset	dbSNP135	Chromosome	Position	Ref	Obs	TFBS	GERP score	RegulomeDB score
ACTC1	intronic	yes	NA	NA	15	35084011	G	A	**STAT3**, E2F6	-2.7	4
ACTC1	intronic	yes	NA	NA	15	35084035	T	A	**STAT3**	-2.7	4
ACTC1	intronic	yes	NA	NA	15	35087530	C	T	CTCF, POLR2A, CCNT2, Ini1, SMARCB1, MAX	1.13	4
ACTC1	intronic	no	NA	NA	15	35087632	C	T	CTCF, POLR2A, CCNT2, Ini1, TAF1, JunD, E2F6, MAX, SMARCB1	-4.53	4
ACTC1	UTR5	yes	NA	NA	15	35087862	C	A	**SRF**	**2.85**	2a
ACTC1	upstream	no	NA	NA	15	35088006	G	C	**SRF**	-1.11	4
MYBPC3	intronic	no	NA	NA	11	47370591	G	A	CTCF, Rad21, **CEBPB**, SMC3	**2.07**	2a
MYBPC3	intronic	no	NA	NA	11	47370618	A	C	CTCF, Rad21, **CEBPB,** SMC3	**2.41**	2b
MYBPC3	intronic	no	NA	NA	11	47370703	A	G	CTCF, Rad21, **CEBPB**	**2.54**	4
MYH7	upstream	yes	NA	NA	14	23905020	T	C	**p300**, SP1, **HDAC2**,HNF4A, HNF4G	-3.29	2a
MYH7	intergenic	no	NA	NA	14	23910572	T	A	ELF1	1.35	2b
MYL2	intronic	no	NA	NA	12	111351152	A	G	POLR2A, EBF1	-8.05	4
MYL3	intronic	yes	NA	NA	3	46902080	C	T	CTCF	1.17	4
MYL3	intronic	no	NA	NA	3	46902091	G	A	CTCF	-1.33	4
MYL3	intronic	yes	NA	NA	3	46902110	A	C	CTCF	-5.6	4
TNNI3	intronic	no	NA	NA	19	55663455	C	T	SETDB1,ELF1, GABP, SPI1	-5.14	2a
TNNT2	intronic	yes	NA	NA	1	201330921	A	G	CTCF, SMC3, Rad21, ZNF143	-3.81	4
TNNT2	intronic	no	NA	NA	1	201337057	G	T	**CEBPB**	-1.01	3a
TNNT2	intronic	no	NA	NA	1	201345879	A	T	POLR2A, **NRSF,** SPI1	-0.355	5

TNNT2	intronic	no	NA	NA	1	201345940	T	C	POLR2A	-2.06	2b
TNNT2	intronic	no	NA	NA	1	201346338	G	A	POLR2A	-2.03	4
TPM1	UTR5	no	NA	NA	15	63334844	G	C	**YY1**, CTCF, RAD21,POLR2A, TAF1	**2.89**	2b
TPM1	UTR5	no	NA	NA	15	63334923	C	T	CTCF, RAD21 POLR2A,TAF1, TBP	**5.02**	2b
TPM1	intronic	no	NA	NA	15	63335343	C	A	TAF7	0.428	4
TPM1	intronic	no	NA	NA	15	63337778	A	T	GATA2, **SRF**	**5.25**	2a
TPM1	intronic	no	0.0011	rs146903018	15	63341426	G	A	CDX2, CTCF, STAT1, GATA1, POLR2A, ETS1, E2F6, SIN3A, RAD21, MXI1, SMC3	-0.215	4
TPM1	intronic	yes	NA	NA	15	63341606	T	C	CDX2, CTCF, STAT1, GATA1, POLR2A, ETS1	-1.54	2b
TPM1	intronic	no	NA	NA	15	63348576	C	T	POLR2A	-0.546	5
TPM1	intronic	yes	0.00181	rs188184852	15	63350150	G	A	POLR2A	-6.1	2b
TPM1	UTR3	no	NA	NA	15	63356374	C	T	POLR2A	-2.14	5
TPM1	UTR3	no	NA	NA	15	63358153	C	G	GR (NR3C1)	**2.79**	4
TPM1	UTR3	yes	NA	NA	15	63358197	C	T	GR (NR3C1)	-1.94	4
TPM1	intergenic	no	NA	NA	15	63368688	G	C	SPI1	0.0837	3a

8.2. NORMALIZING THE NUMBER OF DISTINCT NON-CODING VARIANTS FOR THE SIZE OF EACH GENE

To test if the frequency of the variants in each gene reflects background random variation dependent on the genomic dimension, we normalized the data with respect to the size of the genes. *ACTC1* and *MYL3* showed an excess of candidate non-coding variants compared to gene size, in contrast with the others (shown in **figure 43**).

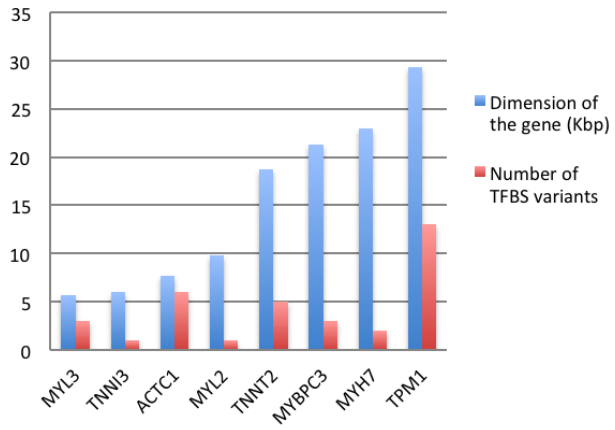

Figure 43. Comparison between the number of distinct variants in each gene and the gene size.

8.3. EVOLUTIONARY CONSERVATION ANALYSIS OF THE GENOMIC COORDINATES

Eight of the TFBS variants (25%) were localized in conserved positions, defined by a genomic evolutionary rate profiling (GERP) conservation score > 2. One in the 5'UTR of *ACTC1* (**figure 44**), three in intronic regions of *MYBPC3* (which correspond to all the noncoding variants in these gene) and four in *TPM1* (one is shown in **figure 45**). Seven (88%) of the variants located in conserved positions are carried by patients that do not have coding variants in sarcomere genes.

8.4. TRANSCRIPTION FACTORS PREVIOUSLY ASSOCIATED WITH CARDIOMYOCYTE HYPERTROPHY AND CARDIOMYOPATHY SIGNALING PATHWAYS

When analysing the TFs that bind to the DNA coordinates where these variants map, we identified seven TFs previously experimentally shown to be involved in hypertrophy signaling: SRF (serum response factor), C/EBPß (CCAAT/enhancer binding protein beta), p300, STAT3

(signal transducer and activator of transcription 3), HDAC2 (histone deacetylase 2), NRSF (neuron-restrictive silencer factor) and YY1.

In total, the 12 variants that are predicted to potentially interfere with the binding and function of these TFs were distributed in 13 patients, nine of which (69%) do not carry coding variants in sarcomere genes. Four are in *ACTC1* (in 4 patients), three in *MYBPC3* (in 4 patients), one in *MYH7*, two in *TNNT2* (in 2 patients) and two in *TPM1* (in 2 patients). Six of these variants (50%) are localized in conserved positions. Again, *ACTC1*, compared to its dimensions, shows excess in non-coding variants mapping to these potentially relevant TF binding sites.

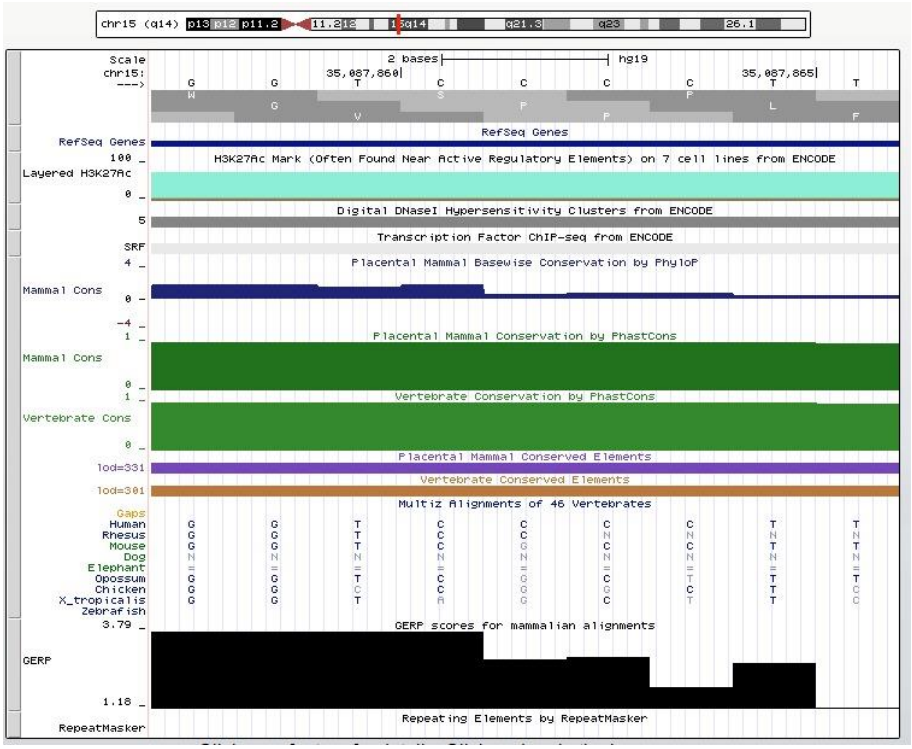

Figure 44. Image from the UCSC genome browser showing the genomic region around the variant 15:35087862C>A, that occurs in a conserved position in the 5'UTR of *ACTC1*. GERP score is 2.85. PhastCons and PhyloP scores also predict the position as conserved, as shown. This position was experimentally demonstrated to be part of an SRF binding site, as illustrated in the track "Transcription factor ChIP-seq from ENCODE". The level of evidence for the transcription factor binding at this position is high, reflected by a RegulomeDB score of 2a (datatypes available: TF binding + matched TF motif + matched DNase Footprint + DNase peak).

Figure 45. Image from the UCSC genome browser showing the genomic region around the variant 15: 63337778A>T, that occurs in a conserved position in an intronic region of *TPM1*. GERP score is 5.25. PhastCons and PhyloP scores also predict the position as conserved, as shown. This position was experimentally demonstrated to be part of an SRF and GATA-2 binding site, as illustrated in the track "Transcription factor ChIP-seq from ENCODE". The level of evidence for the transcription factor binding at this position is high, reflected by a RegulomeDB score of 2a (datatypes available: TF binding + matched TF motif + matched DNase Footprint + DNase peak).

8.5. 3'UTR VARIANTS IN MIRNA TARGET SITES

We identified 119 distinct rare variants in the 3'UTR regions of the eight genes, distributed in 218 of the 233 patients. Of these, only 2 mapped to predicted miRNA target sites (**table 30**). One was localized in the 3'UTR of *MYH7* and predicted to interfere with the binding of miR-516b and miR-28-5p. It was present in two patients and it is identified in the dbSNP135 (rs45548631). It is also listed in the 1000 genomes database (MAF 0.5%) and the exome sequencing project database (MAF 0.6%). Therefore, it seems to be a low frequency variant, most probably a benign polymorphism. The other variant is novel, present in the 3'UTR of *TPM1* and maps to the binding site of miR-30a, miR-30d and miR-30e. These miRNAs are amongst the most abundant in the heart and known to be down-regulated in cardiac

hypertrophy [319]. The patient that carried this variant did not have any sarcomere gene exonic mutation.

Table 30. Rare non-coding variants that map onto predicted miRNA target regions. GERP: genomic evolutionary rate profiling. MAF: minor allele frequency. ESP: exome sequencing project. Ref: reference allele. Obs: observed allele.

Gene	MAF (1000 genomes)	dbSNP135	MAF (ESP)	Chromosome	Start	Ref	Obs	GERP	miRNA
MYH7	0.00463	rs45548631	0.00641	14	23882043	C	T	1.11	hsa-miR-516b, hsa-miR-28-5p
TPM1	NA	NA	NA	15	63362267	A	G	-1.26	hsa-miR-30 a, d, e

8.6. EXPRESSION COMPARISON BETWEEN CASES AND CONTROLS

In two patients with cardiac tissue samples available from myectomy, who carried potentially functional non-coding variants and no candidate variants identified in a sarcomere protein gene, we conducted an array experiment (see Methods Section, chapter 7.3.) comparing expression of sarcomere protein genes between these two patients and controls.

One of the patients carried the *ACTC1* upstream variant g.35088006G>C, position predicted to be involved in the binding of SRF. The other patient had an intronic variant localized in a highly conserved intronic region of *TPM1*: g.63337778A>T, predicted to bind GATA and SRF as illustrated in **figure 45**. No significant differences were found for the RNA expression levels between these patients and the control dataset, either for those two genes or any other sarcomere gene – **table 31**.

Table 31. Raw and normalized values of mRNA expression of the two cases (G18_0952059 and G18_1052131) and the controls (GSM954999-GSM955004) for the eight main sarcomere genes. No significant differences were found between cases and controls.

Gene	G18_09S2059.CEL (raw)	G18_10S2131.CEL (raw)	GSM954999_VC-A1.CEL (raw)	GSM955000_VC-A2.CEL (raw)	GSM955001_VC-A3.CEL (raw)	GSM955002_VC-A4.CEL (raw)	GSM955003_VC-A5.CEL (raw)	GSM955004_VC-A6.CEL (raw)	G18_09S2059.CEL (normalized)	G18_10S2131.CEL (normalized)	GSM954999_VC-A1.CEL (normalized)	GSM955000_VC-A2.CEL (normalized)	GSM955001_VC-A3.CEL (normalized)	GSM955002_VC-A4.CEL (normalized)	GSM955003_VC-A5.CEL (normalized)	GSM955004_VC-A6.CEL (normalized)
ACTC1	**6234,69**	**7083,46**	12199,00	11438,16	7761,55	11055,34	8687,72	7658,49	**-0,40**	**-0,21**	0,57	0,48	-0,08	0,43	0,08	-0,10
MYBPC3	**3743,24**	**5471,78**	4619,76	3386,49	5110,87	4440,73	4335,28	3831,91	**-0,23**	**0,32**	0,07	-0,37	0,22	0,02	-0,02	-0,20
MYH7	**10921,64**	**11903,40**	11668,40	10385,90	13019,74	11708,56	12368,06	10759,60	**-0,10**	**0,03**	0,00	-0,17	0,16	0,00	0,08	-0,12
MYL2	**11507,23**	**11626,74**	13894,04	13586,81	12733,31	13669,90	13482,04	11129,54	**-0,19**	**-0,17**	0,08	0,05	-0,04	0,06	0,04	-0,24
MYL3	**5095,57**	**6315,96**	7552,22	7337,00	7298,29	7986,41	7581,48	6672,58	**-0,52**	**-0,21**	0,05	0,00	0,00	0,13	0,05	-0,13
TNNI3	**6398,24**	**8289,79**	5585,82	4769,70	7149,85	7972,92	7086,78	5802,46	**-0,07**	**0,30**	-0,27	-0,50	0,09	0,24	0,07	-0,21
TNNT2	**9256,75**	**12268,60**	7071,69	7345,94	6065,22	7675,37	8404,19	8217,87	**0,22**	**0,63**	-0,17	-0,11	-0,39	-0,05	0,08	0,05
TPM1	**1598,93**	**1796,87**	1475,61	1512,29	1367,85	1600,32	1630,88	1695,13	**0,00**	**0,17**	-0,12	-0,08	-0,23	0,00	0,03	0,08

9. WHOLE-EXOME SEQUENCING FOR SARCOMERE-NEGATIVE FAMILIES

9.1. QUALITY ASSESSMENT OF THE SEQUENCING DATA

Analysis of the mean depth of coverage per sample revealed adequate coverage of the exome, with a minimum mean read depth per sample of 77.65 and maximum of 118.62, and a minimum coverage of 94.5% (for read depth above 15) and a minimum coverage of 82.4% (for read depth above 30), as shown in **table 32**.

Table 32. Depth of coverage statistics for whole-exome sequencing, as calculated with GATK DepthOfCoverage profiler.

Sample ID	Total coverage	Mean	% bases above 10	% bases above 15	% bases above 30
Family 1 – patient 1	6071881895	118,62	97,8	95,9	87,7
Family 1 – patient 2	5258116701	102,72	98,2	96,6	88,8
Family 2 – patient 1	5184108419	101,27	97,8	96,1	87,6
Family 2 – patient 2	5063555774	98,92	97,9	96	86,8
Family 3 – patient 1	4398764419	85,93	97,1	94,6	83,3
Family 3 – patient 2	3974845771	77,65	97,1	94,5	82,4

9.2. CANDIDATE VARIANTS

Based on the filtering process as described in the Methods Section, chapter 8, we obtained datasets of between 34-68 candidate variants per family (supplementary tables in **Appendix F**). Pedigrees are shown in **figure 46**.

Family 1

34 unique variants were obtained as candidates. From these, only one was localized in a gene previously related to cardiomyopathy (*TTN* T3713I), which is a variant of unknown significance.

Family 2

40 unique variants were filtered as candidates. From these, one was localized in a gene previously related to cardiomyopathy (*OBSCN* T7800I). Additionally, four occurred in

compound heterozygosity: two in *CACNA1A* (H7440Q and E2524K) and two in *LRKK1* (D3009N and K5269R).

Family 3

68 unique variants were candidates. From these, 3 were localized in genes previously related to cardiomyopathy (*OBSCN* A7669T and *TTN* R26175Q and T8910S). Importantly, the *TTN* variants are also included in the list of prioritized variants; the first is a putative phosphorylation site and the second is surface exposed and likely involved in ligand interaction (see chapter 4.6. – **table 14**).

A

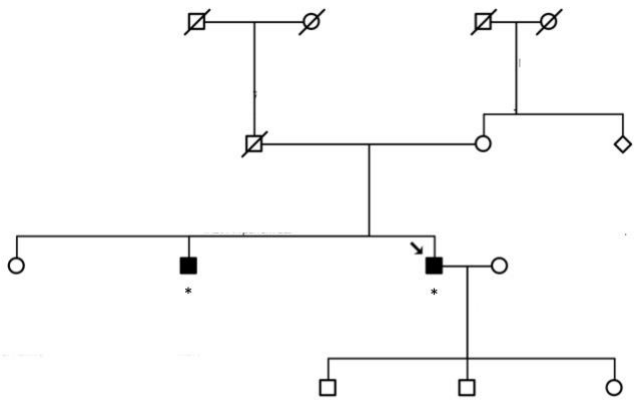

B

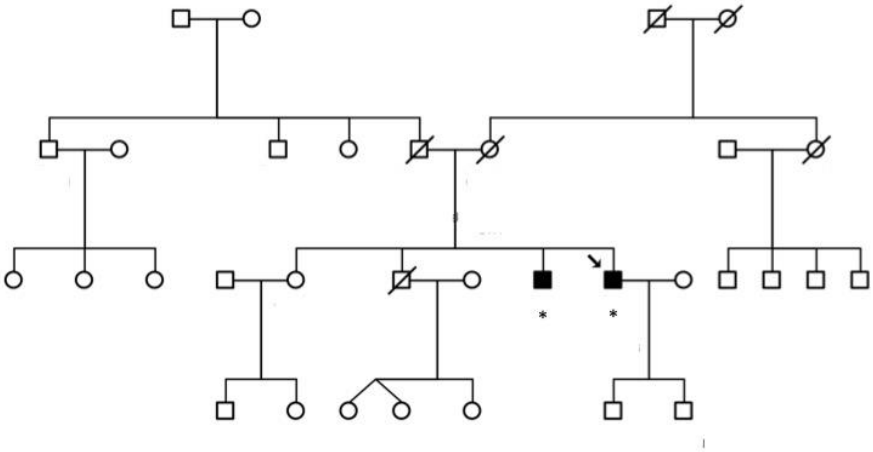

C

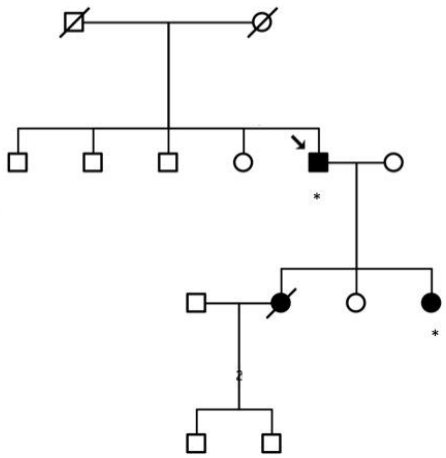

Figure 46. Pedigrees of the families studied with whole-exome sequencing. A: family 1; B: family 2; C: family 3. Arrows point to the proband. Squares – males; circles – females; black-filled shapes – affected; empty-shapes: not affected or not studied; stars signal whole-exome sequenced individuals.

10. *IN SILICO* ANALYSIS OF *MYH7* MISSENSE VARIANTS – PATHOGENICITY AND PHENOTYPE PREDICTION BASED IN THE STRUCTURAL IMPACT OF THE MUTATION

10.1. MANUAL ANALYSIS

A total of 401 mutations in the *MYH7* gene were used to build the dataset (supplementary table in **Appendix G**). More than two-thirds of the variants were published as disease causing (72%), in keeping with the proportion of published mutations if only considering our own cohort, and the others were novel variants. Of the total mutations, 235 mapped to at least one PDB with a total of 806 mappings to (multiple) PDB structures.

More mutations were associated with HCM (n = 292), whereas all other phenotypes were associated with fewer than 50 mutations each, including DCM with the next highest number of mutations (n = 46). Since mutations related to these phenotypes were the most abundant, further analyses were conducted looking specifically at HCM vs DCM and grouping the remaining phenotypes as "others".

Two additional simple phenotype parameters were also available for the HCM-associated variants - maximum wall thickness (20±4 mm) and age at presentation (33±16 years).

Restricting the remaining analyses to the variants that mapped to PDB (Protein Data Bank, http://www.rcsb.org/pdb/home/home.do) structure, we analysed the distribution of the variants amongst the structural and functionally annotated domains of this protein. All of the variants were located in the myosin globular head domain or the neck region. From all variants, 51% were located in functionally annotated domains: 18% mapped to the actin-binding site (residues 655-677); 4% mapped to the ATP-binding region (residues 178-185); 3% were located in the essential and regulatory myosin light chain binding regions (residues 788-801 and 814-827) and 27% mapped to the *MYBPC3* binding region (residues 839-964, mapped to different PDB ID 2FXM and 2FXO).

The predominantly mutated amino acid was arginine (85 variants, expected around 23.53),

followed by methionine (20 variants, expected around 10.84) and Glycine (26 variants, expected around 14.73).

The analyses of the dataset with SAAPdap (data analysis pipeline) showed that a total of 175 variants were classified as likely to be damaging by at least one SAAPdap feature. For 55 variants, no significant structural effect was detected by SAAPdap analysis and 166 failed to be analysed by SAAPdap (i.e. they did not map to a PDB structure). The most frequent features affected were: mutation of a highly conserved residue (Impact) occurring in 138 variants; the mutation of an interface amino acid (Interface) occurring in 48 of the variants and disrupting H-bonds, occurring in 42 of the variants. Other significant mutations effects occurred less frequently, with mutations causing voids or disrupting disulphide bonds not occurring at all.

A significant association was detected between the mutation of a highly conserved residue ("impact") and the presence of a DCM phenotype instead of HCM (90% versus 53%, P-value=0.029). Also, the number of variants with annotated features on UniProt was significantly higher in the presence of a DCM phenotype (20% vs 0%, P-value=0.020).

Furthermore, an association was found between the predicted mutation of an "Interface" aminoacid and the functional domain to which the residue mapped. A mutation affecting "Interface" aminoacids tended to affect the *MYBPC3* binding region (56% in MYBPC3 binding region affected an interface aminoacid vs 0% in the actin-binding domain, P-value=0.001).

Finally, a tendency was observed for an association between the mutation of an "Interface" aminoacid and a higher MLVWT (22±4 vs 19±4mm, P-value=0.051) and the variation of a "Binding" aminoacid and a higher MLVWT (25±5 vs 20±4mm, P-value=0.052).

10.2. MACHINE LEARNING ANALYSIS TO PREDICT PATHOGENICITY

The accuracy (Acc) to predict pathogenicity versus neutral variation, when the best PDB structure for each mutation was chosen, was: Acc = 0.927 for all mutations, Acc = 0.991 for DCM associated mutations and Acc = 0.914 for HCM associated mutations Accuracy for all phenotypes was greater when using a single best resolution PDB chain instead of using multiple PDB chains.

To compare SAAPpred performance with SIFT and Polyphen2 prediction software, 235 of the mutations that mapped to at least one PDB structure were analysed, of which 92.7% were predicted to be damaging by SAAPpred, 69.51% were predicted to be damaging by SIFT, and 90% were predicted to be pathogenic by Polyphen-2.

10.3. MACHINE LEARNING ANALYSIS TO PREDICT PHENOTYPE (HCM VS DCM)

Regarding the most informative features, the highest Chi-square values were obtained for highly conserved "Impact" mutations, followed by mutations to glycines. These results indicate that the mutation of residues affecting these features confers a high probability of a pathogenic phenotype. Mutation of "Binding" residues is also associated with pathogenicity, whereas mutations to proline and introducing hydrophilic residues in the core confers the lowest risk.

Clustering analysis

MYH7 mutations fall into two distinct regions that map to different PDB files, for DCM and HCM mutations. For the more C-terminal structure (PDB ID 2fxm) there are only 2 DCM mutations (compared with 35 HCM), indicating that DCM mutations are rare in this domain. For the N-terminal structure (PDB ID 4db1), there are 16 DCM and 116 HCM mutations.

The data suggest the presence of clusters of residues that are over/under populated with DCM and HCM mutations compared with what is expected. **Figure 47** illustrates the 3 clusters on PDB ID 4db1, colouring the clusters red, green and blue for HCM and orange, yellow and cyan for DCM.

In particular, DCM is highly over-represented in the third (blue/cyan) cluster. DCM mutations in clusters 1 and 2 (orange and yellow) are hardly visible and therefore mostly buried. On the other hand the DCM mutations in cluster 3 (cyan) are largely on the surface.

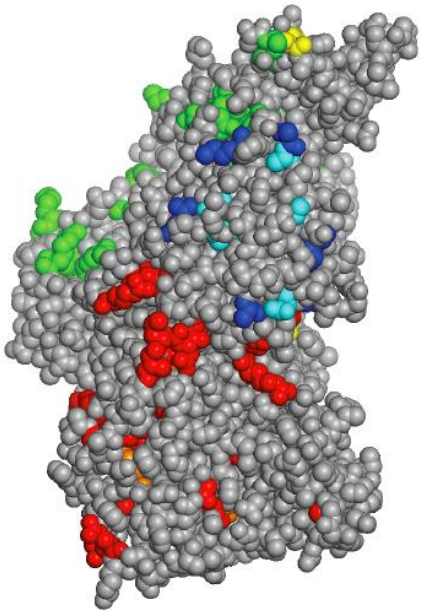

Figure 47. Clustering mutations on PDB ID 4db1 human myosin structure. Colouring the clusters red, green and blue for HCM and orange, yellow and cyan for DCM. Clustering was done on one chain and the results are then shown on the two chains in the 4db1 crystal structure.

HCM vs DCM predictor

Eleven models together with the a set of features (see Methods, chapter 9.2) including Clustering in addition to Binding, RelativeAccess, SurfacePhobic, CorePhilic, Voids, Clash, Proline, CisProline gave an accuracy of 0.75 and a Mathews correlation coefficient (MCC) of 0.531. The best predictive performance was achieved by averaging 10 models using this feature set and using 1000 Trees with 5 features, reaching a final accuracy of 0.79 and MCC of 0.61.

SECTION IV – DISCUSSION

1. TARGETED HIGH-THROUGHPUT SEQUENCING DATA ANALYSIS

1.1. QUALITY ASSESSMENT OF THE SEQUENCING DATA

Our high-throughput sequencing (HTS) protocol achieved adequate coverage of the targeted genomic DNA, which was comparable to the few previously published studies [105],[320]. The accuracy of a targeted HTS methodology is now well established in the literature, if an acceptable mean read-depth and coverage is obtained. The threshold of 15x has been reported [105, 109, 321],[108] to be sufficient for diagnostic testing, with a sensitivity of 99%. In this cohort, 93.5% of the targeted region was covered to a depth of 15 or more. However, the read depth per plate varied widely, from 73.39±108.0 for plate 1 to 500.30±67.50 for plate 9, which was mainly due to differences on the multiplexing methodology and the sequencing platform used, which changed from plate 3 (233th patient) onwards. In each plate, read depth also varied from gene to gene, which is also the case in other HTS studies in cardiovascular disease or otherwise [105].The GC content is one of the main factors responsible for differences in read depth among genes, as it influences the capture efficiency, with regions with higher GC content being less efficiently captured [322]. This occurred in our experiment with some of the *MYBPC3* exons, which needed further validation with Sanger sequencing.

To avoid missing important variation, we screened with Sanger sequencing those exons that presented an average read-depth of 15 or lower. Also, in order to eliminate possible false-positives due to low read-depth, variants called at a read depth of 15 or lower were systematically validated with Sanger. Both the number of false positives and false negatives detected was very low and similar to published reports [109], [108].

One paper [109] stated that with a mean read depth of 100±35 the statistical chance that a variant is missed in a patient is 0.004%. The mean coverage across all the samples is well above this threshold, although the initial three plates had lower values; however, as described (Sections Methods and Results), those plates were submitted to a more extensive validation step. In later plates, while obtaining higher read depth and actually supra-optimal coverage, we increased the number of patients sequenced in the same run (pre-capture multiplexing),

optimizing time and throughput.

One current research - and in the near future possibly clinical - alternative to targeted sequencing is the use of whole-exome sequencing (WES) platforms, which have been suggested as cost-effective, as the coding region corresponds to only 1% of the genome and hence should be able to cover most protein disrupting sequence variation, while providing additional sequence data in all genes. However, some authors have pointed out some disadvantages. WES platforms are generally characterized by lower coverage than targeted sequencing for a defined number of genes, given the amount of DNA to be sequenced, which could either result in lower sensitivity or allow less multiplexing, at the end compromising the throughput [107, 109]. Other limitations are higher costs and more challenges in terms of interpretation and data analysis [109]. Finally, the clinical use of whole-exome platforms raises growing concern and debate surrounding incidental findings [323], because relevant variants in genes not related to the phenotype under study can be discovered (e.g. *BRCA* mutations). Recently, guidelines have been published that address this issue [323].

1.2. GENOTYPING RESULTS

1.2.1. SARCOMERE AND RELATED GENES

I identified likely causal variants in 47% of the patients, if considering the sarcomere genes most robustly associated with HCM (*MYBPC3, MYH7, TNNT2, TNNI3, MYL2, MYL3, ACTC1, TPM1*) -which is in keeping with the published literature on cohorts of unrelated HCM probands [38] and with the meta-analysis presented in the Introduction [172]. Previous studies have used conventional genetic sequencing techniques to screen patients with HCM and most suggest that approximately 50% of individuals carry mutations in one of eight main cardiac sarcomere protein genes [20],[157]. This is also the approximate yield previously described in the same referral centre where this study was conducted, using conventional sequencing methodology [324],[139].

In this study, the distribution of variants amongst individual sarcomere and related protein genes was similar to that reported previously and summarized in my systematic review [172]. The major causal genes in this cohort were *MYBPC3* and *MYH7*, with variation in *MYBPC3* being the most prevalent. I applied both a 0.5% and a 0.2% MAF filter, without any significant

difference in the obtained dataset of variants for sarcomere genes.

As to the distribution of mutations across the domains and regions of each of the sarcomere proteins, I observed an interesting overlap between my single centre data and what is reported as an aggregate from the literature [27],[26],[25]. This is the case of the more prevalent mutations in the beta-myosin head and neck domains, where the functional ATP-binding and actin binding domains reside, compared to the rod region [27]. The C-terminal region is apparently one of the clustering zones for *TNNT2* and *TNNI3* variants [26]. In troponin I, the C-terminal region corresponds to a highly mobile domain, for which experimental evidence has attributed a role in translating towards troponin T the conformational changes provoked by the binding of calcium to troponin C [26]. This could explain an increased pathogenicity for variants occurring in this region. The role and structure of the C-terminal region of troponin T is still to be explored. In general, the distribution of the variants in this single centre cohort data corroborates the putative biologically relevant roles of the domains where the clustering of variants occur. One exception to this overlap is the finding of a significant number of variants located in the alpha-tropomyosin C-terminal domain (period 7 of the coiled-coil structure), whereas the large majority of the published variants reside in period 2 (N-terminal region) or period 5 (middle of the molecule) [26].

Considering other possibly causal but less strongly established sarcomeric and related genes, I reported, for the first time, the prevalence of all types of variants (including missense) in *TTN* in an HCM cohort. Several recent studies have focussed attention on the role of this protein in heart muscle disease [46],[50],[44] . Titin is found in skeletal and cardiac muscle, where it forms an elastic filament, bound at the N-terminus to the Z-disc and at the C-terminus to myosin, myosin-binding protein C and M-band proteins. The inextensible A-band region of the filament consists of regular patterns of immunoglobulin-like and fibronectin repeats, whereas the I band region is composed of multiple extensible segments (or “spring” elements) including PEVK, N2A (skeletal and cardiac muscle) and N2B (cardiac only). Titin is encoded by a single gene on chromosome 2 that undergoes complex differential splicing to produce isoforms with variable elastic properties and has a major role in determining the mechanical properties of the heart through its effects on passive tension during myocardial stretch and restoring forces during early ventricular filling and appears to be an important biomechanical sensor and organisational element within the sarcomere [46]. These multiple and central roles in cardiomyocyte biology make this protein an ideal candidate gene for cardiomyopathy.

Nevertheless, titin has been difficult to sequence and study due to its size, large number of isoforms and mostly unsolved tertiary structure.

In the present study, I identified a large number of novel titin variants, occurring in two thirds of the probands, the majority in association with variants in other candidate genes. Twenty-seven of the titin variants, present in 46 patients (5% of the cohort) are predicted to cause loss-of-function, which is more than the proportion of potentially truncating mutations recently reported in a sub-cohort of patients with HCM [50]. A slight majority of patients (57%) carrying potentially truncating variants do not show any associated rare main sarcomere protein gene variant, which is the reverse of what is observed if considering all titin rare variants.

The significance of the large number of missense SNPs is more difficult to assess. All the individual variants present in this cohort occurred with a frequency less that 0.5% in the 1000 genomes project [111], and the great majority with a frequency lower than 0.0%, suggesting that a proportion are at the very least modulators of the phenotype. However, the overall frequency of variants in the HCM cohort was actually lower than that seen in the control exome population. This finding is difficult to interpret because the annotation of titin variants is made extremely complex by the large number of possible isoforms/transcripts, which are not accounted for in existing databases. Furthermore, some individual variants are enriched in my dataset and have significantly increased frequency compared to the 1000 genomes population.

While this research was ongoing, truncating mutations in *TTN* were published as a major cause of dilated cardiomyopathy (DCM), in a study that detected this type of variants in 25% of familial cases and in 18% of sporadic cases [50]. However, robust evidence for pathogenicity is not present for all the variants reported and caution has been advised in another study [325], that found a truncating variant in 7 of 17 familial DCM cases; however, two of those families also carried novel *TTN* missense variants that co-segregated with the phenotype and in 2 there was no co-segregation.

Further work on understanding the role of titin in cardiomyopathy is clearly necessary. Based in homology modelling, conservation, domain location and predicted effect on protein structure, I have selected a set of around 30 missense variants for future work, including

mechanistic/functional studies and co-segregation.

Rare variation in *MYH6* was also found in a higher number of patients than initially expected. Alpha-myosin and beta-myosin heavy chain are encoded by the tandemly arranged genes *MYH6* and *MYH7* respectively, situated on chromosome 14. As β-myosin heavy chain is the predominantly expressed isoform in human hearts, most studies in patients with HCM have not screened the MYH6 gene and evidence that mutations in *MYH6* can cause HCM only comes from a few case reports [28]. *MYH6* has also been implicated in familial atrial septal defects [301] and sick sinus syndrome [326]. In this study, the frequency of rare *MYH6* variants in patients was similar to the control populations, questioning the importance of this gene in HCM. Further functional studies and family evaluation needs to be performed to determine the pathogenicity of the identified SNPs.

Unlike the main contractile sarcomeric genes, the association between sarcomeric cytoskeleton genes and cardiomyopathies have mainly been suggested by candidate-gene approaches in index-case or only small families, rather than the more classical linkage strategies that established successive contractile proteins as a cause of familial HCM or DCM. As such, even more caution must be used when interpreting variation in these genes.

1.2.2. NON-SARCOMERE GENES

Inclusion of additional genes, implicated in other inherited cardiac diseases, resulted in the identification of a large number of non-synonymous rare variants in ARVC related and/or ion channel genes in 42% of the cohort. While the overall frequency of these variants was similar to the control population, published data and *in silico* prediction tools suggested the hypothesis that some of these have the potential to modify the disease phenotype.

ARVC and ion-channel associated genes showed a significant difference in the number of identified variants when the cut-off for rarity was 0.2% instead of 0.5%, contrary to the findings for sarcomere and related genes. This fact is probably due to the high level of variation in ARVC and ion-channel associated genes in the general population [115], [116], [245].

Heterozygous mutations in genes encoding desmosomal proteins have been identified in up to 70% of patients with non-syndromic autosomal dominant forms of arrhythmogenic right

ventricular cardiomyopathy [327] and latterly in up to 15% of patients with dilated cardiomyopathy [328]. In this cohort, I identified a large number of desmosomal candidate variants, most of which were classified as variants of unknown significance. As with *TTN*, the majority occurred in patients that had at least one sarcomere protein (or related) gene variant, making it difficult to determine their pathogenic role. The same was true for the many variants detected in ion channel genes. I hypothesized that the previously published and other rare variants in ARVC-related and ion channel genes may be potential phenotype modifiers in HCM, given the overlap of some of the downstream pathways.

1.3. DETERMINING PATHOGENICITY OF SEQUENCE VARIANTS

Even when using conventional sequencing technology, the genetic heterogeneity of HCM and the high frequency of novel variants with uncertain effects on gene function present considerable challenges for clinical interpretation. Ideally, novel variants should be subjected to functional studies, but these are costly, time consuming and often impractical in the clinical setting. Similarly, co-segregation analysis within families can be helpful, but is uninformative in small pedigrees –which are increasingly prevalent- and often difficult and time-consuming to orchestrate.

The recent availability of sequence datasets from large healthy and disease cohorts- 1000 genomes project [112], NHLBI exome sequencing project, UK10K - makes it possible to use them as controls for which variant frequency can be used to filter the variants detected in a disease dataset. In this study, I applied both a threshold of 0.5% and 0.2% based on the 1000 genomes project dataset (step I) and NHBLI ESP (step II); this strategy eliminated around 90% of the calls and halved the number of distinct variants, while retaining the most likely causative. A recently published study [329] analysed the presence and frequency of DCM associated variants in the NHLBI exome sequencing project database and in the dbSNP build 131. Based on their findings, the authors proposed a preliminary allele frequency cut-off of 0.04%. However, the majority of the studies published since my own work have used cut-offs of 0.5% or 1% for rare variation [108]. Some of the relevant variants might be lost if a too stringent threshold is applied. For example, if applied to this dataset, the threshold of 0.04% would exclude some clinically important variants, including five disease-causing published sarcomere variants and five published ion-channel disease-causing variants.

As a consequence of the above-mentioned large-scale genomic screening projects, rare variation in sarcomere genes in the "general" population was also scrutinized, as I did in the context of this study (Methods and Results Section) and these data were published concomitantly. In one paper, the authors queried the 1000 genomes database for rare exonic variants in *MYH7*, *MYBPC3* and *TTN* and found previously reported and probable pathogenic variants in *MYH7* and *MYBPC3* at a frequency higher than expected for the prevalence of cardiomyopathy [246]. Similar findings were reported in other papers, including two that analysed the NHLBI exome sequencing population data [330], [245] and another that used the Framingham and Jackson Heart Study cohorts [244] to screen for the presence of previously reported or likely pathogenic variation in sarcomere genes. Possible explanations for these findings are a combination of reduced penetrance for some of these alleles, the possibility of digenic and oligogenic models of inheritance and also erroneous attribution of pathogenicity to previously reported variants [142].

The fact that rare variation is cardiomyopathy associated genes has been described in a much higher prevalence than expected complicates the interpretation of a given genetic result and demonstrates the caution needed when interpreting missense variants, even if they are rare or previously described as causal and the need to develop new tools that calculate a probability that a given variant is disease causing. If using HTS approaches, as in this study, the potential to identify a very large number of rare variants that are also found in the general population and which have little or no effect on disease phenotypes could make attribution of causality to candidate variants using conventional methods such as co-segregation analysis in large pedigrees impractical. The availability of sequencing data from large population cohorts allowed the statistically comparison of the distribution of rare variants between controls and cases. I compared the sequencing results for the first 223 patients with a set of high depth exomes generated by the UK10K sequencing project (www.uk10k.org) and investigated whether I could identify an excess of rare variants in cases that would be consistent with a pathogenic role. Four sarcomeric genes (*MYH7, MYBPC3, TNNI3, TNNT2*) showed a significant excess of rare nsSNPs compared to controls. Assuming a simple dominant model, we estimated that rare nsSNPs in these four genes explained between 13% and 43.7% of HCM cases. Additionally, we proposed a statistical approach that estimated the probability that a nsSNP candidate variant is causal. While this statistical approach cannot on its own identify a variant as causal, it provides insights into the genetic architecture of HCM.

I repeated this approach for the larger cohort of 874 patients, using both a 0.2% and 0.5% threshold for rarity and incorporating small indels and splice-site variants in the analysis and the obtained results were very similar, with the same four sarcomere genes showing a statistically significant difference between cases and controls. However, in this second case-control analysis *MYBPC3* showed the highest difference for the frequency of rare variation (compared to *MYH7* in the previous analysis), which is related to the high prevalence of non-missense variants in *MYBPC3,* that were absent from the first comparison. Additionally, rare variation in *CSRP3* and *PLN* was significantly higher in HCM cases, which suggests an important but incompletely explored role for these genes in HCM genetics. In fact, *CSRP3* has been questioned as a causal gene, namely due to the unexpectedly high prevalence of the W4R variant in the general population [330], but my statistical approach further suggests a pathogenic role for this gene in HCM.

I also detected a few number of individual variants, mainly in *MYBPC3*, to occur at a high frequency in this cohort. Taking into account that the cohort is constituted by unrelated probands only, the high number of individuals with the same variant could be the result of a founder effect.

The case-control comparison for non-sarcomere genes associated with arrhythmogenic right ventricular cardiomyopathy or ion-channel disease showed no significant enrichment of rare variation in patients compared to controls, either from UK10K project or UCLexome. While these data could be interpreted as proving that such variation is purely "background noise", my genotype-phenotype findings seem to suggest otherwise, at least for some of the non-sarcomere genes, such as *ANK2*. A modifier effect on phenotype, rather than a causal one, could be compatible with an absence of enrichment for these variants, which would only exert their effect in the presence of a main and truly causal sarcomere variant.

In conclusion, one approach to the interpretation of variants is purely statistical. Rare genetic variation in healthy populations occurs in a much higher prevalence than expected [246], [244], [330]. But at least in the case of HCM, I showed that the prevalence of rare variants is significantly higher in HCM cases compared to controls for most of the main sarcomeric genes. Interpretation of genetic variants might therefore include a probabilistic element, based on gene, type of mutation and the proportion of rare variation in cases versus controls; this approach was also very recently suggested by other authors [331], [332].

Standard approaches to variant interpretation will increasingly need to be complemented by other strategies and the novel quantitative methods presented in this study provide one way of determining the probability that a variant is disease causing. Additional tools that integrate genetic data with high throughput functional analyses and more sophisticated *in silico* prediction models coupled with improved clinical phenotyping will also be required. In the scientific setting, corroborative information on pathogenicity is derived from functional assays of various kinds but these are expensive, time consuming and difficult to translate into the clinical setting. New animal and cellular models are needed to provide accurate (and hopefully rapid) data on the consequences of sarcomeric mutations in the clinical diagnostic laboratories. Work in iPSCs appears promising [87], as well the use of zebrafish models [333].

Also, new patterns of oligogenetic or non-mendelian inheritance should be considered, which could also justify the high prevalence of rare variants (including published as disease-causing ones) in the general population.

2. NOVEL GENOTYPE-PHENOTYPE ASSOCIATIONS IN HYPERTROPHIC CARDIOMYOPATHY REVEALED BY HIGH-THROUGHPUT SEQUENCING

2.1. INFLUENCE OF SARCOMERIC VARIATION ON PHENOTYPE

In this cohort, the presence of any sarcomere protein (SP) variant was associated with a class-effect consisting of an asymmetric septal hypertrophy pattern, younger age at presentation, family history of HCM and sudden cardiac death (SCD) and higher proportion of female individuals. Three studies, published after my data was generated, broadly confirm these results [334], [335], [336]. All these data also reproduce part of the results presented in my systematic review and meta-analysis (see Introduction) [172]. However, none of these other previous or concomitant studies used massively parallel sequencing technology and all spanned a period of time where different sequencing technologies and heterogeneous gene panels were used, which is a limitation.

I additionally constructed a multivariate regression model based in the variables that individually showed a significant association with a SP - positive genotype. The strongest predictors, which showed the highest score values, were family history of HCM and an asymmetric septal hypertrophy pattern.

Furthermore, this study also showed that patients with sarcomere protein variants had higher cardiovascular and SCD mortality during follow-up. Previous reports have analysed the association of genotype and cardiovascular death, but integrated in a composite end-point, together with other cardiovascular outcomes, such as an evolution to heart failure or stroke [178]. My study was the first to analyse cardiovascular death as an isolated end-point, as well as sudden cardiac death.

Patients with more than one sarcomere protein variant had an increased risk profile for SCD, confirming the suggestion of a gene dose effect, reported in previously published small series [18, 176],[242],[337]. Also, double heterozygotes for *MYH7* and *MYBPC3* were associated with a significantly reduced survival, compared to no variation in these genes or to the presence of

a rare variant in either gene in isolation, which further confirms the deleterious prognostic effect of multiple SP variation.

With regard to individual sarcomere protein genes, some of the effects seem to reproduce the previously mentioned class effect on age, morphology and family history of HCM and SCD, if considering the two most prevalently mutated genes, *MYBPC3* and *MYH7*. However, I have also demonstrated a number of completely novel associations that provide evidence for gene specific effects on clinical phenotype and prognosis. For example, the association between the presence of rare variation in *TNNI3* and right ventricular hypertrophy, the lower blood pressure response to exercise in the presence of *MYH7* rare variants and the higher percentage of patients submitted to invasive gradient reduction therapies when carrying *MYBPC3* splicing variants. This last finding is rather interesting, because despite the loss of statistical power due to only analysing a subset of variants (splicing but not missense or others), an association was discovered with an end-point that is a surrogate to a more severe manifestation of the disease – increased symptoms due to left ventricular outflow tract obstruction, that are not manageable with pharmacological therapy. This may be a consequence of an increased biological effect of these splicing variants, which are particularly prevalent in this gene, where haploinsufficiency is probably the predominant mechanism of pathogenicity [338]. The association of *TNNT2* rare variation and a lower blood pressure response to exercise is another relevant finding, already suggested in a previous work, that only focused in one mutation (R92W) [234].

The presence of a rare variant in *MYBPC3* or *MYH7* was associated with reduced survival (respectively for SCD and cardiovascular death), but only when modelled for time from birth. Interestingly, the presence of rare variation in *TNNT2* was related to increased cardiovascular death, either modelled for follow-up or for time from birth, but not SCD. Although this is in apparent contradiction with earlier reports that associated *TNNT2* mutations with an increased risk of SCD [172], more recent studies with longitudinal follow-up of large cohorts have contested this apparently too simplistic concept [139]. I also compared the survival directly between *MYH7* and *MYBPC3*, without finding any difference.

I opted to model all the conducted survival analyses for both follow-up time and time from birth, as previous work has suggested that the assessment of the influence of genetic [139] and clinical [339] risk factors in mortality can be potentiated by this statistical approach. The

rationale is the fact that being a genetic disease, the risk of adverse outcomes is theoretically present from birth [339].

However, the low number of outcome events during follow-up may have biased the survival analysis and precluded an analysis of other associations, including the effect of carrying multiple compared with single variants. The survival from birth is provided for comparison with the published literature but also introduces an inherent survivor bias.

I also hypothesized that filtering for putatively biologically more relevant variants, by selecting only those that are predicted to be pathogenic *in silico*, could enhance the discovery of genotype-phenotype correlations. However, when the analysis was repeated for only those variants, no additional genotype-phenotype correlations were revealed. This is probably related to the known limitations of bioinformatic tools, such as Polyphen [160] and SIFT [340], that are not directed to a specific phenotype nor validated for clinical use [110].Other possible reason for this negative finding was the loss of statistical power, due to the lower number of variants analysed.

Finally, the genotype-phenotype analysis was repeated in the sarcomere positive sub-cohort alone, with the purpose of limiting the analysis to a more homogeneous population in terms of genetic background, which could reveal additional associations, for example related to a hypothesized modifier effect of non-SP genes. Again, this approach did not reveal additional genotype-phenotype relationships, while reproducing the most significant ones. Again, a loss of statistical power occurred in this sub-analysis, as the sample is reduced by half if only considering the sarcomere positive individuals.

2.2. CARDIAC MAGNETIC RESONANCE PHENOTYPING SUGGESTED ADDITIONAL GENOTYPE-PHENOTYPE ASSOCIATIONS

In the sub-cohort of patients where phenotyping was further refined with cardiac magnetic resonance (CMR), the association between the presence of rare sarcomere variation and left ventricular wall thickness or the pattern of hypertrophy was confirmed, despite the smaller size of the sample. Also, additional genotype-phenotype associations were revealed. Carriers of an SP variant showed lower ejection fraction, an association never described before. Although in of need of confirmation in other cohorts, this clinically relevant association could

prove to be another of the constellation of functional and morphological findings that constitute a class-effect of sarcomere variation. The higher reproducibility of left ventricular function quantification by CMR [341] can partly explain the fact that this finding was not reported in previous echocardiography-based studies of large HCM cohorts. The poorer ventricular systolic function might be explained by a common downstream contractility impairment, resulting from sarcomere malfunction as a consequence of mutations in any of the main sarcomere genes. Interestingly, I have shown that SP genotype-positive patients had worse prognosis, which is commonly correlated with lower LVEF in other cardiovascular diseases.

Furthermore, sarcomere-negative patients had a significantly higher myocardial mass, for the quantification of which CMR is the gold-standard [341]. Again, this is a previously unknown correlation, probably revealed by the higher accuracy of CMR, which is much less dependent on geometrical assumptions and much more reproducible than echocardiography for the calculation of volumes and mass. The increased LV mass observed in the sarcomere-negative patients is difficult to explain biologically, as those patients are probably very heterogeneous in terms of causality and genetic background.

Another advantage of the more detailed phenotyping provided by CMR is the ability to perform tissue characterization [342]. Late-gadolinium enhancement (LGE) has been related to an increased prevalence of ventricular arrhythmias and with a higher risk of heart failure in HCM, although the association with an increased risk of SCD is more debatable [343]. Interestingly, the proportion of individuals with late gadolinium enhancement was increased in sarcomere positive individuals, although not reaching statistical significance.

2.3. EFFECTS OF TITIN ON THE PHENOTYPE

My data on *TTN* variation provides the first evidence for a possible modifier effect of *TTN* loss-of-function variants on the left ventricular systolic function of HCM patients, which showed a lower fractional shortening when carrying such variants. This novel finding is biologically plausible given the central role of titin in sarcomere biology and structure and the proposed position of *TTN* as the major causal gene in DCM [50]. The results from regression analysis demonstrated that right ventricular hypertrophy and maximal LV wall thickness were also predictors of the presence of a potentially loss-of-function titin variant.

Furthermore, I analysed the phenotype of carriers of candidate titin variants that were significantly enriched in this cohort, compared with the 1000 genomes population, and thus hypothesized to exert a functional effect. Male sex, increased left ventricular and left atrial dimensions and higher maximal wall thickness were predictors for the presence of an enriched titin variant.

The presence of any type of rare *TTN* variant was significantly associated with a higher probability of carrying an implantable cardioverter-defibrillator at baseline or having one implanted during follow-up. This suggests an increased SCD risk profile for patients that carry a *TTN* variant, which merits further exploration in future studies.

2.4. MODIFIER EFFECT OF NON-SARCOMERE VARIANTS

I have described that many patients with sarcomere mutations also carry rare variants in genes coding for desmosomal, ion-channel and other proteins implicated in inherited heart disease, but their relevance to disease expression was unknown. Given the phenotypic and genetic overlap between different cardiomyopathies, I have hypothesized that variation in non-sarcomere genes could act as a modifier of the HCM phenotype by acting in common downstream pathways and hence contribute at least partially to explain the phenotypic heterogeneity that characterizes this disease. This was never tested before my work.

The data in this study suggest that rare *ANK2* variants are associated with severe LV hypertrophy. *ANK2*, or *ankyrin B*, stabilises membrane ion channels in cardiomyocytes and mutations cause long QT syndrome 4, ventricular arrhythmias and sinus node disease [344], [345]. I am unaware of any link between *ANK2* expression and changes in LV morphology, but as ankyrins interact with proteins that influence calcium homeostasis and ß-adrenergic signaling, it is conceivable that they eventually affect the cellular expression of sarcomere protein gene variants. The strength of association (P = 0.0005) passes a Bonferroni correction for the number of tested genes, but further replication in independent cohorts will be necessary to confirm these results.

In addition to the association with *ANK2* variation, I detected a number of associations of lower statistical significance with variation in other non-SP genes. Patients with *SCN5A* rare

variants were more likely to have LA enlargement at the final evaluation. A link between *SCN5A* disruption and TGF-beta$_1$-mediated fibrosis has recently been demonstrated in a murine model of sinus node disease [346] and it is possible that *SCN5A* variants influence the pro-fibrotic milieu associated with sarcomere protein mutations. *SCN5A* rare variation was also associated with a higher proportion of significant left ventricular outflow tract obstruction.

Individuals with rare *PLN* variants had a significantly increased proportion of NSVT, which is interesting considering the recently described arrhythmogenic burden risk of a founder *PLN* mutation [347]. Similarly to the association with *ANK2*, further replication will be required to confirm these findings.

2.5. CLINICAL IMPLICATIONS

If genetic variation is to become a clinically relevant biomarker, it is essential that there is a clearer understanding of genotype-phenotype relationships. The associations between sarcomere gene variants and the broader phenotype examined in this study contribute to this understanding and if confirmed in other populations could inform the counselling of patients and relatives who are contemplating predictive genetic testing. The demonstration that non-sarcomeric variants may influence disease expression is an illustration of the complexity that underlies the biology of this genetic disease. New models that incorporate a broad genetic profile and deep clinical phenotyping are necessary to use mutation analysis in prognostic models. Ultimately, the clarification of genotype-phenotype relationships will require collaborative, large-scale research that brings together teams expert in molecular biology, clinical medicine, bioinformatics and population science.

3. COPY NUMBER VARIATION IN HYPERTROPHIC CARDIOMYOPATHY

Motivated by the fact that approximately 50-60% of HCM patients remain genetically undiagnosed [172], a read depth strategy was applied to the targeted high-throughput sequence data generated from the first 505 unrelated and consecutive HCM patients. Such analysis could be hampered by the limitations of short read sequencing approaches, which negatively affect sensitivity/specificity [348]. To avoid false calls, I used an aCGH validation strategy and validated 4 out of 12 CNV calls, in line with the previously reported high false positive rate across all available algorithms [348].

Using this two-step approach, I detected and validated potential disease causing CNVs in 0.8% of the samples, with direct implications for diagnostic and counselling: some patients without mutations on direct sequencing may still have transmissible CNVs in sarcomeric protein genes.

While the limited sensitivity of read depth techniques for CNV detection is an important caveat to consider, the read depth methodology applied here provided reliable data for large CNVs [349]. Hence, the limited proportion of potential disease causing CNVs in the cohort (< 1%) suggests that CNVs are not a major genetic cause of HCM. While the knowledge of the role of CNVs in HCM is scarce, other reports are compatible with this conclusion. These include a single family with a large *MYH7* deletion as the probable cause [350], which was detected using a PCR-based method and more recently a single *MYBPC3* deletion [351] in a cohort of 100 unrelated genotype-negative patients, using multiplex ligation-dependent probe amplification (MPLA). A third study, also using MPLA, was unable to detect any large rearrangement in *MYBPC3* or *TNNT2* in a cohort of around 100 unrelated HCM patients [352].

In other cardiomyopathies, two groups [353],[354] reported on three large *PKP2* deletions in arrhythmogenic right ventricular cardiomyopathy (ARVC) patients, one detected by a SNP array [353] in a single family without point mutations in known ARVC genes and the other [354] in two unrelated probands (one detected by array methodology and the other by MPLA). Another report failed to demonstrate the presence of *LMNA* CNVs in a cohort of dilated cardiomyopathy (DCM) patients [355].

Further work to define the pathogenicity of the discovered CNV candidates is required, but the two deletions – one in *MYBPC3* and the other in *PDLIM3* -are likely to be pathogenic. The large deletion in *MYBPC3*, encompassing 4 exons, is consistent with haploinsufficiency, the most commonly accepted pathogenic mechanism for this protein [35, 356]. The large deletion in *PDLIM3*, involving the last 4 exons, is also very likely to cause a truncated protein or RNA mediated decay, culminating in haploinsufficiency. Interestingly, although previously reported as causal, there are very few data on the association between this gene and HCM (or cardiomyopathy in general) [63] and CNVs might prove to be an important cause of pathogenic variation in *PDLIM3*. *PDLIM3* is a conserved human gene: the NHLBI exome sequencing server [357][74](24) shows a single loss-of-function (LOF) variant in over 12500 alleles– a frameshift insertion (rs199476399; c.178_179insCA; p.(M60Tfs*2)) The observation of a LOF CNV in the cohort of HCM cases is consistent with the possibility that *PDLIM3* LOF alleles cause HCM. However, additional evidence will be necessary to confirm this hypothesis.

The possible causal role of the two large duplications is more difficult to judge. The database of genomic variants (http://www.ncbi.nlm.nih.gov/dbvar/, accessed Aug 2014) lists a single exonic *TNNT2* duplication, (dbVar nsv467961; 218021 bp). This previously reported duplication is large and involves 7 genes. It was originally reported in a CNV screening study of a general population cohort of 1,500 individuals (no detailed phenotypic data available) [358]. A similar dbVar search for exonic *LMNA* CNVs identified a single duplication (dbVar nsv509513; 246469 bp), involving 10 genes, and originally published in a technical report of single molecule analysis of genome structure in 4 samples [359]. Overall and although a proper estimation of control sample size is not possible owing to the heterogeneity of this available database, these data suggest that large duplications in these two genes are rare and could be disease causing.

Structural variation has traditionally been studied using hybridization techniques such as fluorescent in situ hybridization (FISH), only capable of detecting very large structural changes. These approaches have more recently been replaced by aCGH for clinical applications. The development of calling algorithms that can detect CNVs from HTS data [273],[348] means that for the first time larger patient cohorts can be routinely screened for CNV, as demonstrated in this study. Furthermore, while clinically relevant results can be obtained with targeted sequencing data, as applied here, such techniques will be radically improved by the generalization of whole genome sequencing, for which read depth strategies can be used in

combination with read pair and split read methodologies [152] to provide a thorough picture of the contribution of CNVs to inherited cardiac disorders.

4. NON-CODING SEQUENCE DATA ANALYSIS

In this work, I sought to explore, for the first time, the possible contribution of non-coding variation to the genetic architecture of HCM, using targeted HTS. I also proposed a pipeline for the analysis of non-coding variation, based on open-access bioinformatic tools and public databases, which can be used to prioritize candidate variants for future functional studies.

4.1. VARIANTS MAPPING TO TRANSCRIPTION FACTOR BINDING SITES

My results show that a considerable proportion of patients (14%) carry variants that could potentially interfere with the binding of cardiac expressed transcription factors (TF). A majority of these patients do not carry potentially causal mutations in the exonic regions of these genes.

If only considering those transcription factors in which previous experimental evidence shows a role in cardiomyocyte hypertrophy signalling, the proportion of patients without coding candidate variants is higher and even higher if only considering the variants that map to conserved positions.

SRF (serum response factor) has been established as a mediator of hypertrophic signals and its over-expression in transgenic animal models induced cardiac hypertrophy or dilation. Its role in the regulation of cardiac development genetic programs has also been demonstrated, as well as its effect in the induction of the fetal gene program as part of the cardiac hypertrophy response [360],[361],[362]. There is extensive experimental evidence from luciferase reporter gene assays, RT-PCR and microarray analysis in cell lines from animal models, that establishes SRF as binding to the promoter of *ACTC1* and activating the transcription of this gene[363],[364],[365],[366],[367]. In this cohort, three variants were predicted to potentially interfere with the binding of SRF to regulatory regions of sarcomere genes: two are in conserved positions, located in the 5'UTR of *ACTC1* and in an intronic region of *TPM1*. These genomic positions also have a high level of evidence for the transcription factor binding, reflected by a RegulomeDB score of 2a (datatypes available: TF binding + matched TF motif +

matched DNase Footprint + DNase peak). A third SRF-binding variant is located in the upstream region of *ACTC1*.

C/EBPß (CCAAT/enhancer binding protein beta) has recently been implicated in the transcriptional mechanisms and signaling underlying physiological hypertrophy and also cardiomyocyte proliferation during development [368]. Data from genetically modified mice suggested that C/EBPß inhibits cardiomyocyte hypertrophy in the adult mammalian heart. I found three variants that could potentially affect C/EBPß binding to regulatory intronic regions of *MYBPC3* in four patients that did not carry any candidate coding variants in sarcomere genes. All the three positions are conserved.

p300 is a transcription co-activator of GATA4 and myocardin and has histone acetyltransferase activity. Overexpression in cardiomyocytes induces hypertrophy [361]. The p300/GATA4 pathway was also recently suggested to mediate the hypertrophic response to aldosterone/mineralocorticoid receptors [369]. Two of the detected variants map to p300 binding sites, one upstream of *MYH7* and the other in an intronic region of *TPM1*.

STAT3 (signal transducer and activator of transcription 3) over-expression in mice induces cardiac hypertrophy. This signaling pathway has also been implicated in cardiomyocyte survival (e.g. upon anthracycline toxicity), mitochondrial energy metabolism and extracellular matrix composition [370],[371]. I identified two variants potentially affecting the binding of STAT3, both in intronic regions of *ACTC1*.

Activation of HDAC2 (histone deacetylase 2) by hypertrophic stressors has previously been demonstrated. Transgenic mice with HDAC2 over-expression exhibit cardiac hypertrophy and knock-out mice are resistant to hypertrophy [372]. My analysis identified two variants mapping to binding sites for HDAC2. One variant is present in the 3'UTR of *TPM1* and another in the upstream region of *MYH7*.

NSRF (neuronrestrictive silencer factor) is a transcription repressor, with a key role in the induction of the "fetal gene program" in the presence of hypertrophic stimuli. Knock-in mice for a mutant NSRF exhibited a dilated cardiomyopathy phenotype [373]. I detected one variant that could interfere with NSRF binding to an intronic region of *TNNT2*, in a patient without any exonic variant in sarcomere genes.

YY1 was demonstrated to be an anti-hypertrophic factor. Over-expression of YY1 prevents cardiomyocyte hypertrophy and the "fetal gene program" activation in the presence of hypertrophic stimuli [374]. A variant that could potentially affect the binding of YY1 to the 5'UTR of TPM1 was detected in one patient, who did not present any potentially causal variant in the coding region of any sarcomere gene. The variant occurred in a conserved position.

One important limitation for this screening is the absence of suitable controls for comparison of the frequency of non-coding variation. In fact, most of the available databases, such as NHBLI ESP exome sequencing server (http://evs.gs.washington.edu/EVS/) or the 1000 genomes project browser (http://browser.1000genomes.org/index.html) only include exome (coding) sequencing data or in the case of the 1000 genomes, very low read depth data for non-coding regions in phase II of the project, which invalidates a meaningful comparison.

Until the completion of the thesis, additional algorithms were published that allow annotation of non-coding variants and prediction of pathogenicity, such as Combined Annotation-Dependent Depletion (CADD) [375], which also allows annotation of coding regions and Genome-Wide annotation of Variants (GWAVA), specifically developed to annotate the non-coding regions [376]. Future work with the use of these algorithms might help the prioritization of variants for mechanistic studies, which is outside the scope of the current work.

4.2. EXPRESSION COMPARISON BETWEEN CASES AND CONTROLS

I then sought to understand whether the presence of non-coding variants mapping to TF binding sites influenced the expression of the sarcomeric genes where those variants occurred, using tissue from two sarcomere-negative individuals previously submitted to miectomy and additionally if there was a change in the expression of other sarcomere genes in that tissue.

The array expression study showed that the RNA levels for the eight main sarcomeric genes was not different between these two cases and controls. The most likely explanation is that the cause of hypertrophic cardiomyopathy in these two patients resides elsewhere in the coding genome. However, as some of these genes also have an important role during cardiac development, another explanation can be that the effect of the non-coding variation in the expression of these genes could only be verified in earlier stages of development, leading years later to the development of HCM. Another open hypothesis is that non-coding variation

is a modifier and not a cause of the phenotype, which would require much more complex models to evaluate.

5. WHOLE-EXOME SEQUENCING

The emergence of high-throughput sequencing technologies has allowed the possibility of sequencing the entire coding region of the human genome, the exome, a sequencing process called whole-exome sequencing (WES) [377], [107].

In the first few published studies, WES was demonstrated to be useful for new causal gene discovery, in Mendelian diseases where the genetic basis was not (partially or completely) solved, as an alternative to the more classic linkage studies. This was the case of the initial proof-of-concept publications [377],[378] in very rare syndromes such as Miller or Freeman-Sheldon syndrome. WES was then applied for new gene discovery, and also in the cardiovascular setting; one example is the discovery of *BAG3* as causal gene for dilated cardiomyopathy [379].

WES has also been used to screen large populations, in the previously mentioned studies that have been extremely useful for the understanding of the scope of human variation in health and disease, such as the 1000 genomes project [112], the NHBLI ESP [114] and UK10K [380]. Those studies, all conducted while my own research was taking place, were very recently completed and have provided an extraordinary amount of data, for which one of the most useful clinical applications is the ability to filter variants according to their frequency in those populations.

More recently and as a consequence of the technological development of sequencing platforms and bioinformatic algorithms for variant calling and annotation, the use of WES has also been advocated for clinical genetic testing, particularly in diseases characterized by high locus heterogeneity (which is the case of HCM), as an alternative to the targeted sequencing of a limited panel of genes of interest for the disease being studied [107]. The stated advantages are equivalent costs and the gain of extra-information. However, the previously discussed challenges of sequence data interpretation are greatly augmented by this approach, because variants from more than 20,000 genes are obtained. Other limitations are the lower coverage and read depth [109], compared to the more focussed targeted sequencing of a few genes of

interest, and the challenging issue of incidental findings, for which recent guidelines have recommended a list of genes where variation should be reported [323].

As described previously in this text, around half of the studied HCM probands did not carry any candidate variant in a main sarcomere gene. I therefore hypothesized that this could be partially due to previously undiscovered genes - or known genes that were not previously associated with HCM.

As such, WES was used as a pilot study for new causal gene discover, in families where I did not find any candidate variant in the initial targeted sequencing of known causal genes. I selected three of those "genotype-negative" families, where blood was available for two affected relatives. After a process of filtering for shared variants between two relatives, rarity and relevant disease pathways, a list of between 34-68 candidate variants was obtained.

Based on molecular interactions and data from the literature and databases, the strongest candidates obtained were two *OBSCN* (obscurin) variants – T7800I and A7669T – one in each of two families. Furthermore, in one of these families, the phenotype also co-segregates with compound heterozigozity for 2 missense *TTN* variants – R26175Q and T8910S, both predicted to have a functional impact.

Different obscurin isoforms are obtained from differential splicing of the *OBSCN* gene. Most are very large proteins, composed of multiple immunoglobulin domains, a calmodulin/Ca interacting domain, a Rho-guanine nucleotide exchange factor (RhoGEF) and in obscurin B, two C-terminal kinase domains. This protein interacts with M-band proteins, Z-disc proteins, *TTN* and the sarcoplasmic reticulum through ankyrin [381]. Through these multiple interactions, osbcurin is thus believed to exert important roles in myofibrillar and sarcomere organization and signaling. The causal role of obscurin variation in cardiomyopathies has not been systematically explored. There is only one single report of an association with HCM [75], with limited functional data showing impaired interaction with *TTN* and impaired localization to the Z-disc, but co-segregation information is absent. The limited knowledge regarding the pathogenicity contribution of obscurin to cardiomyopathies is probably related to factors in common with titin. Because of its large dimensions, it has been challenging to sequence the gene by previously available conventional sequencing technologies in a significant amount of patients. Also, the complex splicing process and multiple isoforms create annotation problems.

For my own data, functional studies and sequencing of unaffected relatives has to follow, in order to prove pathogenicity and causality for these variants. However it is interesting to notice that I detected two possible candidate *OBSCN* variants in 3 families, suggesting a common genetic cause of HCM. More HCM probands should be screeened for variation in this gene. For the family with the compound heterozigozity for *TTN*, I hypothesize that the triple variation in these two crucial proteins for sarcomere function is ultimately responsible for the phenotype, functioning as an oligogenic mechanism.

6. *IN SILICO* ANALYSIS OF *MYH7* MISSENSE VARIANTS – PATHOGENICITY AND PHENOTYPE PREDICTION BASED IN THE STRUCTURAL IMPACT OF THE MUTATION

Genotype-phenotype analyses, like the one described in previous sections, do not usually account for protein structural data regarding the mutations being analysed, both in terms of the location of the mutated residue in a certain domain or the potential impact of the amino acid substitution regarding conformational changes, interaction with other domains/regions within the same protein, protein-protein interaction or ligand binding. This limitation is probably due to a combination of a still large number of unsolved protein structures and the absence of *in silico* prediction software incorporating structural information. In the cardiomyopathy field, only one report has suggested a prognostic influence of the domain localization of mutations in beta-myosin heavy chain [169], but this was not the object of further studies.

Stimulated by the above limitations and the availability of an *in silico* software – SAAPpred – that predicts the structural impact of an amin oacid change [163], [166] if the residue locates to a solved PDB structure, I hypothesized that the integrated use of such a tool would improve the ability to predict pathogenicity of missense variants and help in the establishment of genotype-phenotype relationships in cardiomyopathy. I used beta-myosin heavy chain as the model of this exploratory work, because its structure is mostly solved and almost all causal mutations are missense, on the contrary to cardiac myosin binding protein C, where truncating mutations are very prevalent. Furthermore, mutations in *MYH7* can give rise to two different phenotypes – HCM and DCM.

An initial manual analysis showed promising associations between some of the structural features and phenotype traits, such as maximal wall thickness or the development of an HCM phenotype vs DCM.

This pilot results suggested the possibility that a more sophisticated approach, for example using machine-learning methods could generate novel results. When the predictive power of the SAAPpred approach was examined by a machine learning approach to discriminate between pathogenic and putatively neutral SNPs in *MYH7*, the dataset gave very reasonable

results for accuracy, above 0.90. This was then followed by the creation of a novel predictor, which attempts to distinguish between HCM and DCM mutations using SAAP analysis. Structural clustering was incorporated as one of the features, because mutations causing HCM and DCM were found to cluster in different regions of the beta-myosin heavy chain head. The best performance currently achieved for distinguishing HCM and DCM mutations, by removing models that perform particularly badly, is an accuracy of 0.79. The reason for removal of the badly performing models must be further explored from a protein structural perspective (i.e some structures appear to make the performance worse).

In conclusion, the use of a machine learning algorithm based on a structural impact prediction tool allowed very reasonable prediction of pathogenicity, at least comparable to the existing tools [166], but with the advantage of having been developed for a single protein and disease group, which is an often cited limitation of the existing *in silico* software[110]. These findings can now be further validated in additional datasets of *MYH7* variants.

Perhaps even more interesting and novel, is the promising ability of predicting phenotype (HCM vs DCM) from the structural impact / location of the mutation. Considering that this is such a complex biological problem, the accuracy of 0.79 was considered surprisingly good and deserves to be further explored for other phenotype traits, such as maximal wall thickness and eventually for other sarcomere proteins. The differential clustering of HCM vs DCM mutations on the beta-myosin heavy chain head should also be studied in terms of the affected sub-domains, which may suggest novel hypothesis regarding downstream pathways, mechanisms of disease and new drug targets in cardiomyopathies.

7. CONCLUSIONS

- This study provided the first large-scale quantitative analysis of the prevalence and effects of sarcomere protein gene variants in patients with HCM using a targeted HTS technology;
- I identified a large number of nsSNPs in sarcomeric and non-sarcomeric genes. Four sarcomeric genes (*MYH7, MYBPC3, TNNI3, TNNT2*), *CSRP3* and *PLN* showed an excess of rare single non-synonymous SNPs (nsSNPs) in cases compared to controls;
- The frequency of non-sarcomeric variants was similar to the control population but some of them are predicted to have functional impact and/or were previously published as pathogenic in other inherited cardiac diseases;
- There is a class effect of sarcomere protein gene variants on the HCM phenotype and I detected novel associations with mutations in individual sarcomere protein genes;
- There is evidence of a modifier effect of variation in non-sarcomere protein genes in HCM expression, that could explain some of the characteristic clinical heterogeneity of the disease;
- Copy number variants are apparently a rare genetic cause of hypertrophic cardiomyopathy, but patients studied with HTS should be screened for this type of variation;
- Rare non-coding variation is present in a substantial proportion of HCM patients; variation in transcription factor binding sites seems to be more important than variation in 3'UTR miRNA target regions.
- *Insilico* tools that integrate structural features potentially enhance the establishment of genotype-phenotype relationships.

REFERENCES

1 Elliott P, Andersson B, Arbustini E, et al. Classification of the cardiomyopathies: a position statement from the European Society Of Cardiology Working Group on Myocardial and Pericardial Diseases. *Eur Heart J* 2008;**29**:270-6.
2 Lopes LR, Elliott PM. A straightforward guide to the sarcomeric basis of cardiomyopathies. *Heart* 2014; **100** (24):1916-1923..
3 Elliott P, McKenna WJ. Hypertrophic cardiomyopathy. *Lancet* 2004;**363**:1881-91.
4 Maron BJ, McKenna WJ, Danielson GK, et al. American College of Cardiology/European Society of Cardiology clinical expert consensus document on hypertrophic cardiomyopathy. A report of the American College of Cardiology Foundation Task Force on Clinical Expert Consensus Documents and the European Society of Cardiology Committee for Practice Guidelines. *J Am Coll Cardiol* 2003;**42**:1687-713.
5 Gersh BJ, Maron BJ, Bonow RO, et al. 2011 ACCF/AHA Guideline for the Diagnosis and Treatment of Hypertrophic Cardiomyopathy: a report of the American College of Cardiology Foundation/American Heart Association Task Force on Practice Guidelines. Developed in collaboration with the American Association for Thoracic Surgery, American Society of Echocardiography, American Society of Nuclear Cardiology, Heart Failure Society of America, Heart Rhythm Society, Society for Cardiovascular Angiography and Interventions, and Society of Thoracic Surgeons. *J Am Coll Cardiol* 2011;**58**:e212-60.
6 Elliott PM, Poloniecki J, Dickie S, et al. Sudden death in hypertrophic cardiomyopathy: identification of high risk patients. *J Am Coll Cardiol* 2000;**36**:2212-8.
7 Elliott PM, Gimeno Blanes JR, Mahon NG, et al. Relation between severity of left-ventricular hypertrophy and prognosis in patients with hypertrophic cardiomyopathy. *Lancet* 2001;**357**:420-4.
8 Elliott PM, Gimeno JR, Thaman R, et al. Historical trends in reported survival rates in patients with hypertrophic cardiomyopathy. *Heart* 2006;**92**:785-91.
9 Varnava AM, Elliott PM, Baboonian C, et al. Hypertrophic cardiomyopathy: histopathological features of sudden death in cardiac troponin T disease. *Circulation* 2001;**104**:1380-4.
10 Gersh BJ, Maron BJ, Bonow RO, et al. 2011 ACCF/AHA guideline for the diagnosis and treatment of hypertrophic cardiomyopathy: executive summary: a report of the American College of Cardiology Foundation/American Heart Association Task Force on Practice Guidelines. *Circulation* 2011;**124**:2761-96.
11 Olivotto I, Cecchi F, Poggesi C, et al. Patterns of disease progression in hypertrophic cardiomyopathy: an individualized approach to clinical staging. *Circ Heart Fail* 2012;**5**:535-46.
12 Harris KM, Spirito P, Maron MS, et al. Prevalence, clinical profile, and significance of left ventricular remodeling in the end-stage phase of hypertrophic cardiomyopathy. *Circulation* 2006;**114**:216-25.
13 Geisterfer-Lowrance AA, Kass S, Tanigawa G, et al. A molecular basis for familial hypertrophic cardiomyopathy: a beta cardiac myosin heavy chain gene missense mutation. *Cell* 1990;**62**:999-1006.
14 Watkins H, Conner D, Thierfelder L, et al. Mutations in the cardiac myosin binding protein-C gene on chromosome 11 cause familial hypertrophic cardiomyopathy. *Nat Genet* 1995;**11**:434-7.
15 Thierfelder L, Watkins H, MacRae C, et al. Alpha-tropomyosin and cardiac troponin T mutations cause familial hypertrophic cardiomyopathy: a disease of the sarcomere. *Cell* 1994;**77**:701-12.
16 Poetter K, Jiang H, Hassanzadeh S, et al. Mutations in either the essential or regulatory light chains of myosin are associated with a rare myopathy in human heart and skeletal muscle. *Nat Genet* 1996;**13**:63-9.
17 Kimura A, Harada H, Park JE, et al. Mutations in the cardiac troponin I gene associated with hypertrophic cardiomyopathy. *Nat Genet* 1997;**16**:379-82.

18 Keren A, Syrris P, McKenna WJ. Hypertrophic cardiomyopathy: the genetic determinants of clinical disease expression. *Nat Clin Pract Cardiovasc Med* 2008;**5**:158-68.
19 Marian AJ, Roberts R. The molecular genetic basis for hypertrophic cardiomyopathy. *J Mol Cell Cardiol* 2001;**33**:655-70.
20 Morita H, Rehm HL, Menesses A, et al. Shared genetic causes of cardiac hypertrophy in children and adults. *N Engl J Med* 2008;**358**:1899-908.
21 Van Driest SL, Ommen SR, Tajik AJ, et al. Yield of genetic testing in hypertrophic cardiomyopathy. *Mayo Clin Proc* 2005;**80**:739-44.
22 Millat G, Bouvagnet P, Chevalier P, et al. Prevalence and spectrum of mutations in a cohort of 192 unrelated patients with hypertrophic cardiomyopathy. *Eur J Med Genet* 2010;**53**:261-7.
23 Richard P, Charron P, Carrier L, et al. Hypertrophic cardiomyopathy: distribution of disease genes, spectrum of mutations, and implications for a molecular diagnosis strategy. *Circulation* 2003;**107**:2227-32.
24 Sequeira V, Nijenkamp LL, Regan JA, et al. The physiological role of cardiac cytoskeleton and its alterations in heart failure. *Biochim Biophys Acta* 2014;**1838**:700-22.
25 Harris SP, Lyons RG, Bezold KL. In the thick of it: HCM-causing mutations in myosin binding proteins of the thick filament. *Circ Res* 2011;**108**:751-64.
26 Tardiff JC. Thin filament mutations: developing an integrative approach to a complex disorder. *Circ Res* 2011;**108**:765-82.
27 Moore JR, Leinwand L, Warshaw DM. Understanding cardiomyopathy phenotypes based on the functional impact of mutations in the myosin motor. *Circ Res* 2012;**111**:375-85.
28 Carniel E, Taylor MR, Sinagra G, et al. Alpha-myosin heavy chain: a sarcomeric gene associated with dilated and hypertrophic phenotypes of cardiomyopathy. *Circulation* 2005;**112**:54-9.
29 Granados-Riveron JT, Ghosh TK, Pope M, et al. Alpha-cardiac myosin heavy chain (MYH6) mutations affecting myofibril formation are associated with congenital heart defects. *Hum Mol Genet* 2010;**19**:4007-16.
30 Muller M, Mazur AJ, Behrmann E, et al. Functional characterization of the human alpha-cardiac actin mutations Y166C and M305L involved in hypertrophic cardiomyopathy. *Cellular and molecular life sciences : CMLS* 2012;**69**:3457-79.
31 Gordon AM, Homsher E, Regnier M. Regulation of contraction in striated muscle. *Physiol Rev* 2000;**80**:853-924.
32 Hershberger RE, Hedges DJ, Morales A. Dilated cardiomyopathy: the complexity of a diverse genetic architecture. *Nat Rev Cardiol* 2013;**10**:531-47.
33 Sen-Chowdhry S, Syrris P, McKenna WJ. Genetics of restrictive cardiomyopathy. *Heart Fail Clin* 2010;**6**:179-86.
34 Seidman JG, Seidman C. The genetic basis for cardiomyopathy: from mutation identification to mechanistic paradigms. *Cell* 2001;**104**:557-67.
35 Marston S, Copeland O, Jacques A, et al. Evidence from human myectomy samples that MYBPC3 mutations cause hypertrophic cardiomyopathy through haploinsufficiency. *Circ Res* 2009;**105**:219-22.
36 Spudich JA. Hypertrophic and Dilated Cardiomyopathy: Four Decades of Basic Research on Muscle Lead to Potential Therapeutic Approaches to These Devastating Genetic Diseases. *Biophys J* 2014;**106**:1236-49.
37 Bonne G, Carrier L, Bercovici J, et al. Cardiac myosin binding protein-C gene splice acceptor site mutation is associated with familial hypertrophic cardiomyopathy. *Nat Genet* 1995;**11**:438-40.
38 Elliott PM, Anastasakis A, Borger MA, Borggrefe M, Cecchi F, Charron P, Hagege AA, Lafont A, Limongelli G, Mahrholdt H, McKenna WJ, Mogensen J, Nihoyannopoulos P, Nistri S, Pieper PG, Pieske B, Rapezzi C, Rutten FH, Tillmanns C, Watkins H; Authors/Task Force

members. 2014 ESC Guidelines on diagnosis and management of hypertrophic cardiomyopathy: The Task Force for the Diagnosis and Management of Hypertrophic Cardiomyopathy of the European Society of Cardiology (ESC). Eur Heart J. 2014; **35**(39):2733-79.

39 Mogensen J, Klausen IC, Pedersen AK, et al. Alpha-cardiac actin is a novel disease gene in familial hypertrophic cardiomyopathy. *J Clin Invest* 1999;**103**:R39-43.

40 Landstrom AP, Parvatiyar MS, Pinto JR, et al. Molecular and functional characterization of novel hypertrophic cardiomyopathy susceptibility mutations in TNNC1-encoded troponin C. *J Mol Cell Cardiol* 2008;**45**:281-8.

41 Mogensen J, Murphy RT, Shaw T, et al. Severe disease expression of cardiac troponin C and T mutations in patients with idiopathic dilated cardiomyopathy. *J Am Coll Cardiol* 2004;**44**:2033-40.

42 Zou P, Pinotsis N, Lange S, et al. Palindromic assembly of the giant muscle protein titin in the sarcomeric Z-disk. *Nature* 2006;**439**:229-33.

43 Fukuzawa A, Lange S, Holt M, et al. Interactions with titin and myomesin target obscurin and obscurin-like 1 to the M-band: implications for hereditary myopathies. *J Cell Sci* 2008;**121**:1841-51.

44 Gautel M. The sarcomeric cytoskeleton: who picks up the strain? *Curr Opin Cell Biol* 2011;**23**:39-46.

45 Muller S, Lange S, Gautel M, et al. Rigid conformation of an immunoglobulin domain tandem repeat in the A-band of the elastic muscle protein titin. *J Mol Biol* 2007;**371**:469-80.

46 LeWinter MM, Granzier H. Cardiac titin: a multifunctional giant. *Circulation* 2010;**121**:2137-45.

47 Lange S, Xiang F, Yakovenko A, et al. The kinase domain of titin controls muscle gene expression and protein turnover. *Science* 2005;**308**:1599-603.

48 Itoh-Satoh M, Hayashi T, Nishi H, et al. Titin mutations as the molecular basis for dilated cardiomyopathy. *Biochem Biophys Res Commun* 2002;**291**:385-93.

49 Gerull B, Gramlich M, Atherton J, et al. Mutations of TTN, encoding the giant muscle filament titin, cause familial dilated cardiomyopathy. *Nat Genet* 2002;**30**:201-4.

50 Herman DS, Lam L, Taylor MR, et al. Truncations of titin causing dilated cardiomyopathy. *N Engl J Med* 2012;**366**:619-28.

51 Arimura T, Bos JM, Sato A, et al. Cardiac ankyrin repeat protein gene (ANKRD1) mutations in hypertrophic cardiomyopathy. *J Am Coll Cardiol* 2009;**54**:334-42.

52 Peled Y, Gramlich M, Yoskovitz G, et al. Titin mutation in familial restrictive cardiomyopathy. *Int J Cardiol* 2014;**171**:24-30.

53 Taylor M, Graw S, Sinagra G, et al. Genetic variation in titin in arrhythmogenic right ventricular cardiomyopathy-overlap syndromes. *Circulation* 2011;**124**:876-85.

54 Knoll R, Buyandelger B, Lab M. The sarcomeric Z-disc and Z-discopathies. *J Biomed Biotechnol* 2011;**2011**:569628.

55 Chiu C, Bagnall RD, Ingles J, et al. Mutations in alpha-actinin-2 cause hypertrophic cardiomyopathy: a genome-wide analysis. *J Am Coll Cardiol* 2010;**55**:1127-35.

56 Mohapatra B, Jimenez S, Lin JH, et al. Mutations in the muscle LIM protein and alpha-actinin-2 genes in dilated cardiomyopathy and endocardial fibroelastosis. *Mol Genet Metab* 2003;**80**:207-15.

57 Geier C, Gehmlich K, Ehler E, et al. Beyond the sarcomere: CSRP3 mutations cause hypertrophic cardiomyopathy. *Hum Mol Genet* 2008;**17**:2753-65.

58 Hayashi T, Arimura T, Itoh-Satoh M, et al. Tcap gene mutations in hypertrophic cardiomyopathy and dilated cardiomyopathy. *J Am Coll Cardiol* 2004;**44**:2192-201.

59 Osio A, Tan L, Chen SN, et al. Myozenin 2 is a novel gene for human hypertrophic cardiomyopathy. *Circ Res* 2007;**100**:766-8.

60 Gossios TD, Lopes LR, Elliott PM. Left ventricular hypertrophy caused by a novel nonsense mutation in FHL1. *Eur J Med Genet* 2013;**56**:251-5.
61 Vatta M, Mohapatra B, Jimenez S, et al. Mutations in Cypher/ZASP in patients with dilated cardiomyopathy and left ventricular non-compaction. *J Am Coll Cardiol* 2003;**42**:2014-27.
62 Theis JL, Bos JM, Bartleson VB, et al. Echocardiographic-determined septal morphology in Z-disc hypertrophic cardiomyopathy. *Biochem Biophys Res Commun* 2006;**351**:896-902.
63 Bagnall RD, Yeates L, Semsarian C. Analysis of the Z-disc genes PDLIM3 and MYPN in patients with hypertrophic cardiomyopathy. *Int J Cardiol* 2010;**145**:601-2.
64 Goldfarb LG, Park KY, Cervenakova L, et al. Missense mutations in desmin associated with familial cardiac and skeletal myopathy. *Nat Genet* 1998;**19**:402-3.
65 Li D, Tapscoft T, Gonzalez O, et al. Desmin mutation responsible for idiopathic dilated cardiomyopathy. *Circulation* 1999;**100**:461-4.
66 Klauke B, Kossmann S, Gaertner A, et al. De novo desmin-mutation N116S is associated with arrhythmogenic right ventricular cardiomyopathy. *Hum Mol Genet* 2010;**19**:4595-607.
67 Lorenzon A, Beffagna G, Bauce B, et al. Desmin mutations and arrhythmogenic right ventricular cardiomyopathy. *Am J Cardiol* 2013;**111**:400-5.
68 Purevjav E, Arimura T, Augustin S, et al. Molecular basis for clinical heterogeneity in inherited cardiomyopathies due to myopalladin mutations. *Hum Mol Genet* 2012;**21**:2039-53.
69 Wang H, Li Z, Wang J, et al. Mutations in NEXN, a Z-disc gene, are associated with hypertrophic cardiomyopathy. *Am J Hum Genet* 2010;**87**:687-93.
70 Hassel D, Dahme T, Erdmann J, et al. Nexilin mutations destabilize cardiac Z-disks and lead to dilated cardiomyopathy. *Nat Med* 2009;**15**:1281-8.
71 Duboscq-Bidot L, Charron P, Ruppert V, et al. Mutations in the ANKRD1 gene encoding CARP are responsible for human dilated cardiomyopathy. *Eur Heart J* 2009;**30**:2128-36.
72 Moulik M, Vatta M, Witt SH, et al. ANKRD1, the gene encoding cardiac ankyrin repeat protein, is a novel dilated cardiomyopathy gene. *J Am Coll Cardiol* 2009;**54**:325-33.
73 Siegert R, Perrot A, Keller S, et al. A myomesin mutation associated with hypertrophic cardiomyopathy deteriorates dimerisation properties. *Biochem Biophys Res Commun* 2011;**405**:473-9.
74 Kho AL, Perera S, Alexandrovich A, et al. The sarcomeric cytoskeleton as a target for pharmacological intervention. *Curr Opin Pharmacol* 2012;**12**:347-54.
75 Arimura T, Matsumoto Y, Okazaki O, et al. Structural analysis of obscurin gene in hypertrophic cardiomyopathy. *Biochem Biophys Res Commun* 2007;**362**:281-7.
76 Cleland JG, Teerlink JR, Senior R, et al. The effects of the cardiac myosin activator, omecamtiv mecarbil, on cardiac function in systolic heart failure: a double-blind, placebo-controlled, crossover, dose-ranging phase 2 trial. *Lancet* 2011;**378**:676-83.
77 Bond LM, Tumbarello DA, Kendrick-Jones J, et al. Small-molecule inhibitors of myosin proteins. *Future medicinal chemistry* 2013;**5**:41-52.
78 Witjas-Paalberends ER, Piroddi N, Stam K, et al. Mutations in MYH7 reduce the force generating capacity of sarcomeres in human familial hypertrophic cardiomyopathy. *Cardiovasc Res* 2013;**99**:432-41.
79 Alves ML, Dias FA, Gaffin RD, et al. Desensitization of Myofilaments to Ca2+ as a Therapeutic Target for Hypertrophic Cardiomyopathy with Mutations in Thin Filament Proteins. *Circ Cardiovasc Genet* 2014; **7**(2):132-43..
80 Ashrafian H, McKenna WJ, Watkins H. Disease pathways and novel therapeutic targets in hypertrophic cardiomyopathy. *Circ Res* 2011;**109**:86-96.
81 Semsarian C, Ahmad I, Giewat M, et al. The L-type calcium channel inhibitor diltiazem prevents cardiomyopathy in a mouse model. *J Clin Invest* 2002;**109**:1013-20.

82 Schober T, Huke S, Venkataraman R, et al. Myofilament Ca sensitization increases cytosolic Ca binding affinity, alters intracellular Ca homeostasis, and causes pause-dependent Ca-triggered arrhythmia. *Circ Res* 2012;**111**:170-9.
83 Fatkin D, McConnell BK, Mudd JO, et al. An abnormal Ca(2+) response in mutant sarcomere protein-mediated familial hypertrophic cardiomyopathy. *J Clin Invest* 2000;**106**:1351-9.
84 Javadpour MM, Tardiff JC, Pinz I, et al. Decreased energetics in murine hearts bearing the R92Q mutation in cardiac troponin T. *J Clin Invest* 2003;**112**:768-75.
85 Knollmann BC, Kirchhof P, Sirenko SG, et al. Familial hypertrophic cardiomyopathy-linked mutant troponin T causes stress-induced ventricular tachycardia and Ca2+-dependent action potential remodeling. *Circ Res* 2003;**92**:428-36.
86 Baudenbacher F, Schober T, Pinto JR, et al. Myofilament Ca2+ sensitization causes susceptibility to cardiac arrhythmia in mice. *J Clin Invest* 2008;**118**:3893-903.
87 Lan F, Lee AS, Liang P, et al. Abnormal calcium handling properties underlie familial hypertrophic cardiomyopathy pathology in patient-specific induced pluripotent stem cells. *Cell stem cell* 2013;**12**:101-13.
88 Westermann D, Knollmann BC, Steendijk P, et al. Diltiazem treatment prevents diastolic heart failure in mice with familial hypertrophic cardiomyopathy. *Eur J Heart Fail* 2006;**8**:115-21.
89 Coppini R, Ferrantini C, Yao L, et al. Late sodium current inhibition reverses electromechanical dysfunction in human hypertrophic cardiomyopathy. *Circulation* 2013;**127**:575-84.
90 Manning G, Whyte DB, Martinez R, et al. The protein kinase complement of the human genome. *Science* 2002;**298**:1912-34.
91 Mumby MC, Walter G. Protein serine/threonine phosphatases: structure, regulation, and functions in cell growth. *Physiol Rev* 1993;**73**:673-99.
92 Carrier L, Schlossarek S, Willis MS, et al. The ubiquitin-proteasome system and nonsense-mediated mRNA decay in hypertrophic cardiomyopathy. *Cardiovasc Res* 2010;**85**:330-8.
93 Chen SN, Czernuszewicz G, Tan Y, et al. Human molecular genetic and functional studies identify TRIM63, encoding Muscle RING Finger Protein 1, as a novel gene for human hypertrophic cardiomyopathy. *Circ Res* 2012;**111**:907-19.
94 Ploski R, Pollak A, Muller S, et al. Does p.Q247X in TRIM63 cause human hypertrophic cardiomyopathy? *Circ Res* 2014;**114**:e2-5.
95 Teekakirikul P, Eminaga S, Toka O, et al. Cardiac fibrosis in mice with hypertrophic cardiomyopathy is mediated by non-myocyte proliferation and requires Tgf-beta. *J Clin Invest* 2010;**120**:3520-9.
96 Ho CY, Lopez B, Coelho-Filho OR, et al. Myocardial fibrosis as an early manifestation of hypertrophic cardiomyopathy. *N Engl J Med* 2010;**363**:552-63.
97 Stanley WC, Recchia FA, Lopaschuk GD. Myocardial substrate metabolism in the normal and failing heart. *Physiological reviews* 2005;**85**:1093-129.
98 Crilley JG, Boehm EA, Blair E, et al. Hypertrophic cardiomyopathy due to sarcomeric gene mutations is characterized by impaired energy metabolism irrespective of the degree of hypertrophy. *J Am Coll Cardiol* 2003;**41**:1776-82.
99 Ashrafian H, Redwood C, Blair E, et al. Hypertrophic cardiomyopathy:a paradigm for myocardial energy depletion. *Trends Genet* 2003;**19**:263-8.
100 Abozguia K, Elliott P, McKenna W, et al. Metabolic modulator perhexiline corrects energy deficiency and improves exercise capacity in symptomatic hypertrophic cardiomyopathy. *Circulation* 2010;**122**:1562-9.

101 Charron P, Arad M, Arbustini E, et al. Genetic counselling and testing in cardiomyopathies: a position statement of the European Society of Cardiology Working Group on Myocardial and Pericardial Diseases. *Eur Heart J* 2010;**31**:2715-26.
102 Hershberger RE, Lindenfeld J, Mestroni L, et al. Genetic evaluation of cardiomyopathy--a Heart Failure Society of America practice guideline. *J Card Fail* 2009;**15**:83-97.
103 Ho CY. Genetics and clinical destiny: improving care in hypertrophic cardiomyopathy. *Circulation* 2010;**122**:2430-40; discussion 40.
104 Metzker ML. Sequencing technologies - the next generation. *Nat Rev Genet* 2010;**11**:31-46.
105 Meder B, Haas J, Keller A, et al. Targeted next-generation sequencing for the molecular genetic diagnostics of cardiomyopathies. *Circ Cardiovasc Genet* 2011;**4**:110-22.
106 Summerer D, Wu H, Haase B, et al. Microarray-based multicycle-enrichment of genomic subsets for targeted next-generation sequencing. *Genome Res* 2009;**19**:1616-21.
107 Dewey FE, Pan S, Wheeler MT, et al. DNA sequencing: clinical applications of new DNA sequencing technologies. *Circulation* 2012;**125**:931-44.
108 D'Argenio V, Frisso G, Precone V, et al. DNA sequence capture and next-generation sequencing for the molecular diagnosis of genetic cardiomyopathies. *J Mol Diagn* 2014;**16**:32-44.
109 Mook OR, Haagmans MA, Soucy JF, et al. Targeted sequence capture and GS-FLX Titanium sequencing of 23 hypertrophic and dilated cardiomyopathy genes: implementation into diagnostics. *J Med Genet* 2013;**50**:614-26.
110 Jordan DM, Kiezun A, Baxter SM, et al. Development and validation of a computational method for assessment of missense variants in hypertrophic cardiomyopathy. *Am J Hum Genet* 2011;**88**:183-92.
111 A map of human genome variation from population-scale sequencing. *Nature* 2010;**467**:1061-73.
112 Abecasis GR, Auton A, Brooks LD, et al. An integrated map of genetic variation from 1,092 human genomes. *Nature* 2012;**491**:56-65.
113 MacArthur DG, Balasubramanian S, Frankish A, et al. A systematic survey of loss-of-function variants in human protein-coding genes. *Science* 2012;**335**:823-8.
114 Tennessen JA, Bigham AW, O'Connor TD, et al. Evolution and Functional Impact of Rare Coding Variation from Deep Sequencing of Human Exomes. *Science* 2012; **337**:64-9..
115 Kapplinger JD, Landstrom AP, Salisbury BA, et al. Distinguishing arrhythmogenic right ventricular cardiomyopathy/dysplasia-associated mutations from background genetic noise. *J Am Coll Cardiol* 2011;**57**:2317-27.
116 Refsgaard L, Holst AG, Sadjadieh G, et al. High prevalence of genetic variants previously associated with LQT syndrome in new exome data. *Eur J Hum Genet* 2012; **20**(8):905-8.
117 Maron BJ, Maron MS, Semsarian C. Genetics of hypertrophic cardiomyopathy after 20 years: clinical perspectives. *J Am Coll Cardiol* 2012;**60**:705-15.
118 Jacoby D, McKenna WJ. Genetics of inherited cardiomyopathy. *Eur Heart J* 2012;**33**:296-304.
119 Epstein ND, Cohn GM, Cyran F, et al. Differences in clinical expression of hypertrophic cardiomyopathy associated with two distinct mutations in the beta-myosin heavy chain gene. A 908Leu----Val mutation and a 403Arg----Gln mutation. *Circulation* 1992;**86**:345-52.
120 Fananapazir L, Epstein ND. Genotype-phenotype correlations in hypertrophic cardiomyopathy. Insights provided by comparisons of kindreds with distinct and identical beta-myosin heavy chain gene mutations. *Circulation* 1994;**89**:22-32.
121 Watkins H, Rosenzweig A, Hwang DS, et al. Characteristics and prognostic implications of myosin missense mutations in familial hypertrophic cardiomyopathy. *N Engl J Med* 1992;**326**:1108-14.

122 Anan R, Greve G, Thierfelder L, et al. Prognostic implications of novel beta cardiac myosin heavy chain gene mutations that cause familial hypertrophic cardiomyopathy. *J Clin Invest* 1994;**93**:280-5.
123 Watkins H, McKenna WJ, Thierfelder L, et al. Mutations in the genes for cardiac troponin T and alpha-tropomyosin in hypertrophic cardiomyopathy. *N Engl J Med* 1995;**332**:1058-64.
124 Tesson F, Richard P, Charron P, et al. Genotype-phenotype analysis in four families with mutations in beta-myosin heavy chain gene responsible for familial hypertrophic cardiomyopathy. *Hum Mutat* 1998;**12**:385-92.
125 Niimura H, Bachinski LL, Sangwatanaroj S, et al. Mutations in the gene for cardiac myosin-binding protein C and late-onset familial hypertrophic cardiomyopathy. *N Engl J Med* 1998;**338**:1248-57.
126 Charron P, Dubourg O, Desnos M, et al. Clinical features and prognostic implications of familial hypertrophic cardiomyopathy related to the cardiac myosin-binding protein C gene. *Circulation* 1998;**97**:2230-6.
127 Maron BJ, Niimura H, Casey SA, et al. Development of left ventricular hypertrophy in adults in hypertrophic cardiomyopathy caused by cardiac myosin-binding protein C gene mutations. *J Am Coll Cardiol* 2001;**38**:315-21.
128 Niimura H, Patton KK, McKenna WJ, et al. Sarcomere protein gene mutations in hypertrophic cardiomyopathy of the elderly. *Circulation* 2002;**105**:446-51.
129 Watkins H. Genotype: phenotype correlations in hypertrophic cardiomyopathy. *Eur Heart J* 1998;**19**:10-2.
130 Moolman JC, Corfield VA, Posen B, et al. Sudden death due to troponin T mutations. *J Am Coll Cardiol* 1997;**29**:549-55.
131 Marian AJ, Mares A, Jr., Kelly DP, et al. Sudden cardiac death in hypertrophic cardiomyopathy. Variability in phenotypic expression of beta-myosin heavy chain mutations. *Eur Heart J* 1995;**16**:368-76.
132 Kokado H, Shimizu M, Yoshio H, et al. Clinical features of hypertrophic cardiomyopathy caused by a Lys183 deletion mutation in the cardiac troponin I gene. *Circulation* 2000;**102**:663-9.
133 Moolman JA, Reith S, Uhl K, et al. A newly created splice donor site in exon 25 of the MyBP-C gene is responsible for inherited hypertrophic cardiomyopathy with incomplete disease penetrance. *Circulation* 2000;**101**:1396-402.
134 Ackerman MJ, VanDriest SL, Ommen SR, et al. Prevalence and age-dependence of malignant mutations in the beta-myosin heavy chain and troponin T genes in hypertrophic cardiomyopathy: a comprehensive outpatient perspective. *J Am Coll Cardiol* 2002;**39**:2042-8.
135 Landstrom AP, Ackerman MJ. Mutation type is not clinically useful in predicting prognosis in hypertrophic cardiomyopathy. *Circulation* 2010;**122**:2441-9; discussion 50.
136 Van Driest SL, Ackerman MJ, Ommen SR, et al. Prevalence and severity of "benign" mutations in the beta-myosin heavy chain, cardiac troponin T, and alpha-tropomyosin genes in hypertrophic cardiomyopathy. *Circulation* 2002;**106**:3085-90.
137 Mogensen J, Murphy RT, Kubo T, et al. Frequency and clinical expression of cardiac troponin I mutations in 748 consecutive families with hypertrophic cardiomyopathy. *J Am Coll Cardiol* 2004;**44**:2315-25.
138 Page SP, Kounas S, Syrris P, et al. Cardiac myosin binding protein-C mutations in families with hypertrophic cardiomyopathy: disease expression in relation to age, gender, and long term outcome. *Circ Cardiovasc Genet* 2012;**5**:156-66.
139 Pasquale F, Syrris P, Kaski JP, et al. Long-term outcomes in hypertrophic cardiomyopathy caused by mutations in the cardiac troponin T gene. *Circ Cardiovasc Genet* 2012;**5**:10-7.

140 Watkins H, Ashrafian H, Redwood C. Inherited cardiomyopathies. *N Engl J Med* 2011;**364**:1643-56.
141 Sen-Chowdhry S, Syrris P, Pantazis A, et al. Mutational heterogeneity, modifier genes, and environmental influences contribute to phenotypic diversity of arrhythmogenic cardiomyopathy. *Circ Cardiovasc Genet* 2010;**3**:323-30.
142 Cooper DN, Krawczak M, Polychronakos C, et al. Where genotype is not predictive of phenotype: towards an understanding of the molecular basis of reduced penetrance in human inherited disease. *Hum Genet* 2013;**132**:1077-130.
143 Osterop AP, Kofflard MJ, Sandkuijl LA, et al. AT1 receptor A/C1166 polymorphism contributes to cardiac hypertrophy in subjects with hypertrophic cardiomyopathy. *Hypertension* 1998;**32**:825-30.
144 Kaufman BD, Auerbach S, Reddy S, et al. RAAS gene polymorphisms influence progression of pediatric hypertrophic cardiomyopathy. *Hum Genet* 2007;**122**:515-23.
145 Funada A, Konno T, Fujino N, et al. Impact of renin-angiotensin system polymorphisms on development of systolic dysfunction in hypertrophic cardiomyopathy. Evidence from a study of genotyped patients. *Circ J* 2010;**74**:2674-80.
146 Daw EW, Chen SN, Czernuszewicz G, et al. Genome-wide mapping of modifier chromosomal loci for human hypertrophic cardiomyopathy. *Hum Mol Genet* 2007;**16**:2463-71.
147 Kolder IC, Michels M, Christiaans I, et al. The role of renin-angiotensin-aldosterone system polymorphisms in phenotypic expression of MYBPC3-related hypertrophic cardiomyopathy. *Eur J Hum Genet* 2012; **20**(10):1071-7.
148 Sudmant PH, Kitzman JO, Antonacci F, et al. Diversity of human copy number variation and multicopy genes. *Science* 2010;**330**:641-6.
149 Girirajan S, Rosenfeld JA, Coe BP, et al. Phenotypic heterogeneity of genomic disorders and rare copy-number variants. *N Engl J Med* 2012;**367**:1321-31.
150 Pankratz N, Dumitriu A, Hetrick KN, et al. Copy number variation in familial Parkinson disease. *PLoS One* 2011;**6**:e20988.
151 Krumm N, Sudmant PH, Ko A, et al. Copy number variation detection and genotyping from exome sequence data. *Genome Res* 2012;**22**:1525-32.
152 Medvedev P, Stanciu M, Brudno M. Computational methods for discovering structural variation with next-generation sequencing. *Nat Methods* 2009;**6**:S13-20.
153 Bernstein BE, Birney E, Dunham I, et al. An integrated encyclopedia of DNA elements in the human genome. *Nature* 2012;**489**:57-74.
154 Huang L, Jolly LA, Willis-Owen S, et al. A Noncoding, Regulatory Mutation Implicates HCFC1 in Nonsyndromic Intellectual Disability. *Am J Hum Genet* 2012;**91**:694-702.
155 A user's guide to the encyclopedia of DNA elements (ENCODE). *PLoS Biol* 2011;**9**:e1001046.
156 Raney BJ, Cline MS, Rosenbloom KR, et al. ENCODE whole-genome data in the UCSC genome browser (2011 update). *Nucleic Acids Res* 2011;**39**:D871-5.
157 Bos JM, Towbin JA, Ackerman MJ. Diagnostic, prognostic, and therapeutic implications of genetic testing for hypertrophic cardiomyopathy. *J Am Coll Cardiol* 2009;**54**:201-11.
158 Kryukov GV, Pennacchio LA, Sunyaev SR. Most rare missense alleles are deleterious in humans: implications for complex disease and association studies. *Am J Hum Genet* 2007;**80**:727-39.
159 Ng PC, Henikoff S. SIFT: Predicting amino acid changes that affect protein function. *Nucleic Acids Res* 2003;**31**:3812-4.
160 Adzhubei IA, Schmidt S, Peshkin L, et al. A method and server for predicting damaging missense mutations. *Nat Methods* 2010;**7**:248-9.
161 Gonzalez-Perez A, Lopez-Bigas N. Improving the assessment of the outcome of nonsynonymous SNVs with a consensus deleteriousness score, Condel. *Am J Hum Genet* 2011;**88**:440-9.

162 Stead LF, Wood IC, Westhead DR. KvSNP: accurately predicting the effect of genetic variants in voltage-gated potassium channels. *Bioinformatics* 2011;**27**:2181-6.
163 Hurst JM, McMillan LE, Porter CT, et al. The SAAPdb web resource: a large-scale structural analysis of mutant proteins. *Hum Mutat* 2009;**30**:616-24.
164 Cuff AL, Janes RW, Martin AC. Analysing the ability to retain sidechain hydrogen-bonds in mutant proteins. *Bioinformatics* 2006;**22**:1464-70.
165 Cuff AL, Martin AC. Analysis of void volumes in proteins and application to stability of the p53 tumour suppressor protein. *J Mol Biol* 2004;**344**:1199-209.
166 Al-Numair NS, Martin AC. The SAAP pipeline and database: tools to analyze the impact and predict the pathogenicity of mutations. *BMC Genomics* 2013;**14 Suppl 3**:S4.
167 Kwok CJ, Martin AC, Au SW, et al. G6PDdb, an integrated database of glucose-6-phosphate dehydrogenase (G6PD) mutations. *Hum Mutat* 2002;**19**:217-24.
168 Martin AC, Facchiano AM, Cuff AL, et al. Integrating mutation data and structural analysis of the TP53 tumor-suppressor protein. *Hum Mutat* 2002;**19**:149-64.
169 Woo A, Rakowski H, Liew JC, et al. Mutations of the beta myosin heavy chain gene in hypertrophic cardiomyopathy: critical functional sites determine prognosis. *Heart* 2003;**89**:1179-85.
170 Moher D, Liberati A, Tetzlaff J, et al. Preferred reporting items for systematic reviews and meta-analyses: the PRISMA statement. *BMJ* 2009;**339**:b2535.
171 DerSimonian R, Laird N. Meta-analysis in clinical trials. *Control Clin Trials* 1986;**7**:177-88.
172 Lopes LR, Rahman MS, Elliott PM. A systematic review and meta-analysis of genotype-phenotype associations in patients with hypertrophic cardiomyopathy caused by sarcomeric protein mutations. *Heart* 2013;**99**:1800-11.
173 Morner S, Richard P, Kazzam E, et al. Identification of the genotypes causing hypertrophic cardiomyopathy in northern Sweden. *J Mol Cell Cardiol* 2003;**35**:841-9.
174 Erdmann J, Daehmlow S, Wischke S, et al. Mutation spectrum in a large cohort of unrelated consecutive patients with hypertrophic cardiomyopathy. *Clin Genet* 2003;**64**:339-49.
175 Van Driest SL, Ellsworth EG, Ommen SR, et al. Prevalence and spectrum of thin filament mutations in an outpatient referral population with hypertrophic cardiomyopathy. *Circulation* 2003;**108**:445-51.
176 Van Driest SL, Vasile VC, Ommen SR, et al. Myosin binding protein C mutations and compound heterozygosity in hypertrophic cardiomyopathy. *J Am Coll Cardiol* 2004;**44**:1903-10.
177 Van Driest SL, Jaeger MA, Ommen SR, et al. Comprehensive analysis of the beta-myosin heavy chain gene in 389 unrelated patients with hypertrophic cardiomyopathy. *J Am Coll Cardiol* 2004;**44**:602-10.
178 Olivotto I, Girolami F, Ackerman MJ, et al. Myofilament protein gene mutation screening and outcome of patients with hypertrophic cardiomyopathy. *Mayo Clin Proc* 2008;**83**:630-8.
179 Garcia-Castro M, Coto E, Reguero JR, et al. [Mutations in sarcomeric genes MYH7, MYBPC3, TNNT2, TNNI3, and TPM1 in patients with hypertrophic cardiomyopathy]. *Rev Esp Cardiol* 2009;**62**:48-56.
180 Andersen PS, Havndrup O, Hougs L, et al. Diagnostic yield, interpretation, and clinical utility of mutation screening of sarcomere encoding genes in Danish hypertrophic cardiomyopathy patients and relatives. *Hum Mutat* 2009;**30**:363-70.
181 Laredo R, Monserrat L, Hermida-Prieto M, et al. [Beta-myosin heavy-chain gene mutations in patients with hypertrophic cardiomyopathy]. *Rev Esp Cardiol* 2006;**59**:1008-18.
182 Rodriguez-Garcia MI, Monserrat L, Ortiz M, et al. Screening mutations in myosin binding protein C3 gene in a cohort of patients with Hypertrophic Cardiomyopathy. *BMC Med Genet* 2010;**11**:67.

183 Waldmuller S, Erdmann J, Binner P, et al. Novel correlations between the genotype and the phenotype of hypertrophic and dilated cardiomyopathy: results from the German Competence Network Heart Failure. *Eur J Heart Fail* 2011;**13**:1185-92.
184 Brito D, Miltenberger-Miltenyi G, Vale Pereira S, et al. Sarcomeric hypertrophic cardiomyopathy: genetic profile in a Portuguese population. *Rev Port Cardiol* 2012;**31**:577-87.
185 Gruner C, Ivanov J, Care M, et al. The Toronto HCM Genotype Score for Prediction of a Positive Genotype in Hypertrophic Cardiomyopathy. *Circ Cardiovasc Genet* 2012; **6**(1):19-26.
186 Zou Y, Wang J, Liu X, et al. Multiple gene mutations, not the type of mutation, are the modifier of left ventricle hypertrophy in patients with hypertrophic cardiomyopathy. *Mol Biol Rep* 2013; **40**(6):3969-76.
187 Charron P, Dubourg O, Desnos M, et al. Genotype-phenotype correlations in familial hypertrophic cardiomyopathy. A comparison between mutations in the cardiac protein-C and the beta-myosin heavy chain genes. *Eur Heart J* 1998;**19**:139-45.
188 Konno T, Shimizu M, Ino H, et al. A novel missense mutation in the myosin binding protein-C gene is responsible for hypertrophic cardiomyopathy with left ventricular dysfunction and dilation in elderly patients. *J Am Coll Cardiol* 2003;**41**:781-6.
189 Kubo T, Kitaoka H, Okawa M, et al. Lifelong left ventricular remodeling of hypertrophic cardiomyopathy caused by a founder frameshift deletion mutation in the cardiac Myosin-binding protein C gene among Japanese. *J Am Coll Cardiol* 2005;**46**:1737-43.
190 Konno T, Shimizu M, Ino H, et al. A novel mutation in the cardiac myosin-binding protein C gene is responsible for hypertrophic cardiomyopathy with severe ventricular hypertrophy and sudden death. *Clin Sci (Lond)* 2006;**110**:125-31.
191 Saltzman AJ, Mancini-DiNardo D, Li C, et al. Short communication: the cardiac myosin binding protein C Arg502Trp mutation: a common cause of hypertrophic cardiomyopathy. *Circ Res* 2010;**106**:1549-52.
192 Oliva-Sandoval MJ, Ruiz-Espejo F, Monserrat L, et al. Insights into genotype-phenotype correlation in hypertrophic cardiomyopathy. Findings from 18 Spanish families with a single mutation in MYBPC3. *Heart* 2010;**96**:1980-4.
193 Choi JO, Yu CW, Chun Nah J, et al. Long-term outcome of 4 Korean families with hypertrophic cardiomyopathy caused by 4 different mutations. *Clin Cardiol* 2010;**33**:430-8.
194 Hirota T, Kubo T, Kitaoka H, et al. A novel cardiac myosin-binding protein C S297X mutation in hypertrophic cardiomyopathy. *J Cardiol* 2010;**56**:59-65.
195 García-Castro M, Reguero JR, Morís C, Alonso-Montes C, Berrazueta JR, Sainz R, Alvarez V, Coto E. Prevalence and spectrum of mutations in the sarcomeric troponin T and I genes in a cohort of Spanish cardiac hypertrophy patients. Int J Cardiol. 2007; 14;**121**(1):115-6.
196 Consevage MW, Salada GC, Baylen BG, et al. A new missense mutation, Arg719Gln, in the beta-cardiac heavy chain myosin gene of patients with familial hypertrophic cardiomyopathy. *Hum Mol Genet* 1994;**3**:1025-6.
197 Marian AJ, Kelly D, Mares A, Jr., et al. A missense mutation in the beta myosin heavy chain gene is a predictor of premature sudden death in patients with hypertrophic cardiomyopathy. *J Sports Med Phys Fitness* 1994;**34**:1-10.
198 Posen BM, Moolman JC, Corfield VA, et al. Clinical and prognostic evaluation of familial hypertrophic cardiomyopathy in two South African families with different cardiac beta myosin heavy chain gene mutations. *Br Heart J* 1995;**74**:40-6.
199 Ko YL, Chen JJ, Tang TK, et al. Malignant familial hypertrophic cardiomyopathy in a family with a 453Arg-->Cys mutation in the beta-myosin heavy chain gene: coexistence of sudden death and end-stage heart failure. *Hum Genet* 1996;**97**:585-90.
200 Hwang TH, Lee WH, Kimura A, et al. Early expression of a malignant phenotype of familial hypertrophic cardiomyopathy associated with a Gly716Arg myosin heavy chain mutation in a Korean family. *Am J Cardiol* 1998;**82**:1509-13.

201 Enjuto M, Francino A, Navarro-Lopez F, et al. Malignant hypertrophic cardiomyopathy caused by the Arg723Gly mutation in beta-myosin heavy chain gene. *J Mol Cell Cardiol* 2000;**32**:2307-13.
202 Havndrup O, Bundgaard H, Andersen PS, et al. The Val606Met mutation in the cardiac beta-myosin heavy chain gene in patients with familial hypertrophic cardiomyopathy is associated with a high risk of sudden death at young age. *Am J Cardiol* 2001;**87**:1315-7.
203 Huang X, Song L, Ma AQ, et al. A malignant phenotype of hypertrophic cardiomyopathy caused by Arg719Gln cardiac beta-myosin heavy-chain mutation in a Chinese family. *Clin Chim Acta* 2001;**310**:131-9.
204 Brito D, Richard P, Isnard R, et al. Familial hypertrophic cardiomyopathy: the same mutation, different prognosis. Comparison of two families with a long follow-up. *Rev Port Cardiol* 2003;**22**:1445-61.
205 Liu SX, Hu SJ, Sun J, et al. Characteristics of the beta myosin heavy chain gene Ala26Val mutation in a Chinese family with hypertrophic cardiomyopathy. *Eur J Intern Med* 2005;**16**:328-33.
206 Perrot A, Schmidt-Traub H, Hoffmann B, et al. Prevalence of cardiac beta-myosin heavy chain gene mutations in patients with hypertrophic cardiomyopathy. *J Mol Med (Berl)* 2005;**83**:468-77.
207 Nakajima-Taniguchi C, Matsui H, Fujio Y, et al. Novel missense mutation in cardiac troponin T gene found in Japanese patient with hypertrophic cardiomyopathy. *J Mol Cell Cardiol* 1997;**29**:839-43.
208 Anan R, Shono H, Kisanuki A, et al. Patients with familial hypertrophic cardiomyopathy caused by a Phe110Ile missense mutation in the cardiac troponin T gene have variable cardiac morphologies and a favorable prognosis. *Circulation* 1998;**98**:391-7.
209 Varnava A, Baboonian C, Davison F, et al. A new mutation of the cardiac troponin T gene causing familial hypertrophic cardiomyopathy without left ventricular hypertrophy. *Heart* 1999;**82**:621-4.
210 Torricelli F, Girolami F, Olivotto I, et al. Prevalence and clinical profile of troponin T mutations among patients with hypertrophic cardiomyopathy in tuscany. *Am J Cardiol* 2003;**92**:1358-62.
211 Theopistou A, Anastasakis A, Miliou A, et al. Clinical features of hypertrophic cardiomyopathy caused by an Arg278Cys missense mutation in the cardiac troponin T gene. *Am J Cardiol* 2004;**94**:246-9.
212 Gimeno JR, Monserrat L, Perez-Sanchez I, et al. Hypertrophic cardiomyopathy. A study of the troponin-T gene in 127 Spanish families. *Rev Esp Cardiol* 2009;**62**:1473-7.
213 Shimizu M, Ino H, Okeie K, et al. Septal wall thinning and systolic dysfunction in patients with hypertrophic cardiomyopathy caused by a cardiac troponin I gene mutation. *Am Heart J* 2002;**143**:690-5.
214 Doolan A, Tebo M, Ingles J, et al. Cardiac troponin I mutations in Australian families with hypertrophic cardiomyopathy: clinical, genetic and functional consequences. *J Mol Cell Cardiol* 2005;**38**:387-93.
215 Flavigny J, Richard P, Isnard R, et al. Identification of two novel mutations in the ventricular regulatory myosin light chain gene (MYL2) associated with familial and classical forms of hypertrophic cardiomyopathy. *J Mol Med (Berl)* 1998;**76**:208-14.
216 Kabaeva ZT, Perrot A, Wolter B, et al. Systematic analysis of the regulatory and essential myosin light chain genes: genetic variants and mutations in hypertrophic cardiomyopathy. *Eur J Hum Genet* 2002;**10**:741-8.
217 Lee W, Hwang TH, Kimura A, et al. Different expressivity of a ventricular essential myosin light chain gene Ala57Gly mutation in familial hypertrophic cardiomyopathy. *Am Heart J* 2001;**141**:184-9.

218 Yamauchi-Takihara K, Nakajima-Taniguchi C, Matsui H, et al. Clinical implications of hypertrophic cardiomyopathy associated with mutations in the alpha-tropomyosin gene. *Heart* 1996;**76**:63-5.
219 Coviello DA, Maron BJ, Spirito P, et al. Clinical features of hypertrophic cardiomyopathy caused by mutation of a "hot spot" in the alpha-tropomyosin gene. *J Am Coll Cardiol* 1997;**29**:635-40.
220 Karibe A, Tobacman LS, Strand J, et al. Hypertrophic cardiomyopathy caused by a novel alpha-tropomyosin mutation (V95A) is associated with mild cardiac phenotype, abnormal calcium binding to troponin, abnormal myosin cycling, and poor prognosis. *Circulation* 2001;**103**:65-71.
221 Jongbloed RJ, Marcelis CL, Doevendans PA, et al. Variable clinical manifestation of a novel missense mutation in the alpha-tropomyosin (TPM1) gene in familial hypertrophic cardiomyopathy. *J Am Coll Cardiol* 2003;**41**:981-6.
222 Makhoul M, Ackerman MJ, Atkins DL, et al. Clinical spectrum in a family with tropomyosin-mediated hypertrophic cardiomyopathy and sudden death in childhood. *Pediatr Cardiol* 2011;**32**:215-20.
223 Wang S, Zou Y, Fu C, et al. Worse prognosis with gene mutations of beta-myosin heavy chain than myosin-binding protein C in Chinese patients with hypertrophic cardiomyopathy. *Clin Cardiol* 2008;**31**:114-8.
224 Mohiddin SA, Begley DA, McLam E, et al. Utility of genetic screening in hypertrophic cardiomyopathy: prevalence and significance of novel and double (homozygous and heterozygous) beta-myosin mutations. *Genet Test* 2003;**7**:21-7.
225 Song L, Zou Y, Wang J, et al. Mutations profile in Chinese patients with hypertrophic cardiomyopathy. *Clin Chim Acta* 2005;**351**:209-16.
226 Garcia-Pavia P, Vazquez ME, Segovia J, et al. Genetic basis of end-stage hypertrophic cardiomyopathy. *Eur J Heart Fail* 2011;**13**:1193-201.
227 Ingles J, Doolan A, Chiu C, et al. Compound and double mutations in patients with hypertrophic cardiomyopathy: implications for genetic testing and counselling. *J Med Genet* 2005;**42**:e59.
228 Binder J, Ommen SR, Gersh BJ, et al. Echocardiography-guided genetic testing in hypertrophic cardiomyopathy: septal morphological features predict the presence of myofilament mutations. *Mayo Clin Proc* 2006;**81**:459-67.
229 Arad M, Penas-Lado M, Monserrat L, et al. Gene mutations in apical hypertrophic cardiomyopathy. *Circulation* 2005;**112**:2805-11.
230 Gruner C, Care M, Siminovitch K, et al. Sarcomere protein gene mutations in patients with apical hypertrophic cardiomyopathy. *Circ Cardiovasc Genet* 2011;**4**:288-95.
231 Olivotto I, Girolami F, Sciagra R, et al. Microvascular function is selectively impaired in patients with hypertrophic cardiomyopathy and sarcomere myofilament gene mutations. *J Am Coll Cardiol* 2011;**58**:839-48.
232 Blauwet LA, Ackerman MJ, Edwards WD, et al. Myocardial fibrosis in patients with symptomatic obstructive hypertrophic cardiomyopathy: correlation with echocardiographic measurements, sarcomeric genotypes, and pro-left ventricular hypertrophy polymorphisms involving the renin-angiotensin-aldosterone system. *Cardiovasc Pathol* 2009;**18**:262-8.
233 McLeod CJ, Bos JM, Theis JL, et al. Histologic characterization of hypertrophic cardiomyopathy with and without myofilament mutations. *Am Heart J* 2009;**158**:799-805.
234 Heradien M, Revera M, van der Merwe L, et al. Abnormal blood pressure response to exercise occurs more frequently in hypertrophic cardiomyopathy patients with the R92W troponin T mutation than in those with myosin mutations. *Heart Rhythm* 2009;**6**:S18-24.
235 Zahka K, Kalidas K, Simpson MA, et al. Homozygous mutation of MYBPC3 associated with severe infantile hypertrophic cardiomyopathy at high frequency among the Amish. *Heart* 2008;**94**:1326-30.

236 Lekanne Deprez RH, Muurling-Vlietman JJ, Hruda J, et al. Two cases of severe neonatal hypertrophic cardiomyopathy caused by compound heterozygous mutations in the MYBPC3 gene. *J Med Genet* 2006;**43**:829-32.
237 Garcia-Castro M, Reguero JR, Alvarez V, et al. Hypertrophic cardiomyopathy linked to homozygosity for a new mutation in the myosin-binding protein C gene (A627V) suggests a dosage effect. *Int J Cardiol* 2005;**102**:501-7.
238 Jeschke B, Uhl K, Weist B, et al. A high risk phenotype of hypertrophic cardiomyopathy associated with a compound genotype of two mutated beta-myosin heavy chain genes. *Hum Genet* 1998;**102**:299-304.
239 Ortiz MF, Rodriguez-Garcia MI, Hermida-Prieto M, et al. A homozygous MYBPC3 gene mutation associated with a severe phenotype and a high risk of sudden death in a family with hypertrophic cardiomyopathy. *Rev Esp Cardiol* 2009;**62**:572-5.
240 Bashyam MD, Savithri GR, Gopikrishna M, et al. A p.R870H mutation in the beta-cardiac myosin heavy chain 7 gene causes familial hypertrophic cardiomyopathy in several members of an Indian family. *Can J Cardiol* 2007;**23**:788-90.
241 Ho CY, Lever HM, DeSanctis R, et al. Homozygous mutation in cardiac troponin T: implications for hypertrophic cardiomyopathy. *Circulation* 2000;**102**:1950-5.
242 Girolami F, Ho CY, Semsarian C, et al. Clinical features and outcome of hypertrophic cardiomyopathy associated with triple sarcomere protein gene mutations. *J Am Coll Cardiol* 2010;**55**:1444-53.
243 Christiaans I, Birnie E, van Langen IM, et al. The yield of risk stratification for sudden cardiac death in hypertrophic cardiomyopathy myosin-binding protein C gene mutation carriers: focus on predictive screening. *Eur Heart J* 2010;**31**:842-8.
244 Bick AG, Flannick J, Ito K, et al. Burden of rare sarcomere gene variants in the Framingham and Jackson Heart Study cohorts. *Am J Hum Genet* 2012;**91**:513-9.
245 Pan S, Caleshu CA, Dunn KE, et al. Cardiac structural and sarcomere genes associated with cardiomyopathy exhibit marked intolerance of genetic variation. *Circ Cardiovasc Genet* 2012;**5**:602-10.
246 Golbus JR, Puckelwartz MJ, Fahrenbach JP, et al. Population-based variation in cardiomyopathy genes. *Circ Cardiovasc Genet* 2012;**5**:391-9.
247 Andreasen C, Nielsen JB, Refsgaard L, et al. New population-based exome data are questioning the pathogenicity of previously cardiomyopathy-associated genetic variants. *Eur J Hum Genet* 2013; **21**(9):918-28.
248 Lahtinen AM, Lehtonen E, Marjamaa A, Kaartinen M, Heliö T, Porthan K, Oikarinen L, Toivonen L, Swan H, Jula A, Peltonen L, Palotie A, Salomaa V, Kontula K. Population-prevalent desmosomal mutations predisposing to arrhythmogenic right ventricular cardiomyopathy. Heart Rhythm. 2011; **8**(8):1214-21.
249 McKenna WJ, Spirito P, Desnos M, et al. Experience from clinical genetics in hypertrophic cardiomyopathy: proposal for new diagnostic criteria in adult members of affected families. *Heart* 1997;77:130-2.
250 Mogensen J, Kubo T, Duque M, et al. Idiopathic restrictive cardiomyopathy is part of the clinical expression of cardiac troponin I mutations. *J Clin Invest* 2003;**111**:209-16.
251 Lopes LR, Zekavati A, Syrris P, et al. Genetic complexity in hypertrophic cardiomyopathy revealed by high-throughput sequencing. *J Med Genet* 2013;**50**:228-39.
252 Li H, Handsaker B, Wysoker A, et al. The Sequence Alignment/Map format and SAMtools. *Bioinformatics* 2009;**25**:2078-9.
253 McKenna A, Hanna M, Banks E, et al. The Genome Analysis Toolkit: a MapReduce framework for analyzing next-generation DNA sequencing data. *Genome Res* 2010;**20**:1297-303.
254 DePristo MA, Banks E, Poplin R, et al. A framework for variation discovery and genotyping using next-generation DNA sequencing data. *Nat Genet* 2011;**43**:491-8.

255 Wang K, Li M, Hakonarson H. ANNOVAR: functional annotation of genetic variants from high-throughput sequencing data. *Nucleic Acids Res* 2010;**38**:e164.
256 Pearson RD. Bias due to selection of rare variants using frequency in controls. *Nat Genet* 2011;**43**:392-3; author reply 4-5.
257 Smigielski EM, Sirotkin K, Ward M, et al. dbSNP: a database of single nucleotide polymorphisms. *Nucleic Acids Res* 2000;**28**:352-5.
258 Robinson JT, Thorvaldsdottir H, Winckler W, et al. Integrative genomics viewer. *Nat Biotechnol* 2011;**29**:24-6.
259 Turner T. Plot protein: visualization of mutations. *Journal of clinical bioinformatics* 2013;**3**:14.
260 Langmead B, Trapnell C, Pop M, et al. Ultrafast and memory-efficient alignment of short DNA sequences to the human genome. *Genome Biol* 2009;**10**:R25.
261 O'Mahony C, Tome-Esteban M, Lambiase PD, et al. A validation study of the 2003 American College of Cardiology/European Society of Cardiology and 2011 American College of Cardiology Foundation/American Heart Association risk stratification and treatment algorithms for sudden cardiac death in patients with hypertrophic cardiomyopathy. *Heart* 2013;**99**:534-41.
262 Shapiro LM, McKenna WJ. Distribution of left ventricular hypertrophy in hypertrophic cardiomyopathy: a two-dimensional echocardiographic study. *J Am Coll Cardiol* 1983;**2**:437-44.
263 Lang RM, Bierig M, Devereux RB, et al. Recommendations for chamber quantification. *Eur J Echocardiogr* 2006;**7**:79-108.
264 Nagueh SF, Appleton CP, Gillebert TC, et al. Recommendations for the evaluation of left ventricular diastolic function by echocardiography. *Eur J Echocardiogr* 2009;**10**:165-93.
265 Lancellotti P, Moura L, Pierard LA, et al. European Association of Echocardiography recommendations for the assessment of valvular regurgitation. Part 2: mitral and tricuspid regurgitation (native valve disease). *Eur J Echocardiogr* 2010;**11**:307-32.
266 Rudski LG, Lai WW, Afilalo J, et al. Guidelines for the echocardiographic assessment of the right heart in adults: a report from the American Society of Echocardiography endorsed by the European Association of Echocardiography, a registered branch of the European Society of Cardiology, and the Canadian Society of Echocardiography. *J Am Soc Echocardiogr* 2010;**23**:685-713; quiz 86-8.
267 Maron BJ, McKenna WJ, Danielson GK, et al. American College of Cardiology/European Society of Cardiology Clinical Expert Consensus Document on Hypertrophic Cardiomyopathy. A report of the American College of Cardiology Foundation Task Force on Clinical Expert Consensus Documents and the European Society of Cardiology Committee for Practice Guidelines. *Eur Heart J* 2003;**24**:1965-91.
268 Monserrat L, Elliott PM, Gimeno JR, et al. Non-sustained ventricular tachycardia in hypertrophic cardiomyopathy: an independent marker of sudden death risk in young patients. *J Am Coll Cardiol* 2003;**42**:873-9.
269 Sadoul N, Prasad K, Elliott PM, et al. Prospective prognostic assessment of blood pressure response during exercise in patients with hypertrophic cardiomyopathy. *Circulation* 1997;**96**:2987-91.
270 Kramer CM, Barkhausen J, Flamm SD, et al. Standardized cardiovascular magnetic resonance imaging (CMR) protocols, society for cardiovascular magnetic resonance: board of trustees task force on standardized protocols. *J Cardiovasc Magn Reson* 2008;**10**:35.
271 Alfakih K, Plein S, Thiele H, et al. Normal human left and right ventricular dimensions for MRI as assessed by turbo gradient echo and steady-state free precession imaging sequences. *J Magn Reson Imaging* 2003;**17**:323-9.
272 Maron MS, Olivotto I, Harrigan C, et al. Mitral valve abnormalities identified by cardiovascular magnetic resonance represent a primary phenotypic expression of hypertrophic cardiomyopathy. *Circulation* 2011;**124**:40-7.

273 Plagnol V, Curtis J, Epstein M, et al. A robust model for read count data in exome sequencing experiments and implications for copy number variant calling. *Bioinformatics* 2012;**28**:2747-54.
274 Smith ML MJ, McKinney S, Hardcastle T and Thorne NP. snapCGH: Segmentation, normalisation and processing of aCGH data. R package version 1.35.0. 2009.
275 Kent WJ, Sugnet CW, Furey TS, et al. The human genome browser at UCSC. *Genome Res* 2002;**12**:996-1006.
276 Boyle AP, Hong EL, Hariharan M, et al. Annotation of functional variation in personal genomes using RegulomeDB. *Genome Res* 2012;**22**:1790-7.
277 Lewis BP, Burge CB, Bartel DP. Conserved seed pairing, often flanked by adenosines, indicates that thousands of human genes are microRNA targets. *Cell* 2005;**120**:15-20.
278 Wu C, Orozco C, Boyer J, et al. BioGPS: an extensible and customizable portal for querying and organizing gene annotation resources. *Genome Biol* 2009;**10**:R130.
279 Su AI, Wiltshire T, Batalov S, et al. A gene atlas of the mouse and human protein-encoding transcriptomes. *Proc Natl Acad Sci U S A* 2004;**101**:6062-7.
280 Ritchie W, Flamant S, Rasko JE. mimiRNA: a microRNA expression profiler and classification resource designed to identify functional correlations between microRNAs and their targets. *Bioinformatics* 2010;**26**:223-7.
281 Davydov EV, Goode DL, Sirota M, et al. Identifying a high fraction of the human genome to be under selective constraint using GERP++. *PLoS Comput Biol* 2010;**6**:e1001025.
282 Pilbrow AP, Folkersen L, Pearson JF, et al. The chromosome 9p21.3 coronary heart disease risk allele is associated with altered gene expression in normal heart and vascular tissues. *PLoS One* 2012;**7**:e39574.
283 Li H, Durbin R. Fast and accurate short read alignment with Burrows-Wheeler transform. *Bioinformatics* 2009;**25**:1754-60.
284 Brito D, Madeira H. Malignant mutations in hypertrophic cardiomyopathy: fact or fancy? *Rev Port Cardiol* 2005;**24**:1137-46.
285 Maron BJ, Maron MS, Semsarian C. Double or compound sarcomere mutations in hypertrophic cardiomyopathy: a potential link to sudden death in the absence of conventional risk factors. *Heart Rhythm* 2012;**9**:57-63.
286 Girolami F, Olivotto I, Passerini I, et al. A molecular screening strategy based on beta-myosin heavy chain, cardiac myosin binding protein C and troponin T genes in Italian patients with hypertrophic cardiomyopathy. *J Cardiovasc Med (Hagerstown)* 2006;**7**:601-7.
287 Zimmerman RS, Cox S, Lakdawala NK, et al. A novel custom resequencing array for dilated cardiomyopathy. *Genet Med* 2010;**12**:268-78.
288 Millat G, Chanavat V, Crehalet H, et al. Development of a high resolution melting method for the detection of genetic variations in hypertrophic cardiomyopathy. *Clin Chim Acta* 2010;**411**:1983-91.
289 Nanni L, Pieroni M, Chimenti C, et al. Hypertrophic cardiomyopathy: two homozygous cases with "typical" hypertrophic cardiomyopathy and three new mutations in cases with progression to dilated cardiomyopathy. *Biochem Biophys Res Commun* 2003;**309**:391-8.
290 Morita H, Larson MG, Barr SC, et al. Single-gene mutations and increased left ventricular wall thickness in the community: the Framingham Heart Study. *Circulation* 2006;**113**:2697-705.
291 Alpert NR, Mohiddin SA, Tripodi D, et al. Molecular and phenotypic effects of heterozygous, homozygous, and compound heterozygote myosin heavy-chain mutations. *Am J Physiol Heart Circ Physiol* 2005;**288**:H1097-102.
292 Gruver EJ, Fatkin D, Dodds GA, et al. Familial hypertrophic cardiomyopathy and atrial fibrillation caused by Arg663His beta-cardiac myosin heavy chain mutation. *Am J Cardiol* 1999;**83**:13H-8H.

293 Kaski JP, Syrris P, Esteban MT, et al. Prevalence of sarcomere protein gene mutations in preadolescent children with hypertrophic cardiomyopathy. *Circ Cardiovasc Genet* 2009;**2**:436-41.
294 Fananapazir L, Dalakas MC, Cyran F, et al. Missense mutations in the beta-myosin heavy-chain gene cause central core disease in hypertrophic cardiomyopathy. *Proc Natl Acad Sci U S A* 1993;**90**:3993-7.
295 Bos JM, Poley RN, Ny M, et al. Genotype-phenotype relationships involving hypertrophic cardiomyopathy-associated mutations in titin, muscle LIM protein, and telethonin. *Mol Genet Metab* 2006;**88**:78-85.
296 Refaat MM, Lubitz SA, Makino S, et al. Genetic variation in the alternative splicing regulator RBM20 is associated with dilated cardiomyopathy. *Heart Rhythm* 2012;**9**:390-6.
297 Knoll R, Hoshijima M, Hoffman HM, et al. The cardiac mechanical stretch sensor machinery involves a Z disc complex that is defective in a subset of human dilated cardiomyopathy. *Cell* 2002;**111**:943-55.
298 Lakdawala NK, Thune JJ, Maron BJ, et al. Electrocardiographic features of sarcomere mutation carriers with and without clinically overt hypertrophic cardiomyopathy. *Am J Cardiol* 2011;**108**:1606-13.
299 Ohsuzu F, Katsushika S, Akanuma M, et al. Hypertrophic obstructive cardiomyopathy due to a novel T-to-A transition at codon 624 in the beta-myosin heavy chain (beta-MHC) gene possibly related to the sudden death. *Int J Cardiol* 1997;**62**:203-9.
300 Waldmuller S, Muller M, Rackebrandt K, et al. Array-based resequencing assay for mutations causing hypertrophic cardiomyopathy. *Clin Chem* 2008;**54**:682-7.
301 Posch MG, Waldmuller S, Muller M, et al. Cardiac alpha-myosin (MYH6) is the predominant sarcomeric disease gene for familial atrial septal defects. *PLoS One* 2011;**6**:e28872.
302 Ohlsson M, Hedberg C, Bradvik B, et al. Hereditary myopathy with early respiratory failure associated with a mutation in A-band titin. *Brain* 2012;**135**:1682-94.
303 Pfeffer G, Elliott HR, Griffin H, et al. Titin mutation segregates with hereditary myopathy with early respiratory failure. *Brain* 2012;**135**:1695-713.
304 Palmio J, Evila A, Chapon F, et al. Hereditary myopathy with early respiratory failure: occurrence in various populations. *J Neurol Neurosurg Psychiatry* 2013; **85**(3):345-53.
305 Quarta G, Muir A, Pantazis A, et al. Familial evaluation in arrhythmogenic right ventricular cardiomyopathy: impact of genetics and revised task force criteria. *Circulation* 2011;**123**:2701-9.
306 Fressart V, Duthoit G, Donal E, et al. Desmosomal gene analysis in arrhythmogenic right ventricular dysplasia/cardiomyopathy: spectrum of mutations and clinical impact in practice. *Europace* 2010;**12**:861-8.
307 Basso C, Czarnowska E, Della Barbera M, et al. Ultrastructural evidence of intercalated disc remodelling in arrhythmogenic right ventricular cardiomyopathy: an electron microscopy investigation on endomyocardial biopsies. *Eur Heart J* 2006;**27**:1847-54.
308 van der Zwaag PA, Jongbloed JD, van den Berg MP, et al. A genetic variants database for arrhythmogenic right ventricular dysplasia/cardiomyopathy. *Hum Mutat* 2009;**30**:1278-83.
309 Medeiros-Domingo A, Bhuiyan ZA, Tester DJ, et al. The RYR2-encoded ryanodine receptor/calcium release channel in patients diagnosed previously with either catecholaminergic polymorphic ventricular tachycardia or genotype negative, exercise-induced long QT syndrome: a comprehensive open reading frame mutational analysis. *J Am Coll Cardiol* 2009;**54**:2065-74.
310 Mohler PJ, Le Scouarnec S, Denjoy I, et al. Defining the cellular phenotype of "ankyrin-B syndrome" variants: human ANK2 variants associated with clinical phenotypes display a spectrum of activities in cardiomyocytes. *Circulation* 2007;**115**:432-41.

311 Mohler PJ, Splawski I, Napolitano C, et al. A cardiac arrhythmia syndrome caused by loss of ankyrin-B function. *Proc Natl Acad Sci U S A* 2004;**101**:9137-42.
312 Wattanasirichaigoon D, Vesely MR, Duggal P, et al. Sodium channel abnormalities are infrequent in patients with long QT syndrome: identification of two novel SCN5A mutations. *Am J Med Genet* 1999;**86**:470-6.
313 Sherman J, Tester DJ, Ackerman MJ. Targeted mutational analysis of ankyrin-B in 541 consecutive, unrelated patients referred for long QT syndrome genetic testing and 200 healthy subjects. *Heart Rhythm* 2005;**2**:1218-23.
314 Cronk LB, Ye B, Kaku T, et al. Novel mechanism for sudden infant death syndrome: persistent late sodium current secondary to mutations in caveolin-3. *Heart Rhythm* 2007;**4**:161-6.
315 Garcia-Pavia P, Syrris P, Salas C, et al. Desmosomal protein gene mutations in patients with idiopathic dilated cardiomyopathy undergoing cardiac transplantation: a clinicopathological study. *Heart* 2011;**97**:1744-52.
316 den Haan AD, Tan BY, Zikusoka MN, et al. Comprehensive desmosome mutation analysis in north americans with arrhythmogenic right ventricular dysplasia/cardiomyopathy. *Circ Cardiovasc Genet* 2009;**2**:428-35.
317 Syrris P, Ward D, Asimaki A, et al. Desmoglein-2 mutations in arrhythmogenic right ventricular cardiomyopathy: a genotype-phenotype characterization of familial disease. *Eur Heart J* 2007;**28**:581-8.
318 Millat G, Chevalier P, Restier-Miron L, et al. Spectrum of pathogenic mutations and associated polymorphisms in a cohort of 44 unrelated patients with long QT syndrome. *Clin Genet* 2006;**70**:214-27.
319 Duisters RF, Tijsen AJ, Schroen B, et al. miR-133 and miR-30 regulate connective tissue growth factor: implications for a role of microRNAs in myocardial matrix remodeling. *Circ Res* 2009;**104**:170-8, 6p following 8.
320 Sikkema-Raddatz B, Johansson LF, de Boer EN, et al. Targeted next-generation sequencing can replace Sanger sequencing in clinical diagnostics. *Hum Mutat* 2013;**34**:1035-42.
321 Hoischen A, Gilissen C, Arts P, et al. Massively parallel sequencing of ataxia genes after array-based enrichment. *Hum Mutat* 2010;**31**:494-9.
322 Valencia CA, Rhodenizer D, Bhide S, et al. Assessment of target enrichment platforms using massively parallel sequencing for the mutation detection for congenital muscular dystrophy. *J Mol Diagn* 2012;**14**:233-46.
323 Green RC, Berg JS, Grody WW, et al. ACMG recommendations for reporting of incidental findings in clinical exome and genome sequencing. *Genet Med* 2013;**15**:565-74.
324 Page SP, Kounas S, Syrris P, et al. Cardiac Myosin Binding Protein-C Mutations in Families with Hypertrophic Cardiomyopathy: Disease Expression in Relation to Age, Gender, and Long Term Outcome. *Circ Cardiovasc Genet* 2012; **5**(2):156-66.
325 Norton N, Li D, Rampersaud E, et al. Exome sequencing and genome-wide linkage analysis in 17 families illustrate the complex contribution of TTN truncating variants to dilated cardiomyopathy. *Circ Cardiovasc Genet* 2013;**6**:144-53.
326 Holm H, Gudbjartsson DF, Sulem P, et al. A rare variant in MYH6 is associated with high risk of sick sinus syndrome. *Nat Genet* 2011;**43**:316-20.
327 Sen-Chowdhry S, Morgan RD, Chambers JC, et al. Arrhythmogenic cardiomyopathy: etiology, diagnosis, and treatment. *Annu Rev Med* 2010;**61**:233-53.
328 Elliott P, O'Mahony C, Syrris P, et al. Prevalence of desmosomal protein gene mutations in patients with dilated cardiomyopathy. *Circ Cardiovasc Genet* 2010;**3**:314-22.
329 Norton N, Robertson PD, Rieder MJ, et al. Evaluating Pathogenicity of Rare Variants from Dilated Cardiomyopathy in the Exome Era. *Circ Cardiovasc Genet* 2012; **5**(2):167-74.

330 Andreasen C, Nielsen JB, Refsgaard L, et al. New population-based exome data are questioning the pathogenicity of previously cardiomyopathy-associated genetic variants. *Eur J Hum Genet* 2013;**21**:918-28.
331 Kapa S, Tester DJ, Salisbury BA, et al. Genetic testing for long-QT syndrome: distinguishing pathogenic mutations from benign variants. *Circulation* 2009;**120**:1752-60.
332 Kapplinger JD, Landstrom AP, Bos JM, et al. Distinguishing hypertrophic cardiomyopathy-associated mutations from background genetic noise. *J Cardiovasc Transl Res* 2014;**7**:347-61.
333 Arndt AK, Schafer S, Drenckhahn JD, et al. Fine mapping of the 1p36 deletion syndrome identifies mutation of PRDM16 as a cause of cardiomyopathy. *Am J Hum Genet* 2013;**93**:67-77.
334 Gruner C, Ivanov J, Care M, et al. Toronto hypertrophic cardiomyopathy genotype score for prediction of a positive genotype in hypertrophic cardiomyopathy. *Circ Cardiovasc Genet* 2013;**6**:19-26.
335 Ingles J, Sarina T, Yeates L, et al. Clinical predictors of genetic testing outcomes in hypertrophic cardiomyopathy. *Genet Med* 2013;**15**:972-7.
336 Bos JM, Will ML, Gersh BJ, et al. Characterization of a phenotype-based genetic test prediction score for unrelated patients with hypertrophic cardiomyopathy. *Mayo Clin Proc* 2014;**89**:727-37.
337 Bauce B, Nava A, Beffagna G, et al. Multiple mutations in desmosomal proteins encoding genes in arrhythmogenic right ventricular cardiomyopathy/dysplasia. *Heart Rhythm* 2010;**7**:22-9.
338 Marston S, Copeland O, Gehmlich K, et al. How do MYBPC3 mutations cause hypertrophic cardiomyopathy? *J Muscle Res Cell Motil* 2011.
339 Dimitrow PP, Chojnowska L, Rudzinski T, et al. Sudden death in hypertrophic cardiomyopathy: old risk factors re-assessed in a new model of maximalized follow-up. *Eur Heart J* 2010;**31**:3084-93.
340 Kumar P, Henikoff S, Ng PC. Predicting the effects of coding non-synonymous variants on protein function using the SIFT algorithm. *Nat Protoc* 2009;**4**:1073-81.
341 Nagueh SF, Bierig SM, Budoff MJ, et al. American Society of Echocardiography clinical recommendations for multimodality cardiovascular imaging of patients with hypertrophic cardiomyopathy: Endorsed by the American Society of Nuclear Cardiology, Society for Cardiovascular Magnetic Resonance, and Society of Cardiovascular Computed Tomography. *J Am Soc Echocardiogr* 2011;**24**:473-98.
342 Moon JC, McKenna WJ, McCrohon JA, et al. Toward clinical risk assessment in hypertrophic cardiomyopathy with gadolinium cardiovascular magnetic resonance. *J Am Coll Cardiol* 2003;**41**:1561-7.
343 Green JJ, Berger JS, Kramer CM, et al. Prognostic value of late gadolinium enhancement in clinical outcomes for hypertrophic cardiomyopathy. *JACC Cardiovasc Imaging* 2012;**5**:370-7.
344 Webster G, Berul CI. An update on channelopathies: from mechanisms to management. *Circulation* 2013;**127**:126-40.
345 Hashemi SM, Hund TJ, Mohler PJ. Cardiac ankyrins in health and disease. *J Mol Cell Cardiol* 2009;**47**:203-9.
346 Hao X, Zhang Y, Zhang X, et al. TGF-beta1-mediated fibrosis and ion channel remodeling are key mechanisms in producing the sinus node dysfunction associated with SCN5A deficiency and aging. *Circ Arrhythm Electrophysiol* 2011;**4**:397-406.
347 van der Zwaag PA, van Rijsingen IA, de Ruiter R, et al. Recurrent and founder mutations in the Netherlands-Phospholamban p.Arg14del mutation causes arrhythmogenic cardiomyopathy. *Neth Heart J* 2013;**21**:286-93.

348 Duan J, Zhang JG, Deng HW, et al. Comparative studies of copy number variation detection methods for next-generation sequencing technologies. *PLoS One* 2013;**8**:e59128.
349 de Ligt J, Boone PM, Pfundt R, et al. Detection of clinically relevant copy number variants with whole-exome sequencing. *Hum Mutat* 2013;**34**:1439-48.
350 Marian AJ, Yu QT, Mares A, Jr., et al. Detection of a new mutation in the beta-myosin heavy chain gene in an individual with hypertrophic cardiomyopathy. *J Clin Invest* 1992;**90**:2156-65.
351 Chanavat V, Seronde MF, Bouvagnet P, et al. Molecular characterization of a large MYBPC3 rearrangement in a cohort of 100 unrelated patients with hypertrophic cardiomyopathy. *Eur J Med Genet* 2012;**55**:163-6.
352 Bagnall RD, Yeates L, Semsarian C. The role of large gene deletions and duplications in MYBPC3 and TNNT2 in patients with hypertrophic cardiomyopathy. *Int J Cardiol* 2010;**145**:150-3.
353 Roberts JD, Herkert JC, Rutberg J, et al. Detection of genomic deletions of PKP2 in arrhythmogenic right ventricular cardiomyopathy. *Clin Genet* 2013;**83**:452-6.
354 Li Mura IE, Bauce B, Nava A, et al. Identification of a PKP2 gene deletion in a family with arrhythmogenic right ventricular cardiomyopathy. *Eur J Hum Genet* 2013.
355 Norton N, Siegfried JD, Li D, et al. Assessment of LMNA copy number variation in 58 probands with dilated cardiomyopathy. *Clin Transl Sci* 2011;**4**:351-2.
356 van Dijk SJ, Dooijes D, dos Remedios C, et al. Cardiac myosin-binding protein C mutations and hypertrophic cardiomyopathy: haploinsufficiency, deranged phosphorylation, and cardiomyocyte dysfunction. *Circulation* 2009;**119**:1473-83.
357 Exome Variant Server, NHLBI GO Exome Sequencing Project (ESP), Seattle, WA (URL: http://evs.gs.washington.edu/EVS/) [accessed 8, 2014].
358 Itsara A, Cooper GM, Baker C, et al. Population analysis of large copy number variants and hotspots of human genetic disease. *Am J Hum Genet* 2009;**84**:148-61.
359 Teague B, Waterman MS, Goldstein S, et al. High-resolution human genome structure by single-molecule analysis. *Proc Natl Acad Sci U S A* 2010;**107**:10848-53.
360 Nelson TJ, Balza R, Jr., Xiao Q, et al. SRF-dependent gene expression in isolated cardiomyocytes: regulation of genes involved in cardiac hypertrophy. *J Mol Cell Cardiol* 2005;**39**:479-89.
361 Xing W, Zhang TC, Cao D, et al. Myocardin induces cardiomyocyte hypertrophy. *Circ Res* 2006;**98**:1089-97.
362 Gary-Bobo G, Huet A, Li Z, et al. [Development and cardiomyopathy: serum response factor, a key protein]. *Arch Mal Coeur Vaiss* 2005;**98**:655-60.
363 Catala F, Wanner R, Barton P, et al. A skeletal muscle-specific enhancer regulated by factors binding to E and CArG boxes is present in the promoter of the mouse myosin light-chain 1A gene. *Mol Cell Biol* 1995;**15**:4585-96.
364 Zhang SX, Garcia-Gras E, Wycuff DR, et al. Identification of direct serum-response factor gene targets during Me2SO-induced P19 cardiac cell differentiation. *J Biol Chem* 2005;**280**:19115-26.
365 Balza RO, Jr., Misra RP. Role of the serum response factor in regulating contractile apparatus gene expression and sarcomeric integrity in cardiomyocytes. *J Biol Chem* 2006;**281**:6498-510.
366 Belaguli NS, Sepulveda JL, Nigam V, et al. Cardiac tissue enriched factors serum response factor and GATA-4 are mutual coregulators. *Mol Cell Biol* 2000;**20**:7550-8.
367 Zhang X, Azhar G, Zhong Y, et al. Identification of a novel serum response factor cofactor in cardiac gene regulation. *J Biol Chem* 2004;**279**:55626-32.
368 Bostrom P, Mann N, Wu J, et al. C/EBPbeta controls exercise-induced cardiac growth and protects against pathological cardiac remodeling. *Cell* 2010;**143**:1072-83.

369 Yoshida Y, Morimoto T, Takaya T, et al. Aldosterone signaling associates with p300/GATA4 transcriptional pathway during the hypertrophic response of cardiomyocytes. *Circ J* 2010;**74**:156-62.
370 Haghikia A, Stapel B, Hoch M, et al. STAT3 and cardiac remodeling. *Heart Fail Rev* 2011;**16**:35-47.
371 Kunisada K, Negoro S, Tone E, et al. Signal transducer and activator of transcription 3 in the heart transduces not only a hypertrophic signal but a protective signal against doxorubicin-induced cardiomyopathy. *Proc Natl Acad Sci U S A* 2000;**97**:315-9.
372 Kee HJ, Kook H. Roles and targets of class I and IIa histone deacetylases in cardiac hypertrophy. *J Biomed Biotechnol* 2011;**2011**:928326.
373 Kuwahara K, Saito Y, Takano M, et al. NRSF regulates the fetal cardiac gene program and maintains normal cardiac structure and function. *EMBO J* 2003;**22**:6310-21.
374 Sucharov CC, Dockstader K, McKinsey TA. YY1 protects cardiac myocytes from pathologic hypertrophy by interacting with HDAC5. *Mol Biol Cell* 2008;**19**:4141-53.
375 Kircher M, Witten DM, Jain P, et al. A general framework for estimating the relative pathogenicity of human genetic variants. *Nat Genet* 2014;**46**:310-5.
376 Ritchie GR, Dunham I, Zeggini E, et al. Functional annotation of noncoding sequence variants. *Nat Methods* 2014;**11**:294-6.
377 Ng SB, Buckingham KJ, Lee C, et al. Exome sequencing identifies the cause of a mendelian disorder. *Nat Genet* 2010;**42**:30-5.
378 Ng SB, Turner EH, Robertson PD, et al. Targeted capture and massively parallel sequencing of 12 human exomes. *Nature* 2009;**461**:272-6.
379 Norton N, Li D, Rieder MJ, et al. Genome-wide studies of copy number variation and exome sequencing identify rare variants in BAG3 as a cause of dilated cardiomyopathy. *Am J Hum Genet* 2011;**88**:273-82.
380 Muddyman D, Smee C, Griffin H, et al. Implementing a successful data-management framework: the UK10K managed access model. *Genome Med* 2013;**5**:100.
381 Perry NA, Ackermann MA, Shriver M, et al. Obscurins: unassuming giants enter the spotlight. *IUBMB Life* 2013;**65**:479-86.

APPENDICES

APPENDIX A – PUBLICATIONS ARISING FROM THIS WORK

1. Lopes LR, Zekavati A, Syrris P, Hubank M, Giambartolomei C, Dalageorgou C, Jenkins S, McKenna W, Uk10k Consortium, Plagnol V, Elliott PM. Genetic complexity in hypertrophic cardiomyopathy revealed by high-throughput sequencing. J Med Genet. 2013 Apr;50(4):228-39.

2. Lopes LR, Rahman MS, Elliott PM. A systematic review and meta-analysis of genotype-phenotype associations in patients with hypertrophic cardiomyopathy caused by sarcomeric protein mutations. Heart. 2013 Dec;99(24):1800-11.

3. Lopes LR, Elliott PM. A straightforward guide to the sarcomeric basis of cardiomyopathies. Heart. 2014 Dec 15;100(24):1916-1923.

4. Lopes LR, Syrris P, Guttmann OP, O'Mahony C, Tang HC, Dalageorgou C, Jenkins S, Hubank M, Monserrat L, McKenna WJ, Plagnol V, Elliott P. Novel genotype-phenotype associations demonstrated by high-throughput sequencing in patients with hypertrophic cardiomyopathy. Heart. 2014 Oct 28. doi: 10.1136/heartjnl-2014-306387.

APPENDIX B – ETHICAL APPROVAL AND CONSENT FORM

St George's Healthcare NHS
NHS Trust

Wandsworth Local Research Ethics Committee
1st Floor Grosvenor

Our Ref: IAS/kl/01.78.10

3 December 2001

St George's Hospital
Blackshaw Road
London
SW17 0QT

Tel: 020 8672 1255
Fax: 020 8672 5304

www.st-georges.org.uk

Professor W McKenna
BHF Professor of Molecular Cardiovascular Sciences
Dept. of Cardiological Sciences
St. George's Hospital Medical School

Dear Professor McKenna

Re: Hypertrophic Cardiomyopathy (HCM): Clinical and Genetic investigation of a hereditary heart disease – 01.78.10

The Local Research Ethics Committee of 28th November 2001 reviewed the re-submission of your application. Following consideration the Committee agreed that you have now fully addressed the issues raised at our earlier meeting and, therefore, final ethical approval is given for the above named study to proceed subject to the Patient Information Sheets and Letters being printed on the appropriate headed paper.

Yours sincerely

Canon Ian Ainsworth-Smith
Chairman
Local Research Ethics Committee

Please Note: All research should be conducted in accordance with the guidelines of the Ethical Committee; the reference number allocated to the project should be used in all correspondence with the Committee and the Committee should be informed:

(a) when the project is complete.

(b) what stage the project is at one year from today's date.

(c) if any alterations are made to the treatment or protocol which might have affected ethical approval being granted.

(d) all investigators whose projects have been approved by this Committee are required to report at once any adverse experience affecting subjects in the study and at the same time state the current total number of Serious Adverse Events that have occurred.

University College London Hospitals NHS

NHS Trust

Co-Chairs: Mr M Harrison and Dr R MacAllister

Please address all correspondence to:
Ms Shelly Moylan - *Ethics Administrator (Temp)*
Email: sabrina.balendra@uclh.org

The Joint UCL/UCLH Ethics Committee: Committee A
Research & Development
1st Floor, Vezey Strong Wing
112 Hampstead Road
London NW1 2LT
Tel: 020 7380 9579
Fax: 020 7380 9937
Website: www.uclh.org

22nd July 2003

Our Ref: RM/ds/03A202

Professor W J McKenna
Professor of Cardiology
The Heart Hospital
16-18 Westmoreland Street
London

Dear Professor McKenna

REC Ref No: 03/0196*(please quote in all correspondence)*
REC Name: Committee A *(please quote in all correspondence)*
Study Title: Hypertrophic cardiomyopathy (HCM): Clinical and genetic investigation of a hereditary heart disease

Thank you for sending us your application for ethical review received on 9th July 2003. The Chair of the Joint UCL/UCLH Committee for Ethics on Human Research reviewed your application on 11th July 2003. The following documents have been reviewed:

- Health Authority Locality Form (signed 02/07/03)
- Patient information sheet (version 1 dated 30.06.03)
- Information Booklet for Patients and their families
- Adult consent form
- Child consent form
- Lead LREC application form (6th November 2001)
- Lead LREC approval letter (reference 01.78.10, dated 03.10.01)
- Investigator's CV

The Chair acting under delegated authority is satisfied that there are no ethical concerns and you are therefore given approval for your research on ethical grounds providing you comply with the conditions of approval set out below. This decision will be notified to the ethics committee at the next ethics committee meeting on 16th September 2003.

- You do not recruit any research subjects unless you have received a notification of no objections from the R&D office.

- You do not undertake this research until the relevant Trust management approval has been received (via the R&D office).

- You complete and return the standard progress report form to the REC one year from the date on this letter and thereafter on an annual basis. This form should also be used to notify the REC

- If this research is terminated prematurely, at this site, you send a report to the REC within 15 days indicating the reason for the early termination.
- The project must be started within three years of the date of this letter.

NHS RECs are compliant with the International Conference on Harmonisation/Good Clinical Practice (ICH GCP) Guidelines for the conduct of trials involving participation of human subjects.

Your application has been given a unique reference number please use it on all correspondence with the REC.

Yours sincerely

pp. Shelley Moyle

Doreen Sharpe
Senior Ethics Administrator

Enclosure: REC Response Form
REC Progress Report Form

NHS
National Research Ethics Service
Central London REC 4
South House, Block A
Royal Free Hospital
Pond Street
London NW3 2QG

11th May 2011
Dr Perry Elliot
The Heart Hospital
16-18 Westmoreland St.
London
W1G 8PH

Dear Dr. Elliot

Study title:	**Hypertrophic cardiomyopathy (HCM): Clinical and genetic investigation of a hereditary heart disease**
REC reference:	**03/0196**
Amendment number:	**1**
Amendment date:	**28/02/2011**

The above amendment was reviewed by the Sub-Committee in correspondence.

Ethical opinion

The members of the Committee taking part in the review gave a favourable ethical opinion of the amendment on the basis described in the notice of amendment form and supporting documentation.

Membership of the Committee

The members of the Committee who took part in the review are listed on the attached sheet.

R&D approval

All investigators and research collaborators in the NHS should notify the R&D office for the relevant NHS care organisation of this amendment and check whether it affects R&D approval of the research.

Statement of compliance

The Committee is constituted in accordance with the Governance Arrangements for Research Ethics Committees (July 2001) and complies fully with the Standard Operating Procedures for Research Ethics Committees in the UK.

03/0196:	Please quote this number on all correspondence

Yours sincerely

Laura Keegan
Committee Co-ordinator

E-mail: laura.keegan@nhs.net

Name	*Profession*	*Capacity*
Professor David Katz	Professor of Immunopathology	Expert
Mrs Michelle McPhail	Lay member	Lay

Also in attendance:

Name	*Position (or reason for attending)*
Miss Laura Keegan	REC Co-ordinator

NHS
National Patient Safety Agency

National Research Ethics Service

NOTICE OF SUBSTANTIAL AMENDMENT

For use in the case of all research other than clinical trials of investigational medicinal products (CTIMPs). For substantial amendments to CTIMPs, please use the EU-approved notice of amendment form (Annex 2 to ENTR/CT1) at http://eudract.emea.eu.int/document.html#guidance.

To be completed in typescript by the Chief Investigator in language comprehensible to a lay person and submitted to the Research Ethics Committee that gave a favourable opinion of the research ("the main REC"). In the case of multi-site studies, there is no need to send copies to other RECs unless specifically required by the main REC.

Further guidance is available at http://www.nres.npsa.nhs.uk/applicants/review/after/amendments.htm.

Details of Chief Investigator:

Name:	Dr Perry Elliott
Address:	The Heart Hospital 16-18 Westmoreland St London W1G 8PH
Telephone:	02075738888
Email:	Perry.elliott@ucl.ac.uk
Fax:	

Full title of study:	Hypertrophic cardiomyopathy (HCM): Clinical and genetic investigation of a hereditary heart disease
Name of main REC:	The Joint UCL/UCLH Ethics Committee: Committee A
REC reference number:	03/0196
Date study commenced:	03.10.01
Protocol reference *(if applicable)*, current version and date:	
Amendment number and date:	1 28.02.11

Type of amendment (indicate all that apply in bold)

(a) Amendment to information previously given on the NRES Application Form

Yes *No*

If yes, please refer to relevant sections of the REC application in the "summary of changes" below.

(b) Amendment to the protocol

Yes *No*

If yes, please submit either the revised protocol with a new version number and date, highlighting changes in bold, or a document listing the changes and giving both the previous and revised text.

(c) Amendment to the information sheet(s) and consent form(s) for participants, or to any other supporting documentation for the study

Yes *No*

If yes, please submit all revised documents with new version numbers and dates, highlighting new text in bold.

Is this a modified version of an amendment previously notified to the REC and given an unfavourable opinion?

Yes ***No***

Summary of changes

Briefly summarise the main changes proposed in this amendment using language comprehensible to a lay person. Explain the purpose of the changes and their significance for the study. In the case of a modified amendment, highlight the modifications that have been made.

If the amendment significantly alters the research design or methodology, or could otherwise affect the scientific value of the study, supporting scientific information should be given (or enclosed separately). Indicate whether or not additional scientific critique has been obtained.

Title: Inherited Cardiac Disease: A Clinical and Genetic Investigation

Research Participants and End Points:

Inherited cardiomyopathy is a myocardial disorder in which heart muscle is structurally and functionally abnormal in the absence of coronary artery disease, hypertension, valvular disease, and congenital heart diseases' (ESC). This umbrella incorporates hypertrophic cardiomyopathy (HCM), dilated cardiomyopathy (DCM), arrhythmogenic right ventricular cardiomyopathy (ARVC), left venticular non compaction (LVNC) and restrictive cardiomyopathy. Although previously classified by morphofunctional phenotype there are many similarities with the clinical manifestation relating to heart failure, arrhythmias and sudden death. With increased understanding of the condition it is also

clear that there is a large overlap in the molecular and genetic basis of the disease.

We therefore propose to extend the investigation to include individuals with a diagnosis of DCM, ARVC, LVNC and restrictive cardiomyopathy to fit with the current paradigm. We aim to enhance the understanding of the genotype and phenotype relationship across inherited cardiomyopathies. The proposed inclusion criteria include:

1. Phenotypic expression of an inherited cardiomyopathy
2. First degree relative of an individual with a diagnosis of inherited cardiomyopathy caused by an identified genetic mutation.

The proposed amendment will aim to amalgamate the current study with other ongoing studies:

Ref 03/0197 Dilated Cardiomyopathy (DMC): Clinical and genetic investigation of a hereditary heart disease.

Ref 03/0306 The identification of abnormal structural protein genes of the cardiac cell junction in autosomal dominant Arrythmogenic right ventricular cardiomyopathy.

The aims of the project and study end points will remain as those identified but will be assessed across the spectrum of cardiomyopathies.

Duration of Study

We propose to extend the study by an additional 5 years for estimated completion 28.02.2018

Research Sites:

The Heart Hospital (University College London Hospitals), 16-18 Westmoreland St, London, W1G 8PH

Great Ormond Street Hospital for Children NHS Trust, Great Ormond Street, London WC1N 3JH

Participant Recruitment:

We propose to investigate a total of 5,000 individuals. A previously published pilot study suggests that disease causing mutations are identified in 50%. By testing 5,000 individuals we aim to identify 2,500 individuals with a genetic mutation which would be sufficient to establish a genotype – phenotype correlation. Participants will be recruited from the inherited cardiac disease Clinics at University College London Hospitals (The Heart Hospital) and Great Ormond Street Hospital.

Storage and Future Use of Samples:

Samples will be securely stored at:

Paul O'Gorman Building, UCL Institute of Cardiovascular
Science, Ground Floor, Room G05, 72 Huntley Street, London, WC1E 6DD.
Tel: 020 7679 6464; Fax: 020 7679 6463.

Samples will be analyzed at UCL research/UCL genomics. Additional analysis may take place at other research laboratories including those located outside the United Kingdom.

Samples may be analysed on multiple occasions for genes relating to inherited cardiomyopathies. Following completion of the study, samples may be transferred to a tissue bank or destroyed in accordance with the Human Tissue Authority's Code of Practice. Access to samples will be restricted to those involved in the study.

Potential Outcomes:

Those with definite or potential genetic mutations will be offered confirmatory testing at an accredited

NHS laboratory. In addition they will be offered genetic counselling and ongoing clinical care at our centre.

Those with no genetic mutation identified will be managed as per clinical indication. Samples may be analysed in the future for genes that have not as yet been identified.

Recruitment of Children:

A separate information sheet and consent form will be provided for parental/legal guardians. Consent for children will be taken at Great Ormond Street Hospital for Children. Children who are able to consent for themselves may do so, however due to the familial nature of the disease we would encourage the involvement of family.

Recruitment of Participants Involved in Other Trials:

Individuals that are involved in other trials will be offered the opportunity to participate. The clinical profiling required for this study would form a part of routine clinical care and thus the time burden for this trial is limited to the process of recruitment and genetic counseling. No therapy will be administered in this trial and therefore we would not have to consider the potential implications on other trials.

Participation in trials which relate inherited cardiomyoapthies (i.e therapeutic trials and other observational studies) will be noted. With the consent of the investigator and participant, outcomes of these trials may be correlated to genotype where possible.

Storage of Research Data:

Data will be stored using a unique participant identifier. Data will be stored on secure and password protected hospital and university networks. Data will not be stored on personal computers. Confidential documents will be stored in a locked filing cabinet located in a secure room. Patients' clinical notes will be handled according to trust protocol and in line with the procedures set out in the original application.

University College London Hospitals NHS
NHS Foundation Trust

Consent form for Genetic Testing

The Heart Hospital
Cardiology Department
16 -18 Westmoreland Street
London W1G 8PH

Telephone: 020 7573 8888
Fax: 020 7573 8838
Web-site: www.uclh.nhs.uk

Purpose(s) of test:

☐ To discover if the patient carries a gene alteration
☐ To enable relatives to benefit from genetic testing
☐ To clarify the implications of a previous test result
☐ To help make a diagnosis
☐ Other:_____

Blood sample to be analysed for: _____

Patient Statement: **(Please delete where appropriate)**

I **agree/do not agree** to the test on this form

I understand that

- This test is voluntary and I can withdraw from the testing process at any time.
- In the future my genetic test results may affect the ability of me or my family members to obtain some types of insurance.
- The test result will not be revealed or made available to any other person/organisation, except with my consent or when disclosure is required by law.
- The sample may be sent to another laboratory outside UCL/UCLH for testing. If testing is currently unavailable, the sample will be stored in UCL/UCLH for possible future use.
- The sample will be transported and stored in good faith but we cannot guarantee its suitability for testing.
- My sample will be disposed of in accordance with standard laboratory practices/regulatory requirements.

I **give/do not give** permission for my blood sample to be tested in the future if new genes are found to be associated with_____(Insert name of condition)

I **give/do not give** permission for my blood sample to be used in the future to benefit my family members.

In the event of my death, I give permission for the results of my test to be given to:

_____(Insert name)

Name of Patient	Date	Signature
Name of Doctor/Counsellor/Nurse	Date	Signature

1 copy for patient; 1 copy for hospital notes

G:\Users\Mturnbul\Forms\Consent\Consent form for genetic testing.doc
Last updated 17 November 2004

University College London Hospitals NHS
NHS Foundation Trust

PATIENT INFORMATION SHEET

Hypertrophic cardiomyopathy (HCM): Clinical and genetic investigation of a hereditary heart disease.

(11 June 2007, version 2)

The Heart Hospital
Outpatients Department
14 – 16 Westmoreland Street
London
W1G 8PH

Switchboard: 020 3456 6222
Fax: 020 3456 4205

What is hypertrophic cardiomyopathy (HCM)?
HCM is a common condition that affects the heart muscle. It affects people in different ways. Some people with the condition do not have any symptoms of disease while others may experience episodes of breathlessness, chest pain, and palpitation or have attacks of dizziness or fainting. These symptoms are usually caused by a thickening of the heart muscle. More details about the condition are provided in the booklet we have given you.

HCM can be inherited. By this, we mean that the condition can be passed down in a family through the genes. Everybody has about 30,000 pairs of genes that contain the instructions (like a recipe) that determine the way we grow and develop. There are genes that contain the instructions for the proper functioning of the heart. If one of these genes has a spelling change in it, which we call a "mutation", it can cause HCM. In recent years it has become possible to test some of the genes for changes.

Our research:

Our research aims to identify changes in the gene that are currently known to cause HCM and understand how these gene changes affect the heart. To identify changes in these genes, we need a blood sample from individuals with the condition. We will test that blood sample for changes in the gene that are currently known to cause HCM. The sample may also be used to identify new genes that cause HCM.

How long will it take and what are the possible outcomes of my test?

This test is being performed on a **research** basis. This means that it could take many years to get an answer. If a gene change is identified, we will contact you. It would be helpful to contact us if you have changed address so that your details are kept current with our program. Any results will be kept **confidential** and will not be revealed to any one else without your consent.

The possible outcomes of your test could be:

- We may identify a gene change that we can confidently say is the cause of HCM in you.
- We may identify a change that could be the cause of HCM in you. In this circumstance, we may need to ask other family members to be investigated to help determine whether the identified change is actually causing the condition or not It will be their choice if they wish to become involved.
- There may be no result. This could occur if testing does not reveal any changes in the genes that were analysed or if by chance, you have a gene change in a HCM gene that has not been discovered and therefore could not be tested.
- Some gene changes can potentially affect other organ systems and therefore may require a change in medical management

What are the implications of the test for you?

If a gene change that causes HCM is identified in you , you will continue to have regular check-ups; the frequency and nature of which will be depend on your symptoms.

What are the implications of the test for your children?

If a gene change that causes HCM is identified in you, your children may or may not have inherited it from you. Some people wish to know if their children have the gene change while others do not. If a gene change is identified in you, you and your partner will be offered the opportunity to discuss your thoughts and feelings about having your children tested. It is not compulsory for children to be tested.

What are the implications for the rest of your family?

In the majority of cases, people identified with a gene change will have inherited it from one of their parents. Each of your brothers and sisters may be at risk of having inherited the gene change and some of your aunts and cousins may have inherited it. Some relatives may wish to know this information, while others will not. If a gene change is identified in you, we will discuss with you ways of informing relatives.

What are the benefits of being involved in this research?

If a gene change is identified in you, other family members at risk of the disease can be identified by having a blood test to identify if they have the same gene change. Those that do not have the gene change will not be at risk of developing the condition and will not have to have heart check ups. Those that are found to have the gene change may or may not have signs of HCM, but will be offered clinical screening as required.

Do I have to take part?

Your participation in this research is absolutely voluntary. If you decide to take part you are free to withdraw at any time and without giving a reason. This will not affect the present standard of care you receive or any future care.

This research has been approved by an ethics committee and is funded by the British Heart Foundation.

Principal Investigator:

Professor W.J McKenna, Professor of Cardiology

Contact people

Simon Waller
020 345 64302
Bleep: 6951

APPENDIX C – ADDITIONAL STATISTICAL METHODS FOR METHODS - CHAPTER 3.4

1 Bringing the data into the R software

We first load the data into R. The numbers below indicate, for each gene, the frequencies of candidate variants (i.e. non-synonymous and rare in the 1,000 genomes dataset) cases and controls.

```
> n1 <- 1287
> n2 <- 180
> genes <- data.frame(gene = c('MYH7', 'TNNT2', 'TNNI3', 'MYBPC3', 'MYL2', 'MYL3', 'ACTC1',
  'TPM1'),
+                     f.controls = c(0.0125, 0.00155, 0.00000, 0.02725, 0.0035, 0.00194, 0.00039, 0.001
+                     f.cases = c(0.086, 0.027, 0.0083, 0.05, 0.011, 0.0055, 0.0027, 0.0027))
> genes
```

	gene	f.controls	f.cases
1	MYH7	0.01250	0.0860
2	TNNT2	0.00155	0.0270
3	TNNI3	0.00000	0.0083
4	MYBPC3	0.02725	0.0500
5	MYL2	0.00350	0.0110
6	MYL3	0.00194	0.0055
7	ACTC1	0.00039	0.0027
8	TPM1	0.00136	0.0027

2 Estimating the proportion of cases explained for each gene

The most difficult question is the following: for a gene of interest, and given the estimated frequencies of candidate variants in controls and cases, how can we estimate the confidence interval for the proportion of HCM cases explained by this class of variants in that gene? Mathematically, we use the following notations: x is the frequency of candidate variants in controls and x + y is the frequency of candidate variants in cases. The parameter y refers to the additional proportion of cases whose disease is caused by mutations in that gene. What we are after is a confidence interval for y.

Here, X is a nuisance parameter and we use a profile likelihood argument to get rid of this parameter. Precisely, we set up a grid of values for y and for each of these we find the value of x that maximizes the lieklihood of the data. The function that we use to obtain the cofidence interval for the parameter y is below. n_1 = 1; is the number of controls and n_2 = 180 is the number of cases.

```
> joint.estimate <- function(n1, n2, x1, x2) {
+     y <- seq(0, 3*x2, x2/100)  ##grid of values for y
+
+     ## Now here is the likelihood function
+     my.fn <- function(x, y) ( -floor(x1*n1)*log(x)
  +                                - (n1    - floor(x1*n1))*log(1-x)
  +                                - floor(x2*n2)*log(x+y)
  +                                - (n2    - floor(x2*n2))*log(1- x - y))
+     prof <- rep(NA, length(y))  ##profile likelihood
```

```
+
+     ## Now loop over all possible values of y and maximise wrt x
+     for (i in 1:length(y)) {
+        prof[i] = optim(par = x1, ##here is the maximisation for x
+                  fn = my.fn,
+                  gr = NULL,
+                  y = y[i],
+                  lower = 0.001,
+                  upper = 1 - y - 0.001,
+                  method = 'Brent')$value
+     }
+     prof <- ifelse (is.nan(prof), -10^6, prof)
+     prof <- -prof
+     prof <- prof - max(prof)
+
+     in.CI <- which(2*prof > -qchisq(df = 1, p = 0.95, lower.tail = TRUE))
+     my.CI <- y[ range( in.CI ) ]
+     return(my.CI)
+ }
```

We can now estimate this confidence interval for each gene in our dataset. Because each control/case has 2 chromosomes, if the frequency of candidate variants is f, then the proportion of cases with at least one causal variant is $f^2 + 2f(1\ f)$.

```
> for  (i in 1:nrow(genes)) {
+     prop.controls <- 2*genes$f.controls[i]*(1-genes$f.controls[i]) + genes$f.controls[i]^2
+     prop.cases <- 2*genes$f.cases[i]*(1-genes$f.cases[i]) + genes$f.cases[i]^2
+
+     my.CI <- joint.estimate (n1 = n1, n2 = n2, x1 = prop.controls, x2 = prop.cases)
+     my.CI <- signif(my.CI, 3)
+     genes$CI.prop.HCM.cases.explained[i] <- paste( '[', my.CI[1], '-', my.CI[2], ']', sep =   )
+ }
> genes
```

	gene	f.controls	f.cases	CI.prop.HCM.cases.explained
1	MYH7	0.01250	0.0860	[0.0889-0.196]
2	TNNT2	0.00155	0.0270	[0.0218-0.0858]
3	TNNI3	0.00000	0.0083	[0.000992-0.0329]
4	MYBPC3	0.02725	0.0500	[0.00195-0.0897]
5	MYL2	0.00350	0.0110	[0-0.0365]
6	MYL3	0.00194	0.0055	[0-0.0213]
7	ACTC1	0.00039	0.0027	[0-0.0106]
8	TPM1	0.00136	0.0027	[0-0.0106]

3 P-values for differences between cases and controls

This computation is done by statistically comparing the number of candidate variants between cases and controls. We use a Fisher exact test to quantify this difference. Because we work at the allele level the observed number of alleles are $2n_1\ f_1$ in controls and $2n_1\ f_2$ in cases, where f_1 and f_2 denote the frequency of candidate variants in cases and controls.

```
> for  (i in 1:nrow(genes)) {
```

```
+     my.mat <- matrix(data = c(2*n1*(1 - genes$f.controls[ i ]),
+                               2*n1*genes$f.controls[i],
+                               2*n2*(1-genes$f.cases[i]),
+                               2*n2*genes$f.cases[i]),
+                              nrow = 2,
+                              ncol = 2,
+                              byrow = TRUE)
+
+     my.mat <- round(my.mat)
+     genes$P.diff[i] <- fisher.test ( my.mat )$p.value
+ }
> genes

      gene f.controls f.cases CI.prop.HCM.cases.explained                P.diff
1     MYH7    0.01250  0.0860                [0.0889-0.196] 3.855666e-13
2    TNNT2    0.00155  0.0270                [0.0218-0.0858] 4.373726e-07
3    TNNI3    0.00000  0.0083              [0.000992-0.0329] 1.833766e-03
4   MYBPC3    0.02725  0.0500               [0.00195-0.0897] 2.987798e-02
5     MYL2    0.00350  0.0110                     [0-0.0365] 6.473193e-02
6     MYL3    0.00194  0.0055                     [0-0.0213] 2.083091e-01
7    ACTC1    0.00039  0.0027                     [0-0.0106] 2.303803e-01
8     TPM1    0.00136  0.0027                     [0-0.0106] 4.805606e-01

>
```

4 **Point estimates for the probability that a candidate variant is causal**

We want to estimate, for each gene, the probability that a candidate variant in a HCM case is causal. This point estimate is straightforward. It is simply:

$$p_{causal} = \frac{\text{Frequency of candidates variants in cases} - \text{Frequency of candidates variants in controls}}{\text{Frequency of candidate variants in cases}}$$

Hence:

```
> genes$prob.causal <- (genes$f.cases - genes$f.controls)/genes$f.cases
> genes

      gene f.controls  f.cases CI.prop.HCM.cases.explained                P.diff
1     MYH7    0.01250  0.0860                [0.0889-0.196] 3.855666e-13
2    TNNT2    0.00155  0.0270                [0.0218-0.0858] 4.373726e-07
3    TNNI3    0.00000  0.0083              [0.000992-0.0329] 1.833766e-03
4   MYBPC3    0.02725  0.0500               [0.00195-0.0897] 2.987798e-02
5     MYL2    0.00350  0.0110                     [0-0.0365] 6.473193e-02
6     MYL3    0.00194  0.0055                     [0-0.0213] 2.083091e-01
7    ACTC1    0.00039  0.0027                     [0-0.0106] 2.303803e-01
8     TPM1    0.00136  0.0027                     [0-0.0106] 4.805606e-01
  prob.causal
1   0.8546512
2   0.9425926
3   1.0000000
4   0.4550000
```

5 0.6818182
6 0.6472727
7 0.8555556
8 0.4962963

APPENDIX D – LIST OF CANDIDATE VARIANTS – EXCLUDING TITIN

Supplementary table 1. List of distinct rare variants detected (MAF<0.2%; see methods). All variants were detected in heterozygozity. Type of variant: D: variant reported on dbSNP137, not predicted *in silico* to be pathogenic, not nonsense, frameshift indel or splice-site and not published in the literature; L: novel (or reported on dbSNP137) nonsense, frameshift indel or splice-site variant; N: novel variant not predicted *in silico* to be pathogenic and not nonsense, frameshift indel or splice-site; P: published variant in the literature; S: novel (or reported on dbSNP137) missense variant predicted *in silico* to be pathogenic. MAF: minor allele frequency.

ACTC1: actin, alpha, cardiac muscle 1; *ANK2*: ankyrin 2, neuronal; *CASQ2*: calsequestrin 2 cardiac muscle; *CAV3*: caveolin 3; *CSRP3*: cysteine and glycine-rich protein 3 cardiac LIM protein; *DES*: desmin; *DSC2*: desmocollin 2; *DSG2*: desmoglein 2; *DSP*: desmoplakin; *JUP*: junction plakoglobin; *KCNE1*: potassium voltage-gated channel, Isk-related family, member 1; *KCNE2*: potassium voltage-gated channel, Isk-related family, member 2; *KCNH2*: potassium voltage-gated channel, subfamily H eag-related, member 2; *KCNJ2*: potassium inwardly-rectifying channel, subfamily J, member 2; *KCNQ1*: potassium voltage-gated channel, KQT-like subfamily, member 1; *LDB3*: LIM domain binding 3; *LMNA*: lamin A/C; *MYBPC3*: myosin binding protein C, cardiac; *MYH6*: myosin, heavy chain 6, cardiac muscle, alpha; *MYH7*: myosin, heavy chain 7, cardiac muscle, beta; *MYL2*: myosin, light chain 2, regulatory, cardiac, slow; *MYL3*: myosin, light chain 3, alkali; *PDLIM3*: PDZ and LIM domain 3; *PKP2*: plakophilin 2; *PLN*, phospholamban; *RBM20*: RNA binding motif protein 20; *RYR2*: ryanodine receptor 2 cardiac; *SCN5A*: sodium channel, voltage-gated, type V, alpha subunit; *TCAP*: titin-cap; *TGFbeta3*: transforming growth factor, beta 3; *TMEM43*: transmembrane protein 43; *TNNC1*: troponin C type 1 slow; *TNNI3*: troponin I type 3 cardiac; *TNNT2*: troponin T type 2 cardiac; *TPM1*: tropomyosin 1 alpha; VCL: vinculin.

Gene	Genomic signature	Transcript / Amino acid change	dbSNP137 ID	Type of variant	MAF- cases
ACTC1	15_35084398_G_A	ENSG00000159251:ENST00000290378:exon5:c.C701T:p.S234F		N	0,00057
ACTC1	15_35085539_T_C	ENSG00000159251:ENST00000290378:exon3:c.A361G:p.M121V		S	0,00058
ACTC1	15_35085599_C_T	ENSG00000159251:ENST00000290378:exon3:c.G301A:p.E101K	rs193922680	P	0,00057
ANK2	4_113970940_G_A	ENSG00000145362:ENST00000264366:exon1:c.G56A:p.S19N,ENSG00000145362:ENST00000357077:exon1:c.G56A:p.S19N,ENSG00000145362:ENST00000394537:exon1:c.G56A:p.S19N,ENSG00000145362:ENST00000504454:exon1:c.G56A:p.S19N		N	0,00057
ANK2	4_114067089_T_A	ENSG00000145362:ENST00000511380:exon1:c.T65A:p.M22K	rs116338686	D	0,00115
ANK2	4_114072285_T_C	ENST00000504454:exon2:c.129+5T>C		L	0,00057

ANK2	4_114158192_C_T	ENSG00000145362:ENST00000264366:exon6:c.C533T:p.A178V,ENSG00000145362:ENST00000357077:exon6:c.C533T:p.A178V,ENSG00000145362:ENST00000394537:exon6:c.C533T:p.A178V,ENSG00000145362:ENST00000515034:exon6:c.C128T:p.A43V,ENSG00000145362:ENST00000503271:exon7:c.C470T:p.A157V,ENSG00000145362:ENST00000503423:exon7:c.C470T:p.A157V,ENSG00000145362:ENST00000504454:exon7:c.C578T:p.A193V,ENSG00000145362:ENST00000506722:exon7:c.C470T:p.A157V		N	0,00058
ANK2	4_114195614_C_G	ENSG00000145362:ENST00000264366:exon15:c.C1492G:p.Q498E,ENSG00000145362:ENST00000357077:exon15:c.C1492G:p.Q498E,ENSG00000145362:ENST00000394537:exon15:c.C1492G:p.Q498E,ENSG00000145362:ENST00000503271:exon16:c.C1429G:p.Q477E,ENSG00000145362:ENST00000503423:exon16:c.C1429G:p.Q477E,ENSG00000145362:ENST00000504454:exon16:c.C1537G:p.Q513E,ENSG00000145362:ENST00000506722:exon16:c.C1429G:p.Q477E		S	0,00057
ANK2	4_114199026_T_C	ENSG00000145362:ENST00000264366:exon16:c.T1717C:p.Y573H,ENSG00000145362:ENST00000357077:exon16:c.T1717C:p.Y573H,ENSG00000145362:ENST00000394537:exon16:c.T1717C:p.Y573H,ENSG00000145362:ENST00000503271:exon17:c.T1654C:p.Y552H,ENSG00000145362:ENST00000503423:exon17:c.T1654C:p.Y552H,ENSG00000145362:ENST00000504454:exon17:c.T1762C:p.Y588H,ENSG00000145362:ENST00000506722:exon17:c.T1654C:p.Y552H		S	0,00057
ANK2	4_114208841_T_A	ENSG00000145362:ENST00000264366:exon19:c.T2160A:p.D720E,ENSG00000145362:ENST00000357077:exon19:c.T2160A:p.D720E,ENSG00000145362:ENST00000394537:exon19:c.T2160A:p.D720E,ENSG00000145362:ENST00000503423:exon19:c.T1998A:p.D666E,ENSG00000145362:ENST00000503271:exon20:c.T2097A:p.D699E,ENSG00000145362:ENST00000504454:exon20:c.T2205A:p.D735E,ENSG00000145362:ENST00000506722:exon20:c.T2097A:p.D699E		N	0,00057
ANK2	4_114239695_C_G	ENSG00000145362:ENST00000509550:exon6:c.C446G:p.A149G,ENSG00000145362:ENST00000264366:exon26:c.C2819G:p.A940G,ENSG00000145362:ENST00000357077:exon26:c.C2819G:p.A940G,ENSG00000145362:ENST00000394537:exon26:c.C2819G:p.A940G,ENSG00000145362:ENST00000503423:exon26:c.C2657G:p.A886G,ENSG00000145362:ENST00000503271:exon27:c.C2756G:p.A919G,ENSG00000145362:ENST00000504454:exon27:c.C2864G:p.A955G,ENSG00000145362:ENST00000506722:exon27:c.C2756G:p.A919G		S	0,00115
ANK2	4_114244911_G_A	ENST00000506722:exon28:-4G>A	rs139641776	L	0,00057
ANK2	4_114244926_C_A	ENSG00000145362:ENST00000506722:exon28:c.C2849A:p.P950Q		N	0,00114
ANK2	4_114251533_G_A	ENSG00000145362:ENST00000509550:exon7:c.G659A:p.R220H,ENSG00000145362:ENST00000264366:exon27:c.G3032A:p.R1011H,ENSG00000145362:ENST00000357077:exon27:c.G3032A:p.R1011H,ENSG00000145362:ENST00000394537:exon27:c.G3032A:p.R1011H,ENSG00000145362:ENST00000503423:exon27:c.G2870A:p.R957H,ENSG00000145362:ENST00000503271:exon28:c.G2969A:p.R990H,ENSG00000145362:ENST00000504454:exon28:c.G3077A:p.R1026H,ENSG00000145362:ENST00000506722:exon29:c.G3005A:p.R1002H		S	0,00058

ANK2	4_114251575_G_C	ENSG00000145362:ENST00000509550:exon7:c.G701C:p.G234A,ENSG00000145362:ENST00000264366:exon27:c.G3074C:p.G1025A,ENSG00000145362:ENST00000357077:exon27:c.G3074C:p.G1025A,ENSG00000145362:ENST00000394537:exon27:c.G3074C:p.G1025A,ENSG00000145362:ENST00000503423:exon27:c.G2912C:p.G971A,ENSG00000145362:ENST00000503271:exon28:c.G3011C:p.G1004A,ENSG00000145362:ENST00000504454:exon28:c.G3119C:p.G1040A,ENSG00000145362:ENST00000506722:exon29:c.G3047C:p.G1016A		S	0,00058
ANK2	4_114263066_T_G	ENSG00000145362:ENST00000510275:exon1:c.T72G:p.D24E,ENSG00000145362:ENST00000509550:exon12:c.T1644G:p.D548E,ENSG00000145362:ENST00000264366:exon32:c.T4017G:p.D1339E,ENSG00000145362:ENST00000503423:exon32:c.T3855G:p.D1285E,ENSG00000145362:ENST00000357077:exon33:c.T4116G:p.D1372E,ENSG00000145362:ENST00000394537:exon33:c.T4116G:p.D1372E,ENSG00000145362:ENST00000504454:exon34:c.T4161G:p.D1387E,ENSG00000145362:ENST00000506722:exon35:c.T4089G:p.D1363E		S	0,00057
ANK2	4_114267117_C_T	ENSG00000145362:ENST00000510275:exon3:c.C266T:p.T89M,ENSG00000145362:ENST00000509550:exon14:c.C1838T:p.T613M,ENSG00000145362:ENST00000264366:exon34:c.C4211T:p.T1404M,ENSG00000145362:ENST00000503423:exon34:c.C4049T:p.T1350M,ENSG00000145362:ENST00000357077:exon35:c.C4310T:p.T1437M,ENSG00000145362:ENST00000394537:exon35:c.C4310T:p.T1437M,ENSG00000145362:ENST00000504454:exon36:c.C4355T:p.T1452M,ENSG00000145362:ENST00000506722:exon37:c.C4283T:p.T1428M	rs142534126	S	0,00057
ANK2	4_114267122_G_T	ENSG00000145362:ENST00000510275:exon3:c.G271T:p.G91C,ENSG00000145362:ENST00000509550:exon14:c.G1843T:p.G615C,ENSG00000145362:ENST00000264366:exon34:c.G4216T:p.G1406C,ENSG00000145362:ENST00000503423:exon34:c.G4054T:p.G1352C,ENSG00000145362:ENST00000357077:exon35:c.G4315T:p.G1439C,ENSG00000145362:ENST00000394537:exon35:c.G4315T:p.G1439C,ENSG00000145362:ENST00000504454:exon36:c.G4360T:p.G1454C,ENSG00000145362:ENST00000506722:exon37:c.G4288T:p.G1430C	rs34591340	P	0,00057
ANK2	4_114267176_A_G	ENSG00000145362:ENST00000510275:exon3:c.A325G:p.K109E,ENSG00000145362:ENST00000509550:exon14:c.A1897G:p.K633E,ENSG00000145362:ENST00000264366:exon34:c.A4270G:p.K1424E,ENSG00000145362:ENST00000503423:exon34:c.A4108G:p.K1370E,ENSG00000145362:ENST00000357077:exon35:c.A4369G:p.K1457E,ENSG00000145362:ENST00000394537:exon35:c.A4369G:p.K1457E,ENSG00000145362:ENST00000504454:exon36:c.A4414G:p.K1472E,ENSG00000145362:ENST00000506722:exon37:c.A4342G:p.K1448E		N	0,00057
ANK2	4_114269433_A_G	ENSG00000145362:ENST00000510275:exon4:c.A329G:p.E110G,ENSG00000145362:ENST00000509550:exon15:c.A1901G:p.E634G,ENSG00000145362:ENST00000264366:exon35:c.A4274G:p.E1425G,ENSG00000145362:ENST00000503423:exon35:c.A4112G:p.E1371G,ENSG00000145362:ENST00000357077:exon36:c.A4373G:p.E1458G,ENSG00000145362:ENST00000394537:exon36:c.A4373G:p.E1458G,ENSG00000145362:ENST00000504454:exon37:c.A4418G:p.E1473G,ENSG00000145362:ENST00000506722:exon38:c.A4346G:p.E1449G	rs72544141	P	0,00172

ANK2	4_114274519_G_A	ENSG00000145362:ENST00000264366:exon37:c.G4646A:p.R1549Q,ENSG00000145362:ENST00000503423:exon37:c.G4484A:p.R1495Q,ENSG00000145362:ENST00000357077:exon38:c.G4745A:p.R1582Q,ENSG00000145362:ENST00000504454:exon39:c.G4790A:p.R1597Q	rs138842207	D	0,00286
ANK2	4_114274546_A_G	ENSG00000145362:ENST00000264366:exon37:c.A4673G:p.E1558G,ENSG00000145362:ENST00000503423:exon37:c.A4511G:p.E1504G,ENSG00000145362:ENST00000357077:exon38:c.A4772G:p.E1591G,ENSG00000145362:ENST00000504454:exon39:c.A4817G:p.E1606G		S	0,00057
ANK2	4_114274806_G_A	ENSG00000145362:ENST00000264366:exon37:c.G4933A:p.E1645K,ENSG00000145362:ENST00000503423:exon37:c.G4771A:p.E1591K,ENSG00000145362:ENST00000357077:exon38:c.G5032A:p.E1678K,ENSG00000145362:ENST00000504454:exon39:c.G5077A:p.E1693K		N	0,00057
ANK2	4_114275005_C_A	ENSG00000145362:ENST00000264366:exon37:c.C5132A:p.A1711D,ENSG00000145362:ENST00000357077:exon38:c.C5231A:p.A1744D	rs147706514	D	0,00057
ANK2	4_114275005_C_T	ENSG00000145362:ENST00000264366:exon37:c.C5132T:p.A1711V,ENSG00000145362:ENST00000357077:exon38:c.C5231T:p.A1744V		N	0,00057
ANK2	4_114275096_G_T	ENSG00000145362:ENST00000264366:exon37:c.G5223T:p.Q1741H,ENSG00000145362:ENST00000357077:exon38:c.G5322T:p.Q1774H		S	0,00057
ANK2	4_114275262_C_T	ENSG00000145362:ENST00000264366:exon37:c.C5389T:p.H1797Y,ENSG00000145362:ENST00000357077:exon38:c.C5488T:p.H1830Y		N	0,00057
ANK2	4_114275344_T_A	ENSG00000145362:ENST00000264366:exon37:c.T5471A:p.V1824E,ENSG00000145362:ENST00000357077:exon38:c.T5570A:p.V1857E	rs141212932	D	0,00057
ANK2	4_114275425_C_T	ENSG00000145362:ENST00000264366:exon37:c.C5552T:p.S1851L,ENSG00000145362:ENST00000357077:exon38:c.C5651T:p.S1884L	rs150737736	D	0,00057
ANK2	4_114275688_C_A	ENSG00000145362:ENST00000264366:exon37:c.C5815A:p.Q1939K,ENSG00000145362:ENST00000357077:exon38:c.C5914A:p.Q1972K		N	0,00057
ANK2	4_114275852_A_T	ENSG00000145362:ENST00000264366:exon37:c.A5979T:p.K1993N,ENSG00000145362:ENST00000357077:exon38:c.A6078T:p.K2026N		N	0,00115
ANK2	4_114275950_C_T	ENSG00000145362:ENST00000264366:exon37:c.C6077T:p.T2026M,ENSG00000145362:ENST00000357077:exon38:c.C6176T:p.T2059M	rs200765866	S	0,00058
ANK2	4_114275980_G_A	ENSG00000145362:ENST00000264366:exon37:c.G6107A:p.R2036H,ENSG00000145362:ENST00000357077:exon38:c.G6206A:p.R2069H	rs149645600	S	0,00058
ANK2	4_114276279_G_A	ENSG00000145362:ENST00000264366:exon37:c.G6406A:p.V2136I,ENSG00000145362:ENST00000357077:exon38:c.G6505A:p.V2169I	rs149292242	S	0,00057
ANK2	4_114276360_G_A	ENSG00000145362:ENST00000264366:exon37:c.G6487A:p.G2163S,ENSG00000145362:ENST00000357077:exon38:c.G6586A:p.G2196S		N	0,00057
ANK2	4_114276657_A_G	ENSG00000145362:ENST00000264366:exon37:c.A6784G:p.T2262A,ENSG00000145362:ENST00000357077:exon38:c.A6883G:p.T2295A		N	0,00058
ANK2	4_114276879_G_T	ENSG00000145362:ENST00000264366:exon37:c.G7006T:p.V2336F,ENSG00000145362:ENST00000357077:exon38:c.G7105T:p.V2369F		N	0,00130

ANK2	4_114276891_A_G	ENSG00000145362:ENST00000264366:exon37:c.A7018G:p.T2340A,ENSG00000145362:ENST00000357077:exon38:c.A7117G:p.T2373A	rs184514058	D	0,00066
ANK2	4_114276922_C_T	ENSG00000145362:ENST00000264366:exon37:c.C7049T:p.P2350L,ENSG00000145362:ENST00000357077:exon38:c.C7148T:p.P2383L	rs35960628	D	0,00066
ANK2	4_114276957_A_C	ENSG00000145362:ENST00000264366:exon37:c.A7084C:p.T2362P,ENSG00000145362:ENST00000357077:exon38:c.A7183C:p.T2395P	rs201693280	D	0,00133
ANK2	4_114277041_G_A	ENSG00000145362:ENST00000264366:exon37:c.G7168A:p.A2390T,ENSG00000145362:ENST00000357077:exon38:c.G7267A:p.A2423T	rs3733616	D	0,00062
ANK2	4_114277108_A_G	ENSG00000145362:ENST00000264366:exon37:c.A7235G:p.D2412G,ENSG00000145362:ENST00000357077:exon38:c.A7334G:p.D2445G		S	0,00059
ANK2	4_114277642_C_G	ENSG00000145362:ENST00000264366:exon37:c.C7769G:p.S2590C,ENSG00000145362:ENST00000357077:exon38:c.C7868G:p.S2623C	rs116253689	D	0,00057
ANK2	4_114277871_G_A	ENSG00000145362:ENST00000264366:exon37:c.G7998A:p.M2666I,ENSG00000145362:ENST00000357077:exon38:c.G8097A:p.M2699I	rs148904454	D	0,00058
ANK2	4_114278014_G_A	ENSG00000145362:ENST00000264366:exon37:c.G8141A:p.R2714H,ENSG00000145362:ENST00000357077:exon38:c.G8240A:p.R2747H	rs142137451	D	0,00057
ANK2	4_114278542_A_G	ENSG00000145362:ENST00000264366:exon37:c.A8669G:p.Q2890R,ENSG00000145362:ENST00000357077:exon38:c.A8768G:p.Q2923R		S	0,00057
ANK2	4_114278701_C_G	ENSG00000145362:ENST00000264366:exon37:c.C8828G:p.S2943C,ENSG00000145362:ENST00000357077:exon38:c.C8927G:p.S2976C		S	0,00057
ANK2	4_114278820_G_A	ENSG00000145362:ENST00000505342:exon1:c.G76A:p.E26K,ENSG00000145362:ENST00000264366:exon37:c.G8947A:p.E2983K,ENSG00000145362:ENST00000357077:exon38:c.G9046A:p.E3016K	rs149963885	D	0,00057
ANK2	4_114279054_C_G	ENSG00000145362:ENST00000505342:exon1:c.C310G:p.P104A,ENSG00000145362:ENST00000264366:exon37:c.C9181G:p.P3061A,ENSG00000145362:ENST00000357077:exon38:c.C9280G:p.P3094A		S	0,00115
ANK2	4_114279615_C_G	ENSG00000145362:ENST00000505342:exon1:c.C871G:p.Q291E,ENSG00000145362:ENST00000264366:exon37:c.C9742G:p.Q3248E,ENSG00000145362:ENST00000357077:exon38:c.C9841G:p.Q3281E		N	0,00057
ANK2	4_114279646_C_G	ENSG00000145362:ENST00000505342:exon1:c.C902G:p.P301R,ENSG00000145362:ENST00000264366:exon37:c.C9773G:p.P3258R,ENSG00000145362:ENST00000357077:exon38:c.C9872G:p.P3291R		N	0,00057
ANK2	4_114279892_C_T	ENSG00000145362:ENST00000505342:exon1:c.C1148T:p.A383V,ENSG00000145362:ENST00000264366:exon37:c.C10019T:p.A3340V,ENSG00000145362:ENST00000357077:exon38:c.C10118T:p.A3373V		N	0,00059
ANK2	4_114280441_A_G	ENSG00000145362:ENST00000505342:exon1:c.A1697G:p.H566R,ENSG00000145362:ENST00000264366:exon37:c.A10568G:p.H3523R,ENSG00000145362:ENST00000357077:exon38:c.A10667G:p.H3556R		S	0,00057

ANK2	4_114281999_C_T	ENSG00000145362:ENST00000505342:exon2:c.C1732T:p.R578W,ENSG00000145362:ENST00000510275:exon6:c.C403T:p.R135W,ENSG00000145362:ENST00000509550:exon17:c.C1975T:p.R659W,ENSG00000145362:ENST00000264366:exon38:c.C10603T:p.R3535W,ENSG00000145362:ENST00000394537:exon38:c.C4447T:p.R1483W,ENSG00000145362:ENST00000357077:exon39:c.C10702T:p.R3568W,ENSG00000145362:ENST00000506722:exon40:c.C4420T:p.R1474W	rs72556376	P	0,00057
ANK2	4_114282005_G_A	ENSG00000145362:ENST00000505342:exon2:c.G1738A:p.E580K,ENSG00000145362:ENST00000510275:exon6:c.G409A:p.E137K,ENSG00000145362:ENST00000509550:exon17:c.G1981A:p.E661K,ENSG00000145362:ENST00000264366:exon38:c.G10609A:p.E3537K,ENSG00000145362:ENST00000394537:exon38:c.G4453A:p.E1485K,ENSG00000145362:ENST00000357077:exon39:c.G10708A:p.E3570K,ENSG00000145362:ENST00000506722:exon40:c.G4426A:p.E1476K	rs180843436	P	0,00057
ANK2	4_114290677_A_G	ENSG00000145362:ENST00000505342:exon6:c.A2356G:p.T786A,ENSG00000145362:ENST00000510275:exon10:c.A1027G:p.T343A,ENSG00000145362:ENST00000509550:exon21:c.A2599G:p.T867A,ENSG00000145362:ENST00000264366:exon42:c.A11227G:p.T3743A,ENSG00000145362:ENST00000394537:exon42:c.A5071G:p.T1691A,ENSG00000145362:ENST00000357077:exon43:c.A11326G:p.T3776A,ENSG00000145362:ENST00000506722:exon44:c.A5044G:p.T1682A		S	0,00057
ANK2	4_114290837_C_T	ENSG00000145362:ENST00000505342:exon6:c.C2516T:p.P839L,ENSG00000145362:ENST00000510275:exon10:c.C1187T:p.P396L,ENSG00000145362:ENST00000509550:exon21:c.C2759T:p.P920L,ENSG00000145362:ENST00000264366:exon42:c.C11387T:p.P3796L,ENSG00000145362:ENST00000394537:exon42:c.C5231T:p.P1744L,ENSG00000145362:ENST00000357077:exon43:c.C11486T:p.P3829L,ENSG00000145362:ENST00000506722:exon44:c.C5204T:p.P1735L		N	0,00058
ANK2	4_114290844_G_T	ENSG00000145362:ENST00000505342:exon6:c.G2523T:p.E841D,ENSG00000145362:ENST00000510275:exon10:c.G1194T:p.E398D,ENSG00000145362:ENST00000509550:exon21:c.G2766T:p.E922D,ENSG00000145362:ENST00000264366:exon42:c.G11394T:p.E3798D,ENSG00000145362:ENST00000394537:exon42:c.G5238T:p.E1746D,ENSG00000145362:ENST00000357077:exon43:c.G11493T:p.E3831D,ENSG00000145362:ENST00000506722:exon44:c.G5211T:p.E1737D	rs144046572	S	0,00058
ANK2	4_114290875_C_T	ENSG00000145362:ENST00000505342:exon6:c.C2554T:p.R852W,ENSG00000145362:ENST00000510275:exon10:c.C1225T:p.R409W,ENSG00000145362:ENST00000509550:exon21:c.C2797T:p.R933W,ENSG00000145362:ENST00000264366:exon42:c.C11425T:p.R3809W,ENSG00000145362:ENST00000394537:exon42:c.C5269T:p.R1757W,ENSG00000145362:ENST00000357077:exon43:c.C11524T:p.R3842W,ENSG00000145362:ENST00000506722:exon44:c.C5242T:p.R1748W	rs139797180	S	0,00057
ANK2	4_114293765_G_A	ENSG00000145362:ENST00000510275:exon11:c.G1388A:p.R463Q		N	0,00057
ANK2	4_114294276_A_G	ENSG00000145362:ENST00000505342:exon7:c.A2671G:p.T891A,ENSG00000145362:ENST00000510275:exon12:c.A1435G:p.T479A,ENSG00000145362:ENST00000509550:exon22:c.A2914G:p.T972A,ENSG00000145362:ENST00000264366:exon43:c.A11542G:p.T3848A,ENSG00000145362:ENST00000394537:exon43:c.A5386G:p.T1796A,ENSG00000145362:ENST00000357077:exon44:c.A11641G:p.T3881A,ENSG00000145362:ENST00000506722:exon45:c.A5359G:p.T1787A		N	0,00057

ANK2	4_114294462_C_T	ENSG00000145362:ENST00000505342:exon8:c.C2746T:p.R916W,ENSG00000145362:ENST00000510275:exon13:c.C1510T:p.R504W,ENSG00000145362:ENST00000509550:exon23:c.C2989T:p.R997W,ENSG00000145362:ENST00000264366:exon44:c.C11617T:p.R3873W,ENSG00000145362:ENST00000394537:exon44:c.C5461T:p.R1821W,ENSG00000145362:ENST00000357077:exon45:c.C11716T:p.R3906W,ENSG00000145362:ENST00000506722:exon46:c.C5434T:p.R1812W	rs121912706	P	0,00172
ANK2	4_114294488_G_C	ENSG00000145362:ENST00000505342:exon8:c.G2772C:p.E924D,ENSG00000145362:ENST00000510275:exon13:c.G1536C:p.E512D,ENSG00000145362:ENST00000509550:exon23:c.G3015C:p.E1005D,ENSG00000145362:ENST00000264366:exon44:c.G11643C:p.E3881D,ENSG00000145362:ENST00000394537:exon44:c.G5487C:p.E1829D,ENSG00000145362:ENST00000357077:exon45:c.G11742C:p.E3914D,ENSG00000145362:ENST00000506722:exon46:c.G5460C:p.E1820D		S	0,00057
ANK2	4_114295915_A_G	ENST00000514960:exon19:c.2702-5A>G,ENST00000505342:exon9:c.2890-5A>G,ENST00000506344:exon2:c.134-5A>G		L	0,00057
ANK2	4_114296105_A_G	ENST00000514960:exon19:c.2884+3A>G,ENST00000505342:exon9:c.3072+3A>G,ENST00000506344:exon2:c.316+3A>G		L	0,00057
ANK2	4_114299338_G_A	ENST00000506344:exon3:c.408+1G>A,ENST00000514167:exon2:c.183+1G>A	rs180914830	L	0,00057
CASQ2	1_116243897_C_A	ENSG00000118729:ENST00000456138:exon9:c.G952T:p.D318Y,ENSG00000118729:ENST00000261448:exon11:c.G1165T:p.D389Y		N	0,00061
CASQ2	1_116243928_ATC_-	ENSG00000118729:ENST00000456138:exon9:c.919_921del:p.307_307del,ENSG00000118729:ENST00000261448:exon11:c.1132_1134del:p.378_378del		N	0,00060
CASQ2	1_116247824_C_T	ENSG00000118729:ENST00000456138:exon7:c.G715A:p.D239N,ENSG00000118729:ENST00000261448:exon9:c.G928A:p.D310N	rs141314684	D	0,00057
CASQ2	1_116269737_T_C	ENSG00000118729:ENST00000456138:exon4:c.A400G:p.K134E,ENSG00000118729:ENST00000261448:exon6:c.A613G:p.K205E		S	0,00057
CASQ2	1_116275587_C_G	ENSG00000118729:ENST00000456138:exon3:c.G328C:p.A110P,ENSG00000118729:ENST00000261448:exon5:c.G541C:p.A181P		N	0,00057
CASQ2	1_116283431_C_T	ENSG00000118729:ENST00000261448:exon3:c.G338A:p.S113N	rs199750975	D	0,00057
CASQ2	1_116287470_C_T	ENSG00000118729:ENST00000261448:exon2:c.G298A:p.A100T,ENSG00000118729:ENST00000456138:exon2:c.G298A:p.A100T		N	0,00057
CASQ2	1_116310926_T_C	ENST00000261448:exon2:c.234+3A>G,ENST00000456138:exon2:c.234+3A>G		L	0,00057
CAV3	3_8775602_G_A	ENSG00000182533:ENST00000343849:exon1:c.G40A:p.V14I,ENSG00000182533:ENST00000397368:exon1:c.G40A:p.V14I	rs121909281	D	0,00115
CAV3	3_8787374_G_A	ENSG00000182533:ENST00000343849:exon2:c.G277A:p.A93T,ENSG00000182533:ENST00000397368:exon2:c.G277A:p.A93T	rs28936686	P	0,00063
CSRP3	11_19204270_G_A	ENSG00000129170:ENST00000265968:exon6:c.C532T:p.P178S,ENSG00000129170:ENST00000533783:exon7:c.C532T:p.P178S		S	0,00057

CSRP3	11_19206558_C_T	ENSG00000129170:ENST00000265968:exon5:c.G449A:p.C150Y,ENSG00000129170:ENST00000533783:exon6:c.G449A:p.C150Y		S	0,00172
CSRP3	11_19206593_C_A	ENST00000265968:exon6:c.415-1G>T,ENST00000533783:exon7:c.415-1G>T		L	0,00115
CSRP3	11_19209682_C_G	ENST00000265968:exon4:c.281+1G>C,ENST00000533783:exon5:c.281+1G>C		L	0,00057
CSRP3	11_19209752_A_G	ENSG00000129170:ENST00000265968:exon3:c.T212C:p.I71T,ENSG00000129170:ENST00000533783:exon4:c.T212C:p.I71T		N	0,00057
CSRP3	11_19209773_C_T	ENSG00000129170:ENST00000265968:exon3:c.G191A:p.R64H,ENSG00000129170:ENST00000533783:exon4:c.G191A:p.R64H		S	0,00057
CSRP3	11_19209833_A_G	ENSG00000129170:ENST00000265968:exon3:c.T131C:p.L44P,ENSG00000129170:ENST00000533783:exon4:c.T131C:p.L44P	rs104894205	P	0,00172
CSRP3	11_19213968_A_G	ENSG00000129170:ENST00000265968:exon2:c.T28C:p.C10R,ENSG00000129170:ENST00000533783:exon3:c.T28C:p.C10R		S	0,00057
CSRP3	11_19213974_C_T	ENSG00000129170:ENST00000265968:exon2:c.G22A:p.A8T,ENSG00000129170:ENST00000533783:exon3:c.G22A:p.A8T	rs45531937	D	0,00057
DES	2_220284854_A_G	ENSG00000175084:ENST00000373960:exon2:c.A616G:p.N206D		N	0,00058
DES	2_220285382_GG_-			L	0,00059
DES	2_220288540_G_A	ENSG00000175084:ENST00000373960:exon7:c.G1286A:p.R429Q	rs200580581	D	0,00059
DSC2	18_28648063_C_T	ENSG00000134755:ENST00000280904:exon16:c.G2624A:p.R875Q		N	0,00057
DSC2	18_28648870_C_T	ENSG00000134755:ENST00000251081:exon15:c.G2498A:p.R833H,ENSG00000134755:ENST00000280904:exon15:c.G2498A:p.R833H		P	0,00058
DSC2	18_28648998_TCC_-	ENSG00000134755:ENST00000251081:exon15:c.2368_2370del:p.790_790del,ENSG00000134755:ENST00000280904:exon15:c.2368_2370del:p.790_790del		N	0,00058
DSC2	18_28649002_CCT_-	ENSG00000134755:ENST00000251081:exon15:c.2364_2366del:p.788_789del,ENSG00000134755:ENST00000280904:exon15:c.2364_2366del:p.788_789del		P	0,00058
DSC2	18_28649033_C_T	ENSG00000134755:ENST00000251081:exon15:c.G2335A:p.G779R,ENSG00000134755:ENST00000280904:exon15:c.G2335A:p.G779R	rs139290300	S	0,00058
DSC2	18_28649081_C_T	ENSG00000134755:ENST00000251081:exon15:c.G2287A:p.A763T,ENSG00000134755:ENST00000280904:exon15:c.G2287A:p.A763T		N	0,00057
DSC2	18_28650748_A_C	ENSG00000134755:ENST00000251081:exon14:c.T2194G:p.L732V,ENSG00000134755:ENST00000280904:exon14:c.T2194G:p.L732V	rs151024019	P	0,00458
DSC2	18_28651640_C_T	ENSG00000134755:ENST00000251081:exon13:c.G2056A:p.G686S,ENSG00000134755:ENST00000280904:exon13:c.G2056A:p.G686S		N	0,00057
DSC2	18_28654750_G_A	ENSG00000134755:ENST00000251081:exon12:c.C1787T:p.A596V,ENSG00000134755:ENST00000280904:exon12:c.C1787T:p.A596V	rs148185335	P	0,00115
DSC2	18_28654874_C_A	ENST00000251081:exon13:c.1664-1G>T,ENST00000280904:exon13:c.1664-1G>T		L	0,00058

DSC2	18_28662896_G_A	ENSG00000134755:ENST00000251081:exon8:c.C1073T:p.T358I,ENSG00000134755:ENST00000280904:exon8:c.C1073T:p.T358I	rs139399951	D	0,00057
DSC2	18_28666574_C_T	ENSG00000134755:ENST00000251081:exon7:c.G907A:p.V303M,ENSG00000134755:ENST00000280904:exon7:c.G907A:p.V303M	rs145560678	P	0,00229
DSC2	18_28666624_C_A	ENSG00000134755:ENST00000251081:exon7:c.G857T:p.G286V,ENSG00000134755:ENST00000280904:exon7:c.G857T:p.G286V	rs199682735	D	0,00057
DSC2	18_28666627_A_G	ENSG00000134755:ENST00000251081:exon7:c.T854C:p.I285T,ENSG00000134755:ENST00000280904:exon7:c.T854C:p.I285T	rs199918720	D	0,00057
DSC2	18_28666657_G_A	ENSG00000134755:ENST00000251081:exon7:c.C824T:p.T275M,ENSG00000134755:ENST00000280904:exon7:c.C824T:p.T275M		P	0,00057
DSC2	18_28671095_G_A	ENSG00000134755:ENST00000251081:exon4:c.C370T:p.H124Y,ENSG00000134755:ENST00000280904:exon4:c.C370T:p.H124Y		N	0,00057
DSC2	18_28672152_G_A	ENSG00000134755:ENST00000251081:exon3:c.C266T:p.S89L,ENSG00000134755:ENST00000280904:exon3:c.C266T:p.S89L	rs141379407	P	0,00057
DSC2	18_28672246_A_C	ENSG00000134755:ENST00000251081:exon3:c.T172G:p.F58V,ENSG00000134755:ENST00000280904:exon3:c.T172G:p.F58V	rs138749562	P	0,00057
DSC2	18_28681901_C_T	ENSG00000134755:ENST00000251081:exon1:c.G34A:p.G12R,ENSG00000134755:ENST00000280904:exon1:c.G34A:p.G12R		N	0,00127
DSC2	18_28681932_C_A	ENSG00000134755:ENST00000251081:exon1:c.G3T:p.M1I,ENSG00000134755:ENST00000280904:exon1:c.G3T:p.M1I		S	0,00153
DSG2	18_29099805_C_A	ENSG00000046604:ENST00000261590:exon3:c.C121A:p.H41N,ENSG00000046604:ENST00000585206:exon3:c.C121A:p.H41N	rs201499704	P	0,00114
DSG2	18_29101120_G_A	ENSG00000046604:ENST00000261590:exon5:c.G437A:p.R146H,ENSG00000046604:ENST00000585206:exon5:c.G437A:p.R146H		P	0,00058
DSG2	18_29102067_A_G	ENSG00000046604:ENST00000261590:exon6:c.A545G:p.N182S,ENSG00000046604:ENST00000585206:exon6:c.A545G:p.N182S		N	0,00057
DSG2	18_29104717_A_G	ENSG00000046604:ENST00000261590:exon8:c.A880G:p.K294E		P	0,00057
DSG2	18_29104798_T_A	ENSG00000046604:ENST00000261590:exon8:c.T961A:p.F321I	rs201040643	P	0,00057
DSG2	18_29104840_A_G	ENSG00000046604:ENST00000261590:exon8:c.A1003G:p.T335A	rs191564916	P	0,00057
DSG2	18_29110986_-_C	ENSG00000046604:ENST00000261590:exon9:c.1051_1052insC:p.S351fs		L	0,00057
DSG2	18_29110986_A_C	ENSG00000046604:ENST00000261590:exon9:c.A1051C:p.S351R		N	0,00057
DSG2	18_29115255_G_A	ENSG00000046604:ENST00000261590:exon10:c.G1303A:p.D435N		P	0,00057
DSG2	18_29115328_A_G	ENSG00000046604:ENST00000261590:exon10:c.A1376G:p.Y459C		S	0,00057
DSG2	18_29122591_A_G	ENSG00000046604:ENST00000261590:exon14:c.A2110G:p.I704V	rs141388237	D	0,00174

DSG2	18_29122696_A_T	ENSG00000046604:ENST00000261590:exon14:c.A2215T:p.I739F		N	0,00059
DSG2	18_29126099_C_T	ENSG00000046604:ENST00000261590:exon15:c.C2750T:p.A917V		P	0,00057
DSG2	18_29126255_C_T	ENSG00000046604:ENST00000261590:exon15:c.C2906T:p.A969V		S	0,00057
DSG2	18_29126389_G_A	ENSG00000046604:ENST00000261590:exon15:c.G3040A:p.V1014I	rs200830807	P	0,00057
DSG2	18_29126426_G_A	ENSG00000046604:ENST00000261590:exon15:c.G3077A:p.S1026N		S	0,00057
DSG2	18_29126458_A_G	ENSG00000046604:ENST00000261590:exon15:c.A3109G:p.N1037D		N	0,00057
DSG2	18_29126475_G_C	ENSG00000046604:ENST00000261590:exon15:c.G3126C:p.Q1042H		S	0,00057
DSG2	18_29126516_C_T	ENSG00000046604:ENST00000261590:exon15:c.C3167T:p.T1056I		P	0,00057
DSP	6_7562969_A_G	ENSG00000096696:ENST00000379802:exon5:c.A682G:p.I228V,ENSG00000096696:ENST00000418664:exon5:c.A682G:p.I228V		N	0,00058
DSP	6_7562975_G_A	ENSG00000096696:ENST00000379802:exon5:c.G688A:p.D230N,ENSG00000096696:ENST00000418664:exon5:c.G688A:p.D230N	rs147315869	P	0,00172
DSP	6_7564006_A_T	ENSG00000096696:ENST00000379802:exon6:c.A764T:p.Y255F,ENSG00000096696:ENST00000418664:exon6:c.A764T:p.Y255F		S	0,00057
DSP	6_7565758_G_T	ENST00000379802:exon7:c.939+5G>T,ENST00000418664:exon7:c.939+5G>T		L	0,00058
DSP	6_7569444_G_A	ENSG00000096696:ENST00000379802:exon12:c.G1445A:p.C482Y,ENSG00000096696:ENST00000418664:exon12:c.G1445A:p.C482Y		S	0,00058
DSP	6_7569482_G_A	ENSG00000096696:ENST00000379802:exon12:c.G1483A:p.V495M,ENSG00000096696:ENST00000418664:exon12:c.G1483A:p.V495M		N	0,00058
DSP	6_7570791_G_A	ENSG00000096696:ENST00000379802:exon13:c.G1696A:p.A566T,ENSG00000096696:ENST00000418664:exon13:c.G1696A:p.A566T	rs148147581	P	0,00059
DSP	6_7571692_A_G	ENSG00000096696:ENST00000379802:exon14:c.A1778G:p.N593S,ENSG00000096696:ENST00000418664:exon14:c.A1778G:p.N593S	rs34239595	D	0,00057
DSP	6_7574937_A_G	ENSG00000096696:ENST00000379802:exon17:c.A2345G:p.D782G,ENSG00000096696:ENST00000418664:exon17:c.A2345G:p.D782G		S	0,00057
DSP	6_7575014_C_T	ENSG00000096696:ENST00000379802:exon17:c.C2422T:p.R808C,ENSG00000096696:ENST00000418664:exon17:c.C2422T:p.R808C	rs150339369	S	0,00172
DSP	6_7576669_C_T	ENSG00000096696:ENST00000379802:exon19:c.C2773T:p.R925W,ENSG00000096696:ENST00000418664:exon19:c.C2773T:p.R925W	rs145933612	S	0,00057
DSP	6_7578770_T_C	ENSG00000096696:ENST00000379802:exon22:c.T3059C:p.M1020T,ENSG00000096696:ENST00000418664:exon22:c.T3059C:p.M1020T		N	0,00057
DSP	6_7580129_A_G	ENSG00000096696:ENST00000379802:exon23:c.A3706G:p.R1236G		S	0,00115
DSP	6_7580528_G_A	ENSG00000096696:ENST00000379802:exon23:c.G4105A:p.E1369K	rs141805096	D	0,00058

DSP	6_7580810_G_A	ENSG00000096696:ENST00000379802:exon23:c.G4387A:p.V1463I		N	0,00058
DSP	6_7580912_C_T	ENSG00000096696:ENST00000379802:exon23:c.C4489T:p.R1497W	rs148041814	D	0,00057
DSP	6_7580913_G_A	ENSG00000096696:ENST00000379802:exon23:c.G4490A:p.R1497Q		N	0,00057
DSP	6_7580981_A_T	ENSG00000096696:ENST00000379802:exon23:c.A4558T:p.S1520C		S	0,00058
DSP	6_7581198_A_G	ENSG00000096696:ENST00000379802:exon23:c.A4775G:p.K1592R	rs200421954	P	0,00120
DSP	6_7581420_G_A	ENSG00000096696:ENST00000379802:exon23:c.G4997A:p.R1666Q		N	0,00058
DSP	6_7581543_A_G	ENSG00000096696:ENST00000379802:exon23:c.A5120G:p.Q1707R		S	0,00057
DSP	6_7581601_C_A	ENSG00000096696:ENST00000379802:exon23:c.C5178A:p.N1726K	rs147415451	P	0,00057
DSP	6_7581644_G_A	ENSG00000096696:ENST00000379802:exon23:c.G5221A:p.A1741T		N	0,00057
DSP	6_7581786_A_G	ENSG00000096696:ENST00000379802:exon23:c.A5363G:p.Q1788R	rs139673146	D	0,00057
DSP	6_7583299_A_G	ENSG00000096696:ENST00000379802:exon24:c.A5804G:p.Y1935C,ENSG00000096696:ENST00000418664:exon24:c.A4007G:p.Y1336C		N	0,00058
DSP	6_7583347_G_A	ENSG00000096696:ENST00000379802:exon24:c.G5852A:p.R1951Q,ENSG00000096696:ENST00000418664:exon24:c.G4055A:p.R1352Q		N	0,00058
DSP	6_7583376_G_A	ENSG00000096696:ENST00000379802:exon24:c.G5881A:p.V1961I,ENSG00000096696:ENST00000418664:exon24:c.G4084A:p.V1362I		N	0,00058
DSP	6_7584376_C_G	ENSG00000096696:ENST00000379802:exon24:c.C6881G:p.A2294G,ENSG00000096696:ENST00000418664:exon24:c.C5084G:p.A1695G	rs147000526	P	0,00115
DSP	6_7584845_G_C	ENSG00000096696:ENST00000379802:exon24:c.G7350C:p.K2450N,ENSG00000096696:ENST00000418664:exon24:c.G5553C:p.K1851N		S	0,00057
DSP	6_7584922_A_T	ENSG00000096696:ENST00000379802:exon24:c.A7427T:p.E2476V,ENSG00000096696:ENST00000418664:exon24:c.A5630T:p.E1877V		S	0,00057
DSP	6_7585127_T_G	ENSG00000096696:ENST00000379802:exon24:c.T7632G:p.F2544L,ENSG00000096696:ENST00000418664:exon24:c.T5835G:p.F1945L		N	0,00057
DSP	6_7585233_G_T	ENSG00000096696:ENST00000379802:exon24:c.G7738T:p.D2580Y,ENSG00000096696:ENST00000418664:exon24:c.G5941T:p.D1981Y		N	0,00057
DSP	6_7585612_A_T	ENSG00000096696:ENST00000379802:exon24:c.A8117T:p.K2706M,ENSG00000096696:ENST00000418664:exon24:c.A6320T:p.K2107M		N	0,00059
DSP	6_7585686_T_C	ENSG00000096696:ENST00000379802:exon24:c.T8191C:p.Y2731H,ENSG00000096696:ENST00000418664:exon24:c.T6394C:p.Y2132H	rs201397978	D	0,00240
DSP	6_7585774_C_T	ENSG00000096696:ENST00000379802:exon24:c.C8279T:p.A2760V,ENSG00000096696:ENST00000418664:exon24:c.C6482T:p.A2161V		N	0,00058

DSP	6_7585921_C_T	ENSG00000096696:ENST00000379802:exon24:c.C8426T:p.S2809L,ENSG00000096696:ENST00000418664:exon24:c.C6629T:p.S2210L		N	0,00058
DSP	6_7585962_C_G	ENSG00000096696:ENST00000379802:exon24:c.C8467G:p.P2823A,ENSG00000096696:ENST00000418664:exon24:c.C6670G:p.P2224A	rs142717240	S	0,00115
DSP	6_7586019_C_T	ENSG00000096696:ENST00000379802:exon24:c.C8524T:p.R2842C,ENSG00000096696:ENST00000418664:exon24:c.C6727T:p.R2243C	rs144850908	D	0,00058
JUP	17_39912055_C_T	ENSG00000173801:ENST00000310706:exon14:c.G2179A:p.D727N,ENSG00000173801:ENST00000393930:exon14:c.G2179A:p.D727N,ENSG00000173801:ENST00000393931:exon14:c.G2179A:p.D727N		N	0,00093
JUP	17_39912444_T_C	ENSG00000173801:ENST00000310706:exon13:c.A2069G:p.N690S,ENSG00000173801:ENST00000393930:exon13:c.A2069G:p.N690S,ENSG00000173801:ENST00000393931:exon13:c.A2069G:p.N690S	rs147628503	D	0,00070
JUP	17_39919360_C_T	ENSG00000173801:ENST00000310706:exon8:c.G1372A:p.A458T,ENSG00000173801:ENST00000393930:exon8:c.G1372A:p.A458T,ENSG00000173801:ENST00000393931:exon8:c.G1372A:p.A458T	rs139559495	D	0,00080
JUP	17_39919408_T_A	ENSG00000173801:ENST00000310706:exon8:c.A1324T:p.I442F,ENSG00000173801:ENST00000393930:exon8:c.A1324T:p.I442F,ENSG00000173801:ENST00000393931:exon8:c.A1324T:p.I442F	rs142213474	S	0,00064
JUP	17_39921027_G_C	ENSG00000173801:ENST00000310706:exon7:c.C1096G:p.P366A,ENSG00000173801:ENST00000393930:exon7:c.C1096G:p.P366A,ENSG00000173801:ENST00000393931:exon7:c.C1096G:p.P366A		N	0,00070
JUP	17_39925401_C_T	ENSG00000173801:ENST00000540235:exon3:c.G527A:p.R176Q,ENSG00000173801:ENST00000310706:exon4:c.G527A:p.R176Q,ENSG00000173801:ENST00000393930:exon4:c.G527A:p.R176Q,ENSG00000173801:ENST00000393931:exon4:c.G527A:p.R176Q,ENSG00000173801:ENST00000420370:exon4:c.G527A:p.R176Q,ENSG00000173801:ENST00000437187:exon4:c.G527A:p.R176Q,ENSG00000173801:ENST00000449889:exon4:c.G527A:p.R176Q,ENSG00000173801:ENST00000424457:exon5:c.G527A:p.R176Q	rs144171604	D	0,00107
JUP	17_39925704_G_C	ENSG00000173801:ENST00000540235:exon2:c.C434G:p.P145R,ENSG00000173801:ENST00000310706:exon3:c.C434G:p.P145R,ENSG00000173801:ENST00000393930:exon3:c.C434G:p.P145R,ENSG00000173801:ENST00000393931:exon3:c.C434G:p.P145R,ENSG00000173801:ENST00000420370:exon3:c.C434G:p.P145R,ENSG00000173801:ENST00000437187:exon3:c.C434G:p.P145R,ENSG00000173801:ENST00000449889:exon3:c.C434G:p.P145R,ENSG00000173801:ENST00000424457:exon4:c.C434G:p.P145R		S	0,00085
KCNE1	21_35821619_G_A	ENSG00000180509:ENST00000416357:exon2:c.C314T:p.S105L,ENSG00000180509:ENST00000337385:exon3:c.C314T:p.S105L,ENSG00000180509:ENST00000399284:exon3:c.C314T:p.S105L,ENSG00000180509:ENST00000399289:exon3:c.C314T:p.S105L,ENSG00000180509:ENST00000432085:exon3:c.C314T:p.S105L,ENSG00000180509:ENST00000399286:exon4:c.C314T:p.S105L		N	0,00057
KCNE1	21_35821827_G_A	ENSG00000180509:ENST00000416357:exon2:c.C106T:p.R36C,ENSG00000180509:ENST00000337385:exon3:c.C106T:p.R36C,ENSG00000180509:ENST00000399284:exon3:c.C106T:p.R36C,ENSG00000180509:ENST00000399289:exon3:c.C106T:p.R36C,ENSG00000180509:ENST00000432085:exon3:c.C106T:p.R36C,ENSG00000180509:ENST00000399286:exon4:c.C106T:p.R36C		N	0,00058

KCNE1	21_35821850_G_A	ENSG00000180509:ENST00000416357:exon2:c.C83T:p.S28L,ENSG00000180509:ENST00000337385:exon3:c.C83T:p.S28L,ENSG00000180509:ENST00000399284:exon3:c.C83T:p.S28L,ENSG00000180509:ENST00000399289:exon3:c.C83T:p.S28L,ENSG00000180509:ENST00000432085:exon3:c.C83T:p.S28L,ENSG00000180509:ENST00000399286:exon4:c.C83T:p.S28L	rs199473350	P	0,00058
KCNE1	21_35821916_G_T	ENSG00000180509:ENST00000416357:exon2:c.C17A:p.T6N,ENSG00000180509:ENST00000337385:exon3:c.C17A:p.T6N,ENSG00000180509:ENST00000399284:exon3:c.C17A:p.T6N,ENSG00000180509:ENST00000399289:exon3:c.C17A:p.T6N,ENSG00000180509:ENST00000432085:exon3:c.C17A:p.T6N,ENSG00000180509:ENST00000399286:exon4:c.C17A:p.T6N		N	0,00058
KCNE2	21_35736455_G_A			L	0,00057
KCNE2	21_35742806_C_T	ENSG00000159197:ENST00000290310:exon2:c.C29T:p.T10M	rs199473648	P	0,00057
KCNE2	21_35742817_G_A	ENSG00000159197:ENST00000290310:exon2:c.G40A:p.V14I	rs142153692	P	0,00115
KCNE2	21_35742938_T_C	ENSG00000159197:ENST00000290310:exon2:c.T161C:p.M54T	rs74315447	P	0,00057
KCNE2	21_35742947_T_C	ENSG00000159197:ENST00000290310:exon2:c.T170C:p.I57T	rs74315448	P	0,00057
KCNE2	21_35743134_C_A	ENSG00000159197:ENST00000290310:exon2:c.C357A:p.F119L	rs139202426	D	0,00058
KCNH2	7_150642517_G_A	ENSG00000055118:ENST00000330883:exon11:c.C2396T:p.P799L,ENSG00000055118:ENST00000392968:exon13:c.C3128T:p.P1043L,ENSG00000055118:ENST00000262186:exon15:c.C3416T:p.P1139L		N	0,00093
KCNH2	7_150644131_C_T	ENSG00000055118:ENST00000330883:exon10:c.G2144A:p.R715Q,ENSG00000055118:ENST00000392968:exon12:c.G2876A:p.R959Q,ENSG00000055118:ENST00000262186:exon14:c.G3164A:p.R1055Q	rs41307270	S	0,00063
KCNH2	7_150644718_T_C	ENSG00000055118:ENST00000330883:exon8:c.A1921G:p.S641G,ENSG00000055118:ENST00000392968:exon10:c.A2653G:p.S885G,ENSG00000055118:ENST00000262186:exon12:c.A2941G:p.S981G	rs76649554	D	0,00111
KCNH2	7_150645607_C_T	ENSG00000055118:ENST00000330883:exon7:c.G1597A:p.G533S,ENSG00000055118:ENST00000392968:exon9:c.G2329A:p.G777S,ENSG00000055118:ENST00000262186:exon11:c.G2617A:p.G873S	rs41314354	D	0,00117
KCNH2	7_150647078_G_A	ENSG00000055118:ENST00000430723:exon9:c.C2576T:p.T859M	rs41314366	S	0,00059
KCNH2	7_150647144_C_A	ENSG00000055118:ENST00000430723:exon9:c.G2510T:p.G837V		N	0,00060
KCNH2	7_150647353_GT_-	ENSG00000055118:ENST00000330883:exon5:c.1280_1281del:p.427_427del,ENSG00000055118:ENST00000392968:exon7:c.2012_2013del:p.671_671del,ENSG00000055118:ENST00000262186:exon9:c.2300_2301del:p.767_767del,ENSG00000055118:ENST00000430723:exon9:c.2300_2301del:p.767_767del		N	0,00073
KCNH2	7_150654468_G_A	ENSG00000055118:ENST00000392968:exon3:c.C751T:p.P251S,ENSG00000055118:ENST00000262186:exon5:c.C1039T:p.P347S,ENSG00000055118:ENST00000430723:exon5:c.C1039T:p.P347S	rs138776684	P	0,00118
KCNH2	7_150655425_T_C	ENSG00000055118:ENST00000392968:exon2:c.A350G:p.D117G,ENSG00000055118:ENST00000262186:exon4:c.A638G:p.D213G,ENSG00000055118:ENST00000430723:exon4:c.A638G:p.D213G		N	0,00148

KCNH2	7_150655495_CGCCCGCGC_-	ENSG00000055118:ENST00000392968:exon2:c.272_280del:p.91_94del,ENSG00000055118:ENST00000262186:exon4:c.560_568del:p.187_190del,ENSG00000055118:ENST00000430723:exon4:c.560_568del:p.187_190del		P	0,01220
KCNH2	7_150655510_CGCCGCCCG_-	ENSG00000055118:ENST00000392968:exon2:c.257_265del:p.86_89del,ENSG00000055118:ENST00000262186:exon4:c.545_553del:p.182_185del,ENSG00000055118:ENST00000430723:exon4:c.545_553del:p.182_185del		N	0,01124
KCNH2	7_150655521_C_T	ENSG00000055118:ENST00000392968:exon2:c.G254A:p.R85Q,ENSG00000055118:ENST00000262186:exon4:c.G542A:p.R181Q,ENSG00000055118:ENST00000430723:exon4:c.G542A:p.R181Q	rs41308954	D	0,01099
KCNH2	7_150655537_G_A	ENSG00000055118:ENST00000392968:exon2:c.C238T:p.R80W,ENSG00000055118:ENST00000262186:exon4:c.C526T:p.R176W,ENSG00000055118:ENST00000430723:exon4:c.C526T:p.R176W	rs36210422	S	0,00543
KCNH2	7_150656690_G_A	ENSG00000055118:ENST00000392968:exon1:c.C154T:p.R52W,ENSG00000055118:ENST00000262186:exon3:c.C442T:p.R148W,ENSG00000055118:ENST00000430723:exon3:c.C442T:p.R148W	rs139544114	D	0,00140
KCNH2	7_150674983_G_A	ENSG00000055118:ENST00000262186:exon1:c.C19T:p.H7Y,ENSG00000055118:ENST00000430723:exon1:c.C19T:p.H7Y		S	0,00175
KCNJ2	17_68172133_A_G	ENSG00000123700:ENST00000243457:exon2:c.A953G:p.N318S,ENSG00000123700:ENST00000535240:exon2:c.A953G:p.N318S		N	0,00057
KCNQ1	11_2466480_-_CGCGCCCAT	ENSG00000053918:ENST00000155840:exon1:c.152_153insCGCGCCCAT:p.Y51delinsYAPI		N	0,01376
KCNQ1	11_2466545_C_A	ENSG00000053918:ENST00000155840:exon1:c.C217A:p.P73T	rs199472676	P	0,00110
KCNQ1	11_2542757_C_T	ENSG00000053918:ENST00000380776:exon2:c.C133T:p.R45C	rs80269976	D	0,00058
KCNQ1	11_2542793_G_A	ENSG00000053918:ENST00000380776:exon2:c.G169A:p.D57N	rs10400212	D	0,00059
KCNQ1	11_2549229_C_T	ENSG00000053918:ENST00000155840:exon2:c.C458T:p.T153M,ENSG00000053918:ENST00000335475:exon2:c.C77T:p.T26M,ENSG00000053918:ENST00000496887:exon3:c.C197T:p.T66M	rs143709408	P	0,00068
KCNQ1	11_2591921_C_T	ENSG00000053918:ENST00000155840:exon3:c.C541T:p.R181C,ENSG00000053918:ENST00000335475:exon3:c.C160T:p.R54C,ENSG00000053918:ENST00000496887:exon4:c.C280T:p.R94C	rs199473395	P	0,00094
KCNQ1	11_2594092_T_G	ENSG00000053918:ENST00000155840:exon6:c.T797G:p.L266R,ENSG00000053918:ENST00000335475:exon6:c.T416G:p.L139R,ENSG00000053918:ENST00000496887:exon7:c.T536G:p.L179R		S	0,00062
KCNQ1	11_2604687_A_T	ENSG00000053918:ENST00000155840:exon7:c.A944T:p.Y315F,ENSG00000053918:ENST00000335475:exon7:c.A563T:p.Y188F	rs74462309	P	0,00074
KCNQ1	11_2608850_G_T	ENSG00000053918:ENST00000155840:exon9:c.G1179T:p.K393N,ENSG00000053918:ENST00000335475:exon9:c.G798T:p.K266N	rs12720457	D	0,00158
KCNQ1	11_2790079_G_A	ENSG00000053918:ENST00000155840:exon12:c.G1520A:p.R507Q,ENSG00000053918:ENST00000335475:exon12:c.G1139A:p.R380Q		N	0,00058
KCNQ1	11_2797186_G_A	ENST00000155840:exon13:c.1591-4G>A,ENST00000335475:exon13:c.1210-4G>A		L	0,00085
KCNQ1	11_2869087_G_A	ENSG00000053918:ENST00000155840:exon16:c.G1885A:p.G629S,ENSG00000053918:ENST00000335475:exon16:c.G1504A:p.G502S		N	0,00097

KCNQ1	11_2869105_G_A	ENSG00000053918:ENST00000155840:exon16:c.G1903A:p.G635R,ENSG00000053918:ENST00000335475:exon16:c.G1522A:p.G508R	rs199473484	P	0,00097
KCNQ1	11_2869127_G_T	ENSG00000053918:ENST00000155840:exon16:c.G1925T:p.C642F,ENSG00000053918:ENST00000335475:exon16:c.G1544T:p.C515F		N	0,00096
LDB3	10_88428332_G_C			L	0,00070
LDB3	10_88439193_G_A	ENSG00000122367:ENST00000263066:exon2:c.G163A:p.V55I,ENSG00000122367:ENST00000310944:exon2:c.G163A:p.V55I,ENSG00000122367:ENST00000361373:exon2:c.G163A:p.V55I,ENSG00000122367:ENST00000372056:exon2:c.G163A:p.V55I,ENSG00000122367:ENST00000372066:exon2:c.G163A:p.V55I,ENSG00000122367:ENST00000542786:exon2:c.G163A:p.V55I,ENSG00000122367:ENST00000352360:exon3:c.G163A:p.V55I,ENSG00000122367:ENST00000429277:exon3:c.G163A:p.V55I,ENSG00000122367:ENST00000458213:exon3:c.G163A:p.V55I	rs3740343	P	0,00115
LDB3	10_88441437_C_T	ENSG00000122367:ENST00000310944:exon4:c.C566T:p.S189L,ENSG00000122367:ENST00000361373:exon4:c.C566T:p.S189L,ENSG00000122367:ENST00000372056:exon4:c.C566T:p.S189L,ENSG00000122367:ENST00000542786:exon4:c.C566T:p.S189L,ENSG00000122367:ENST00000429277:exon5:c.C566T:p.S189L	rs45487699	P	0,00072
LDB3	10_88441535_G_A	ENSG00000122367:ENST00000310944:exon4:c.G664A:p.A222T,ENSG00000122367:ENST00000361373:exon4:c.G664A:p.A222T,ENSG00000122367:ENST00000372056:exon4:c.G664A:p.A222T,ENSG00000122367:ENST00000542786:exon4:c.G664A:p.A222T,ENSG00000122367:ENST00000429277:exon5:c.G664A:p.A222T	rs139922045	D	0,00066
LDB3	10_88446940_G_C	ENSG00000122367:ENST00000263066:exon5:c.G459C:p.Q153H,ENSG00000122367:ENST00000372056:exon5:c.G804C:p.Q268H,ENSG00000122367:ENST00000372066:exon5:c.G459C:p.Q153H,ENSG00000122367:ENST00000429277:exon6:c.G804C:p.Q268H,ENSG00000122367:ENST00000458213:exon6:c.G459C:p.Q153H		N	0,00067
LDB3	10_88446992_G_A	ENSG00000122367:ENST00000263066:exon5:c.G511A:p.A171T,ENSG00000122367:ENST00000372056:exon5:c.G856A:p.A286T,ENSG00000122367:ENST00000372066:exon5:c.G511A:p.A171T,ENSG00000122367:ENST00000429277:exon6:c.G856A:p.A286T,ENSG00000122367:ENST00000458213:exon6:c.G511A:p.A171T		N	0,00066
LDB3	10_88466427_G_A	ENSG00000122367:ENST00000361373:exon7:c.G1036A:p.A346T	rs201968775	D	0,00094
LDB3	10_88466440_C_T	ENSG00000122367:ENST00000361373:exon7:c.C1049T:p.T350I	rs200796750	P	0,00092
LDB3	10_88469687_G_A	ENSG00000122367:ENST00000352360:exon5:c.G340A:p.A114T,ENSG00000122367:ENST00000263066:exon8:c.G781A:p.A261T,ENSG00000122367:ENST00000361373:exon8:c.G1111A:p.A371T,ENSG00000122367:ENST00000429277:exon9:c.G1126A:p.A376T,ENSG00000122367:ENST00000458213:exon9:c.G781A:p.A261T	rs45539535	P	0,00143

LDB3	10_88476312_G_A	ENSG00000122367:ENST00000352360:exon6:c.G689A:p.R230H,ENSG00000122367:ENST00000263066:exon9:c.G1130A:p.R377H,ENSG00000122367:ENST00000361373:exon9:c.G1460A:p.R487H,ENSG00000122367:ENST00000429277:exon10:c.G1475A:p.R492H,ENSG00000122367:ENST00000458213:exon10:c.G1130A:p.R377H	rs146265188	S	0,00088
LDB3	10_88476339_T_C	ENSG00000122367:ENST00000352360:exon6:c.T716C:p.F239S,ENSG00000122367:ENST00000263066:exon9:c.T1157C:p.F386S,ENSG00000122367:ENST00000361373:exon9:c.T1487C:p.F496S,ENSG00000122367:ENST00000429277:exon10:c.T1502C:p.F501S,ENSG00000122367:ENST00000458213:exon10:c.T1157C:p.F386S	rs147072071	D	0,00083
LDB3	10_88476446_G_C	ENSG00000122367:ENST00000352360:exon6:c.G823C:p.A275P,ENSG00000122367:ENST00000263066:exon9:c.G1264C:p.A422P,ENSG00000122367:ENST00000361373:exon9:c.G1594C:p.A532P,ENSG00000122367:ENST00000429277:exon10:c.G1609C:p.A537P,ENSG00000122367:ENST00000458213:exon10:c.G1264C:p.A422P	rs143764931	S	0,00258
LDB3	10_88476524_A_G	ENSG00000122367:ENST00000352360:exon6:c.A901G:p.I301V,ENSG00000122367:ENST00000263066:exon9:c.A1342G:p.I448V,ENSG00000122367:ENST00000361373:exon9:c.A1672G:p.I558V,ENSG00000122367:ENST00000429277:exon10:c.A1687G:p.I563V,ENSG00000122367:ENST00000458213:exon10:c.A1342G:p.I448V		P	0,00079
LMNA	1_156096679_G_A	ENSG00000160789:ENST00000392353:exon1:c.G86A:p.R29K,ENSG00000160789:ENST00000368297:exon2:c.G86A:p.R29K,ENSG00000160789:ENST00000515459:exon2:c.G86A:p.R29K		N	0,00123
LMNA	1_156096738_C_T			L	0,00067
LMNA	1_156105051_C_T	ENSG00000160789:ENST00000347559:exon5:c.C884T:p.S295L,ENSG00000160789:ENST00000361308:exon5:c.C884T:p.S295L,ENSG00000160789:ENST00000368299:exon5:c.C884T:p.S295L,ENSG00000160789:ENST00000368300:exon5:c.C884T:p.S295L,ENSG00000160789:ENST00000392353:exon5:c.C641T:p.S214L,ENSG00000160789:ENST00000448611:exon5:c.C548T:p.S183L,ENSG00000160789:ENST00000368297:exon6:c.C641T:p.S214L,ENSG00000160789:ENST00000473598:exon6:c.C587T:p.S196L,ENSG00000160789:ENST00000368301:exon8:c.C884T:p.S295L		N	0,00081
LMNA	1_156105062_A_G	ENSG00000160789:ENST00000347559:exon5:c.A895G:p.I299V,ENSG00000160789:ENST00000361308:exon5:c.A895G:p.I299V,ENSG00000160789:ENST00000368299:exon5:c.A895G:p.I299V,ENSG00000160789:ENST00000368300:exon5:c.A895G:p.I299V,ENSG00000160789:ENST00000392353:exon5:c.A652G:p.I218V,ENSG00000160789:ENST00000448611:exon5:c.A559G:p.I187V,ENSG00000160789:ENST00000368297:exon6:c.A652G:p.I218V,ENSG00000160789:ENST00000473598:exon6:c.A598G:p.I200V,ENSG00000160789:ENST00000368301:exon8:c.A895G:p.I299V	rs150924946	D	0,00083
LMNA	1_156105708_C_T	ENSG00000160789:ENST00000347559:exon6:c.C953T:p.A318V,ENSG00000160789:ENST00000361308:exon6:c.C953T:p.A318V,ENSG00000160789:ENST00000368299:exon6:c.C953T:p.A318V,ENSG00000160789:ENST00000368300:exon6:c.C953T:p.A318V,ENSG00000160789:ENST00000392353:exon6:c.C710T:p.A237V,ENSG00000160789:ENST00000448611:exon6:c.C617T:p.A206V,ENSG00000160789:ENST00000368297:exon7:c.C710T:p.A237V,ENSG00000160789:ENST00000473598:exon7:c.C656T:p.A219V,ENSG00000160789:ENST00000368301:exon9:c.C953T:p.A318V		N	0,00063

LMNA	1_156106078_G_T	ENSG00000160789:ENST00000508500:exon2:c.G109T:p.G37C,ENSG00000160789:ENST00000347559:exon7:c.G1231T:p.G411C,ENSG00000160789:ENST00000361308:exon7:c.G1231T:p.G411C,ENSG00000160789:ENST00000368299:exon7:c.G1231T:p.G411C,ENSG00000160789:ENST00000368300:exon7:c.G1231T:p.G411C,ENSG00000160789:ENST00000392353:exon7:c.G988T:p.G330C,ENSG00000160789:ENST00000448611:exon7:c.G895T:p.G299C,ENSG00000160789:ENST00000368297:exon8:c.G988T:p.G330C,ENSG00000160789:ENST00000473598:exon8:c.G934T:p.G312C,ENSG00000160789:ENST00000368301:exon10:c.G1231T:p.G411C		N	0,00076
LMNA	1_156108453_A_C	ENSG00000160789:ENST00000508500:exon5:c.A661C:p.S221R,ENSG00000160789:ENST00000347559:exon10:c.A1783C:p.S595R,ENSG00000160789:ENST00000368300:exon11:c.A1873C:p.S625R,ENSG00000160789:ENST00000448611:exon11:c.A1537C:p.S513R,ENSG00000160789:ENST00000473598:exon12:c.A1576C:p.S526R		N	0,00076
LMNA	1_156108454_G_C	ENSG00000160789:ENST00000508500:exon5:c.G662C:p.S221T,ENSG00000160789:ENST00000347559:exon10:c.G1784C:p.S595T,ENSG00000160789:ENST00000368300:exon11:c.G1874C:p.S625T,ENSG00000160789:ENST00000448611:exon11:c.G1538C:p.S513T,ENSG00000160789:ENST00000473598:exon12:c.G1577C:p.S526T		N	0,00076
LMNA	1_156108510_C_T	ENSG00000160789:ENST00000508500:exon5:c.C718T:p.R240C,ENSG00000160789:ENST00000347559:exon10:c.C1840T:p.R614C,ENSG00000160789:ENST00000368300:exon11:c.C1930T:p.R644C,ENSG00000160789:ENST00000448611:exon11:c.C1594T:p.R532C,ENSG00000160789:ENST00000473598:exon12:c.C1633T:p.R545C	rs142000963	S	0,00151
MYBPC3	11_47353626_G_A	ENSG00000134571:ENST00000256993:exon31:c.C3808T:p.R1270X,ENSG00000134571:ENST00000399249:exon32:c.C3811T:p.R1271X,ENSG00000134571:ENST00000545968:exon33:c.C3811T:p.R1271X		P	0,00061
MYBPC3	11_47353639_G_C	ENSG00000134571:ENST00000256993:exon31:c.C3795G:p.C1265W,ENSG00000134571:ENST00000399249:exon32:c.C3798G:p.C1266W,ENSG00000134571:ENST00000545968:exon33:c.C3798G:p.C1266W		S	0,00060
MYBPC3	11_47353666_G_T	ENSG00000134571:ENST00000256993:exon31:c.C3768A:p.N1256K,ENSG00000134571:ENST00000399249:exon32:c.C3771A:p.N1257K,ENSG00000134571:ENST00000545968:exon33:c.C3771A:p.N1257K		S	0,00237
MYBPC3	11_47353674_C_T	ENSG00000134571:ENST00000256993:exon31:c.G3760A:p.A1254T,ENSG00000134571:ENST00000399249:exon32:c.G3763A:p.A1255T,ENSG00000134571:ENST00000545968:exon33:c.G3763A:p.A1255T		P	0,00117
MYBPC3	11_47353685_T_C	ENSG00000134571:ENST00000256993:exon31:c.A3749G:p.Y1250C,ENSG00000134571:ENST00000399249:exon32:c.A3752G:p.Y1251C,ENSG00000134571:ENST00000545968:exon33:c.A3752G:p.Y1251C		P	0,00059
MYBPC3	11_47353686_A_G	ENSG00000134571:ENST00000256993:exon31:c.T3748C:p.Y1250H,ENSG00000134571:ENST00000399249:exon32:c.T3751C:p.Y1251H,ENSG00000134571:ENST00000545968:exon33:c.T3751C:p.Y1251H		S	0,00058

MYBPC3	11_47353709_G_C	ENSG00000134571:ENST00000256993:exon31:c.C3725G:p.P1242R,ENSG00000134571:ENST00000399249:exon32:c.C3728G:p.P1243R,ENSG00000134571:ENST00000545968:exon33:c.C3728G:p.P1243R		S	0,00058
MYBPC3	11_47353740_G_A	ENSG00000134571:ENST00000256993:exon31:c.C3694T:p.Q1232X,ENSG00000134571:ENST00000399249:exon32:c.C3697T:p.Q1233X,ENSG00000134571:ENST00000545968:exon33:c.C3697T:p.Q1233X		P	0,00058
MYBPC3	11_47353755_G_A	ENSG00000134571:ENST00000256993:exon31:c.C3679T:p.R1227C,ENSG00000134571:ENST00000399249:exon32:c.C3682T:p.R1228C,ENSG00000134571:ENST00000545968:exon33:c.C3682T:p.R1228C	rs201312636	S	0,00057
MYBPC3	11_47354116_C_T	ENST00000256993:exon31:c.3624+1G>A,ENST00000399249:exon32:c.3627+1G>A,ENST00000545968:exon33:c.3627+1G>A		P	0,00059
MYBPC3	11_47354123_G_-	ENSG00000134571:ENST00000256993:exon30:c.3618delC:p.S1206fs,ENSG00000134571:ENST00000399249:exon31:c.3621delC:p.S1207fs,ENSG00000134571:ENST00000545968:exon32:c.3621delC:p.S1207fs		L	0,00059
MYBPC3	11_47354139_CAGCAGAGCA_-	ENSG00000134571:ENST00000256993:exon30:c.3593_3602del:p.1198_1201del,ENSG00000134571:ENST00000399249:exon31:c.3596_3605del:p.1199_1202del,ENSG00000134571:ENST00000545968:exon32:c.3596_3605del:p.1199_1202del		L	0,00059
MYBPC3	11_47354151_GCAGTGTAGCCC_-	ENSG00000134571:ENST00000256993:exon30:c.3579_3590del:p.1193_1197del,ENSG00000134571:ENST00000399249:exon31:c.3582_3593del:p.1194_1198del,ENSG00000134571:ENST00000545968:exon32:c.3582_3593del:p.1194_1198del		N	0,00118
MYBPC3	11_47354172_G_A	ENSG00000134571:ENST00000256993:exon30:c.C3569T:p.S1190L,ENSG00000134571:ENST00000399249:exon31:c.C3572T:p.S1191L,ENSG00000134571:ENST00000545968:exon32:c.C3572T:p.S1191L		P	0,00060
MYBPC3	11_47354209_C_T	ENSG00000134571:ENST00000256993:exon30:c.G3532A:p.E1178K,ENSG00000134571:ENST00000399249:exon31:c.G3535A:p.E1179K,ENSG00000134571:ENST00000545968:exon32:c.G3535A:p.E1179K	rs199669878	P	0,00059
MYBPC3	11_47354256_G_C	ENST00000256993:exon31:c.3488-3C>G,ENST00000399249:exon32:c.3491-3C>G,ENST00000545968:exon33:c.3491-3C>G		L	0,00059
MYBPC3	11_47354389_CCTTGGTGGTGG_-	ENSG00000134571:ENST00000256993:exon29:c.3452_3463del:p.1151_1155del,ENSG00000134571:ENST00000399249:exon30:c.3455_3466del:p.1152_1156del,ENSG00000134571:ENST00000545968:exon31:c.3455_3466del:p.1152_1156del		N	0,00059
MYBPC3	11_47354451_TAG_-	ENSG00000134571:ENST00000256993:exon29:c.3399_3401del:p.1133_1134del,ENSG00000134571:ENST00000399249:exon30:c.3402_3404del:p.1134_1135del,ENSG00000134571:ENST00000545968:exon31:c.3402_3404del:p.1134_1135del		N	0,00059
MYBPC3	11_47354471_C_G	ENSG00000134571:ENST00000256993:exon29:c.G3381C:p.E1127D,ENSG00000134571:ENST00000399249:exon30:c.G3384C:p.E1128D,ENSG00000134571:ENST00000545968:exon31:c.G3384C:p.E1128D		N	0,00059

MYBPC3	11_47354522_-_CAC	ENSG00000134571:ENST00000256993:exon29:c.3330_3331insGTG:p.E1110delinsEW,ENSG00000134571:ENST00000399249:exon30:c.3333_3334insGTG:p.E1111delinsEW,ENSG00000134571:ENST00000545968:exon31:c.3333_3334insGTG:p.E1111delinsEW		N	0,00062
MYBPC3	11_47354740_C_G	ENST00000256993:exon29:c.3327+5G>C,ENST00000399249:exon30:c.3330+5G>C,ENST00000545968:exon31:c.3330+5G>C		P	0,00348
MYBPC3	11_47354749_G_A	ENSG00000134571:ENST00000256993:exon28:c.C3323T:p.T1108I,ENSG00000134571:ENST00000399249:exon29:c.C3326T:p.T1109I,ENSG00000134571:ENST00000545968:exon30:c.C3326T:p.T1109I		P	0,00138
MYBPC3	11_47354781_C_T	ENSG00000134571:ENST00000256993:exon28:c.G3291A:p.W1097X,ENSG00000134571:ENST00000399249:exon29:c.G3294A:p.W1098X,ENSG00000134571:ENST00000545968:exon30:c.G3294A:p.W1098X		P	0,00071
MYBPC3	11_47354818_C_T	ENSG00000134571:ENST00000256993:exon28:c.G3254A:p.W1085X,ENSG00000134571:ENST00000399249:exon29:c.G3257A:p.W1086X,ENSG00000134571:ENST00000545968:exon30:c.G3257A:p.W1086X		L	0,00075
MYBPC3	11_47354848_-_A	ENSG00000134571:ENST00000256993:exon28:c.3224_3225insT:p.D1075fs,ENSG00000134571:ENST00000399249:exon29:c.3227_3228insT:p.D1076fs,ENSG00000134571:ENST00000545968:exon30:c.3227_3228insT:p.D1076fs		P	0,00378
MYBPC3	11_47355103_C_T	ENST00000256993:exon28:c.3187+5G>A,ENST00000399249:exon29:c.3190+5G>A,ENST00000545968:exon30:c.3190+5G>A		P	0,00134
MYBPC3	11_47355191_C_T	ENSG00000134571:ENST00000256993:exon27:c.G3104A:p.R1035H,ENSG00000134571:ENST00000399249:exon28:c.G3107A:p.R1036H,ENSG00000134571:ENST00000545968:exon29:c.G3107A:p.R1036H		N	0,00062
MYBPC3	11_47355233_C_G	ENSG00000134571:ENST00000256993:exon27:c.G3062C:p.R1021P,ENSG00000134571:ENST00000399249:exon28:c.G3065C:p.R1022P,ENSG00000134571:ENST00000545968:exon29:c.G3065C:p.R1022P		P	0,00063
MYBPC3	11_47355249_C_T	ENSG00000134571:ENST00000256993:exon27:c.G3046A:p.E1016K,ENSG00000134571:ENST00000399249:exon28:c.G3049A:p.E1017K,ENSG00000134571:ENST00000545968:exon29:c.G3049A:p.E1017K		P	0,00064
MYBPC3	11_47355294_G_A	ENSG00000134571:ENST00000256993:exon27:c.C3001T:p.R1001W,ENSG00000134571:ENST00000399249:exon28:c.C3004T:p.R1002W,ENSG00000134571:ENST00000545968:exon29:c.C3004T:p.R1002W	rs3729799	D	0,00065
MYBPC3	11_47355304_C_T	ENST00000256993:exon28:c.2992-1G>A,ENST00000399249:exon29:c.2995-1G>A,ENST00000545968:exon30:c.2995-1G>A		L	0,00066
MYBPC3	11_47355514_T_A	ENSG00000134571:ENST00000256993:exon26:c.A2950T:p.K984X,ENSG00000134571:ENST00000399249:exon27:c.A2953T:p.K985X,ENSG00000134571:ENST00000545968:exon28:c.A2953T:p.K985X		L	0,00068
MYBPC3	11_47356588_C_A	ENST00000256993:exon26:c.2902+5G>T,ENST00000399249:exon27:c.2905+5G>T,ENST00000545968:exon28:c.2905+5G>T		L	0,00074

MYBPC3	11_47356592_C_T	ENST00000256993:exon26:c.2902+1G>A,ENST00000399249:exon27:c.2905+1G>A,ENST00000545968:exon28:c.2905+1G>A		P	0,00147
MYBPC3	11_47356633_AG_-	ENSG00000134571:ENST00000256993:exon25:c.2861_2862del:p.954_954del,ENSG00000134571:ENST00000399249:exon26:c.2864_2865del:p.955_955del,ENSG00000134571:ENST00000545968:exon27:c.2864_2865del:p.955_955del		L	0,00156
MYBPC3	11_47356671_G_A	ENSG00000134571:ENST00000256993:exon25:c.C2824T:p.R942X,ENSG00000134571:ENST00000399249:exon26:c.C2827T:p.R943X,ENSG00000134571:ENST00000545968:exon27:c.C2827T:p.R943X		P	0,00312
MYBPC3	11_47356710_G_C	ENSG00000134571:ENST00000256993:exon25:c.C2785G:p.L929V,ENSG00000134571:ENST00000399249:exon26:c.C2788G:p.L930V,ENSG00000134571:ENST00000545968:exon27:c.C2788G:p.L930V		N	0,00082
MYBPC3	11_47357425_CA_-			P	0,00061
MYBPC3	11_47357437_G_T	ENSG00000134571:ENST00000256993:exon24:c.C2725A:p.P909T,ENSG00000134571:ENST00000399249:exon25:c.C2728A:p.P910T,ENSG00000134571:ENST00000545968:exon26:c.C2728A:p.P910T		P	0,00060
MYBPC3	11_47357547_G_T	ENSG00000134571:ENST00000256993:exon24:c.C2615A:p.P872H,ENSG00000134571:ENST00000399249:exon25:c.C2618A:p.P873H,ENSG00000134571:ENST00000545968:exon26:c.C2618A:p.P873H		P	0,00063
MYBPC3	11_47357555_G_-	ENSG00000134571:ENST00000256993:exon24:c.2607delC:p.P869fs,ENSG00000134571:ENST00000399249:exon25:c.2610delC:p.P870fs,ENSG00000134571:ENST00000545968:exon26:c.2610delC:p.P870fs		P	0,00252
MYBPC3	11_47357560_G_T	ENSG00000134571:ENST00000256993:exon24:c.C2602A:p.P868T,ENSG00000134571:ENST00000399249:exon25:c.C2605A:p.P869T,ENSG00000134571:ENST00000545968:exon26:c.C2605A:p.P869T		P	0,00188
MYBPC3	11_47357560_GA_GGA	ENSG00000134571:ENST00000256993:exon24:c.2601_2602TCC,ENSG00000134571:ENST00000399249:exon25:c.2604_2605TCC,ENSG00000134571:ENST00000545968:exon26:c.2604_2605TCC		N	0,00063
MYBPC3	11_47357561_A_-	ENSG00000134571:ENST00000256993:exon24:c.2601delT:p.G867fs,ENSG00000134571:ENST00000399249:exon25:c.2604delT:p.G868fs,ENSG00000134571:ENST00000545968:exon26:c.2604delT:p.G868fs		P	0,00253
MYBPC3	11_47357563_C_G	ENST00000256993:exon25:c.2600-1G>C,ENST00000399249:exon26:c.2603-1G>C,ENST00000545968:exon27:c.2603-1G>C,ENST00000544791:exon27:c.2535-1G>C		L	0,00062
MYBPC3	11_47357564_T_C	ENST00000256993:exon25:c.2600-2A>G,ENST00000399249:exon26:c.2603-2A>G,ENST00000545968:exon27:c.2603-2A>G,ENST00000544791:exon27:c.2535-2A>G		L	0,00125
MYBPC3	11_47358987_C_-	ENSG00000134571:ENST00000256993:exon23:c.2554delG:p.G852fs,ENSG00000134571:ENST00000399249:exon24:c.2557delG:p.G853fs,ENSG00000134571:ENST00000545968:exon25:c.2557delG:p.G853fs		P	0,00080
MYBPC3	11_47358999_C_-	ENSG00000134571:ENST00000256993:exon23:c.2542delG:p.V848fs,ENSG00000134571:ENST00000399249:exon24:c.2545delG:p.V849fs,ENSG00000134571:ENST00000545968:exon25:c.2545delG:p.V849fs		L	0,00152

MYBPC3	11_47359000_C_-	ENSG00000134571:ENST00000256993:exon23:c.2541delG:p.A847fs,ENSG00000134571:ENST00000399249:exon24:c.2544delG:p.A848fs,ENSG00000134571:ENST00000545968:exon25:c.2544delG:p.A848fs		P	0,00151
MYBPC3	11_47359020_-_A	ENSG00000134571:ENST00000256993:exon23:c.2521_2522insT:p.Y841fs,ENSG00000134571:ENST00000399249:exon24:c.2524_2525insT:p.Y842fs,ENSG00000134571:ENST00000545968:exon25:c.2524_2525insT:p.Y842fs		L	0,00072
MYBPC3	11_47359032_-_C	ENSG00000134571:ENST00000256993:exon23:c.2509_2510insG:p.E837fs,ENSG00000134571:ENST00000399249:exon24:c.2512_2513insG:p.E838fs,ENSG00000134571:ENST00000545968:exon25:c.2512_2513insG:p.E838fs		L	0,00071
MYBPC3	11_47359047_C_T	ENSG00000134571:ENST00000256993:exon23:c.G2494A:p.A832T,ENSG00000134571:ENST00000399249:exon24:c.G2497A:p.A833T,ENSG00000134571:ENST00000545968:exon25:c.G2497A:p.A833T	rs199865688	P	0,00138
MYBPC3	11_47359085_C_T	ENSG00000134571:ENST00000256993:exon23:c.G2456A:p.R819Q,ENSG00000134571:ENST00000399249:exon24:c.G2459A:p.R820Q,ENSG00000134571:ENST00000545968:exon25:c.G2459A:p.R820Q	rs2856655	P	0,00142
MYBPC3	11_47359095_G_A	ENSG00000134571:ENST00000256993:exon23:c.C2446T:p.R816W,ENSG00000134571:ENST00000399249:exon24:c.C2449T:p.R817W,ENSG00000134571:ENST00000545968:exon25:c.C2449T:p.R817W		S	0,00071
MYBPC3	11_47359109_T_C	ENSG00000134571:ENST00000256993:exon23:c.A2432G:p.K811R,ENSG00000134571:ENST00000399249:exon24:c.A2435G:p.K812R,ENSG00000134571:ENST00000545968:exon25:c.A2435G:p.K812R		N	0,00072
MYBPC3	11_47359115_C_T	ENSG00000134571:ENST00000256993:exon23:c.G2426A:p.R809H,ENSG00000134571:ENST00000399249:exon24:c.G2429A:p.R810H,ENSG00000134571:ENST00000545968:exon25:c.G2429A:p.R810H		P	0,00218
MYBPC3	11_47359116_G_A	ENSG00000134571:ENST00000256993:exon23:c.C2425T:p.R809C,ENSG00000134571:ENST00000399249:exon24:c.C2428T:p.R810C,ENSG00000134571:ENST00000545968:exon25:c.C2428T:p.R810C		S	0,00074
MYBPC3	11_47359251_C_G	ENSG00000134571:ENST00000256993:exon22:c.G2400C:p.Q800H,ENSG00000134571:ENST00000399249:exon23:c.G2403C:p.Q801H,ENSG00000134571:ENST00000544791:exon24:c.G2403C:p.Q801H,ENSG00000134571:ENST00000545968:exon24:c.G2403C:p.Q801H		N	0,00073
MYBPC3	11_47359280_-_C	ENSG00000134571:ENST00000256993:exon22:c.2371_2372insG:p.W791fs,ENSG00000134571:ENST00000399249:exon23:c.2374_2375insG:p.W792fs,ENSG00000134571:ENST00000544791:exon24:c.2374_2375insG:p.W792fs,ENSG00000134571:ENST00000545968:exon24:c.2374_2375insG:p.W792fs		P	0,00645
MYBPC3	11_47359281_-_C	ENSG00000134571:ENST00000256993:exon22:c.2370_2371insG:p.Q790fs,ENSG00000134571:ENST00000399249:exon23:c.2373_2374insG:p.Q791fs,ENSG00000134571:ENST00000544791:exon24:c.2373_2374insG:p.Q791fs,ENSG00000134571:ENST00000545968:exon24:c.2373_2374insG:p.Q791fs		P	0,00646

MYBPC3	11_47359347_T_C	ENST00000256993:exon23:c.2306-2A>G,ENST00000399249:exon24:c.2309-2A>G,ENST00000545968:exon25:c.2309-2A>G,ENST00000544791:exon25:c.2309-2A>G		P	0,00064
MYBPC3	11_47360071_C_T	ENSG00000134571:ENST00000256993:exon21:c.G2305A:p.D769N,ENSG00000134571:ENST00000399249:exon22:c.G2308A:p.D770N,ENSG00000134571:ENST00000544791:exon23:c.G2308A:p.D770N,ENSG00000134571:ENST00000545968:exon23:c.G2308A:p.D770N	rs36211723	P	0,00064
MYBPC3	11_47360104_C_T	ENSG00000134571:ENST00000256993:exon21:c.G2272A:p.E758K,ENSG00000134571:ENST00000399249:exon22:c.G2275A:p.E759K,ENSG00000134571:ENST00000544791:exon23:c.G2275A:p.E759K,ENSG00000134571:ENST00000545968:exon23:c.G2275A:p.E759K		S	0,00062
MYBPC3	11_47360110_C_T	ENSG00000134571:ENST00000256993:exon21:c.G2266A:p.V756M,ENSG00000134571:ENST00000399249:exon22:c.G2269A:p.V757M,ENSG00000134571:ENST00000544791:exon23:c.G2269A:p.V757M,ENSG00000134571:ENST00000545968:exon23:c.G2269A:p.V757M		P	0,00061
MYBPC3	11_47360200_C_T	ENSG00000134571:ENST00000256993:exon21:c.G2176A:p.V726M,ENSG00000134571:ENST00000399249:exon22:c.G2179A:p.V727M,ENSG00000134571:ENST00000544791:exon23:c.G2179A:p.V727M,ENSG00000134571:ENST00000545968:exon23:c.G2179A:p.V727M		S	0,00066
MYBPC3	11_47360235_G_A	ENST00000256993:exon22:c.2146-5C>T,ENST00000399249:exon23:c.2149-5C>T,ENST00000545968:exon24:c.2149-5C>T,ENST00000544791:exon24:c.2149-5C>T	rs36211722	P	0,00139
MYBPC3	11_47360927_G_-	ENSG00000134571:ENST00000256993:exon20:c.2093delC:p.P698fs,ENSG00000134571:ENST00000399249:exon21:c.2096delC:p.P699fs,ENSG00000134571:ENST00000544791:exon22:c.2096delC:p.P699fs,ENSG00000134571:ENST00000545968:exon22:c.2096delC:p.P699fs		P	0,00173
MYBPC3	11_47360930_G_-	ENSG00000134571:ENST00000256993:exon20:c.2090delC:p.A697fs,ENSG00000134571:ENST00000399249:exon21:c.2093delC:p.A698fs,ENSG00000134571:ENST00000544791:exon22:c.2093delC:p.A698fs,ENSG00000134571:ENST00000545968:exon22:c.2093delC:p.A698fs		P	0,00173
MYBPC3	11_47361309_G_A	ENSG00000134571:ENST00000256993:exon19:c.C1957T:p.R653C,ENSG00000134571:ENST00000399249:exon20:c.C1960T:p.R654C,ENSG00000134571:ENST00000544791:exon21:c.C1960T:p.R654C,ENSG00000134571:ENST00000545968:exon21:c.C1960T:p.R654C		P	0,00059
MYBPC3	11_47361343_T_C	ENST00000256993:exon20:c.1925-2A>G,ENST00000399249:exon21:c.1928-2A>G,ENST00000545968:exon22:c.1928-2A>G,ENST00000544791:exon22:c.1928-2A>G		P	0,00061
MYBPC3	11_47362731_C_T	ENSG00000134571:ENST00000256993:exon17:c.G1852A:p.E618K,ENSG00000134571:ENST00000399249:exon18:c.G1855A:p.E619K,ENSG00000134571:ENST00000544791:exon19:c.G1855A:p.E619K,ENSG00000134571:ENST00000545968:exon19:c.G1855A:p.E619K	rs200352299	P	0,00065
MYBPC3	11_47363546_C_T	ENSG00000134571:ENST00000256993:exon16:c.G1783A:p.G595R,ENSG00000134571:ENST00000399249:exon17:c.G1786A:p.G596R,ENSG00000134571:ENST00000544791:exon18:c.G1786A:p.G596R,ENSG00000134571:ENST00000545968:exon18:c.G1786A:p.G596R	rs199728019	P	0,00116
MYBPC3	11_47363567_G_A	ENSG00000134571:ENST00000256993:exon16:c.C1762T:p.R588C,ENSG00000134571:ENST00000399249:exon17:c.C1765T:p.R589C,ENSG00000134571:ENST00000544791:exon18:c.C1765T:p.R589C,ENSG00000134571:ENST00000545968:exon18:c.C1765T:p.R589C		S	0,00058

MYBPC3	11_47363704_T_-	ENSG00000134571:ENST00000256993:exon16:c.1625delA:p.K542fs,ENSG00000134571:ENST00000399249:exon17:c.1628delA:p.K543fs,ENSG00000134571:ENST00000544791:exon18:c.1628delA:p.K543fs,ENSG00000134571:ENST00000545968:exon18:c.1628delA:p.K543fs		L	0,00058
MYBPC3	11_47364125_T_A	ENST00000256993:exon16:c.1621+4A>T,ENST00000399249:exon17:c.1624+4A>T,ENST00000545968:exon18:c.1624+4A>T,ENST00000544791:exon18:c.1624+4A>T		P	0,01346
MYBPC3	11_47364129_C_A	ENSG00000134571:ENST00000256993:exon15:c.G1621T:p.E541X,ENSG00000134571:ENST00000399249:exon16:c.G1624T:p.E542X,ENSG00000134571:ENST00000544791:exon17:c.G1624T:p.E542X,ENSG00000134571:ENST00000545968:exon17:c.G1624T:p.E542X		L	0,00090
MYBPC3	11_47364129_C_G	ENSG00000134571:ENST00000256993:exon15:c.G1621C:p.E541Q,ENSG00000134571:ENST00000399249:exon16:c.G1624C:p.E542Q,ENSG00000134571:ENST00000544791:exon17:c.G1624C:p.E542Q,ENSG00000134571:ENST00000545968:exon17:c.G1624C:p.E542Q	rs121909374	P	0,00269
MYBPC3	11_47364162_C_G	ENSG00000134571:ENST00000256993:exon15:c.G1588C:p.G530R,ENSG00000134571:ENST00000399249:exon16:c.G1591C:p.G531R,ENSG00000134571:ENST00000544791:exon17:c.G1591C:p.G531R,ENSG00000134571:ENST00000545968:exon17:c.G1591C:p.G531R		P	0,00083
MYBPC3	11_47364173_A_G	ENSG00000134571:ENST00000256993:exon15:c.T1577C:p.L526P,ENSG00000134571:ENST00000399249:exon16:c.T1580C:p.L527P,ENSG00000134571:ENST00000544791:exon17:c.T1580C:p.L527P,ENSG00000134571:ENST00000545968:exon17:c.T1580C:p.L527P		P	0,00078
MYBPC3	11_47364180_A_G	ENSG00000134571:ENST00000256993:exon15:c.T1570C:p.Y524H,ENSG00000134571:ENST00000399249:exon16:c.T1573C:p.Y525H,ENSG00000134571:ENST00000544791:exon17:c.T1573C:p.Y525H,ENSG00000134571:ENST00000545968:exon17:c.T1573C:p.Y525H		S	0,00076
MYBPC3	11_47364204_C_G	ENSG00000134571:ENST00000256993:exon15:c.G1546C:p.A516P,ENSG00000134571:ENST00000399249:exon16:c.G1549C:p.A517P,ENSG00000134571:ENST00000544791:exon17:c.G1549C:p.A517P,ENSG00000134571:ENST00000545968:exon17:c.G1549C:p.A517P		N	0,00071
MYBPC3	11_47364249_G_A	ENSG00000134571:ENST00000256993:exon15:c.C1501T:p.R501W,ENSG00000134571:ENST00000399249:exon16:c.C1504T:p.R502W,ENSG00000134571:ENST00000544791:exon17:c.C1504T:p.R502W,ENSG00000134571:ENST00000545968:exon17:c.C1504T:p.R502W		P	0,01038
MYBPC3	11_47364269_C_T	ENSG00000134571:ENST00000256993:exon15:c.G1481A:p.R494Q,ENSG00000134571:ENST00000399249:exon16:c.G1484A:p.R495Q,ENSG00000134571:ENST00000544791:exon17:c.G1484A:p.R495Q,ENSG00000134571:ENST00000545968:exon17:c.G1484A:p.R495Q	rs200411226	P	0,00319
MYBPC3	11_47364270_G_A	ENSG00000134571:ENST00000256993:exon15:c.C1480T:p.R494W,ENSG00000134571:ENST00000399249:exon16:c.C1483T:p.R495W,ENSG00000134571:ENST00000544791:exon17:c.C1483T:p.R495W,ENSG00000134571:ENST00000545968:exon17:c.C1483T:p.R495W		P	0,00064
MYBPC3	11_47364270_G_C	ENSG00000134571:ENST00000256993:exon15:c.C1480G:p.R494G,ENSG00000134571:ENST00000399249:exon16:c.C1483G:p.R495G,ENSG00000134571:ENST00000544791:exon17:c.C1483G:p.R495G,ENSG00000134571:ENST00000545968:exon17:c.C1483G:p.R495G		N	0,00256
MYBPC3	11_47364282_C_T	ENSG00000134571:ENST00000256993:exon15:c.G1468A:p.V490M,ENSG00000134571:ENST00000399249:exon16:c.G1471A:p.V491M,ENSG00000134571:ENST00000544791:exon17:c.G1471A:p.V491M,ENSG00000134571:ENST00000545968:exon17:c.G1471A:p.V491M		P	0,00064

MYBPC3	11_47364376_C_G	ENST00000256993:exon15:c.1454+5G>C,ENST00000399249:exon16:c.1457+5G>C,ENST00000545968:exon17:c.1457+5G>C,ENST00000544791:exon17:c.1457+5G>C		L	0,00060
MYBPC3	11_47364377_T_C	ENST00000256993:exon15:c.1454+4A>G,ENST00000399249:exon16:c.1457+4A>G,ENST00000545968:exon17:c.1457+4A>G,ENST00000544791:exon17:c.1457+4A>G		L	0,00120
MYBPC3	11_47364393_G_A	ENSG00000134571:ENST00000256993:exon14:c.C1442T:p.A481V,ENSG00000134571:ENST00000399249:exon15:c.C1445T:p.A482V,ENSG00000134571:ENST00000544791:exon16:c.C1445T:p.A482V,ENSG00000134571:ENST00000545968:exon16:c.C1445T:p.A482V		S	0,00060
MYBPC3	11_47364479_A_-	ENSG00000134571:ENST00000256993:exon14:c.1356delT:p.P452fs,ENSG00000134571:ENST00000399249:exon15:c.1359delT:p.P453fs,ENSG00000134571:ENST00000544791:exon16:c.1359delT:p.P453fs,ENSG00000134571:ENST00000545968:exon16:c.1359delT:p.P453fs		L	0,00061
MYBPC3	11_47364620_G_A	ENSG00000134571:ENST00000256993:exon13:c.C1300T:p.Q434X,ENSG00000134571:ENST00000399249:exon14:c.C1303T:p.Q435X,ENSG00000134571:ENST00000544791:exon15:c.C1303T:p.Q435X,ENSG00000134571:ENST00000545968:exon15:c.C1303T:p.Q435X		L	0,00063
MYBPC3	11_47364621_G_C	ENSG00000134571:ENST00000256993:exon13:c.C1299G:p.Y433X,ENSG00000134571:ENST00000399249:exon14:c.C1302G:p.Y434X,ENSG00000134571:ENST00000544791:exon15:c.C1302G:p.Y434X,ENSG00000134571:ENST00000545968:exon15:c.C1302G:p.Y434X		L	0,00063
MYBPC3	11_47364621_G_T	ENSG00000134571:ENST00000256993:exon13:c.C1299A:p.Y433X,ENSG00000134571:ENST00000399249:exon14:c.C1302A:p.Y434X,ENSG00000134571:ENST00000544791:exon15:c.C1302A:p.Y434X,ENSG00000134571:ENST00000545968:exon15:c.C1302A:p.Y434X		L	0,00063
MYBPC3	11_47364650_G_A	ENSG00000134571:ENST00000256993:exon13:c.C1270T:p.Q424X,ENSG00000134571:ENST00000399249:exon14:c.C1273T:p.Q425X,ENSG00000134571:ENST00000544791:exon15:c.C1273T:p.Q425X,ENSG00000134571:ENST00000545968:exon15:c.C1273T:p.Q425X		P	0,00063
MYBPC3	11_47364677_C_T	ENSG00000134571:ENST00000256993:exon13:c.G1243A:p.G415S,ENSG00000134571:ENST00000399249:exon14:c.G1246A:p.G416S,ENSG00000134571:ENST00000544791:exon15:c.G1246A:p.G416S,ENSG00000134571:ENST00000545968:exon15:c.G1246A:p.G416S		P	0,00066
MYBPC3	11_47364686_-_A	ENSG00000134571:ENST00000256993:exon13:c.1234_1235insT:p.E412_S413delinsX,ENSG00000134571:ENST00000399249:exon14:c.1237_1238insT:p.E413_S414delinsX,ENSG00000134571:ENST00000544791:exon15:c.1237_1238insT:p.E413_S414delinsX,ENSG00000134571:ENST00000545968:exon15:c.1237_1238insT:p.E413_S414delinsX		L	0,00137
MYBPC3	11_47364689_-_A	ENSG00000134571:ENST00000256993:exon13:c.1231_1232insT:p.F411fs,ENSG00000134571:ENST00000399249:exon14:c.1234_1235insT:p.F412fs,ENSG00000134571:ENST00000544791:exon15:c.1234_1235insT:p.F412fs,ENSG00000134571:ENST00000545968:exon15:c.1234_1235insT:p.F412fs		P	0,00137
MYBPC3	11_47364698_T_C	ENST00000256993:exon14:c.1224-2A>G,ENST00000399249:exon15:c.1227-2A>G,ENST00000545968:exon16:c.1227-2A>G,ENST00000544791:exon16:c.1227-2A>G		L	0,00070
MYBPC3	11_47365143_C_T	ENSG00000134571:ENST00000256993:exon12:c.G1123A:p.V375M,ENSG00000134571:ENST00000399249:exon12:c.G1123A:p.V375M,ENSG00000134571:ENST00000544791:exon13:c.G1123A:p.V375M,ENSG00000134571:ENST00000545968:exon13:c.G1123A:p.V375M		S	0,00095

MYBPC3	11_47367757_C_A	ENST00000256993:exon12:c.1090+1G>T,ENST00000399249:exon12:c.1090+1G>T,ENST00000545968:exon13:c.1090+1G>T,ENST00000544791:exon13:c.1090+1G>T		P	0,00231
MYBPC3	11_47367757_C_T	ENST00000256993:exon12:c.1090+1G>A,ENST00000399249:exon12:c.1090+1G>A,ENST00000545968:exon13:c.1090+1G>A,ENST00000544791:exon13:c.1090+1G>A		P	0,00058
MYBPC3	11_47367764_T_C	ENSG00000134571:ENST00000256993:exon11:c.A1084G:p.S362G,ENSG00000134571:ENST00000399249:exon11:c.A1084G:p.S362G,ENSG00000134571:ENST00000544791:exon12:c.A1084G:p.S362G,ENSG00000134571:ENST00000545968:exon12:c.A1084G:p.S362G		S	0,00058
MYBPC3	11_47367776_C_T	ENSG00000134571:ENST00000256993:exon11:c.G1072A:p.D358N,ENSG00000134571:ENST00000399249:exon11:c.G1072A:p.D358N,ENSG00000134571:ENST00000544791:exon12:c.G1072A:p.D358N,ENSG00000134571:ENST00000545968:exon12:c.G1072A:p.D358N		N	0,00058
MYBPC3	11_47367822_GACGCCGT_-	ENSG00000134571:ENST00000256993:exon11:c.1019_1026del:p.340_342del,ENSG00000134571:ENST00000399249:exon11:c.1019_1026del:p.340_342del,ENSG00000134571:ENST00000544791:exon12:c.1019_1026del:p.340_342del,ENSG00000134571:ENST00000545968:exon12:c.1019_1026del:p.340_342del		L	0,00058
MYBPC3	11_47367848_C_T	ENSG00000134571:ENST00000256993:exon11:c.G1000A:p.E334K,ENSG00000134571:ENST00000399249:exon11:c.G1000A:p.E334K,ENSG00000134571:ENST00000544791:exon12:c.G1000A:p.E334K,ENSG00000134571:ENST00000545968:exon12:c.G1000A:p.E334K		P	0,00061
MYBPC3	11_47367849_G_C	ENSG00000134571:ENST00000256993:exon11:c.C999G:p.Y333X,ENSG00000134571:ENST00000399249:exon11:c.C999G:p.Y333X,ENSG00000134571:ENST00000544791:exon12:c.C999G:p.Y333X,ENSG00000134571:ENST00000545968:exon12:c.C999G:p.Y333X		L	0,00061
MYBPC3	11_47367887_C_T	ENSG00000134571:ENST00000256993:exon11:c.G961A:p.V321M,ENSG00000134571:ENST00000399249:exon11:c.G961A:p.V321M,ENSG00000134571:ENST00000544791:exon12:c.G961A:p.V321M,ENSG00000134571:ENST00000545968:exon12:c.G961A:p.V321M	rs200119454	P	0,00187
MYBPC3	11_47367923_T_C	ENST00000256993:exon12:c.927-2A>G,ENST00000399249:exon12:c.927-2A>G,ENST00000545968:exon13:c.927-2A>G,ENST00000544791:exon13:c.927-2A>G		P	0,00132
MYBPC3	11_47368187_C_T	ENSG00000134571:ENST00000256993:exon10:c.G917A:p.R306Q,ENSG00000134571:ENST00000399249:exon10:c.G917A:p.R306Q,ENSG00000134571:ENST00000544791:exon11:c.G917A:p.R306Q,ENSG00000134571:ENST00000545968:exon11:c.G917A:p.R306Q		N	0,00059
MYBPC3	11_47368202_C_T	ENST00000256993:exon11:c.906-4G>A,ENST00000399249:exon11:c.906-4G>A		L	0,00060
MYBPC3	11_47369023_G_A	ENSG00000134571:ENST00000256993:exon9:c.C859T:p.H287Y,ENSG00000134571:ENST00000399249:exon9:c.C859T:p.H287Y,ENSG00000134571:ENST00000544791:exon9:c.C859T:p.H287Y,ENSG00000134571:ENST00000545968:exon9:c.C859T:p.H287Y		P	0,00066
MYBPC3	11_47369406_A_G	ENST00000256993:exon8:c.821+2T>C,ENST00000399249:exon8:c.821+2T>C,ENST00000545968:exon8:c.821+2T>C,ENST00000544791:exon8:c.821+2T>C		P	0,00087
MYBPC3	11_47369975_C_T	ENSG00000134571:ENST00000256993:exon6:c.G772A:p.E258K,ENSG00000134571:ENST00000399249:exon6:c.G772A:p.E258K,ENSG00000134571:ENST00000544791:exon6:c.G772A:p.E258K,ENSG00000134571:ENST00000545968:exon6:c.G772A:p.E258K		P	0,00616

MYBPC3	11_47370037_T_G	ENSG00000134571:ENST00000256993:exon6:c.A710C:p.Y237S,ENSG00000134571:ENST00000399249:exon6:c.A710C:p.Y237S,ENSG00000134571:ENST00000544791:exon6:c.A710C:p.Y237S,ENSG00000000134571:ENST00000545968:exon6:c.A710C:p.Y237S		P	0,00140
MYBPC3	11_47370092_C_G	ENSG00000134571:ENST00000256993:exon6:c.G655C:p.V219L,ENSG00000134571:ENST00000399249:exon6:c.G655C:p.V219L,ENSG00000134571:ENST00000544791:exon6:c.G655C:p.V219L,ENSG00000000134571:ENST00000545968:exon6:c.G655C:p.V219L		P	0,00442
MYBPC3	11_47371330_T_C	ENSG00000134571:ENST00000256993:exon5:c.A649G:p.S217G,ENSG00000134571:ENST00000399249:exon5:c.A649G:p.S217G,ENSG00000134571:ENST00000544791:exon5:c.A649G:p.S217G,ENSG00000000134571:ENST00000545968:exon5:c.A649G:p.S217G	rs138753870	P	0,00067
MYBPC3	11_47371366_G_A	ENSG00000134571:ENST00000256993:exon5:c.C613T:p.Q205X,ENSG00000134571:ENST00000399249:exon5:c.C613T:p.Q205X,ENSG00000134571:ENST00000544791:exon5:c.C613T:p.Q205X,ENSG00000000134571:ENST00000545968:exon5:c.C613T:p.Q205X		L	0,00068
MYBPC3	11_47371390_CCCATTTG_-	ENSG00000134571:ENST00000256993:exon5:c.582_589del:p.194_197del,ENSG00000134571:ENST00000399249:exon5:c.582_589del:p.194_197del,ENSG00000134571:ENST00000544791:exon5:c.582_589del:p.194_197del,ENSG00000134571:ENST00000545968:exon5:c.582_589del:p.194_197del		L	0,00071
MYBPC3	11_47371560_C_T	ENST00000256993:exon5:c.505+5G>A,ENST00000399249:exon5:c.505+5G>A,ENST00000545968:exon5:c.505+5G>A,ENST00000544791:exon5:c.505+5G>A		L	0,00096
MYBPC3	11_47372107_CA_-	ENSG00000134571:ENST00000256993:exon3:c.351_352del:p.117_118del,ENSG00000134571:ENST00000399249:exon3:c.351_352del:p.117_118del,ENSG00000134571:ENST00000544791:exon3:c.351_352del:p.117_118del,ENSG00000134571:ENST00000545968:exon3:c.351_352del:p.117_118del		L	0,00182
MYBPC3	11_47372859_C_T	ENSG00000134571:ENST00000256993:exon2:c.G223A:p.D75N,ENSG00000134571:ENST00000399249:exon2:c.G223A:p.D75N,ENSG00000134571:ENST00000544791:exon2:c.G223A:p.D75N,ENSG00000000134571:ENST00000545968:exon2:c.G223A:p.D75N		P	0,00082
MYBPC3	11_47372866_-_CC	ENSG00000134571:ENST00000256993:exon2:c.216_217insGG:p.G72fs,ENSG00000134571:ENST00000399249:exon2:c.216_217insGG:p.G72fs,ENSG00000134571:ENST00000544791:exon2:c.216_217insGG:p.G72fs,ENSG00000000134571:ENST00000545968:exon2:c.216_217insGG:p.G72fs		L	0,00081
MYBPC3	11_47372898_TGCCCTCTGTG_-	ENSG00000134571:ENST00000256993:exon2:c.174_184del:p.58_62del,ENSG00000134571:ENST00000399249:exon2:c.174_184del:p.58_62del,ENSG00000134571:ENST00000544791:exon2:c.174_184del:p.58_62del,ENSG00000000134571:ENST00000545968:exon2:c.174_184del:p.58_62del		P	0,00319
MYBPC3	11_47372956_C_T	ENSG00000134571:ENST00000256993:exon2:c.G126A:p.W42X,ENSG00000134571:ENST00000399249:exon2:c.G126A:p.W42X,ENSG00000134571:ENST00000544791:exon2:c.G126A:p.W42X,ENSG00000000134571:ENST00000545968:exon2:c.G126A:p.W42X		L	0,00078
MYBPC3	11_47372961_-_G	ENSG00000134571:ENST00000256993:exon2:c.121_122insC:p.R41fs,ENSG00000134571:ENST00000399249:exon2:c.121_122insC:p.R41fs,ENSG00000134571:ENST00000544791:exon2:c.121_122insC:p.R41fs,ENSG00000000134571:ENST00000545968:exon2:c.121_122insC:p.R41fs		L	0,00077
MYBPC3	11_47374186_C_G	ENSG00000134571:ENST00000256993:exon1:c.G13C:p.G5R,ENSG00000134571:ENST00000399249:exon1:c.G13C:p.G5R,ENSG00000134571:ENST00000544791:exon1:c.G13C:p.G5R,ENSG00000000134571:ENST00000545968:exon1:c.G13C:p.G5R	rs201278114	P	0,00117

MYH6	14_23852451_G_T	ENSG00000197616:ENST00000356287:exon36:c.C5644A:p.R1882S,ENSG00000197616:ENST00000405093:exon37:c.C5644A:p.R1882S		S	0,00058
MYH6	14_23852501_C_T	ENSG00000197616:ENST00000356287:exon36:c.G5594A:p.R1865Q,ENSG00000197616:ENST00000405093:exon37:c.G5594A:p.R1865Q	rs138720701	P	0,00059
MYH6	14_23852520_C_T	ENSG00000197616:ENST00000356287:exon36:c.G5575A:p.D1859N,ENSG00000197616:ENST00000405093:exon37:c.G5575A:p.D1859N		S	0,00069
MYH6	14_23853739_C_T	ENSG00000197616:ENST00000356287:exon35:c.G5477A:p.G1826D,ENSG00000197616:ENST00000405093:exon36:c.G5477A:p.G1826D	rs200260229	D	0,00119
MYH6	14_23853740_C_T	ENSG00000197616:ENST00000356287:exon35:c.G5476A:p.G1826S,ENSG00000197616:ENST00000405093:exon36:c.G5476A:p.G1826S	rs202141059	D	0,00119
MYH6	14_23853806_G_T	ENSG00000197616:ENST00000356287:exon35:c.C5410A:p.Q1804K,ENSG00000197616:ENST00000405093:exon36:c.C5410A:p.Q1804K	rs144571463	D	0,00060
MYH6	14_23854220_TCT_-	ENSG00000197616:ENST00000356287:exon34:c.5192_5194del:p.1731_1732del,ENSG00000197616:ENST00000405093:exon35:c.5192_5194del:p.1731_1732del		N	0,00057
MYH6	14_23855136_C_A	ENST00000405093:exon35:c.5163+1G>T,ENST00000356287:exon34:c.5163+1G>T		L	0,00058
MYH6	14_23855160_G_A	ENSG00000197616:ENST00000356287:exon33:c.C5140T:p.R1714W,ENSG00000197616:ENST00000405093:exon34:c.C5140T:p.R1714W	rs140651265	S	0,00058
MYH6	14_23855228_C_T	ENSG00000197616:ENST00000356287:exon33:c.G5072A:p.R1691H,ENSG00000197616:ENST00000405093:exon34:c.G5072A:p.R1691H		S	0,00060
MYH6	14_23855609_T_C	ENSG00000197616:ENST00000356287:exon32:c.A4874G:p.N1625S,ENSG00000197616:ENST00000405093:exon33:c.A4874G:p.N1625S		S	0,00058
MYH6	14_23855779_G_T	ENSG00000197616:ENST00000356287:exon32:c.C4704A:p.N1568K,ENSG00000197616:ENST00000405093:exon33:c.C4704A:p.N1568K	rs149771264	S	0,00058
MYH6	14_23856786_C_G	ENSG00000197616:ENST00000356287:exon31:c.G4602C:p.Q1534H,ENSG00000197616:ENST00000405093:exon32:c.G4602C:p.Q1534H	rs199600772	S	0,00057
MYH6	14_23856987_C_T	ENSG00000197616:ENST00000356287:exon30:c.G4505A:p.R1502Q,ENSG00000197616:ENST00000405093:exon31:c.G4505A:p.R1502Q	rs199936506	D	0,00115
MYH6	14_23857371_A_T	ENSG00000197616:ENST00000356287:exon29:c.T4352A:p.F1451Y,ENSG00000197616:ENST00000405093:exon30:c.T4352A:p.F1451Y		N	0,00058
MYH6	14_23857395_G_T	ENSG00000197616:ENST00000356287:exon29:c.C4328A:p.A1443D,ENSG00000197616:ENST00000405093:exon30:c.C4328A:p.A1443D		P	0,00058
MYH6	14_23857530_C_T	ENSG00000197616:ENST00000356287:exon29:c.G4193A:p.R1398Q,ENSG00000197616:ENST00000405093:exon30:c.G4193A:p.R1398Q	rs150815925	D	0,00058
MYH6	14_23858107_G_A	ENSG00000197616:ENST00000356287:exon28:c.C4136T:p.T1379M,ENSG00000197616:ENST00000405093:exon29:c.C4136T:p.T1379M	rs145611185	P	0,00058
MYH6	14_23858161_C_T	ENSG00000197616:ENST00000356287:exon28:c.G4082A:p.R1361H,ENSG00000197616:ENST00000405093:exon29:c.G4082A:p.R1361H		S	0,00058

MYH6	14_23858648_G_A	ENSG00000197616:ENST00000356287:exon27:c.C3932T:p.T1311I,ENSG00000197616:ENST00000405093:exon28:c.C3932T:p.T1311I		S	0,00058
MYH6	14_23858687_G_A	ENSG00000197616:ENST00000356287:exon27:c.C3893T:p.A1298V,ENSG00000197616:ENST00000405093:exon28:c.C3893T:p.A1298V		N	0,00058
MYH6	14_23858720_C_T	ENSG00000197616:ENST00000356287:exon27:c.G3860A:p.G1287E,ENSG00000197616:ENST00000405093:exon28:c.G3860A:p.G1287E		N	0,00058
MYH6	14_23859370_C_T	ENSG00000197616:ENST00000356287:exon25:c.G3628A:p.D1210N,ENSG00000197616:ENST00000405093:exon26:c.G3628A:p.D1210N		S	0,00065
MYH6	14_23859484_C_T	ENSG00000197616:ENST00000356287:exon25:c.G3514A:p.E1172K,ENSG00000197616:ENST00000405093:exon26:c.G3514A:p.E1172K		S	0,00092
MYH6	14_23859571_G_A	ENSG00000197616:ENST00000356287:exon25:c.C3427T:p.R1143W,ENSG00000197616:ENST00000405093:exon26:c.C3427T:p.R1143W		S	0,00093
MYH6	14_23859652_G_T	ENSG00000197616:ENST00000356287:exon25:c.C3346A:p.R1116S,ENSG00000197616:ENST00000405093:exon26:c.C3346A:p.R1116S		P	0,00080
MYH6	14_23861814_T_A	ENSG00000197616:ENST00000356287:exon24:c.A3299T:p.Q1100L,ENSG00000197616:ENST00000405093:exon25:c.A3299T:p.Q1100L		S	0,00057
MYH6	14_23862208_C_T	ENSG00000197616:ENST00000356287:exon23:c.G3164A:p.R1055Q,ENSG00000197616:ENST00000405093:exon24:c.G3164A:p.R1055Q		N	0,00057
MYH6	14_23862646_C_A	ENSG00000197616:ENST00000356287:exon22:c.G3010T:p.A1004S,ENSG00000197616:ENST00000405093:exon23:c.G3010T:p.A1004S	rs143978652	P	0,00057
MYH6	14_23862870_C_T	ENST00000405093:exon23:c.2928+5G>A,ENST00000356287:exon22:c.2928+5G>A	rs28730772	L	0,00400
MYH6	14_23863087_G_A	ENSG00000197616:ENST00000356287:exon21:c.C2716T:p.R906C,ENSG00000197616:ENST00000405093:exon22:c.C2716T:p.R906C	rs143928061	S	0,00057
MYH6	14_23863348_G_A	ENSG00000197616:ENST00000356287:exon20:c.C2614T:p.R872C,ENSG00000197616:ENST00000405093:exon21:c.C2614T:p.R872C	rs201193346	S	0,00058
MYH6	14_23863384_G_A	ENSG00000197616:ENST00000356287:exon20:c.C2578T:p.R860C,ENSG00000197616:ENST00000405093:exon21:c.C2578T:p.R860C		S	0,00057
MYH6	14_23865497_G_A	ENSG00000197616:ENST00000356287:exon19:c.C2425T:p.R809C,ENSG00000197616:ENST00000405093:exon20:c.C2425T:p.R809C		S	0,00057
MYH6	14_23865569_G_A	ENSG00000197616:ENST00000356287:exon19:c.C2353T:p.R785C,ENSG00000197616:ENST00000405093:exon20:c.C2353T:p.R785C		S	0,00058
MYH6	14_23866275_G_T	ENSG00000197616:ENST00000356287:exon17:c.C2065A:p.P689T,ENSG00000197616:ENST00000405093:exon18:c.C2065A:p.P689T		N	0,00060
MYH6	14_23868065_T_G	ENSG00000197616:ENST00000356287:exon14:c.A1763C:p.D588A,ENSG00000197616:ENST00000405093:exon15:c.A1763C:p.D588A	rs142992009	D	0,00057
MYH6	14_23869462_C_T	ENST00000405093:exon15:c.1581+3G>A,ENST00000356287:exon14:c.1581+3G>A		L	0,00057

MYH6	14_23869967_C_A	ENSG00000197616:ENST00000356287:exon12:c.G1361T:p.R454L,ENSG00000197616:ENST00000405093:exon13:c.G1361T:p.R454L		S	0,00058
MYH6	14_23870001_G_A	ENSG00000197616:ENST00000356287:exon12:c.C1327T:p.R443C,ENSG00000197616:ENST00000405093:exon13:c.C1327T:p.R443C	rs182373896	S	0,00058
MYH6	14_23870012_C_T	ENSG00000197616:ENST00000356287:exon12:c.G1316A:p.W439X,ENSG00000197616:ENST00000405093:exon13:c.G1316A:p.W439X		L	0,00058
MYH6	14_23870034_C_G	ENSG00000197616:ENST00000356287:exon12:c.G1294C:p.V432L,ENSG00000197616:ENST00000405093:exon13:c.G1294C:p.V432L		N	0,00057
MYH6	14_23870151_A_C	ENSG00000197616:ENST00000356287:exon12:c.T1177G:p.S393A,ENSG00000197616:ENST00000405093:exon13:c.T1177G:p.S393A	rs199877580	D	0,00057
MYH6	14_23871758_C_G	ENSG00000197616:ENST00000356287:exon11:c.G1056C:p.K352N,ENSG00000197616:ENST00000405093:exon12:c.G1056C:p.K352N		S	0,00058
MYH6	14_23871766_C_T	ENSG00000197616:ENST00000356287:exon11:c.G1048A:p.V350I,ENSG00000197616:ENST00000405093:exon12:c.G1048A:p.V350I	rs200260629	D	0,00058
MYH6	14_23872631_A_T	ENSG00000197616:ENST00000356287:exon9:c.T824A:p.I275N,ENSG00000197616:ENST00000405093:exon10:c.T824A:p.I275N	rs201327273	P	0,00120
MYH6	14_23874309_G_A	ENSG00000197616:ENST00000356287:exon5:c.C530T:p.T177M,ENSG00000197616:ENST00000405093:exon6:c.C530T:p.T177M		S	0,00058
MYH6	14_23874525_C_T	ENSG00000197616:ENST00000356287:exon4:c.G409A:p.E137K,ENSG00000197616:ENST00000405093:exon5:c.G409A:p.E137K		N	0,00061
MYH6	14_23874889_C_T	ENSG00000197616:ENST00000356287:exon3:c.G292A:p.E98K,ENSG00000197616:ENST00000405093:exon4:c.G292A:p.E98K	rs140596256	D	0,00059
MYH6	14_23874936_G_A	ENSG00000197616:ENST00000356287:exon3:c.C245T:p.P82L,ENSG00000197616:ENST00000405093:exon4:c.C245T:p.P82L		S	0,00058
MYH6	14_23876352_C_G	ENSG00000197616:ENST00000356287:exon2:c.G81C:p.Q27H,ENSG00000197616:ENST00000405093:exon3:c.G81C:p.Q27H		N	0,00058
MYH6	14_23876363_G_T	ENSG00000197616:ENST00000356287:exon2:c.C70A:p.L24I,ENSG00000197616:ENST00000405093:exon3:c.C70A:p.L24I		N	0,00115
MYH6	14_23876785_C_T			L	0,00059
MYH7	14_23882979_T_A	ENSG00000092054:ENST00000355349:exon39:c.A5779T:p.I1927F		P	0,00058
MYH7	14_23883068_C_T	ENSG00000092054:ENST00000355349:exon39:c.G5690A:p.R1897H		S	0,00058
MYH7	14_23883217_G_A	ENSG00000092054:ENST00000355349:exon38:c.C5654T:p.A1885V		N	0,00059
MYH7	14_23884200_G_A	ENST00000355349:exon38:c.5559+4C>T		L	0,00058
MYH7	14_23884421_C_T	ENSG00000092054:ENST00000355349:exon37:c.G5342A:p.R1781H		P	0,00058
MYH7	14_23884469_A_T	ENSG00000092054:ENST00000355349:exon37:c.T5294A:p.M1765K		S	0,00058

MYH7	14_23884860_C_T	ENSG00000092054:ENST00000355349:exon35:c.G5135A:p.R1712Q	rs193922390	P	0,00063
MYH7	14_23885349_C_T	ENSG00000092054:ENST00000355349:exon34:c.G4817A:p.R1606H		N	0,00058
MYH7	14_23885502_T_C	ENSG00000092054:ENST00000355349:exon34:c.A4664G:p.E1555G		P	0,00058
MYH7	14_23886806_C_T	ENSG00000092054:ENST00000355349:exon31:c.G4259A:p.R1420Q		P	0,00058
MYH7	14_23886815_G_A	ENSG00000092054:ENST00000355349:exon31:c.C4250T:p.T1417I		S	0,00058
MYH7	14_23887522_C_T	ENSG00000092054:ENST00000355349:exon30:c.G4066A:p.E1356K		P	0,00296
MYH7	14_23887607_G_T	ENSG00000092054:ENST00000355349:exon30:c.C3981A:p.N1327K	rs141764279	D	0,00058
MYH7	14_23888775_T_C	ENSG00000092054:ENST00000355349:exon28:c.A3770G:p.N1257S		N	0,00058
MYH7	14_23889158_C_T	ENSG00000092054:ENST00000355349:exon27:c.G3622A:p.D1208N		S	0,00062
MYH7	14_23889187_T_C	ENSG00000092054:ENST00000355349:exon27:c.A3593G:p.D1198G		S	0,00070
MYH7	14_23892910_A_G	ENSG00000092054:ENST00000355349:exon24:c.T2945C:p.M982T	rs145532615	P	0,00057
MYH7	14_23893148_C_G	ENSG00000092054:ENST00000355349:exon23:c.G2890C:p.V964L	rs45496496	P	0,00344
MYH7	14_23893192_T_A	ENSG00000092054:ENST00000355349:exon23:c.A2846T:p.E949V		S	0,00057
MYH7	14_23893246_T_C	ENSG00000092054:ENST00000355349:exon23:c.A2792G:p.E931G		S	0,00057
MYH7	14_23893255_T_C	ENSG00000092054:ENST00000355349:exon23:c.A2783G:p.D928G		S	0,00057
MYH7	14_23893268_C_G	ENSG00000092054:ENST00000355349:exon23:c.G2770C:p.E924Q		P	0,00057
MYH7	14_23893268_C_T	ENSG00000092054:ENST00000355349:exon23:c.G2770A:p.E924K	rs121913628	P	0,00057
MYH7	14_23893316_G_C	ENSG00000092054:ENST00000355349:exon23:c.C2722G:p.L908V	rs121913631	P	0,00057
MYH7	14_23893321_T_C	ENSG00000092054:ENST00000355349:exon23:c.A2717G:p.D906G		P	0,00286
MYH7	14_23893357_T_C	ENSG00000092054:ENST00000355349:exon23:c.A2681G:p.E894G		P	0,00172
MYH7	14_23893988_T_G	ENSG00000092054:ENST00000355349:exon22:c.A2669C:p.Q890P		S	0,00060
MYH7	14_23894048_C_T	ENSG00000092054:ENST00000355349:exon22:c.G2609A:p.R870H	rs36211715	P	0,00293
MYH7	14_23894051_C_G	ENSG00000092054:ENST00000355349:exon22:c.G2606C:p.R869P		N	0,00117
MYH7	14_23894051_C_T	ENSG00000092054:ENST00000355349:exon22:c.G2606A:p.R869H	rs202141173	P	0,00058
MYH7	14_23894052_G_A	ENSG00000092054:ENST00000355349:exon22:c.C2605T:p.R869C		P	0,00117
MYH7	14_23894052_G_T	ENSG00000092054:ENST00000355349:exon22:c.C2605A:p.R869S		N	0,00058
MYH7	14_23894084_C_T	ENSG00000092054:ENST00000355349:exon22:c.G2573A:p.R858H	rs2856897	P	0,00058

MYH7	14_23894118_T_C	ENSG00000092054:ENST00000355349:exon22:c.A2539G:p.K847E		P	0,00116
MYH7	14_23894118_TCT_-	ENSG00000092054:ENST00000355349:exon22:c.2537_2539del:p.846_847del		N	0,00058
MYH7	14_23894123_C_T	ENSG00000092054:ENST00000355349:exon22:c.G2534A:p.R845K		N	0,00058
MYH7	14_23894193_T_A	ENSG00000092054:ENST00000355349:exon22:c.A2464T:p.M822L		P	0,00058
MYH7	14_23894525_C_T	ENSG00000092054:ENST00000355349:exon21:c.G2389A:p.A797T	rs3218716	P	0,00172
MYH7	14_23894539_G_T	ENSG00000092054:ENST00000355349:exon21:c.C2375A:p.S792Y		N	0,00058
MYH7	14_23894554_C_T	ENSG00000092054:ENST00000355349:exon21:c.G2360A:p.R787H		P	0,00173
MYH7	14_23894566_C_T	ENSG00000092054:ENST00000355349:exon21:c.G2348A:p.R783H		P	0,00058
MYH7	14_23894969_C_A	ENSG00000092054:ENST00000355349:exon20:c.G2221T:p.G741W		P	0,00057
MYH7	14_23894969_C_G	ENSG00000092054:ENST00000355349:exon20:c.G2221C:p.G741R	rs121913632	P	0,00057
MYH7	14_23895023_G_A	ENSG00000092054:ENST00000355349:exon20:c.C2167T:p.R723C	rs121913630	P	0,00230
MYH7	14_23895023_G_C	ENSG00000092054:ENST00000355349:exon20:c.C2167G:p.R723G		P	0,00057
MYH7	14_23895179_C_T	ENSG00000092054:ENST00000355349:exon19:c.G2156A:p.R719Q	rs121913641	P	0,00118
MYH7	14_23895180_G_A	ENSG00000092054:ENST00000355349:exon19:c.C2155T:p.R719W	rs121913637	P	0,00059
MYH7	14_23895243_C_G	ENSG00000092054:ENST00000355349:exon19:c.G2092C:p.V698L		N	0,00065
MYH7	14_23895254_C_T	ENSG00000092054:ENST00000355349:exon19:c.G2081A:p.R694H		P	0,00065
MYH7	14_23896042_C_T	ENSG00000092054:ENST00000355349:exon18:c.G1988A:p.R663H		P	0,00287
MYH7	14_23896043_G_A	ENSG00000092054:ENST00000355349:exon18:c.C1987T:p.R663C		P	0,00172
MYH7	14_23896812_A_T	ENSG00000092054:ENST00000355349:exon16:c.T1870A:p.Y624N		P	0,00057
MYH7	14_23896866_C_T	ENSG00000092054:ENST00000355349:exon16:c.G1816A:p.V606M	rs121913627	P	0,00229
MYH7	14_23897796_C_A	ENSG00000092054:ENST00000355349:exon15:c.G1491T:p.E497D		P	0,00057
MYH7	14_23897840_C_T	ENSG00000092054:ENST00000355349:exon15:c.G1447A:p.E483K	rs121913651	P	0,00057
MYH7	14_23897854_A_T	ENSG00000092054:ENST00000355349:exon15:c.T1433A:p.I478N		S	0,00057
MYH7	14_23898213_C_A	ENSG00000092054:ENST00000355349:exon14:c.G1358T:p.R453L		S	0,00057
MYH7	14_23898240_T_C	ENSG00000092054:ENST00000355349:exon14:c.A1331G:p.N444S		P	0,00057
MYH7	14_23898292_G_T	ENSG00000092054:ENST00000355349:exon14:c.C1279A:p.L427M		P	0,00230
MYH7	14_23898464_C_T	ENSG00000092054:ENST00000355349:exon13:c.G1231A:p.V411I		P	0,00057

MYH7	14_23898487_C_T	ENSG00000092054:ENST00000355349:exon13:c.G1208A:p.R403Q	rs121913624	P	0,00057
MYH7	14_23898488_G_A	ENSG00000092054:ENST00000355349:exon13:c.C1207T:p.R403W	rs3218714	P	0,00172
MYH7	14_23898551_C_A	ENSG00000092054:ENST00000355349:exon13:c.G1144T:p.D382Y		P	0,00115
MYH7	14_23899059_C_A	ENSG00000092054:ENST00000355349:exon12:c.G1063T:p.A355S		N	0,00115
MYH7	14_23899059_C_T	ENSG00000092054:ENST00000355349:exon12:c.G1063A:p.A355T		P	0,00229
MYH7	14_23899071_T_C	ENSG00000092054:ENST00000355349:exon12:c.A1051G:p.K351E		P	0,00115
MYH7	14_23899101_A_G	ENSG00000092054:ENST00000355349:exon12:c.T1021C:p.F341L		S	0,00057
MYH7	14_23899864_G_T	ENSG00000092054:ENST00000355349:exon11:c.C904A:p.L302M		S	0,00057
MYH7	14_23900635_A_G	ENSG00000092054:ENST00000355349:exon9:c.T788C:p.I263T		P	0,00057
MYH7	14_23900656_C_T	ENSG00000092054:ENST00000355349:exon9:c.G767A:p.G256E	rs121913633	P	0,00057
MYH7	14_23900677_C_T	ENSG00000092054:ENST00000355349:exon9:c.G746A:p.R249Q	rs3218713	P	0,00057
MYH7	14_23900811_C_T	ENSG00000092054:ENST00000355349:exon8:c.G715A:p.D239N		P	0,00058
MYH7	14_23901712_C_T	ENSG00000092054:ENST00000355349:exon6:c.G506A:p.R169K		N	0,00058
MYH7	14_23901922_C_T	ENSG00000092054:ENST00000355349:exon5:c.G428A:p.R143Q		P	0,00059
MYH7	14_23902293_G_T	ENSG00000092054:ENST00000355349:exon4:c.C345A:p.Y115X		L	0,00058
MYH7	14_23902340_C_T	ENSG00000092054:ENST00000355349:exon4:c.G298A:p.A100T		S	0,00058
MYH7	14_23902892_C_T	ENSG00000092054:ENST00000355349:exon3:c.G50A:p.R17H		S	0,00058
MYH7	14_23903456_G_A		rs45566639	L	0,00401
MYL2	12_111350901_T_G	ENSG00000111245:ENST00000548438:exon5:c.A359C:p.E120A,ENSG00000111245:ENST00000228841:exon6:c.A401C:p.E134A	rs143139258	S	0,00115
MYL2	12_111350926_G_C	ENSG00000111245:ENST00000548438:exon5:c.C334G:p.Q112E,ENSG00000111245:ENST00000550439:exon5:c.C319G:p.Q107E,ENSG00000111245:ENST00000228841:exon6:c.C376G:p.Q126E		S	0,00058
MYL2	12_111352004_C_G	ENSG00000111245:ENST00000548438:exon3:c.G218C:p.G73A,ENSG00000111245:ENST00000550439:exon3:c.G203C:p.G68A,ENSG00000111245:ENST00000228841:exon4:c.G260C:p.G87A		S	0,00058
MYL2	12_111352091_C_T	ENSG00000111245:ENST00000548438:exon3:c.G131A:p.R44Q,ENSG00000111245:ENST00000550439:exon3:c.G116A:p.R39Q,ENSG00000111245:ENST00000228841:exon4:c.G173A:p.R58Q	rs104894369	P	0,00057
MYL2	12_111353547_G_T	ENSG00000111245:ENST00000550439:exon2:c.C84A:p.N28K,ENSG00000111245:ENST00000228841:exon3:c.C141A:p.N47K	rs199474808	P	0,00057
MYL2	12_111356937_C_T	ENSG00000111245:ENST00000550439:exon1:c.G7A:p.E3K,ENSG00000111245:ENST00000228841:exon2:c.G64A:p.E22K,ENSG00000111245:ENST00000548438:exon2:c.G64A:p.E22K	rs104894368	P	0,00057

MYL2	12_111356964_C_T	ENSG00000111245:ENST00000228841:exon2:c.G37A:p.A13T,ENSG00000111245:ENST00000548438:exon2:c.G37A:p.A13T	rs104894363	P	0,00115
MYL3	3_46899903_T_C	ENSG00000160808:ENST00000292327:exon5:c.A530G:p.E177G,ENSG00000160808:ENST00000395869:exon5:c.A530G:p.E177G	rs193922391	S	0,00058
MYL3	3_46900970_G_A	ENSG00000160808:ENST00000292327:exon4:c.C476T:p.T159M,ENSG00000160808:ENST00000395869:exon4:c.C476T:p.T159M		S	0,00058
MYL3	3_46900986_G_A	ENSG00000160808:ENST00000292327:exon4:c.C460T:p.R154C,ENSG00000160808:ENST00000395869:exon4:c.C460T:p.R154C	rs143852164	S	0,00115
MYL3	3_46901009_C_T	ENSG00000160808:ENST00000292327:exon4:c.G437A:p.G146D,ENSG00000160808:ENST00000395869:exon4:c.G437A:p.G146D		S	0,00058
MYL3	3_46902285_C_T	ENSG00000160808:ENST00000292327:exon3:c.G188A:p.R63H,ENSG00000160808:ENST00000395869:exon3:c.G188A:p.R63H	rs139354105	S	0,00058
PDLIM3	4_186423516_T_C	ENSG00000154553:ENST00000284771:exon7:c.A883G:p.T295A,ENSG00000154553:ENST00000284770:exon8:c.A1027G:p.T343A		N	0,00172
PDLIM3	4_186423579_C_T	ENSG00000154553:ENST00000284771:exon7:c.G820A:p.D274N,ENSG00000154553:ENST00000284770:exon8:c.G964A:p.D322N		S	0,00057
PDLIM3	4_186427754_C_T	ENSG00000154553:ENST00000284771:exon5:c.G571A:p.D191N,ENSG00000154553:ENST00000284770:exon6:c.G715A:p.D239N	rs142143310	D	0,00058
PDLIM3	4_186427786_G_A	ENSG00000154553:ENST00000284771:exon5:c.C539T:p.P180L,ENSG00000154553:ENST00000284770:exon6:c.C683T:p.P228L	rs201185673	D	0,00115
PDLIM3	4_186429568_C_A	ENSG00000154553:ENST00000284770:exon5:c.G547T:p.V183L		N	0,00057
PDLIM3	4_186435447_A_G	ENSG00000154553:ENST00000284767:exon5:c.T563C:p.L188P		N	0,00057
PDLIM3	4_186435483_G_C	ENSG00000154553:ENST00000284770:exon4:c.C339G:p.N113K,ENSG00000154553:ENST00000284767:exon5:c.C527G:p.T176S		N	0,00057
PDLIM3	4_186444600_C_T	ENSG00000154553:ENST00000505886:exon2:c.G94A:p.G32R,ENSG00000154553:ENST00000512293:exon2:c.G94A:p.G32R	rs200354645	D	0,00115
PDLIM3	4_186446250_T_C	ENSG00000154553:ENST00000284767:exon2:c.A169G:p.T57A,ENSG00000154553:ENST00000284770:exon2:c.A169G:p.T57A,ENSG00000154553:ENST00000284771:exon2:c.A169G:p.T57A	rs142951316	D	0,00115
PKP2	12_32949101_G_T	ENSG00000057294:ENST00000340811:exon11:c.C2299A:p.R767S,ENSG00000057294:ENST00000070846:exon12:c.C2431A:p.R811S	rs139734328	D	0,00058
PKP2	12_32955491_C_G	ENST00000340811:exon11:c.2014-1G>C,ENST00000070846:exon12:c.2146-1G>C	rs193922674	P	0,00057
PKP2	12_32975431_A_C	ENSG00000057294:ENST00000340811:exon8:c.T1809G:p.C603W,ENSG00000057294:ENST00000070846:exon9:c.T1941G:p.C647W	rs149392678	S	0,00114
PKP2	12_32994007_C_-	ENSG00000057294:ENST00000340811:exon6:c.1511delG:p.G504fs,ENSG00000057294:ENST00000070846:exon7:c.1643delG:p.G548fs		P	0,00057

PKP2	12_32994100_T_C	ENSG00000057294:ENST00000340811:exon6:c.A1418G:p.N473S,ENSG00000057294:ENST00000070846:exon7:c.A1550G:p.N517S	rs144536197	D	0,00115
PKP2	12_32996206_C_T	ENSG00000057294:ENST00000070846:exon6:c.G1420A:p.A474T	rs138538072	D	0,00193
PKP2	12_33021936_C_T	ENSG00000057294:ENST00000070846:exon4:c.G1095A:p.M365I,ENSG00000057294:ENST00000340811:exon4:c.G1095A:p.M365I		N	0,00058
PKP2	12_33021997_C_G	ENST00000340811:exon5:c.1035-1G>C,ENST00000070846:exon5:c.1035-1G>C		L	0,00057
PKP2	12_33030850_C_A	ENSG00000057294:ENST00000070846:exon3:c.G964T:p.G322C,ENSG00000057294:ENST00000340811:exon3:c.G964T:p.G322C		S	0,00064
PKP2	12_33031039_C_A	ENSG00000057294:ENST00000070846:exon3:c.G775T:p.E259X,ENSG00000057294:ENST00000340811:exon3:c.G775T:p.E259X		P	0,00062
PKP2	12_33031321_C_T	ENSG00000057294:ENST00000070846:exon3:c.G493A:p.D165N,ENSG00000057294:ENST00000340811:exon3:c.G493A:p.D165N		S	0,00118
PKP2	12_33031329_G_A	ENSG00000057294:ENST00000070846:exon3:c.C485T:p.T162M,ENSG00000057294:ENST00000340811:exon3:c.C485T:p.T162M		N	0,00059
PKP2	12_33031468_T_C	ENSG00000057294:ENST00000070846:exon3:c.A346G:p.T116A,ENSG00000057294:ENST00000340811:exon3:c.A346G:p.T116A		N	0,00057
PKP2	12_33031883_G_C	ENSG00000057294:ENST00000070846:exon2:c.C307G:p.P103A,ENSG00000057294:ENST00000340811:exon2:c.C307G:p.P103A		N	0,00057
PKP2	12_33031883_G_T	ENSG00000057294:ENST00000070846:exon2:c.C307A:p.P103T,ENSG00000057294:ENST00000340811:exon2:c.C307A:p.P103T	rs139215336	D	0,00057
PKP2	12_33031888_C_T	ENSG00000057294:ENST00000070846:exon2:c.G302A:p.R101H,ENSG00000057294:ENST00000340811:exon2:c.G302A:p.R101H	rs149542398	P	0,00115
PKP2	12_33031931_C_G	ENSG00000057294:ENST00000070846:exon2:c.G259C:p.V87L,ENSG00000057294:ENST00000340811:exon2:c.G259C:p.V87L		P	0,00057
PKP2	12_33049492_C_A	ENSG00000057294:ENST00000070846:exon1:c.G174T:p.E58D,ENSG00000057294:ENST00000340811:exon1:c.G174T:p.E58D	rs146708884	P	0,00771
PKP4	2_159313728_A_C			L	0,00993
PKP4	2_159459593_A_G	ENSG00000144283:ENST00000389757:exon4:c.A257G:p.K86R,ENSG00000144283:ENST00000389759:exon4:c.A257G:p.K86R,ENSG00000144283:ENST00000421462:exon4:c.A257G:p.K86R,ENSG00000144283:ENST00000426248:exon4:c.A257G:p.K86R	rs144452632	D	0,00057
PKP4	2_159459601_C_T	ENSG00000144283:ENST00000389757:exon4:c.C265T:p.P89S,ENSG00000144283:ENST00000389759:exon4:c.C265T:p.P89S,ENSG00000144283:ENST00000421462:exon4:c.C265T:p.P89S,ENSG00000144283:ENST00000426248:exon4:c.C265T:p.P89S	rs141436976	D	0,00057
PKP4	2_159477550_A_G	ENSG00000144283:ENST00000389757:exon5:c.A329G:p.Q110R,ENSG00000144283:ENST00000389759:exon5:c.A329G:p.Q110R,ENSG00000144283:ENST00000421462:exon5:c.A329G:p.Q110R,ENSG00000144283:ENST00000426248:exon5:c.A329G:p.Q110R	rs148019751	D	0,00057

PKP4	2_159477598_A_G	ENSG00000144283:ENST00000389757:exon5:c.A377G:p.Y126C,ENSG00000144283:ENST00000389759:exon5:c.A377G:p.Y126C,ENSG00000144283:ENST00000421462:exon5:c.A377G:p.Y126C,ENSG00000144283:ENST00000426248:exon5:c.A377G:p.Y126C		S	0,00114
PKP4	2_159481523_G_C	ENSG00000144283:ENST00000389757:exon7:c.G737C:p.G246A,ENSG00000144283:ENST00000389759:exon7:c.G737C:p.G246A		N	0,00058
PKP4	2_159481526_C_T	ENSG00000144283:ENST00000389757:exon7:c.C740T:p.S247F,ENSG00000144283:ENST00000389759:exon7:c.C740T:p.S247F		N	0,00058
PKP4	2_159481840_C_A	ENSG00000144283:ENST00000389757:exon7:c.C1054A:p.P352T,ENSG00000144283:ENST00000389759:exon7:c.C1054A:p.P352T		N	0,00058
PKP4	2_159481864_G_T	ENSG00000144283:ENST00000389757:exon7:c.G1078T:p.D360Y,ENSG00000144283:ENST00000389759:exon7:c.G1078T:p.D360Y	rs147567711	S	0,00058
PKP4	2_159481865_A_G	ENSG00000144283:ENST00000389757:exon7:c.A1079G:p.D360G,ENSG00000144283:ENST00000389759:exon7:c.A1079G:p.D360G	rs147809285	D	0,00058
PKP4	2_159497153_G_A	ENSG00000144283:ENST00000389757:exon10:c.G1577A:p.R526H,ENSG00000144283:ENST00000389759:exon10:c.G1577A:p.R526H	rs144253065	S	0,00057
PKP4	2_159499094_G_A	ENSG00000144283:ENST00000389757:exon11:c.G1792A:p.V598I,ENSG00000144283:ENST00000389759:exon11:c.G1792A:p.V598I		N	0,00057
PKP4	2_159499181_A_G	ENSG00000144283:ENST00000389757:exon11:c.A1879G:p.I627V,ENSG00000144283:ENST00000389759:exon11:c.A1879G:p.I627V		N	0,00057
PKP4	2_159517919_A_G	ENSG00000144283:ENST00000389757:exon13:c.A2168G:p.Y723C,ENSG00000144283:ENST00000389759:exon13:c.A2168G:p.Y723C	rs150425961	S	0,00057
PKP4	2_159519410_C_T	ENSG00000144283:ENST00000389757:exon14:c.C2213T:p.T738M,ENSG00000144283:ENST00000389759:exon14:c.C2213T:p.T738M	rs201257617	S	0,00058
PKP4	2_159519557_G_A	ENSG00000144283:ENST00000389757:exon14:c.G2360A:p.G787E,ENSG00000144283:ENST00000389759:exon14:c.G2360A:p.G787E		S	0,00057
PKP4	2_159519581_G_A	ENSG00000144283:ENST00000389757:exon14:c.G2384A:p.R795K,ENSG00000144283:ENST00000389759:exon14:c.G2384A:p.R795K	rs139221917	D	0,00115
PKP4	2_159519846_G_T	ENSG00000144283:ENST00000389757:exon15:c.G2466T:p.W822C,ENSG00000144283:ENST00000389759:exon15:c.G2466T:p.W822C		S	0,00058
PKP4	2_159523058_G_A	ENSG00000144283:ENST00000389757:exon16:c.G2711A:p.R904H,ENSG00000144283:ENST00000389759:exon16:c.G2711A:p.R904H		S	0,00057
PKP4	2_159530233_C_T	ENSG00000144283:ENST00000389757:exon18:c.C2969T:p.T990I,ENSG00000144283:ENST00000389759:exon18:c.C2969T:p.T990I	rs190318071	D	0,00057
PKP4	2_159530257_G_A	ENSG00000144283:ENST00000389757:exon18:c.G2993A:p.R998Q,ENSG00000144283:ENST00000389759:exon18:c.G2993A:p.R998Q		S	0,00057
PKP4	2_159536972_C_G	ENSG00000144283:ENST00000389757:exon21:c.C3233G:p.S1078C,ENSG00000144283:ENST00000389759:exon22:c.C3362G:p.S1121C		S	0,00114

PKP4	2_159537050_G_A	ENSG00000144283:ENST00000389757:exon21:c.G3311A:p.R1104Q,ENSG00000144283:ENST00000389759:exon22:c.G3440A:p.R1147Q		N	0,00057
PLN	6_118879986_A_T			L	0,00057
PLN	6_118880110_G_A	ENSG00000198523:ENST00000357525:exon2:c.G26A:p.R9H		S	0,00057
PLN	6_118880137_T_C	ENSG00000198523:ENST00000357525:exon2:c.T53C:p.I18T		N	0,00057
PLN	6_118880145_-_CT	ENSG00000198523:ENST00000357525:exon2:c.61_62insCT:p.P21fs		L	0,00057
PLN	6_118880157_C_T	ENSG00000198523:ENST00000357525:exon2:c.C73T:p.R25C		N	0,00057
PLN	6_118880158_G_A	ENSG00000198523:ENST00000357525:exon2:c.G74A:p.R25H		N	0,00057
PLN	6_118880236_T_C	ENSG00000198523:ENST00000357525:exon2:c.T152C:p.L51P		S	0,00057
PNN	14_39646638_A_G	ENSG00000100941:ENST00000216832:exon4:c.A277G:p.R93G,ENSG00000100941:ENST00000553331:exon4:c.A277G:p.R93G,ENSG00000100941:ENST00000556530:exon4:c.A277G:p.R93G		N	0,00058
PNN	14_39649827_C_T	ENSG00000100941:ENST00000216832:exon9:c.C914T:p.A305V	rs140529795	D	0,00057
PNN	14_39650139_A_G	ENSG00000100941:ENST00000216832:exon9:c.A1226G:p.N409S	rs143201887	D	0,00057
PNN	14_39650169_A_G	ENSG00000100941:ENST00000216832:exon9:c.A1256G:p.N419S	rs145173115	D	0,00057
PNN	14_39650261_A_G	ENSG00000100941:ENST00000216832:exon9:c.A1348G:p.S450G	rs145827544	D	0,00057
PNN	14_39650320_A_T	ENSG00000100941:ENST00000216832:exon9:c.A1407T:p.Q469H	rs148193612	D	0,00058
PNN	14_39650334_CTCAAC_-	ENSG00000100941:ENST00000216832:exon9:c.1421_1426del:p.474_476del		N	0,00058
PNN	14_39650338_ACCTCA_-	ENSG00000100941:ENST00000216832:exon9:c.1425_1430del:p.475_477del		N	0,00058
PNN	14_39650559_A_C	ENSG00000100941:ENST00000216832:exon9:c.A1646C:p.H549P		N	0,00057
PNN	14_39650883_C_G	ENSG00000100941:ENST00000216832:exon9:c.C1970G:p.T657S		N	0,00057
RBM20	10_112404334_-_GCA	ENSG00000203867:ENST00000369519:exon1:c.122_123insGCA:p.M41delinsMQ		N	0,01980
RBM20	10_112404342_-_AGC	ENSG00000203867:ENST00000369519:exon1:c.130_131insAGC:p.P44delinsQP		N	0,01754
RBM20	10_112541047_G_T	ENSG00000203867:ENST00000369519:exon2:c.G680T:p.G227V	rs202238753	D	0,00058
RBM20	10_112541290_T_C	ENSG00000203867:ENST00000369519:exon2:c.T923C:p.V308A		N	0,00059
RBM20	10_112541394_C_T	ENSG00000203867:ENST00000369519:exon2:c.C1027T:p.H343Y	rs112226602	D	0,00058
RBM20	10_112541424_G_A	ENSG00000203867:ENST00000369519:exon2:c.G1057A:p.E353K		S	0,00058
RBM20	10_112541460_G_A	ENSG00000203867:ENST00000369519:exon2:c.G1093A:p.G365R	rs201047984	S	0,00058
RBM20	10_112541502_G_A	ENSG00000203867:ENST00000369519:exon2:c.G1135A:p.G379R	rs199842148	D	0,00057

RBM20	10_112541511_G_T	ENSG00000203867:ENST00000369519:exon2:c.G1144T:p.A382S		N	0,00057
RBM20	10_112541568_G_A	ENSG00000203867:ENST00000369519:exon2:c.G1201A:p.D401N		S	0,00057
RBM20	10_112541632_T_C	ENSG00000203867:ENST00000369519:exon2:c.T1265C:p.F422S		S	0,00057
RBM20	10_112544571_C_T	ENSG00000203867:ENST00000369519:exon5:c.C1451T:p.T484I	rs116442272	D	0,00057
RBM20	10_112557371_G_A	ENSG00000203867:ENST00000369519:exon6:c.G1633A:p.V545I		N	0,00057
RBM20	10_112559642_G_A	ENSG00000203867:ENST00000369519:exon7:c.G1766A:p.R589Q		N	0,00115
RBM20	10_112572113_C_T	ENSG00000203867:ENST00000369519:exon9:c.C1958T:p.T653I		S	0,00060
RBM20	10_112572169_G_A	ENSG00000203867:ENST00000369519:exon9:c.G2014A:p.G672S		N	0,00061
RBM20	10_112572271_C_A	ENSG00000203867:ENST00000369519:exon9:c.C2116A:p.P706T		N	0,00059
RBM20	10_112572356_G_A	ENSG00000203867:ENST00000369519:exon9:c.G2201A:p.R734Q		S	0,00059
RBM20	10_112572368_C_T	ENSG00000203867:ENST00000369519:exon9:c.C2213T:p.P738L		N	0,00059
RBM20	10_112572394_C_T	ENSG00000203867:ENST00000369519:exon9:c.C2239T:p.H747Y		S	0,00059
RBM20	10_112572419_G_A	ENSG00000203867:ENST00000369519:exon9:c.G2264A:p.R755H		S	0,00058
RBM20	10_112572473_A_G	ENSG00000203867:ENST00000369519:exon9:c.A2318G:p.K773R	rs181769913	D	0,00058
RBM20	10_112572488_C_T	ENSG00000203867:ENST00000369519:exon9:c.C2333T:p.A778V		N	0,00058
RBM20	10_112581039_G_A	ENSG00000203867:ENST00000369519:exon11:c.G2662A:p.D888N	rs201370621	P	0,00344
RBM20	10_112581264_A_G	ENSG00000203867:ENST00000369519:exon11:c.A2887G:p.K963E		N	0,00057
RBM20	10_112581282_G_A	ENSG00000203867:ENST00000369519:exon11:c.G2905A:p.V969I		N	0,00057
RBM20	10_112581381_C_G	ENSG00000203867:ENST00000369519:exon11:c.C3004G:p.L1002V		N	0,00115
RBM20	10_112581391_A_G	ENSG00000203867:ENST00000369519:exon11:c.A3014G:p.D1005G		S	0,00057
RBM20	10_112581400_G_A	ENSG00000203867:ENST00000369519:exon11:c.G3023A:p.R1008Q		N	0,00115
RBM20	10_112581424_G_C	ENSG00000203867:ENST00000369519:exon11:c.G3047C:p.G1016A		S	0,00057
RBM20	10_112581492_C_T	ENSG00000203867:ENST00000369519:exon11:c.C3115T:p.P1039S		N	0,00057
RBM20	10_112581642_C_G	ENSG00000203867:ENST00000369519:exon11:c.C3265G:p.P1089A	rs147356378	D	0,00058
RBM20	10_112581643_C_G	ENSG00000203867:ENST00000369519:exon11:c.C3266G:p.P1089R		N	0,00057
RYR2	1_237538086_G_A	ENSG00000198626:ENST00000542537:exon6:c.G406A:p.D136N,ENSG00000198626:ENST00000366574:exon7:c.G454A:p.D152N,ENSG00000198626:ENST00000360064:exon8:c.G448A:p.D150N		N	0,00058

RYR2	1_237608773_A_G	ENSG00000198626:ENST00000542537:exon13:c.A1195G:p.T399A,ENSG00000198626:ENST00000366574:exon14:c.A1243G:p.T415A,ENSG00000198626:ENST00000360064:exon15:c.A1237G:p.T413A		N	0,00057
RYR2	1_237619933_C_G	ENSG00000198626:ENST00000542537:exon15:c.C1462G:p.R488G,ENSG00000198626:ENST00000366574:exon16:c.C1510G:p.R504G,ENSG00000198626:ENST00000360064:exon17:c.C1504G:p.R502G		S	0,00057
RYR2	1_237619982_G_T	ENSG00000198626:ENST00000542537:exon15:c.G1511T:p.R504L,ENSG00000198626:ENST00000366574:exon16:c.G1559T:p.R520L,ENSG00000198626:ENST00000360064:exon17:c.G1553T:p.R518L		N	0,00057
RYR2	1_237659825_T_G	ENSG00000198626:ENST00000542537:exon19:c.T1928G:p.I643S,ENSG00000198626:ENST00000366574:exon20:c.T1976G:p.I659S,ENSG00000198626:ENST00000360064:exon21:c.T1970G:p.I657S		S	0,00057
RYR2	1_237659929_C_T	ENSG00000198626:ENST00000542537:exon19:c.C2032T:p.R678X,ENSG00000198626:ENST00000366574:exon20:c.C2080T:p.R694X,ENSG00000198626:ENST00000360064:exon21:c.C2074T:p.R692X		L	0,00057
RYR2	1_237659953_G_A	ENSG00000198626:ENST00000542537:exon19:c.G2056A:p.G686R,ENSG00000198626:ENST00000366574:exon20:c.G2104A:p.G702R,ENSG00000198626:ENST00000360064:exon21:c.G2098A:p.G700R		S	0,00057
RYR2	1_237660057_G_A	ENST00000366574:exon20:c.2203+5G>A,ENST00000360064:exon21:c.2197+5G>A,ENST00000542537:exon19:c.2155+5G>A		L	0,00057
RYR2	1_237664074_G_A	ENSG00000198626:ENST00000542537:exon20:c.G2219A:p.S740N,ENSG00000198626:ENST00000366574:exon21:c.G2267A:p.S756N,ENSG00000198626:ENST00000360064:exon22:c.G2261A:p.S754N	rs193922623	S	0,00057
RYR2	1_237664112_C_G	ENSG00000198626:ENST00000542537:exon20:c.C2257G:p.R753G,ENSG00000198626:ENST00000366574:exon21:c.C2305G:p.R769G,ENSG00000198626:ENST00000360064:exon22:c.C2299G:p.R767G		S	0,00057
RYR2	1_237664149_A_G	ENSG00000198626:ENST00000542537:exon20:c.A2294G:p.N765S,ENSG00000198626:ENST00000366574:exon21:c.A2342G:p.N781S,ENSG00000198626:ENST00000360064:exon22:c.A2336G:p.N779S		S	0,00057
RYR2	1_237666593_C_T	ENSG00000198626:ENST00000542537:exon21:c.C2353T:p.R785C,ENSG00000198626:ENST00000366574:exon22:c.C2401T:p.R801C,ENSG00000198626:ENST00000360064:exon23:c.C2395T:p.R799C		S	0,00057
RYR2	1_237666731_A_G	ENSG00000198626:ENST00000542537:exon21:c.A2491G:p.T831A,ENSG00000198626:ENST00000366574:exon22:c.A2539G:p.T847A,ENSG00000198626:ENST00000360064:exon23:c.A2533G:p.T845A		N	0,00057
RYR2	1_237670112_C_G	ENSG00000198626:ENST00000542537:exon22:c.C2668G:p.P890A,ENSG00000198626:ENST00000366574:exon23:c.C2716G:p.P906A,ENSG00000198626:ENST00000360064:exon24:c.C2710G:p.P904A		S	0,00057
RYR2	1_237693732_T_C	ENSG00000198626:ENST00000542537:exon24:c.T2780C:p.L927S,ENSG00000198626:ENST00000366574:exon25:c.T2828C:p.L943S,ENSG00000198626:ENST00000360064:exon26:c.T2822C:p.L941S		S	0,00058

RYR2	1_237711759_G_T	ENSG00000198626:ENST00000542537:exon25:c.G2887T:p.A963S,ENSG00000198626:ENST00000366574:exon26:c.G2935T:p.A979S,ENSG00000198626:ENST00000360064:exon27:c.G2929T:p.A977S	rs202015519	D	0,00057
RYR2	1_237711861_C_T	ENSG00000198626:ENST00000542537:exon25:c.C2989T:p.R997W,ENSG00000198626:ENST00000366574:exon26:c.C3037T:p.R1013W,ENSG00000198626:ENST00000360064:exon27:c.C3031T:p.R1011W		N	0,00057
RYR2	1_237711862_G_A	ENSG00000198626:ENST00000542537:exon25:c.G2990A:p.R997Q,ENSG00000198626:ENST00000366574:exon26:c.G3038A:p.R1013Q,ENSG00000198626:ENST00000360064:exon27:c.G3032A:p.R1011Q	rs149514924	P	0,00115
RYR2	1_237713928_C_T	ENSG00000198626:ENST00000542537:exon26:c.C3103T:p.R1035C,ENSG00000198626:ENST00000366574:exon27:c.C3151T:p.R1051C,ENSG00000198626:ENST00000360064:exon28:c.C3145T:p.R1049C		N	0,00057
RYR2	1_237713940_C_T	ENSG00000198626:ENST00000542537:exon26:c.C3115T:p.R1039C,ENSG00000198626:ENST00000366574:exon27:c.C3163T:p.R1055C,ENSG00000198626:ENST00000360064:exon28:c.C3157T:p.R1053C		S	0,00057
RYR2	1_237730008_G_A	ENSG00000198626:ENST00000542537:exon27:c.G3308A:p.R1103H,ENSG00000198626:ENST00000366574:exon28:c.G3356A:p.R1119H,ENSG00000198626:ENST00000360064:exon29:c.G3350A:p.R1117H	rs201312753	S	0,00116
RYR2	1_237732502_G_C	ENSG00000198626:ENST00000542537:exon28:c.G3433C:p.V1145L,ENSG00000198626:ENST00000366574:exon29:c.G3481C:p.V1161L,ENSG00000198626:ENST00000360064:exon30:c.G3475C:p.V1159L		S	0,00057
RYR2	1_237754201_G_C	ENSG00000198626:ENST00000542537:exon30:c.G4021C:p.D1341H,ENSG00000198626:ENST00000366574:exon31:c.G4069C:p.D1357H,ENSG00000198626:ENST00000360064:exon32:c.G4063C:p.D1355H	rs193922626	D	0,00114
RYR2	1_237758826_T_C	ENSG00000198626:ENST00000542537:exon33:c.T4417C:p.C1473R,ENSG00000198626:ENST00000366574:exon34:c.T4465C:p.C1489R,ENSG00000198626:ENST00000360064:exon35:c.T4459C:p.C1487R	rs200450676	S	0,00058
RYR2	1_237777530_G_C	ENSG00000198626:ENST00000542537:exon36:c.G5054C:p.G1685A,ENSG00000198626:ENST00000366574:exon37:c.G5102C:p.G1701A,ENSG00000198626:ENST00000360064:exon38:c.G5096C:p.G1699A		S	0,00057
RYR2	1_237777694_T_G	ENSG00000198626:ENST00000542537:exon36:c.T5218G:p.S1740A,ENSG00000198626:ENST00000366574:exon37:c.T5266G:p.S1756A,ENSG00000198626:ENST00000360064:exon38:c.T5260G:p.S1754A		S	0,00057
RYR2	1_237777722_C_G	ENSG00000198626:ENST00000542537:exon36:c.C5246G:p.S1749C,ENSG00000198626:ENST00000366574:exon37:c.C5294G:p.S1765C,ENSG00000198626:ENST00000360064:exon38:c.C5288G:p.S1763C		S	0,00057
RYR2	1_237778090_C_T	ENSG00000198626:ENST00000542537:exon36:c.C5614T:p.R1872W,ENSG00000198626:ENST00000366574:exon37:c.C5662T:p.R1888W,ENSG00000198626:ENST00000360064:exon38:c.C5656T:p.R1886W		N	0,00058

RYR2	1_237778108_C_A	ENSG00000198626:ENST00000542537:exon36:c.C5632A:p.L1878I,ENSG00000198626:ENST00000366574:exon37:c.C5680A:p.L1894I,ENSG00000198626:ENST00000360064:exon38:c.C5674A:p.L1892I		S	0,00057
RYR2	1_237787064_G_C	ENST00000366574:exon39:c.5917-1G>C,ENST00000360064:exon40:c.5911-1G>C,ENST00000542537:exon38:c.5869-1G>C		L	0,00057
RYR2	1_237794736_G_A	ENSG00000198626:ENST00000542537:exon41:c.G6402A:p.M2134I,ENSG00000198626:ENST00000366574:exon42:c.G6450A:p.M2150I,ENSG00000198626:ENST00000360064:exon43:c.G6444A:p.M2148I		N	0,00057
RYR2	1_237813288_G_A	ENSG00000198626:ENST00000542537:exon49:c.G7576A:p.A2526T,ENSG00000198626:ENST00000366574:exon50:c.G7624A:p.A2542T,ENSG00000198626:ENST00000360064:exon51:c.G7618A:p.A2540T		N	0,00057
RYR2	1_237814727_A_G	ENSG00000198626:ENST00000542537:exon50:c.A7702G:p.M2568V,ENSG00000198626:ENST00000366574:exon51:c.A7750G:p.M2584V,ENSG00000198626:ENST00000360064:exon52:c.A7744G:p.M2582V		N	0,00057
RYR2	1_237821276_T_C	ENSG00000198626:ENST00000542537:exon53:c.T8114C:p.I2705T,ENSG00000198626:ENST00000366574:exon54:c.T8162C:p.I2721T,ENSG00000198626:ENST00000360064:exon55:c.T8156C:p.I2719T	rs201500134	D	0,00230
RYR2	1_237823350_G_T	ENSG00000198626:ENST00000542537:exon54:c.G8226T:p.K2742N,ENSG00000198626:ENST00000366574:exon55:c.G8274T:p.K2758N,ENSG00000198626:ENST00000360064:exon56:c.G8268T:p.K2756N		S	0,00057
RYR2	1_237868518_G_T	ENSG00000198626:ENST00000540213:exon5:c.G440T:p.R147L,ENSG00000198626:ENST00000542288:exon6:c.G320T:p.R107L,ENSG00000198626:ENST00000542537:exon66:c.G9407T:p.R3136L,ENSG00000198626:ENST00000366574:exon67:c.G9455T:p.R3152L,ENSG00000198626:ENST00000360064:exon68:c.G9449T:p.R3150L		N	0,00057
RYR2	1_237868623_A_G	ENSG00000198626:ENST00000540213:exon5:c.A545G:p.K182R,ENSG00000198626:ENST00000542288:exon6:c.A425G:p.K142R,ENSG00000198626:ENST00000542537:exon66:c.A9512G:p.K3171R,ENSG00000198626:ENST00000366574:exon67:c.A9560G:p.K3187R,ENSG00000198626:ENST00000360064:exon68:c.A9554G:p.K3185R	rs184218219	S	0,00057
RYR2	1_237868632_G_A	ENSG00000198626:ENST00000540213:exon5:c.G554A:p.R185Q,ENSG00000198626:ENST00000542288:exon6:c.G434A:p.R145Q,ENSG00000198626:ENST00000542537:exon66:c.G9521A:p.R3174Q,ENSG00000198626:ENST00000366574:exon67:c.G9569A:p.R3190Q,ENSG00000198626:ENST00000360064:exon68:c.G9563A:p.R3188Q		S	0,00057
RYR2	1_237875041_T_C	ENST00000366574:exon71:c.10231-4T>C,ENST00000360064:exon72:c.10225-4T>C,ENST00000542537:exon70:c.10183-4T>C,ENST00000542288:exon10:c.1096-4T>C,ENST00000540213:exon9:c.1216-4T>C	rs117180147	L	0,00058
RYR2	1_237886554_C_G	ENSG00000198626:ENST00000542288:exon13:c.C1546G:p.L516V,ENSG00000198626:ENST00000542537:exon73:c.C10633G:p.L3545V,ENSG00000198626:ENST00000366574:exon74:c.C10681G:p.L3561V,ENSG00000198626:ENST00000360064:exon75:c.C10675G:p.L3559V		N	0,00057

RYR2	1_237947785_T_A	ENSG00000198626:ENST00000542288:exon30:c.T3695A:p.M1232K,ENSG00000198626:ENST00000542537:exon89:c.T12725A:p.M4242K,ENSG00000198626:ENST00000366574:exon90:c.T12773A:p.M4258K,ENSG00000198626:ENST00000360064:exon92:c.T12791A:p.M4264K		N	0,00058
RYR2	1_237948105_G_A	ENSG00000198626:ENST00000542288:exon30:c.G4015A:p.D1339N,ENSG00000198626:ENST00000542537:exon89:c.G13045A:p.D4349N,ENSG00000198626:ENST00000366574:exon90:c.G13093A:p.D4365N,ENSG00000198626:ENST00000360064:exon92:c.G13111A:p.D4371N		N	0,00058
RYR2	1_237948273_-_TAAT	ENST00000366574:exon90:c.13260+1->TAAT,ENST00000360064:exon92:c.13278+1->TAAT,ENST00000542537:exon89:c.13212+1->TAAT,ENST00000542288:exon30:c.4182+1->TAAT		L	0,00057
RYR2	1_237961442_C_G	ENSG00000198626:ENST00000536033:exon5:c.C361G:p.P121A,ENSG00000198626:ENST00000542537:exon96:c.C14014G:p.P4672A,ENSG00000198626:ENST00000366574:exon97:c.C14062G:p.P4688A,ENSG00000198626:ENST00000360064:exon99:c.C14080G:p.P4694A		N	0,00057
RYR2	1_237969434_T_C	ENST00000366574:exon99:c.14152-3T>C,ENST00000360064:exon101:c.14170-3T>C,ENST00000542537:exon98:c.14104-3T>C,ENST00000536033:exon7:c.451-3T>C		L	0,00058
SCN5A	3_38591847_G_C	ENSG00000183873:ENST00000414099:exon26:c.C5962G:p.P1988A,ENSG00000183873:ENST00000449557:exon26:c.C5854G:p.P1952A,ENSG00000183873:ENST00000450102:exon26:c.C5854G:p.P1952A,ENSG00000183873:ENST00000423572:exon27:c.C6013G:p.P2005A,ENSG00000183873:ENST00000425664:exon27:c.C5962G:p.P1988A,ENSG00000183873:ENST00000451551:exon27:c.C5854G:p.P1952A,ENSG00000183873:ENST00000455624:exon27:c.C5917G:p.P1973A,ENSG00000183873:ENST00000333535:exon28:c.C6016G:p.P2006A,ENSG00000183873:ENST00000413689:exon28:c.C6016G:p.P2006A,ENSG00000183873:ENST00000443581:exon28:c.C6013G:p.P2005A	rs45489199	D	0,00060
SCN5A	3_38591895_C_G	ENSG00000183873:ENST00000414099:exon26:c.G5914C:p.V1972L,ENSG00000183873:ENST00000449557:exon26:c.G5806C:p.V1936L,ENSG00000183873:ENST00000450102:exon26:c.G5806C:p.V1936L,ENSG00000183873:ENST00000423572:exon27:c.G5965C:p.V1989L,ENSG00000183873:ENST00000425664:exon27:c.G5914C:p.V1972L,ENSG00000183873:ENST00000451551:exon27:c.G5806C:p.V1936L,ENSG00000183873:ENST00000455624:exon27:c.G5869C:p.V1957L,ENSG00000183873:ENST00000333535:exon28:c.G5968C:p.V1990L,ENSG00000183873:ENST00000413689:exon28:c.G5968C:p.V1990L,ENSG00000183873:ENST00000443581:exon28:c.G5965C:p.V1989L		N	0,00060
SCN5A	3_38591978_G_A	ENSG00000183873:ENST00000414099:exon26:c.C5831T:p.P1944L,ENSG00000183873:ENST00000449557:exon26:c.C5723T:p.P1908L,ENSG00000183873:ENST00000450102:exon26:c.C5723T:p.P1908L,ENSG00000183873:ENST00000423572:exon27:c.C5882T:p.P1961L,ENSG00000183873:ENST00000425664:exon27:c.C5831T:p.P1944L,ENSG00000183873:ENST00000451551:exon27:c.C5723T:p.P1908L,ENSG00000183873:ENST00000455624:exon27:c.C5786T:p.P1929L,ENSG00000183873:ENST00000333535:exon28:c.C5885T:p.P1962L,ENSG00000183873:ENST00000413689:exon28:c.C5885T:p.P1962L,ENSG00000183873:ENST00000443581:exon28:c.C5882T:p.P1961L	rs199473638	P	0,00061

SCN5A	3_38592120_G_A	ENSG00000183873:ENST00000414099:exon26:c.C5689T:p.H1897Y,ENSG00000183873:ENST00000449557:exon26:c.C5581T:p.H1861Y,ENSG00000183873:ENST00000450102:exon26:c.C5581T:p.H1861Y,ENSG00000183873:ENST00000423572:exon27:c.C5740T:p.H1914Y,ENSG00000183873:ENST00000425664:exon27:c.C5689T:p.H1897Y,ENSG00000183873:ENST00000451551:exon27:c.C5581T:p.H1861Y,ENSG00000183873:ENST00000455624:exon27:c.C5644T:p.H1882Y,ENSG00000183873:ENST00000333535:exon28:c.C5743T:p.H1915Y,ENSG00000183873:ENST00000413689:exon28:c.C5743T:p.H1915Y,ENSG00000183873:ENST00000443581:exon28:c.C5740T:p.H1914Y		N	0,00058
SCN5A	3_38592408_C_T	ENSG00000183873:ENST00000414099:exon26:c.G5401A:p.D1801N,ENSG00000183873:ENST00000449557:exon26:c.G5293A:p.D1765N,ENSG00000183873:ENST00000450102:exon26:c.G5293A:p.D1765N,ENSG00000183873:ENST00000423572:exon27:c.G5452A:p.D1818N,ENSG00000183873:ENST00000425664:exon27:c.G5401A:p.D1801N,ENSG00000183873:ENST00000451551:exon27:c.G5293A:p.D1765N,ENSG00000183873:ENST00000455624:exon27:c.G5356A:p.D1786N,ENSG00000183873:ENST00000333535:exon28:c.G5455A:p.D1819N,ENSG00000183873:ENST00000413689:exon28:c.G5455A:p.D1819N,ENSG00000183873:ENST00000443581:exon28:c.G5452A:p.D1818N	rs137854619	P	0,00058
SCN5A	3_38592503_C_T	ENSG00000183873:ENST00000414099:exon26:c.G5306A:p.S1769N,ENSG00000183873:ENST00000449557:exon26:c.G5198A:p.S1733N,ENSG00000183873:ENST00000450102:exon26:c.G5198A:p.S1733N,ENSG00000183873:ENST00000423572:exon27:c.G5357A:p.S1786N,ENSG00000183873:ENST00000425664:exon27:c.G5306A:p.S1769N,ENSG00000183873:ENST00000451551:exon27:c.G5198A:p.S1733N,ENSG00000183873:ENST00000455624:exon27:c.G5261A:p.S1754N,ENSG00000183873:ENST00000333535:exon28:c.G5360A:p.S1787N,ENSG00000183873:ENST00000413689:exon28:c.G5360A:p.S1787N,ENSG00000183873:ENST00000443581:exon28:c.G5357A:p.S1786N	rs199473316	P	0,00172
SCN5A	3_38592527_G_A	ENSG00000183873:ENST00000414099:exon26:c.C5282T:p.T1761M,ENSG00000183873:ENST00000449557:exon26:c.C5174T:p.T1725M,ENSG00000183873:ENST00000450102:exon26:c.C5174T:p.T1725M,ENSG00000183873:ENST00000423572:exon27:c.C5333T:p.T1778M,ENSG00000183873:ENST00000425664:exon27:c.C5282T:p.T1761M,ENSG00000183873:ENST00000451551:exon27:c.C5174T:p.T1725M,ENSG00000183873:ENST00000455624:exon27:c.C5237T:p.T1746M,ENSG00000183873:ENST00000333535:exon28:c.C5336T:p.T1779M,ENSG00000183873:ENST00000413689:exon28:c.C5336T:p.T1779M,ENSG00000183873:ENST00000443581:exon28:c.C5333T:p.T1778M	rs199473634	S	0,00058
SCN5A	3_38597928_G_A	ENST00000414099:exon24:c.4383+4C>T,ENST00000425664:exon25:c.4383+4C>T,ENST00000443581:exon26:c.4434+4C>T,ENST00000451551:exon25:c.4275+4C>T,ENST00000413689:exon26:c.4437+4C>T,ENST00000423572:exon25:c.4434+4C>T,ENST00000333535:exon26:c.4437+4C>T,ENST00000455624:exon25:c.4434+4C>T,ENST00000450102:exon24:c.4275+4C>T,ENST00000449557:exon24:c.4275+4C>T		L	0,00066

SCN5A	3_38598027_T_G	ENSG00000183873:ENST00000414099:exon23:c.A4288C:p.I1430L,ENSG00000183873:ENST00000449557:exon23:c.A4180C:p.I1394L,ENSG00000183873:ENST00000450102:exon23:c.A4180C:p.I1394L,ENSG00000183873:ENST00000423572:exon24:c.A4339C:p.I1447L,ENSG00000183873:ENST00000425664:exon24:c.A4288C:p.I1430L,ENSG00000183873:ENST00000451551:exon24:c.A4180C:p.I1394L,ENSG00000183873:ENST00000455624:exon24:c.A4339C:p.I1447L,ENSG00000183873:ENST00000333535:exon25:c.A4342C:p.I1448L,ENSG00000183873:ENST00000413689:exon25:c.A4342C:p.I1448L,ENSG00000183873:ENST00000443581:exon25:c.A4339C:p.I1447L	rs199473250	D	0,00059
SCN5A	3_38603947_G_A	ENSG00000183873:ENST00000449557:exon20:c.C3760T:p.L1254F,ENSG00000183873:ENST00000450102:exon20:c.C3760T:p.L1254F,ENSG00000183873:ENST00000414099:exon21:c.C3922T:p.L1308F,ENSG00000183873:ENST00000423572:exon21:c.C3919T:p.L1307F,ENSG00000183873:ENST00000451551:exon21:c.C3760T:p.L1254F,ENSG00000183873:ENST00000455624:exon21:c.C3919T:p.L1307F,ENSG00000183873:ENST00000333535:exon22:c.C3922T:p.L1308F,ENSG00000183873:ENST00000413689:exon22:c.C3922T:p.L1308F,ENSG00000183873:ENST00000425664:exon22:c.C3922T:p.L1308F,ENSG00000183873:ENST00000443581:exon22:c.C3919T:p.L1307F	rs41313031	P	0,00079
SCN5A	3_38603958_G_A	ENSG00000183873:ENST00000449557:exon20:c.C3749T:p.T1250M,ENSG00000183873:ENST00000450102:exon20:c.C3749T:p.T1250M,ENSG00000183873:ENST00000414099:exon21:c.C3911T:p.T1304M,ENSG00000183873:ENST00000423572:exon21:c.C3908T:p.T1303M,ENSG00000183873:ENST00000451551:exon21:c.C3749T:p.T1250M,ENSG00000183873:ENST00000455624:exon21:c.C3908T:p.T1303M,ENSG00000183873:ENST00000333535:exon22:c.C3911T:p.T1304M,ENSG00000183873:ENST00000413689:exon22:c.C3911T:p.T1304M,ENSG00000183873:ENST00000425664:exon22:c.C3911T:p.T1304M,ENSG00000183873:ENST00000443581:exon22:c.C3908T:p.T1303M	rs199473603	P	0,00153
SCN5A	3_38603991_A_G	ENSG00000183873:ENST00000449557:exon20:c.T3716C:p.F1239S,ENSG00000183873:ENST00000450102:exon20:c.T3716C:p.F1239S,ENSG00000183873:ENST00000414099:exon21:c.T3878C:p.F1293S,ENSG00000183873:ENST00000423572:exon21:c.T3875C:p.F1292S,ENSG00000183873:ENST00000451551:exon21:c.T3716C:p.F1239S,ENSG00000183873:ENST00000455624:exon21:c.T3875C:p.F1292S,ENSG00000183873:ENST00000333535:exon22:c.T3878C:p.F1293S,ENSG00000183873:ENST00000413689:exon22:c.T3878C:p.F1293S,ENSG00000183873:ENST00000425664:exon22:c.T3878C:p.F1293S,ENSG00000183873:ENST00000443581:exon22:c.T3875C:p.F1292S	rs41311127	P	0,00076
SCN5A	3_38607905_C_T	ENSG00000183873:ENST00000449557:exon19:c.G3673A:p.V1225I,ENSG00000183873:ENST00000450102:exon19:c.G3673A:p.V1225I,ENSG00000183873:ENST00000414099:exon20:c.G3835A:p.V1279I,ENSG00000183873:ENST00000423572:exon20:c.G3832A:p.V1278I,ENSG00000183873:ENST00000451551:exon20:c.G3673A:p.V1225I,ENSG00000183873:ENST00000455624:exon20:c.G3832A:p.V1278I,ENSG00000183873:ENST00000333535:exon21:c.G3835A:p.V1279I,ENSG00000183873:ENST00000413689:exon21:c.G3835A:p.V1279I,ENSG00000183873:ENST00000425664:exon21:c.G3835A:p.V1279I,ENSG00000183873:ENST00000443581:exon21:c.G3832A:p.V1278I	rs199473341	P	0,00059

SCN5A	3_38608022_C_G	ENSG00000183873:ENST00000449557:exon19:c.G3556C:p.E1186Q,ENSG00000183873:ENST00000450102:exon19:c.G3556C:p.E1186Q,ENSG00000183873:ENST00000414099:exon20:c.G3718C:p.E1240Q,ENSG00000183873:ENST00000423572:exon20:c.G3715C:p.E1239Q,ENSG00000183873:ENST00000451551:exon20:c.G3556C:p.E1186Q,ENSG00000183873:ENST00000455624:exon20:c.G3715C:p.E1239Q,ENSG00000183873:ENST00000333535:exon21:c.G3718C:p.E1240Q,ENSG00000183873:ENST00000413689:exon21:c.G3718C:p.E1240Q,ENSG00000183873:ENST00000425664:exon21:c.G3718C:p.E1240Q,ENSG00000183873:ENST00000443581:exon21:c.G3715C:p.E1239Q	rs199473211	P	0,00058
SCN5A	3_38608058_A_G	ENSG00000183873:ENST00000449557:exon19:c.T3520C:p.Y1174H,ENSG00000183873:ENST00000450102:exon19:c.T3520C:p.Y1174H,ENSG00000183873:ENST00000414099:exon20:c.T3682C:p.Y1228H,ENSG00000183873:ENST00000423572:exon20:c.T3679C:p.Y1227H,ENSG00000183873:ENST00000451551:exon20:c.T3520C:p.Y1174H,ENSG00000183873:ENST00000455624:exon20:c.T3679C:p.Y1227H,ENSG00000183873:ENST00000333535:exon21:c.T3682C:p.Y1228H,ENSG00000183873:ENST00000413689:exon21:c.T3682C:p.Y1228H,ENSG00000183873:ENST00000425664:exon21:c.T3682C:p.Y1228H,ENSG00000183873:ENST00000443581:exon21:c.T3679C:p.Y1227H	rs199473205	P	0,00059
SCN5A	3_38622640_A_G	ENSG00000183873:ENST00000414099:exon16:c.T3010C:p.C1004R,ENSG00000183873:ENST00000423572:exon16:c.T3010C:p.C1004R,ENSG00000183873:ENST00000449557:exon16:c.T3010C:p.C1004R,ENSG00000183873:ENST00000450102:exon16:c.T3010C:p.C1004R,ENSG00000183873:ENST00000455624:exon16:c.T3010C:p.C1004R,ENSG00000183873:ENST00000333535:exon17:c.T3010C:p.C1004R,ENSG00000183873:ENST00000413689:exon17:c.T3010C:p.C1004R,ENSG00000183873:ENST00000425664:exon17:c.T3010C:p.C1004R,ENSG00000183873:ENST00000443581:exon17:c.T3010C:p.C1004R,ENSG00000183873:ENST00000451551:exon17:c.T3010C:p.C1004R	rs199473183	P	0,00157
SCN5A	3_38622706_A_G	ENSG00000183873:ENST00000414099:exon16:c.T2944C:p.C982R,ENSG00000183873:ENST00000423572:exon16:c.T2944C:p.C982R,ENSG00000183873:ENST00000449557:exon16:c.T2944C:p.C982R,ENSG00000183873:ENST00000450102:exon16:c.T2944C:p.C982R,ENSG00000183873:ENST00000455624:exon16:c.T2944C:p.C982R,ENSG00000183873:ENST00000333535:exon17:c.T2944C:p.C982R,ENSG00000183873:ENST00000413689:exon17:c.T2944C:p.C982R,ENSG00000183873:ENST00000425664:exon17:c.T2944C:p.C982R,ENSG00000183873:ENST00000443581:exon17:c.T2944C:p.C982R,ENSG00000183873:ENST00000451551:exon17:c.T2944C:p.C982R	rs199473182	P	0,00080
SCN5A	3_38627537_G_T	ENST00000414099:exon16:c.2437-5C>A,ENST00000425664:exon17:c.2437-5C>A,ENST00000443581:exon17:c.2437-5C>A,ENST00000451551:exon17:c.2437-5C>A,ENST00000413689:exon17:c.2437-5C>A,ENST00000423572:exon16:c.2437-5C>A,ENST00000333535:exon17:c.2437-5C>A,ENST00000455624:exon16:c.2437-5C>A,ENST00000450102:exon16:c.2437-5C>A,ENST00000449557:exon16:c.2437-5C>A	rs72549411	L	0,00174

SCN5A	3_38628928_C_A	ENSG00000183873:ENST00000414099:exon14:c.G2399T:p.R800L,ENSG00000183873:ENST00000423572:exon14:c.G2399T:p.R800L,ENSG00000183873:ENST00000449557:exon14:c.G2399T:p.R800L,ENSG00000183873:ENST00000450102:exon14:c.G2399T:p.R800L,ENSG00000183873:ENST00000455624:exon14:c.G2399T:p.R800L,ENSG00000183873:ENST00000333535:exon15:c.G2399T:p.R800L,ENSG00000183873:ENST00000413689:exon15:c.G2399T:p.R800L,ENSG00000183873:ENST00000425664:exon15:c.G2399T:p.R800L,ENSG00000183873:ENST00000443581:exon15:c.G2399T:p.R800L,ENSG00000183873:ENST00000451551:exon15:c.G2399T:p.R800L		N	0,00070
SCN5A	3_38639408_G_T	ENSG00000183873:ENST00000414099:exon13:c.C2074A:p.Q692K,ENSG00000183873:ENST00000423572:exon13:c.C2074A:p.Q692K,ENSG00000183873:ENST00000449557:exon13:c.C2074A:p.Q692K,ENSG00000183873:ENST00000450102:exon13:c.C2074A:p.Q692K,ENSG00000183873:ENST00000455624:exon13:c.C2074A:p.Q692K,ENSG00000183873:ENST00000333535:exon14:c.C2074A:p.Q692K,ENSG00000183873:ENST00000413689:exon14:c.C2074A:p.Q692K,ENSG00000183873:ENST00000425664:exon14:c.C2074A:p.Q692K,ENSG00000183873:ENST00000443581:exon14:c.C2074A:p.Q692K,ENSG00000183873:ENST00000451551:exon14:c.C2074A:p.Q692K	rs45553235	P	0,00124
SCN5A	3_38639443_C_T	ENSG00000183873:ENST00000414099:exon13:c.G2039A:p.R680H,ENSG00000183873:ENST00000423572:exon13:c.G2039A:p.R680H,ENSG00000183873:ENST00000449557:exon13:c.G2039A:p.R680H,ENSG00000183873:ENST00000450102:exon13:c.G2039A:p.R680H,ENSG00000183873:ENST00000455624:exon13:c.G2039A:p.R680H,ENSG00000183873:ENST00000333535:exon14:c.G2039A:p.R680H,ENSG00000183873:ENST00000413689:exon14:c.G2039A:p.R680H,ENSG00000183873:ENST00000425664:exon14:c.G2039A:p.R680H,ENSG00000183873:ENST00000443581:exon14:c.G2039A:p.R680H,ENSG00000183873:ENST00000451551:exon14:c.G2039A:p.R680H	rs199473142	P	0,00061
SCN5A	3_38640418_C_T	ENSG00000183873:ENST00000414099:exon12:c.G2014A:p.A672T,ENSG00000183873:ENST00000423572:exon12:c.G2014A:p.A672T,ENSG00000183873:ENST00000449557:exon12:c.G2014A:p.A672T,ENSG00000183873:ENST00000450102:exon12:c.G2014A:p.A672T,ENSG00000183873:ENST00000455624:exon12:c.G2014A:p.A672T,ENSG00000183873:ENST00000333535:exon13:c.G2014A:p.A672T,ENSG00000183873:ENST00000413689:exon13:c.G2014A:p.A672T,ENSG00000183873:ENST00000425664:exon13:c.G2014A:p.A672T,ENSG00000183873:ENST00000443581:exon13:c.G2014A:p.A672T,ENSG00000183873:ENST00000451551:exon13:c.G2014A:p.A672T	rs199473140	P	0,00062
SCN5A	3_38640450_C_T	ENSG00000183873:ENST00000414099:exon12:c.G1982A:p.R661Q,ENSG00000183873:ENST00000423572:exon12:c.G1982A:p.R661Q,ENSG00000183873:ENST00000449557:exon12:c.G1982A:p.R661Q,ENSG00000183873:ENST00000450102:exon12:c.G1982A:p.R661Q,ENSG00000183873:ENST00000455624:exon12:c.G1982A:p.R661Q,ENSG00000183873:ENST00000333535:exon13:c.G1982A:p.R661Q,ENSG00000183873:ENST00000413689:exon13:c.G1982A:p.R661Q,ENSG00000183873:ENST00000425664:exon13:c.G1982A:p.R661Q,ENSG00000183873:ENST00000443581:exon13:c.G1982A:p.R661Q,ENSG00000183873:ENST00000451551:exon13:c.G1982A:p.R661Q		N	0,00067

SCN5A	3_38645332_GAGGGC_-	ENSG00000183873:ENST00000414099:exon11:c.1756_1761del:p.586_587del,ENSG00000183873:ENST00000423572:exon11:c.1756_1761del:p.586_587del,ENSG00000183873:ENST00000449557:exon11:c.1756_1761del:p.586_587del,ENSG00000183873:ENST00000450102:exon11:c.1756_1761del:p.586_587del,ENSG00000183873:ENST00000455624:exon11:c.1756_1761del:p.586_587del,ENSG00000183873:ENST00000333535:exon12:c.1756_1761del:p.586_587del,ENSG00000183873:ENST00000413689:exon12:c.1756_1761del:p.586_587del,ENSG00000183873:ENST00000425664:exon12:c.1756_1761del:p.586_587del,ENSG00000183873:ENST00000443581:exon12:c.1756_1761del:p.586_587del,ENSG00000183873:ENST00000451551:exon12:c.1756_1761del:p.586_587del		N	0,00062
SCN5A	3_38645333_AGGGCG_-	ENSG00000183873:ENST00000414099:exon11:c.1755_1760del:p.585_587del,ENSG00000183873:ENST00000423572:exon11:c.1755_1760del:p.585_587del,ENSG00000183873:ENST00000449557:exon11:c.1755_1760del:p.585_587del,ENSG00000183873:ENST00000450102:exon11:c.1755_1760del:p.585_587del,ENSG00000183873:ENST00000455624:exon11:c.1755_1760del:p.585_587del,ENSG00000183873:ENST00000333535:exon12:c.1755_1760del:p.585_587del,ENSG00000183873:ENST00000413689:exon12:c.1755_1760del:p.585_587del,ENSG00000183873:ENST00000425664:exon12:c.1755_1760del:p.585_587del,ENSG00000183873:ENST00000443581:exon12:c.1755_1760del:p.585_587del,ENSG00000183873:ENST00000451551:exon12:c.1755_1760del:p.585_587del		P	0,00062
SCN5A	3_38645438_C_G	ENSG00000183873:ENST00000414099:exon11:c.G1655C:p.G552A,ENSG00000183873:ENST00000423572:exon11:c.G1655C:p.G552A,ENSG00000183873:ENST00000449557:exon11:c.G1655C:p.G552A,ENSG00000183873:ENST00000450102:exon11:c.G1655C:p.G552A,ENSG00000183873:ENST00000455624:exon11:c.G1655C:p.G552A,ENSG00000183873:ENST00000333535:exon12:c.G1655C:p.G552A,ENSG00000183873:ENST00000413689:exon12:c.G1655C:p.G552A,ENSG00000183873:ENST00000425664:exon12:c.G1655C:p.G552A,ENSG00000183873:ENST00000443581:exon12:c.G1655C:p.G552A,ENSG00000183873:ENST00000451551:exon12:c.G1655C:p.G552A		N	0,00061
SCN5A	3_38646398_G_C	ENSG00000183873:ENST00000414099:exon10:c.C1340G:p.A447G,ENSG00000183873:ENST00000423572:exon10:c.C1340G:p.A447G,ENSG00000183873:ENST00000449557:exon10:c.C1340G:p.A447G,ENSG00000183873:ENST00000450102:exon10:c.C1340G:p.A447G,ENSG00000183873:ENST00000455624:exon10:c.C1340G:p.A447G,ENSG00000183873:ENST00000333535:exon11:c.C1340G:p.A447G,ENSG00000183873:ENST00000413689:exon11:c.C1340G:p.A447G,ENSG00000183873:ENST00000425664:exon11:c.C1340G:p.A447G,ENSG00000183873:ENST00000443581:exon11:c.C1340G:p.A447G,ENSG00000183873:ENST00000451551:exon11:c.C1340G:p.A447G	rs199473113	D	0,00057
SCN5A	3_38647444_C_T	ENSG00000183873:ENST00000414099:exon9:c.G1336A:p.E446K,ENSG00000183873:ENST00000423572:exon9:c.G1336A:p.E446K,ENSG00000183873:ENST00000449557:exon9:c.G1336A:p.E446K,ENSG00000183873:ENST00000450102:exon9:c.G1336A:p.E446K,ENSG00000183873:ENST00000455624:exon9:c.G1336A:p.E446K,ENSG00000183873:ENST00000333535:exon10:c.G1336A:p.E446K,ENSG00000183873:ENST00000413689:exon10:c.G1336A:p.E446K,ENSG00000183873:ENST00000425664:exon10:c.G1336A:p.E446K,ENSG00000183873:ENST00000443581:exon10:c.G1336A:p.E446K,ENSG00000183873:ENST00000451551:exon10:c.G1336A:p.E446K	rs199473339	P	0,00115

SCN5A	3_38655278_G_A	ENSG00000183873:ENST00000423572:exon5:c.C659T:p.T220I,ENSG00000183873:ENST00000449557:exon5:c.C659T:p.T220I,ENSG00000183873:ENST00000333535:exon6:c.C659T:p.T220I,ENSG00000183873:ENST00000443581:exon6:c.C659T:p.T220I	rs45620037	P	0,00116
SCN5A	3_38655318_T_C	ENSG00000183873:ENST00000423572:exon5:c.A619G:p.T207A,ENSG00000183873:ENST00000449557:exon5:c.A619G:p.T207A,ENSG00000183873:ENST00000333535:exon6:c.A619G:p.T207A,ENSG00000183873:ENST00000443581:exon6:c.A619G:p.T207A		N	0,00058
SCN5A	3_38662449_C_T	ENSG00000183873:ENST00000414099:exon4:c.G496A:p.A166T,ENSG00000183873:ENST00000423572:exon4:c.G496A:p.A166T,ENSG00000183873:ENST00000449557:exon4:c.G496A:p.A166T,ENSG00000183873:ENST00000450102:exon4:c.G496A:p.A166T,ENSG00000183873:ENST00000455624:exon4:c.G496A:p.A166T,ENSG00000183873:ENST00000333535:exon5:c.G496A:p.A166T,ENSG00000183873:ENST00000413689:exon5:c.G496A:p.A166T,ENSG00000183873:ENST00000425664:exon5:c.G496A:p.A166T,ENSG00000183873:ENST00000443581:exon5:c.G496A:p.A166T,ENSG00000183873:ENST00000451551:exon5:c.G496A:p.A166T	rs201232332	S	0,00060
SCN5A	3_38671821_C_G	ENSG00000183873:ENST00000414099:exon2:c.G373C:p.V125L,ENSG00000183873:ENST00000423572:exon2:c.G373C:p.V125L,ENSG00000183873:ENST00000449557:exon2:c.G373C:p.V125L,ENSG00000183873:ENST00000450102:exon2:c.G373C:p.V125L,ENSG00000183873:ENST00000455624:exon2:c.G373C:p.V125L,ENSG00000183873:ENST00000333535:exon3:c.G373C:p.V125L,ENSG00000183873:ENST00000413689:exon3:c.G373C:p.V125L,ENSG00000183873:ENST00000425664:exon3:c.G373C:p.V125L,ENSG00000183873:ENST00000443581:exon3:c.G373C:p.V125L,ENSG00000183873:ENST00000451551:exon3:c.G373C:p.V125L	rs199473059	P	0,00115
SCN5A	3_38674747_G_A	ENSG00000183873:ENST00000414099:exon1:c.C52T:p.R18W,ENSG00000183873:ENST00000423572:exon1:c.C52T:p.R18W,ENSG00000183873:ENST00000449557:exon1:c.C52T:p.R18W,ENSG00000183873:ENST00000450102:exon1:c.C52T:p.R18W,ENSG00000183873:ENST00000455624:exon1:c.C52T:p.R18W,ENSG00000183873:ENST00000327956:exon2:c.C52T:p.R18W,ENSG00000183873:ENST00000333535:exon2:c.C52T:p.R18W,ENSG00000183873:ENST00000413689:exon2:c.C52T:p.R18W,ENSG00000183873:ENST00000425664:exon2:c.C52T:p.R18W,ENSG00000183873:ENST00000443581:exon2:c.C52T:p.R18W,ENSG00000183873:ENST00000451551:exon2:c.C52T:p.R18W	rs199473044	P	0,00128
TCAP	17_37821616_G_A	ENSG00000173991:ENST00000309889:exon1:c.G4A:p.A2T,ENSG00000173991:ENST00000578283:exon1:c.G4A:p.A2T		N	0,00062
TCAP	17_37821644_C_T	ENSG00000173991:ENST00000309889:exon1:c.C32T:p.S11L,ENSG00000173991:ENST00000578283:exon1:c.C32T:p.S11L	rs45495192	D	0,00126
TCAP	17_37821645_GGA_-	ENSG00000173991:ENST00000309889:exon1:c.33_35del:p.11_12del,ENSG00000173991:ENST00000578283:exon1:c.33_35del:p.11_12del		N	0,00063
TCAP	17_37821649_GAG_-	ENSG00000173991:ENST00000309889:exon1:c.37_39del:p.13_13del,ENSG00000173991:ENST00000578283:exon1:c.37_39del:p.13_13del		P	0,00063
TCAP	17_37822175_G_T	ENSG00000173991:ENST00000309889:exon2:c.G317T:p.R106L,ENSG00000173991:ENST00000578283:exon3:c.G245T:p.R82L		N	0,00092

TCAP	17_37822195_C_T	ENSG00000173991:ENST00000309889:exon2:c.C337T:p.L113F,ENSG00000173991:ENST00000578283:exon3:c.C265T:p.L89F		N	0,00091
TCAP	17_37822211_C_T	ENSG00000173991:ENST00000309889:exon2:c.C353T:p.A118V,ENSG00000173991:ENST00000578283:exon3:c.C281T:p.A94V	rs143233087	D	0,00090
TGFB3	14_76429772_C_G	ENSG00000119699:ENST00000238682:exon5:c.G813C:p.K271N,ENSG00000119699:ENST00000556285:exon5:c.G813C:p.K271N	rs147601018	D	0,00058
TGFB3	14_76437523_C_T	ENSG00000119699:ENST00000238682:exon3:c.G592A:p.E198K,ENSG00000119699:ENST00000556285:exon3:c.G592A:p.E198K		N	0,00058
TGFB3	14_76437535_G_A	ENSG00000119699:ENST00000238682:exon3:c.C580T:p.R194W,ENSG00000119699:ENST00000556285:exon3:c.C580T:p.R194W		S	0,00058
TGFB3	14_76438059_C_T	ENSG00000119699:ENST00000238682:exon2:c.G355A:p.E119K,ENSG00000119699:ENST00000556285:exon2:c.G355A:p.E119K		N	0,00059
TGFB3	14_76446944_G_A	ENSG00000119699:ENST00000238682:exon1:c.C293T:p.S98L,ENSG00000119699:ENST00000556285:exon1:c.C293T:p.S98L	rs142047577	D	0,00059
TMEM43	3_14170982_G_A	ENSG00000170876:ENST00000306077:exon2:c.G83A:p.R28Q		S	0,00058
TMEM43	3_14170990_G_A	ENSG00000170876:ENST00000306077:exon2:c.G91A:p.E31K		N	0,00058
TMEM43	3_14172439_G_A	ENSG00000170876:ENST00000306077:exon3:c.G280A:p.A94T		N	0,00088
TMEM43	3_14175244_T_C	ENSG00000170876:ENST00000306077:exon7:c.T518C:p.M173T		S	0,00093
TMEM43	3_14176287_G_A	ENSG00000170876:ENST00000306077:exon8:c.G601A:p.D201N	rs138182276	D	0,00063
TMEM43	3_14177355_A_T	ENSG00000170876:ENST00000306077:exon10:c.A829T:p.T277S		N	0,00059
TNNC1	3_52485431_T_C	ENSG00000114854:ENST00000232975:exon5:c.A430G:p.N144D		N	0,00060
TNNC1	3_52485805_C_T	ENSG00000114854:ENST00000496590:exon3:c.G140A:p.G47E,ENSG00000114854:ENST00000232975:exon4:c.G272A:p.G91E		S	0,00057
TNNC1	3_52485879_G_A	ENST00000232975:exon5:c.203-5C>T,ENST00000496590:exon4:c.71-5C>T	rs142519988	L	0,00058
TNNC1	3_52486194_C_T	ENSG00000114854:ENST00000232975:exon3:c.G130A:p.V44M		S	0,00063
TNNI3	19_55663243_G_C	ENSG00000129991:ENST00000588882:exon5:c.C517G:p.L173V,ENSG00000129991:ENST00000344887:exon8:c.C592G:p.L198V		P	0,00057
TNNI3	19_55663249_C_T	ENSG00000129991:ENST00000588882:exon5:c.G511A:p.D171N,ENSG00000129991:ENST00000344887:exon8:c.G586A:p.D196N	rs104894727	P	0,00115
TNNI3	19_55663278_C_T	ENSG00000129991:ENST00000588882:exon5:c.G482A:p.R161Q,ENSG00000129991:ENST00000344887:exon8:c.G557A:p.R186Q		P	0,00057
TNNI3	19_55665421_C_T	ENSG00000129991:ENST00000588882:exon4:c.G451A:p.V151M,ENSG00000129991:ENST00000344887:exon7:c.G526A:p.V176M		S	0,00115

TNNI3	19_55665436_C_T	ENSG00000129991:ENST00000588882:exon4:c.G436A:p.A146T,ENSG00000129991:ENST00000344887:exon7:c.G511A:p.A171T	rs121917761	P	0,00057
TNNI3	19_55665462_C_T	ENSG00000129991:ENST00000588882:exon4:c.G410A:p.R137Q,ENSG00000129991:ENST00000344887:exon7:c.G485A:p.R162Q		P	0,00173
TNNI3	19_55665463_G_A	ENSG00000129991:ENST00000588882:exon4:c.C409T:p.R137W,ENSG00000129991:ENST00000344887:exon7:c.C484T:p.R162W		P	0,00115
TNNI3	19_55665477_G_A	ENSG00000129991:ENST00000588882:exon4:c.C395T:p.A132V,ENSG00000129991:ENST00000344887:exon7:c.C470T:p.A157V		P	0,00057
TNNI3	19_55665514_G_A	ENSG00000129991:ENST00000588882:exon4:c.C358T:p.R120W,ENSG00000129991:ENST00000344887:exon7:c.C433T:p.R145W	rs104894724	P	0,00229
TNNI3	19_55665525_C_T	ENSG00000129991:ENST00000588882:exon4:c.G347A:p.R116Q,ENSG00000129991:ENST00000344887:exon7:c.G422A:p.R141Q		P	0,00057
TNNI3	19_55667616_G_A	ENSG00000129991:ENST00000588882:exon2:c.C160T:p.R54C,ENSG00000129991:ENST00000344887:exon5:c.C235T:p.R79C	rs3729712	D	0,00082
TNNI3	19_55668007_T_A	ENSG00000129991:ENST00000586858:exon1:c.A39T:p.K13N,ENSG00000129991:ENST00000588882:exon1:c.A39T:p.K13N,ENSG00000129991:ENST00000344887:exon4:c.A114T:p.K38N		S	0,00062
TNNI3	19_55668029_G_T	ENSG00000129991:ENST00000586858:exon1:c.C17A:p.S6Y,ENSG00000129991:ENST00000588882:exon1:c.C17A:p.S6Y	rs139150276	D	0,00245
TNNT2	1_201328345_C_T	ENSG00000118194:ENST00000360372:exon14:c.G845A:p.W282X,ENSG00000118194:ENST00000367315:exon14:c.G851A:p.W284X,ENSG00000118194:ENST00000236918:exon15:c.G875A:p.W292X,ENSG00000118194:ENST00000367317:exon15:c.G860A:p.W287X,ENSG00000118194:ENST00000367320:exon15:c.G761A:p.W254X,ENSG00000118194:ENST00000367322:exon15:c.G851A:p.W284X,ENSG00000118194:ENST00000421663:exon15:c.G869A:p.W290X,ENSG00000118194:ENST00000367318:exon16:c.G860A:p.W287X,ENSG00000118194:ENST00000458432:exon16:c.G887A:p.W296X,ENSG00000118194:ENST00000509001:exon16:c.G860A:p.W287X		P	0,00061
TNNT2	1_201328348_C_T	ENSG00000118194:ENST00000360372:exon14:c.G842A:p.R281H,ENSG00000118194:ENST00000367315:exon14:c.G848A:p.R283H,ENSG00000118194:ENST00000236918:exon15:c.G872A:p.R291H,ENSG00000118194:ENST00000367317:exon15:c.G857A:p.R286H,ENSG00000118194:ENST00000367320:exon15:c.G758A:p.R253H,ENSG00000118194:ENST00000367322:exon15:c.G848A:p.R283H,ENSG00000118194:ENST00000421663:exon15:c.G866A:p.R289H,ENSG00000118194:ENST00000367318:exon16:c.G857A:p.R286H,ENSG00000118194:ENST00000458432:exon16:c.G884A:p.R295H,ENSG00000118194:ENST00000509001:exon16:c.G857A:p.R286H	rs141121678	P	0,00122

TNNT2	1_201328372_C_G	ENSG00000118194:ENST00000360372:exon14:c.G818C:p.R273P,ENSG00000118194:ENST00000367315:exon14:c.G824C:p.R275P,ENSG00000118194:ENST00000236918:exon15:c.G848C:p.R283P,ENSG00000118194:ENST00000367317:exon15:c.G833C:p.R278P,ENSG00000118194:ENST00000367320:exon15:c.G734C:p.R245P,ENSG00000118194:ENST00000367322:exon15:c.G824C:p.R275P,ENSG00000118194:ENST00000421663:exon15:c.G842C:p.R281P,ENSG00000118194:ENST00000367318:exon16:c.G833C:p.R278P,ENSG00000118194:ENST00000458432:exon16:c.G860C:p.R287P,ENSG00000118194:ENST00000509001:exon16:c.G833C:p.R278P		N	0,00062
TNNT2	1_201328373_G_A	ENSG00000118194:ENST00000360372:exon14:c.C817T:p.R273C,ENSG00000118194:ENST00000367315:exon14:c.C823T:p.R275C,ENSG00000118194:ENST00000236918:exon15:c.C847T:p.R283C,ENSG00000118194:ENST00000367317:exon15:c.C832T:p.R278C,ENSG00000118194:ENST00000367320:exon15:c.C733T:p.R245C,ENSG00000118194:ENST00000367322:exon15:c.C823T:p.R275C,ENSG00000118194:ENST00000421663:exon15:c.C841T:p.R281C,ENSG00000118194:ENST00000367318:exon16:c.C832T:p.R278C,ENSG00000118194:ENST00000458432:exon16:c.C859T:p.R287C,ENSG00000118194:ENST00000509001:exon16:c.C832T:p.R278C	rs121964857	P	0,00498
TNNT2	1_201328386_G_T	ENST00000367322:exon16:c.813-3C>A,ENST00000367318:exon17:c.822-3C>A,ENST00000360372:exon15:c.807-3C>A,ENST00000367315:exon15:c.813-3C>A,ENST00000367317:exon16:c.822-3C>A,ENST00000236918:exon16:c.837-3C>A,ENST00000421663:exon16:c.831-3C>A,ENST00000458432:exon17:c.849-3C>A,ENST00000367320:exon16:c.723-3C>A,ENST00000509001:exon17:c.822-3C>A,ENST00000438742:exon16:c.804-3C>A		L	0,00062
TNNT2	1_201328760_T_A	ENSG00000118194:ENST00000360372:exon13:c.A797T:p.N266I,ENSG00000118194:ENST00000367315:exon13:c.A803T:p.N268I,ENSG00000118194:ENST00000236918:exon14:c.A827T:p.N276I,ENSG00000118194:ENST00000367317:exon14:c.A812T:p.N271I,ENSG00000118194:ENST00000367320:exon14:c.A713T:p.N238I,ENSG00000118194:ENST00000367322:exon14:c.A803T:p.N268I,ENSG00000118194:ENST00000421663:exon14:c.A821T:p.N274I,ENSG00000118194:ENST00000438742:exon14:c.A794T:p.N265I,ENSG00000118194:ENST00000367318:exon15:c.A812T:p.N271I,ENSG00000118194:ENST00000458432:exon15:c.A839T:p.N280I,ENSG00000118194:ENST00000509001:exon15:c.A812T:p.N271I		P	0,00059
TNNT2	1_201328787_T_C	ENSG00000118194:ENST00000360372:exon13:c.A770G:p.N257S,ENSG00000118194:ENST00000367315:exon13:c.A776G:p.N259S,ENSG00000118194:ENST00000236918:exon14:c.A800G:p.N267S,ENSG00000118194:ENST00000367317:exon14:c.A785G:p.N262S,ENSG00000118194:ENST00000367320:exon14:c.A686G:p.N229S,ENSG00000118194:ENST00000367322:exon14:c.A776G:p.N259S,ENSG00000118194:ENST00000421663:exon14:c.A794G:p.N265S,ENSG00000118194:ENST00000438742:exon14:c.A767G:p.N256S,ENSG00000118194:ENST00000367318:exon15:c.A785G:p.N262S,ENSG00000118194:ENST00000458432:exon15:c.A812G:p.N271S,ENSG00000118194:ENST00000509001:exon15:c.A785G:p.N262S		P	0,00117

TNNT2	1_201331150_T_C	ENSG00000118194:ENST00000360372:exon11:c.A565G:p.T189A,ENSG00000118194:ENST00000367315:exon11:c.A571G:p.T191A,ENSG00000118194:ENST00000236918:exon12:c.A595G:p.T199A,ENSG00000118194:ENST00000367317:exon12:c.A580G:p.T194A,ENSG00000118194:ENST00000367320:exon12:c.A481G:p.T161A,ENSG00000118194:ENST00000367322:exon12:c.A571G:p.T191A,ENSG00000118194:ENST00000421663:exon12:c.A589G:p.T197A,ENSG00000118194:ENST00000438742:exon12:c.A562G:p.T188A,ENSG00000118194:ENST00000367318:exon13:c.A580G:p.T194A,ENSG00000118194:ENST00000458432:exon13:c.A607G:p.T203A,ENSG00000118194:ENST00000509001:exon13:c.A580G:p.T194A		N	0,00058
TNNT2	1_201332459_A_C	ENSG00000118194:ENST00000360372:exon9:c.T520G:p.S174A,ENSG00000118194:ENST00000236918:exon10:c.T550G:p.S184A,ENSG00000118194:ENST00000367315:exon10:c.T535G:p.S179A,ENSG00000118194:ENST00000367317:exon10:c.T535G:p.S179A,ENSG00000118194:ENST00000438742:exon10:c.T520G:p.S174A,ENSG00000118194:ENST00000367318:exon11:c.T535G:p.S179A,ENSG00000118194:ENST00000367320:exon11:c.T445G:p.S149A,ENSG00000118194:ENST00000367322:exon11:c.T535G:p.S179A,ENSG00000118194:ENST00000421663:exon11:c.T541G:p.S181A,ENSG00000118194:ENST00000509001:exon11:c.T535G:p.S179A,ENSG00000118194:ENST00000458432:exon12:c.T571G:p.S191A		N	0,00057
TNNT2	1_201332505_CTC_-	ENSG00000118194:ENST00000360372:exon9:c.472_474del:p.158_158del,ENSG00000118194:ENST00000236918:exon10:c.502_504del:p.168_168del,ENSG00000118194:ENST00000367315:exon10:c.487_489del:p.163_163del,ENSG00000118194:ENST00000367317:exon10:c.487_489del:p.163_163del,ENSG00000118194:ENST00000438742:exon10:c.472_474del:p.158_158del,ENSG00000118194:ENST00000367318:exon11:c.487_489del:p.163_163del,ENSG00000118194:ENST00000367320:exon11:c.397_399del:p.133_133del,ENSG00000118194:ENST00000367322:exon11:c.487_489del:p.163_163del,ENSG00000118194:ENST00000421663:exon11:c.493_495del:p.165_165del,ENSG00000118194:ENST00000509001:exon11:c.487_489del:p.163_163del,ENSG00000118194:ENST00000455702:exon12:c.517_519del:p.173_173del,ENSG00000118194:ENST00000458432:exon12:c.523_525del:p.175_175del		P	0,00172
TNNT2	1_201332514_CTC_-	ENSG00000118194:ENST00000360372:exon9:c.463_465del:p.155_155del,ENSG00000118194:ENST00000236918:exon10:c.493_495del:p.165_165del,ENSG00000118194:ENST00000367315:exon10:c.478_480del:p.160_160del,ENSG00000118194:ENST00000367317:exon10:c.478_480del:p.160_160del,ENSG00000118194:ENST00000438742:exon10:c.463_465del:p.155_155del,ENSG00000118194:ENST00000367318:exon11:c.478_480del:p.160_160del,ENSG00000118194:ENST00000367320:exon11:c.388_390del:p.130_130del,ENSG00000118194:ENST00000367322:exon11:c.478_480del:p.160_160del,ENSG00000118194:ENST00000421663:exon11:c.484_486del:p.162_162del,ENSG00000118194:ENST00000509001:exon11:c.478_480del:p.160_160del,ENSG00000118194:ENST00000455702:exon12:c.508_510del:p.170_170del,ENSG00000118194:ENST00000458432:exon12:c.514_516del:p.172_172del		P	0,00172

TNNT2	1_201334389_G_A	ENSG00000118194:ENST00000360372:exon7:c.C296T:p.A99V,ENSG00000118194:ENST00000236918:exon8:c.C326T:p.A109V,ENSG00000118194:ENST00000367315:exon8:c.C311T:p.A104V,ENSG00000118194:ENST00000367317:exon8:c.C311T:p.A104V,ENSG00000118194:ENST00000438742:exon8:c.C296T:p.A99V,ENSG00000118194:ENST00000367318:exon9:c.C311T:p.A104V,ENSG00000118194:ENST00000367322:exon9:c.C311T:p.A104V,ENSG00000118194:ENST00000421663:exon9:c.C317T:p.A106V,ENSG00000118194:ENST00000422165:exon9:c.C326T:p.A109V,ENSG00000118194:ENST00000509001:exon9:c.C311T:p.A104V,ENSG00000118194:ENST00000455702:exon10:c.C341T:p.A114V,ENSG00000118194:ENST00000458432:exon10:c.C347T:p.A116V		P	0,00174
TNNT2	1_201334419_C_T	ENSG00000118194:ENST00000360372:exon7:c.G266A:p.R89H,ENSG00000118194:ENST00000236918:exon8:c.G296A:p.R99H,ENSG00000118194:ENST00000367315:exon8:c.G281A:p.R94H,ENSG00000118194:ENST00000367317:exon8:c.G281A:p.R94H,ENSG00000118194:ENST00000438742:exon8:c.G266A:p.R89H,ENSG00000118194:ENST00000367318:exon9:c.G281A:p.R94H,ENSG00000118194:ENST00000367322:exon9:c.G281A:p.R94H,ENSG00000118194:ENST00000412633:exon9:c.G278A:p.R93H,ENSG00000118194:ENST00000421663:exon9:c.G287A:p.R96H,ENSG00000118194:ENST00000422165:exon9:c.G296A:p.R99H,ENSG00000118194:ENST00000509001:exon9:c.G281A:p.R94H,ENSG00000118194:ENST00000455702:exon10:c.G311A:p.R104H,ENSG00000118194:ENST00000458432:exon10:c.G317A:p.R106H		P	0,00059
TNNT2	1_201334425_C_T	ENSG00000118194:ENST00000360372:exon7:c.G260A:p.R87Q,ENSG00000118194:ENST00000236918:exon8:c.G290A:p.R97Q,ENSG00000118194:ENST00000367315:exon8:c.G275A:p.R92Q,ENSG00000118194:ENST00000367317:exon8:c.G275A:p.R92Q,ENSG00000118194:ENST00000438742:exon8:c.G260A:p.R87Q,ENSG00000118194:ENST00000367318:exon9:c.G275A:p.R92Q,ENSG00000118194:ENST00000367322:exon9:c.G275A:p.R92Q,ENSG00000118194:ENST00000412633:exon9:c.G272A:p.R91Q,ENSG00000118194:ENST00000421663:exon9:c.G281A:p.R94Q,ENSG00000118194:ENST00000422165:exon9:c.G290A:p.R97Q,ENSG00000118194:ENST00000509001:exon9:c.G275A:p.R92Q,ENSG00000118194:ENST00000455702:exon10:c.G305A:p.R102Q,ENSG00000118194:ENST00000458432:exon10:c.G311A:p.R104Q	rs121964856	P	0,00059
TNNT2	1_201334426_G_A	ENSG00000118194:ENST00000360372:exon7:c.C259T:p.R87W,ENSG00000118194:ENST00000236918:exon8:c.C289T:p.R97W,ENSG00000118194:ENST00000367315:exon8:c.C274T:p.R92W,ENSG00000118194:ENST00000367317:exon8:c.C274T:p.R92W,ENSG00000118194:ENST00000438742:exon8:c.C259T:p.R87W,ENSG00000118194:ENST00000367318:exon9:c.C274T:p.R92W,ENSG00000118194:ENST00000367322:exon9:c.C274T:p.R92W,ENSG00000118194:ENST00000412633:exon9:c.C271T:p.R91W,ENSG00000118194:ENST00000421663:exon9:c.C280T:p.R94W,ENSG00000118194:ENST00000422165:exon9:c.C289T:p.R97W,ENSG00000118194:ENST00000509001:exon9:c.C274T:p.R92W,ENSG00000118194:ENST00000455702:exon10:c.C304T:p.R102W,ENSG00000118194:ENST00000458432:exon10:c.C310T:p.R104W		P	0,00118

TNNT2	1_201334766_A_T	ENSG00000118194:ENST00000360372:exon6:c.T221A:p.I74N,ENSG00000118194:ENST00000236918:exon7:c.T251A:p.I84N,ENSG00000118194:ENST00000367315:exon7:c.T236A:p.I79N,ENSG00000118194:ENST00000367317:exon7:c.T236A:p.I79N,ENSG00000118194:ENST00000438742:exon7:c.T221A:p.I74N,ENSG00000118194:ENST00000367318:exon8:c.T236A:p.I79N,ENSG00000118194:ENST00000367322:exon8:c.T236A:p.I79N,ENSG00000118194:ENST00000412633:exon8:c.T233A:p.I78N,ENSG00000118194:ENST00000421663:exon8:c.T242A:p.I81N,ENSG00000118194:ENST00000422165:exon8:c.T251A:p.I84N,ENSG00000118194:ENST00000509001:exon8:c.T236A:p.I79N,ENSG00000118194:ENST00000367320:exon9:c.T263A:p.I88N,ENSG00000118194:ENST00000455702:exon9:c.T266A:p.I89N,ENSG00000118194:ENST00000458432:exon9:c.T272A:p.I91N	rs121964855	P	0,00058
TNNT2	1_201337340_G_A	ENSG00000118194:ENST00000360372:exon3:c.C68T:p.A23V,ENSG00000118194:ENST00000236918:exon4:c.C98T:p.A33V,ENSG00000118194:ENST00000367315:exon4:c.C83T:p.A28V,ENSG00000118194:ENST00000367317:exon4:c.C83T:p.A28V,ENSG00000118194:ENST00000438742:exon4:c.C68T:p.A23V,ENSG00000118194:ENST00000367318:exon5:c.C83T:p.A28V,ENSG00000118194:ENST00000367322:exon5:c.C83T:p.A28V,ENSG00000118194:ENST00000412633:exon5:c.C83T:p.A28V,ENSG00000118194:ENST00000421663:exon5:c.C89T:p.A30V,ENSG00000118194:ENST00000422165:exon5:c.C98T:p.A33V,ENSG00000118194:ENST00000509001:exon5:c.C83T:p.A28V,ENSG00000118194:ENST00000367320:exon6:c.C113T:p.A38V,ENSG00000118194:ENST00000455702:exon6:c.C113T:p.A38V,ENSG00000118194:ENST00000458432:exon6:c.C119T:p.A40V	rs200754249	P	0,00058
TNNT2	1_201337541_G_A	ENST00000360372:exon3:c.52+5C>T		L	0,00058
TNNT2	1_201338976_G_-	ENST00000236918:exon4:c.52-2C>-,ENST00000458432:exon6:c.74-3C>-,ENST00000367320:exon6:c.68-3C>-,ENST00000455702:exon6:c.68-3C>-,ENST00000422165:exon5:c.53-3C>-	rs200153031	D	0,00184
TNNT2	1_201338976_G_A	ENST00000236918:exon4:c.52-2C>T,ENST00000458432:exon6:c.74-3C>T,ENST00000367320:exon6:c.68-3C>T,ENST00000455702:exon6:c.68-3C>T,ENST00000422165:exon5:c.53-3C>T		N	0,00122
TNNT2	1_201338978_G_A	ENST00000236918:exon4:c.52-4C>T,ENST00000458432:exon6:c.74-5C>T,ENST00000367320:exon6:c.68-5C>T,ENST00000455702:exon6:c.68-5C>T,ENST00000422165:exon5:c.53-5C>T		L	0,00061
TNNT2	1_201338979_G_-	ENST00000236918:exon4:c.52-5C>-		L	0,00183
TPM1	15_63335110_G_A	ENSG00000140416:ENST00000267996:exon1:c.G82A:p.D28N,ENSG00000140416:ENST00000288398:exon1:c.G82A:p.D28N,ENSG00000140416:ENST00000357980:exon1:c.G82A:p.D28N,ENSG00000140416:ENST00000358278:exon1:c.G82A:p.D28N,ENSG00000140416:ENST00000403994:exon1:c.G82A:p.D28N,ENSG00000140416:ENST00000558347:exon1:c.G82A:p.D28N,ENSG00000140416:ENST00000559397:exon1:c.G82A:p.D28N,ENSG00000140416:ENST00000559556:exon1:c.G82A:p.D28N,ENSG00000140416:ENST00000560445:exon1:c.G82A:p.D28N,ENSG00000140416:ENST00000561425:exon1:c.G82A:p.D28N		N	0,00187

TPM1	15_63335138_A_C	ENSG00000140416:ENST00000267996:exon1:c.A110C:p.K37T,ENSG00000140416:ENST00000288398:exon1:c.A110C:p.K37T,ENSG00000140416:ENST00000357980:exon1:c.A110C:p.K37T,ENSG00000140416:ENST00000358278:exon1:c.A110C:p.K37T,ENSG00000140416:ENST00000403994:exon1:c.A110C:p.K37T,ENSG00000140416:ENST00000558347:exon1:c.A110C:p.K37T,ENSG00000140416:ENST00000559397:exon1:c.A110C:p.K37T,ENSG00000140416:ENST00000559556:exon1:c.A110C:p.K37T,ENSG00000140416:ENST00000560445:exon1:c.A110C:p.K37T,ENSG00000140416:ENST00000561425:exon1:c.A110C:p.K37T		N	0,00094
TPM1	15_63336299_C_T	ENSG00000140416:ENST00000288398:exon2:c.C188T:p.A63V,ENSG00000140416:ENST00000358278:exon2:c.C188T:p.A63V,ENSG00000140416:ENST00000403994:exon2:c.C188T:p.A63V,ENSG00000140416:ENST00000558347:exon2:c.C188T:p.A63V,ENSG00000140416:ENST00000559556:exon2:c.C188T:p.A63V,ENSG00000140416:ENST00000357980:exon3:c.C314T:p.A105V	rs199476306	P	0,00057
TPM1	15_63351757_T_C	ENST00000288398:exon4:c.375-5T>C,ENST00000358278:exon4:c.375-5T>C,ENST00000403994:exon4:c.375-5T>C,ENST00000357980:exon5:c.501-5T>C,ENST00000267996:exon4:c.375-5T>C,ENST00000559397:exon4:c.375-5T>C,ENST00000559556:exon4:c.375-5T>C,ENST00000560970:exon4:c.317-5T>C,ENST00000561266:exon3:c.191-5T>C,ENST00000559831:exon3:c.147-5T>C,ENST00000334895:exon3:c.267-5T>C,ENST00000404484:exon3:c.267-5T>C,ENST00000558544:exon2:c.133-5T>C,ENST00000560959:exon3:c.267-5T>C,ENST00000317516:exon3:c.267-5T>C,ENST00000559281:exon3:c.267-5T>C,ENST00000561395:exon2:c.114-5T>C		P	0,00057
TPM1	15_63353123_C_T	ENSG00000140416:ENST00000558264:exon3:c.C170T:p.A57V,ENSG00000140416:ENST00000317516:exon4:c.C440T:p.A147V,ENSG00000140416:ENST00000334895:exon4:c.C440T:p.A147V,ENSG00000140416:ENST00000404484:exon4:c.C440T:p.A147V,ENSG00000140416:ENST00000559281:exon4:c.C440T:p.A147V,ENSG00000140416:ENST00000559831:exon4:c.C320T:p.A107V,ENSG00000140416:ENST00000560615:exon4:c.C170T:p.A57V,ENSG00000140416:ENST00000560959:exon4:c.C440T:p.A147V,ENSG00000140416:ENST00000267996:exon5:c.C548T:p.A183V,ENSG00000140416:ENST00000288398:exon5:c.C548T:p.A183V,ENSG00000140416:ENST00000358278:exon5:c.C548T:p.A183V,ENSG00000140416:ENST00000403994:exon5:c.C548T:p.A183V,ENSG00000140416:ENST00000559397:exon5:c.C548T:p.A183V,ENSG00000140416:ENST00000559556:exon5:c.C548T:p.A183V,ENSG00000140416:ENST00000357980:exon6:c.C674T:p.A225V		S	0,00058
TPM1	15_63353922_G_A	ENSG00000140416:ENST00000561395:exon3:c.G200A:p.R67Q,ENSG00000140416:ENST00000334895:exon5:c.G466A:p.E156K,ENSG00000140416:ENST00000558264:exon5:c.G272A:p.R91Q,ENSG00000140416:ENST00000559281:exon5:c.G466A:p.E156K,ENSG00000140416:ENST00000267996:exon6:c.G574A:p.E192K,ENSG00000140416:ENST00000403994:exon6:c.G574A:p.E192K,ENSG00000140416:ENST00000559556:exon6:c.G574A:p.E192K,ENSG00000140416:ENST00000559831:exon6:c.G422A:p.R141Q,ENSG00000140416:ENST00000357980:exon7:c.G700A:p.E234K	rs199476315	P	0,00115

TPM1	15_63354818_T_G	ENSG00000140416:ENST00000317516:exon7:c.T638G:p.L213W,ENSG00000140416:ENST00000334895:exon7:c.T638G:p.L213W,ENSG00000140416:ENST00000404484:exon7:c.T638G:p.L213W,ENSG00000140416:ENST00000559281:exon7:c.T638G:p.L213W,ENSG00000140416:ENST00000560959:exon7:c.T638G:p.L213W,ENSG00000140416:ENST00000267996:exon8:c.T746G:p.L249W,ENSG00000140416:ENST00000288398:exon8:c.T746G:p.L249W,ENSG00000140416:ENST00000358278:exon8:c.T746G:p.L249W,ENSG00000140416:ENST00000403994:exon8:c.T746G:p.L249W,ENSG00000140416:ENST00000559397:exon8:c.T746G:p.L249W,ENSG00000140416:ENST00000559556:exon8:c.T746G:p.L249W,ENSG00000140416:ENST00000357980:exon9:c.T872G:p.L291W		S	0,00057
TPM1	15_63354833_A_G	ENSG00000140416:ENST00000317516:exon7:c.A653G:p.D218G,ENSG00000140416:ENST00000334895:exon7:c.A653G:p.D218G,ENSG00000140416:ENST00000404484:exon7:c.A653G:p.D218G,ENSG00000140416:ENST00000559281:exon7:c.A653G:p.D218G,ENSG00000140416:ENST00000560959:exon7:c.A653G:p.D218G,ENSG00000140416:ENST00000267996:exon8:c.A761G:p.D254G,ENSG00000140416:ENST00000288398:exon8:c.A761G:p.D254G,ENSG00000140416:ENST00000358278:exon8:c.A761G:p.D254G,ENSG00000140416:ENST00000403994:exon8:c.A761G:p.D254G,ENSG00000140416:ENST00000559397:exon8:c.A761G:p.D254G,ENSG00000140416:ENST00000559556:exon8:c.A761G:p.D254G,ENSG00000140416:ENST00000357980:exon9:c.A887G:p.D296G		S	0,00057
TPM1	15_63354907_A_G	ENSG00000140416:ENST00000560959:exon7:c.A727G:p.I243V		N	0,00057
TPM1	15_63354938_CGCT_-	ENSG00000140416:ENST00000560959:exon7:c.758_761del:p.253_254del		L	0,00114
TPM1	15_63354943_C_T	ENSG00000140416:ENST00000560959:exon7:c.C763T:p.L255F	rs56054026	D	0,00114
TPM1	15_63356281_A_G	ENSG00000140416:ENST00000559281:exon8:c.A683G:p.K228R,ENSG00000140416:ENST00000288398:exon9:c.A791G:p.K264R,ENSG00000140416:ENST00000403994:exon9:c.A791G:p.K264R		S	0,00057
TPM1	15_63358166_A_G	ENSG00000140416:ENST00000560445:exon3:c.A193G:p.I65V		N	0,00057
VCL	10_75832551_G_A	ENSG00000035403:ENST00000211998:exon5:c.G563A:p.R188Q,ENSG00000035403:ENST00000372755:exon5:c.G563A:p.R188Q		N	0,00057
VCL	10_75832578_C_T	ENSG00000035403:ENST00000211998:exon5:c.C590T:p.T197I,ENSG00000035403:ENST00000372755:exon5:c.C590T:p.T197I	rs189242810	S	0,00057
VCL	10_75834522_C_T	ENSG00000035403:ENST00000211998:exon6:c.C644T:p.T215I,ENSG00000035403:ENST00000372755:exon6:c.C644T:p.T215I		N	0,00057
VCL	10_75849088_A_G	ENSG00000035403:ENST00000436396:exon2:c.A173G:p.K58R,ENSG00000035403:ENST00000211998:exon9:c.A1157G:p.K386R,ENSG00000035403:ENST00000372755:exon9:c.A1157G:p.K386R	rs200342284	D	0,00115
VCL	10_75849097_A_G	ENSG00000035403:ENST00000436396:exon2:c.A182G:p.D61G,ENSG00000035403:ENST00000211998:exon9:c.A1166G:p.D389G,ENSG00000035403:ENST00000372755:exon9:c.A1166G:p.D389G		N	0,00115
VCL	10_75849776_T_C	ENST00000211998:exon10:c.1177-5T>C,ENST00000372755:exon10:c.1177-5T>C,ENST00000436396:exon3:c.193-5T>C		L	0,00057
VCL	10_75849841_G_A	ENSG00000035403:ENST00000436396:exon3:c.G253A:p.A85T,ENSG00000035403:ENST00000211998:exon10:c.G1237A:p.A413T,ENSG00000035403:ENST00000372755:exon10:c.G1237A:p.A413T	rs146278697	D	0,00057

VCL	10_75855425_A_C	ENSG00000035403:ENST00000436396:exon5:c.A571C:p.I191L,ENSG00000035403:ENST00000211998:exon12:c.A1555C:p.I519L,ENSG00000035403:ENST00000372755:exon12:c.A1555C:p.I519L	rs141033098	S	0,00173
VCL	10_75855491_C_G	ENSG00000035403:ENST00000436396:exon5:c.C637G:p.L213V,ENSG00000035403:ENST00000211998:exon12:c.C1621G:p.L541V,ENSG00000035403:ENST00000372755:exon12:c.C1621G:p.L541V		N	0,00058
VCL	10_75857050_T_C	ENSG00000035403:ENST00000436396:exon6:c.T848C:p.V283A,ENSG00000035403:ENST00000211998:exon13:c.T1832C:p.V611A,ENSG00000035403:ENST00000372755:exon13:c.T1832C:p.V611A		N	0,00057
VCL	10_75857059_C_T	ENSG00000035403:ENST00000436396:exon6:c.C857T:p.T286M,ENSG00000035403:ENST00000211998:exon13:c.C1841T:p.T614M,ENSG00000035403:ENST00000372755:exon13:c.C1841T:p.T614M		S	0,00057
VCL	10_75860740_A_G	ENSG00000035403:ENST00000436396:exon7:c.A923G:p.H308R,ENSG00000035403:ENST00000211998:exon14:c.A1907G:p.H636R,ENSG00000035403:ENST00000372755:exon14:c.A1907G:p.H636R	rs71579374	D	0,00057
VCL	10_75860750_G_T	ENSG00000035403:ENST00000436396:exon7:c.G933T:p.K311N,ENSG00000035403:ENST00000211998:exon14:c.G1917T:p.K639N,ENSG00000035403:ENST00000372755:exon14:c.G1917T:p.K639N		S	0,00057
VCL	10_75860773_C_T	ENSG00000035403:ENST00000436396:exon7:c.C956T:p.A319V,ENSG00000035403:ENST00000211998:exon14:c.C1940T:p.A647V,ENSG00000035403:ENST00000372755:exon14:c.C1940T:p.A647V		N	0,00057
VCL	10_75860806_T_C	ENSG00000035403:ENST00000436396:exon7:c.T989C:p.V330A,ENSG00000035403:ENST00000211998:exon14:c.T1973C:p.V658A,ENSG00000035403:ENST00000372755:exon14:c.T1973C:p.V658A		N	0,00172
VCL	10_75871695_TAGGTG_-	ENSG00000035403:ENST00000436396:exon12:c.1790_1795del:p.597_599del,ENSG00000035403:ENST00000211998:exon19:c.2774_2779del:p.925_927del		N	0,00057
VCL	10_75871722_C_T	ENSG00000035403:ENST00000436396:exon12:c.C1817T:p.A606V,ENSG00000035403:ENST00000211998:exon19:c.C2801T:p.A934V	rs16931179	P	0,00057
VCL	10_75871748_C_G	ENSG00000035403:ENST00000436396:exon12:c.C1843G:p.P615A,ENSG00000035403:ENST00000211998:exon19:c.C2827G:p.P943A	rs71579375	P	0,00057
VCL	10_75871782_TGT_-	ENSG00000035403:ENST00000436396:exon12:c.1877_1879del:p.626_627del,ENSG00000035403:ENST00000211998:exon19:c.2861_2863del:p.954_955del		P	0,00057
VCL	10_75873951_A_G	ENSG00000035403:ENST00000417648:exon5:c.A538G:p.I180V,ENSG00000035403:ENST00000436396:exon13:c.A1975G:p.I659V,ENSG00000035403:ENST00000372755:exon19:c.A2755G:p.I919V,ENSG00000035403:ENST00000211998:exon20:c.A2959G:p.I987V		N	0,00057

APPENDIX E – LIST OF CANDIDATE TITIN VARIANTS

Supplementary table 2. List of candidate titin variants L : predicted loss-of-function variant; E: enriched variant; P: published in the literature as associated with hypertrophic cardiomyopathy. All the types of variants are defined in the Methods Section, chapter 3.3.

Genomic signature	Transcript / Amino acid change	Type of variant	dbSNP137 ID
2_179392277_A_G	ENSG00000155657:ENST00000460472:exon190:c.T80381C:p.M26794T,ENSG00000155657:ENST00000342175:exon191:c.T80957C:p.M26986T,ENSG00000155657:ENST00000359218:exon191:c.T80756C:p.M26919T,ENSG00000155657:ENST00000342992:exon311:c.T99872C:p.M33291T,ENSG00000155657:ENST00000591111:exon312:c.T102653C:p.M34218T,ENSG00000155657:ENST00000589042:exon362:c.T107576C:p.M35859T		rs72629793
2_179393373_G_A	ENSG00000155657:ENST00000460472:exon188:c.C79910T:p.P26637L,ENSG00000155657:ENST00000342175:exon189:c.C80486T:p.P26829L,ENSG00000155657:ENST00000359218:exon189:c.C80285T:p.P26762L,ENSG00000155657:ENST00000342992:exon309:c.C99401T:p.P33134L,ENSG00000155657:ENST00000591111:exon310:c.C102182T:p.P34061L,ENSG00000155657:ENST00000589042:exon360:c.C107105T:p.P35702L		
2_179393622_T_A	NM_003319:c.A79661T:p.N26554I		NA
2_179393898_T_A	ENSG00000155657:ENST00000460472:exon188:c.A79385T:p.E26462V,ENSG00000155657:ENST00000342175:exon189:c.A79961T:p.E26654V,ENSG00000155657:ENST00000359218:exon189:c.A79760T:p.E26587V,ENSG00000155657:ENST00000342992:exon309:c.A98876T:p.E32959V,ENSG00000155657:ENST00000591111:exon310:c.A101657T:p.E33886V,ENSG00000155657:ENST00000589042:exon360:c.A106580T:p.E35527V		rs55725279
2_179394779_T_C	NM_003319:c.A79244G:p.H26415R		
2_179395251_T_C	NM_003319:c.A78896G:p.E26299G		
2_179395550_-_A	ENSG00000155657:ENST00000460472:exon186:c.78597_78598insT:p.V26199fs,ENSG00000155657:ENST00000342175:exon187:c.79173_79174insT:p.V26391fs,ENSG00000155657:ENST00000359218:exon187:c.78972_78973insT:p.V26324fs,ENSG00000155657:ENST00000342992:exon307:c.98088_98089insT:p.V32696fs,ENSG00000155657:ENST00000591111:exon308:c.100869_100870insT:p.V33623fs,ENSG00000155657:ENST00000589042:exon358:c.105792_105793insT:p.V35264fs	L	
2_179395623_C_T	NM_003319:c.C26729G:p.T8910S		

2_179395826_AGA_-	ENSG00000155657:ENST00000460472:exon186:c.78319_78321del:p.26107_26107del,ENSG00000155657:ENST00000342175:exon187:c.78895_78897del:p.26299_26299del,ENSG00000155657:ENST00000359218:exon187:c.78694_78696del:p.26232_26232del,ENSG00000155657:ENST00000342992:exon307:c.97810_97812del:p.32604_32604del,ENSG00000155657:ENST00000591111:exon308:c.100591_100593del:p.33531_33531del,ENSG00000155657:ENST00000589042:exon358:c.105514_105516del:p.35172_35172del		
2_179395930_T_C	NM_003319:c.A78217G:p.M26073V		
2_179395936_G_A	NM_003319:c.C19652T:p.T6551M		
2_179395959_G_A	NM_003319:c.C78188T:p.A26063V		
2_179396215_G_A	NM_003319:c.C77932T:p.R25978C		
2_179396479_A_C	NM_003319:c.T77668G:p.C25890G		
2_179396496_C_T	NM_003319:c.G77651A:p.R25884H		
2_179396568_T_G	NM_003319:c.A77579C:p.E25860A		
2_179396648_T_G	ENSG00000155657:ENST00000460472:exon186:c.A77499C:p.R25833S,ENSG00000155657:ENST00000342175:exon187:c.A78075C:p.R26025S,ENSG00000155657:ENST00000359218:exon187:c.A77874C:p.R25958S,ENSG00000155657:ENST00000342992:exon307:c.A96990C:p.R32330S,ENSG00000155657:ENST00000591111:exon308:c.A99771C:p.R33257S,ENSG00000155657:ENST00000589042:exon358:c.A104694C:p.R34898S		
2_179396995_G_A	ENSG00000155657:ENST00000460472:exon186:c.C77152T:p.L25718F,ENSG00000155657:ENST00000342175:exon187:c.C77728T:p.L25910F,ENSG00000155657:ENST00000359218:exon187:c.C77527T:p.L25843F,ENSG00000155657:ENST00000342992:exon307:c.C96643T:p.L32215F,ENSG00000155657:ENST00000591111:exon308:c.C99424T:p.L33142F,ENSG00000155657:ENST00000589042:exon358:c.C104347T:p.L34783F		
2_179397010_T_C	ENSG00000155657:ENST00000460472:exon186:c.A77137G:p.T25713A,ENSG00000155657:ENST00000342175:exon187:c.A77713G:p.T25905A,ENSG00000155657:ENST00000359218:exon187:c.A77512G:p.T25838A,ENSG00000155657:ENST00000342992:exon307:c.A96628G:p.T32210A,ENSG00000155657:ENST00000591111:exon308:c.A99409G:p.T33137A,ENSG00000155657:ENST00000589042:exon358:c.A104332G:p.T34778A		
2_179397081_G_A	NM_003319:c.G60895A:p.G20299S		
2_179397091_C_G	NM_003319:c.G77056C:p.A25686P	E	

2_179397416_AGG_-	ENSG00000155657:ENST00000460472:exon186:c.76729_76731del:p.25577_25577del,ENSG00000155657:ENST00000342175:exon187:c.77305_77307del:p.25769_25769del,ENSG00000155657:ENST00000359218:exon187:c.77104_77106del:p.25702_25702del,ENSG00000155657:ENST00000342992:exon307:c.96220_96222del:p.32074_32074del,ENSG00000155657:ENST00000591111:exon308:c.99001_99003del:p.33001_33001del,ENSG00000155657:ENST00000589042:exon358:c.103924_103926del:p.34642_34642del		
2_179397654_A_G	NM_003319:c.T76493C:p.V25498A		rs55945684
2_179397706_G_A	NM_003319:c.C76441T:p.R25481C		
2_179397733_G_A	NM_003319:c.C76414T:p.R25472W		
2_179397979_G_A	ENSG00000155657:ENST00000460472:exon186:c.C76168T:p.R25390C,ENSG00000155657:ENST00000342175:exon187:c.C76744T:p.R25582C,ENSG00000155657:ENST00000359218:exon187:c.C76543T:p.R25515C,ENSG00000155657:ENST00000342992:exon307:c.C95659T:p.R31887C,ENSG00000155657:ENST00000591111:exon308:c.C98440T:p.R32814C,ENSG00000155657:ENST00000589042:exon358:c.C103363T:p.R34455C		rs72629785
2_179398050_G_A	NM_003319:c.C76097T:p.T25366M		
2_179398186_C_T	NM_003319:c.G75961A:p.V25321M		
2_179398386_G_A	NM_003319:c.C75761T:p.T25254I		
2_179398465_T_C	NM_003319:c.A75682G:p.K25228E		rs72629783
2_179398591_T_C	ENSG00000155657:ENST00000460472:exon186:c.A75556G:p.M25186V,ENSG00000155657:ENST00000342175:exon187:c.A76132G:p.M25378V,ENSG00000155657:ENST00000359218:exon187:c.A75931G:p.M25311V,ENSG00000155657:ENST00000342992:exon307:c.A95047G:p.M31683V,ENSG00000155657:ENST00000591111:exon308:c.A97828G:p.M32610V,ENSG00000155657:ENST00000589042:exon358:c.A102751G:p.M34251V		rs56173891
2_179398747_T_C	NM_003319:c.G74696A:p.R24899H		rs56347248
2_179399071_G_A	ENSG00000155657:ENST00000460472:exon186:c.C75076T:p.R25026W,ENSG00000155657:ENST00000342175:exon187:c.C75652T:p.R25218W,ENSG00000155657:ENST00000359218:exon187:c.C75451T:p.R25151W,ENSG00000155657:ENST00000342992:exon307:c.C94567T:p.R31523W,ENSG00000155657:ENST00000591111:exon308:c.C97348T:p.R32450W,ENSG00000155657:ENST00000589042:exon358:c.C102271T:p.R34091W		rs140319117
2_179399406_G_C	NM_003319:c.A58496T:p.K19499I		
2_179399451_C_T	NM_133378:c.C19806G:p.F6602L		rs55669553

2_179399687_C_T	NM_003319:c.G74460A:p.M24820I		
2_179400016_-_ATCTGAAGG	NM_003319:c.74131_74132insCCTTCAGAT:p.P24711delinsPSDP		
2_179400027_-_CTGAAGGCT	NM_003319:c.74120_74121insAGCCTTCAG:p.K24707delinsKPSE		
2_179400097_C_T	NM_003319:c.G74050A:p.V24684M		
2_179400261_C_T	NM_003319:c.G73886A:p.R24629K		
2_179400360_C_T	ENSG00000155657:ENST00000460472:exon186:c.G73787A:p.R24596K,ENSG00000155657:ENST00000342175:exon187:c.G74363A:p.R24788K,ENSG00000155657:ENST00000359218:exon187:c.G74162A:p.R24721K,ENSG00000155657:ENST00000342992:exon307:c.G93278A:p.R31093K,ENSG00000155657:ENST00000591111:exon308:c.G96059A:p.R32020K,ENSG00000155657:ENST00000589042:exon358:c.G100982A:p.R33661K		rs201857158
2_179400396_G_A	NM_003319:c.C73751T:p.S24584F		
2_179401084_C_T	ENSG00000155657:ENST00000460472:exon185:c.G73195A:p.E24399K,ENSG00000155657:ENST00000342175:exon186:c.G73771A:p.E24591K,ENSG00000155657:ENST00000359218:exon186:c.G73570A:p.E24524K,ENSG00000155657:ENST00000342992:exon306:c.G92686A:p.E30896K,ENSG00000155657:ENST00000591111:exon307:c.G95467A:p.E31823K,ENSG00000155657:ENST00000589042:exon357:c.G100390A:p.E33464K		
2_179401935_C_T	NM_003319:c.G72706A:p.E24236K		rs72648278
2_179402104_C_T	NM_003319:c.G72635A:p.G24212E		
2_179402266_C_T	NM_003319:c.G72473A:p.R24158H		
2_179403525_A_T	ENSG00000155657:ENST00000460472:exon182:c.T71836A:p.S23946T,ENSG00000155657:ENST00000342175:exon183:c.T72412A:p.S24138T,ENSG00000155657:ENST00000359218:exon183:c.T72211A:p.S24071T,ENSG00000155657:ENST00000342992:exon303:c.T91327A:p.S30443T,ENSG00000155657:ENST00000591111:exon304:c.T94108A:p.S31370T,ENSG00000155657:ENST00000589042:exon354:c.T99031A:p.S33011T		rs78814506
2_179403769_C_G	NM_003319:c.G71698C:p.D23900H		
2_179403836_G_C	ENSG00000155657:ENST00000460472:exon181:c.C71631G:p.D23877E,ENSG00000155657:ENST00000342175:exon182:c.C72207G:p.D24069E,ENSG00000155657:ENST00000359218:exon182:c.C72006G:p.D24002E,ENSG00000155657:ENST00000342992:exon302:c.C91122G:p.D30374E,ENSG00000155657:ENST00000591111:exon303:c.C93903G:p.D31301E,ENSG00000155657:ENST00000589042:exon353:c.C98826G:p.D32942E		rs190967471

2_179403946_C_T	ENSG00000155657:ENST00000460472:exon181:c.G71521A:p.V23841I,ENSG00000155657:ENST00000342175:exon182:c.G72097A:p.V24033I,ENSG00000155657:ENST00000359218:exon182:c.G71896A:p.V23966I,ENSG00000155657:ENST00000342992:exon302:c.G91012A:p.V30338I,ENSG00000155657:ENST00000591111:exon303:c.G93793A:p.V31265I,ENSG00000155657:ENST00000589042:exon353:c.G98716A:p.V32906I		rs182683829
2_179404151_G_A	ENSG00000155657:ENST00000460472:exon180:c.C71446T:p.P23816S,ENSG00000155657:ENST00000342175:exon181:c.C72022T:p.P24008S,ENSG00000155657:ENST00000359218:exon181:c.C71821T:p.P23941S,ENSG00000155657:ENST00000342992:exon301:c.C90937T:p.P30313S,ENSG00000155657:ENST00000591111:exon302:c.C93718T:p.P31240S,ENSG00000155657:ENST00000589042:exon352:c.C98641T:p.P32881S		
2_179404361_G_A	NM_003319:c.C71236T:p.R23746C		
2_179404451_A_G	NM_003319:c.T71146C:p.C23716R		
2_179404525_G_A	ENSG00000155657:ENST00000460472:exon180:c.C71072T:p.T23691I,ENSG00000155657:ENST00000342175:exon181:c.C71648T:p.T23883I,ENSG00000155657:ENST00000359218:exon181:c.C71447T:p.T23816I,ENSG00000155657:ENST00000342992:exon301:c.C90563T:p.T30188I,ENSG00000155657:ENST00000591111:exon302:c.C93344T:p.T31115I,ENSG00000155657:ENST00000589042:exon352:c.C98267T:p.T32756I		rs199805060
2_179404549_C_T	ENSG00000155657:ENST00000460472:exon180:c.G71048A:p.R23683H,ENSG00000155657:ENST00000342175:exon181:c.G71624A:p.R23875H,ENSG00000155657:ENST00000359218:exon181:c.G71423A:p.R23808H,ENSG00000155657:ENST00000342992:exon301:c.G90539A:p.R30180H,ENSG00000155657:ENST00000591111:exon302:c.G93320A:p.R31107H,ENSG00000155657:ENST00000589042:exon352:c.G98243A:p.R32748H		
2_179404550_G_A	ENSG00000155657:ENST00000460472:exon180:c.C71047T:p.R23683C,ENSG00000155657:ENST00000342175:exon181:c.C71623T:p.R23875C,ENSG00000155657:ENST00000359218:exon181:c.C71422T:p.R23808C,ENSG00000155657:ENST00000342992:exon301:c.C90538T:p.R30180C,ENSG00000155657:ENST00000591111:exon302:c.C93319T:p.R31107C,ENSG00000155657:ENST00000589042:exon352:c.C98242T:p.R32748C		rs72648272
2_179404673_C_G	ENSG00000155657:ENST00000460472:exon180:c.G70924C:p.D23642H,ENSG00000155657:ENST00000342175:exon181:c.G71500C:p.D23834H,ENSG00000155657:ENST00000359218:exon181:c.G71299C:p.D23767H,ENSG00000155657:ENST00000342992:exon301:c.G90415C:p.D30139H,ENSG00000155657:ENST00000591111:exon302:c.G93196C:p.D31066H,ENSG00000155657:ENST00000589042:exon352:c.G98119C:p.D32707H		
2_179406044_C_G	ENSG00000155657:ENST00000460472:exon178:c.G70565C:p.R23522P,ENSG00000155657:ENST00000342175:exon179:c.G71141C:p.R23714P,ENSG00000155657:ENST00000359218:exon179:c.G70940C:p.R23647P,ENSG00000155657:ENST00000342992:exon299:c.G90056C:p.R30019P,ENSG00000155657:ENST00000591111:exon300:c.G92837C:p.R30946P,ENSG00000155657:ENST00000589042:exon350:c.G97760C:p.R32587P		

2_179406044_C_T	NM_003319:c.G70565A:p.R23522H		rs55704830
2_179406131_C_T	NM_003319:c.G70478A:p.R23493Q		
2_179406177_C_T	NM_003319:c.G70432A:p.A23478T		
2_179406266_C_T	NM_003319:c.G70343A:p.R23448H		
2_179406993_A_G	NM_003319:c.T70295C:p.I23432TTTN;TTN		rs55660660
2_179407041_C_T	NM_003319:c.G70247A:p.G23416E		
2_179407047_C_T	NM_003319:c.G70241A:p.R23414H		
2_179407065_C_T	ENSG00000155657:ENST00000460472:exon177:c.G70223A:p.R23408H,ENSG00000155657:ENST00000342175:exon178:c.G70799A:p.R23600H,ENSG00000155657:ENST00000359218:exon178:c.G70598A:p.R23533H,ENSG00000155657:ENST00000342992:exon298:c.G89714A:p.R29905H,ENSG00000155657:ENST00000591111:exon299:c.G92495A:p.R30832H,ENSG00000155657:ENST00000589042:exon349:c.G97418A:p.R32473H		
2_179407293_A_G	NM_133437:exon179:c.70574-3T>C,NM_133432:exon179:c.70373-3T>C,NM_003319:exon178:c.69998-3T>C,NM_133378:exon299:c.89489-3T>C	L	
2_179407482_G_A	ENSG00000155657:ENST00000460472:exon176:c.C69904T:p.R23302C,ENSG00000155657:ENST00000342175:exon177:c.C70480T:p.R23494C,ENSG00000155657:ENST00000359218:exon177:c.C70279T:p.R23427C,ENSG00000155657:ENST00000342992:exon297:c.C89395T:p.R29799C,ENSG00000155657:ENST00000591111:exon298:c.C92176T:p.R30726C,ENSG00000155657:ENST00000589042:exon348:c.C97099T:p.R32367C		rs202064385
2_179407592_A_G	NM_003319:c.T69794C:p.I23265T		
2_179407662_C_T	NM_003319:c.G69724A:p.D23242N		
2_179407984_A_G	ENSG00000155657:ENST00000460472:exon175:c.T69521C:p.L23174P,ENSG00000155657:ENST00000342175:exon176:c.T70097C:p.L23366P,ENSG00000155657:ENST00000359218:exon176:c.T69896C:p.L23299P,ENSG00000155657:ENST00000342992:exon296:c.T89012C:p.L29671P,ENSG00000155657:ENST00000591111:exon297:c.T91793C:p.L30598P,ENSG00000155657:ENST00000589042:exon347:c.T96716C:p.L32239P		
2_179408096_C_A	NM_003319:c.G69409T:p.V23137L		
2_179408557_T_A	NM_133437:exon176:c.69691+4A>T,NM_133432:exon176:c.69490+4A>T,NM_003319:exon175:c.69115+4A>T,NM_133378:exon296:c.88606+4A>T	L	

2_179408636_C_T	ENSG00000155657:ENST00000460472:exon174:c.G69040A:p.D23014N,ENSG00000155657:ENST00000342175:exon175:c.G69616A:p.D23206N,ENSG00000155657:ENST00000359218:exon175:c.G69415A:p.D23139N,ENSG00000155657:ENST00000342992:exon295:c.G88531A:p.D29511N,ENSG00000155657:ENST00000591111:exon296:c.G91312A:p.D30438N,ENSG00000155657:ENST00000589042:exon346:c.G96235A:p.D32079N		
2_179408731_G_A	NM_003319:c.C68945T:p.T22982M		
2_179408940_C_T	NM_003319:c.G68821A:p.V22941M		rs191786700
2_179408964_C_T	NM_003319:c.G68797A:p.E22933K		
2_179410115_A_G	NM_003319:c.T68527C:p.Y22843H		
2_179410184_C_T	ENSG00000155657:ENST00000460472:exon172:c.G68458A:p.A22820T,ENSG00000155657:ENST00000342175:exon173:c.G69034A:p.A23012T,ENSG00000155657:ENST00000359218:exon173:c.G68833A:p.A22945T,ENSG00000155657:ENST00000342992:exon293:c.G87949A:p.A29317T,ENSG00000155657:ENST00000591111:exon294:c.G90730A:p.A30244T,ENSG00000155657:ENST00000589042:exon344:c.G95653A:p.A31885T		rs72648263
2_179410255_T_C	ENSG00000155657:ENST00000460472:exon172:c.A68387G:p.Y22796C,ENSG00000155657:ENST00000342175:exon173:c.A68963G:p.Y22988C,ENSG00000155657:ENST00000359218:exon173:c.A68762G:p.Y22921C,ENSG00000155657:ENST00000342992:exon293:c.A87878G:p.Y29293C,ENSG00000155657:ENST00000591111:exon294:c.A90659G:p.Y30220C,ENSG00000155657:ENST00000589042:exon344:c.A95582G:p.Y31861C		rs59148238
2_179410286_TCT_-	ENSG00000155657:ENST00000460472:exon172:c.68354_68356del:p.22785_22786del,ENSG00000155657:ENST00000342175:exon173:c.68930_68932del:p.22977_22978del,ENSG00000155657:ENST00000359218:exon173:c.68729_68731del:p.22910_22911del,ENSG00000155657:ENST00000342992:exon293:c.87845_87847del:p.29282_29283del,ENSG00000155657:ENST00000591111:exon294:c.90626_90628del:p.30209_30210del,ENSG00000155657:ENST00000589042:exon344:c.95549_95551del:p.31850_31851del		
2_179410548_G_T	NM_003319:c.C68220A:p.F22740LTTN;TTN		
2_179410568_T_C	NM_003319:c.A68200G:p.I22734V		
2_179410666_G_A	NM_003319:c.G64570A:p.A21524T		
2_179410693_A_G	NM_003319:c.A42481G:p.S14161G	E	rs72648259

2_179410721_G_A	ENSG00000155657:ENST00000460472:exon171:c.C68047T:p.R22683C,ENSG00000155657:ENST00000342175:exon172:c.C68623T:p.R22875C,ENSG00000155657:ENST00000359218:exon172:c.C68422T:p.R22808C,ENSG00000155657:ENST00000342992:exon292:c.C87538T:p.R29180C,ENSG00000155657:ENST00000591111:exon293:c.C90319T:p.R30107C,ENSG00000155657:ENST00000589042:exon343:c.C95242T:p.R31748C		rs142525903
2_179411023_C_T	ENSG00000155657:ENST00000460472:exon170:c.G67840A:p.D22614N,ENSG00000155657:ENST00000342175:exon171:c.G68416A:p.D22806N,ENSG00000155657:ENST00000359218:exon171:c.G68215A:p.D22739N,ENSG00000155657:ENST00000342992:exon291:c.G87331A:p.D29111N,ENSG00000155657:ENST00000591111:exon292:c.G90112A:p.D30038N,ENSG00000155657:ENST00000589042:exon342:c.G95035A:p.D31679N		rs116567963
2_179411126_T_G	ENSG00000155657:ENST00000460472:exon170:c.A67737C:p.E22579D,ENSG00000155657:ENST00000342175:exon171:c.A68313C:p.E22771D,ENSG00000155657:ENST00000359218:exon171:c.A68112C:p.E22704D,ENSG00000155657:ENST00000342992:exon291:c.A87228C:p.E29076D,ENSG00000155657:ENST00000591111:exon292:c.A90009C:p.E30003D,ENSG00000155657:ENST00000589042:exon342:c.A94932C:p.E31644D		
2_179411207_A_T	NM_003319:c.T67656A:p.D22552E		rs72648256
2_179411455_T_C	ENSG00000155657:ENST00000460472:exon169:c.A67505G:p.N22502S,ENSG00000155657:ENST00000342175:exon170:c.A68081G:p.N22694S,ENSG00000155657:ENST00000359218:exon170:c.A67880G:p.N22627S,ENSG00000155657:ENST00000342992:exon290:c.A86996G:p.N28999S,ENSG00000155657:ENST00000591111:exon291:c.A89777G:p.N29926S,ENSG00000155657:ENST00000589042:exon341:c.A94700G:p.N31567S		
2_179411522_G_A	ENSG00000155657:ENST00000460472:exon169:c.C67438T:p.R22480C,ENSG00000155657:ENST00000342175:exon170:c.C68014T:p.R22672C,ENSG00000155657:ENST00000359218:exon170:c.C67813T:p.R22605C,ENSG00000155657:ENST00000342992:exon290:c.C86929T:p.R28977C,ENSG00000155657:ENST00000591111:exon291:c.C89710T:p.R29904C,ENSG00000155657:ENST00000589042:exon341:c.C94633T:p.R31545C		rs202187398
2_179411602_A_G	NM_003319:c.A3557T:p.D1186V		
2_179412307_C_T	NM_003319:c.G66851A:p.R22284H		
2_179412679_A_G	ENSG00000155657:ENST00000460472:exon167:c.T66479C:p.I22160T,ENSG00000155657:ENST00000342175:exon168:c.T67055C:p.I22352T,ENSG00000155657:ENST00000359218:exon168:c.T66854C:p.I22285T,ENSG00000155657:ENST00000342992:exon288:c.T85970C:p.I28657T,ENSG00000155657:ENST00000591111:exon289:c.T88751C:p.I29584T,ENSG00000155657:ENST00000589042:exon339:c.T93674C:p.I31225T		
2_179413138_C_T	NM_003319:c.G66020A:p.R22007H		rs141817409
2_179413348_C_A	NM_003319:c.G65810T:p.S21937I	E	rs180975448

2_179413547_C_T	NM_003319:c.G65611A:p.V21871I		
2_179413573_A_T	ENSG00000155657:ENST00000460472:exon167:c.T65585A:p.I21862K,ENSG00000155657:ENST00000342175:exon168:c.T66161A:p.I22054K,ENSG00000155657:ENST00000359218:exon168:c.T65960A:p.I21987K,ENSG00000155657:ENST00000342992:exon288:c.T85076A:p.I28359K,ENSG00000155657:ENST00000591111:exon289:c.T87857A:p.I29286K,ENSG00000155657:ENST00000589042:exon339:c.T92780A:p.I30927K		
2_179413729_G_C	NM_003319:c.C65429G:p.A21810G		
2_179413789_C_A	ENSG00000155657:ENST00000460472:exon167:c.G65369T:p.G21790V,ENSG00000155657:ENST00000342175:exon168:c.G65945T:p.G21982V,ENSG00000155657:ENST00000359218:exon168:c.G65744T:p.G21915V,ENSG00000155657:ENST00000342992:exon288:c.G84860T:p.G28287V,ENSG00000155657:ENST00000591111:exon289:c.G87641T:p.G29214V,ENSG00000155657:ENST00000589042:exon339:c.G92564T:p.G30855V		
2_179413902_C_A	NM_003319:c.G65256T:p.E21752D		
2_179413970_C_G	ENSG00000155657:ENST00000460472:exon167:c.G65188C:p.V21730L,ENSG00000155657:ENST00000342175:exon168:c.G65764C:p.V21922L,ENSG00000155657:ENST00000359218:exon168:c.G65563C:p.V21855L,ENSG00000155657:ENST00000342992:exon288:c.G84679C:p.V28227L,ENSG00000155657:ENST00000591111:exon289:c.G87460C:p.V29154L,ENSG00000155657:ENST00000589042:exon339:c.G92383C:p.V30795L		
2_179414059_C_G	NM_003319:c.G65099C:p.R21700T		
2_179414177_G_A	NM_003319:c.C64981T:p.P21661S		rs72648247
2_179414791_C_T	ENSG00000155657:ENST00000460472:exon165:c.G64579A:p.D21527N,ENSG00000155657:ENST00000342175:exon166:c.G65155A:p.D21719N,ENSG00000155657:ENST00000359218:exon166:c.G64954A:p.D21652N,ENSG00000155657:ENST00000342992:exon286:c.G84070A:p.D28024N,ENSG00000155657:ENST00000591111:exon287:c.G86851A:p.D28951N,ENSG00000155657:ENST00000589042:exon337:c.G91774A:p.D30592N		
2_179414800_C_T	NM_003319:c.C20350A:p.P6784T		
2_179414955_A_T	NM_003319:c.T64415A:p.I21472N		
2_179414964_T_A	NM_133378:c.C15300G:p.D5100E		
2_179415859_G_A	ENSG00000155657:ENST00000460472:exon164:c.C64204T:p.R21402C,ENSG00000155657:ENST00000342175:exon165:c.C64780T:p.R21594C,ENSG00000155657:ENST00000359218:exon165:c.C64579T:p.R21527C,ENSG00000155657:ENST00000342992:exon285:c.C83695T:p.R27899C,ENSG00000155657:ENST00000591111:exon286:c.C86476T:p.R28826C,ENSG00000155657:ENST00000589042:exon336:c.C91399T:p.R30467C		

2_179415952_G_A	NM_003319:c.C61405T:p.P20469S		
2_179416454_T_G	ENSG00000155657:ENST00000460472:exon163:c.A63978C:p.E21326D,ENSG00000155657:ENST00000342175:exon164:c.A64554C:p.E21518D,ENSG00000155657:ENST00000359218:exon164:c.A64353C:p.E21451D,ENSG00000155657:ENST00000342992:exon284:c.A83469C:p.E27823D,ENSG00000155657:ENST00000591111:exon285:c.A86250C:p.E28750D,ENSG00000155657:ENST00000589042:exon335:c.A91173C:p.E30391D		rs199505541
2_179416703_G_T	ENSG00000155657:ENST00000460472:exon163:c.C63729A:p.S21243R,ENSG00000155657:ENST00000342175:exon164:c.C64305A:p.S21435R,ENSG00000155657:ENST00000359218:exon164:c.C64104A:p.S21368R,ENSG00000155657:ENST00000342992:exon284:c.C83220A:p.S27740R,ENSG00000155657:ENST00000591111:exon285:c.C86001A:p.S28667R,ENSG00000155657:ENST00000589042:exon335:c.C90924A:p.S30308R		
2_179416801_A_C	NM_003319:c.G63341A:p.R21114H		
2_179416861_CTC_-	ENSG00000155657:ENST00000460472:exon163:c.63569_63571del:p.21190_21191del,ENSG00000155657:ENST00000342175:exon164:c.64145_64147del:p.21382_21383del,ENSG00000155657:ENST00000359218:exon164:c.63944_63946del:p.21315_21316del,ENSG00000155657:ENST00000342992:exon284:c.83060_83062del:p.27687_27688del,ENSG00000155657:ENST00000591111:exon285:c.85841_85843del:p.28614_28615del,ENSG00000155657:ENST00000589042:exon335:c.90764_90766del:p.30255_30256del		
2_179416912_C_T	ENSG00000155657:ENST00000460472:exon163:c.G63520A:p.A21174T,ENSG00000155657:ENST00000342175:exon164:c.G64096A:p.A21366T,ENSG00000155657:ENST00000359218:exon164:c.G63895A:p.A21299T,ENSG00000155657:ENST00000342992:exon284:c.G83011A:p.A27671T,ENSG00000155657:ENST00000591111:exon285:c.G85792A:p.A28598T,ENSG00000155657:ENST00000589042:exon335:c.G90715A:p.A30239T		
2_179417033_A_T	NM_003319:c.T63399A:p.H21133Q		
2_179417043_T_C	NM_003319:c.A63389G:p.K21130R		
2_179417091_C_T	NM_133378:c.A16443G:p.I5481M		
2_179417295_A_G	NM_003319:c.T63137C:p.L21046P		
2_179417428_C_T	ENSG00000155657:ENST00000460472:exon163:c.G63004A:p.V21002I,ENSG00000155657:ENST00000342175:exon164:c.G63580A:p.V21194I,ENSG00000155657:ENST00000359218:exon164:c.G63379A:p.V21127I,ENSG00000155657:ENST00000342992:exon284:c.G82495A:p.V27499I,ENSG00000155657:ENST00000591111:exon285:c.G85276A:p.V28426I,ENSG00000155657:ENST00000589042:exon335:c.G90199A:p.V30067I		
2_179417463_T_A	NM_003319:c.A62969T:p.D20990V		

2_179417586_C_T	ENSG00000155657:ENST00000460472:exon163:c.G62846A:p.G20949E,ENSG00000155657:ENST00000342175:exon164:c.G63422A:p.G21141E,ENSG00000155657:ENST00000359218:exon164:c.G63221A:p.G21074E,ENSG00000155657:ENST00000342992:exon284:c.G82337A:p.G27446E,ENSG00000155657:ENST00000591111:exon285:c.G85118A:p.G28373E,ENSG00000155657:ENST00000589042:exon335:c.G90041A:p.G30014E		
2_179417638_A_T	NM_003319:c.T62794A:p.L20932M		
2_179417643_A_G	NM_003319:c.T62789C:p.I20930T		
2_179417703_G_A	NM_003319:c.C62729T:p.A20910V		rs117097948
2_179418306_C_T	NM_003319:c.G62231A:p.R20744Q		rs72648238
2_179418346_C_T	ENSG00000155657:ENST00000460472:exon162:c.G62191A:p.V20731M,ENSG00000155657:ENST00000342175:exon163:c.G62767A:p.V20923M,ENSG00000155657:ENST00000359218:exon163:c.G62566A:p.V20856M,ENSG00000155657:ENST00000342992:exon283:c.G81682A:p.V27228M,ENSG00000155657:ENST00000591111:exon284:c.G84463A:p.V28155M,ENSG00000155657:ENST00000589042:exon334:c.G89386A:p.V29796M	E	rs72648237
2_179419323_A_G	NM_003319:c.T61556C:p.V20519A		
2_179419354_G_A	ENSG00000155657:ENST00000460472:exon160:c.C61525T:p.R20509C,ENSG00000155657:ENST00000342175:exon161:c.C62101T:p.R20701C,ENSG00000155657:ENST00000359218:exon161:c.C61900T:p.R20634C,ENSG00000155657:ENST00000342992:exon281:c.C81016T:p.R27006C,ENSG00000155657:ENST00000591111:exon282:c.C83797T:p.R27933C,ENSG00000155657:ENST00000589042:exon332:c.C88720T:p.R29574C		rs200513274
2_179419366_T_C	NM_003319:c.A61513G:p.I20505V		rs139506970
2_179419370_G_T	NM_003319:c.C61509A:p.H20503Q		
2_179419389_C_T	ENSG00000155657:ENST00000460472:exon160:c.G61490A:p.G20497D,ENSG00000155657:ENST00000342175:exon161:c.G62066A:p.G20689D,ENSG00000155657:ENST00000359218:exon161:c.G61865A:p.G20622D,ENSG00000155657:ENST00000342992:exon281:c.G80981A:p.G26994D,ENSG00000155657:ENST00000591111:exon282:c.G83762A:p.G27921D,ENSG00000155657:ENST00000589042:exon332:c.G88685A:p.G29562D		rs72648235
2_179419474_G_A	NM_003319:c.C64111T:p.R21371W		
2_179419655_A_G	ENSG00000155657:ENST00000460472:exon159:c.T61336C:p.Y20446H,ENSG00000155657:ENST00000342175:exon160:c.T61912C:p.Y20638H,ENSG00000155657:ENST00000359218:exon160:c.T61711C:p.Y20571H,ENSG00000155657:ENST00000342992:exon280:c.T80827C:p.Y26943H,ENSG00000155657:ENST00000591111:exon281:c.T83608C:p.Y27870H,ENSG00000155657:ENST00000589042:exon331:c.T88531C:p.Y29511H		

2_179419679_C_T	ENSG00000155657:ENST00000460472:exon159:c.G61312A:p.A20438T,ENSG00000155657:ENST00000342175:exon160:c.G61888A:p.A20630T,ENSG00000155657:ENST00000359218:exon160:c.G61687A:p.A20563T,ENSG00000155657:ENST00000342992:exon280:c.G80803A:p.A26935T,ENSG00000155657:ENST00000591111:exon281:c.G83584A:p.A27862T,ENSG00000155657:ENST00000589042:exon331:c.G88507A:p.A29503T		
2_179419792_G_A	NM_003319:c.C61199T:p.S20400F		rs146181116
2_179421596_T_C	NM_003319:c.A61090G:p.I20364V		
2_179421791_C_T	NM_003319:c.C77066T:p.A25689V		
2_179422112_G_A	NM_003319:c.C60682T:p.R20228C		rs191482653
2_179422181_C_T	NM_003319:c.G60613A:p.V20205I		rs141624266
2_179422286_C_A	NA	L	rs201770959
2_179422450_G_A	NM_003319:c.C60436T:p.R20146C		
2_179422470_G_C	NM_003319:c.C60416G:p.T20139R		rs72648228
2_179422612_G_A	NM_003319:c.A31229G:p.N10410S		
2_179422669_G_T	NM_133378:c.G17911A:p.A5971T		rs72648227
2_179424176_C_T	NM_003319:c.G59488A:p.V19830M		
2_179424188_C_A	ENSG00000155657:ENST00000460472:exon154:c.G59476T:p.A19826S,ENSG00000155657:ENST00000342175:exon155:c.G60052T:p.A20018S,ENSG00000155657:ENST00000359218:exon155:c.G59851T:p.A19951S,ENSG00000155657:ENST00000342992:exon275:c.G78967T:p.A26323S,ENSG00000155657:ENST00000591111:exon276:c.G81748T:p.A27250S,ENSG00000155657:ENST00000589042:exon326:c.G86671T:p.A28891S		
2_179424363_A_T	NM_003319:c.T59301A:p.S19767R		
2_179424625_G_A	NM_003319:c.C59039T:p.A19680V		
2_179425063_C_T	NM_003319:c.G19060T:p.A6354S		
2_179425168_T_A	NM_003319:c.G30488A:p.R10163H		
2_179425438_C_T	ENSG00000155657:ENST00000460472:exon154:c.G58226A:p.R19409H,ENSG00000155657:ENST00000342175:exon155:c.G58802A:p.R19601H,ENSG00000155657:ENST00000359218:exon155:c.G58601A:p.R19534H,ENSG00000155657:ENST00000342992:exon275:c.G77717A:p.R25906H,ENSG00000155657:ENST00000591111:exon276:c.G80498A:p.R26833H,ENSG00000155657:ENST00000589042:exon326:c.G85421A:p.R28474H		

2_179425744_C_T	ENSG00000155657:ENST00000460472:exon154:c.G57920A:p.G19307E,ENSG00000155657:ENST00000342175:exon155:c.G58496A:p.G19499E,ENSG00000155657:ENST00000359218:exon155:c.G58295A:p.G19432E,ENSG00000155657:ENST00000342992:exon275:c.G77411A:p.G25804E,ENSG00000155657:ENST00000591111:exon276:c.G80192A:p.G26731E,ENSG00000155657:ENST00000589042:exon326:c.G85115A:p.G28372E		rs190721759
2_179425894_C_T	ENSG00000155657:ENST00000460472:exon154:c.G57770A:p.R19257H,ENSG00000155657:ENST00000342175:exon155:c.G58346A:p.R19449H,ENSG00000155657:ENST00000359218:exon155:c.G58145A:p.R19382H,ENSG00000155657:ENST00000342992:exon275:c.G77261A:p.R25754H,ENSG00000155657:ENST00000591111:exon276:c.G80042A:p.R26681H,ENSG00000155657:ENST00000589042:exon326:c.G84965A:p.R28322H		
2_179425895_G_A	NM_003319:c.C57769T:p.R19257C		
2_179425988_G_A	NM_003319:c.C57676T:p.R19226C		rs192152102
2_179426020_C_A	NM_003319:c.G13480A:p.V4494I		
2_179426219_T_C	NM_003319:c.A57445G:p.M19149V		rs72648221
2_179426225_T_G	ENSG00000155657:ENST00000460472:exon154:c.A57439C:p.T19147P,ENSG00000155657:ENST00000342175:exon155:c.A58015C:p.T19339P,ENSG00000155657:ENST00000359218:exon155:c.A57814C:p.T19272P,ENSG00000155657:ENST00000342992:exon275:c.A76930C:p.T25644P,ENSG00000155657:ENST00000591111:exon276:c.A79711C:p.T26571P,ENSG00000155657:ENST00000589042:exon326:c.A84634C:p.T28212P		
2_179426596_C_T	NM_133378:c.G17066C:p.G5689A		
2_179426702_G_A	NM_003319:c.C56962T:p.L18988F		
2_179426711_T_C	NM_003319:c.A56953G:p.I18985V		
2_179426787_T_G	ENSG00000155657:ENST00000460472:exon154:c.A56877C:p.E18959D,ENSG00000155657:ENST00000342175:exon155:c.A57453C:p.E19151D,ENSG00000155657:ENST00000359218:exon155:c.A57252C:p.E19084D,ENSG00000155657:ENST00000342992:exon275:c.A76368C:p.E25456D,ENSG00000155657:ENST00000591111:exon276:c.A79149C:p.E26383D,ENSG00000155657:ENST00000589042:exon326:c.A84072C:p.E28024D		
2_179427119_T_C	NM_003319:c.A56545G:p.T18849A		rs188370772
2_179427578_C_T	NM_003319:c.G56086A:p.V18696I		
2_179427688_A_C	ENSG00000155657:ENST00000460472:exon154:c.T55976G:p.V18659G,ENSG00000155657:ENST00000342175:exon155:c.T56552G:p.V18851G,ENSG00000155657:ENST00000359218:exon155:c.T56351G:p.V18784G,ENSG00000155657:ENST00000342992:exon275:c.T75467G:p.V25156G,ENSG00000155657:ENST00000591111:exon276:c.T78248G:p.V26083G,ENSG00000155657:ENST00000589042:exon326:c.T83171G:p.V27724G		rs201896662

2_179427796_C_T	NM_003319:c.G55868A:p.R18623H		
2_179427985_C_T	ENSG00000155657:ENST00000460472:exon154:c.G55679A:p.G18560E,ENSG00000155657:ENST00000342175:exon155:c.G56255A:p.G18752E,ENSG00000155657:ENST00000359218:exon155:c.G56054A:p.G18685E,ENSG00000155657:ENST00000342992:exon275:c.G75170A:p.G25057E,ENSG00000155657:ENST00000591111:exon276:c.G77951A:p.G25984E,ENSG00000155657:ENST00000589042:exon326:c.G82874A:p.G27625E		
2_179428049_C_T	NM_133378:c.G16579C:p.E5527Q		
2_179428168_G_A	ENSG00000155657:ENST00000460472:exon154:c.C55496T:p.A18499V,ENSG00000155657:ENST00000342175:exon155:c.C56072T:p.A18691V,ENSG00000155657:ENST00000359218:exon155:c.C55871T:p.A18624V,ENSG00000155657:ENST00000342992:exon275:c.C74987T:p.A24996V,ENSG00000155657:ENST00000591111:exon276:c.C77768T:p.A25923V,ENSG00000155657:ENST00000589042:exon326:c.C82691T:p.A27564V		rs55634791
2_179428175_A_G	ENSG00000155657:ENST00000460472:exon154:c.T55489C:p.Y18497H,ENSG00000155657:ENST00000342175:exon155:c.T56065C:p.Y18689H,ENSG00000155657:ENST00000359218:exon155:c.T55864C:p.Y18622H,ENSG00000155657:ENST00000342992:exon275:c.T74980C:p.Y24994H,ENSG00000155657:ENST00000591111:exon276:c.T77761C:p.Y25921H,ENSG00000155657:ENST00000589042:exon326:c.T82684C:p.Y27562H		
2_179428299_G_T	NM_133378:c.G21758A:p.R7253H		rs56264840
2_179428474_G_A	ENSG00000155657:ENST00000460472:exon154:c.C55190T:p.T18397M,ENSG00000155657:ENST00000342175:exon155:c.C55766T:p.T18589M,ENSG00000155657:ENST00000359218:exon155:c.C55565T:p.T18522M,ENSG00000155657:ENST00000342992:exon275:c.C74681T:p.T24894M,ENSG00000155657:ENST00000591111:exon276:c.C77462T:p.T25821M,ENSG00000155657:ENST00000589042:exon326:c.C82385T:p.T27462M		
2_179428778_G_C	ENSG00000155657:ENST00000460472:exon154:c.C54886G:p.P18296A,ENSG00000155657:ENST00000342175:exon155:c.C55462G:p.P18488A,ENSG00000155657:ENST00000359218:exon155:c.C55261G:p.P18421A,ENSG00000155657:ENST00000342992:exon275:c.C74377G:p.P24793A,ENSG00000155657:ENST00000591111:exon276:c.C77158G:p.P25720A,ENSG00000155657:ENST00000589042:exon326:c.C82081G:p.P27361A		rs56137800
2_179428921_C_T	NM_003319:c.G54743A:p.G18248E		
2_179429015_T_C	NM_003319:c.A54649G:p.K18217E		
2_179429017_T_C	NM_003319:c.A54647G:p.Y18216C		
2_179429320_A_G	NM_003319:c.T54344C:p.I18115T		rs182126530
2_179429356_C_T	NM_003319:c.G54308A:p.R18103H		
2_179429387_G_C	NM_003319:c.C54277G:p.P18093A		

2_179429577_A_C	NM_003319:c.T54087G:p.H18029Q		
2_179429577_A_T	NM_003319:c.A7085G:p.Q2362R		
2_179429823_C_A	ENSG00000155657:ENST00000460472:exon154:c.G53841T:p.K17947N,ENSG00000155657:ENST00000342175:exon155:c.G54417T:p.K18139N,ENSG00000155657:ENST00000359218:exon155:c.G54216T:p.K18072N,ENSG00000155657:ENST00000342992:exon275:c.G73332T:p.K24444N,ENSG00000155657:ENST00000591111:exon276:c.G76113T:p.K25371N,ENSG00000155657:ENST00000589042:exon326:c.G81036T:p.K27012N		
2_179429915_A_G	NM_003319:c.T53749C:p.F17917L		
2_179430001_G_A	ENSG00000155657:ENST00000460472:exon154:c.C53663T:p.T17888M,ENSG00000155657:ENST00000342175:exon155:c.C54239T:p.T18080M,ENSG00000155657:ENST00000359218:exon155:c.C54038T:p.T18013M,ENSG00000155657:ENST00000342992:exon275:c.C73154T:p.T24385M,ENSG00000155657:ENST00000591111:exon276:c.C75935T:p.T25312M,ENSG00000155657:ENST00000589042:exon326:c.C80858T:p.T26953M		
2_179430067_G_A	NM_003319:c.C53597T:p.T17866I		
2_179430158_T_C	ENSG00000155657:ENST00000460472:exon154:c.A53506G:p.I17836V,ENSG00000155657:ENST00000342175:exon155:c.A54082G:p.I18028V,ENSG00000155657:ENST00000359218:exon155:c.A53881G:p.I17961V,ENSG00000155657:ENST00000342992:exon275:c.A72997G:p.I24333V,ENSG00000155657:ENST00000591111:exon276:c.A75778G:p.I25260V,ENSG00000155657:ENST00000589042:exon326:c.A80701G:p.I26901V		rs201562505
2_179430434_C_T	ENSG00000155657:ENST00000460472:exon154:c.G53230A:p.G17744S,ENSG00000155657:ENST00000342175:exon155:c.G53806A:p.G17936S,ENSG00000155657:ENST00000359218:exon155:c.G53605A:p.G17869S,ENSG00000155657:ENST00000342992:exon275:c.G72721A:p.G24241S,ENSG00000155657:ENST00000591111:exon276:c.G75502A:p.G25168S,ENSG00000155657:ENST00000589042:exon326:c.G80425A:p.G26809S		
2_179430442_T_C	NM_003319:c.A53222G:p.H17741R		rs181766682
2_179430596_A_G	ENSG00000155657:ENST00000460472:exon154:c.T53068C:p.F17690L,ENSG00000155657:ENST00000342175:exon155:c.T53644C:p.F17882L,ENSG00000155657:ENST00000359218:exon155:c.T53443C:p.F17815L,ENSG00000155657:ENST00000342992:exon275:c.T72559C:p.F24187L,ENSG00000155657:ENST00000591111:exon276:c.T75340C:p.F25114L,ENSG00000155657:ENST00000589042:exon326:c.T80263C:p.F26755L		rs200181804
2_179430699_A_C	ENSG00000155657:ENST00000460472:exon154:c.T52965G:p.I17655M,ENSG00000155657:ENST00000342175:exon155:c.T53541G:p.I17847M,ENSG00000155657:ENST00000359218:exon155:c.T53340G:p.I17780M,ENSG00000155657:ENST00000342992:exon275:c.T72456G:p.I24152M,ENSG00000155657:ENST00000591111:exon276:c.T75237G:p.I25079M,ENSG00000155657:ENST00000589042:exon326:c.T80160G:p.I26720M		

2_179430976_C_T	NM_003319:c.G52688A:p.R17563Q		
2_179431159_T_C	NM_003319:c.A52505G:p.N17502S		rs183844833
2_179431247_T_C	ENSG00000155657:ENST00000460472:exon154:c.A52417G:p.T17473A,ENSG00000155657:ENST00000342175:exon155:c.A52993G:p.T17665A,ENSG00000155657:ENST00000359218:exon155:c.A52792G:p.T17598A,ENSG00000155657:ENST00000342992:exon275:c.A71908G:p.T23970A,ENSG00000155657:ENST00000591111:exon276:c.A74689G:p.T24897A,ENSG00000155657:ENST00000589042:exon326:c.A79612G:p.T26538A		rs150682764
2_179431633_C_T	ENSG00000155657:ENST00000460472:exon154:c.G52031A:p.R17344H,ENSG00000155657:ENST00000342175:exon155:c.G52607A:p.R17536H,ENSG00000155657:ENST00000359218:exon155:c.G52406A:p.R17469H,ENSG00000155657:ENST00000342992:exon275:c.G71522A:p.R23841H,ENSG00000155657:ENST00000591111:exon276:c.G74303A:p.R24768H,ENSG00000155657:ENST00000589042:exon326:c.G79226A:p.R26409H		rs72648206
2_179431847_C_A	ENSG00000155657:ENST00000460472:exon154:c.G51817T:p.A17273S,ENSG00000155657:ENST00000342175:exon155:c.G52393T:p.A17465S,ENSG00000155657:ENST00000359218:exon155:c.G52192T:p.A17398S,ENSG00000155657:ENST00000342992:exon275:c.G71308T:p.A23770S,ENSG00000155657:ENST00000591111:exon276:c.G74089T:p.A24697S,ENSG00000155657:ENST00000589042:exon326:c.G79012T:p.A26338S		
2_179431871_T_C	NM_003319:c.A51793G:p.S17265G		
2_179431967_C_T	NM_003319:c.G51697A:p.G17233R		rs72648205
2_179432458_C_T	ENSG00000155657:ENST00000460472:exon154:c.G51206A:p.R17069H,ENSG00000155657:ENST00000342175:exon155:c.G51782A:p.R17261H,ENSG00000155657:ENST00000359218:exon155:c.G51581A:p.R17194H,ENSG00000155657:ENST00000342992:exon275:c.G70697A:p.R23566H,ENSG00000155657:ENST00000591111:exon276:c.G73478A:p.R24493H,ENSG00000155657:ENST00000589042:exon326:c.G78401A:p.R26134H		
2_179432791_A_G	NM_003319:c.T50873C:p.I16958T		
2_179432795_C_T	ENSG00000155657:ENST00000460472:exon154:c.G50869A:p.V16957I,ENSG00000155657:ENST00000342175:exon155:c.G51445A:p.V17149I,ENSG00000155657:ENST00000359218:exon155:c.G51244A:p.V17082I,ENSG00000155657:ENST00000342992:exon275:c.G70360A:p.V23454I,ENSG00000155657:ENST00000591111:exon276:c.G73141A:p.V24381I,ENSG00000155657:ENST00000589042:exon326:c.G78064A:p.V26022I		
2_179433557_G_T	NM_003319:c.C50107A:p.L16703I		
2_179433672_T_A	NM_003319:c.A49992T:p.K16664N		
2_179433674_T_A	NM_003319:c.A49990T:p.K16664X	L	

2_179433937_C_T	ENSG00000155657:ENST00000460472:exon154:c.G49727A:p.R16576H,ENSG00000155657:ENST00000342175:exon155:c.G50303A:p.R16768H,ENSG00000155657:ENST00000359218:exon155:c.G50102A:p.R16701H,ENSG00000155657:ENST00000342992:exon275:c.G69218A:p.R23073H,ENSG00000155657:ENST00000591111:exon276:c.G71999A:p.R24000H,ENSG00000155657:ENST00000589042:exon326:c.G76922A:p.R25641H		
2_179434120_G_T	ENSG00000155657:ENST00000460472:exon154:c.C49544A:p.T16515K,ENSG00000155657:ENST00000342175:exon155:c.C50120A:p.T16707K,ENSG00000155657:ENST00000359218:exon155:c.C49919A:p.T16640K,ENSG00000155657:ENST00000342992:exon275:c.C69035A:p.T23012K,ENSG00000155657:ENST00000591111:exon276:c.C71816A:p.T23939K,ENSG00000155657:ENST00000589042:exon326:c.C76739A:p.T25580K		rs56372592
2_179434336_G_T	NM_003319:c.C49328A:p.P16443Q		rs188085512
2_179434437_C_A	ENSG00000155657:ENST00000460472:exon154:c.G49227T:p.K16409N,ENSG00000155657:ENST00000342175:exon155:c.G49803T:p.K16601N,ENSG00000155657:ENST00000359218:exon155:c.G49602T:p.K16534N,ENSG00000155657:ENST00000342992:exon275:c.G68718T:p.K22906N,ENSG00000155657:ENST00000591111:exon276:c.G71499T:p.K23833N,ENSG00000155657:ENST00000589042:exon326:c.G76422T:p.K25474N		
2_179434538_T_C	ENSG00000155657:ENST00000460472:exon154:c.A49126G:p.I16376V,ENSG00000155657:ENST00000342175:exon155:c.A49702G:p.I16568V,ENSG00000155657:ENST00000359218:exon155:c.A49501G:p.I16501V,ENSG00000155657:ENST00000342992:exon275:c.A68617G:p.I22873V,ENSG00000155657:ENST00000591111:exon276:c.A71398G:p.I23800V,ENSG00000155657:ENST00000589042:exon326:c.A76321G:p.I25441V		
2_179434840_A_T	NM_003319:c.T48824A:p.V16275D		
2_179435114_G_A	NM_003319:c.C48550T:p.R16184C		
2_179435332_C_T	NM_003319:c.G48332A:p.R16111H		
2_179435401_G_A	NM_003319:c.C48263T:p.S16088L		
2_179435764_T_C	NM_003319:c.A47900G:p.Y15967C		
2_179435825_G_A	ENSG00000155657:ENST00000460472:exon154:c.C47839T:p.R15947W,ENSG00000155657:ENST00000342175:exon155:c.C48415T:p.R16139W,ENSG00000155657:ENST00000359218:exon155:c.C48214T:p.R16072W,ENSG00000155657:ENST00000342992:exon275:c.C67330T:p.R22444W,ENSG00000155657:ENST00000591111:exon276:c.C70111T:p.R23371W,ENSG00000155657:ENST00000589042:exon326:c.C75034T:p.R25012W		
2_179435894_C_T	NM_003319:c.G47770A:p.V15924M		
2_179435964_T_G	NM_003319:c.A47700C:p.Q15900H		

2_179435968_G_A	ENSG00000155657:ENST00000460472:exon154:c.C47696T:p.P15899L,ENSG00000155657:ENST00000342175:exon155:c.C48272T:p.P16091L,ENSG00000155657:ENST00000359218:exon155:c.C48071T:p.P16024L,ENSG00000155657:ENST00000342992:exon275:c.C67187T:p.P22396L,ENSG00000155657:ENST00000591111:exon276:c.C69968T:p.P23323L,ENSG00000155657:ENST00000589042:exon326:c.C74891T:p.P24964L		rs72646899
2_179436257_T_C	NM_003319:c.A47407G:p.I15803V		rs72646898
2_179436257_TTG_-	ENSG00000155657:ENST00000460472:exon154:c.47405_47407del:p.15802_15803del,ENSG00000155657:ENST00000342175:exon155:c.47981_47983del:p.15994_15995del,ENSG00000155657:ENST00000359218:exon155:c.47780_47782del:p.15927_15928del,ENSG00000155657:ENST00000342992:exon275:c.66896_66898del:p.22299_22300del,ENSG00000155657:ENST00000591111:exon276:c.69677_69679del:p.23226_23227del,ENSG00000155657:ENST00000589042:exon326:c.74600_74602del:p.24867_24868del		
2_179436261_TGT_-	NM_003319:c.T67358C:p.V22453A		
2_179436310_T_C	ENSG00000155657:ENST00000460472:exon154:c.A47354G:p.D15785G,ENSG00000155657:ENST00000342175:exon155:c.A47930G:p.D15977G,ENSG00000155657:ENST00000359218:exon155:c.A47729G:p.D15910G,ENSG00000155657:ENST00000342992:exon275:c.A66845G:p.D22282G,ENSG00000155657:ENST00000591111:exon276:c.A69626G:p.D23209G,ENSG00000155657:ENST00000589042:exon326:c.A74549G:p.D24850G		
2_179437034_C_G	ENSG00000155657:ENST00000460472:exon154:c.G46630C:p.E15544Q,ENSG00000155657:ENST00000342175:exon155:c.G47206C:p.E15736Q,ENSG00000155657:ENST00000359218:exon155:c.G47005C:p.E15669Q,ENSG00000155657:ENST00000342992:exon275:c.G66121C:p.E22041Q,ENSG00000155657:ENST00000591111:exon276:c.G68902C:p.E22968Q,ENSG00000155657:ENST00000589042:exon326:c.G73825C:p.E24609Q		rs55762754
2_179437525_G_A	NM_003319:c.C46139T:p.T15380I		
2_179437691_T_C	ENSG00000155657:ENST00000460472:exon154:c.A45973G:p.T15325A,ENSG00000155657:ENST00000342175:exon155:c.A46549G:p.T15517A,ENSG00000155657:ENST00000359218:exon155:c.A46348G:p.T15450A,ENSG00000155657:ENST00000342992:exon275:c.A65464G:p.T21822A,ENSG00000155657:ENST00000591111:exon276:c.A68245G:p.T22749A,ENSG00000155657:ENST00000589042:exon326:c.A73168G:p.T24390A		rs182491843
2_179437868_G_A	NM_003319:c.C45796T:p.R15266C		
2_179437928_T_C	NM_003319:c.A45736G:p.T15246A		rs56201325
2_179438035_T_A	NM_003319:c.A45629T:p.K15210I		

2_179438093_T_C	ENSG00000155657:ENST00000460472:exon154:c.A45571G:p.N15191D,ENSG00000155657:ENST00000342175:exon155:c.A46147G:p.N15383D,ENSG00000155657:ENST00000359218:exon155:c.A45946G:p.N15316D,ENSG00000155657:ENST00000342992:exon275:c.A65062G:p.N21688D,ENSG00000155657:ENST00000591111:exon276:c.A67843G:p.N22615D,ENSG00000155657:ENST00000589042:exon326:c.A72766G:p.N24256D		rs187868672
2_179438252_A_G	NM_003319:c.T45412C:p.Y15138H		
2_179438557_G_T	NM_003319:c.C45107A:p.T15036N		rs192962624
2_179438710_T_C	NM_003319:c.A44954G:p.E14985G		
2_179438713_A_G	NM_003319:c.T44951C:p.L14984P		rs56399205
2_179438746_G_A	NM_003319:c.C44918T:p.T14973M		
2_179438858_C_T	ENSG00000155657:ENST00000460472:exon154:c.G44806A:p.A14936T,ENSG00000155657:ENST00000342175:exon155:c.G45382A:p.A15128T,ENSG00000155657:ENST00000359218:exon155:c.G45181A:p.A15061T,ENSG00000155657:ENST00000342992:exon275:c.G64297A:p.A21433T,ENSG00000155657:ENST00000591111:exon276:c.G67078A:p.A22360T,ENSG00000155657:ENST00000589042:exon326:c.G72001A:p.A24001T		rs180828370
2_179439151_G_C	NM_003319:c.G38281A:p.E12761K		
2_179439154_A_G	NM_003319:c.T44510C:p.I14837T		rs55837610
2_179439383_C_G	ENSG00000155657:ENST00000460472:exon154:c.G44281C:p.V14761L,ENSG00000155657:ENST00000342175:exon155:c.G44857C:p.V14953L,ENSG00000155657:ENST00000359218:exon155:c.G44656C:p.V14886L,ENSG00000155657:ENST00000342992:exon275:c.G63772C:p.V21258L,ENSG00000155657:ENST00000591111:exon276:c.G66553C:p.V22185L,ENSG00000155657:ENST00000589042:exon326:c.G71476C:p.V23826L		
2_179439490_C_T	ENSG00000155657:ENST00000460472:exon154:c.G44174A:p.R14725H,ENSG00000155657:ENST00000342175:exon155:c.G44750A:p.R14917H,ENSG00000155657:ENST00000359218:exon155:c.G44549A:p.R14850H,ENSG00000155657:ENST00000342992:exon275:c.G63665A:p.R21222H,ENSG00000155657:ENST00000591111:exon276:c.G66446A:p.R22149H,ENSG00000155657:ENST00000589042:exon326:c.G71369A:p.R23790H		rs55677134
2_179439491_G_A	ENSG00000155657:ENST00000460472:exon154:c.C44173T:p.R14725C,ENSG00000155657:ENST00000342175:exon155:c.C44749T:p.R14917C,ENSG00000155657:ENST00000359218:exon155:c.C44548T:p.R14850C,ENSG00000155657:ENST00000342992:exon275:c.C63664T:p.R21222C,ENSG00000155657:ENST00000591111:exon276:c.C66445T:p.R22149C,ENSG00000155657:ENST00000589042:exon326:c.C71368T:p.R23790C		

2_179439755_C_A	ENSG00000155657:ENST00000460472:exon154:c.G43909T:p.G14637W,ENSG00000155657:ENST00000342175:exon155:c.G44485T:p.G14829W,ENSG00000155657:ENST00000359218:exon155:c.G44284T:p.G14762W,ENSG00000155657:ENST00000342992:exon275:c.G63400T:p.G21134W,ENSG00000155657:ENST00000591111:exon276:c.G66181T:p.G22061W,ENSG00000155657:ENST00000589042:exon326:c.G71104T:p.G23702W		
2_179439823_C_T	NM_003319:c.G43841A:p.R14614K		
2_179440027_G_A	ENSG00000155657:ENST00000460472:exon154:c.C43637T:p.A14546V,ENSG00000155657:ENST00000342175:exon155:c.C44213T:p.A14738V,ENSG00000155657:ENST00000359218:exon155:c.C44012T:p.A14671V,ENSG00000155657:ENST00000342992:exon275:c.C63128T:p.A21043V,ENSG00000155657:ENST00000591111:exon276:c.C65909T:p.A21970V,ENSG00000155657:ENST00000589042:exon326:c.C70832T:p.A23611V		rs72646891
2_179440028_C_T	NM_003319:c.G43636A:p.A14546T		
2_179440609_A_G	NM_003319:c.T43055C:p.I14352T		
2_179440757_T_C	ENSG00000155657:ENST00000460472:exon154:c.A42907G:p.I14303V,ENSG00000155657:ENST00000342175:exon155:c.A43483G:p.I14495V,ENSG00000155657:ENST00000359218:exon155:c.A43282G:p.I14428V,ENSG00000155657:ENST00000342992:exon275:c.A62398G:p.I20800V,ENSG00000155657:ENST00000591111:exon276:c.A65179G:p.I21727V,ENSG00000155657:ENST00000589042:exon326:c.A70102G:p.I23368V		
2_179440995_T_C	ENSG00000155657:ENST00000460472:exon154:c.A42669G:p.I14223M,ENSG00000155657:ENST00000342175:exon155:c.A43245G:p.I14415M,ENSG00000155657:ENST00000359218:exon155:c.A43044G:p.I14348M,ENSG00000155657:ENST00000342992:exon275:c.A62160G:p.I20720M,ENSG00000155657:ENST00000591111:exon276:c.A64941G:p.I21647M,ENSG00000155657:ENST00000589042:exon326:c.A69864G:p.I23288M		
2_179441038_C_T	NM_003319:c.G42626A:p.G14209D		
2_179441148_G_C	NM_133437:exon156:c.43097-5C>G,NM_133432:exon156:c.42896-5C>G,NM_003319:exon155:c.42521-5C>G,NM_133378:exon276:c.62012-5C>G	L	
2_179441724_C_T	ENSG00000155657:ENST00000460472:exon152:c.G42143A:p.R14048Q,ENSG00000155657:ENST00000342175:exon153:c.G42719A:p.R14240Q,ENSG00000155657:ENST00000359218:exon153:c.G42518A:p.R14173Q,ENSG00000155657:ENST00000342992:exon273:c.G61634A:p.R20545Q,ENSG00000155657:ENST00000591111:exon274:c.G64415A:p.R21472Q,ENSG00000155657:ENST00000589042:exon324:c.G69338A:p.R23113Q		
2_179441932_G_A	NM_003319:c.C41935T:p.P13979S		rs55980498
2_179442329_C_T	NM_003319:c.G41629A:p.E13877KTTN;TTN		
2_179442784_C_G	NM_003319:c.G20528A:p.R6843H		rs72646880

2_179442825_G_A	NM_003319:c.C41222T:p.T13741I		
2_179443533_C_T	NM_003319:c.G41029A:p.D13677NTTN;TTN		
2_179443626_C_T	NM_003319:c.G40936A:p.G13646S		
2_179444421_C_T	ENSG00000155657:ENST00000460472:exon147:c.G40308A:p.M13436I,ENSG00000155657:ENST00000342175:exon148:c.G40884A:p.M13628I,ENSG00000155657:ENST00000359218:exon148:c.G40683A:p.M13561I,ENSG00000155657:ENST00000342992:exon268:c.G59799A:p.M19933I,ENSG00000155657:ENST00000591111:exon269:c.G62580A:p.M20860I,ENSG00000155657:ENST00000589042:exon319:c.G67503A:p.M22501I		
2_179444437_T_C	NM_003319:c.A40292G:p.K13431R		
2_179444480_G_A	ENSG00000155657:ENST00000460472:exon147:c.C40249T:p.R13417W,ENSG00000155657:ENST00000342175:exon148:c.C40825T:p.R13609W,ENSG00000155657:ENST00000359218:exon148:c.C40624T:p.R13542W,ENSG00000155657:ENST00000342992:exon268:c.C59740T:p.R19914W,ENSG00000155657:ENST00000591111:exon269:c.C62521T:p.R20841W,ENSG00000155657:ENST00000589042:exon319:c.C67444T:p.R22482W		
2_179444915_A_G	NM_003319:c.T39904C:p.S13302P		rs72646873
2_179446322_C_T	NM_003319:c.G39478A:p.D13160N		rs72646870
2_179446418_C_T	NM_003319:c.G39382A:p.V13128I		
2_179446770_G_A	NM_003319:c.C39131T:p.P13044L		
2_179446813_G_A	NM_003319:c.C39088T:p.R13030W		
2_179446903_T_A	NM_003319:c.A38998T:p.S13000C		
2_179447197_G_A	ENSG00000155657:ENST00000460472:exon142:c.C38791T:p.R12931C,ENSG00000155657:ENST00000342175:exon143:c.C39367T:p.R13123C,ENSG00000155657:ENST00000359218:exon143:c.C39166T:p.R13056C,ENSG00000155657:ENST00000342992:exon263:c.C58282T:p.R19428C,ENSG00000155657:ENST00000591111:exon264:c.C61063T:p.R20355C,ENSG00000155657:ENST00000589042:exon314:c.C65986T:p.R21996C		
2_179447220_A_G	ENSG00000155657:ENST00000460472:exon142:c.T38768C:p.I12923T,ENSG00000155657:ENST00000342175:exon143:c.T39344C:p.I13115T,ENSG00000155657:ENST00000359218:exon143:c.T39143C:p.I13048T,ENSG00000155657:ENST00000342992:exon263:c.T58259C:p.I19420T,ENSG00000155657:ENST00000591111:exon264:c.T61040C:p.I20347T,ENSG00000155657:ENST00000589042:exon314:c.T65963C:p.I21988T		
2_179447261_C_T	NM_003319:c.G38727A:p.M12909I		
2_179447849_G_C	NM_003319:c.C38486G:p.T12829R		

2_179447858_G_A	ENSG00000155657:ENST00000460472:exon141:c.C38477T:p.P12826L,ENSG00000155657:ENST00000342175:exon142:c.C39053T:p.P13018L,ENSG00000155657:ENST00000359218:exon142:c.C38852T:p.P12951L,ENSG00000155657:ENST00000342992:exon262:c.C57968T:p.P19323L,ENSG00000155657:ENST00000591111:exon263:c.C60749T:p.P20250L,ENSG00000155657:ENST00000589042:exon313:c.C65672T:p.P21891L		
2_179447940_C_G	NM_003319:c.G38395C:p.D12799H		
2_179448375_G_A	NM_003319:c.C38339T:p.P12780L		
2_179448433_C_T	NM_003319:c.C44513G:p.A14838G		
2_179448450_G_A	ENSG00000155657:ENST00000460472:exon140:c.C38264T:p.T12755I,ENSG00000155657:ENST00000342175:exon141:c.C38840T:p.T12947I,ENSG00000155657:ENST00000359218:exon141:c.C38639T:p.T12880I,ENSG00000155657:ENST00000342992:exon261:c.C57755T:p.T19252I,ENSG00000155657:ENST00000591111:exon262:c.C60536T:p.T20179I,ENSG00000155657:ENST00000589042:exon312:c.C65459T:p.T21820I		rs56130023
2_179448570_C_T	NM_003319:c.G38144A:p.R12715H		
2_179449026_T_A	ENSG00000155657:ENST00000460472:exon139:c.A38057T:p.Y12686F,ENSG00000155657:ENST00000342175:exon140:c.A38633T:p.Y12878F,ENSG00000155657:ENST00000359218:exon140:c.A38432T:p.Y12811F,ENSG00000155657:ENST00000342992:exon260:c.A57548T:p.Y19183F,ENSG00000155657:ENST00000591111:exon261:c.A60329T:p.Y20110F,ENSG00000155657:ENST00000589042:exon311:c.A65252T:p.Y21751F		
2_179449084_A_G	ENSG00000155657:ENST00000460472:exon139:c.T37999C:p.F12667L,ENSG00000155657:ENST00000342175:exon140:c.T38575C:p.F12859L,ENSG00000155657:ENST00000359218:exon140:c.T38374C:p.F12792L,ENSG00000155657:ENST00000342992:exon260:c.T57490C:p.F19164L,ENSG00000155657:ENST00000591111:exon261:c.T60271C:p.F20091L,ENSG00000155657:ENST00000589042:exon311:c.T65194C:p.F21732L		
2_179449231_G_T	NM_003319:c.C37852A:p.P12618T		
2_179449452_C_T	NM_003319:c.G37721A:p.R12574Q		
2_179449606_C_T	NM_003319:c.G37567A:p.G12523R		rs181717727
2_179451454_G_A	NM_003319:c.C36979T:p.R12327C		rs72646859
2_179452021_C_T	NM_003319:c.G36722A:p.R12241H		
2_179452243_C_T	NM_003319:c.G36598A:p.D12200N		

2_179452410_C_T	ENSG00000155657:ENST00000460472:exon134:c.G36431A:p.R12144Q,ENSG00000155657:ENST00000342175:exon135:c.G37007A:p.R12336Q,ENSG00000155657:ENST00000359218:exon135:c.G36806A:p.R12269Q,ENSG00000155657:ENST00000342992:exon255:c.G55922A:p.R18641Q,ENSG00000155657:ENST00000591111:exon256:c.G58703A:p.R19568Q,ENSG00000155657:ENST00000589042:exon306:c.G63626A:p.R21209Q		rs148684589
2_179452447_T_C	NM_003319:c.A36394G:p.I12132V		rs72646855
2_179452459_G_A	NM_003319:c.C36382T:p.R12128C		
2_179452695_C_T	ENSG00000155657:ENST00000460472:exon133:c.G36244A:p.A12082T,ENSG00000155657:ENST00000342175:exon134:c.G36820A:p.A12274T,ENSG00000155657:ENST00000359218:exon134:c.G36619A:p.A12207T,ENSG00000155657:ENST00000342992:exon254:c.G55735A:p.A18579T,ENSG00000155657:ENST00000591111:exon255:c.G58516A:p.A19506T,ENSG00000155657:ENST00000589042:exon305:c.G63439A:p.A21147T		rs72646853
2_179452782_G_A	ENSG00000155657:ENST00000460472:exon133:c.C36157T:p.R12053W,ENSG00000155657:ENST00000342175:exon134:c.C36733T:p.R12245W,ENSG00000155657:ENST00000359218:exon134:c.C36532T:p.R12178W,ENSG00000155657:ENST00000342992:exon254:c.C55648T:p.R18550W,ENSG00000155657:ENST00000591111:exon255:c.C58429T:p.R19477W,ENSG00000155657:ENST00000589042:exon305:c.C63352T:p.R21118W		rs200726948
2_179452853_G_C	NM_003319:c.C36086G:p.A12029G		
2_179453771_C_A	NM_003319:c.G35486T:p.C11829F		
2_179453841_G_C	NM_003319:c.C35416G:p.L11806V		
2_179453997_T_C	NM_003319:c.A35260G:p.K11754E		
2_179454020_T_C	NM_003319:c.A35237G:p.D11746G		rs72646849
2_179454135_G_T	ENSG00000155657:ENST00000460472:exon132:c.C35122A:p.L11708M,ENSG00000155657:ENST00000342175:exon133:c.C35698A:p.L11900M,ENSG00000155657:ENST00000359218:exon133:c.C35497A:p.L11833M,ENSG00000155657:ENST00000342992:exon253:c.C54613A:p.L18205M,ENSG00000155657:ENST00000591111:exon254:c.C57394A:p.L19132M,ENSG00000155657:ENST00000589042:exon304:c.C62317A:p.L20773M		
2_179454263_A_G	NM_003319:c.T34994C:p.V11665A		
2_179454383_C_T	NM_003319:c.G34874A:p.R11625Q		
2_179454530_C_T	NM_003319:c.C71099G:p.A23700G		

2_179455043_A_G	ENSG00000155657:ENST00000460472:exon132:c.T34214C:p.I11405T,ENSG00000155657:ENST00000342175:exon133:c.T34790C:p.I11597T,ENSG00000155657:ENST00000359218:exon133:c.T34589C:p.I11530T,ENSG00000155657:ENST00000342992:exon253:c.T53705C:p.I17902T,ENSG00000155657:ENST00000591111:exon254:c.T56486C:p.I18829T,ENSG00000155657:ENST00000589042:exon304:c.T61409C:p.I20470T		rs202012910
2_179455133_C_T	NM_003319:c.G34124A:p.G11375E		
2_179455352_C_T	NM_003319:c.G33905A:p.R11302Q		rs141973925
2_179455520_C_T	ENSG00000155657:ENST00000460472:exon132:c.G33737A:p.R11246Q,ENSG00000155657:ENST00000342175:exon133:c.G34313A:p.R11438Q,ENSG00000155657:ENST00000359218:exon133:c.G34112A:p.R11371Q,ENSG00000155657:ENST00000342992:exon253:c.G53228A:p.R17743Q,ENSG00000155657:ENST00000591111:exon254:c.G56009A:p.R18670Q,ENSG00000155657:ENST00000589042:exon304:c.G60932A:p.R20311Q		
2_179455631_G_A	NM_003319:c.C33626T:p.P11209L	E	rs72646845
2_179455731_C_G	NM_003319:c.G33526C:p.E11176Q		
2_179456349_G_A	ENSG00000155657:ENST00000460472:exon131:c.C33002T:p.P11001L,ENSG00000155657:ENST00000342175:exon132:c.C33578T:p.P11193L,ENSG00000155657:ENST00000359218:exon132:c.C33377T:p.P11126L,ENSG00000155657:ENST00000342992:exon252:c.C52493T:p.P17498L,ENSG00000155657:ENST00000591111:exon253:c.C55274T:p.P18425L,ENSG00000155657:ENST00000589042:exon303:c.C60197T:p.P20066L		
2_179456491_C_T	NM_003319:c.G32860A:p.E10954K		
2_179456541_T_C	NM_133378:c.G18902A:p.R6301Q		
2_179456756_G_A	ENSG00000155657:ENST00000460472:exon130:c.C32680T:p.R10894C,ENSG00000155657:ENST00000342175:exon131:c.C33256T:p.R11086C,ENSG00000155657:ENST00000359218:exon131:c.C33055T:p.R11019C,ENSG00000155657:ENST00000342992:exon251:c.C52171T:p.R17391C,ENSG00000155657:ENST00000591111:exon252:c.C54952T:p.R18318C,ENSG00000155657:ENST00000589042:exon302:c.C59875T:p.R19959C		
2_179456968_T_G	NM_003319:c.A32468C:p.E10823A		
2_179457531_G_A	ENSG00000155657:ENST00000460472:exon128:c.C32120T:p.P10707L,ENSG00000155657:ENST00000342175:exon129:c.C32696T:p.P10899L,ENSG00000155657:ENST00000359218:exon129:c.C32495T:p.P10832L,ENSG00000155657:ENST00000342992:exon249:c.C51611T:p.P17204L,ENSG00000155657:ENST00000591111:exon250:c.C54392T:p.P18131L,ENSG00000155657:ENST00000589042:exon300:c.C59315T:p.P19772L		rs72646840
2_179457598_C_T	NM_003319:c.G25901A:p.R8634H		

2_179458369_C_T	ENSG00000155657:ENST00000460472:exon126:c.G31463A:p.R10488Q,ENSG00000155657:ENST00000342175:exon127:c.G32039A:p.R10680Q,ENSG00000155657:ENST00000359218:exon127:c.G31838A:p.R10613Q,ENSG00000155657:ENST00000342992:exon247:c.G50954A:p.R16985Q,ENSG00000155657:ENST00000591111:exon248:c.G53735A:p.R17912Q,ENSG00000155657:ENST00000589042:exon298:c.G58658A:p.R19553Q		
2_179458391_C_G	NM_003319:c.G22676A:p.R7559Q		
2_179458694_C_T	ENSG00000155657:ENST00000460472:exon125:c.G31231A:p.V10411I,ENSG00000155657:ENST00000342175:exon126:c.G31807A:p.V10603I,ENSG00000155657:ENST00000359218:exon126:c.G31606A:p.V10536I,ENSG00000155657:ENST00000342992:exon246:c.G50722A:p.V16908I,ENSG00000155657:ENST00000591111:exon247:c.G53503A:p.V17835I,ENSG00000155657:ENST00000589042:exon297:c.G58426A:p.V19476I		
2_179458696_T_C	NM_133378:c.A17270G:p.K5757R		
2_179458723_C_G	NM_003319:c.G31202C:p.G10401A		
2_179458757_C_T	ENSG00000155657:ENST00000460472:exon125:c.G31168A:p.G10390S,ENSG00000155657:ENST00000342175:exon126:c.G31744A:p.G10582S,ENSG00000155657:ENST00000359218:exon126:c.G31543A:p.G10515S,ENSG00000155657:ENST00000342992:exon246:c.G50659A:p.G16887S,ENSG00000155657:ENST00000591111:exon247:c.G53440A:p.G17814S,ENSG00000155657:ENST00000589042:exon297:c.G58363A:p.G19455S		rs191927501
2_179458894_C_T	ENSG00000155657:ENST00000460472:exon125:c.G31031A:p.R10344H,ENSG00000155657:ENST00000342175:exon126:c.G31607A:p.R10536H,ENSG00000155657:ENST00000359218:exon126:c.G31406A:p.R10469H,ENSG00000155657:ENST00000342992:exon246:c.G50522A:p.R16841H,ENSG00000155657:ENST00000591111:exon247:c.G53303A:p.R17768H,ENSG00000155657:ENST00000589042:exon297:c.G58226A:p.R19409H		rs201505306
2_179459202_A_T	ENSG00000155657:ENST00000460472:exon124:c.T30824A:p.L10275H,ENSG00000155657:ENST00000342175:exon125:c.T31400A:p.L10467H,ENSG00000155657:ENST00000359218:exon125:c.T31199A:p.L10400H,ENSG00000155657:ENST00000342992:exon245:c.T50315A:p.L16772H,ENSG00000155657:ENST00000591111:exon246:c.T53096A:p.L17699H,ENSG00000155657:ENST00000589042:exon296:c.T58019A:p.L19340H		
2_179459370_A_C	ENSG00000155657:ENST00000460472:exon124:c.T30656G:p.V10219G,ENSG00000155657:ENST00000342175:exon125:c.T31232G:p.V10411G,ENSG00000155657:ENST00000359218:exon125:c.T31031G:p.V10344G,ENSG00000155657:ENST00000342992:exon245:c.T50147G:p.V16716G,ENSG00000155657:ENST00000591111:exon246:c.T52928G:p.V17643G,ENSG00000155657:ENST00000589042:exon296:c.T57851G:p.V19284G		
2_179460227_TACT_TTACT	TTN	L	

2_179460255_G_A	ENSG00000155657:ENST00000460472:exon123:c.C30631T:p.L10211F,ENSG00000155657:ENST00000342175:exon124:c.C31207T:p.L10403F,ENSG00000155657:ENST00000359218:exon124:c.C31006T:p.L10336F,ENSG00000155657:ENST00000342992:exon244:c.C50122T:p.L16708F,ENSG00000155657:ENST00000591111:exon245:c.C52903T:p.L17635F,ENSG00000155657:ENST00000589042:exon295:c.C57826T:p.L19276F		
2_179460332_T_G	NM_003319:c.G34727A:p.R11576Q		
2_179460398_C_T	ENSG00000155657:ENST00000460472:exon123:c.G30488A:p.R10163H,ENSG00000155657:ENST00000342175:exon124:c.G31064A:p.R10355H,ENSG00000155657:ENST00000359218:exon124:c.G30863A:p.R10288H,ENSG00000155657:ENST00000342992:exon244:c.G49979A:p.R16660H,ENSG00000155657:ENST00000591111:exon245:c.G52760A:p.R17587H,ENSG00000155657:ENST00000589042:exon295:c.G57683A:p.R19228H		rs114711705
2_179460425_T_A	ENSG00000155657:ENST00000460472:exon123:c.A30461T:p.Y10154F,ENSG00000155657:ENST00000342175:exon124:c.A31037T:p.Y10346F,ENSG00000155657:ENST00000359218:exon124:c.A30836T:p.Y10279F,ENSG00000155657:ENST00000342992:exon244:c.A49952T:p.Y16651F,ENSG00000155657:ENST00000591111:exon245:c.A52733T:p.Y17578F,ENSG00000155657:ENST00000589042:exon295:c.A57656T:p.Y19219F		rs201541213
2_179460488_T_C	NM_003319:c.A30398G:p.N10133S		
2_179462367_T_C	NM_003319:c.A30247G:p.M10083V		
2_179462655_A_G	ENSG00000155657:ENST00000460472:exon121:c.T30047C:p.I10016T,ENSG00000155657:ENST00000342175:exon122:c.T30623C:p.I10208T,ENSG00000155657:ENST00000359218:exon122:c.T30422C:p.I10141T,ENSG00000155657:ENST00000342992:exon242:c.T49538C:p.I16513T,ENSG00000155657:ENST00000591111:exon243:c.T52319C:p.I17440T,ENSG00000155657:ENST00000589042:exon293:c.T57242C:p.I19081T		rs78509062
2_179462685_A_G	NM_003319:c.T30017C:p.I10006T		
2_179463490_C_T	NM_003319:c.G29752A:p.A9918T		
2_179463526_C_T	ENSG00000155657:ENST00000460472:exon119:c.G29716A:p.V9906M,ENSG00000155657:ENST00000342175:exon120:c.G30292A:p.V10098M,ENSG00000155657:ENST00000359218:exon120:c.G30091A:p.V10031M,ENSG00000155657:ENST00000342992:exon240:c.G49207A:p.V16403M,ENSG00000155657:ENST00000591111:exon241:c.G51988A:p.V17330M,ENSG00000155657:ENST00000589042:exon291:c.G56911A:p.V18971M		
2_179465706_A_T	NM_003319:c.T28730A:p.L9577Q		rs140714512
2_179465721_C_T	NM_003319:c.G28715A:p.R9572H		
2_179465893_G_A	NM_003319:c.C28543T:p.P9515S		

2_179466400_T_C	ENSG00000155657:ENST00000460472:exon114:c.A28222G:p.R9408G,ENSG00000155657:ENST00000342175:exon115:c.A28798G:p.R9600G,ENSG00000155657:ENST00000359218:exon115:c.A28597G:p.R9533G,ENSG00000155657:ENST00000342992:exon235:c.A47713G:p.R15905G,ENSG00000155657:ENST00000591111:exon236:c.A50494G:p.R16832G,ENSG00000155657:ENST00000589042:exon286:c.A55417G:p.R18473G		rs72646822
2_179466463_A_G	ENSG00000155657:ENST00000460472:exon114:c.T28159C:p.S9387P,ENSG00000155657:ENST00000342175:exon115:c.T28735C:p.S9579P,ENSG00000155657:ENST00000359218:exon115:c.T28534C:p.S9512P,ENSG00000155657:ENST00000342992:exon235:c.T47650C:p.S15884P,ENSG00000155657:ENST00000591111:exon236:c.T50431C:p.S16811P,ENSG00000155657:ENST00000589042:exon286:c.T55354C:p.S18452P		
2_179467275_G_A	NM_003319:c.C27659T:p.T9220M		
2_179468618_C_A	NM_003319:c.G27601T:p.A9201S		
2_179469013_T_C	NM_003319:c.A27206G:p.N9069S		
2_179469756_G_A	NM_003319:c.C26953T:p.R8985C		rs55734111
2_179469764_G_A	NM_003319:c.C26945T:p.A8982V		
2_179469960_C_T	NM_003319:c.G26749A:p.E8917K		
2_179469980_G_C	NM_003319:c.G78524A:p.R26175Q		
2_179470001_C_T	ENSG00000155657:ENST00000460472:exon108:c.G26708A:p.R8903H,ENSG00000155657:ENST00000342175:exon109:c.G27284A:p.R9095H,ENSG00000155657:ENST00000359218:exon109:c.G27083A:p.R9028H,ENSG00000155657:ENST00000342992:exon229:c.G46199A:p.R15400H,ENSG00000155657:ENST00000591111:exon230:c.G48980A:p.R16327H,ENSG00000155657:ENST00000589042:exon280:c.G53903A:p.R17968H		rs200100660
2_179471822_C_T	NM_003319:c.G26312A:p.R8771H		
2_179472155_A_G	ENSG00000155657:ENST00000460472:exon105:c.T26065C:p.F8689L,ENSG00000155657:ENST00000342175:exon106:c.T26641C:p.F8881L,ENSG00000155657:ENST00000359218:exon106:c.T26440C:p.F8814L,ENSG00000155657:ENST00000342992:exon226:c.T45556C:p.F15186L,ENSG00000155657:ENST00000591111:exon227:c.T48337C:p.F16113L,ENSG00000155657:ENST00000589042:exon277:c.T53260C:p.F17754L		
2_179472293_T_C	NM_003319:c.A25927G:p.K8643E		rs185913848
2_179472360_C_T	ENSG00000155657:ENST00000460472:exon105:c.G25860A:p.M8620I,ENSG00000155657:ENST00000342175:exon106:c.G26436A:p.M8812I,ENSG00000155657:ENST00000359218:exon106:c.G26235A:p.M8745I,ENSG00000155657:ENST00000342992:exon226:c.G45351A:p.M15117I,ENSG00000155657:ENST00000591111:exon227:c.G48132A:p.M16044I,ENSG00000155657:ENST00000589042:exon277:c.G53055A:p.M17685I		rs200387466

2_179472662_G_A	NM_003319:c.G11659A:p.V3887M		
2_179473066_T_C	NM_003319:c.A25349G:p.H8450R		
2_179473074_G_C	ENSG00000155657:ENST00000460472:exon103:c.C25341G:p.N8447K,ENSG00000155657:ENST00000342175:exon104:c.C25917G:p.N8639K,ENSG00000155657:ENST00000359218:exon104:c.C25716G:p.N8572K,ENSG00000155657:ENST00000342992:exon224:c.C44832G:p.N14944K,ENSG00000155657:ENST00000591111:exon225:c.C47613G:p.N15871K,ENSG00000155657:ENST00000589042:exon275:c.C52536G:p.N17512K		rs199615557
2_179473094_G_T	ENSG00000155657:ENST00000460472:exon103:c.C25321A:p.L8441I,ENSG00000155657:ENST00000342175:exon104:c.C25897A:p.L8633I,ENSG00000155657:ENST00000359218:exon104:c.C25696A:p.L8566I,ENSG00000155657:ENST00000342992:exon224:c.C44812A:p.L14938I,ENSG00000155657:ENST00000591111:exon225:c.C47593A:p.L15865I,ENSG00000155657:ENST00000589042:exon275:c.C52516A:p.L17506I		
2_179474015_C_T	ENSG00000155657:ENST00000460472:exon101:c.G24827A:p.R8276Q,ENSG00000155657:ENST00000342175:exon102:c.G25403A:p.R8468Q,ENSG00000155657:ENST00000359218:exon102:c.G25202A:p.R8401Q,ENSG00000155657:ENST00000342992:exon222:c.G44318A:p.R14773Q,ENSG00000155657:ENST00000591111:exon223:c.G47099A:p.R15700Q,ENSG00000155657:ENST00000589042:exon273:c.G52022A:p.R17341Q		
2_179474046_C_G	NM_003319:c.G24796C:p.E8266Q		
2_179474150_C_T	ENSG00000155657:ENST00000460472:exon101:c.G24692A:p.R8231H,ENSG00000155657:ENST00000342175:exon102:c.G25268A:p.R8423H,ENSG00000155657:ENST00000359218:exon102:c.G25067A:p.R8356H,ENSG00000155657:ENST00000342992:exon222:c.G44183A:p.R14728H,ENSG00000155657:ENST00000591111:exon223:c.G46964A:p.R15655H,ENSG00000155657:ENST00000589042:exon273:c.G51887A:p.R17296H		rs200456782
2_179474255_C_T	NM_003319:c.G24587A:p.R8196Q		
2_179474468_C_T	ENSG00000155657:ENST00000460472:exon100:c.G24487A:p.A8163T,ENSG00000155657:ENST00000342175:exon101:c.G25063A:p.A8355T,ENSG00000155657:ENST00000359218:exon101:c.G24862A:p.A8288T,ENSG00000155657:ENST00000342992:exon221:c.G43978A:p.A14660T,ENSG00000155657:ENST00000591111:exon222:c.G46759A:p.A15587T,ENSG00000155657:ENST00000589042:exon272:c.G51682A:p.A17228T		
2_179474525_C_T	ENSG00000155657:ENST00000460472:exon100:c.G24430A:p.A8144T,ENSG00000155657:ENST00000342175:exon101:c.G25006A:p.A8336T,ENSG00000155657:ENST00000359218:exon101:c.G24805A:p.A8269T,ENSG00000155657:ENST00000342992:exon221:c.G43921A:p.A14641T,ENSG00000155657:ENST00000591111:exon222:c.G46702A:p.A15568T,ENSG00000155657:ENST00000589042:exon272:c.G51625A:p.A17209T		
2_179475068_C_T	NM_003319:c.G23990A:p.S7997N		

2_179475722_A_G	NM_003319:c.T23939C:p.I7980TTTN;TTN		rs111933113
2_179476106_G_T	ENSG00000155657:ENST00000460472:exon97:c.C23655A:p.D7885E,ENSG00000155657:ENST00000342175:exon98:c.C24231A:p.D8077E,ENSG00000155657:ENST00000359218:exon98:c.C24030A:p.D8010E,ENSG00000155657:ENST00000342992:exon218:c.C43146A:p.D14382E,ENSG00000155657:ENST00000591111:exon219:c.C45927A:p.D15309E,ENSG00000155657:ENST00000589042:exon269:c.C50850A:p.D16950E		rs200700386
2_179476342_C_G	NM_003319:c.G23419C:p.A7807P		
2_179476619_C_T	NM_003319:c.G23222A:p.G7741E		
2_179476646_C_T	NM_003319:c.G23195A:p.R7732H		
2_179476673_A_G	ENSG00000155657:ENST00000460472:exon96:c.T23168C:p.I7723T,ENSG00000155657:ENST00000342175:exon97:c.T23744C:p.I7915T,ENSG00000155657:ENST00000359218:exon97:c.T23543C:p.I7848T,ENSG00000155657:ENST00000342992:exon217:c.T42659C:p.I14220T,ENSG00000155657:ENST00000591111:exon218:c.T45440C:p.I15147T,ENSG00000155657:ENST00000589042:exon268:c.T50363C:p.I16788T		
2_179477040_C_T	NM_003319:c.G23017A:p.E7673K		rs148018042
2_179477175_C_T	NM_003319:c.G22882A:p.V7628I		
2_179477286_G_T	ENSG00000155657:ENST00000460472:exon94:c.C22771A:p.R7591S,ENSG00000155657:ENST00000342175:exon95:c.C23347A:p.R7783S,ENSG00000155657:ENST00000359218:exon95:c.C23146A:p.R7716S,ENSG00000155657:ENST00000342992:exon215:c.C42262A:p.R14088S,ENSG00000155657:ENST00000591111:exon216:c.C45043A:p.R15015S,ENSG00000155657:ENST00000589042:exon266:c.C49966A:p.R16656S		
2_179477529_C_G	NM_003319:c.G12770A:p.G4257D		rs55663050
2_179477577_C_T	NM_003319:c.C60274T:p.L20092F		
2_179478597_C_A	NM_003319:c.G22218T:p.W7406C		
2_179478647_T_C	ENSG00000155657:ENST00000460472:exon91:c.A22168G:p.T7390A,ENSG00000155657:ENST00000342175:exon92:c.A22744G:p.T7582A,ENSG00000155657:ENST00000359218:exon92:c.A22543G:p.T7515A,ENSG00000155657:ENST00000342992:exon212:c.A41659G:p.T13887A,ENSG00000155657:ENST00000591111:exon213:c.A44440G:p.T14814A,ENSG00000155657:ENST00000589042:exon263:c.A49363G:p.T16455A		
2_179479064_G_A	NM_003319:c.C21865T:p.P7289S		

2_179479241_C_T	ENSG00000155657:ENST00000460472:exon89:c.G21805A:p.V7269M,ENSG00000155657:ENST00000342175:exon90:c.G22381A:p.V7461M,ENSG00000155657:ENST00000359218:exon90:c.G22180A:p.V7394M,ENSG00000155657:ENST00000342992:exon210:c.G41296A:p.V13766M,ENSG00000155657:ENST00000591111:exon211:c.G44077A:p.V14693M,ENSG00000155657:ENST00000589042:exon261:c.G49000A:p.V16334M		
2_179479288_A_G	ENSG00000155657:ENST00000460472:exon89:c.T21758C:p.I7253T,ENSG00000155657:ENST00000342175:exon90:c.T22334C:p.I7445T,ENSG00000155657:ENST00000359218:exon90:c.T22133C:p.I7378T,ENSG00000155657:ENST00000342992:exon210:c.T41249C:p.I13750T,ENSG00000155657:ENST00000591111:exon211:c.T44030C:p.I14677T,ENSG00000155657:ENST00000589042:exon261:c.T48953C:p.I16318T		rs72677243
2_179479607_G_A	ENSG00000155657:ENST00000460472:exon88:c.C21532T:p.P7178S,ENSG00000155657:ENST00000342175:exon89:c.C22108T:p.P7370S,ENSG00000155657:ENST00000359218:exon89:c.C21907T:p.P7303S,ENSG00000155657:ENST00000342992:exon209:c.C41023T:p.P13675S,ENSG00000155657:ENST00000591111:exon210:c.C43804T:p.P14602S,ENSG00000155657:ENST00000589042:exon260:c.C48727T:p.P16243S		rs72677242
2_179480377_T_C	NM_003319:c.A21256G:p.T7086A		rs186497293
2_179480475_T_C	ENSG00000155657:ENST00000460472:exon86:c.A21158G:p.D7053G,ENSG00000155657:ENST00000342175:exon87:c.A21734G:p.D7245G,ENSG00000155657:ENST00000359218:exon87:c.A21533G:p.D7178G,ENSG00000155657:ENST00000342992:exon207:c.A40649G:p.D13550G,ENSG00000155657:ENST00000591111:exon208:c.A43430G:p.D14477G,ENSG00000155657:ENST00000589042:exon258:c.A48353G:p.D16118G		
2_179481223_G_A	NM_003319:c.C21100T:p.R7034W		
2_179481467_A_C	NM_003319:c.T20954G:p.V6985G		
2_179481618_C_G	NM_003319:c.G20803C:p.D6935H		
2_179481666_C_G	ENSG00000155657:ENST00000460472:exon84:c.G20755C:p.V6919L,ENSG00000155657:ENST00000342175:exon85:c.G21331C:p.V7111L,ENSG00000155657:ENST00000359218:exon85:c.G21130C:p.V7044L,ENSG00000155657:ENST00000342992:exon205:c.G40246C:p.V13416L,ENSG00000155657:ENST00000591111:exon206:c.G43027C:p.V14343L,ENSG00000155657:ENST00000589042:exon256:c.G47950C:p.V15984L		
2_179482089_C_T	NM_003319:c.G62191A:p.V20731M		rs72677237
2_179482533_G_T	NM_133379:c.G14492A:p.C4831Y		
2_179482565_C_T	NM_003319:c.G20318A:p.R6773Q		

2_179482763_C_T	ENSG00000155657:ENST00000460472:exon81:c.G20120A:p.R6707Q,ENSG00000155657:ENST00000342175:exon82:c.G20696A:p.R6899Q,ENSG00000155657:ENST00000359218:exon82:c.G20495A:p.R6832Q,ENSG00000155657:ENST00000342992:exon202:c.G39611A:p.R13204Q,ENSG00000155657:ENST00000591111:exon203:c.G42392A:p.R14131Q,ENSG00000155657:ENST00000589042:exon253:c.G47315A:p.R15772Q		rs72677233
2_179482937_C_T	NM_003319:c.G20053A:p.V6685I		rs72677232
2_179482994_G_A	ENSG00000155657:ENST00000460472:exon80:c.C19996T:p.R6666C,ENSG00000155657:ENST00000342175:exon81:c.C20572T:p.R6858C,ENSG00000155657:ENST00000359218:exon81:c.C20371T:p.R6791C,ENSG00000155657:ENST00000342992:exon201:c.C39487T:p.R13163C,ENSG00000155657:ENST00000591111:exon202:c.C42268T:p.R14090C,ENSG00000155657:ENST00000589042:exon252:c.C47191T:p.R15731C	E	rs72677231
2_179483108_C_T	ENSG00000155657:ENST00000460472:exon80:c.G19882A:p.V6628I,ENSG00000155657:ENST00000342175:exon81:c.G20458A:p.V6820I,ENSG00000155657:ENST00000359218:exon81:c.G20257A:p.V6753I,ENSG00000155657:ENST00000342992:exon201:c.G39373A:p.V13125I,ENSG00000155657:ENST00000591111:exon202:c.G42154A:p.V14052I,ENSG00000155657:ENST00000589042:exon252:c.G47077A:p.V15693I		rs201717871
2_179483349_T_C	NM_003319:c.A19733G:p.H6578R		
2_179483375_C_A	NM_003319:c.G19707T:p.R6569S		
2_179483384_G_C	NM_003319:c.C19698G:p.D6566E		
2_179483430_G_A	NM_003319:c.C78211T:p.R26071W		
2_179484376_TTT_-	ENSG00000155657:ENST00000460472:exon78:c.19471_19473del:p.6491_6491del,ENSG00000155657:ENST00000342175:exon79:c.20047_20049del:p.6683_6683del,ENSG00000155657:ENST00000359218:exon79:c.19846_19848del:p.6616_6616del,ENSG00000155657:ENST00000342992:exon199:c.38962_38964del:p.12988_12988del,ENSG00000155657:ENST00000591111:exon200:c.41743_41745del:p.13915_13915del,ENSG00000155657:ENST00000589042:exon250:c.46666_46668del:p.15556_15556del		
2_179484555_C_A	NM_003319:c.G19294T:p.V6432F		
2_179484593_C_T	NM_003319:c.G19256A:p.R6419K		
2_179484757_C_T	ENSG00000155657:ENST00000460472:exon77:c.G19192A:p.G6398R,ENSG00000155657:ENST00000342175:exon78:c.G19768A:p.G6590R,ENSG00000155657:ENST00000359218:exon78:c.G19567A:p.G6523R,ENSG00000155657:ENST00000342992:exon198:c.G38683A:p.G12895R,ENSG00000155657:ENST00000591111:exon199:c.G41464A:p.G13822R,ENSG00000155657:ENST00000589042:exon249:c.G46387A:p.G15463R		rs200042932
2_179484993_C_A	NM_003319:c.G58601A:p.R19534H		

2_179485026_C_T	ENSG00000155657:ENST00000460472:exon76:c.G19027A:p.A6343T,ENSG00000155657:ENST00000342175:exon77:c.G19603A:p.A6535T,ENSG00000155657:ENST00000359218:exon77:c.G19402A:p.A6468T,ENSG00000155657:ENST00000342992:exon197:c.G38518A:p.A12840T,ENSG00000155657:ENST00000591111:exon198:c.G41299A:p.A13767T,ENSG00000155657:ENST00000589042:exon248:c.G46222A:p.A15408T		
2_179485196_A_C	NM_003319:c.T18857G:p.V6286G		
2_179485268_C_T	NM_003319:c.G18785A:p.R6262H		
2_179485304_T_C	NM_003319:c.A18749G:p.E6250G		
2_179485589_T_A	NM_003319:c.A18553T:p.S6185C		
2_179485846_G_C	NM_003319:c.C18404G:p.A6135G		
2_179486037_C_A	NM_003319:c.G18213T:p.K6071N		rs72677225
2_179486376_C_T	NM_003319:c.G17980A:p.A5994T		rs144668626
2_179486699_C_G	ENSG00000155657:ENST00000460472:exon72:c.G17755C:p.G5919R,ENSG00000155657:ENST00000342175:exon73:c.G18331C:p.G6111R,ENSG00000155657:ENST00000359218:exon73:c.G18130C:p.G6044R,ENSG00000155657:ENST00000342992:exon193:c.G37246C:p.G12416R,ENSG00000155657:ENST00000591111:exon194:c.G40027C:p.G13343R,ENSG00000155657:ENST00000589042:exon244:c.G44950C:p.G14984R		
2_179494968_G_A	NM_003319:c.C17086T:p.P5696STTN;TTN		rs192766485
2_179495607_C_T	ENSG00000155657:ENST00000460472:exon66:c.G16883A:p.R5628H,ENSG00000155657:ENST00000342175:exon67:c.G17459A:p.R5820H,ENSG00000155657:ENST00000359218:exon67:c.G17258A:p.R5753H,ENSG00000155657:ENST00000342992:exon187:c.G36374A:p.R12125H,ENSG00000155657:ENST00000591111:exon188:c.G39155A:p.R13052H,ENSG00000155657:ENST00000589042:exon238:c.G44078A:p.R14693H		
2_179495936_ATCTGC_-	NM_003319:c.16639_16644del:p.5547_5548del		
2_179497042_C_T	NM_003319:c.G16384A:p.V5462I		
2_179497134_C_T	NM_003319:c.G16292A:p.R5431Q		
2_179497457_T_C	NM_003319:c.A16081G:p.K5361E		
2_179497478_C_T	NM_003319:c.G16060A:p.V5354I		
2_179497720_A_G	ENSG00000155657:ENST00000460472:exon62:c.T15943C:p.C5315R,ENSG00000155657:ENST00000342175:exon63:c.T16519C:p.C5507R,ENSG00000155657:ENST00000359218:exon63:c.T16318C:p.C5440R,ENSG00000155657:ENST00000342992:exon183:c.T35434C:p.C11812R,ENSG00000155657:ENST00000591111:exon184:c.T38215C:p.C12739R,ENSG00000155657:ENST00000589042:exon234:c.T43138C:p.C14380R		

2_179497918_G_T	NM_003319:c.C15887A:p.S5296YTTN;TTN		
2_179499545_C_T	ENSG00000155657:ENST00000460472:exon57:c.G14861A:p.R4954H,ENSG00000155657:ENST00000342175:exon58:c.G15437A:p.R5146H,ENSG00000155657:ENST00000359218:exon58:c.G15236A:p.R5079H,ENSG00000155657:ENST00000342992:exon178:c.G34352A:p.R11451H,ENSG00000155657:ENST00000591111:exon179:c.G37133A:p.R12378H,ENSG00000155657:ENST00000589042:exon229:c.G42056A:p.R14019H		
2_179499960_C_T	NM_003319:c.G14761A:p.A4921T		
2_179500241_G_A	ENSG00000155657:ENST00000460472:exon55:c.C14615T:p.A4872V,ENSG00000155657:ENST00000342175:exon56:c.C15191T:p.A5064V,ENSG00000155657:ENST00000359218:exon56:c.C14990T:p.A4997V,ENSG00000155657:ENST00000342992:exon176:c.C34106T:p.A11369V,ENSG00000155657:ENST00000591111:exon177:c.C36887T:p.A12296V,ENSG00000155657:ENST00000589042:exon227:c.C41810T:p.A13937V		
2_179500777_C_T	NM_003319:c.G14326A:p.D4776N		
2_179501156_T_G	ENSG00000155657:ENST00000460472:exon53:c.A14103C:p.E4701D,ENSG00000155657:ENST00000342175:exon54:c.A14679C:p.E4893D,ENSG00000155657:ENST00000359218:exon54:c.A14478C:p.E4826D,ENSG00000155657:ENST00000342992:exon174:c.A33594C:p.E11198D,ENSG00000155657:ENST00000591111:exon175:c.A36375C:p.E12125D,ENSG00000155657:ENST00000589042:exon225:c.A41298C:p.E13766D		
2_179501161_T_C	ENSG00000155657:ENST00000460472:exon53:c.A14098G:p.K4700E,ENSG00000155657:ENST00000342175:exon54:c.A14674G:p.K4892E,ENSG00000155657:ENST00000359218:exon54:c.A14473G:p.K4825E,ENSG00000155657:ENST00000342992:exon174:c.A33589G:p.K11197E,ENSG00000155657:ENST00000591111:exon175:c.A36370G:p.K12124E,ENSG00000155657:ENST00000589042:exon225:c.A41293G:p.K13765E		
2_179501481_T_C	NM_003319:c.A13778G:p.K4593R		rs184713215
2_179505316_C_T	NM_003319:c.T5227G:p.S1743A		
2_179506001_G_A	ENSG00000155657:ENST00000414766:exon28:c.C2563T:p.P855S,ENSG00000155657:ENST00000460472:exon48:c.C13405T:p.P4469S,ENSG00000155657:ENST00000342175:exon49:c.C13981T:p.P4661S,ENSG00000155657:ENST00000359218:exon49:c.C13780T:p.P4594S,ENSG00000155657:ENST00000342992:exon169:c.C32896T:p.P10966S,ENSG00000155657:ENST00000591111:exon170:c.C35677T:p.P11893S,ENSG00000155657:ENST00000589042:exon220:c.C40600T:p.P13534S		

2_179507024_C_A	ENSG00000155657:ENST00000414766:exon27:c.G2461T:p.V821F,ENSG00000155657:ENST00000460472:exon47:c.G13303T:p.V4435F,ENSG00000155657:ENST00000342175:exon48:c.G13879T:p.V4627F,ENSG00000155657:ENST00000359218:exon48:c.G13678T:p.V4560F,ENSG00000155657:ENST00000342992:exon168:c.G32794T:p.V10932F,ENSG00000155657:ENST00000591111:exon169:c.G35575T:p.V11859F,ENSG00000155657:ENST00000589042:exon219:c.G40498T:p.V13500F		rs201944202
2_179511286_T_C	ENSG00000155657:ENST00000446966:exon10:c.A740G:p.E247G,ENSG00000155657:ENST00000589042:exon216:c.A40223G:p.E13408G		rs183950862
2_179514582_A_G	NM_133378:c.T32555C:p.V10852A		
2_179515498_G_A	NM_133378:c.C32387T:p.A10796V		
2_179516689_C_T	NM_133378:c.G31999A:p.E10667K		
2_179517227_G_T	ENSG00000155657:ENST00000342992:exon156:c.C31783A:p.P10595T,ENSG00000155657:ENST00000591111:exon157:c.C34564A:p.P11522T,ENSG00000155657:ENST00000589042:exon202:c.C39085A:p.P13029T		
2_179517425_C_T	ENSG00000155657:ENST00000589042:exon201:c.G38998A:p.V13000M		
2_179518992_G_A	ENSG00000155657:ENST00000589042:exon193:c.C38323T:p.L12775F		rs186232617
2_179518994_A_G	ENSG00000155657:ENST00000589042:exon193:c.T38321C:p.V12774A		
2_179527707_G_A	ENSG00000155657:ENST00000342992:exon153:c.C31559T:p.A10520V,ENSG00000155657:ENST00000589042:exon174:c.C36776T:p.A12259V		
2_179527775_T_A	NM_133378:c.A31491T:p.E10497D		rs1883088
2_179528017_T_C	ENSG00000155657:ENST00000589042:exon173:c.A36676G:p.K12226E		rs200815663
2_179528377_T_A	ENSG00000155657:ENST00000589042:exon171:c.A36509T:p.E12170V		rs200840285
2_179528759_T_C	ENSG00000155657:ENST00000589042:exon169:c.A36347G:p.E12116G		rs200513156
2_179528793_T_C	ENSG00000155657:ENST00000589042:exon169:c.A36313G:p.K12105E		
2_179534380_A_C	ENSG00000155657:ENST00000589042:exon158:c.T35409G:p.I11803M		rs186992412
2_179535861_T_G	ENSG00000155657:ENST00000342992:exon151:c.A31361C:p.K10454T,ENSG00000155657:ENST00000591111:exon152:c.A34142C:p.K11381T,ENSG00000155657:ENST00000589042:exon156:c.A35264C:p.K11755T		rs189966800
2_179537200_C_T	NM_133378:c.G30961A:p.V10321I		
2_179537434_T_C	NM_133378:exon149:c.30884-4A>G	L	
2_179538377_T_C	NM_133378:c.A30866G:p.E10289G		

2_179538378_C_G	NM_133378:c.G30865C:p.E10289Q		
2_179538425_A_G	NM_133378:c.T30818C:p.I10273T		
2_179539812_T_G	NM_133378:c.A30663C:p.E10221D		
2_179540461_G_T	ENSG00000155657:ENST00000589042:exon149:c.C34474A:p.P11492T		rs182428755
2_179541999_T_C	ENSG00000155657:ENST00000589042:exon147:c.A34307G:p.K11436R		
2_179542350_G_T	ENSG00000155657:ENST00000342992:exon143:c.C30557A:p.P10186Q,ENSG00000155657:ENST00000591111:exon144:c.C33338A:p.P11113Q,ENSG00000155657:ENST00000589042:exon146:c.C34289A:p.P11430Q		
2_179542390_CTT_-	ENSG00000155657:ENST00000342992:exon143:c.30515_30517del:p.10172_10173del,ENSG00000155657:ENST00000591111:exon144:c.33296_33298del:p.11099_11100del,ENSG00000155657:ENST00000589042:exon146:c.34247_34249del:p.11416_11417del		
2_179542397_TTC_-	NM_133378:c.30508_30510del:p.10170_10170del		
2_179542423_G_T	NM_133378:c.C30484A:p.P10162T		
2_179544077_G_A	NM_133378:c.C29999T:p.P10000L		
2_179544685_-_CCT	NM_133378:c.29784_29785insAGG:p.E9928delinsEG		
2_179544689_-_ATT	NM_133378:c.29780_29781insAAT:p.E9927delinsEX	L	
2_179544700_-_TCT	NM_133378:c.29769_29770insAGA:p.V9923delinsVE		
2_179544983_C_G	NM_133378:c.G29684C:p.R9895TTTN;TTN		rs72650040
2_179545841_C_T	ENSG00000155657:ENST00000342992:exon135:c.G29573A:p.R9858H,ENSG00000155657:ENST00000591111:exon136:c.G32354A:p.R10785H,ENSG00000155657:ENST00000589042:exon138:c.G33305A:p.R11102H		
2_179547466_G_A	NM_133378:c.C29320T:p.R9774W		
2_179547531_TCATATTCTTCATATTCC_- ENSG00000155657:ENST00000414766:exon20:c.1812_1829del:p.604_610del,ENSG00000155657:ENST00000342992:exon132:c.29238_29255del:p.9746_9752del,ENSG00000155657:ENST00000591111:exon133:c.32019_32036del:p.10673_10679del,ENSG00000155657:ENST00000589042:exon135:c.32970_32987del:p.10990_10996del			
2_179548782_G_A	ENSG00000155657:ENST00000342992:exon130:c.C29018T:p.P9673L,ENSG00000155657:ENST00000591111:exon131:c.C31799T:p.P10600L,ENSG00000155657:ENST00000589042:exon133:c.C32750T:p.P10917L		rs73973137
2_179548789_C_G	ENSG00000155657:ENST00000342992:exon130:c.G29011C:p.A9671P,ENSG00000155657:ENST00000591111:exon131:c.G31792C:p.A10598P,ENSG00000155657:ENST00000589042:exon133:c.G32743C:p.A10915P		rs72650032

2_179548809_A_T	NM_133378:c.T28991A:p.V9664ETTN;TTN		
2_179549407_G_A	NM_133378:c.C28892T:p.P9631L		het
2_179549438_C_G	ENSG00000155657:ENST00000342992:exon128:c.G28861C:p.V9621L,ENSG00000155657:ENST00000591111:exon129:c.G31642C:p.V10548L,ENSG00000155657:ENST00000589042:exon131:c.G32593C:p.V10865L		rs150733188
2_179549474_G_A	ENSG00000155657:ENST00000342992:exon128:c.C28825T:p.P9609S,ENSG00000155657:ENST00000591111:exon129:c.C31606T:p.P10536S,ENSG00000155657:ENST00000589042:exon131:c.C32557T:p.P10853S		rs201738153
2_179549707_G_A	NM_133378:c.C28748T:p.A9583V		rs72650030
2_179553415_G_A	NM_133378:c.C28454T:p.T9485M		rs115119858
2_179553443_A_G	ENSG00000155657:ENST00000342992:exon123:c.T28426C:p.F9476L,ENSG00000155657:ENST00000591111:exon124:c.T31207C:p.F10403L,ENSG00000155657:ENST00000589042:exon126:c.T32158C:p.F10720L		
2_179553510_A_C	NM_133378:exon124:c.28364-5T>G	L	
2_179554549_G_C	ENSG00000155657:ENST00000414766:exon16:c.C1471G:p.P491A,ENSG00000155657:ENST00000342992:exon119:c.C28105G:p.P9369A,ENSG00000155657:ENST00000591111:exon120:c.C30886G:p.P10296A,ENSG00000155657:ENST00000589042:exon122:c.C31837G:p.P10613A		rs200213832
2_179554624_C_T	NM_133378:exon120:c.28031-1G>A	L	
2_179556769_-_TAG	ENSG00000155657:ENST00000414766:exon15:c.1370_1371insCTA:p.K457delinsTK,ENSG00000155657:ENST00000342992:exon118:c.28004_28005insCTA:p.K9335delinsTK,ENSG00000155657:ENST00000591111:exon119:c.30785_30786insCTA:p.K10262delinsTK,ENSG00000155657:ENST00000589042:exon121:c.31736_31737insCTA:p.K10579delinsTK		
2_179556770_T_G	ENSG00000155657:ENST00000414766:exon15:c.A1369C:p.K457Q,ENSG00000155657:ENST00000342992:exon118:c.A28003C:p.K9335Q,ENSG00000155657:ENST00000591111:exon119:c.A30784C:p.K10262Q,ENSG00000155657:ENST00000589042:exon121:c.A31735C:p.K10579Q		
2_179557257_T_C	ENSG00000155657:ENST00000414766:exon14:c.A1279G:p.I427V,ENSG00000155657:ENST00000342992:exon117:c.A27913G:p.I9305V,ENSG00000155657:ENST00000591111:exon118:c.A30694G:p.I10232V,ENSG00000155657:ENST00000589042:exon120:c.A31645G:p.I10549V		
2_179558657_G_A	NM_133378:c.C27773T:p.S9258L		

2_179559353_C_T	ENSG00000155657:ENST00000414766:exon11:c.G1033A:p.V345I,ENSG00000155657:ENST00000342992:exon114:c.G27667A:p.V9223I,ENSG00000155657:ENST00000591111:exon115:c.G30448A:p.V10150I,ENSG00000155657:ENST00000589042:exon117:c.G31399A:p.V10467I		rs72650019
2_179560717_T_C	NM_133378:c.A27350G:p.E9117G		
2_179563575_C_T	NM_133378:c.G27017A:p.R9006H		
2_179563582_T_C	ENSG00000155657:ENST00000414766:exon6:c.A376G:p.T126A,ENSG00000155657:ENST00000342992:exon109:c.A27010G:p.T9004A,ENSG00000155657:ENST00000591111:exon110:c.A29791G:p.T9931A,ENSG00000155657:ENST00000589042:exon112:c.A30742G:p.T10248A		
2_179563611_T_C	NM_133378:c.A26981G:p.K8994R		
2_179566792_T_A	NM_133378:c.A26781T:p.E8927DTTN;TTN		
2_179567202_T_G	NM_133378:c.A26680C:p.N8894H		
2_179567340_G_A	ENSG00000155657:ENST00000342992:exon104:c.C26542T:p.H8848Y,ENSG00000155657:ENST00000591111:exon105:c.C29323T:p.H9775Y,ENSG00000155657:ENST00000589042:exon107:c.C30274T:p.H10092Y		rs72650011
2_179569416_G_A	ENSG00000155657:ENST00000342992:exon102:c.C26051T:p.P8684L,ENSG00000155657:ENST00000591111:exon103:c.C28832T:p.P9611L,ENSG00000155657:ENST00000589042:exon105:c.C29783T:p.P9928L		
2_179570048_C_A	ENSG00000155657:ENST00000342992:exon100:c.G25725T:p.E8575D,ENSG00000155657:ENST00000591111:exon101:c.G28506T:p.E9502D,ENSG00000155657:ENST00000589042:exon103:c.G29457T:p.E9819D		
2_179571284_C_T	NM_133378:c.G25585A:p.A8529T		
2_179571370_C_T	NM_133378:c.G25499A:p.R8500H	P	
2_179571661_C_G	NM_133378:c.G25330C:p.A8444P		
2_179571683_T_G	NM_133378:exon99:c.25310-2A>C	L	rs6716782
2_179572324_G_A	NM_133378:c.C25238T:p.S8413L		
2_179574313_G_A	NM_133378:c.C25001T:p.T8334M		rs184923756
2_179576026_T_C	NM_133378:c.A24205G:p.T8069A		
2_179576881_A_G	ENSG00000155657:ENST00000342992:exon93:c.T23944C:p.C7982R,ENSG00000155657:ENST00000591111:exon94:c.T26725C:p.C8909R,ENSG00000155657:ENST00000589042:exon96:c.T27676C:p.C9226R		
2_179576932_T_C	NM_133378:c.A23893G:p.K7965E		rs148355969

2_179577281_A_G	ENSG00000155657:ENST00000342992:exon92:c.T23636C:p.I7879T,ENSG00000155657:ENST00000591111:exon93:c.T26417C:p.I8806T,ENSG00000155657:ENST00000589042:exon95:c.T27368C:p.I9123T		
2_179577535_C_G	NM_133378:c.G23485C:p.V7829L		
2_179577979_T_C	ENSG00000155657:ENST00000342992:exon90:c.A23150G:p.H7717R,ENSG00000155657:ENST00000591111:exon91:c.A25931G:p.H8644R,ENSG00000155657:ENST00000589042:exon93:c.A26882G:p.H8961R		
2_179577984_C_A	ENSG00000155657:ENST00000342992:exon90:c.G23145T:p.W7715C,ENSG00000155657:ENST00000591111:exon91:c.G25926T:p.W8642C,ENSG00000155657:ENST00000589042:exon93:c.G26877T:p.W8959C		
2_179578012_T_C	ENSG00000155657:ENST00000342992:exon90:c.A23117G:p.Y7706C,ENSG00000155657:ENST00000591111:exon91:c.A25898G:p.Y8633C,ENSG00000155657:ENST00000589042:exon93:c.A26849G:p.Y8950C		rs199557654
2_179578043_C_T	ENSG00000155657:ENST00000342992:exon90:c.G23086A:p.G7696S,ENSG00000155657:ENST00000591111:exon91:c.G25867A:p.G8623S,ENSG00000155657:ENST00000589042:exon93:c.G26818A:p.G8940S		rs201005813
2_179578857_G_A	ENSG00000155657:ENST00000342992:exon89:c.C22796T:p.T7599M,ENSG00000155657:ENST00000591111:exon90:c.C25577T:p.T8526M,ENSG00000155657:ENST00000589042:exon92:c.C26528T:p.T8843M		rs72648990
2_179578891_T_C	NM_133378:c.G16609A:p.E5537K		rs72648989
2_179578900_G_A	ENSG00000155657:ENST00000342992:exon89:c.C22753T:p.P7585S,ENSG00000155657:ENST00000591111:exon90:c.C25534T:p.P8512S,ENSG00000155657:ENST00000589042:exon92:c.C26485T:p.P8829S		
2_179579211_G_A	NM_133378:c.C22558T:p.P7520S		
2_179579957_T_C	ENSG00000155657:ENST00000342992:exon87:c.A22224G:p.I7408M,ENSG00000155657:ENST00000591111:exon88:c.A25005G:p.I8335M,ENSG00000155657:ENST00000589042:exon90:c.A25956G:p.I8652M		
2_179580264_T_C	ENSG00000155657:ENST00000342992:exon86:c.A22145G:p.N7382S,ENSG00000155657:ENST00000591111:exon87:c.A24926G:p.N8309S,ENSG00000155657:ENST00000589042:exon89:c.A25877G:p.N8626S		rs200355367
2_179581842_G_A	ENSG00000155657:ENST00000342992:exon85:c.C21887T:p.S7296F,ENSG00000155657:ENST00000591111:exon86:c.C24668T:p.S8223F,ENSG00000155657:ENST00000589042:exon88:c.C25619T:p.S8540F		rs201523784
2_179581878_C_T	ENSG00000155657:ENST00000342992:exon85:c.G21851A:p.C7284Y,ENSG00000155657:ENST00000591111:exon86:c.G24632A:p.C8211Y,ENSG00000155657:ENST00000589042:exon88:c.G25583A:p.C8528Y		

2_179581897_C_T	NM_133378:c.G21832A:p.D7278N		
2_179581971_C_T	NM_133378:c.A15092G:p.N5031S		
2_179582687_G_C	ENSG00000155657:ENST00000342992:exon83:c.C21314G:p.A7105G,ENSG00000155657:ENST00000591111:exon84:c.C24095G:p.A8032G,ENSG00000155657:ENST00000589042:exon86:c.C25046G:p.A8349G		
2_179582760_T_C	NM_133378:c.A21241G:p.K7081E		rs72648984
2_179582769_C_A	ENSG00000155657:ENST00000342992:exon83:c.G21232T:p.V7078L,ENSG00000155657:ENST00000591111:exon84:c.G24013T:p.V8005L,ENSG00000155657:ENST00000589042:exon86:c.G24964T:p.V8322L		rs201571580
2_179582913_C_T	NM_133378:c.G21088A:p.E7030K		rs72648981
2_179583152_T_C	ENSG00000155657:ENST00000342992:exon82:c.A20949G:p.I6983M,ENSG00000155657:ENST00000591111:exon83:c.A23730G:p.I7910M,ENSG00000155657:ENST00000589042:exon85:c.A24681G:p.I8227M		
2_179583960_C_T	NM_133378:c.G20425A:p.G6809S		
2_179584042_A_C	NM_133378:c.T20343G:p.I6781M		
2_179584302_T_C	ENSG00000155657:ENST00000342992:exon79:c.A20185G:p.T6729A,ENSG00000155657:ENST00000591111:exon80:c.A22966G:p.T7656A,ENSG00000155657:ENST00000589042:exon82:c.A23917G:p.T7973A		
2_179584550_C_A	NM_133378:c.G19937T:p.R6646I		
2_179584752_C_T	ENSG00000155657:ENST00000342992:exon78:c.G19885A:p.D6629N,ENSG00000155657:ENST00000591111:exon79:c.G22666A:p.D7556N,ENSG00000155657:ENST00000589042:exon81:c.G23617A:p.D7873N		
2_179584831_G_C	NM_003319:c.G37594A:p.V12532M		
2_179585187_C_T	NM_133378:c.G19570A:p.D6524N		rs72648973
2_179585257_G_C	NM_133378:c.C19500G:p.N6500K		het
2_179585717_C_T	ENSG00000155657:ENST00000342992:exon76:c.G19297A:p.G6433R,ENSG00000155657:ENST00000591111:exon77:c.G22078A:p.G7360R,ENSG00000155657:ENST00000589042:exon79:c.G23029A:p.G7677R		
2_179586723_C_T	ENSG00000155657:ENST00000342992:exon75:c.G18935A:p.R6312H,ENSG00000155657:ENST00000591111:exon76:c.G21716A:p.R7239H,ENSG00000155657:ENST00000589042:exon78:c.G22667A:p.R7556H		
2_179586756_C_T	NM_003319:c.A32810G:p.D10937G		rs72648969

2_179587934_C_T	ENSG00000155657:ENST00000342992:exon72:c.G18068A:p.G6023D,ENSG00000155657:ENST00000591111:exon73:c.G20849A:p.G6950D,ENSG00000155657:ENST00000589042:exon75:c.G21800A:p.G7267D		
2_179587955_G_T	NM_133378:c.C18047A:p.S6016Y		rs187925021
2_179588184_C_T	NM_003319:c.C60217A:p.P20073T		
2_179588279_C_T	NM_133378:c.G17816A:p.C5939Y		rs189951108
2_179588622_C_T	NM_133378:c.G17632A:p.A5878T		
2_179589100_T_C	NM_003319:c.G31441C:p.E10481Q		
2_179589103_T_C	NM_133378:c.A17267G:p.N5756S		
2_179590133_C_G	NM_003319:c.A5126G:p.N1709S		
2_179590695_G_A	NM_133378:c.C16622T:p.S5541L		
2_179590708_C_T	NM_133378:c.A22762G:p.I7588V		rs72648958
2_179590714_T_A	ENSG00000155657:ENST00000342992:exon67:c.A16603T:p.S5535C,ENSG00000155657:ENST00000591111:exon68:c.A19384T:p.S6462C,ENSG00000155657:ENST00000589042:exon70:c.A20335T:p.S6779C		rs149470241
2_179590738_C_G	NM_003319:c.G55615A:p.G18539S		
2_179590756_T_A	ENSG00000155657:ENST00000342992:exon67:c.A16561T:p.S5521C,ENSG00000155657:ENST00000591111:exon68:c.A19342T:p.S6448C,ENSG00000155657:ENST00000589042:exon70:c.A20293T:p.S6765C		
2_179591917_T_C	NM_003319:c.A75400G:p.I25134V		
2_179591997_C_T	ENSG00000155657:ENST00000342992:exon66:c.G16363A:p.V5455I,ENSG00000155657:ENST00000591111:exon67:c.G19144A:p.V6382I,ENSG00000155657:ENST00000589042:exon69:c.G20095A:p.V6699I		
2_179592507_T_C	ENSG00000155657:ENST00000342992:exon65:c.A16066G:p.T5356A,ENSG00000155657:ENST00000591111:exon66:c.A18847G:p.T6283A,ENSG00000155657:ENST00000589042:exon68:c.A19798G:p.T6600A		
2_179592561_G_A	ENSG00000155657:ENST00000342992:exon65:c.C16012T:p.R5338X,ENSG00000155657:ENST00000591111:exon66:c.C18793T:p.R6265X,ENSG00000155657:ENST00000589042:exon68:c.C19744T:p.R6582X	L	
2_179592888_C_T	ENSG00000155657:ENST00000342992:exon64:c.G15931A:p.V5311M,ENSG00000155657:ENST00000591111:exon65:c.G18712A:p.V6238M,ENSG00000155657:ENST00000589042:exon67:c.G19663A:p.V6555M		

2_179593004_T_A	ENSG00000155657:ENST00000342992:exon64:c.A15815T:p.K5272M,ENSG00000155657:ENST00000591111:exon65:c.A18596T:p.K6199M,ENSG00000155657:ENST00000589042:exon67:c.A19547T:p.K6516M		rs199796249
2_179593110_G_T	NM_133378:c.C15709A:p.P5237T		
2_179593503_G_T	NM_133378:c.C15418A:p.P5140T		rs72648953
2_179593702_C_A	NM_133378:c.G15331T:p.D5111Y		rs188878341
2_179593733_G_C	NM_003319:c.G2962A:p.V988M		
2_179593804_T_C	ENSG00000155657:ENST00000342992:exon62:c.A15229G:p.I5077V,ENSG00000155657:ENST00000591111:exon63:c.A18010G:p.I6004V,ENSG00000155657:ENST00000589042:exon65:c.A18961G:p.I6321V		rs145204073
2_179594059_T_C	NM_003319:c.C68102T:p.S22701F		
2_179594107_G_C	ENSG00000155657:ENST00000342992:exon61:c.C15044G:p.T5015S,ENSG00000155657:ENST00000591111:exon62:c.C17825G:p.T5942S,ENSG00000155657:ENST00000589042:exon64:c.C18776G:p.T6259S		rs72648949
2_179594164_C_T	NM_133378:c.G14987A:p.R4996Q		
2_179594220_T_G	NM_133378:c.A14931C:p.E4977D		
2_179594430_C_T	NM_133378:c.G14818A:p.A4940T		rs72648947
2_179594655_T_C	ENSG00000155657:ENST00000342992:exon60:c.A14593G:p.K4865E,ENSG00000155657:ENST00000591111:exon61:c.A17374G:p.K5792E,ENSG00000155657:ENST00000589042:exon63:c.A18325G:p.K6109E		rs73973139
2_179595247_G_C	NM_133378:c.C14281G:p.H4761D		
2_179595892_C_T	ENSG00000155657:ENST00000342992:exon57:c.G13768A:p.V4590I,ENSG00000155657:ENST00000591111:exon58:c.G16549A:p.V5517I,ENSG00000155657:ENST00000589042:exon60:c.G17500A:p.V5834I		
2_179596269_G_A	NM_133378:c.C13492T:p.L4498F		rs72648943
2_179596554_T_C	NM_133378:c.A13316G:p.Y4439C		het
2_179596614_G_A	ENSG00000155657:ENST00000342992:exon55:c.C13256T:p.T4419I,ENSG00000155657:ENST00000591111:exon56:c.C16037T:p.T5346I,ENSG00000155657:ENST00000589042:exon58:c.C16988T:p.T5663I		
2_179596668_G_A	ENSG00000155657:ENST00000342992:exon55:c.C13202T:p.P4401L,ENSG00000155657:ENST00000591111:exon56:c.C15983T:p.P5328L,ENSG00000155657:ENST00000589042:exon58:c.C16934T:p.P5645L		
2_179597606_T_C	NM_133378:c.A12565G:p.N4189D		

2_179597691_C_G	NM_133378:c.G12480C:p.R4160S		
2_179598064_T_C	ENSG00000155657:ENST00000342992:exon51:c.A12224G:p.K4075R,ENSG00000155657:ENST00000591111:exon52:c.A15005G:p.K5002R,ENSG00000155657:ENST00000589042:exon54:c.A15956G:p.K5319R		
2_179598532_T_C	ENSG00000155657:ENST00000342992:exon50:c.A11852G:p.E3951G,ENSG00000155657:ENST00000591111:exon51:c.A14633G:p.E4878G,ENSG00000155657:ENST00000589042:exon53:c.A15584G:p.E5195G		rs72648931
2_179598553_T_G	NM_133378:c.A11831C:p.Q3944P		rs72648930
2_179599298_C_T	NM_133378:c.G11521A:p.D3841N		
2_179599455_T_C	ENSG00000155657:ENST00000342992:exon48:c.A11464G:p.S3822G,ENSG00000155657:ENST00000591111:exon49:c.A14245G:p.S4749G,ENSG00000155657:ENST00000589042:exon51:c.A15196G:p.S5066G		
2_179599473_C_G	ENSG00000155657:ENST00000342992:exon48:c.G11446C:p.V3816L,ENSG00000155657:ENST00000591111:exon49:c.G14227C:p.V4743L,ENSG00000155657:ENST00000589042:exon51:c.G15178C:p.V5060L		rs72648929
2_179599473_C_T	ENSG00000155657:ENST00000342992:exon48:c.G11446A:p.V3816I,ENSG00000155657:ENST00000591111:exon49:c.G14227A:p.V4743I,ENSG00000155657:ENST00000589042:exon51:c.G15178A:p.V5060I		rs72648929
2_179599565_C_T	NM_133378:c.G11354A:p.R3785Q		
2_179599697_T_G	NM_133378:c.A11222C:p.K3741T		
2_179600303_G_A	NM_133378:c.C11138T:p.T3713I		
2_179600303_G_C	NM_133378:c.C11138G:p.T3713S		rs72648925
2_179600360_A_G	ENSG00000155657:ENST00000342992:exon47:c.T11081C:p.F3694S,ENSG00000155657:ENST00000591111:exon48:c.T13862C:p.F4621S,ENSG00000155657:ENST00000589042:exon50:c.T14813C:p.F4938S		
2_179600385_G_T	NM_133378:c.C11056A:p.P3686T		
2_179600475_C_T	ENSG00000155657:ENST00000342992:exon47:c.G10966A:p.A3656T,ENSG00000155657:ENST00000591111:exon48:c.G13747A:p.A4583T,ENSG00000155657:ENST00000589042:exon50:c.G14698A:p.A4900T		rs72648923
2_179602850_T_G	NM_003319:c.G77051A:p.R25684Q		

2_179602878_C_T	ENSG00000155657:ENST00000342992:exon46:c.G10570A:p.G3524S,ENSG00000155657:ENST00000460472:exon46:c.G13213A:p.G4405S,ENSG00000155657:ENST00000342175:exon47:c.G13789A:p.G4597S,ENSG00000155657:ENST00000359218:exon47:c.G13588A:p.G4530S,ENSG00000155657:ENST00000591111:exon47:c.G13351A:p.G4451S,ENSG00000155657:ENST00000589042:exon49:c.G14302A:p.G4768S		
2_179603001_G_A	ENSG00000155657:ENST00000342992:exon46:c.C10447T:p.P3483S,ENSG00000155657:ENST00000460472:exon46:c.C13090T:p.P4364S,ENSG00000155657:ENST00000342175:exon47:c.C13666T:p.P4556S,ENSG00000155657:ENST00000359218:exon47:c.C13465T:p.P4489S,ENSG00000155657:ENST00000591111:exon47:c.C13228T:p.P4410S,ENSG00000155657:ENST00000589042:exon49:c.C14179T:p.P4727S		
2_179603028_T_C	NM_003319:c.A13063G:p.K4355E		
2_179603984_T_C	ENSG00000155657:ENST00000460472:exon45:c.A12887G:p.Y4296C,ENSG00000155657:ENST00000342175:exon46:c.A13463G:p.Y4488C,ENSG00000155657:ENST00000359218:exon46:c.A13262G:p.Y4421C,ENSG00000155657:ENST00000591111:exon46:c.A13025G:p.Y4342C,ENSG00000155657:ENST00000589042:exon48:c.A13976G:p.Y4659C		rs34706803
2_179603991_T_G	NM_003319:c.A12880C:p.N4294H		
2_179604063_T_C	NM_003319:c.A12808G:p.K4270E		
2_179604101_C_T	NM_003319:c.G22724C:p.S7575T		rs55857742
2_179604366_T_C	NM_003319:c.A12505G:p.T4169A		
2_179604440_A_G	ENSG00000155657:ENST00000460472:exon45:c.T12431C:p.M4144T,ENSG00000155657:ENST00000342175:exon46:c.T13007C:p.M4336T,ENSG00000155657:ENST00000359218:exon46:c.T12806C:p.M4269T,ENSG00000155657:ENST00000591111:exon46:c.T12569C:p.M4190T,ENSG00000155657:ENST00000589042:exon48:c.T13520C:p.M4507T		rs191968963
2_179604698_T_C	ENSG00000155657:ENST00000460472:exon45:c.A12173G:p.N4058S,ENSG00000155657:ENST00000342175:exon46:c.A12749G:p.N4250S,ENSG00000155657:ENST00000359218:exon46:c.A12548G:p.N4183S,ENSG00000155657:ENST00000591111:exon46:c.A12311G:p.N4104S,ENSG00000155657:ENST00000589042:exon48:c.A13262G:p.N4421S		rs72648922
2_179605004_G_A	ENSG00000155657:ENST00000460472:exon45:c.C11867T:p.A3956V,ENSG00000155657:ENST00000342175:exon46:c.C12443T:p.A4148V,ENSG00000155657:ENST00000359218:exon46:c.C12242T:p.A4081V,ENSG00000155657:ENST00000591111:exon46:c.C12005T:p.A4002V,ENSG00000155657:ENST00000589042:exon48:c.C12956T:p.A4319V		

2_179605139_C_T	NM_003319:c.G11732A:p.S3911N		
2_179605212_C_T	NM_003319:c.C25657T:p.R8553C		
2_179605280_G_T	ENSG00000155657:ENST00000460472:exon45:c.C11591A:p.T3864N,ENSG00000155657:ENST00000342175:exon46:c.C12167A:p.T4056N,ENSG00000155657:ENST00000359218:exon46:c.C11966A:p.T3989N,ENSG00000155657:ENST00000591111:exon46:c.C11729A:p.T3910N,ENSG00000155657:ENST00000589042:exon48:c.C12680A:p.T4227N		
2_179605727_G_A	ENSG00000155657:ENST00000460472:exon45:c.C11144T:p.T3715I,ENSG00000155657:ENST00000342175:exon46:c.C11720T:p.T3907I,ENSG00000155657:ENST00000359218:exon46:c.C11519T:p.T3840I,ENSG00000155657:ENST00000591111:exon46:c.C11282T:p.T3761I,ENSG00000155657:ENST00000589042:exon48:c.C12233T:p.T4078I		rs80136515
2_179605964_T_C	ENSG00000155657:ENST00000460472:exon45:c.A10907G:p.N3636S,ENSG00000155657:ENST00000342175:exon46:c.A11483G:p.N3828S,ENSG00000155657:ENST00000359218:exon46:c.A11282G:p.N3761S,ENSG00000155657:ENST00000591111:exon46:c.A11045G:p.N3682S,ENSG00000155657:ENST00000589042:exon48:c.A11996G:p.N3999S		rs199844346
2_179606118_G_A	NM_003319:c.C10753T:p.R3585C		
2_179606124_G_T	ENSG00000155657:ENST00000460472:exon45:c.C10747A:p.P3583T,ENSG00000155657:ENST00000342175:exon46:c.C11323A:p.P3775T,ENSG00000155657:ENST00000359218:exon46:c.C11122A:p.P3708T,ENSG00000155657:ENST00000591111:exon46:c.C10885A:p.P3629T,ENSG00000155657:ENST00000589042:exon48:c.C11836A:p.P3946T		
2_179610391_C_G	NM_133379:c.G16736C:p.S5579T		
2_179610514_C_T	ENSG00000155657:ENST00000360870:exon46:c.G16613A:p.R5538H		rs145932311
2_179610658_A_G	NM_133379:c.T16469C:p.L5490S		
2_179610806_G_A	NM_133379:c.C16321T:p.R5441X	L	
2_179610967_C_T	NM_133379:c.G16160A:p.C5387Y		rs72648913
2_179610985_C_T	NM_133379:c.G16142A:p.R5381H		
2_179611046_AATCCATATTTG_-	NM_133379:c.16070_16081del:p.5357_5361del		
2_179611126_G_A	NM_133379:c.C16001T:p.P5334L		rs151253841
2_179611340_C_T	NM_133379:c.G15787A:p.E5263K		
2_179611825_T_C	NM_133379:c.A15302G:p.E5101G		rs142973956
2_179612005_G_C	NM_133379:c.C15122G:p.T5041R		

2_179612313_C_T	NM_133379:c.G14814A:p.M4938I		
2_179612315_T_C	NM_133379:c.A14812G:p.M4938V		rs145581345
2_179612321_T_A	NM_133379:c.A14806T:p.T4936S		rs72648909
2_179612414_G_C	NM_133379:c.C14713G:p.L4905V		
2_179612521_G_T	ENSG00000155657:ENST00000360870:exon46:c.C14606A:p.A4869D		
2_179612635_C_T	NM_003319:c.T63631G:p.C21211G		
2_179612678_G_A	ENSG00000155657:ENST00000360870:exon46:c.C14449T:p.Q4817X	L	
2_179613049_A_G	NM_133379:c.T14078C:p.I4693T		rs139486133
2_179613264_C_T	ENSG00000155657:ENST00000360870:exon46:c.G13863A:p.M4621I		rs77419653
2_179613268_T_G	NM_133379:c.A13859C:p.Q4620P		rs139172299
2_179613376_T_C	ENSG00000155657:ENST00000360870:exon46:c.A13751G:p.K4584R		
2_179613494_C_T	ENSG00000155657:ENST00000360870:exon46:c.G13633A:p.A4545T		rs147884688
2_179613541_G_C	NM_133379:c.C13586G:p.A4529G		rs138927584
2_179613763_T_C	NM_133379:c.A13364G:p.K4455R		rs142304137
2_179613780_T_C	NM_133379:c.A13347G:p.I4449M		rs144539321
2_179614099_G_T	NM_133379:c.C13028A:p.T4343N		
2_179614148_T_C	NM_133379:c.A12979G:p.I4327V		rs144226338
2_179614901_C_T	NM_133379:c.G12226A:p.E4076K		rs144690298
2_179615024_C_T	NM_133379:c.G12103A:p.A4035T		
2_179615318_T_G	ENSG00000155657:ENST00000360870:exon46:c.A11809C:p.K3937Q		
2_179615844_C_G	ENSG00000155657:ENST00000360870:exon46:c.G11283C:p.K3761N		rs200816462
2_179616052_C_G	ENSG00000155657:ENST00000360870:exon46:c.G11075C:p.S3692T		rs147314430
2_179616073_C_A	ENSG00000155657:ENST00000360870:exon46:c.G11054T:p.G3685V		
2_179616248_C_T	NM_133379:c.G10879A:p.G3627R		
2_179616296_T_C	NM_133379:c.A10831G:p.K3611E		
2_179616345_T_-	ENSG00000155657:ENST00000360870:exon46:c.10782delA:p.S3594fs	L	
2_179616394_T_C	NM_133379:c.A10733G:p.Y3578C		

2_179616481_C_T	NM_133379:c.G10646A:p.R3549H		rs148115514
2_179616490_G_A	ENSG00000155657:ENST00000360870:exon46:c.C10637T:p.T3546I		
2_179616716_C_T	NM_133379:c.G10411A:p.A3471T		rs149878929
2_179621021_-_C	NM_133437:c.10669_10670insG:p.G3557fs	L	
2_179622440_G_T	ENSG00000155657:ENST00000359218:exon44:c.C10369A:p.Q3457K,ENSG00000155657:ENST00000589042:exon45:c.C10507A:p.Q3503K		
2_179622508_T_A	ENSG00000155657:ENST00000359218:exon44:c.A10301T:p.E3434V,ENSG00000155657:ENST00000589042:exon45:c.A10439T:p.E3480V		
2_179622577_T_C	NM_133432:c.A10232G:p.K3411R		
2_179623878_C_T	NM_003319:c.G9998A:p.S3333N		
2_179623903_C_T	NM_133437:exon44:c.9977-4G>A,NM_133432:exon44:c.9977-4G>A,NM_003319:exon44:c.9977-4G>A,NM_133378:exon45:c.10115-4G>A,NM_133379:exon45:c.10115-4G>A	L	
2_179628899_C_T		L	rs115985443
2_179628930_C_T	ENSG00000155657:ENST00000342175:exon42:c.G9950A:p.R3317H,ENSG00000155657:ENST00000359218:exon42:c.G9950A:p.R3317H,ENSG00000155657:ENST00000460472:exon42:c.G9950A:p.R3317H,ENSG00000155657:ENST00000342992:exon43:c.G10088A:p.R3363H,ENSG00000155657:ENST00000360870:exon43:c.G10088A:p.R3363H,ENSG00000155657:ENST00000589042:exon43:c.G10088A:p.R3363H,ENSG00000155657:ENST00000591111:exon43:c.G10088A:p.R3363H		rs148169214
2_179629385_T_C	NM_003319:c.A9719G:p.K3240R		
2_179629415_T_C	NM_003319:c.A9689G:p.E3230G		
2_179631324_G_A	ENSG00000155657:ENST00000342175:exon40:c.C9349T:p.R3117C,ENSG00000155657:ENST00000359218:exon40:c.C9349T:p.R3117C,ENSG00000155657:ENST00000460472:exon40:c.C9349T:p.R3117C,ENSG00000155657:ENST00000342992:exon41:c.C9487T:p.R3163C,ENSG00000155657:ENST00000360870:exon41:c.C9487T:p.R3163C,ENSG00000155657:ENST00000589042:exon41:c.C9487T:p.R3163C,ENSG00000155657:ENST00000591111:exon41:c.C9487T:p.R3163C		rs140664731
2_179632598_C_T	ENSG00000155657:ENST00000342175:exon39:c.G9221A:p.R3074Q,ENSG00000155657:ENST00000359218:exon39:c.G9221A:p.R3074Q,ENSG00000155657:ENST00000460472:exon39:c.G9221A:p.R3074Q,ENSG00000155657:ENST00000342992:exon40:c.G9359A:p.R3120Q,ENSG00000155657:ENST00000360870:exon40:c.G9359A:p.R3120Q,ENSG00000155657:ENST00000589042:exon40:c.G9359A:p.R3120Q,ENSG00000155657:ENST00000591111:exon40:c.G9359A:p.R3120Q		rs72647894

2_179632619_C_T	ENSG00000155657:ENST00000342175:exon39:c.G9200A:p.R3067H,ENSG00000155657:ENST00000359218:exon39:c.G9200A:p.R3067H,ENSG00000155657:ENST00000460472:exon39:c.G9200A:p.R3067H,ENSG00000155657:ENST00000342992:exon40:c.G9338A:p.R3113H,ENSG00000155657:ENST00000360870:exon40:c.G9338A:p.R3113H,ENSG00000155657:ENST00000589042:exon40:c.G9338A:p.R3113H,ENSG00000155657:ENST00000591111:exon40:c.G9338A:p.R3113H		rs141258018
2_179634955_C_G	NM_003319:c.G8335C:p.V2779L		
2_179635205_C_T	NM_003319:c.G8176A:p.V2726M		
2_179636183_T_C	ENSG00000155657:ENST00000342175:exon33:c.A7733G:p.K2578R,ENSG00000155657:ENST00000359218:exon33:c.A7733G:p.K2578R,ENSG00000155657:ENST00000460472:exon33:c.A7733G:p.K2578R,ENSG00000155657:ENST00000342992:exon34:c.A7871G:p.K2624R,ENSG00000155657:ENST00000360870:exon34:c.A7871G:p.K2624R,ENSG00000155657:ENST00000589042:exon34:c.A7871G:p.K2624R,ENSG00000155657:ENST00000591111:exon34:c.A7871G:p.K2624R		
2_179637933_T_C	NM_003319:c.A7620G:p.I2540M		
2_179638249_C_T	NM_003319:c.G7396A:p.E2466K		rs116049561
2_179638672_T_C	NM_003319:c.G73852A:p.E24618K		
2_179638750_T_C	NM_003319:c.A7007G:p.E2336G		
2_179639020_G_A	NM_003319:c.C6833T:p.T2278M		
2_179639042_G_A	NM_003319:c.C6811T:p.R2271C		
2_179640101_C_T	NM_003319:c.G6352A:p.A2118T		rs56285559
2_179640146_T_C	NM_003319:c.A6307G:p.I2103V		
2_179640396_T_G	ENSG00000155657:ENST00000342175:exon27:c.A6057C:p.K2019N,ENSG00000155657:ENST00000359218:exon27:c.A6057C:p.K2019N,ENSG00000155657:ENST00000460472:exon27:c.A6057C:p.K2019N,ENSG00000155657:ENST00000342992:exon28:c.A6195C:p.K2065N,ENSG00000155657:ENST00000360870:exon28:c.A6195C:p.K2065N,ENSG00000155657:ENST00000589042:exon28:c.A6195C:p.K2065N,ENSG00000155657:ENST00000591111:exon28:c.A6195C:p.K2065N		
2_179640598_C_A	NM_003319:c.G5855T:p.R1952L		
2_179640716_A_T	NM_003319:c.T5737A:p.F1913I		
2_179640893_C_T	NM_003319:c.G5560A:p.V1854M		

2_179641112_C_A	ENSG00000155657:ENST00000342175:exon27:c.G5341T:p.A1781S,ENSG00000155657:ENST00000359218:exon27:c.G5341T:p.A1781S,ENSG00000155657:ENST00000460472:exon27:c.G5341T:p.A1781S,ENSG00000155657:ENST00000342992:exon28:c.G5479T:p.A1827S,ENSG00000155657:ENST00000360870:exon28:c.G5479T:p.A1827S,ENSG00000155657:ENST00000589042:exon28:c.G5479T:p.A1827S,ENSG00000155657:ENST00000591111:exon28:c.G5479T:p.A1827S		rs141213991
2_179641173_C_A	ENSG00000155657:ENST00000342175:exon27:c.G5280T:p.L1760F,ENSG00000155657:ENST00000359218:exon27:c.G5280T:p.L1760F,ENSG00000155657:ENST00000460472:exon27:c.G5280T:p.L1760F,ENSG00000155657:ENST00000342992:exon28:c.G5418T:p.L1806F,ENSG00000155657:ENST00000360870:exon28:c.G5418T:p.L1806F,ENSG00000155657:ENST00000589042:exon28:c.G5418T:p.L1806F,ENSG00000155657:ENST00000591111:exon28:c.G5418T:p.L1806F		
2_179641226_A_C	NM_003319:c.G57644T:p.G19215V		
2_179641327_T_C	NM_003319:c.G57068A:p.S19023N		
2_179641518_T_A	NM_003319:c.A4935T:p.E1645D		
2_179641646_C_T	NM_003319:c.G4807A:p.V1603I		rs138931943
2_179642019_C_T	NM_003319:c.G4533A:p.M1511I		rs139192633
2_179642173_G_A	ENSG00000155657:ENST00000342175:exon25:c.C4481T:p.S1494L,ENSG00000155657:ENST00000359218:exon25:c.C4481T:p.S1494L,ENSG00000155657:ENST00000460472:exon25:c.C4481T:p.S1494L,ENSG00000155657:ENST00000342992:exon26:c.C4619T:p.S1540L,ENSG00000155657:ENST00000360870:exon26:c.C4619T:p.S1540L,ENSG00000155657:ENST00000589042:exon26:c.C4619T:p.S1540L,ENSG00000155657:ENST00000591111:exon26:c.C4619T:p.S1540L		
2_179642260_C_T	NM_003319:c.G4394A:p.G1465D		
2_179642515_A_G	NM_003319:c.T4258C:p.F1420L		
2_179642552_T_A	NM_003319:c.C4151A:p.A1384E		
2_179642621_TGCAGGAGACATCCT_-	ENSG00000155657:ENST00000342175:exon24:c.4138_4152del:p.1380_1384del,ENSG00000155657:ENST00000359218:exon24:c.4138_4152del:p.1380_1384del,ENSG00000155657:ENST00000460472:exon24:c.4138_4152del:p.1380_1384del,ENSG00000155657:ENST00000342992:exon25:c.4276_4290del:p.1426_1430del,ENSG00000155657:ENST00000360870:exon25:c.4276_4290del:p.1426_1430del,ENSG00000155657:ENST00000589042:exon25:c.4276_4290del:p.1426_1430del,ENSG00000155657:ENST00000591111:exon25:c.4276_4290del:p.1426_1430del		
2_179642622_G_T	NM_003319:c.A4221T:p.R1407S		

2_179643601_C_G	NM_003319:c.G4070C:p.R1357TTTN;TTN		
2_179643610_C_G	NM_003319:c.G4061C:p.S1354T		rs138506461
2_179643649_A_G	ENSG00000155657:ENST00000342175:exon23:c.T4022C:p.L1341P,ENSG00000155657:ENST00000359218:exon23:c.T4022C:p.L1341P,ENSG00000155657:ENST00000460472:exon23:c.T4022C:p.L1341P,ENSG00000155657:ENST00000342992:exon24:c.T4160C:p.L1387P,ENSG00000155657:ENST00000360870:exon24:c.T4160C:p.L1387P,ENSG00000155657:ENST00000589042:exon24:c.T4160C:p.L1387P,ENSG00000155657:ENST00000591111:exon24:c.T4160C:p.L1387P		rs115303497
2_179643761_G_A	NM_003319:c.C3910T:p.R1304C		
2_179644761_T_A	NM_003319:c.47401_47403del:p.15801_15801del		
2_179644788_G_A	ENSG00000155657:ENST00000342175:exon21:c.C3530T:p.A1177V,ENSG00000155657:ENST00000359218:exon21:c.C3530T:p.A1177V,ENSG00000155657:ENST00000460472:exon21:c.C3530T:p.A1177V,ENSG00000155657:ENST00000342992:exon22:c.C3668T:p.A1223V,ENSG00000155657:ENST00000360870:exon22:c.C3668T:p.A1223V,ENSG00000155657:ENST00000589042:exon22:c.C3668T:p.A1223V,ENSG00000155657:ENST00000591111:exon22:c.C3668T:p.A1223V		rs78269740
2_179644851_A_G	NM_003319:c.T3467C:p.V1156A		rs150667217
2_179645857_G_T	NM_003319:c.C3376A:p.L1126I		
2_179645962_C_G	NM_003319:c.G3271C:p.G1091R		rs72647870
2_179645983_C_G	NM_003319:c.G3250C:p.V1084L		
2_179647000_C_T	ENSG00000155657:ENST00000342175:exon19:c.G3181A:p.G1061S,ENSG00000155657:ENST00000359218:exon19:c.G3181A:p.G1061S,ENSG00000155657:ENST00000460472:exon19:c.G3181A:p.G1061S,ENSG00000155657:ENST00000342992:exon20:c.G3319A:p.G1107S,ENSG00000155657:ENST00000360870:exon20:c.G3319A:p.G1107S,ENSG00000155657:ENST00000589042:exon20:c.G3319A:p.G1107S,ENSG00000155657:ENST00000591111:exon20:c.G3319A:p.G1107S		
2_179647078_C_T	ENSG00000155657:ENST00000342175:exon19:c.G3103A:p.A1035T,ENSG00000155657:ENST00000359218:exon19:c.G3103A:p.A1035T,ENSG00000155657:ENST00000460472:exon19:c.G3103A:p.A1035T,ENSG00000155657:ENST00000342992:exon20:c.G3241A:p.A1081T,ENSG00000155657:ENST00000360870:exon20:c.G3241A:p.A1081T,ENSG00000155657:ENST00000589042:exon20:c.G3241A:p.A1081T,ENSG00000155657:ENST00000591111:exon20:c.G3241A:p.A1081T		rs55914517
2_179647533_C_T	NM_003319:c.A64406T:p.D21469V		
2_179647666_G_T	NM_003319:c.C2829A:p.F943L		

2_179648807_C_T	NM_003319:c.G2627A:p.R876H		rs56046320
2_179648808_G_A	NM_003319:c.C2626T:p.R876C		rs72647862
2_179648837_C_T	ENSG00000155657:ENST00000342175:exon15:c.G2597A:p.R866H,ENSG00000155657:ENST00000359218:exon15:c.G2597A:p.R866H,ENSG00000155657:ENST00000460472:exon15:c.G2597A:p.R866H,ENSG00000155657:ENST00000342992:exon16:c.G2735A:p.R912H,ENSG00000155657:ENST00000360870:exon16:c.G2735A:p.R912H,ENSG00000155657:ENST00000589042:exon16:c.G2735A:p.R912H,ENSG00000155657:ENST00000591111:exon16:c.G2735A:p.R912H		
2_179648841_C_T	ENSG00000155657:ENST00000342175:exon15:c.G2593A:p.V865I,ENSG00000155657:ENST00000359218:exon15:c.G2593A:p.V865I,ENSG00000155657:ENST00000460472:exon15:c.G2593A:p.V865I,ENSG00000155657:ENST00000342992:exon16:c.G2731A:p.V911I,ENSG00000155657:ENST00000360870:exon16:c.G2731A:p.V911I,ENSG00000155657:ENST00000589042:exon16:c.G2731A:p.V911I,ENSG00000155657:ENST00000591111:exon16:c.G2731A:p.V911I		rs141961878
2_179648886_C_A	NM_003319:c.G2548T:p.V850F		
2_179648967_T_A	NM_003319:c.A2467T:p.T823S		
2_179650635_C_A	NM_003319:c.G2172T:p.Q724H		
2_179650727_G_T	NM_003319:c.C2080A:p.R694S		
2_179650807_C_T	ENSG00000155657:ENST00000342175:exon13:c.G2000A:p.R667Q,ENSG00000155657:ENST00000359218:exon13:c.G2000A:p.R667Q,ENSG00000155657:ENST00000460472:exon13:c.G2000A:p.R667Q,ENSG00000155657:ENST00000342992:exon14:c.G2138A:p.R713Q,ENSG00000155657:ENST00000360870:exon14:c.G2138A:p.R713Q,ENSG00000155657:ENST00000589042:exon14:c.G2138A:p.R713Q,ENSG00000155657:ENST00000591111:exon14:c.G2138A:p.R713Q		
2_179658217_C_T	ENSG00000155657:ENST00000436599:exon3:c.G238A:p.D80N,ENSG00000155657:ENST00000342175:exon9:c.G1450A:p.D484N,ENSG00000155657:ENST00000342992:exon9:c.G1450A:p.D484N,ENSG00000155657:ENST00000359218:exon9:c.G1450A:p.D484N,ENSG00000155657:ENST00000360870:exon9:c.G1450A:p.D484N,ENSG00000155657:ENST00000460472:exon9:c.G1450A:p.D484N,ENSG00000155657:ENST00000589042:exon9:c.G1450A:p.D484N,ENSG00000155657:ENST00000591111:exon9:c.G1450A:p.D484N		
2_179659122_G_A	NM_133437:exon9:c.1398+4C>T,NM_133432:exon9:c.1398+4C>T,NM_003319:exon9:c.1398+4C>T,NM_133378:exon9:c.1398+4C>T,NM_133379:exon9:c.1398+4C>T	L	

2_179659133_T_C	ENSG00000155657:ENST00000436599:exon2:c.A179G:p.Q60R,ENSG00000155657:ENST00000342175:exon8:c.A1391G:p.Q464R,ENSG00000155657:ENST00000342992:exon8:c.A1391G:p.Q464R,ENSG00000155657:ENST00000359218:exon8:c.A1391G:p.Q464R,ENSG00000155657:ENST00000360870:exon8:c.A1391G:p.Q464R,ENSG00000155657:ENST00000460472:exon8:c.A1391G:p.Q464R,ENSG00000155657:ENST00000589042:exon8:c.A1391G:p.Q464R,ENSG00000155657:ENST00000591111:exon8:c.A1391G:p.Q464R		
2_179659160_G_C	ENSG00000155657:ENST00000436599:exon2:c.C152G:p.T51R,ENSG00000155657:ENST00000342175:exon8:c.C1364G:p.T455R,ENSG00000155657:ENST00000342992:exon8:c.C1364G:p.T455R,ENSG00000155657:ENST00000359218:exon8:c.C1364G:p.T455R,ENSG00000155657:ENST00000360870:exon8:c.C1364G:p.T455R,ENSG00000155657:ENST00000460472:exon8:c.C1364G:p.T455R,ENSG00000155657:ENST00000589042:exon8:c.C1364G:p.T455R,ENSG00000155657:ENST00000591111:exon8:c.C1364G:p.T455R		
2_179659924_G_A	ENSG00000155657:ENST00000342175:exon7:c.C970T:p.P324S,ENSG00000155657:ENST00000342992:exon7:c.C970T:p.P324S,ENSG00000155657:ENST00000359218:exon7:c.C970T:p.P324S,ENSG00000155657:ENST00000360870:exon7:c.C970T:p.P324S,ENSG00000155657:ENST00000460472:exon7:c.C970T:p.P324S,ENSG00000155657:ENST00000589042:exon7:c.C970T:p.P324S,ENSG00000155657:ENST00000591111:exon7:c.C970T:p.P324S		rs72647845
2_179664293_G_A	ENSG00000155657:ENST00000342175:exon6:c.C835T:p.R279W,ENSG00000155657:ENST00000342992:exon6:c.C835T:p.R279W,ENSG00000155657:ENST00000359218:exon6:c.C835T:p.R279W,ENSG00000155657:ENST00000360870:exon6:c.C835T:p.R279W,ENSG00000155657:ENST00000460472:exon6:c.C835T:p.R279W,ENSG00000155657:ENST00000589042:exon6:c.C835T:p.R279W,ENSG00000155657:ENST00000591111:exon6:c.C835T:p.R279W		rs138060032
2_179664373_T_C	NM_003319:c.A755G:p.K252R		
2_179665117_C_T	NM_133437:exon5:c.583+5G>A,NM_133432:exon5:c.583+5G>A,NM_003319:exon5:c.583+5G>A,NM_133378:exon5:c.583+5G>A,NM_133379:exon5:c.583+5G>A	L	
2_179665170_T_C	ENSG00000155657:ENST00000342175:exon4:c.A535G:p.T179A,ENSG00000155657:ENST00000342992:exon4:c.A535G:p.T179A,ENSG00000155657:ENST00000359218:exon4:c.A535G:p.T179A,ENSG00000155657:ENST00000360870:exon4:c.A535G:p.T179A,ENSG00000155657:ENST00000460472:exon4:c.A535G:p.T179A,ENSG00000155657:ENST00000589042:exon4:c.A535G:p.T179A,ENSG00000155657:ENST00000591111:exon4:c.A535G:p.T179A		

APPENDIX F – LISTS OF CANDIDATE VARIANTS FROM WHOLE-EXOME SEQUENCING

Supplementary table 3. List of candidate variants for family 1. *In silico* prediction of pathogenicity as descibed in the Methods Section, chapter 3.2.

Chromosome	Genomic position	Gene name	Type of variant	Amino acid change	*In silico* prediction of pathogenicity
1	179095724	*ABL2*	missense	S159G	Damaging
2	21266783	*APOB*	missense	L4198P	Damaging
17	1933455	*DPH1*	missense	R417W	Damaging
1	157667701	*FCRL3*	missense	I103V	Damaging
6	26234977	*HIST1H2APS3*	missense	A62E	
6	160390393	*IGF2R*	missense	Q39E	
6	52130931	*MCM3*	missense	K724E	Tolerated
1	1563501	*MIB2*	missense	A706T	Tolerated
17	36873726	*MLLT6*	missense	G565R	Damaging
13	33110187	*N4BP2L2*	missense	W326C	Damaging
17	45699167	*NPEPPS*	missense	E877K	Damaging
4	129793236	*PHF17*	missense	R783Q	Tolerated
17	4714242	*PLD2*	missense	R336G	Tolerated
1	204199701	*PLEKHA6*	missense	S808T	Damaging
2	209308218	*PTH2R*	missense	P219S	
5	53815614	*SNX18*	missense	E611A	
2	179600301	*TTN-AS1*	missense	T3713I	
3	151545773	*AADAC*	missense	I338T	Damaging
2	37428927	*CEBPZ*	in-frame	1048delK	
1	26510311	*CNKSR1*	frameshift	P284fs	
6	151627014	*AKAP12*	in-frame	99delE	
18	9258690	*ANKRD12*	missense	T1809A	Tolerated
17	42988667	*GFAP*	frameshift	L346fs	
6	26234977	*HIST1H1D*	missense	A62E	Damaging
11	61915962	*INCENP*	missense	R740Q	Tolerated

8	41790762	*KAT6A*	in-frame	1652_1659delPPPPPQQP	
7	138665900	*KIAA1549*	missense	R39H	Tolerated
5	56177849	*MAP3K1*	in-frame	942_943insT	
15	31775991	*OTUD7A*	missense	P763S	Tolerated
3	126733201	*PLXNA1*	missense	D863N	Damaging
3	157823589	*SHOX2*	in-frame	75_76insGGG	
22	38121208	*TRIOBP*	missense	S882Y	Damaging
8	37555624	*ZNF703*	frameshift	H402fs	
2	20175310	*WDR35*	missense	D184G	Damaging

Supplementary table 4. List of candidate variants for family 2. In silico prediction of pathogenicity as descibed in the Methods Section, chapter 3.2.

Chromosome	Genomic position	Gene name	Type of variant	Amino acid change	*In silico* prediction of pathogenicity
5	125930883	*ALDH7A1*	missense	R3H	Damaging
2	29420448	*ALK*	missense	G1345R	
1	3390007	*ARHGEF16*	missense	P409L	Damaging
15	73009153	*BBS4*	missense	V123I	Tolerated
7	34118681	*BMPER*	missense	S431G	Tolerated
19	13318208	*CACNA1A*	missense	H2480Q	Tolerated
19	13409923	*CACNA1A*	missense	E842K	Tolerated
2	109421373	*CCDC138*	missense	T255I	Damaging
1	180062301	*CEP350*	missense	K2354R	Tolerated
6	39851777	*DAAM2*	missense	M629V	Tolerated
3	52430697	*DNAH1*	missense	H3832N	
17	62122829	*ERN1*	missense	R848T	
19	8137051	*FBN3*	missense	G2657R	
6	89891741	*GABRR1*	missense	R278C	Damaging
15	101567966	*LRRK1*	missense	D884N	Tolerated
15	101602891	*LRRK1*	missense	K1637R	Tolerated
3	47912584	*MAP4*	missense	R588C	Damaging
3	195510085	*MUC4*	missense	S2789I	
11	73914789	*PPME1*	missense	D40N	Damaging
1	156756827	*PRCC*	missense	D315V	Tolerated
6	7231679	*RREB1*	missense	T1116I	Tolerated
2	65571917	*SPRED2*	missense	M47K	Tolerated
2	179447849	*TTN-AS1*	missense	T19326R	
11	124012430	*VWA5A*	missense	K669E	Tolerated
12	7045892	*ATN1*	in-frame	494_495insQQQ	
2	201683051	*BZW1*	missense	G256R	Tolerated
17	5389469	*DERL2; MIS12*	missense	S5G	Tolerated
16	12009531	*GSPT1*	in-frame	16_17insG	
12	108956408	*ISCU*	missense	A4P	Tolerated
1	156707446	*MRPL24*	missense	T169M	Tolerated

1	156641755	*NES*	missense	K742T	Tolerated
1	228559007	*OBSCN*	missense	T7800I	Tolerated
20	1895825	*SIRPA*	missense	R54C	Damaging
15	90144561	*TICRR*	missense	M729T	Damaging
2	179647666	*TTN*	missense	F943L	
11	46726193	*ZNF408*	missense	Q307E	Damaging
3	52430697	*DNAH1*	missense	R3832S	
1	156707446	*MRPL24*	missense	T169M	Tolerated
1	114523963	*OLFML3*	missense	P265S	Tolerated
1	151263678	*ZNF687*	in-frame	1237_1238insN	

Supplementary table 5. List of candidate variants for family 3. *In silico* prediction of pathogenicity as descibed in the Methods Section, chapter 3.2.

Chromosome	Genomic position	Gene name	Type of variant	Amino acid change	*In silico* prediction of pathogenicity
4	657634	*PDE6B*	missense	A666T	Damaging
16	1129292	*SSTR5-AS1*	missense	V142M	Damaging
12	1192430	*ERC1*	missense	P257L	Tolerated
7	1510287	*INTS1*	missense	M2167L	Tolerated
6	7727612	*BMP6*	missense	A142T	
20	8639220	*PLCB1*	missense	Q244R	Tolerated
12	9227259	*A2M*	missense	T1218M	
19	15278138	*NOTCH3*	missense	V1762M	
19	18879577	*CRTC1*	missense	P448S	Tolerated
13	25671834	*PABPC3*	missense	V500M	
8	28574330	*EXTL3*	missense	R252W	
2	32445307	*SLC30A6*	missense	R344Q	Damaging
20	35060823	*DLGAP4*	missense	E235Q	Tolerated
22	43026923	*CYB5R3*	missense	D133N	Damaging
15	43815184	*MAP1A*	missense	P743S	
11	46388005	*DGKZ*	missense	A67P	
3	47125674	*SETD2*	missense	T1866A	
3	47787459	*SMARCC1*	missense	A114T	
17	48602268	*MYCBPAP*	missense	V599I	Tolerated
3	48610326	*COL7A1*	missense	K2267R	
2	48698319	*PPP1R21*	missense	T331S	Tolerated
15	48755314	*FBN1*	missense	N1730T	
12	56333949	*DGKA*	missense	I265V	Tolerated
10	64952781	*JMJD1C*	missense	N1998T	Tolerated
17	67302933	*ABCA5*	missense	V241I	Tolerated
16	69748946	*NQO1*	missense	L113P	Damaging
17	73969720	*ACOX1*	missense	T139M	Damaging
2	101096985	*NMS*	missense	T122P	
3	119256163	*CD80*	missense	S174F	Tolerated
12	124111643	*EIF2B1*	missense	A144T	Tolerated

2	152520109	*NEB*	missense	A1906T	Tolerated
2	153003680	*STAM2*	missense	S148C	
7	158902557	*VIPR2*	missense	E69K	Tolerated
5	171766091	*SH3PXD2B*	missense	A673V	
2	179395623	*TTN-AS1*	missense	R32672Q	
2	179469980	*TTN-AS1*	missense	T15407S	
3	183469964	*YEATS2*	missense	T358S	Tolerated
4	184615778	*TRAPPC11*	missense	R844C	Damaging
4	186533089	*SORBS2*	missense	E977Q	Damaging
2	215593705	*BARD1*	missense	F677L	Damaging
1	228559348	*OBSCN*	missense	A7669T	Tolerated
1	229477857	*CCSAP*	missense	A119G	Tolerated
2	233714978	*GIGYF2*	missense	V1253L	Tolerated
1	240256439	*FMN2*	missense	D344N	
2	242072365	*PASK*	missense	I463V	Tolerated
9	35660840	*ARHGEF39; CCDC107*	missense	E170K	Tolerated
19	58864466	*A1BG*	frameshift	P56fs	
6	157527493	*ARID1B*	in-frame	1740delD	
1	176934357	*ASTN1*	missense	I514V	Tolerated
4	42588463	*ATP8A1*	missense	V209I	Tolerated
7	122526234	*CADPS2*	in-frame	52_53insV	
8	2976054	*CSMD1*	missense	I2099M	Tolerated
1	85029497	*CTBS*	missense	K239R	Tolerated
2	240056115	*HDAC4*	missense	E374K	Tolerated
16	30004967	*HIRIP3*	missense	M155L	Tolerated
1	186101518	*HMCN1*	missense	R4430H	
2	201756818	*NIF3L1*	missense	N24S	Damaging
22	36157297	*RBFOX2*	missense	V306M	Tolerated
22	31957335	*SFI1*	missense	H217R	Tolerated
9	71835968	*TJP2*	missense	S147G	Tolerated
4	69202912	*YTHDC1*	in-frame	239delE	
16	72821594	*ZFHX3*	in-frame	2605_2613delGGGGGGGGG	

11	6422635	*APBB1*	missense	R251C	Damaging
1	151288179	*PI4KB*	missense	A272G	Tolerated
3	127339941	*MCM2*	missense	R825Q	Tolerated
22	30069405	*NF2*	missense	R424C	Tolerated
1	14105122	*PRDM2*	in-frame	282_283insE	
1	14105137	*PRDM2*	in-frame	287_288insD	

APPENDIX G – LIST OF *MYH7* VARIANTS USED FOR PATHOGENICITY AND PHENOTYPE PREDICTION BASED IN THE STRUCTURAL IMPACT OF THE MUTATION

Supplementary table 6. List of *MYH7* missense variants used for pathogenicity and phenotype prediction based in the structural impact of the mutation. AA1 – reference amino acid; AA2: observed amino acid.

Position	AA1	AA2
4	S	L
13	A	T
17	R	H
26	A	V
39	V	M
59	V	I
81	P	S
100	A	T
115	Y	H
124	T	I
142	Y	H
143	R	Q
143	R	G
143	R	W
146	K	N
148	S	I
162	Y	C
162	Y	H
169	R	K
177	T	I
178	G	R
181	G	R
185	T	S
186	V	L
187	N	K
188	T	N
190	R	T
194	Y	S
196	A	T
201	I	T
204	R	H
207	K	Q
211	P	L
214	G	D
216	L	V
219	Q	E
219	Q	L
222	Q	K
223	A	T

227	L	V
232	N	S
233	A	S
237	R	W
239	D	N
243	R	C
243	R	H
244	F	L
246	K	Q
247	F	L
249	R	Q
251	H	N
252	F	L
256	G	E
259	A	E
263	I	T
266	Y	C
270	K	R
272	R	T
281	R	T
283	Y	D
291	S	F
301	L	Q
312	F	C
320	V	M
322	S	F
325	D	G
326	A	P
328	E	G
338	V	M
349	M	T
350	Y	N
351	K	E
355	A	T
355	A	T
369	R	Q
377	G	R
377	G	S
382	D	Y
383	K	N
385	A	V
386	Y	H
388	M	T
390	L	P

390	L	V
398	G	E
403	R	W
403	R	W
403	R	Q
403	R	L
404	V	L
404	V	M
406	V	M
407	G	V
411	V	I
412	T	N
425	G	R
427	L	M
427	L	M
428	A	V
430	A	E
435	M	T
440	V	M
441	T	M
442	R	H
442	R	C
443	I	T
444	N	S
450	K	E
450	K	T
453	R	C
453	R	H
453	R	L
453	R	S
457	I	T
467	I	T
475	Q	H
475	Q	K
478	I	N
479	N	S
483	E	K
484	K	N
489	F	I
493	M	L
497	E	D
499	E	K
500	E	A
501	Y	H

501	Y	C
511	I	F
511	I	T
513	F	C
515	M	R
515	M	T
516	D	E
517	L	M
525	E	K
528	M	I
529	G	D
531	M	R
532	S	P
539	M	L
540	F	L
542	K	R
543	A	T
545	D	N
550	A	V
561	A	T
564	Q	E
576	H	R
583	A	V
584	G	R
584	G	S
587	D	H
587	D	V
591	I	T
601	L	V
601	L	F
602	N	S
606	V	M
609	Y	C
615	K	N
615	K	Q
624	Y	N
637	K	E
642	S	L
652	R	K
652	R	G
658	L	V
659	M	I
663	R	H
663	R	S

671	R	C
694	R	H
694	R	C
694	R	L
695	N	S
698	V	A
705	C	W
710	P	R
712	R	L
716	G	R
719	R	Q
719	R	W
719	R	P
721	R	K
723	R	C
723	R	G
723	R	H
728	A	V
729	A	P
730	I	N
731	P	L
733	G	R
733	G	E
734	Q	E
734	Q	P
736	I	M
736	I	T
736	I	L
738	R	H
741	G	R
741	G	W
741	G	A
742	A	E
743	E	D
763	V	G
763	V	M
764	F	L
768	G	R
771	G	A
774	E	V
778	D	E
778	D	G
778	D	V
779	E	D

782	S	R
782	S	N
783	R	H
783	R	P
787	R	H
787	R	C
793	R	Q
796	L	F
797	A	T
797	A	P
814	I	S
818	I	N
822	M	L
822	M	T
822	M	V
823	G	E
824	V	I
835	K	T
838	P	L
844	E	K
845	R	K
845	R	G
846	E	Q
846	E	K
847	K	E
849	M	T
850	A	D
850	A	T
852	M	T
858	R	C
858	R	H
858	R	P
865	K	R
866	S	Y
868	A	P
869	R	H
869	R	C
869	R	G
870	R	H
870	R	C
877	M	K
878	V	A
878	V	G
882	Q	E

889	L	H
890	Q	P
894	E	G
901	A	P
901	A	G
903	E	K
903	E	G
903	E	K
904	R	H
904	R	C
905	C	F
906	D	G
906	D	G
908	L	V
909	I	M
910	K	Q
921	E	K
924	E	K
924	E	Q
927	E	K
927	W	C
928	D	G
928	D	N
928	D	V
930	E	Q
930	E	K
931	E	G
932	M	K
935	E	K
949	E	K
949	E	V
953	D	H
955	D	N
961	L	R
964	V	L
965	E	K
970	A	V
982	M	T
1019	T	N
1027	L	P
1038	L	P
1042	K	N
1044	V	L
1044	V	A

1045	R	H
1045	R	C
1053	R	Q
1057	G	D
1057	G	S
1067	M	T
1069	D	Y
1079	R	Q
1101	G	S
1116	E	K
1128	A	T
1135	L	R
1169	A	S
1193	R	C
1193	R	S
1205	E	K
1208	D	N
1218	E	Q
1223	E	Q
1250	R	W
1263	A	E
1327	N	K
1332	A	T
1351	T	M
1352	E	Q
1356	E	K
1359	R	C
1377	T	M
1378	D	H
1379	A	T
1382	R	Q
1382	R	W
1414	L	M
1420	R	Q
1420	R	W
1426	E	K
1434	R	C
1454	A	T
1459	K	N
1465	S	L
1474	A	D
1475	R	C
1481	L	P
1488	Y	C

1490	E	K
1491	S	C
1496	E	A
1500	R	W
1500	R	P
1513	T	S
1536	E	K
1555	E	G
1555	E	K
1573	E	K
1619	E	K
1634	R	C
1637	A	T
1652	D	Y
1660	A	E
1662	R	H
1663	A	P
1677	R	C
1677	R	H
1691	V	M
1706	L	P
1712	R	Q
1712	R	W
1751	A	D
1752	E	V
1753	E	K
1760	T	M
1764	M	K
1766	A	T
1768	E	K
1769	L	M
1776	S	G
1777	A	T
1781	R	H
1792	D	G
1793	L	P
1801	E	K
1801	E	G
1808	G	A
1832	R	C
1836	S	L
1838	K	R
1845	R	W
1846	R	C

1854	T	M
1863	R	Q
1883	E	K
1901	H	Q
1901	H	L
1918	N	K
1925	R	G
1927	I	F
1929	T	M
1931	G	C